

Strong-Coupling Solution of the Dynamical Mean-Field Equations for the Mott-Hubbard Insulator on a Bethe Lattice



Dissertation
zur
Erlangung des Doktorgrades
der Naturwissenschaften
(Dr. rer. nat.)

dem
Fachbereich Physik
der Philipps-Universität Marburg
vorgelegt

von
Diplom-Physiker
Daniel F. Ruhl
aus
Kassel

Marburg/Lahn 2010

Vom Fachbereich Physik der Philipps-Universität Marburg
als Dissertation angenommen am 11.06.2010

Erstgutachter: Prof. Dr. Florian Gebhard
Zweitgutachter: Prof. Dr. Peter Lenz

Tag der mündlichen Prüfung: 22.06.2010

Zusammenfassung

Die Geburtsstunde der Physik korrelierter Elektronensysteme datiert in das Jahr 1937. De Boer und Verwey erkannten, dass viele Übergangsmetalloxide wie NiO schlechte elektrische Leiter, ja sogar Isolatoren sind, ganz im Gegensatz zu den Vorhersagen der Bandstrukturberechnungen. Erste theoretische Ansätze von Sir Nevill Mott wiesen auf die entscheidende Bedeutung der Wechselwirkung zwischen den Elektronen hin, so dass diese sich nicht unabhängig voneinander, sondern *korreliert* bewegen.

Trotz intensiver Forschungen in den letzten Jahrzehnten bleiben korrelierte Vielteilchensysteme ein schwieriges und faszinierendes Teilgebiet der Physik kondensierter Materie. Es umfasst heute so diverse Phänomene wie Magnetismus, Hochtemperatursupraleiter, Störstellenmodelle, "Schwere Fermionen" und nicht zuletzt den Metall-Isolator Übergang und die damit verbundene Beschreibung des Mott Isolators.

Viele Fragen sind bis heute nicht oder nur unzureichend geklärt. Das Hauptproblem bei der theoretischen Beschreibung solcher Systeme ist unser Unvermögen, wechselwirkende Vielteilchensysteme exakt lösen zu können. Lediglich Modelle wechselwirkender Elektronen in einer Raumdimension konnten bisher exakt behandelt werden. Aufgrund der niedrigen Dimension ist die Physik dieser Modelle jedoch nicht auf höhere Dimensionen übertragbar. Es gibt kaum analytische Methoden, die zwei- oder dreidimensionale Systeme beschreiben können. Auch die Zahl der aussagekräftigen numerischen Methoden ist sehr begrenzt. Diese Tatsachen machen deutlich, dass wir auf zuverlässige Methoden angewiesen sind, vereinfachende Vielteilchenmodelle kontrolliert näherungsweise zu lösen.

Eine solche Methode ist die Dynamische Molekularfeldtheorie (DMFT), welche in den letzten zwei Jahrzehnten vor allem durch Arbeiten von Vollhardt, Metzner, Brandt, Mielsch, Georges, Kotliar und Jarrell entwickelt wurde. Die DMFT erlaubt es, ein Gittermodell itineranter Elektronen mit lokaler Wechselwirkung auf ein effektives Störstellenmodell abzubilden. Diese Abbildung ist exakt im Grenzfall eines Gitters mit unendlicher Koordination, liefert aber auch verlässliche, approximative Aussagen über die Physik endlichdimensionaler Gitter. Obwohl die Störstellenmodelle konzeptionell einfacher sind als die Gittermodelle, stellen sie dennoch sehr komplizierte Vielteilchenprobleme dar. Die Störstellenmodelle enthalten zwar keine räumlichen Korrelationen mehr, beschreiben aber die zeitlichen Korrelationen des Gittermodells vollständig.

In dieser Arbeit beschäftigen wir uns mit der theoretischen Beschreibung des korrelierten Mott-Hubbard Isolators. Obwohl das Hubbard Modell das konzeptionell einfachste Modell korrelierter Elektronen darstellt, wurde bisher nur in einer Dimension eine exakte Lösung gefunden. Auch das Modell in unendlichen Dimensionen ist bisher nicht exakt gelöst. Zielsetzung unserer Arbeit ist die analytische Berechnung der Einteilchen-Zustandsdichte sowie der Lücke für Ladungsanregungen des Mott-Hubbard Isolators in unendlichen Dimensionen. Hierzu berechnen wir die lokale Greenfunktion des Hubbard Modells auf dem Bethegitter mit unendlich vielen nächsten Nachbarn bei der Temperatur $T = 0$.

Unser Startpunkt ist die Dynamische Molekularfeldtheorie (DMFT), um das auf dem Gitter definierte Hubbard Modell auf das *Single Impurity Anderson Model* (SIAM) abzubilden. Da der Mott-Hubbard Isolator durch eine Lücke in seinem Anregungsspektrum der Größenordnung U charakterisiert ist, formulieren wir das SIAM mit zwei Elektronen-Bädern, welche ebenfalls in der Energie um U voneinander separiert sind. Es ist wichtig an dieser Stelle anzumerken, daß die Parameter des effektiven Störstellenmodells nicht bekannt sind, sondern selbstkonsistent bestimmt werden müssen. Mit Hilfe einer Störungstheorie, welche von dem japanischen, mathematischen Physiker Tosio Kato entwickelt und später von Minoru Takahashi auf das Hubbard Modell in niedrigen Dimensionen angewandt wurde, sind wir in der Lage die Lösungen der Selbstkonsistenzgleichungen der DMFT bis zur dritten Ordnung in $1/U$ anzugeben. Hiermit präsentieren wir zum ersten Mal eine analytische Lösung der Selbstkonsistenzgleichungen der DMFT für den Mott-Hubbard Isolator.

Die Lösungen der Selbstkonsistenzgleichungen können als ein diskretisiertes, auf einer halbunendlichen, eindimensionalen Kette definiertes Streuproblem aufgefaßt werden. Wir berechnen die lokale Greenfunktion des ersten Gitterplatzes dieses Modells und erhalten auf diese Weise die Greenfunktion des Hubbard Modells auf dem Bethegitter mit unendlich vielen nächsten Nachbarn.

Wir vergleichen unsere analytischen Ergebnisse für die Zustandsdichte und die Einteilchenlücke mit nu-

merischen Daten aus der Dynamischen Dichtematrix Renormierungsgruppenmethode (DDMRG). Wir finden ausgezeichnete Übereinstimmung bis zu Werten der Zweiteilchenwechselwirkung von $U \approx 5$, bei einer Bandbreite des nicht-wechselwirkenden Systems von $W = 4$. Zusätzlich sind wir dank der Anregungslücke des Isolators in der Lage, eine genäherte Matsubara-Greenfunktion für Temperaturen $T \ll U - W$ zu berechnen. Diese gestattet uns einen Vergleich mit Daten der Quanten-Monte-Carlo (QMC) Methode, ohne dass diese (numerisch) analytisch fortgesetzt werden müssen. Wir finden hervorragende Übereinstimmung bei einer Temperatur von $T = 0.05$ und Wechselwirkungs-Stärken bis zu $U \approx 5$.

Trotz zwei Jahrzehnten intensiver Forschung und Weiterentwicklung der DMFT ist bisher keine exakte Lösung der Selbstkonsistenzgleichungen für das Hubbard Modell bekannt. Insbesondere wurden bisher keine analytischen Lösungen für den Mott-Hubbard Isolator angegeben. Unsere analytischen, bis einschließlich zur dritten Ordnung in $1/U$ exakte Lösungen der DMFT-Selbstkonsistenzgleichungen sind daher sicher ein bemerkenswertes Ergebnis. Da sie für den thermodynamischen Limes gelten, unterliegen sie insbesondere nicht den ‘finite-size’ Effekten, die letztendlich bei allen numerischen Methoden auftreten und durch Extrapolation minimiert werden müssen. Dies ist sehr aufwendig und oftmals nicht befriedigend durchführbar. Unsere Ergebnisse stellen somit einen verlässlichen Benchmark-Test dar, der helfen kann, die Genauigkeit numerischer Methoden besser abzuschätzen. Darüberhinaus gibt unsere analytische Methode Einblicke in die Physik des korrelierten Mott-Hubbard Isolators. Eine Weiterentwicklung zur Ordnung $1/U^4$ könnte etwa anzeigen, ob im Mott-Hubbard Isolator Bänder existieren, die bei höheren Anregungsstufen des atomaren Limes-Modells zentriert wären. Dies wäre im Hinblick auf die Diskussion der Art des Isolator-Metall-Übergangs sicher von Interesse.

Contents

1. Introduction	1
1.1. Metals and Insulators	2
1.2. Mott Insulator and Single-Particle Gap	3
1.3. Aim of this Thesis	4
1.4. Structure of the Thesis	5
I. Models	9
2. Electrons in Solids	11
2.1. Drude Model	11
2.2. First Principles Hamiltonian	13
2.2.1. Adiabatic Approximation	13
2.2.2. Hartree-Fock Approximation	14
3. Tight-Binding Model	17
3.1. Motivation of the Hamiltonian	17
3.2. Tight-Binding Model on Hypercubic Lattices	20
3.3. Tight-Binding Model on Bethe Lattices	23
3.3.1. Digression on Graph Theory	24
3.3.2. Electron Motion on Bethe Lattices	28
4. Single Impurity Anderson Model	31
4.1. Hamiltonian and Model Parameters	31
4.2. Non-Interacting Limit (Fano-Anderson Model)	32
4.3. Limiting Cases	34
4.3.1. Deep Impurity Limit (Local-Moment Regime)	35
4.3.2. Resonance Limit (Mixed-Valence Regime)	35
5. Hubbard Model	37
5.1. Basic Derivation of the Hubbard Hamiltonian	37
5.1.1. Hubbard's First Assumption (Single Band)	38
5.1.2. Hubbard's Second Assumption (Local Interaction)	38
5.1.3. Hubbard Hamiltonian	39
5.2. Symmetries	39
5.2.1. $SO(4)$ Symmetry	40
5.2.2. Electron-Hole Transformations	41
5.3. Limiting Cases	42
5.3.1. Band Limit	42
5.3.2. Atomic Limit	43
5.3.3. Strong-Coupling Limit	45
5.4. Mott-Hubbard Transition	46
II. Methods	49
6. Dynamical Mean-Field Theory	51
6.1. Ising Model	51
6.1.1. Free Energy in One Dimension	51
6.1.2. Mean-Field Theory of the Ising Model	53
6.1.3. Limits of High Dimensions and Large Coordination Number	55

Contents

6.2. Limit of Infinite Dimensions for Itinerant Electron Systems	56
6.2.1. Hypercubic Lattices	56
6.2.2. Bethe Lattices	57
6.2.3. Simplifications	58
6.2.4. Remarks on the Correct Scaling	59
6.3. Self-Consistency Equations of the Dynamical Mean-Field Theory	59
6.3.1. Self-Consistency in the Paramagnetic Case	60
6.3.2. Self-Consistency on the Infinitely Connected Bethe Lattice	60
6.4. Summary	61
7. Kato Perturbation Theory	63
7.1. Basic Definitions	63
7.2. Perturbational Setup	65
7.3. Eigenvalues and Eigenspaces	66
7.4. Perturbative Expansions	67
7.4.1. Projection Operator	67
7.4.2. Calculation of the Residue for the Projector	68
7.4.3. Hamiltonian	69
7.4.4. Calculation of the Residue for the Hamiltonian	70
7.5. Summary	71
8. Kato-Takahashi Formalism	73
8.1. Fundamental Quantities	73
8.2. Leading-Order Terms	75
8.2.1. Takahashi's Operator	75
8.2.2. Transformed Energy Operator	76
III. Calculations and Results	77
9. Theoretical Setup	79
9.1. Hubbard Lattice Model	79
9.2. Mapping onto the Impurity Problem	81
9.2.1. Local Impurity Green Function	82
9.2.2. Chain Geometry of the SIAM	83
9.3. Application of Kato-Takahashi Perturbation Theory	84
9.3.1. Starting Hamiltonian H_0	85
9.3.2. Perturbation V	86
9.3.3. Systematic Expansion of the Green Function	87
9.4. Matrix Representation via the Lanczos Iteration	89
9.4.1. Hybridization Function	90
9.4.2. Green Function	91
9.4.3. Self-Consistency Equation	91
10. Results	93
10.1. Solution of the Self-Consistency Equation	93
10.1.1. Calculations to Leading Order	93
10.1.2. Remarks on the Higher-Order Calculations	99
10.1.3. Results up to Third Order	102
10.2. Impurity Scattering Model	103
10.3. Green Function	104
10.3.1. Band-Part Contribution	105

10.3.2. Full Green Function	109
10.3.3. Summary	111
10.4. Single-Particle Gap	112
10.5. Density of States	114
10.5.1. Full Density of States	114
10.5.2. Resonance Contribution	116
10.6. Comparisons	116
10.6.1. Charge Gap	117
10.6.2. Density of States	117
10.6.3. Matsubara Green Function	119
11. Conclusions	121
11.1. Achievements	121
11.2. Outlook	122
Appendices	123
A. Use of Green Functions	125
A.1. Classical Green Functions	125
A.2. Green Functions in Single-Particle Quantum Mechanics	125
A.3. Green Functions in Many-Body Problems	127
A.3.1. Self-Energy	129
A.3.2. Summary of Diagrammatic Notions	129
A.4. Local Green Function of the Infinitely Connected Bethe Lattice	130
B. Applications of Symmetries of the Hubbard Model	133
B.1. Irrelevance of the Sign of the Electron Transfer Amplitude	133
B.2. Chemical Potential at Half Band-Filling	133
C. Calculation of the Mappings in the Kato-Takahashi Formalism	135
C.1. Expansion of Takahashi's operator	135
C.1.1. Calculations	135
C.1.2. Summary	139
C.2. Expansion of the Transformed Energy Operator	140
C.2.1. Calculations	140
C.2.2. Summary	146
C.3. Implementation of the SIAM	147
C.3.1. Simplifications in Two-Chain Geometry	147
C.3.2. Operators at Arbitrary Filling	149
C.3.3. Operators at Half Band-Filling	150
D. Multichain Approach to the SIAM	153
D.1. Multichain Setup of the SIAM Hamiltonian	154
D.2. Calculation of the Weights g_n by Perturbation Theory	155
E. Explicit Calculations	157
E.1. Definitions	157
E.2. Starting Vector for the Lanczos Iteration	158
E.2.1. Ground-State Vectors at Half Filling	158
E.2.2. Transformed Hole States	162
E.2.3. Starting Vector	163

Contents

E.3. Ground-State Energy of the SIAM at Half Filling	164
E.4. Operator for the Lanczos Procedure	165
E.5. Action of Operators	166
E.5.1. On-site Energy Operator	166
E.5.2. Intra-Chain Hopping	166
E.5.3. Restricted Hamiltonians	167
E.5.4. Operator for the Lanczos Procedure	177
E.6. Lanczos Iteration	179
E.6.1. Leading Order	180
E.6.2. First Order	183
E.6.3. Second Order	188
E.6.4. Third Order	197
F. Chebyshev Polynomials	211
F.1. Chebyshev Polynomials of the First Kind	211
F.2. Chebyshev Polynomials of the Second Kind	212
F.3. Electron Transport Along a Semi-Infinite Chain	213
F.3.1. Green Functions	215
F.3.2. Products of Green Functions	219
Bibliography	221
Acknowledgements	229
Curriculum Vitae	231

List of Figures

1.1.	Gedankenexperiment for making the single-particle gap plausible.	4
3.1.	Density of states of the one- and two-dimensional tight-binding model.	21
3.2.	Density of states of H_{TB} on the simple cubic lattice.	21
3.3.	Evolution of the density of states with d of H_{TB} on hypercubic lattices.	23
3.4.	Example for a simple graph.	24
3.5.	Examples for simple bipartite graphs.	25
3.6.	The 3-regular cube.	25
3.7.	Definition of trees.	26
3.8.	First Z -Cayley trees.	27
3.9.	Density of states of H_{TB} on Bethe lattices for $Z = 2, 3, 4$ and 5	29
3.10.	Density of states of H_{TB} on Bethe lattices with $Z = 6, 7, 10$ and 35	30
4.1.	Energy-level diagram of the SIAM in the local-moment regime.	35
4.2.	Energy-level diagram of the SIAM in the mixed-valence regime.	35
5.1.	‘Single-particle’ spectrum of the Hubbard model in the atomic limit.	43
5.2.	Local spectral function of the Hubbard model in the limit $t \rightarrow 0$	44
5.3.	Hubbard model in the metallic phase.	46
5.4.	Hubbard model at strong coupling.	47
6.1.	Magnetization density of the one-dimensional Ising model.	53
6.2.	Magnetization density of the Ising model in mean-field theory.	54
6.3.	Density of states in finite and infinite dimensions on hypercubic lattices.	57
6.4.	Visualization of the DMFT mapping.	59
7.1.	Path γ_i of definition 7.1.2.	64
7.2.	Normal energy-level structure without level-crossing.	66
7.3.	Level-crossing at the energies $E_1(b)$ and $E_2(a)$	66
9.1.	Sketch of the density of states of the Mott-Hubbard insulator at strong coupling.	80
9.2.	Mapping of the discretized SIAM in star geometry to a semi-infinite chain.	83
9.3.	Two-Chain mapping.	84
10.1.	Impurity scattering model to third order in $1/U$	103
10.2.	Green function of the lower Hubbard band in the limit of infinite coupling strength.	106
10.3.	Band-part contribution to first order.	107
10.4.	Band-part contribution to second order.	108
10.5.	Band-part contribution to third order.	109
10.6.	Single-particle gap.	113
10.7.	Dependence of the full density of states on the on-site interaction U	115
10.8.	Resonance contribution to the density of states for $U = 5.5$	116
10.9.	Single-particle gap: comparison with DDMRG data.	117
10.10.	Comparison of the density of states with DDMRG data for $U = 6$ and $U = 5$	118
10.11.	Comparison of the density of states with DDMRG data for $U = 4.8$	118
10.12.	Comparison of the logarithm of the Matsubara Green function with QMC data.	120
10.13.	Deviation from QMC.	120
A.1.	First-order self-energy diagrams.	129
A.2.	Contributions to the self-energy in second order.	130
A.3.	Explaining the skeleton expansion of the self-energy.	130

The beginner [...] should not be discouraged if [...] he finds that he does not have the prerequisites for reading the prerequisites.

Paul Halmos



Introduction

Contrary to other divisions of modern physics, the fundamental interaction which governs condensed-matter physics is known very well. It is the Coulomb interaction which acts between the electrons and ions constituting the ‘atomic’ parts of matter at the energy scales of interest in condensed-matter physics. The basic Hamiltonian of solid-state physics, see chapter 2 for details,

$$H = \sum_{i=1}^L \frac{\mathbf{p}_i^2}{2M_i} + \sum_{j=1}^N \frac{\mathbf{p}_j^2}{2m} - \sum_{i,j} \frac{C_i e^2}{|\mathbf{r}_j - \mathbf{R}_i|} + \sum_{i < j} \frac{C_i C_j e^2}{|\mathbf{R}_i - \mathbf{R}_j|} + \sum_{i < j} \frac{e^2}{|\mathbf{r}_i - \mathbf{r}_j|} \quad (1.1)$$

looks rather innocent and unspectacular. One might naively conclude that solid-state physics is a rather boring and uninteresting part of contemporary physics as only a very limited number of different phenomena could possibly be contained within the solution of (1.1). This would be perfectly wrong as a brief glance in a textbook of modern solid-state physics reveals. However, this naive conclusion expresses somewhat the fact that we have no imagination of a complete solution of (1.1). The solution of the Schrödinger equation with the Hamiltonian (1.1) for $N = 10^{19} \dots 10^{23}$ must cover phenomena such as the formation of the solid, its lattice dynamics, magnetism, and electrical (super-) conductivity. In order to understand individual aspects of the physics of solids, we have to resort to approximations to (1.1) and approximate solutions of the simplified Hamiltonians. After all, it were approximate treatments of (1.1) which promoted our understanding of the solid state.

A particularly fascinating example is the field of metals, insulators, and the transition between these two states of matter. The first attempts to describe metals microscopically was put forward by Drude at the beginning of the 20th century. As quantum mechanics had not yet been discovered, he used a purely classical picture which ultimately was responsible for the shortcomings of his theory. The first successful theoretical description of metals, insulators, and the transition between them was based on non-interacting electrons in the periodic potentials of the ions. Nowadays, this theory is called band-theory. It was quite surprising that non-interacting or weakly interacting electrons can successfully describe real materials at least qualitatively. An explanation was given by Landau by means of his phenomenological Fermi-Liquid theory. The low-lying excitations of the interacting system are adiabatically connected with the excitations of the non-interacting ones. The theory was later re-formulated microscopically by Nozières, Pines, and Luttinger. Except for one spatial dimension, the Fermi-Liquid theory provided valuable insights into interacting systems. The band-structure theories were also linked with the Hartree-Fock approximation to include the effects of the electron-electron interactions on average. Despite its successes, band-theory (including Hartree-Fock theory) failed for certain transition-metal oxides which were poor conductors or even insulators while band-theory predicted metallic behavior for them. These observations opened the new field of electron-electron correlations which even today is one of the most challenging fields in condensed-matter theory [1]:

“The insulating phase and its fluctuations in metals are indeed the most outstanding and prominent features of strongly correlated electrons ...”

In this thesis we contribute to this field by providing a new analytical method for the calculation of the density of states of a correlated insulator, namely the Mott-Hubbard insulator. Moreover, we give

1. Introduction

the first analytical solution of the self-consistency equations of Dynamical Mean-Field Theory for the insulating state.

Before we describe the aim of our thesis, we briefly explain what we understand under the notions ‘metal’ and ‘insulator’. Moreover, we discuss various scenarios of metal-to-insulator transitions.

1.1. Metals and Insulators

We begin this section with a definition of metals and insulators at zero temperature and weak external fields. Then, we briefly classify insulators according to the dominant interaction which drives the metal-to-insulator transition. As a consequence, we can distinguish between the Mott transition, subject of this thesis, and other types of transitions. We closely follow Ref. [2] in our presentation.

Definition of Insulator and Metal

The specific characterization of a ‘metal’ depends on the material properties for the specific discipline. For example, in chemistry it is important that a metal forms cations and ionic bonds with non-metallic elements, whereas in material sciences the ability of metals to be deformed under stress without cleaving is of major importance. For the purpose of this work, we are mainly interested in the property of a metal to conduct electrical currents which will therefore serve as our definition of the metallic state. At weak externally applied fields Ohm’s law holds. It reads in momentum and frequency space [3]

$$j_\alpha(\mathbf{k}, \omega) = \sum_\beta \sigma_{\alpha\beta}(\mathbf{k}, \omega) E_\beta(\mathbf{k}, \omega). \quad (1.2)$$

Here, $j_\alpha(\mathbf{k}, \omega)$ denotes the electrical current density in the direction of the k th axis, $\sigma_{\alpha\beta}(\mathbf{k}, \omega)$ gives the conductivity tensor and $E_\alpha(\mathbf{k}, \omega)$ is the α -component of the externally applied electric field. Note that a precise distinction between a metal and an insulator can only be made at absolute zero of temperature, $T = 0$. At every finite temperature there are always excitations present in an electronic system such that one may only speak of ‘good’ and ‘bad’ conductors. With these introductory remarks we are finally able to state the definition of an insulator and a metal.

Definition 1.1.1. At absolute zero of temperature and weak externally applied electric fields an insulator is a system with vanishing static electrical conductivity,

$$\sigma_{\alpha\beta}^{\text{DC}}(T = 0) = \lim_{T \rightarrow 0} \lim_{\omega \rightarrow 0} \lim_{\mathbf{k} \rightarrow 0} \Re \sigma_{\alpha\beta}(\mathbf{k}, \omega) = 0. \quad (1.3a)$$

On the other hand, a (Drude) metal is a system where the static electrical conductivity obeys

$$\sigma_{\alpha\beta}^{\text{DC}}(T = 0) = (D_c)_{\alpha\beta} \frac{\tau}{\pi(1 + \omega^2 \tau^2)}. \quad (1.3b)$$

We calculate the Drude weight D_c in Sect. 2.1 within the framework of the simple classical Drude theory. The symbol τ denotes the scattering time for uncorrelated collisions of the electrons, see chapter 2 for details.

Note that we defined metals and insulators according to the behavior of their conductivity in weak external fields. In linear response theory, the conductivity is given in terms of an equilibrium two-particle correlation function [4]. We show in the following section 1.2 that under special circumstances we can classify a given system as a metal or as an insulator by means of its single-electron excitation spectrum.

Classes of Insulators

According to Ref. [2], at zero temperature and weak external fields there are exactly two basic categories of insulators:

- (a) Insulators due to the ion-electron interaction, and
- (b) insulators due to the electron-electron interaction.

At zero temperature, the ion configurations can be considered as static, see also our discussion of the adiabatic approximation in chapter 2. Consequently, the first class (a) can be understood in terms of single-particle models. Prominent examples are [2]

1. Bloch-Wilson or band insulators due to the motion of the electron in the periodic potential of the ions,
2. Peierls insulators due to interactions of the electron with static lattice deformations, and
3. Anderson insulators due to the localization of the electron as a consequence of disorder.

Especially the band picture was quite successful in describing real materials. However, in 1937 de Boer and Verwey [5] reported that many transition-metal oxides with only partly filled bands were often insulators. A typical example was NiO. As a consequence, Peierls pointed out the importance of electron-electron interactions. According to Mott [6] Peierls noted

“... it is quite possible that the electrostatic interaction between the electrons prevents them from moving at all. At low temperatures the majority of the electrons are in their proper places in the ions. The minority which have happened to cross the potential barrier find therefore all the other atoms occupied, and in order to get through the lattice have to spend a long time in ions already occupied by other electrons. This needs a considerable addition of energy and so is extremely improbable at low temperatures.”

These observation opened a new field in solid-state theory, namely the field of strongly correlated electrons. The first person who was able to come up with a theoretically explanation of how electron-electron interactions can lead to insulating behavior was Sir Nevill Mott [7–10]. In his honor the fourth class of insulators constitute the

4. Mott insulators due to the electron-electron interactions.

Note that in real materials the interactions used above to classify the insulators are always more or less simultaneously present. Thus, the classification of experimentally analyzed systems according to these four classes is only unambiguously possible if one interaction clearly dominates.

In this thesis we analyze the insulator due to electron-electron interactions, following Mott’s idea that the existence of the insulator does not depend on whether the system under consideration is magnetic or not. Using the nomenclature of Ref. [2], we analyze the so-called Mott-Hubbard insulator, where symmetry breaking is absent.

1.2. Mott Insulator and Single-Particle Gap

As we have already noted in the last section, a metal should be characterized by a Drude peak in the static electrical conductivity, whereas, for an insulator, this quantity vanishes. In a weak externally applied electric field the conductivity $\sigma_{\alpha\beta}(\mathbf{q}, \omega)$ at zero temperature can be obtained by means of the Kubo formula [4]

$$\sigma_{\alpha\beta}(\mathbf{q}, \omega) = \frac{1}{\omega V} \int_0^\infty dt e^{i\omega t} \langle \Psi | [j_\alpha^\dagger(\mathbf{q}, t), j_\beta(\mathbf{q}, 0)] | \Psi \rangle + i \frac{ne^2}{m\omega} \delta_{\alpha\beta}, \quad (1.4)$$

1. Introduction

where the current operator $j_\alpha(\mathbf{q}, t)$ is a single-particle operator, see [4] for details. To calculate the conductivity it is therefore necessary to evaluate a two-particle, current-current correlation function in the ground state, which describes the propagation of electron-hole excitations of the system. In order to obtain a metallic ground state $|\Psi\rangle$, two fundamental conditions have to be fulfilled [2]:

- (a) Since a vanishing ($\omega \rightarrow 0$) electrical field provides vanishingly small energy, there must be available states for electron-hole excitations immediately above the ground state.
- (b) The states mentioned in (a) have to be extended over the hole sample size.

The evaluation of the two-particle correlation function in (1.4) is very difficult due to the interaction of the electron and the hole, the so-called vertex corrections [11, 12]. Thus, the two-particle correlation function is not simply the product of two single-particle correlation functions. However, it would be desirable to be able to predict the conducting properties of the system solely by analyzing its single-particle excitation spectrum. As the example of BCS theory of superconductivity immediately shows, this is certainly not possible under all circumstances: The Cooper pairs are mobile and contribute to an infinite conductivity at zero field but one finds a gap in the single-particle excitation spectrum as it requires a finite amount of energy to break a pair. This example makes clear that in every case where pairing between electrons or electrons and holes takes place, we can not draw conclusions about two-particle quantities from single-particle ones.

For cases where electron pairing is absent, we consider the Gedankenexperiment depicted in figure 1.1.

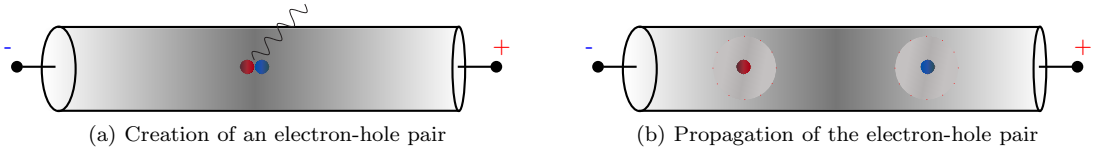


Figure 1.1.: Gedankenexperiment for making the single-particle gap plausible.

In some material, an electron-hole pair is created by means of an optical excitation, as depicted in figure 1.1a. We apply a small electric field along the piece of material. The hole (red) will get shifted in the field direction while the electron moves against it. For a finite electrical conductivity, the electron and hole must become macroscopically separated because they must reach the cathode and anode. At macroscopic distances, their mutual interaction must become negligible and we may consider two independent subsystems with an additional hole and electron, respectively. These systems must permit ungapped charge excitations, otherwise, the electron and hole would not have been able to separate from each other. In turn, a gap for single-particle excitations implies that the DC conductivity vanishes, $\sigma(\omega \rightarrow 0) = 0$, and we observe an insulator.

We therefore conclude that a gap for charge-carrying single-particle excitations indicates an insulator, provided we exclude pairing phenomena. We note that the absence of a single-particle gap does not necessarily imply that the system is a metal. In disordered systems, the single-particle gap can be zero but the gap to macroscopically extended states between the Fermi energy and the mobility edge can be finite. For details, see [2].

1.3. Aim of this Thesis

In this work we analyze the single-particle Green function of the Hubbard model on the Bethe lattice with $Z \rightarrow \infty$ nearest neighbors at zero temperature. The Hubbard model constitutes a drastic approximation to the Hamiltonian (1.1) of condensed-matter physics. Though conceptually the simplest many-electron model, it poses a most difficult many-body problem. Except for one spatial dimension, no exact solution

is known up to today. Therefore, systematic analytical approximations are of major importance as they provide results in the thermodynamic limit against which numerical methods can be tested.

We aim at the calculation of the single-particle density of states and the gap for single-particle, charge excitations. Both of which are rather difficult to obtain by means of numerical studies because those necessarily deal with rather small system sizes. Reliable analytical results provide reliable benchmark tests for the numerics.

We employ the Dynamical Mean-Field theory (DMFT) which permits the mapping of the Hubbard model in infinite dimensions or, equivalently, with an infinite number of nearest neighbors, onto an effective quantum impurity system. We use the Single Impurity Anderson Model (SIAM) as the quantum impurity model. New to our approach is the fact that we solve the DMFT equations for the Mott-Hubbard insulator up to third order in $1/U$. We achieve this goal with the help of a perturbation theory originally developed by Kato and later applied to the Hubbard model in low dimensions by Takahashi. This is the first time an analytical solutions of the DMFT self-consistency equations for the insulator is given.

Having solved the self-consistency equations, we know the parameters of the effective SIAM. The result can be interpreted as a single-particle scattering problem on a semi-infinite chain which we solve for the local Green function of the first site. This gives the Green function of the Hubbard model we originally started with. We discuss the Green function and, in particular, its imaginary part which gives the density of states. From this we can draw conclusions about the single-particle gap for charge-carrying excitations. In the end, we compare our analytical results with numerical data from the Dynamical Density Matrix Renormalization Group (DDMRG) method and the Quantum Monte Carlo (QMC) method. We find excellent agreement with our analytical results down to values of $U \approx 5$, where $W = 4$ is the bare bandwidth. Please note that we set the reduced Planck constant to one, $\hbar \equiv 1$, and use $k_B \equiv 1$ for the Boltzmann constant throughout this work. Thus, we measure frequencies and temperatures in units of energies. The fracture letter i will exclusively denote the imaginary unit, $i^2 = -1$.

1.4. Structure of the Thesis

The thesis is subdivided into three parts and ends with several appendices.

Part I: Models

The first part contains information about the various models used in this work. Except for the particular composition of the various informations and results, none of the material presented is based on our own efforts.

Chapter 2 First, we briefly discuss the Drude model of electrical conductivity as mentioned in Sect. 1.1. Second, we introduce the basic Hamiltonian of solid-state physics. Though this Hamiltonian is well known and easily stated, it is much to complicated to be dealt with. It describes the correlated motion of $N \approx 10^{19} \dots 10^{23}$ electrons and ions. Thus, a complete solution is illusive already at this point because we are unable to cope with all the necessary boundary and/or initial conditions. Approximation schemes and modellings are therefore of utter importance for the progress of our understanding of the solid state. As a second step, we therefore discuss two prominent approximations to the basic Hamiltonian which both are nearly always implicitly present in analyses of electronic systems. These are the adiabatic and the Hartree-Fock approximations. With the Hartree-Fock result we are able to define the notion of ‘electron-electron correlations’.

Chapter 3 In chapter 3 we introduce the tight-binding model, a quantum-mechanical, single-particle model which is capable of describing electronic motion on lattices. As the tight-binding model is a major part of the Hubbard model we are ultimately interested in, we discuss it in considerable detail. First, we calculate the local density of single-particle states on hypercubic lattices in d dimensions and

1. Introduction

discuss its form. In this work we analyze the Hubbard model on the Bethe lattice with $Z \rightarrow \infty$ nearest neighbors. As non-Bravais lattices are usually not considered in textbooks on solid-state theory, we introduce some concepts from mathematical graph theory. This enables us to unambiguously define Bethe lattices with Z nearest neighbors. Finally, we discuss the tight-binding model on Bethe lattices and calculate its local Green function as a function of Z and discuss its form.

Chapter 4 In this chapter we introduce our first model which can describe electron-electron correlations, namely the Single Impurity Anderson Model (SIAM). Though the SIAM is a fascinating model in its own right, we need it as an essential part of the Dynamical Mean-Field Theory for the Hubbard model. After describing the Hamiltonian and its parameters, we discuss its solution in the non-interacting limit to introduce, in particular, the hybridization function. We end the chapter with a brief discussion of some limiting cases of the SIAM.

Chapter 5 Chapter 5 constitutes the end of part I. Here, we introduce the model nowadays known as the ‘paradigm’ of correlated electrons, namely the Hubbard model. First, we give a brief justification of the Hubbard Hamiltonian, following the work of Hubbard. Second, we discuss some of its major symmetries: the invariance under transformations of the group $SO(4)$ and its behavior under various electron-hole transformations. Third, we introduce and discuss some limiting cases of the Hubbard Hamiltonian. As our work deals with the Hubbard model in its insulating phase, we discuss the atomic and strong-coupling limit in more detail. Finally, we discuss the Mott-Hubbard transition following a Gedankenexperiment of Mott.

Part II: Methods

The second part of our thesis deals with the methods we employ to analyze the Mott-Hubbard insulator in infinite dimensions.

Chapter 6 In chapter 6 we discuss the Dynamical Mean-Field Theory (DMFT), a method to map the lattice Hubbard model in infinite dimensions onto an effective impurity model.

To understand the basic ideas of a mean-field theory and some of its drawbacks, we first analyze the one-dimensional Ising model and obtain the magnetization density in zero magnetic field. Then, we briefly review the Weiss or Bragg-Williams mean-field theory of the Ising model and compare its prediction of the magnetization density with the Ising result. As already the classical example shows, a mean-field theory of the ‘Weiss’-type becomes exact in infinite dimensions. We therefore briefly discuss the limit of infinite spatial dimensions, $d \rightarrow \infty$, and compare it to the limit of infinite coordination, $Z \rightarrow \infty$. Afterwards, we discuss the density of states of the tight-binding model on hypercubic lattices in the limit $d \rightarrow \infty$ and on Bethe lattices with $Z \rightarrow \infty$. To obtain sensible results, we need to scale the electron transfer amplitude which, as a consequence, leads to drastic simplifications in the limit of infinite dimensions. Finally, we discuss the self-consistency equations of the DMFT for the general paramagnetic case and the paramagnetic case on the Bethe lattice with infinite coordination.

Chapter 7 In this chapter we formulate and derive a perturbation theory which originates from the mathematical physicist Tosio Kato. This chapter is rather mathematical. For readers who do not wish to follow the derivations, we provide a summary of the results at the end of the chapter.

Chapter 8 The theoretical physicist Minoru Takahashi was the first to apply Kato’s perturbation theory to the Hubbard model. In chapter 8 we first introduce some of Takahashi’s concepts and try to clarify them. Then, we derive the leading-order expressions for ‘Takahashi’s operator’ and, as we call it, the ‘transformed energy operator’. We derive higher-order contributions in appendix C.

Part III: Calculations and Results

The third part of this thesis finally contains our calculations and results for the local Green function of the Mott-Hubbard insulator.

Chapter 9 In chapter 9 we explain how we utilize the methods described in part II to calculate the local Green function of the Hubbard model on the Bethe lattice with infinite coordination.

Therefore, we first introduce the single-particle, local Green function of the lattice Hubbard model and identify the contributions of the lower and upper Hubbard bands. With the help of particle-hole symmetry we can draw our attention to the lower Hubbard band. Then, we describe how we map the lattice model onto the quantum impurity system. Here, we use the Single Impurity Anderson Model (SIAM). In order to solve the SIAM at zero temperature we discuss the mapping of the discretized impurity model onto chain geometries. Since, in the insulator, the lower and upper Hubbard band are well separated in energy from each other, we can use an effective impurity model with two electron baths. We map each of these onto a semi-infinite chain. As the two chains are coupled via the impurity, we call this setup the two-chain geometry.

Then, we separate the SIAM-Hamiltonian in two-chain geometry into a starting Hamiltonian and a perturbation in order to be able to apply the Kato-Takahashi perturbation theory. We discuss the starting Hamiltonian and the perturbation separately. Afterwards, we show how to utilize the perturbation theory for the calculation of the local impurity Green function of the SIAM in two-chain geometry.

Finally, we explain how we utilize the Lanczos algorithm to cast the self-consistency equation of the DMFT into a matrix form. This leads to considerable simplifications because it enables us to satisfy the self-consistency equation by equating a countable set of numbers.

Chapter 10 In this chapter we present the solution of the DMFT equation for the Mott-Hubbard insulator up to third order in $1/U$. As the calculations are technical and rather tedious we show how to solve the DMFT equation to lowest order only. The higher-order calculations are presented in detail in appendix E. In chapter 10, we only briefly comment on them. After having obtained the self-consistent parameters of the effective SIAM, we discuss the emerging impurity scattering problem and solve it for the single-particle Green function. In this way, we obtain the local Green function of the Mott-Hubbard insulator and, in particular, its density of states. We discuss the form of the density of states for various values of U . From the density of states we derive the single-particle gap for charge-carrying excitations. We end the chapter with a favorable comparison of our analytical results with numerical data of DDMRG and QMC calculations.

Chapter 11 We conclude our results and give a short outlook.

Appendices

The appendices contain technical aspects we include for completeness and documentary purposes.

Appendix A This appendix briefly summarizes the use of Green functions in classical and quantum mechanics. It provides some information used throughout the thesis but it certainly is not meant as an introduction into the topic. We also recall some concepts of diagrammatic perturbation theory, namely the self-energy and the skeleton expansion.

Appendix B We use some particle-hole transformations introduced in chapter 5 in order to prove that

- (a) the sign of the electron transfer amplitude of the Hubbard model is irrelevant on bipartite lattices, and that
- (b) a choice of $\mu = 0$ for the chemical potential guarantees a half-filled band at all temperatures.

1. Introduction

Appendix C Here, we derive the explicit expressions for the expansions up to fourth order of ‘Takahashi’s operator’ and the ‘transformed energy operator’.

Appendix D In appendix D we discuss the multichain-setup of the effective Single Impurity Anderson Model for the Mott-Hubbard insulator in more detail.

Appendix E We give the explicit calculations for the solution of the DMFT self-consistency equation up to third order in $1/U$. This appendix is highly technical. We include it first and foremost for documentary purposes.

Appendix F In the last appendix of this thesis, we first summarize properties of the Chebyshev polynomials of the first and second kind. Then, we analyze electron transport along a semi-infinite chain and calculate the Green function of simple tight-binding models on such a chain. The formulae for the Green functions and their powers are proven by means of mathematical induction.

Part I.
Models

One never notices what has been done; one can only see what remains to be done.

Marie Curie

2

Electrons in Solids

A solid is composed of atomic nuclei and electrons. For the energy scales of interest in solid-state physics, we can gather the electrons into two groups. The first group is composed of the so-called *core* electrons which are tightly bound to the nuclei, thereby forming the ions of the solid. The second group consists of the so-called *valence* electrons. We know today that most of the macroscopic properties of solids, such as structural and mechanical properties, thermal and optical features and, in particular, the electrical properties are mainly attributable to the valence electrons.

The first attempt to understand the behavior of electrons in solids was put forward by Drude at the beginning of the last century [13]. Though his ideas were purely classical, his theory was successful in describing qualitatively some features of a metal. For example, he gave an explanation of the law of Wiedemann and Franz [3]. However, it turned out that the successes of his theory were more or less fortuitous [3]. The most important drawback of his theory was the purely classical approach. Since some of the notions of Drude's theory are still in use today [2], we begin the present chapter with a short discussion of his theory of electrical conduction. Then, we leave the realm of classical physics and introduce the basic quantum-mechanical Hamiltonian of solid-state physics. This basic Hamiltonian describes the motion of the electrons as well as of the ions. In this work we will only be interested in the electronic degrees of freedom. Therefore we explain, following Born and Oppenheimer [14], that as a first approximation we are allowed to investigate on a solely electronic problem. This electronic problem will turn out to be intractable without further approximations. Before we introduce more simplified model Hamiltonians in later parts of this thesis, we conclude this chapter with a brief discussion of a very common approximation in solid-state physics, the so-called *Hartree-Fock* theory [15–17]. With the definition of this approximation, we can refine the problem we are interested in, namely *electron correlations*.

2.1. Drude Model

The Drude model [13] was the first theoretical description of metallic (and thermal) conduction. It is based on the ideas of the kinetic theory of gases and therefore is a purely classical model. Drude assumed some of the electrons of the metal, the so-called *conduction* electrons, to form a 'gas'. They can move freely between the positively charged ionic cores. More explicitly, the basic assumptions of the Drude theory are the following.

1. In contrast to the ordinary kinetic theory of gases, the electrons scatter solely from the ionic cores (assumption of *independent electrons*).
2. The (conduction) electrons do not interact with the ions except for occasional collisions (*free electron approximation*).
3. Between two collisions, the electrons move according to Newton's laws (assumption of *short range ionic potentials*). An electron will, on average, travel a time τ before its next and after its last collision. τ is known as the relaxation time and can be considered as the average lifetime of an electron in a state of particular momentum (*relaxation-time approximation*).

2. Electrons in Solids

4. Thermal equilibrium of the electrons is achieved solely through collisions with their surroundings (assumption of *elastic scattering*).

Under these assumptions we can calculate the electrical conductivity for a Drude metal. We consider a metal with an average conduction electron density n , where the electrons with charge $q = -e$ and mass m have average momentum p_k in direction of the k th axis. The current density j_k in this direction is then given by

$$j_k = -\frac{ne}{m}p_k. \quad (2.1)$$

During the short time interval δt we find a collision probability of $\delta t/\tau$ due to the relaxation-time approximation, which implies a probability of surviving without a collision of $(1 - \delta t/\tau)$. In an external force field $f_k(t)$ the momentum $p_k(t + \delta t)$ is therefore given by

$$p_k(t + \delta t) = \left(1 - \frac{\delta t}{\tau}\right)(p_k(t) + f_k(t)\delta t + \mathcal{O}(\delta t^2)), \quad (2.2)$$

which leads in the limit $\delta t \rightarrow 0$ to the force $F_k(t)$ on the electrons,

$$F_k(t) = \frac{dp_k(t)}{dt} = -\frac{p_k(t)}{\tau} + f_k(t). \quad (2.3)$$

As expected, the collisions produce a damping term. Using $f_k = -eE_k$ and assuming a time-dependent electric field

$$E_k(t) = \Re(E_k(\omega)e^{i\omega t}), \quad (2.4)$$

we find under the assumption of a steady-state solution $p_k(t) = \Re(p_k(\omega)e^{i\omega t})$ that

$$i\omega p_k(\omega) = -\frac{p_k(\omega)}{\tau} - eE_k(\omega). \quad (2.5)$$

The frequency-dependent electrical conductivity $\sigma_{kl}(\omega)$ is defined as

$$j_k(\omega) = \sum_l \sigma_{kl}(\omega)E_l(\omega), \quad (2.6)$$

where the current density is given by

$$j_k(\omega) = -\frac{ne}{m}p_k(\omega). \quad (2.7)$$

Together with (2.5) we obtain the Drude result

$$\sigma_{kl}(\omega) = \delta_{kl} \frac{\pi n e^2}{m} \frac{\tau}{\pi(1 + i\omega\tau)}. \quad (2.8)$$

Since in Drude's picture the electrons are considered to be classical particles, the Drude estimate for τ is inaccurate, but the form (2.8) is applicable for metals at low frequencies. A quantum-mechanical treatment of electrons in a periodic potential together with a semi-classical treatment of their motion in external fields and their collisions leads to (2.8) together with an explicit formula for the calculation of the collision time τ . The concepts introduced by Drude a long time ago are still useful in contemporary physics [2], see our discussion on classification of metals and insulators in Sect. 1.1. Of course, a deeper understanding of electrons in solids requires a full quantum-mechanical description.

2.2. First Principles Hamiltonian

A quantitative quantum-mechanical description of the solid state starts from the Schrödinger equation and thus with setting up the Hamiltonian for the problem. In general, a solid consists of L atomic cores of valence C_i and N electrons, such that for the purpose of charge neutrality we have

$$N = \sum_{i=1}^L C_i. \quad (2.9)$$

The electrons may be grouped into two classes: the *core* electrons and the *valence* electrons. The former are considered to be tightly bound in closed shells of the atomic cores, such that they hardly influence the low-energy properties of the solid. Therefore, one usually considers the valence electrons, which contribute to chemical bonding and to transport phenomena, and the lattice ions as the independent constituents of the solid [18]. Then C_i denotes the charge of the ions. Let $(\mathbf{r}_i, \mathbf{p}_i, m)$ and $(\mathbf{R}_i, \mathbf{P}_i, M_i)$ denote the position operator, momentum operator and mass of the valence electrons and ions, respectively. Without taking relativistic effects into account, which is a valid assumption at least for the lighter elements [19], the basic Hamiltonian governing the motion of these constituents of the solid can therefore be written as

$$\begin{aligned} H &= \sum_{i=1}^L \frac{\mathbf{P}_i^2}{2M_i} + \sum_{j=1}^N \frac{\mathbf{p}_j^2}{2m} - \sum_{i,j} \frac{C_i e^2}{|\mathbf{r}_j - \mathbf{R}_i|} + \sum_{i<j} \frac{C_i C_j e^2}{|\mathbf{R}_i - \mathbf{R}_j|} + \sum_{i<j} \frac{e^2}{|\mathbf{r}_i - \mathbf{r}_j|} \\ &=: T_I + T_e + V_{I-e} + V_I + V_{e-e}. \end{aligned} \quad (2.10)$$

The first two terms, T_I and T_e , describe the kinetic energy of the ions and electrons, respectively. The third term, V_{I-e} , denotes the attractive interaction between the negatively charged electrons and the positively charged ions. The last two terms, V_I and V_{e-e} , represent the mutual interaction of the ions and electrons, respectively. We note that all the interactions in the Hamiltonian (2.10) are Coulomb interactions and are therefore *a priori* equally strong [18].

This basic Hamiltonian is much too complicated to be dealt with even numerically. One therefore has to rely on approximation strategies. Two of the most fundamental ones which are nearly always implicitly present in every approximate or exemplary treatment of quantum-mechanical analyses, are the *adiabatic* and the *Hartree-Fock* approximations.

2.2.1. Adiabatic Approximation

As a starting point we rephrase the basic Hamiltonian (2.10) in atomic units [20]. The basic length scale in solid-state physics is the Bohr radius

$$a_0 = \frac{\hbar^2}{me^2}, \quad (2.11)$$

and the basic unit of energy should therefore be given in Rydbergs

$$E_0 = \frac{me^4}{\hbar^2} = 2Ry. \quad (2.12)$$

A general position \mathbf{r} is therefore expressible as $\mathbf{r} = a_0 \tilde{\mathbf{r}}$, which allows us to write (2.10) as

$$\frac{H}{E_0} = -\frac{1}{2} \sum_{i=1}^L \frac{m}{M_i} \frac{\partial^2}{\partial \tilde{\mathbf{R}}_i^2} - \frac{1}{2} \sum_{j=1}^N \frac{\partial^2}{\partial \tilde{\mathbf{r}}_j^2} - \sum_{i,j} \frac{C_i}{|\tilde{\mathbf{r}}_j - \tilde{\mathbf{R}}_i|} + \sum_{i<j} \frac{C_i C_j}{|\tilde{\mathbf{R}}_i - \tilde{\mathbf{R}}_j|} + \sum_{i<j} \frac{1}{|\tilde{\mathbf{r}}_i - \tilde{\mathbf{r}}_j|}. \quad (2.13)$$

The relative contribution of the kinetic energy of the ions is smaller by the ratio of the electron mass to the ion masses

$$\frac{m}{M_i} \approx 10^{-4} \dots 10^{-5}, \quad (2.14)$$

2. Electrons in Solids

which suggests to consider the ions' kinetic energy as a perturbation. Therefore, it is advisable to expand the Hamiltonian into a power series of m/M_i . The analysis has first been carried out by Born and Oppenheimer [14], which is the reason why the adiabatic approximation is also-called *Born-Oppenheimer* approximation. One decomposes the Hamiltonian (2.10) according to

$$H = H_0 + T_I. \quad (2.15)$$

Since the momenta of the ions are not part of H_0 , the corresponding Schrödinger equation depends only parametrically on the positions of the ions and we assume

$$H_0\phi_{\mathbf{e}}(\mathbf{r}, \mathbf{R}) = \epsilon_{\mathbf{e}}(\mathbf{R})\phi_{\mathbf{e}}(\mathbf{r}, \mathbf{R}) \quad (2.16)$$

to be the form of its solution. Here \mathbf{e} denotes a complete set of electronic quantum numbers and \mathbf{r} and \mathbf{R} denote multidimensional vectors containing the positions of all the electrons and ions, respectively. For the wave function of the full problem we may use the Ansatz

$$\Psi(\mathbf{r}, \mathbf{R}) = \sum_{\mathbf{e}} c_{\mathbf{e}}(\mathbf{R})\phi_{\mathbf{e}}(\mathbf{r}, \mathbf{R}) \quad (2.17)$$

resulting in [20]

$$(T_I + \epsilon_{\mathbf{e}}(\mathbf{R}))c_{\mathbf{e}}(\mathbf{R}) + \sum_{\mathbf{f}} t_{\mathbf{e}\mathbf{f}}(\mathbf{R})c_{\mathbf{f}}(\mathbf{R}) = Ec_{\mathbf{e}}(\mathbf{R}), \quad (2.18)$$

with the transition matrix elements between different electronic levels

$$t_{\mathbf{e}\mathbf{f}}(\mathbf{R}) = - \sum_i \frac{\hbar^2}{2M_i} \int \left\{ \phi_{\mathbf{e}}^*(\mathbf{r}, \mathbf{R}) \frac{\partial^2}{\partial \mathbf{R}_i^2} \phi_{\mathbf{f}}(\mathbf{r}, \mathbf{R}) + 2\phi_{\mathbf{e}}^*(\mathbf{r}, \mathbf{R}) \left(\frac{\partial}{\partial \mathbf{R}_i} \phi_{\mathbf{f}}(\mathbf{r}, \mathbf{R}) \right) \frac{\partial}{\partial \mathbf{R}_i} \right\} d^N r. \quad (2.19)$$

The Born-Oppenheimer approximation now consists in neglecting these transition matrix elements completely, which results in

$$(T_I + \epsilon_{\mathbf{e}}(\mathbf{R}))c_{\mathbf{e}}(\mathbf{R}) = Ec_{\mathbf{e}}(\mathbf{R}). \quad (2.20)$$

Equation (2.20) is a Schrödinger equation for the ions in an effective potential $\epsilon_{\mathbf{e}}(\mathbf{R})$, determined by the parametrical dependence of the electronic eigenenergies on the positions of the ions. A detailed estimate [20, 21] of the various energy scales shows that the neglect of the transition matrix elements is valid up to order $(m/M_i)^{1/4} \approx 10^{-1} \dots 10^{-2}$. Figuratively speaking, the adiabatic approximation assumes that the ionic system evolves on a much slower time scale than the electronic system, such that the electrons always experience quasi-stationary positions of the ions.

The derivation above shows that the perturbative treatment of the motion of the ions is justified but it also makes clear that the total separation of lattice dynamics and electronic motion is not possible in every case. For example, the BCS theory [22-24] of conventional superconductors depends vitally on the electron-phonon coupling in a non-perturbative way [4]. Since in this thesis we do not need to consider the lattice dynamics nor its coupling to the electronic degrees of freedom, we do not go into this topic further. The interested reader may find a good introduction in [4, 20].

2.2.2. Hartree-Fock Approximation

The adiabatic approximation discussed in the last subsection allows us to separate the lattice dynamics from the electronic motion. It permits us to analyse the purely electronic Hamiltonian

$$H = \sum_{j=1}^N \left\{ \frac{\mathbf{p}_j^2}{2m} - \sum_i \frac{C_i e^2}{|\mathbf{r}_j - \mathbf{R}_i|} \right\} + \sum_{i < j} \frac{e^2}{|\mathbf{r}_i - \mathbf{r}_j|}, \quad (2.21)$$

where the position of the ions are considered to be fixed and one tries to solve for the electronic levels. The Hamiltonian (2.21) reads in second-quantized form [4, 11, 12]

$$H = \sum_{\alpha,\beta} c_{\alpha}^{\dagger} \langle \alpha | \frac{\mathbf{p}^2}{2m} - \sum_i \frac{C_i e^2}{|\mathbf{r} - \mathbf{R}_i|} | \beta \rangle c_{\beta} + \frac{1}{2} \sum_{\alpha,\beta,\gamma,\delta} c_{\alpha}^{\dagger} c_{\beta}^{\dagger} (\alpha\beta) \frac{e^2}{|\mathbf{r}_1 - \mathbf{r}_2|} |\gamma\delta\rangle c_{\delta} c_{\gamma}, \quad (2.22)$$

where $c_{\alpha}^{\dagger}/c_{\alpha}$ creates/annihilates an electron in the one-particle state $|\alpha\rangle$. The ket $|\alpha\beta\rangle$ denotes a non-symmetrized state of the two-particle Hilbert space. Note that due to the spin independence of the mutual Coulomb interaction, the spin associated with α is the same as that associated with γ and analogously for β and δ . The problem posed by (2.22) is still very complicated because it involves the mutual electron-electron interaction and we have to implement further approximations. If the electron-electron interaction was absent, the Hamiltonian would reduce to a one-body problem which would be much easier to solve.

One of the first quantum-mechanical approximations for the many-body problem defined by (2.21) is the so-called *Hartree-Fock* approximation [15–17, 25]. In this approximation one reduces the many-body problem to an effective one-body problem: The effect of the mutual electron-electron interaction is described by the motion of one electron in an effective field. This field is produced by all the electrons in the system and the actual problem consists of finding it. Technically one adds an auxiliary potential $V_a(\mathbf{r})$ to the single-particle part of (2.21) and subtracts it again from its interaction part,

$$H = \sum_{j=1}^N \left\{ \frac{\mathbf{p}_j^2}{2m} - \sum_i \frac{C_i e^2}{|\mathbf{r}_j - \mathbf{R}_i|} + V_a(\mathbf{r}_j) \right\} + \sum_{i < j} \left\{ \frac{e^2}{|\mathbf{r}_i - \mathbf{r}_j|} - \frac{1}{N-1} (V_a(\mathbf{r}_i) + V_a(\mathbf{r}_j)) \right\}. \quad (2.23)$$

In all Hartree-Fock type approximations one then neglects the second parenthesis in (2.23) completely. For this to be a sensible approach, one must choose $V_a(\mathbf{r})$ in such a way that the matrix elements of the second sum in (2.23), taken in the eigenstates of

$$H_{\text{HF}} = \sum_{j=1}^N \left\{ \frac{\mathbf{p}_j^2}{2m} - \sum_i \frac{C_i e^2}{|\mathbf{r}_j - \mathbf{R}_i|} + V_a(\mathbf{r}) \right\} \quad (2.24)$$

are small. In the remaining part of this section we describe how one solves the problem of finding the appropriate auxiliary potential.

In the Hartree-Fock approximation it is assumed that the exact ground state $|\Psi_0\rangle$ of the Hamiltonian (2.22) can be approximated by a single Slater determinant

$$|\Psi_0\rangle \approx |\alpha_1 \dots \alpha_N\rangle, \quad (2.25)$$

such that the ground-state wave function reads

$$\Psi_0(\mathbf{r}) = (\mathbf{r}_1 \dots \mathbf{r}_N | \Psi_0\rangle = \frac{1}{\sqrt{N!}} \det(\phi_{\alpha_i}(\mathbf{r}_j)). \quad (2.26)$$

The expectation value of the interaction may then be calculated using Wick's theorem [26]. The ground-state energy E_{HF} in Hartree-Fock approximation becomes

$$\begin{aligned} E_{\text{HF}} = & \sum_{\alpha} \int \phi_{\alpha}(\mathbf{r}) \left(\frac{\mathbf{p}^2}{2m} - \sum_i \frac{C_i e^2}{|\mathbf{r} - \mathbf{R}_i|} \right) \phi_{\alpha}^*(\mathbf{r}) d^3r + \frac{e^2}{2} \sum_{\alpha,\beta} \int \frac{|\phi_{\alpha}(\mathbf{r})|^2 |\phi_{\beta}(\mathbf{r}')|^2}{|\mathbf{r} - \mathbf{r}'|} d^3r d^3r' \\ & - \frac{e^2}{2} \sum_{\alpha,\beta} \delta_{\sigma_{\alpha},\sigma_{\beta}} \int \frac{\phi_{\alpha}^*(\mathbf{r}) \phi_{\beta}^*(\mathbf{r}') \phi_{\beta}(\mathbf{r}) \phi_{\alpha}(\mathbf{r}')}{|\mathbf{r} - \mathbf{r}'|} d^3r d^3r'. \end{aligned} \quad (2.27)$$

The one-particle wave functions $\phi_{\alpha}(\mathbf{r}) \equiv \langle \mathbf{r} | \alpha \rangle$ are not known a priori. They are determined by minimizing the ground-state energy E_{HF} with respect to them, subject to the condition that the one-particle

2. Electrons in Solids

wave functions remain normalized. The self-consistency equations read [18]

$$\begin{aligned} & \left(\frac{\mathbf{p}^2}{2m} - \sum_i \frac{C_i e^2}{|\mathbf{r} - \mathbf{R}_i|} + e^2 \sum_\beta \int \frac{|\phi_\beta(\mathbf{r}')|^2}{|\mathbf{r} - \mathbf{r}'|} d^3 r' \right) \phi_\alpha(\mathbf{r}) \\ & - e^2 \sum_\beta \delta_{\sigma_\alpha, \sigma_\beta} \int \frac{\phi_\beta^*(\mathbf{r}') \phi_\alpha(\mathbf{r}')}{|\mathbf{r} - \mathbf{r}'|} d^3 r' \phi_\beta(\mathbf{r}) = \epsilon_\alpha(\mathbf{r}) \phi_\alpha(\mathbf{r}). \end{aligned} \quad (2.28)$$

The so-called Hartree-Fock single-particle energies $\epsilon_\alpha(\mathbf{r})$ are Lagrange multipliers. They can be physically interpreted with Koopmans' theorem as ionization energies [27]. The solution of these equations is very complicated due to the periodic potential of the ionic cores. In the case of a homogeneous electron gas (jellium model) the equations may be solved analytically [12]. Note that the Hartree-Fock approximation can as well be formulated on the level of the Hamiltonian (2.22), where one has to replace the interaction term with

$$\begin{aligned} c_\alpha^\dagger c_\beta^\dagger c_\delta c_\gamma & \mapsto c_\alpha^\dagger c_\gamma \langle c_\beta^\dagger c_\delta \rangle + \langle c_\alpha^\dagger c_\gamma \rangle c_\beta^\dagger c_\delta \\ & - c_\alpha^\dagger c_\delta \langle c_\beta^\dagger c_\gamma \rangle - \langle c_\alpha^\dagger c_\delta \rangle c_\beta^\dagger c_\gamma \\ & - \langle c_\alpha^\dagger c_\gamma \rangle \langle c_\beta^\dagger c_\delta \rangle + \langle c_\alpha^\dagger c_\delta \rangle \langle c_\beta^\dagger c_\gamma \rangle. \end{aligned} \quad (2.29)$$

The self-consistency results from the fact that the expectation values in the Hartree-Fock decoupling (2.29) have to be calculated with respect to the new Hamiltonian containing them. This leads back to the self-consistency equations (2.28).

The Hartree-Fock approximation is sometimes called a *mean-field* approximation [20, 28]. Another way to formulate the Hartree-Fock theory is by means of many-body perturbation theory [12], which shows that it can (and should) be considered as a first-order approximation to the proper self-energy. For details on the notion mean-field theory as we understand it, see chapter 6.

As already stated above, the Hartree-Fock approximation is often employed in band-structure calculations to take some part of the electron-electron interaction into account [3, 20]. These approximations still belong to the class of independent-electron theories. It has been known for a long time that the predictions of these theories fail completely in a number of cases [7], especially in metal oxides such as CoO. The Hartree-Fock theory described in this section fails to classify CoO as an insulator and it is doubtful that an extension like *unrestricted* Hartree-Fock, which allows for symmetry breaking such as the formation of magnetic superstructures, gives a consistent explanation [29]. Nevertheless, we should not overlook that the Hartree-Fock approximation is quite common in solid-state physics and often allows for a first insight into the physics of a model. A particular successful example is the above mentioned BCS theory of (normal) superconductivity, where the Hartree-Fock type mean-field treatment differs only slightly from the form derived above [20].

In 1933 and 1934, Wigner and Seitz [30, 31] introduced the notion of *correlation energy* to name the energy difference between the Hartree-Fock result and the exact value. The term correlation is since then used to describe all effects which are not contained in a Hartree-Fock treatment. This thesis deals exclusively with such electron-electron correlations.

In fact, the mere act of opening the box will determine the state of the cat, although in this case there were three determinate states the cat could be in: these being Alive, Dead, and Bloody Furious.

Schrödinger's cat explained in **Lords and Ladies** by Terry Pratchett

3

Tight-Binding Model

In Sect. 2.2 of the last chapter, we described two commonly used approximations for the basic Hamiltonian (2.10) of solid-state physics, the adiabatic and the Hartree-Fock approximation. The adiabatic approximation allowed us to decouple the electronic motion from the degrees of freedom of the underlying lattice ions. The resulting electronic problem, still far too complicated to be of much use, was mapped by means of the Hartree-Fock, self-consistent theory onto an effective single-particle problem, describing the motion of a single electron on a lattice in an effective field. However, we have not yet discussed any quantum-mechanical single-particle model which describes electronic motion on a lattice. A simple albeit powerful model for this purpose is the so-called *tight-binding* model. As it is one part of the Hubbard model, we are ultimately interested in, we discuss its properties in this chapter.

Beginning with a short motivation of the Hamiltonian of the tight-binding model, we discuss its properties on hypercubic lattices in dimension d . Next, we introduce some basic notions of mathematical graph theory to introduce the so-called *Bethe lattice*, on which we analyze the Hubbard model in its insulating phase in this work. We end the chapter with a derivation and discussion of the local Green function of the tight-binding model on Bethe lattices with Z nearest neighbors.

3.1. Motivation of the Hamiltonian

There are two opposite methods for describing a solid within the independent electron approximation: the method of nearly free electrons and the tight-binding approximation. The method of nearly free electrons views the conduction electrons in the solid as a gas of nearly free particles, weakly perturbed by the periodic potentials of the ions [3]. Though one can qualitatively explain the formation of energy bands, the method is usually not adequate for band-structure calculations [20], though developments on this method have led to the method of pseudopotentials [32].

Instead of trying to understand the solid as a collection of ions between which the electrons move as a gas of nearly free particles, one may also try to visualize the solid as an aggregation of weakly interacting neutral atoms [3]. The isolated atom at position \mathbf{R} is described by the atomic Hamiltonian

$$H_{\text{at},\mathbf{R}} = \frac{\mathbf{p}^2}{2m} + v(\mathbf{r} - \mathbf{R}), \quad (3.1)$$

where $v(\mathbf{r} - \mathbf{R})$ denotes the interaction potential between the valence electrons and the ionic core. The eigenstates ϕ_n and eigenenergies E_n of the isolated atoms are considered to be known:

$$H_{\text{at},\mathbf{R}}\phi_n(\mathbf{r} - \mathbf{R}) = E_n\phi_n(\mathbf{r} - \mathbf{R}). \quad (3.2)$$

The index n denotes as usual a complete set of quantum numbers, e.g. principal quantum number, angular momentum and spin. One wants to study the changes in ϕ_n and E_n upon bringing the isolated atoms in close contact. One therefore considers the one-particle Hamiltonian

$$H = H_{\text{at},\mathbf{R}} + \delta_{\mathbf{R}}(\mathbf{r}), \quad (3.3)$$

3. Tight-Binding Model

where $\delta_{\mathbf{R}}(\mathbf{r})$ describes the interaction of the electron at position \mathbf{r} with all ions except that located at position \mathbf{R} ,

$$\delta_{\mathbf{R}}(\mathbf{r}) = \sum_{\mathbf{R}' \neq \mathbf{R}} v(\mathbf{r} - \mathbf{R}'). \quad (3.4)$$

If the atomic wave functions $\phi_n(\mathbf{r} - \mathbf{R})$ decay fast enough to vanish within the area where $\delta_{\mathbf{R}}(\mathbf{r}) \neq 0$, they are also eigenfunctions of the full Hamiltonian (3.3),

$$H\phi_n(\mathbf{r}) = E_n\phi_n(\mathbf{r}). \quad (3.5)$$

To obtain functions fulfilling the fundamental Bloch theorem [3, 33], one introduces the Bloch functions

$$\Phi_{n\mathbf{k}}(\mathbf{r}) = \frac{1}{\sqrt{L}} \sum_{\mathbf{R}} e^{i\mathbf{k}\mathbf{R}} \phi_n(\mathbf{r} - \mathbf{R}). \quad (3.6)$$

Due to (3.5) these states form dispersionless bands, which therefore can describe the inner core electrons only. For the conduction electrons we must assume overlap of their wave functions in order to describe the formation of bonds. This means that the assumption

$$\delta_{\mathbf{R}}(\mathbf{r})\phi_n(\mathbf{r} - \mathbf{R}) = 0 \quad (3.7)$$

does not hold anymore. Nevertheless, the ansatz (3.6) may be used as an approximation, the so-called *linear combination of atomic orbitals* (LCAO) method [18, 20].

The functions (3.6) do not form an orthogonal set. Their overlap is given by

$$\langle \Phi_{n\mathbf{k}} | \Phi_{n'\mathbf{k}'} \rangle = \delta_{nn'} + \sum_{\mathbf{R} \neq 0} e^{-i\mathbf{k}\mathbf{R}} \int \phi_n^*(\mathbf{r} - \mathbf{R}) \phi_n(\mathbf{r}) d^3r. \quad (3.8)$$

It is much more appealing to use an orthonormal set of wave functions to approach the problem. Such a set is provided by the Wannier functions [20]

$$w_n(\mathbf{r}, \mathbf{R}) = \frac{1}{L} \sum_{\mathbf{k}} e^{-i(\mathbf{k}\mathbf{R} + \chi(\mathbf{k}))} \Phi_{n\mathbf{k}}(\mathbf{r}), \quad (3.9)$$

where the function $\chi(\mathbf{k})$ may be tuned to make the $w_n(\mathbf{r}, \mathbf{R})$ drop off as fast as possible when \mathbf{r} moves away from \mathbf{R} [34]. The Wannier functions $w_n(\mathbf{r}, \mathbf{R})$ are therefore usually considered to be exponentially localized around the lattice site \mathbf{R} [35, 36].

The energy levels are given by

$$\epsilon_n(\mathbf{k}) = \langle \Phi_{n\mathbf{k}} | H | \Phi_{n\mathbf{k}} \rangle. \quad (3.10)$$

The expectation value may be written as

$$\langle \Phi_{n\mathbf{k}} | H | \Phi_{n\mathbf{k}} \rangle = \langle \Phi_{n\mathbf{k}} | \frac{\mathbf{p}^2}{2m} | \Phi_{n\mathbf{k}} \rangle + \frac{1}{L} \sum_{\mathbf{R}_1, \mathbf{R}_2} e^{i\mathbf{k}(\mathbf{R}_1 - \mathbf{R}_2)} \int w_n^*(\mathbf{r} - \mathbf{R}_2) \sum_{\mathbf{R}_3} v(\mathbf{r} - \mathbf{R}_3) w_n(\mathbf{r} - \mathbf{R}_1) d^3r. \quad (3.11)$$

Every \mathbf{r} -dependent function in (3.11) is localized around the corresponding center \mathbf{R}_i , $i = 1, 2, 3$. One has to distinguish three cases [20]:

1. $\mathbf{R}_1 = \mathbf{R}_2 \neq \mathbf{R}_3$

$$\frac{1}{L} \sum_{\mathbf{R}} \int w_n^*(\mathbf{r} - \mathbf{R}) \sum_{\mathbf{R}'} v(\mathbf{r} - \mathbf{R}') w_n(\mathbf{r} - \mathbf{R}) d^3r = \int w_n^*(\mathbf{r}) \sum_{\mathbf{R}} v(\mathbf{r} - \mathbf{R}) w_n(\mathbf{r}) d^3r \quad (3.12)$$

This is a constant shift of the energy levels.

2. $\mathbf{R}_2 = \mathbf{R}_3 \neq \mathbf{R}_1$

$$\frac{1}{L} \sum_{\mathbf{R}_1 \neq \mathbf{R}_2} e^{i\mathbf{k}(\mathbf{R}_1 - \mathbf{R}_2)} \int w_n^*(\mathbf{r} - \mathbf{R}_2) v(\mathbf{r} - \mathbf{R}_2) w_n(\mathbf{r} - \mathbf{R}_1) \quad (3.13)$$

This expression can be thought of as describing electron transfer from site \mathbf{R}_1 to site \mathbf{R}_2 .

3. Three-center contributions

All three \mathbf{R}_i 's are mutually distinct.

The tight-binding approximation consists of neglecting the three-center contributions, so that the dispersion relation can be written as

$$\epsilon_n(\mathbf{k}) = \tilde{E}_n + \frac{1}{L} \sum_{\mathbf{R}_1 \neq \mathbf{R}_2} e^{-i\mathbf{k}(\mathbf{R}_1 - \mathbf{R}_2)} t(\mathbf{R}_1 - \mathbf{R}_2), \quad (3.14)$$

where \tilde{E}_n is (for our purposes) an unimportant constant

$$\tilde{E}_n = \int w_n^*(\mathbf{r}) \left(\frac{\mathbf{p}^2}{2m} + \sum_{\mathbf{R}} v(\mathbf{r} - \mathbf{R}) \right) w_n(\mathbf{r}) d^3r \quad (3.15)$$

and

$$t_n(\mathbf{R}_1 - \mathbf{R}_2) = \int w_n^*(\mathbf{r} - \mathbf{R}_2) v(\mathbf{r} - \mathbf{R}_2) w_n(\mathbf{r} - \mathbf{R}_1) d^3r \quad (3.16)$$

is the so-called *hopping* or *electron transfer amplitude*. The general tight-binding Hamiltonian includes spin degrees of freedom and an in principle site-dependent (non-translational symmetry) on-site energy $\epsilon_{\mathbf{R}n}$. In second quantized form it is written as

$$H = \sum_{\mathbf{R}_1, \mathbf{R}_2, n, \sigma} t_n(\mathbf{R}_1 - \mathbf{R}_2) c_{n\mathbf{R}_1\sigma}^\dagger c_{n\mathbf{R}_2\sigma} + \sum_{\mathbf{R}, n, \sigma} \epsilon_{\mathbf{R}n} c_{n\mathbf{R}\sigma}^\dagger c_{n\mathbf{R}\sigma}. \quad (3.17)$$

Note that we do not assume inter-band hopping which could in principle be included.

Consistent with the neglect of the three-center contributions is the assumption that $t(\mathbf{R})$ is distinctly different from zero only for *nearest* or at most *next-nearest* neighbors. In the nearest neighbor tight-binding model as used in this work, we do not try to calculate the hopping amplitude from first principles via (3.16) but consider it to be parametrized as

$$t(\mathbf{R}) = \begin{cases} t & \text{if } \mathbf{R} \text{ denotes a nearest-neighbor vector,} \\ 0 & \text{otherwise.} \end{cases} \quad (3.18)$$

In this thesis we will refer to the following one-orbital, nearest-neighbor hopping Hamiltonian

$$H_{\text{TB}} = \sum_{\mathbf{R}_1, \mathbf{R}_2, \sigma} t(\mathbf{R}_1 - \mathbf{R}_2) c_{\mathbf{R}_1\sigma}^\dagger c_{\mathbf{R}_2\sigma} \quad (3.19)$$

as the tight-binding Hamiltonian. For ease of notation we usually index every lattice site with an integer and write

$$H_{\text{TB}} = \sum_{i,j,\sigma} t_{ij} c_{i\sigma}^\dagger c_{j\sigma}. \quad (3.20)$$

The hopping amplitude t_{ij} has to fulfill some obvious symmetries in order for H_{TB} to be Hermitian.

3.2. Tight-Binding Model on Hypercubic Lattices

In this section we want to discuss the spectrum of the tight-binding model (3.20) on d -dimensional hypercubic lattices. For this purpose the method of Green functions is ideally suited. The local one-particle Green function is defined as

$$G_{ij}(z) = \langle i | (z - H_{\text{TB}})^{-1} | j \rangle, \quad (3.21)$$

where the resolvent operator $R(z) := (z - H_{\text{TB}})^{-1}$ is defined for all $z \in \mathbb{C}$ not part of the spectrum $\sigma(H_{\text{TB}})$. For a short summary of the use of Green functions in quantum physics, see appendix A. Note that the spin degrees of freedom do not couple in the tight-binding Hamiltonian, so it suffices to calculate the Green function with only one spin species taken into consideration. The resolvent can be calculated in momentum representation via

$$R(z) = \sum_{\mathbf{k}} \frac{|\mathbf{k}\rangle\langle\mathbf{k}|}{z - \epsilon(\mathbf{k})}, \quad (3.22)$$

where $|\mathbf{k}\rangle$ denotes a Bloch state (we drop the band index)

$$\Phi_{\mathbf{k}}(\mathbf{r}) \equiv \langle \mathbf{r} | \mathbf{k} \rangle = \frac{1}{\sqrt{L}} \sum_{\mathbf{R}} e^{i\mathbf{k}\mathbf{R}} w(\mathbf{r}, \mathbf{R}), \quad (3.23)$$

and $\epsilon(\mathbf{k})$ is the dispersion relation (3.14). The matrix elements of the resolvent, i.e. the Green functions, read,

$$G_{ij}(z) = \sum_{\mathbf{k}} \frac{\langle \mathbf{R}_i | \mathbf{k} \rangle \langle \mathbf{k} | \mathbf{R}_j \rangle}{z - \epsilon(\mathbf{k})} \rightarrow \frac{L}{(2\pi)^d} \int \frac{\langle \mathbf{R}_i | \mathbf{k} \rangle \langle \mathbf{k} | \mathbf{R}_j \rangle}{z - \epsilon(\mathbf{k})} d^d k, \quad (3.24)$$

where the second equality denotes the expression in the thermodynamic limit. The density of states per unit volume and lattice site, $\rho(\omega)$, is the imaginary part of the retarded local Green function (A.21),

$$\rho(\omega) = -\frac{1}{\pi} \lim_{\eta \searrow 0} \Im G_{ii}(\omega + i\eta). \quad (3.25)$$

One-dimensional Lattice In the one-dimensional case the evaluation of (3.25) is straightforward [32] and results in

$$\rho(\omega) = \frac{1}{\pi \sqrt{4t^2 - \omega^2}} \theta(2t - |\omega|). \quad (3.26)$$

In figure 3.1a we show this function. The energy ω is given in multiples of half the bandwidth $W = 4t$. In one dimension we find two square root singularities at the band edges [32].

Two-dimensional Lattice The calculations for the square lattice are considerably more involved but one can find an analytical expression for the density of states which reads [32]

$$\rho(\omega) = \frac{1}{\pi^2 2t} K\left(1 - \frac{\omega^2}{16t^2}\right) \theta(4t - |\omega|). \quad (3.27)$$

$K(z)$ denotes the complete elliptic integral of the first kind [37],

$$K(z) := \int_0^{\pi/2} \frac{1}{\sqrt{1 - z \sin^2(\vartheta)}} d\vartheta. \quad (3.28)$$

Equation (3.27) is plotted in figure 3.1b. The bandwidth is given by $W = 8t$. Not unique to the square lattice but characteristic for a two-dimensional system [29, 38], we find step discontinuities at the band

3.2. Tight-Binding Model on Hypercubic Lattices

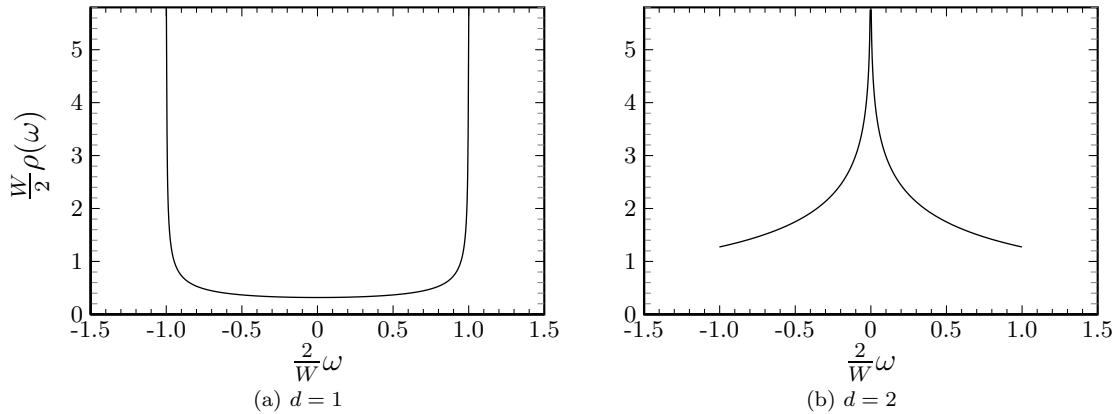


Figure 3.1.: Density of states of the tight-binding model on hypercubic lattices in (a) one dimension and (b) two dimensions.

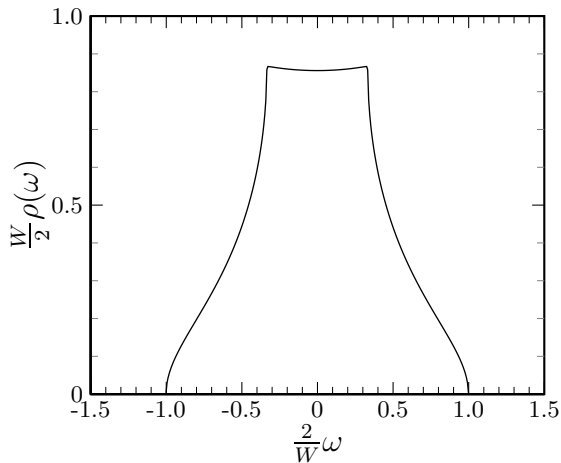


Figure 3.2: The density of states of the tight-binding model on the simple cubic lattice. The bandwidth is given by $W = 12t$.

edges and a logarithmic singularity at $\omega = 0$. This claim can be proved by an expansion of (3.27) in ω around $\omega = 0$,

$$\lim_{\omega \rightarrow 0} \rho(\omega) = \frac{1}{\pi^2 2t} \ln \left(\frac{t}{|\omega|} \right). \quad (3.29)$$

These *van-Hove singularities* stem from maxima, minima and saddle points of the dispersion $\epsilon(\mathbf{k})$ and occur for all dimensions $d < \infty$ [3]. For the case of the square lattice, the step-like discontinuities at the band edges belong to the minimum and maximum of $\epsilon(\mathbf{k})$ whereas the logarithmic divergence results from a saddle point [29].

Three-dimensional Lattice For the simple cubic lattice the local Green function can be simplified to give [39]

$$G_{ii}(z) = \frac{1}{\pi^2 2t} \int_0^\pi k(x; z) K(k^2(x; z)) dx, \quad (3.30)$$

where $k(x; z) = 4t(z - 2t \cos(x))^{-1}$. Formula (3.30) can be integrated numerically. The result for the density of states is shown in figure 3.2. A rather complicated analytical solution for the local Green function is also available [40]. We include it for completeness:

$$G_{ii}(z) = \frac{1}{z} P \left(\frac{6t}{z} \right), \quad (3.31)$$

3. Tight-Binding Model

where

$$P(z) = \frac{4}{\pi^2} \frac{\sqrt{1 - \frac{3}{4}x_1(z)}}{z(1 - x_1(z))} K(k_+^2(z)) K(k_-^2(z)), \quad (3.31a)$$

$$k_{\pm}^2(z) = \frac{1}{2} \pm \frac{1}{4} x_2(z) \sqrt{4 - x_2(z)} - \frac{1}{4} (2 - x_2(z)) \sqrt{1 - x_2(z)}, \quad (3.31b)$$

$$x_1(z) = \frac{1}{2} + \frac{1}{6} z^2 - \frac{1}{2} \sqrt{1 - z^2} \sqrt{1 - \frac{1}{9} z^2} \quad (3.31c)$$

and

$$x_2(z) = \frac{x_1(z)}{x_1(z) - 1}. \quad (3.31d)$$

From (3.31) one can readily prove that there are two van-Hove singularities within the band, where the first derivative becomes singular. As is typical for a three-dimensional system, the density of state approaches zero continuously as $\sqrt{|\omega - \omega_{\text{be}\pm}|}$, where $\omega_{\text{be}\pm}$ denotes the two band edges [32].

Higher-dimensional Lattices The results for the density of states so far have all been obtained via a Green function approach. The analytical expression for the three-dimensional Green function and the expression for the square lattice are rather involved. In this section we present a method which allows for straightforward numerical calculations of the density of states on hypercubes and additionally plays an important role in the discussion of the limit of infinite dimensions, see Sect. 6.2.1.

The tight-binding model reads in momentum representation

$$H_{\text{TB}} = \sum_{\mathbf{k}, \sigma} \epsilon(\mathbf{k}) c_{\mathbf{k}\sigma}^\dagger c_{\mathbf{k}\sigma}, \quad (3.32)$$

with the dispersion on a hypercubic, d -dimensional lattice

$$\epsilon(\mathbf{k}) = -2t \sum_{n=1}^d \cos(k_n), \quad \text{with } -\pi < k_n \leq \pi \text{ for all } n. \quad (3.33)$$

The bandwidth W reads

$$W = 4td. \quad (3.34)$$

The density of states is given by

$$\rho_d(\omega) = \frac{1}{L} \sum_{\mathbf{k}} \delta(\omega - \epsilon(\mathbf{k})), \quad (3.35)$$

see e.g. (A.22) of appendix A. Note that (3.35) describes the probability density that, for a random choice of $\mathbf{k} = (k_1, \dots, k_n)$, one finds $\omega = \epsilon(\mathbf{k})$ [41]. Consider the Fourier transform $\Phi_d(s)$ of the density of states (3.35) [42]

$$\Phi_d(s) = \int_{-\infty}^{\infty} \rho_d(\omega) e^{-is\omega} d\omega. \quad (3.36)$$

Since the dispersion (3.33) is composed additively of cosines, we find

$$\Phi_d(s) = \int_{-\infty}^{\infty} \rho_d(\omega) e^{-is\omega} d\omega \quad (3.37)$$

$$= \frac{1}{L} \sum_{\mathbf{k}} \int_{-\infty}^{\infty} \delta(\omega - \epsilon(\mathbf{k})) e^{-is\omega} d\omega = \frac{1}{L} \sum_{\mathbf{k}} e^{-is\epsilon(\mathbf{k})} \rightarrow \frac{1}{(2\pi)^d} \int e^{-is\epsilon(\mathbf{k})} d^d k \quad (3.38)$$

$$= \left(\int_{-\pi}^{\pi} \frac{dk}{2\pi} e^{i2st \cos(k)} \right)^d = \left(\int_0^{\pi} \frac{dk}{\pi} e^{i2st \cos(k)} \right)^d \quad (3.39)$$

$$= \left(J_0(2st) \right)^d, \quad (3.40)$$

where $J_0(z)$ denotes the zero order Bessel function [37]

$$J_0(z) = \frac{1}{\pi} \int_0^\pi e^{iz \cos(\vartheta)} d\vartheta. \quad (3.41)$$

The density of states in d dimensions $\rho_d(\omega)$ can therefore be obtained via Fourier inversion and reads

$$\rho_d(\omega) = \frac{1}{2\pi} \int_{-\infty}^{\infty} e^{is\omega} \left(J_0(2st) \right)^d ds. \quad (3.42)$$

In figure 3.3 we show how the density of states evolves with increasing dimension d .

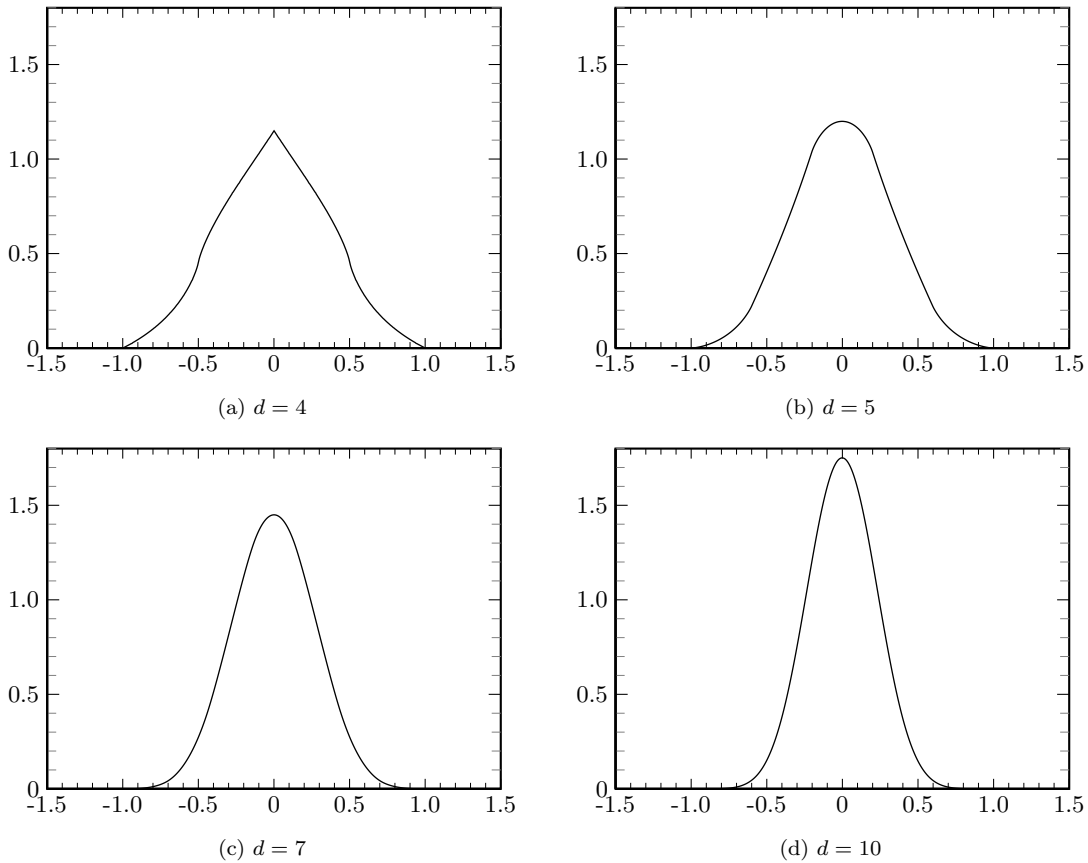


Figure 3.3.: The density of states $\rho_d(\omega)$ has been scaled with half the bandwidth W : $W/2\rho_d(\omega)$. The energy ω is measured in multiples of half the bandwidth $W/2 = 2td$.

Note that the band always has finite width and that the characteristics of the van-Hove singularities decrease with increasing dimension. The density of states becomes smoother and apparently approaches a Gaussian shape, see Sect. 6.2.1 for details.

3.3. Tight-Binding Model on Bethe Lattices

Crystalline materials show periodic and translational invariant arrays of their atoms. In the physical literature these arrays are denoted by *Bravais* lattices. From a mathematical point of view, Bravais

3. Tight-Binding Model

lattices are first of all configurations of nodes and connections between them which together represent the underlying lattice structure. In the simplest case, the nodes represent the positions of the atoms of the solid. The naturally occurring Bravais lattices may be classified according to their behavior under the symmetry operations of translation, rotation and combinations thereof. All operations which transform the lattice under consideration into itself form the so-called space group of the Bravais lattice. In three dimensions there are exactly 230 different space groups and 14 different Bravais lattices [43]. In some cases, however, it might be of interest to discuss physical models on ‘lattices’ which do not have all the symmetries of Bravais lattices but lead to much simpler mathematical problems which might be solvable or at least analytically tractable more easily.

In any case, the underlying configurations of every ‘lattice’ in the above sense are modeled by combinatorial structures called *graphs*. The mathematical discipline which describes and analyzes these structures is part of discrete mathematics and is called graph theory.

3.3.1. Digression on Graph Theory

In order to define physical problems on graphs and to better understand the various terms used to describe them, it seems desirable to introduce some of the concepts and definitions of the mathematical theory, especially because these terms are usually not discussed in textbooks on solid-state theory.

First, we introduce the concept of a graph [44].

Definition 3.3.1. A graph $G = (V, E)$ is a pair consisting of two finite sets V and E . The elements of V are called vertices (or nodes) of G and the elements of E are called the edges of G . Each edge has a set of one or two vertices associated to it, which are called its endpoints. A proper edge is an edge that joins two distinct vertices.

Note that we will always assume a graph to be finite, i.e. the set V of vertices is finite. We shall denote a graph with an infinite set V as a lattice. This means that the notion of a lattice does not immediately imply any kind of symmetry. As an example consider figure 3.4, where $E = \{e_1, e_2, e_3, e_4\}$ and $V = \{v_1, v_2, v_3\}$. The edge e_3 is not proper but joins a single endpoint and is therefore called a *self-loop* [44]. As the degree $deg(v)$ of a vertex $v \in V$ one understands the number of incident proper edges on v plus twice the number of self-loops. The degree of the vertex v_3 in figure 3.4 is $deg(v_3) = 4$.

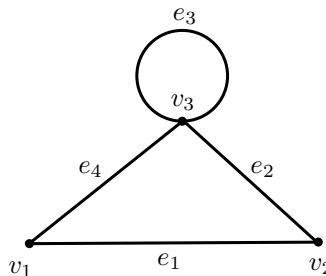


Figure 3.4.: Example for a simple graph.

Second, we introduce a very useful and particularly important family of graphs, the so-called bipartite graphs [44].

Definition 3.3.2. A bipartite graph $G = (V, E)$ is a graph whose vertex set V can be partitioned into two subsets U and W , such that each edge of G has exactly one endpoint in U and exactly one in W .

Figure 3.5 shows some simple examples of bipartite graphs. Note that, by definition, self-loops have to be absent in bipartite graphs.

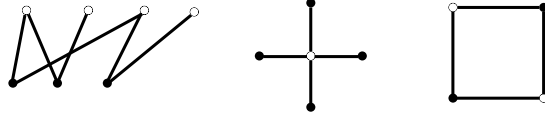


Figure 3.5.: Examples for simple bipartite graphs.

An additional useful class of graphs are the regular graphs whose vertices all have equal degree [44]. Figure 3.6 shows a cube which is a 3-regular graph and, additionally, bipartite.

Third, we consider a subfamily of regular graphs, the hypercubic graphs Q_n [44].

Definition 3.3.3. A hypercubic graph Q_n is an n -regular graph whose vertex set is the set of bitstrings of length n , such that there is an edge between two vertices if and only if they differ in exactly one bit.

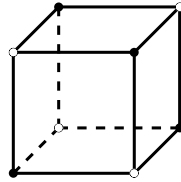


Figure 3.6.: The 3-regular cube.

We have analyzed the tight-binding model on the corresponding lattices in the last section. Many applications, especially in physics, call for graph models that can incorporate the notion of distance and allow for the description of motion on them, as is the case for every model of itinerant electrons on lattices. In order to introduce these concepts we start by defining walks on a graph [44].

Definition 3.3.4 (Walks and paths).

- (i) On a graph $G = (V, E)$ a walk w from vertex $v_0 \in V$ to vertex $v_n \in V$ is a sequence

$$w = \langle v_0, e_1, v_1, \dots, e_n, v_n \rangle \quad (3.43)$$

of vertices and edges such that the endpoints of $e_i \in E$ are given by v_{i-1} and v_i .

- (ii) A path is a walk without repeated vertices.

- (iii) The length $l(w)$ of a walk w is the number of edge-steps in the walk sequence.

- (iv) A closed walk is a walk w with $l(w) > 0$ that begins and ends on the same vertex, whereas an open walk begins and ends at different vertices.

- (v) A closed path of length $l > 0$ is called a cycle.

Note that with the notion of a walk one may introduce connectedness: A graph $G = (V, E)$ is said to be connected if for every pair $(u, v) \in V \times V$ there is a walk from u to v .

The last family of graphs which we need for this thesis are the trees [44].

Definition 3.3.5 (Trees).

- (i) A tree is a connected graph that has no cycles.

- (ii) A leaf of a tree is a vertex v of degree $\text{deg}(v) = 1$.

3. Tight-Binding Model

Note that the deletion of a leaf from a tree leads to a tree with one vertex less. In [44] it is shown that every tree with at least one edge has at least two leaves. This shows that mathematical induction and recursion relations are natural approaches for solving problems defined on trees. Figure 3.7 summarizes the important points of the definition of trees.

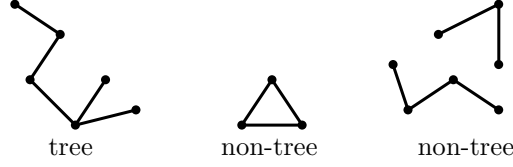


Figure 3.7.: Definition of trees.

For the purpose of this thesis it will not be necessary to embed a given graph into some particular metric space. Only topological properties of a graph will be of importance and we therefore give here the definition of (topological) distance on a graph [45].

Definition 3.3.6. The (topological) distance $d(v_i, v_j)$ from vertex v_i to vertex v_j on a graph G is given by

$$d_{ij} \equiv d(v_i, v_j) := \begin{cases} \min_l \{l(w) | w \text{ walk from } v_i \text{ to } v_j\} & \text{if existent,} \\ \infty & \text{otherwise.} \end{cases} \quad (3.44)$$

Except for very small graphs like in the figures presented so far, line drawings are not an adequate tool for representing these graphs. An especially useful representation of a graph G is its *adjacency matrix* $A(G) = (a_{ij})$ which is a square matrix with $|V(G)| = n$ rows and columns such that a_{ij} gives the number of edges between vertices v_i and v_j [45]. The graph in figure 3.4 has the adjacency matrix

$$A = \begin{pmatrix} 0 & 1 & 1 \\ 1 & 0 & 1 \\ 1 & 1 & 1 \end{pmatrix}. \quad (3.45)$$

The adjacency matrix is of particular use for the analysis of hopping Hamiltonians on a graph G , since the element $a_{ij}^{(k)}$ of the k -th power of $A(G)$

$$A^k(G) = (a_{ij}^{(k)}) \quad (3.46)$$

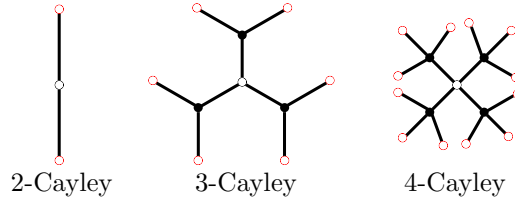
gives the number of walks of length k between the vertices v_i and v_j [45]. Since we will only consider connected graphs we may formulate additionally [45]: The number of shortest paths from v_i to v_j is given by

$$a_{ij}^{(k)}, k = \min_l \{l \in \mathbb{N} | a_{ij}^{(l)} > 0\}. \quad (3.47)$$

We are now in a position to define *Cayley trees*.

Definition 3.3.7 (Cayley Tree). A tree in which every non-leaf has a constant number Z of edges is called a Z -Cayley tree.

Figure 3.8 shows examples for the first Z -Cayley trees. Note that all these trees are bipartite. One can think of constructing such a tree by starting with a central vertex v_0 and add Z new vertices connected to v_0 . These Z vertices constitute the first ‘shell’ and one creates further shells by adding $Z - 1$ new vertices to every vertex in shell s [46]. The leaves are drawn in red and can be thought of as being boundary ‘atoms’ in the outermost shell.


 Figure 3.8.: First Z -Cayley trees.

As is shown in [46], the number $\#_s$ of vertices in shell s of a Z -Cayley tree is given by $\#_s = Z(Z-1)^{s-1}$. The total number of vertices in the tree with q shells is therefore

$$\#_\Sigma := 1 + \sum_{s=1}^q \#_s = 1 + \frac{Z[(Z-1)^q - 1]}{(Z-2)}. \quad (3.48)$$

Note that (3.48) is not directly valid for the one-dimensional chain, where $Z = 2$. In this case one has to take the limit $Z \rightarrow 2$ in all the formulas presented. For example, the total number of vertices in a tree with $Z = 2$, consisting of q shells, is given by

$$\#_\Sigma(Z = 2) = \lim_{Z \rightarrow 2} \#_\Sigma(Z) = 1 + 2q. \quad (3.49)$$

In the limit of an infinite number of shells, i.e., in the thermodynamic limit, the ratio of leafs (boundary sites) to the total number of sites becomes

$$\lim_{q \rightarrow \infty} \frac{\#_q}{\#_\Sigma} = \lim_{q \rightarrow \infty} \frac{Z(Z-1)^{q-1}(Z-2)}{(Z-2) + Z[(Z-1)^q - 1]} \stackrel{Z \geq 2}{=} \lim_{q \rightarrow \infty} \frac{(Z-1)^q}{(Z-1)^q} = 1. \quad (3.50)$$

This large surface contribution is unusual, since one typically assumes that the contributions of boundary terms may be neglected for large systems. It is the reason for the unusual behavior of statistical models in the thermodynamic limit defined on such a tree [46–50].

Note that for the one-dimensional chain ($Z = 2$) the ratio approaches

$$\lim_{Z \rightarrow 2} \frac{\#_q}{\#_\Sigma} = \frac{2}{1 + 2q}, \quad (3.51)$$

which vanishes in the thermodynamic limit as expected.

To overcome the problems arising from the giant surface one ‘throws away’ all surface terms and thinks of the lattice as being formed only by the sites deep within the tree. These sites are all equivalent, have coordination number Z and form the so-called *Bethe lattice* [4, 46].

Definition 3.3.8 (Bethe Lattice). As a Bethe lattice with coordination number Z we denote a Z -Cayley tree with an infinite vertex set and without leafs.

The notion ‘Bethe lattice’ has probably been used for the first time by Domb in [51, 52] and originates from the fact that the Bethe approximation of the Ising model [53] becomes exact on this lattice [52]. Despite the fact that the Bethe lattice is an infinitely extended tree without the usual translational symmetry of (Bravais) lattices (which implies that Fourier transformation does not lead to simplifications), it has been used extensively in physics: For the analysis of the Ising model [4, 46, 53, 54], percolations problems [55–57], Anderson localization [58–61], electron motion [62–64] and correlated electronic systems [65–67] to name but a few.

The definitions presented in this subsection have been chosen with the applications in mind described in the next section. They do not serve as an introduction into graph theory, especially because some

3. Tight-Binding Model

of the definitions have not been formulated in their broadest range. For a thorough introduction, the reader should consult some of the textbooks on this topic, e.g. [44, 45, 68]. Note that graph theory does not only appear in physics in the context of solid-state theory but also within the broad field of quantum-mechanical/field-theoretical perturbation theory in the shape of Feynman diagrams [11, 12].

3.3.2. Electron Motion on Bethe Lattices

In this section, we use some of the concepts introduced in Sect. 3.3.1 and derive the density of states of the nearest-neighbor tight-binding model on Bethe lattices with coordination number Z . The number of publications on methods to derive the spectrum of nearest-neighbor hopping Hamiltonians is quite large. For example, Brinkman and Rice in [69] derived the density of states by examining the self-energy from hopping, Economou [32] derived the spectrum by means of the so-called renormalized perturbation expansion, Mahan [4, 62] introduced the idea of energy bands and Chen and Onsager [70] derived the density of states by means of a transfer matrix approach. Here, we follow the derivation given by Kollar et al. in [64].

Consider a Bethe lattice $G = (V, E)$ with vertex set $V = \{i, j, k, \dots\}$. Since the electron transfer amplitude t_{ij} is assumed to depend only on the distance between the vertices, the general tight-binding Hamiltonian with arbitrary hopping can be written in first-quantized form as

$$H = \sum_{i,j \in V} t_{ij} |i\rangle\langle j| = \sum_{d \geq 0} t_d H_d, \quad (3.52a)$$

where

$$H_d := \sum_{\substack{i,j \in V \\ d_{ij} = d}} |i\rangle\langle j| \quad (3.52b)$$

describes hopping between vertices i and j , a topological distance of d_{ij} apart. Note that the matrix representation of H_0 is the identity matrix whereas the matrix representation of H_1 gives the adjacency matrix

$$a_{ij} = (H_1)_{ij} = \langle i | H_1 | j \rangle = \begin{cases} 1 & \text{for } d_{ij} = 1, \\ 0 & \text{otherwise.} \end{cases} \quad (3.53)$$

As has already been pointed out in Sect. 3.3.1, the matrix elements of H_1^n give the number of walks between vertices i and j . Since on the Bethe lattice $(H_1^n)_{ij}$ is a function solely of d_{ij} (distance regularity), one may express the hopping Hamiltonian H_d as a polynomial in H_1 [64],

$$H_d = \sum_{n=0}^d A_d^{(n)} H_1^n, \quad (3.54)$$

with coefficients $A_d^{(n)}$ to be calculated from the operator identity [64]

$$\frac{1 - x^2}{1 - xH_1 + (Z - 1)x^2} = \sum_{d=0}^{\infty} H_d x^d. \quad (3.55)$$

The single-particle Green function for nearest-neighbor hopping

$$G_{ij}(z) = \langle i | (z - tH_1)^{-1} | j \rangle \quad (3.56)$$

can be expressed via equation (3.55) if we set

$$z = \frac{t(1 + (Z - 1)x^2)}{x} \Rightarrow x(z) = \frac{2t}{z + \sqrt{z^2 - 4(Z - 1)t^2}}, \quad (3.57)$$

3.3. Tight-Binding Model on Bethe Lattices

where the complex square root is chosen such that the sign of its imaginary part equals the sign of $\Im z$. Due to the tree structure of the Bethe lattice, there is only one path connecting vertices i and j . This implies that

$$\langle i|H_d|j\rangle = \delta_{d,d_{ij}}, \quad (3.58)$$

where $\delta_{x,y}$ denotes the Kronecker delta. Applied to the single-particle Green function one finds

$$G_{ij}(z) = \langle i|\frac{1}{t}\frac{x(z)}{1-x^2(z)}\sum_{d=0}^{\infty}H_dx^d(z)|j\rangle = \frac{1}{t}\frac{x^{d_{ij}+1}(z)}{1-x^2(z)}, \quad (3.59)$$

which simplifies after some algebra to

$$G_{ij}(z) = \frac{2(Z-1)}{(Z-2)z + Z\sqrt{z^2 - 4(Z-1)t^2}} \left\{ \frac{2t}{z + Z\sqrt{z^2 - 4(Z-1)t^2}} \right\}^{d_{ij}}. \quad (3.60)$$

The local Green function $G_{ii}(z)$ therefore reads

$$G_{\text{local},Z}(z) := G_{ii}(z) = \frac{2(Z-1)}{(Z-2)z + Z\sqrt{z^2 - 4(Z-1)t^2}}. \quad (3.61)$$

Using relation (A.21) of appendix A,

$$\rho_Z(\omega) = -\frac{1}{\pi} \lim_{\eta \searrow 0} \Im G_{\text{local},Z}(\omega + i\eta), \quad (3.62)$$

we obtain the density of states

$$\rho_Z(\omega) = \frac{Z\sqrt{4(Z-1)t^2 - \omega^2}}{2\pi(Z^2t^2 - \omega^2)} \Theta(4(Z-1)t^2 - \omega^2). \quad (3.63)$$

This density of states is shown in figure 3.9 for $Z = 2, 3, 4$ and 5 .

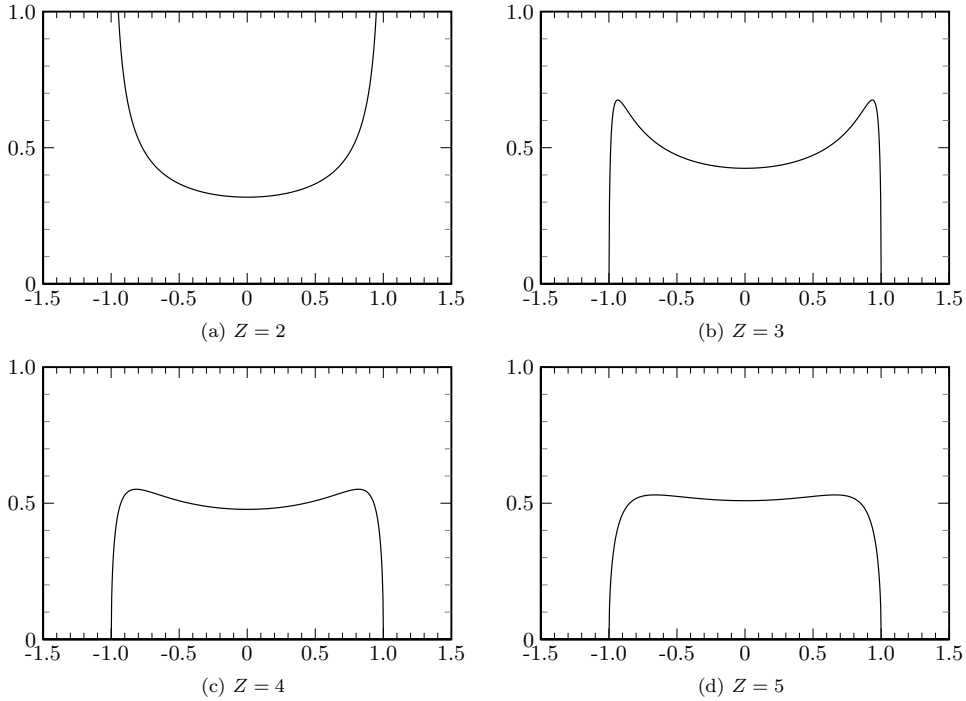


Figure 3.9.: Density of states $(W/2)\rho_Z(2\omega/W)$ for Bethe lattices with various values of Z .

3. Tight-Binding Model

As already mentioned above, we find for $Z = 2$ the same density of states as in the one-dimensional, cubic case. The van-Hove singularities at the band edges for $Z = 2$ are already suppressed in the case of $Z = 3$. For all $Z > 2$ the density of states is a smooth function of the energy and does not show any van-Hove singularities. According to (3.65) the bandwidth is finite for finite Z . At the band edges $\omega_{\text{be}\pm} = \pm 2t\sqrt{Z-1}$ the density of states behaves as

$$\rho(\omega \xrightarrow{|\omega| < |\omega_{\text{be}\pm}|} \omega_{\text{be}\pm}) = \frac{(Z-1)^{1/4} Z \sqrt{t|\omega - \omega_{\text{be}\pm}|}}{\pi t^2 (Z-2)^2}. \quad (3.64)$$

This square root behavior is important as it is typical for three dimensional lattices [32] which shows that the density of states on Bethe lattices for $Z > 2$ can be used as a simple approximation for these lattices, provided details (such as encoded in van-Hove singularities) play no role.

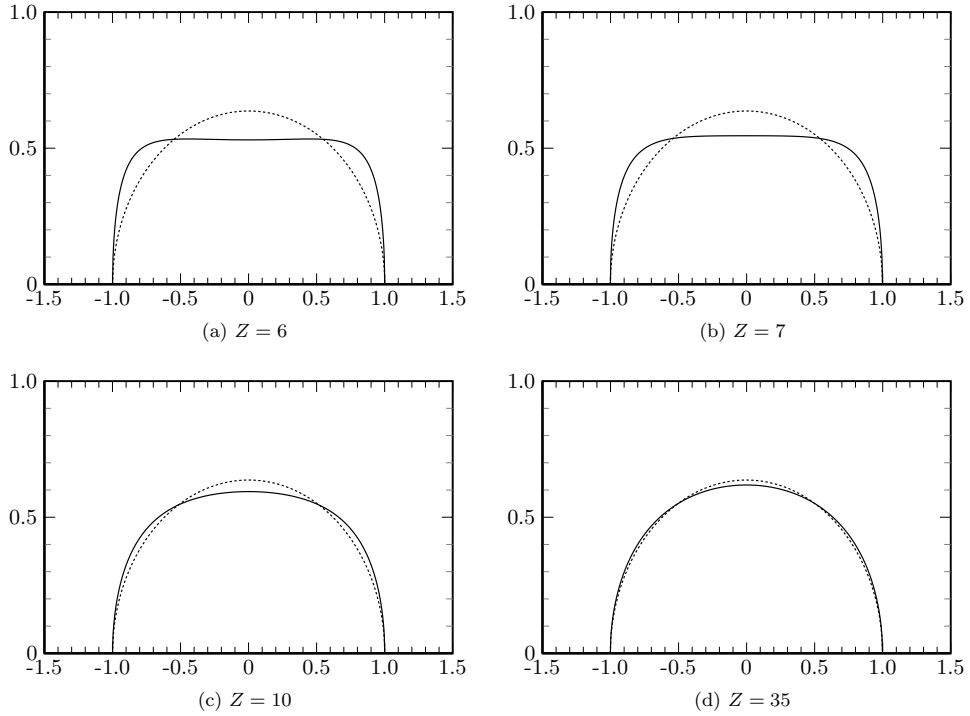


Figure 3.10.: Density of states for Bethe lattices, scaled with half the bandwidth $(W/2)\rho_Z(2\omega/W)$. The dashed curve represents the limiting result (3.66).

In figure 3.10 we show the density of states for $Z = 6, 7, 10$ and 35 . According to (3.63), the bandwidth W of the tight-binding model on Bethe lattices with coordination number Z is given by

$$W = 4t\sqrt{Z-1}. \quad (3.65)$$

Note that that in contrast to (3.34) the bandwidth scales with the square root of the number of nearest-neighbors. This remark will be of some importance in Sect. 6.2. As can be seen from the figure, the density of states approaches rapidly its limiting value for $Z \rightarrow \infty$,

$$\lim_{Z \rightarrow \infty} \frac{W}{2} \rho_Z\left(\frac{2\omega}{W}\right) = \frac{2}{\pi} \sqrt{1 - \left(\frac{2\omega}{W}\right)^2}. \quad (3.66)$$

*Simple things should be simple and
complex things should be possible.*

Alan Kay

4

Single Impurity Anderson Model

In the last chapters we have discussed the properties of some single-particle models. Here we like to introduce a first model capable of describing electron-electron correlations, the *Single Impurity Anderson Model* (SIAM). The SIAM, fascinating in its own right, is an essential part of the Dynamical Mean-Field Theory for the Hubbard model.

In the early 60ies of the last century, non-magnetic metals were studied in which small amounts of iron-group elements were dissolved. A series of electron-spin resonance (ESR) and nuclear magnetic resonance (NMR) experiments [71, 72] proved the appearance of local magnetic moments which drastically influenced the conductivity at low temperatures. The first phenomenological model to explain the onset of local moments was given by Friedel [73–75] who described the effect of the impurity as generating an attractive one-body potential. Such a potential can support bound states if it is deep enough but can always sustain virtual bound states, i.e., scattering resonances. When the lifetime of the resonance is larger than the experimental observation time and the level of up and down spins are non-degenerate, one may observe a local moment. A detailed discussion of these ideas can be found in Ref. [76]. Anderson [77] argued that the formation of localized moments cannot be satisfactorily described within a single-electron theory. Instead, he developed a new one-band model, the so-called Single Impurity Anderson Model, which we introduce and discuss next. In the subsequent presentation we follow [77] and [78].

4.1. Hamiltonian and Model Parameters

The SIAM has originally been introduced to describe the formation of local magnetic moments sustained by magnetic ions such as Fe or Ni dissolved in non-magnetic host metals. These metals (usually transition elements) can have wide conduction bands, describable by a set of Bloch states as expressed by the Hamiltonian

$$H = \sum_{\mathbf{k}, \sigma} \epsilon_{\mathbf{k}} c_{\mathbf{k}\sigma}^\dagger c_{\mathbf{k}\sigma} \equiv \sum_{\mathbf{k}, \sigma} \epsilon_{\mathbf{k}} n_{\mathbf{k}\sigma} \quad (4.1)$$

with energy dispersion $\epsilon_{\mathbf{k}} \equiv \epsilon(\mathbf{k})$. Instead of ‘conduction’ or ‘band’ electrons, one also speaks of ‘bath’ electrons in this context. The bandwidth W of the band electrons can be finite or even (in some cases) free-electron like. Usually one describes the band by its density of states

$$\rho_{\sigma}(\omega) = \frac{1}{L} \sum_{\mathbf{k}} \delta(\omega - \epsilon_{\mathbf{k}}). \quad (4.2)$$

The impurity is treated as a local site with a single electronic orbital $\langle \mathbf{r} | d \rangle \equiv \varphi_d(\mathbf{r})$. As has already been pointed out by Anderson, the restriction to a single orbital is not crucial but keeps the model as simple as possible. The isolated impurity is described by the Hamiltonian

$$H = \sum_{\sigma} E_d d_{\sigma}^\dagger d_{\sigma} + U d_{\uparrow}^\dagger d_{\uparrow} d_{\downarrow}^\dagger d_{\downarrow} \equiv \sum_{\sigma} E_d n_{d\sigma} + U n_{d\uparrow} n_{d\downarrow}. \quad (4.3)$$

4. Single Impurity Anderson Model

The first term describes the position of the impurity level relative to the Fermi energy. In most cases of interest it will be located within the band of conduction electrons. As remarked by Anderson, the localized state $|d\rangle$ should be orthogonal to all the Wannier states belonging to the band. Then, one can neglect the direct perturbation of the band energy levels by the impurity.

The second term in (4.3) gives the on-site Coulomb repulsion between two impurity electrons of anti-parallel spin,

$$U = \langle dd|v_{ee}|dd\rangle = \int d^3r d^3r' |\varphi_d(\mathbf{r})|^2 \frac{e^2}{|\mathbf{r} - \mathbf{r}'|} |\varphi_d(\mathbf{r}')|^2. \quad (4.4)$$

For a discussion of this term and a justification of the neglected terms, such as the Coulomb interaction of the impurity electrons and the band electrons, see our discussion in chapter 5 on the Hubbard model. The inclusion of the interaction term is crucial for local moment formation as we will demonstrate in Sect. 4.2. The two-particle interaction generates a complicated many-particle problem.

The last ingredient we need is a band-impurity hybridization part

$$H_{\text{Hyb}} = \sum_{\mathbf{k}, \sigma} V_{\mathbf{k}} (c_{\mathbf{k}\sigma}^\dagger d_\sigma + d_\sigma^\dagger c_{\mathbf{k}\sigma}). \quad (4.5)$$

For the purpose of this thesis we shall consider the $V_{\mathbf{k}}$ as given parameters.

The Single Impurity Anderson Model is therefore defined by the Hamiltonian

$$H_{\text{SIAM}} = \sum_{\mathbf{k}, \sigma} \epsilon_{\mathbf{k}} n_{\mathbf{k}\sigma} + \sum_{\sigma} E_d n_{d\sigma} + \sum_{\mathbf{k}, \sigma} V_{\mathbf{k}} (c_{\mathbf{k}\sigma}^\dagger d_\sigma + d_\sigma^\dagger c_{\mathbf{k}\sigma}) + U n_{d\uparrow} n_{d\downarrow}. \quad (4.6)$$

4.2. Non-Interacting Limit (Fano-Anderson Model)

In the absence of the on-site interaction, the SIAM Hamiltonian (4.6) reduces to a model introduced by Fano in the context of atomic spectra [79]. The corresponding model

$$H_{\text{FA}} = \sum_{\mathbf{k}, \sigma} \epsilon_{\mathbf{k}} n_{\mathbf{k}\sigma} + \sum_{\sigma} E_d n_{d\sigma} + \sum_{\mathbf{k}, \sigma} V_{\mathbf{k}} (c_{\mathbf{k}\sigma}^\dagger d_\sigma + d_\sigma^\dagger c_{\mathbf{k}\sigma}) \quad (4.7)$$

is also called the Fano-Anderson model. We discuss its solution to introduce some important concepts also used in later parts of the thesis.

We aim at the calculation of the local density of impurity states, see (A.21) of appendix A,

$$D_\sigma(\omega) = \sum_n \delta(\omega - \bar{\epsilon}_n) |\langle d_\sigma | n\sigma \rangle|^2, \quad (4.8)$$

where $|n\sigma\rangle$ is an exact eigenstate of H_{FA} with energy $\bar{\epsilon}_n$. We start from the local, one-particle impurity Green function, see (A.31) of appendix A,

$$G_\sigma(t) := G_\sigma^{\text{ret}}(dd, t) = -i\Theta(t) \langle \{d_\sigma(t), d_\sigma^\dagger\} \rangle = -i\Theta(t) \langle d_\sigma(t) d_\sigma^\dagger \rangle, \quad (4.9)$$

where the expectation value is taken in the vacuum. Taking the Fourier transform according to (A.26) of appendix A we obtain, see (A.14) of appendix A,

$$G_\sigma(\omega) = \lim_{\eta \searrow 0} \langle d_\sigma(\omega - H_{\text{FA}} + i\eta)^{-1} d_\sigma^\dagger \rangle. \quad (4.10)$$

Thus, from the local Green function we indeed obtain the local density of states as

$$D_\sigma(\omega) = -\frac{1}{\pi} \Im G_\sigma(\omega) = \langle d_\sigma \delta(\omega - H_{\text{FA}}) d_\sigma^\dagger \rangle = \sum_n \delta(\omega - \bar{\epsilon}_n) |\langle d_\sigma | n\sigma \rangle|^2. \quad (4.11)$$

4.2. Non-Interacting Limit (Fano-Anderson Model)

A quick way to obtain the impurity Green function is the equation of motion technique:

$$i\frac{\partial G_\sigma(t)}{\partial t} = \delta(t) - i\Theta(t)\langle\{[d_\sigma(t), H_{\text{FA}}], d_\sigma^\dagger\}\rangle \quad (4.12)$$

$$= \delta(t) + E_d G_\sigma(t) + \sum_{\mathbf{k}} V_{\mathbf{k}} G_\sigma(\mathbf{k}d, t), \quad (4.13)$$

where

$$G_\sigma(\mathbf{k}d, t) = -i\Theta(t)\langle\{c_{\mathbf{k}\sigma}(t), d_\sigma^\dagger\}\rangle \quad (4.14)$$

is the impurity-band Green function with the equation of motion

$$i\frac{\partial G_\sigma(\mathbf{k}d, t)}{\partial t} = \epsilon_{\mathbf{k}} G_\sigma(\mathbf{k}d, t) + V_{\mathbf{k}} G_\sigma(t). \quad (4.15)$$

After Fourier transformation one therefore finds the following coupled algebraic equations

$$\lim_{\eta \searrow 0} (\omega - E_d + i\eta) G_\sigma(\omega) = 1 + \sum_{\mathbf{k}} V_{\mathbf{k}} G_\sigma(\mathbf{k}d, \omega), \quad (4.16)$$

$$\lim_{\eta \searrow 0} (\omega - \epsilon_{\mathbf{k}} + i\eta) G_\sigma(\mathbf{k}d, \omega) = V_{\mathbf{k}} G_\sigma(\omega). \quad (4.17)$$

The impurity Green function can be cast into the form

$$G_\sigma(\omega) = (\omega - E_d - \Delta^{\text{ret}}(\omega))^{-1}, \quad (4.18)$$

where

$$\Delta^{\text{ret}}(\omega) := \lim_{\eta \searrow 0} \sum_{\mathbf{k}} \frac{V_{\mathbf{k}}^2}{\omega - \epsilon_{\mathbf{k}} + i\eta} \quad (4.19)$$

is called the *hybridization function*. Since we introduced it by calculating the retarded Green function, it is also given in its retarded form. The causal form reads

$$\Delta(\omega) = \lim_{\eta \searrow 0} \sum_{\mathbf{k}} \frac{V_{\mathbf{k}}^2}{\omega - \epsilon_{\mathbf{k}} + i \operatorname{sgn}(\omega)\eta}. \quad (4.20)$$

We write the retarded function as

$$\begin{aligned} \Delta^{\text{ret}}(\omega) &= \mathcal{P} \sum_{\mathbf{k}} \frac{V_{\mathbf{k}}^2}{\omega - \epsilon_{\mathbf{k}}} - i\pi \sum_{\mathbf{k}} V_{\mathbf{k}}^2 \delta(\omega - \epsilon_{\mathbf{k}}) \\ &=: F(d, \omega) - i\pi \Delta(d, \omega). \end{aligned} \quad (4.21)$$

In order to illustrate the meaning of the hybridization function, let us assume $V_{\mathbf{k}}$ to be constant, $V_{\mathbf{k}} \equiv V$, which corresponds to short-range overlap matrix elements and permits us to write, see (4.2),

$$-\frac{1}{\pi} \Im \Delta^{\text{ret}}(\omega) = V^2 L\rho_\sigma(\omega). \quad (4.22)$$

The imaginary part of the hybridization function is proportional to the density of the band states. In this case the real part $F(d, \omega)$ becomes

$$F(d, \omega) = V^2 \mathcal{P} \sum_{\mathbf{k}} \frac{1}{\omega - \epsilon_{\mathbf{k}}} = V^2 L\mathcal{P} \int_{-\infty}^{\infty} \frac{\rho_\sigma(\epsilon)}{\omega - \epsilon} d\epsilon, \quad (4.23)$$

the Hilbert transform of the band density of states. This clearly shows that the hybridization function is the relevant quantity, describing the host band and its coupling to the impurity.

4. Single Impurity Anderson Model

The local density of impurity states, calculated via (4.11), becomes

$$D_\sigma(\omega) = \frac{\Delta(d, \omega)}{(\omega - E_d - F(d, \omega))^2 + \pi^2 \Delta^2(d, \omega)}. \quad (4.24)$$

The poles ω_p of the Green function are obtained from

$$\omega_p - E_d - F(d, \omega_p) - i\pi\Delta(d, \omega_p) = 0 \quad (4.25)$$

and give the resonances of the system. We see that, for $\Delta(d, \omega_p) \rightarrow 0$, the unperturbed energy level E_d of the impurity is shifted to a new value

$$\bar{E}_d \approx E_d + F(d, \bar{E}_d) \quad (4.26)$$

with a lifetime proportional to $\Delta(d, \bar{E}_d)^{-1}$. If the shifted level \bar{E}_d lies outside the continuum of band states, we find a bound state with infinite lifetime. We can readily see this in our simplified description because

$$\Delta(d, \omega) \propto \rho_\sigma(\omega) \quad (4.27)$$

and, thus, $\Delta(d, \bar{E}_d) = 0$ due to the location of \bar{E}_d . In the opposite case that \bar{E}_d lies within the conduction band we obtain a scattering resonance.

The results of the Fano-Anderson model are similar to those obtained by Friedel [76]. Since both spin sectors are completely decoupled we find no magnetic moment on the impurity.

Though the electron-electron interaction only acts on a single site, the SIAM is much harder to solve. In fact, even today the only exact solution of the model is by means of the Bethe ansatz for special forms of the hybridization function [80]. In particular, we may state that no one has achieved an exact solution of the general model.

The local Green function of the SIAM can be stated in the form of (A.40) of appendix A as

$$G_\sigma^{\text{SIAM}}(\omega) = \frac{1}{\omega - E_d - \Delta(\omega) - \Sigma_\sigma^*(\omega)}. \quad (4.28)$$

However this form is of limited use, because the proper self-energy $\Sigma_\sigma^*(\omega)$ is not known. Since the interaction is only present at a single site, the self-energy is independent of momentum, a property which will be used in the context of the Dynamical Mean-Field Theory for the Hubbard model, see chapter 6. Nevertheless, we can gain some qualitative results.

4.3. Limiting Cases

The Coulomb interaction tends to inhibit double occupancy on the impurity orbital. Therefore, single-electron occupation and thus configurations with a local spin moment are dominant. In contrast, the hybridization part causes charge fluctuations which tend to reduce local moments. Therefore, we have two *non-commuting* terms in the Hamiltonian with opposite tendencies. Examining the Hamiltonian, we realize that the physics of the SIAM is governed by

- the position of the impurity level relative to the Fermi level E_F ,
- the magnitude of the on-site repulsion U ,
- the transition rate between the impurity state $|d\rangle$ and a band state $|\mathbf{k}\sigma\rangle$ which, according to Fermi's Golden Rule [81], can be estimated as

$$\Gamma_{d \rightarrow \mathbf{k}} \propto |V_{\mathbf{k}}|^2 \rho_\sigma(E_d), \quad (4.29)$$

with the unperturbed density of band states $\rho_\sigma(\omega)$.

4.3.1. Deep Impurity Limit (Local-Moment Regime)

Let the impurity level be well below the Fermi energy (E_F) and consider first the case $U \gg |E_d| \gg |V_{\mathbf{k}}|^2 \rho_{\sigma}(E_d)$. Here, the physics is dominated by the local Coulomb repulsion U . Since $E_d < E_F$ the impurity level will definitely be singly occupied. To put a second electron of opposite spin onto it, one has to pay the energy $E_d + U$. For the case at hand the energy level diagram is shown in figure 4.1. Apparently, we find a local moment. Note that the level spectrum cannot be understood in terms of a single-particle because the upper level does not exist when the lower one is not occupied, see also our discussion in Sect. 5.3.2.

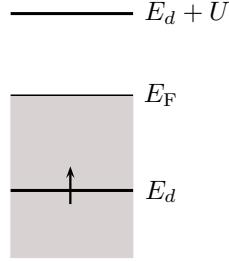


Figure 4.1.: Energy-level diagram of the SIAM for $U \gg |E_d| \gg |V_{\mathbf{k}}|^2 \rho_{\sigma}(E_d)$ and $E_d \ll E_F$.

Now consider the case where the on-site repulsion U is small compared to $|V_{\mathbf{k}}|^2 \rho_{\sigma}(E_d)$. Because of the transitions between the impurity and the band states, the impurity level will be broadened. Its width is proportional to $\Gamma_{d \rightarrow \mathbf{k}}$. In the regime $|E_d| \gg |V_{\mathbf{k}}|^2 \rho_{\sigma}(E_d) \gg U$, the width of the impurity level exceeds the energy cost of double occupancy. This implies that the impurity will be equally occupied with a spin up and a spin down electron and therefore nonmagnetic. This situation is sometimes called a ‘localized spin fluctuation’.

4.3.2. Resonance Limit (Mixed-Valence Regime)

In some rare-earth compounds it might happen that the impurity level(s) are close to the Fermi energy. Such a situation is commonly called ‘mixed-valence regime’. Here, very small alternations in $|V_{\mathbf{k}}|^2 \rho_{\sigma}(E_d)$ might lead to a loss of magnetic moments. Consider the case $U \gg |V_{\mathbf{k}}|^2 \rho_{\sigma}(E_d) \gg E_d$ such that the upper level is still well above the Fermi energy. Due to the hybridization $|V_{\mathbf{k}}|^2 \rho_{\sigma}(E_d) \gg E_d$ we find rapid charge fluctuations on the impurity which also lead to spin fluctuations.

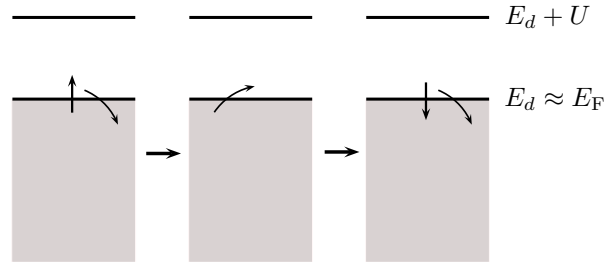


Figure 4.2.: Energy-level diagram of the SIAM for $U \gg |V_{\mathbf{k}}|^2 \rho_{\sigma}(E_d) \gg |E_d|$ and $E_d \approx E_F$.

As a consequence, the state is nonmagnetic. The situation is depicted in figure 4.2.

'While I'm still confused and uncertain, it's on a much higher plane, d'you see, and at least I know I'm bewildered about the really fundamental and important facts of the universe.' Treatle nodded. 'I hadn't looked at it like that,' he said, 'But you're absolutely right. He's really pushed back the boundaries of ignorance.'

Discworld scientists at work in **Equal Rites** by Terry Pratchett

5

Hubbard Model

In March 1963, Gutzwiller [82] and Kanamori [83] and later the same year, starting a seminal series of papers, Hubbard [84–89] have independently introduced a model of locally interacting, itinerant electrons on a lattice. At that time they may not have anticipated that this model will eventually become one of the most studied models of correlated electrons. One might even say that it has become the paradigm of interacting electrons just as the Ising model for classical statistical mechanics [2]. The model is known today as the *Hubbard model*. Though conceptually the simplest model for the description of electron correlations, an exact solution is only known for one spatial dimension in the thermodynamic limit [90, 91].

As we will outline below, the Hubbard model itself cannot properly describe a real material. Nevertheless, the Hubbard interaction is an important ingredient in a vast amount of publications concerning transition metals and their oxides, Fullerenes, heavy fermion materials, high-temperature superconductivity, and the Mott-Hubbard metal-to-insulator transition [2].

In the following chapter we present a short motivation of the Hubbard Hamiltonian, starting with the general electronic problem of solid-state physics. Then, we discuss some of its important symmetries and limiting cases and the problems in their theoretical description. Finally, we conclude this chapter with a sketch of Mott's ideas concerning the metal-to-insulator transition [2, 8] on the basis of the example of the Hubbard model.

5.1. Basic Derivation of the Hubbard Hamiltonian

We start with a short motivation of the Hubbard Hamiltonian. As detailed in Sect. 2.2.2, the basic electronic Hamiltonian in solid-state physics within the adiabatic approximation is given by

$$H = \sum_{j=1}^N \left\{ \underbrace{\frac{\mathbf{p}_j^2}{2m} - V_I(\mathbf{r}_j) + V_a(\mathbf{r}_j)}_{h_{\text{band}}(\mathbf{r}_j)} \right\} + \sum_{i < j} \left\{ \underbrace{V_{e-e}(\mathbf{r}_i - \mathbf{r}_j) - \frac{1}{N-1}(V_a(\mathbf{r}_i) + V_a(\mathbf{r}_j))}_{\tilde{V}_{e-e}(\mathbf{r}_i - \mathbf{r}_j)} \right\}, \quad (5.1)$$

where the auxiliary potential $V_a(\mathbf{r})$ is chosen in order to minimize the matrix elements of $\tilde{V}_{e-e}(\mathbf{r}_i - \mathbf{r}_j)$ in the eigenstates of the one-particle Hamiltonian h_{band} . These eigenstates are given by Bloch states (\mathbf{b} denotes the band index)

$$h_{\text{band}}\Phi_{\mathbf{b}\mathbf{k}}(\mathbf{r}) = \epsilon_{\mathbf{b}}(\mathbf{k})\Phi_{\mathbf{b}\mathbf{k}}(\mathbf{r}). \quad (5.2)$$

As already explained in Sect. 3.1, it is sometimes useful to work in the complementary basis of Wannier functions (3.9) because every Wannier function is centered around a particular lattice site. Introducing creation and annihilation operators with respect to the Wannier basis, we may write the Hamiltonian (5.1) in the tight-binding approximation as

$$H = \sum_{\substack{i,j \\ \mathbf{b},\sigma}} \tilde{t}_{ij}^{\mathbf{b}} c_{\mathbf{b}i\sigma}^\dagger c_{\mathbf{b}j\sigma} + \sum_{\substack{\mathbf{b}_1, \mathbf{b}_2, \mathbf{b}_3, \mathbf{b}_4 \\ i,j,k,l}} \sum_{\sigma, \sigma'} \tilde{V}_{i,j,k,l}^{\mathbf{b}_1 \mathbf{b}_2 \mathbf{b}_3 \mathbf{b}_4} c_{\mathbf{b}_1 i \sigma}^\dagger c_{\mathbf{b}_2 j \sigma'}^\dagger c_{\mathbf{b}_3 k \sigma'} c_{\mathbf{b}_4 l \sigma}. \quad (5.3)$$

5. Hubbard Model

The hopping matrix elements are given by (3.16) and the matrix elements of the interaction \tilde{V}_{e-e} read

$$\tilde{V}_{i,j,k,l}^{b_1 b_2 b_3 b_4} = \int d^3 r d^3 r' w_{b_1}^*(\mathbf{r} - \mathbf{R}_i) w_{b_2}^*(\mathbf{r}' - \mathbf{R}_j) \tilde{V}_{e-e}(\mathbf{r} - \mathbf{r}') w_{b_3}(\mathbf{r}' - \mathbf{R}_k) w_{b_4}(\mathbf{r} - \mathbf{R}_l). \quad (5.4)$$

As explained in Sect. 2.2.2, an optimal choice of the auxiliary potential lessens the influence of the mutual electron-electron interaction. As already stated at the end of Sect. 2.2.2, band structure calculations completely neglect \tilde{V}_{e-e} .

To go on in the derivation, we utilize for the auxiliary potential the Hartree decoupling, see (2.29),

$$c_\alpha^\dagger c_\beta^\dagger c_\delta c_\gamma \mapsto c_\alpha^\dagger c_\gamma \langle c_\beta^\dagger c_\delta \rangle + \langle c_\alpha^\dagger c_\gamma \rangle c_\beta^\dagger c_\delta - \langle c_\alpha^\dagger c_\gamma \rangle \langle c_\beta^\dagger c_\delta \rangle. \quad (5.5)$$

The Fock term is not included because in strongly correlated systems, the exchange and correlation contributions to the energy levels are comparable in magnitude [2]. Moreover, for the purely local Hubbard interaction, the Fock term does not contribute anyway. The Hamiltonian (5.3) thus becomes

$$H = \sum_{\substack{i,j \\ b,\sigma}} t_{ij}^b c_{b i \sigma}^\dagger c_{b j \sigma} + \sum_{\substack{b_1, b_2, b_3, b_4 \\ i,j,k,l}} \sum_{\sigma, \sigma'} \bar{V}_{i,j,k,l}^{b_1 b_2 b_3 b_4} \{ c_{b_1 i \sigma}^\dagger c_{b_2 j \sigma'}^\dagger c_{b_3 k \sigma'} c_{b_4 l \sigma} - c_{b_1 i \sigma}^\dagger c_{b_4 l \sigma} \langle c_{b_2 j \sigma'}^\dagger c_{b_3 k \sigma'} \rangle \\ - \langle c_{b_1 i \sigma}^\dagger c_{b_4 l \sigma} \rangle c_{b_2 j \sigma'}^\dagger c_{b_3 k \sigma'} + \langle c_{b_1 i \sigma}^\dagger c_{b_4 l \sigma} \rangle \langle c_{b_2 j \sigma'}^\dagger c_{b_3 k \sigma'} \rangle \}. \quad (5.6)$$

This Hamiltonian is still intractable. In order to proceed, Hubbard introduced two drastic simplifications [2, 84].

5.1.1. Hubbard's First Assumption (Single Band)

The Hamiltonian (5.6) describes multiple electron bands which is generic for the d-bands in transition metals or f-bands in rare earth compounds. The position of the various bands relative to each other is given by

$$t_{ii}^b = \frac{1}{L} \sum_{\mathbf{k}} \epsilon_b(\mathbf{k}), \quad (5.7)$$

as may be seen by means of (3.14). Typically [2] one only finds few partly filled bands at the Fermi level E_F and bands far away from E_F will only slightly be altered by the electron-electron interaction because it is not effective due to screening [2, 92].

Hubbard assumed the simple case of only one band at the Fermi energy with all other bands being well separated in energy from E_F . This assumption is a drastic oversimplification for a quantitative description of transition metals. Nevertheless, one may hope to capture some of the main features qualitatively. In any case, it permits us to drop the band index b .

5.1.2. Hubbard's Second Assumption (Local Interaction)

According to Hubbard's first assumption, the Hamiltonian reduces to

$$H = \sum_{\substack{i,j \\ \sigma}} t_{ij} c_{i \sigma}^\dagger c_{j \sigma} \\ + \sum_{\substack{i,j,k,l \\ \sigma, \sigma'}} \bar{V}_{i,j,k,l} \{ c_{i \sigma}^\dagger c_{j \sigma'}^\dagger c_{k \sigma'} c_{l \sigma} - c_{i \sigma}^\dagger c_{l \sigma} \langle c_{j \sigma'}^\dagger c_{k \sigma'} \rangle - \langle c_{i \sigma}^\dagger c_{l \sigma} \rangle c_{j \sigma'}^\dagger c_{k \sigma'} + \langle c_{i \sigma}^\dagger c_{l \sigma} \rangle \langle c_{j \sigma'}^\dagger c_{k \sigma'} \rangle \}, \quad (5.8)$$

which still contains long-ranged Coulomb terms. To estimate the various contributions, Hubbard used weakly overlapping, hydrogen-like wave functions, and calculated matrix elements of the interaction in order to estimate their magnitude in materials with small bandwidths [2]. We have summarized some of his results in table 5.1. Here, the indices i and j always denote nearest-neighbor pairs. Matrix elements not shown in the table are exponentially small [2]. For small bandwidths, the on-site Coulomb interaction, also called the *Hubbard interaction*, dominates. In his second assumption Hubbard neglected all terms of the Coulomb interaction except for the intra-orbital part U .

Symbol	Mathematical Expression	Type	Approximate Value
U	$V_{i,i,i,i}$	on-site	20 eV
V	$\bar{V}_{i,j,j,i}$	nearest-neighbor	6 eV
X	$\bar{V}_{i,i,j,i}$	Hubbard- X	0.5 eV
W	$\bar{V}_{i,j,i,j}$	Hubbard- W	1/40 eV

Table 5.1.: Approximate values of the Coulomb matrix elements as calculated by Hubbard [2].

5.1.3. Hubbard Hamiltonian

For a translational invariant, paramagnetic system, where $\langle c_{i\sigma}^\dagger c_{i\sigma} \rangle = n/2$ with n being the electron density, the Hubbard model thus reads

$$H = \sum_{\substack{i,j \\ \sigma}} t_{ij} c_{i\sigma}^\dagger c_{j\sigma} + U \sum_i (c_{i\uparrow}^\dagger c_{i\uparrow} - n/2)(c_{i\downarrow}^\dagger c_{i\downarrow} - n/2). \quad (5.9)$$

The Hubbard Hamiltonian is frequently cast into the form

$$H = \sum_{\substack{i,j \\ \sigma}} t_{ij} c_{i\sigma}^\dagger c_{j\sigma} + U \sum_i n_{i\uparrow} n_{i\downarrow} =: T + UD, \quad (5.10)$$

with T denoting the electron transfer operator and

$$D = \sum_i n_{i\uparrow} n_{i\downarrow} \quad (5.11)$$

defines the operator for counting the number of double occupancies. The Hamiltonian (5.10) describes the same electron-electron correlations as (5.9) since both only differ by single-particle terms which may be included into the chemical potential in a grand-canonical description.

5.2. Symmetries

In this thesis we will be dealing exclusively with the so-called particle-hole symmetric form of the Hubbard model

$$H_{\text{Hubbard}} = \sum_{\substack{i,j \\ \sigma}} t_{ij} c_{i\sigma}^\dagger c_{j\sigma} + U \sum_i (n_{i\uparrow} - 1/2)(n_{i\downarrow} - 1/2) =: T + UD - N/2 + U/4, \quad (5.12)$$

which has the same eigenfunctions as (5.10) since the Hubbard Hamiltonian commutes with the operator of the total number of electrons,

$$N = \sum_i (n_{i\uparrow} + n_{i\downarrow}). \quad (5.13)$$

The Hamiltonian (5.12) is of higher symmetry and therefore has some advantages over (5.10):

- It exhibits particle-hole symmetry on bipartite lattices at all fillings.
- At half band-filling the Hamiltonians (5.12) and (5.9) coincide, which implies that there will be no ‘Hartree-bubbles’ in a diagrammatic perturbation expansion.
- For (5.12) a chemical potential $\mu = 0$ guarantees half-filled bands at all temperatures.

The exactly solvable one-dimensional Hubbard model is integrable. Therefore, it possesses an infinite number of conserved quantities [93]. However, the situation in all higher dimensions is not so clear. In the following sections we will present some selected symmetries of the Hubbard Hamiltonian (5.12). For a more extensive list see [2, 93, 94].

5. Hubbard Model

5.2.1. $SO(4)$ Symmetry

$SU(2)$ Spin-Rotational Invariance

The Hubbard Hamiltonian H_{Hubbard} is invariant under rotations in spin space, generated by the operators of the components of the total spin,

$$S^\alpha = \frac{1}{2} \sum_{\substack{l \\ \mu, \nu}} c_{l\mu}^\dagger (\boldsymbol{\sigma}^\alpha)_{\mu\nu} c_{l\nu}, \quad (5.14)$$

where $\boldsymbol{\sigma}^\alpha$ denotes one of the three Pauli spin matrices, satisfying the commutation relations of the Lie algebra $\mathfrak{su}(2)$ which generates the group $SU(2)$:

$$[\boldsymbol{\sigma}^\alpha, \boldsymbol{\sigma}^\beta] = 2i \sum_{\gamma} \varepsilon_{\alpha\beta\gamma} \boldsymbol{\sigma}^\gamma. \quad (5.15)$$

The proof for $[H_{\text{Hubbard}}, S^\alpha] = 0$ for all α may be found in [93]. This symmetry implies that the z -component and the square of the total spin are good quantum numbers.

η -Pairing symmetry

According to definition (3.3.2), lattices are called bipartite when they consist of two inter-penetrating sub-lattices \mathcal{A} and \mathcal{B} , so that all nearest neighbors of the \mathcal{A} -sites are given by the \mathcal{B} -sites and vice versa. The following considerations are restricted to bipartite lattices and to models with symmetric hopping amplitude $t_{ij} = t_{ji}$, where the hopping is allowed only between \mathcal{A} and \mathcal{B} lattice sites (so-called *non-frustrated* hopping). With the agreement

$$(-1)^l = \begin{cases} +1 & \text{if } l \in \mathcal{A}, \\ -1 & \text{if } l \in \mathcal{B}, \end{cases} \quad (5.16)$$

one defines the operators

$$\eta^z = \frac{1}{2} \sum_l (n_{l\uparrow} + n_{l\downarrow} - 1), \quad (5.17a)$$

$$\eta^+ = - \sum_l (-1)^l c_{l\uparrow}^\dagger c_{l\downarrow}^\dagger, \quad (5.17b)$$

$$\eta^- = (\eta^+)^\dagger, \quad (5.17c)$$

which obey the commutation relations [93]

$$[\eta^z, \eta^\pm] = \pm \eta^\pm, \quad [\eta^+, \eta^-] = 2\eta^z. \quad (5.18)$$

The η -operators therefore form a representation of the Lie algebra $\mathfrak{su}(2)$. One may introduce analogues of S^x and S^y by

$$\eta^\pm = \eta^x \pm i\eta^y. \quad (5.19)$$

It is shown in [93] that the η -operators commute with the Hubbard Hamiltonian in the form (5.12),

$$[H_{\text{Hubbard}}, \eta^\alpha] = 0 \quad \forall \alpha. \quad (5.20)$$

Since the two sets of operators $\{S^\alpha\}$ and $\{\eta^\beta\}$ mutually commute [93], the Hubbard Hamiltonian commutes with the direct sum of two representations of $\mathfrak{su}(2)$. However, the symmetry group of the Hubbard Hamiltonian (5.12) on a bipartite lattice with symmetric, nearest-neighbor hopping is not $SU(2) \times SU(2)$ but $SO(4) \cong SU(2) \times SU(2)/\mathbb{Z}_2$ because η^z and S^z are simultaneously either integer or half odd-integer [93].

It is amusing to note that the Hubbard model (5.12) shares the same symmetry group as an important model of atomic physics, namely the quantum-mechanical Kepler problem [95].

5.2.2. Electron-Hole Transformations

Electron-hole transformations are mappings of the creation and annihilation operators onto each other. In this section we use the notation of [2]. The various symbols \mathcal{T} denote linear operators acting on the algebra of creation and destruction operators. By declaring their action on the vacuum state and by means of the Fock space [12] they can also act on any state defined in Fock space.

Electron-Hole Transformation \mathcal{T}_1

The basic electron-hole transformation \mathcal{T}_1 is given by the following mapping:

$$\begin{aligned} \mathcal{T}_{1,\sigma} : \quad c_{l\sigma}^\dagger &\mapsto c_{l\sigma}, \quad c_{l\sigma} \mapsto c_{l\sigma}^\dagger, \\ \mathcal{T}_1 &:= \prod_{\sigma} \mathcal{T}_{1,\sigma}. \end{aligned} \quad (5.21)$$

Creation operators are transformed into annihilators and vice versa. The local number operators $n_{l\sigma}$ transform according to

$$\mathcal{T}_1^\dagger n_{l\sigma} \mathcal{T}_1 = c_{l\sigma} c_{l\sigma}^\dagger = 1 - n_{l\sigma}, \quad (5.22)$$

so that the Hubbard interaction in the form (5.12) remains unchanged. Note that the operator D , counting the number of double occupancies, see (5.11), is not invariant but transforms according to

$$D = \sum_l n_{l\uparrow} n_{l\downarrow} \mapsto \sum_l (1 - n_{l\uparrow})(1 - n_{l\downarrow}) = L - N + D, \quad (5.23)$$

where L denotes the number of lattice sites and N is defined in (5.13). The kinetic energy transforms according to

$$\mathcal{T}_1^\dagger T \mathcal{T}_1 = \sum_{\substack{m,n \\ \sigma}} t_{m,n} c_{m\sigma} c_{n\sigma}^\dagger \quad (5.24a)$$

$$= - \sum_{\substack{m,n \\ \sigma}} t_{m,n}^* c_{m\sigma}^\dagger c_{n\sigma}. \quad (5.24b)$$

In the last line we have used that $t_{ii} = 0$ and $t_{ij} = t_{ji}^*$.

This shows that the Hubbard model is in general not invariant under an electron-hole transformation. Only for a symmetric hopping amplitude the Hubbard Hamiltonian (5.12) exhibits particle-hole invariance.

Sign Transformation \mathcal{T}_2

This transformation is only defined on bipartite lattices and reads

$$\begin{aligned} \mathcal{T}_{2,\sigma} : \quad c_{l\sigma}^\dagger &\mapsto (-1)^l c_{l\sigma}^\dagger, \quad c_{l\sigma} \mapsto (-1)^l c_{l\sigma}, \\ \mathcal{T}_2 &:= \prod_{\sigma} \mathcal{T}_{2,\sigma}, \end{aligned} \quad (5.25)$$

with the definition (5.16) for $(-1)^l$. The local number operators $n_{l\sigma}$ are invariant,

$$\mathcal{T}_{2,\sigma}^\dagger n_{l\sigma} \mathcal{T}_{2,\sigma} = (-1)^l (-1)^l n_{l\sigma} = n_{l\sigma}, \quad (5.26)$$

which also implies invariance of the number operators N_σ and N as well as invariance of the double occupancy D .

As an application of \mathcal{T}_2 , we show in Sect. B.1 of appendix B that on bipartite lattices the sign of the hopping amplitude t may be chosen at will, if electron transfer is allowed between \mathcal{A} and \mathcal{B} lattice sites only.

5. Hubbard Model

Electron-Hole Transformation \mathcal{T}_3

The last electron-hole transformation to be discussed in this work is the mapping

$$\begin{aligned}\mathcal{T}_{3,\sigma} : c_{l\sigma}^\dagger &\mapsto (-1)^l c_{l\sigma}, & c_{l\sigma} &\mapsto (-1)^l c_{l\sigma}^\dagger, \\ \mathcal{T}_3 &:= \prod_{\sigma} \mathcal{T}_{3,\sigma},\end{aligned}\tag{5.27}$$

which is defined on bipartite lattices only. For symmetric hopping only between \mathcal{A} and \mathcal{B} sites, the kinetic energy T stays invariant under this transformation, since the additional factor (-1) compensates for the sign change which originates from the commutation of the two fermion operators,

$$\mathcal{T}_3^\dagger T \mathcal{T}_3 = \sum_{\substack{m,n \\ \sigma}} t_{m,n} \mathcal{T}_{3,\sigma}^\dagger c_{m\sigma}^\dagger \mathcal{T}_{3,\sigma} c_{n\sigma} \mathcal{T}_{3,\sigma}^\dagger c_{n\sigma} \mathcal{T}_{3,\sigma}\tag{5.28a}$$

$$= \sum_{\substack{m,n \\ \sigma}} t_{m,n} \underbrace{(-1)^m (-1)^n}_{=-1} c_{m\sigma} c_{n\sigma}^\dagger\tag{5.28b}$$

$$= \sum_{\substack{m,n \\ \sigma}} t_{m,n} (-1) (-1) c_{n\sigma}^\dagger c_{m\sigma}\tag{5.28c}$$

$$= \sum_{\substack{m,n \\ \sigma}} t_{n,m} c_{n\sigma}^\dagger c_{m\sigma} = T.\tag{5.28d}$$

The local number operators $n_{l\sigma}$ transform according to

$$\mathcal{T}_{3,\sigma}^\dagger n_{l\sigma} \mathcal{T}_{3,\sigma} = 1 - n_{l\sigma},\tag{5.29}$$

which implies that the interaction changes its sign,

$$\sum_l \mathcal{T}_{3,\sigma}^\dagger (n_{l\sigma} - 1/2) \mathcal{T}_{3,\sigma} (n_{l,-\sigma} - 1/2) = \sum_l (1 - n_{l\sigma} - 1/2) (n_{l,-\sigma} - 1/2)\tag{5.30a}$$

$$= - \sum_l (n_{l\sigma} - 1/2) (n_{l,-\sigma} - 1/2).\tag{5.30b}$$

In the present thesis we deal exclusively with the Hubbard model (5.12), which we from now on assume to be invariant under the particle-hole transformation \mathcal{T}_3 .

5.3. Limiting Cases

Since the Hubbard model poses a difficult many-body problem it is important for its understanding to discuss some limiting cases.

5.3.1. Band Limit

In the limit $U \rightarrow 0$ the Hubbard model (5.12) reduces to

$$H_{\text{TB}} = \sum_{\substack{i,j \\ \sigma}} t_{ij} c_{i\sigma}^\dagger c_{j\sigma}\tag{5.31}$$

which we recognize as the tight-binding model described in considerable detail in chapter 3. We note in passing that the tight-binding model and thus the Hubbard model in the band limit describe a metal in every dimension.

A Note on Names In many publications concerning the one-orbital Hubbard model, one customarily speaks of the *one-band* or *single-band* Hubbard model. However, as is pointed out in [29], the one-orbital model with one Wannier state for each lattice site may possess several electronic bands if the underlying lattice is non-Bravais. Only for Bravais lattices, the one-orbital models will always have exactly one energy band.

The kinetic part H_{TB} is diagonal in momentum space, whereas the interaction term is diagonal in position space. Since $[H_{\text{TB}}, D] \neq 0$ we find a nontrivial competition between both terms: It would be energetically favorable for D to minimize the number of double occupancies while the kinetic part de-localizes the electrons, thereby introducing a vast amount of charge fluctuations.

In the weak-coupling limit, the (single-particle) band aspects will dominate and the model might be tackled by means of perturbation theory: Starting from the Fermi gas one expands in U/W using the standard techniques of Feynman-Dyson perturbation theory [12], as has been done for example by [96]. In this approach the one-particle character of H_{TB} is of great importance for it allows the use of Wick's theorem [26].

5.3.2. Atomic Limit

When we set the hopping amplitude $t = 0$, we obtain the atomic limit of the Hubbard model, where the individual lattice sites are decoupled. When we introduce an on-site energy $t_{ii} = \varepsilon$ (we assume translational invariance), the Hamiltonian in the atomic limit can be written as

$$H_{\text{atomic}} = \sum_i H_i := \sum_i \{ \varepsilon(n_{i\uparrow} + n_{i\downarrow}) + U(n_{i\uparrow} - 1/2)(n_{i\downarrow} - 1/2) \}. \quad (5.32)$$

Energy Spectrum and its Peculiarities The energy spectrum of a single site is very simple. The empty atom has the energy $U/4$. The first electron on site i has an energy $\varepsilon - U/4$. Adding a second electron to that site we end up with the total site energy $2\varepsilon + U/4$. This can be visualized as the result of adding the second electron to the 'one-particle' energy level $\varepsilon + U/2$ as we have done in the case of the Anderson model in Sect. 4.3.1.

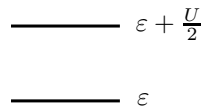


Figure 5.1.: 'Single-particle' spectrum of the Hubbard model in the atomic limit.

Note, however, that the level scheme given in figure 5.1 is fundamentally distinct from the single-electron spectra as they arise in band theory. In the latter case, the energy levels correspond to the eigenenergies of a single particle and we may distribute the available electrons freely to all levels. In particular, we may place the first electron at every level we desire. However, we cannot do this in the case of the spectrum given in figure 5.1, for it depends on the occupation numbers: The energy level $\varepsilon + U/2$ does not exist unless the Wannier orbital at the site under consideration is already occupied by one electron.

One-Particle Green Function and Spectral Function Equation (5.32) describes a two-particle Hamiltonian. Therefore, the concept of single-particle levels, as described by the density of states (A.22) of appendix A, does not work, and we have to use the techniques of many-particle theory to calculate the local spectral function (A.35) of appendix A,

$$D_{\sigma}(\omega) = -\frac{1}{\pi} \Im G_{\text{local},\sigma}^{\text{ret}}(\omega). \quad (5.33)$$

5. Hubbard Model

Note that we will always distinguish it from a single-particle density of states, as given in (A.22) of appendix A, by using the symbol $D(\omega)$. The one-particle Green function

$$G_{ij\sigma}^{\text{ret}}(t) = -i\Theta(t)\langle\{c_{i\sigma}(t), c_{j\sigma}^\dagger\}\rangle \quad (5.34)$$

is a purely local function in the atomic limit, because the different lattice sites are decoupled. In the Hubbard model, we have exactly four different configurations per site: the empty site, a site with a spin up or spin down, and a doubly occupied site. The Green function is therefore given by

$$G_{ij\sigma}^{\text{ret}}(t) = -i\delta_{ij}\Theta(t)\left[e^{-i(\varepsilon-\frac{U}{2})t}\langle 1 - n_{i,-\sigma}\rangle + e^{-i(\varepsilon+\frac{U}{2})t}\langle n_{i,-\sigma}\rangle\right], \quad (5.35)$$

which, after Fourier transforming, leads to

$$G_{\text{local},\sigma}^{\text{ret}}(\omega) = \lim_{\eta\searrow 0} \left[\frac{\langle 1 - n_{-\sigma}\rangle}{\omega - (\varepsilon - \frac{U}{2}) + i\eta} + \frac{\langle n_{-\sigma}\rangle}{\omega - (\varepsilon + \frac{U}{2}) + i\eta}\right]. \quad (5.36)$$

$\langle n_{\sigma}\rangle$ denotes the occupation of any lattice site of the translational invariant system.

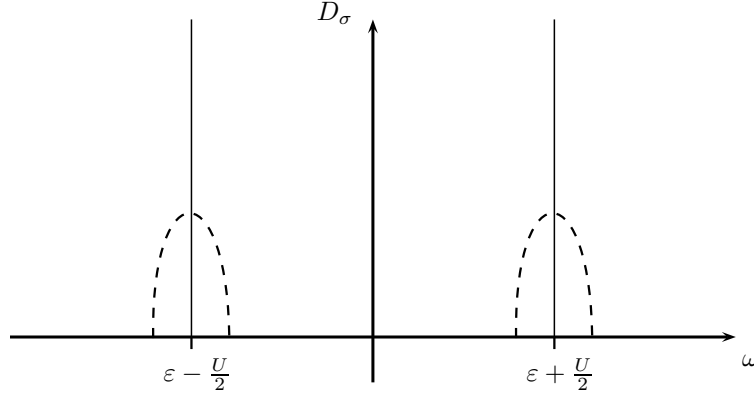


Figure 5.2.: The graphic shows the local spectral function of the Hubbard model in the atomic limit. The dashed curves sketch the situation in the limit $U \rightarrow \infty$ with finite hopping t , to be described in the next section.

As can be seen by means of figure 5.2, the density of states displays two peaks:

- one at the energy $\varepsilon - \frac{U}{2}$, corresponding to a process where one adds an electron to an empty site,
- one at the energy $\varepsilon + \frac{U}{2}$, if one adds an electron to an already singly occupied site.

The ground state of H_{atomic} is vastly degenerate. For $N \leq L$ electrons there are exactly $\binom{L}{N}$ ways to choose the singly occupied sites and every such site can hold an electron with spin up or spin down. The total ground state degeneracy $\#_G$ is therefore given by

$$\#_G = \binom{L}{N} 2^N. \quad (5.37)$$

Here, we note that this ground-state degeneracy of the atomic limit of the Hubbard model makes the analysis of the strong coupling limit, $t \ll U$, a very complicated quantum-mechanical problem.

Concerning the magnetic properties of the model, we may state that the system is paramagnetic as there is no communication between the lattice sites. Obviously, we need a finite electron transfer amplitude $t \neq 0$ or a non-zero range interaction to get an ordered ground state [29]. The lack of communication between the different lattice sites also shows that the atomic limit of the Hubbard model describes necessarily an insulator at all values of U in all dimensions.

5.3.3. Strong-Coupling Limit

The Hubbard model (5.12) consists of two parts: the kinetic part H_{TB} which is quantified in terms of the bandwidth W and an interaction part with coupling U . The case where $W \gg U$ is called *weak-coupling* regime, whereas $U \gg W$ denotes the *strong-coupling* limit. In this limit, we expect a broadening of the atomic levels into so-called Hubbard bands [84], as sketched in Fig. 5.2. The strong-coupling limit will be analyzed in detail in the present work.

In the strong-coupling regime the physics is controlled by the interaction, which suppresses the number of double occupancies. To describe the physics, a real-space picture should therefore be used and the atomic limit $t = 0$ should be used as a starting point for a perturbative treatment. Unfortunately, there exist a number of complications which make a straightforward approach practically impossible:

- The starting point for a straightforward perturbative expansion is the atomic Hamiltonian. Since it is a two-particle Hamiltonian, one cannot use Wick's theorem and an organized, diagrammatic formulation becomes extremely difficult [97–99].
- In the atomic limit, the ground-state degeneracy (5.37) is huge and becomes infinite in the thermodynamic limit. When a finite hopping $0 < t \ll U$ is switched on, the atomic levels will broaden into the Hubbard bands. The degeneracy is partly lifted, and more importantly, the electronic motion is constrained to avoid the creation of double occupancies. A simple application of degenerate perturbation theory, as for example described in [81] will not work because it requires the exact solution of an effective many-particle Hamiltonian. For the Hubbard model this is the t - J model which is not considerably simpler than the Hubbard model itself [100].

The t - J and Heisenberg Model As already stated above, a straightforward application of degenerate perturbation theory is not feasible. One possibility to find a systematic expansion in $t/U \ll 1$ is the use of canonical transformations.

The degenerate, leading-order eigenstates of D are mixed by the perturbation H_{TB} . If one knew the exact eigenstates one could rotate to the corresponding basis. Since an exact solution is normally not available, one proceeds iteratively and, as a first step, rotates the basis such that there is no mixing to $\mathcal{O}(t)$. Then, one proceeds by suppressing the mixing to second order and so on. A detailed presentation of such a procedure can be found in [101].

Another possibility is to project onto subspaces of the Hilbert space of the model, for example the subspace without double occupancy, and to allow only virtual creations of doubly occupied sites. We use such an approach in this work, as we will explain in detail in Part II and Part III of this thesis. For $U \gg W$ one can derive an effective Hamiltonian which is equivalent to the Hubbard model, so that

$$\langle \Psi | H_{\text{Hubbard}} | \Psi \rangle = \langle \Phi | H_{\text{eff}} | \Phi \rangle. \quad (5.38)$$

The state $|\Psi\rangle$ denotes the exact ground state of the Hubbard model, and $|\Phi\rangle$ gives the exact ground state of the effective model. In case of the Hubbard model, the exact ground-state will contain double occupancies even in the strong-coupling regime which, however, are more and more suppressed when U is increased. To obtain the Hamiltonian describing the physics at strong coupling, one starts by projecting onto the subspace without double occupancies. Within this subspace one then finds as effective Hamiltonian, the so-called t - J model [100],

$$H_{t-J} := -t \sum_{\langle i,j \rangle} \sum_{\sigma} (1 - n_{i,-\sigma}) c_{i\sigma}^{\dagger} c_{j\sigma} (1 - n_{j,-\sigma}) + J \sum_{\langle i,j \rangle} (\mathbf{S}_i \cdot \mathbf{S}_j - \frac{1}{4} n_i n_j) + \mathcal{O}\left(\frac{t^3}{U^2}, \frac{\delta t^2}{U}\right), \quad (5.39)$$

where $\delta = 1 - n$ measures the deviation from half band-filling. The first part of (5.39) is called the T -model and describes (correlated) hole motion in a nearly half-filled band. Except for one dimension, there exists no complete solution of this Hamiltonian [100]. The second part contains an anti-ferromagnetic, isotropic Heisenberg model with coupling $J = 4t^2/U$. Due to the condition $U \gg W$, the coupling

5. Hubbard Model

constant J is a small quantity when the model is considered as the strong-coupling limit of the Hubbard model.

Exactly at half band-filling the t - J model is reduced to a Heisenberg-type Hamiltonian [102]

$$H_J = J \sum_{\langle i,j \rangle} \mathbf{S}_i \cdot \mathbf{S}_j, \quad (5.40)$$

where $J = 4t^2/U$ and the term $n_i n_j$ in (5.39) is usually neglected for $n_i = 1$.

The appearance of the anti-ferromagnetic model can easily be understood in terms of second-order perturbation theory: When neighbouring spins are anti-parallel, a virtual hopping process creates an intermediate double occupancy of energy U , and a second virtual hopping brings the state back to the subspace without doubly occupied site. This process leads to an energy gain of $\mathcal{O}(-t^2/U)$. For a ferromagnetic alignment of the neighboring spins, such hopping processes are impossible due to Pauli blocking.

This clearly shows that the Hubbard model, at least in the limit $U \rightarrow \infty$ at half filling, is capable of describing the formation of magnetically ordered states. In this thesis, we will analyse the Hubbard model in its paramagnetic state, so we do not enlarge upon this topic. The reader may find an introduction in [2, 4].

5.4. Mott-Hubbard Transition

In the limit $U \rightarrow 0$ the Hubbard model reduces to the tight-binding model which, as has been shown in chapter 3, describes a metal. The density of states $\rho_\infty(\omega)$ on the Bethe lattice with $Z \rightarrow \infty$ is shown in figure 5.3b, see Sect. 3.3.2. It will be re-derived in Sect. 6.2.2. The gray shading indicates that we are considering the case of half band-filling. The electrons hop from one lattice site to the next and are therefore de-localized. A real-space snapshot at one instant of time might look like figure 5.3a.

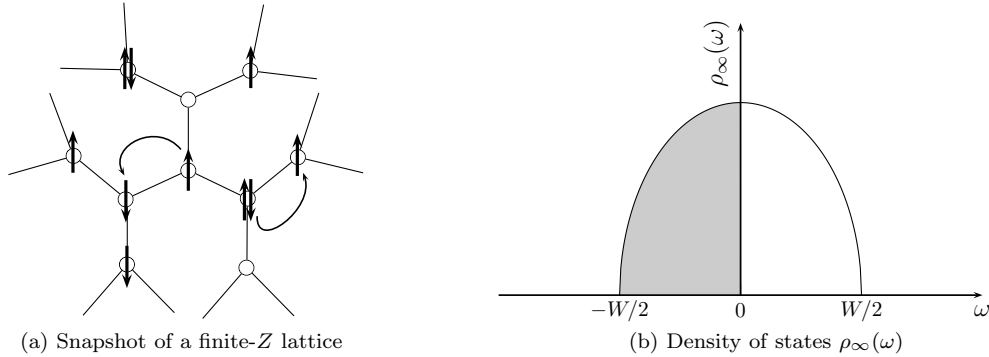


Figure 5.3.: Hubbard model in the metallic phase on the infinitely connected Bethe lattice.

As the ground state of the tight-binding model is a Slater determinant, the snapshot is likely to show massive charge fluctuations [29]: Since the probability that a site is occupied by a σ -electron is $1/2$, we will find on average 25% of the sites empty or doubly occupied and 50% singly occupied. Now imagine that we switch on the interaction U gradually. For every double occupancy, one has to pay the energy $U/2$. As long as $W \gg U$ the gain in kinetic energy will still be greater and the qualitative picture of figure 5.3a remains valid.

On the other hand, in the atomic limit $t = 0$, the density of states has the form depicted in figure 5.2. When we switch on a small but finite electron transfer amplitude t , every hopping process at half filling will lead to a double occupied site and therefore to the energy investment of $U/2$. For $0 < W \ll U$, such processes cannot occur and we necessarily find insulating behavior.

A snapshot of the insulating ground state on a finite- Z Bethe lattice is presented in figure 5.4a. The

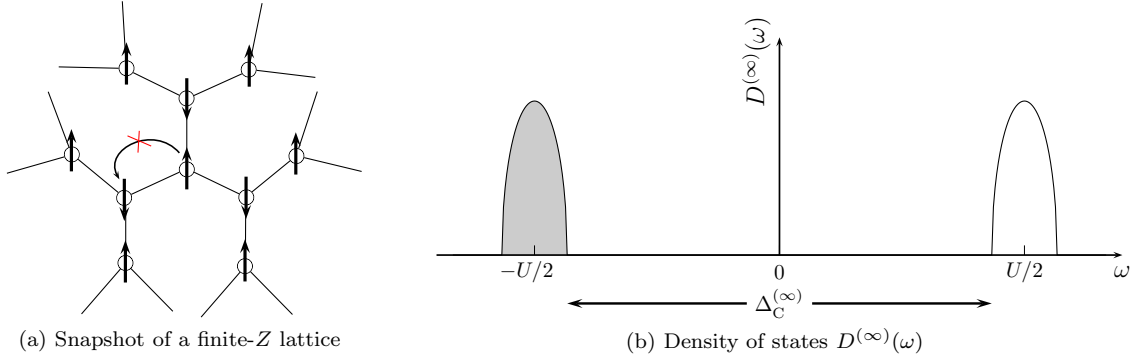


Figure 5.4.: Hubbard model at $0 < W \ll U \rightarrow \infty$ on the infinitely connected Bethe lattice.

density of states $D^{(\infty)}(\omega)$, as sketched in figure 5.4b, can qualitatively be understood as follows: By inserting an electron at half band-filling one has to pay the energy

$$\mu_{\text{UHB}}^+ := E_0(L+1) - E_0(L) = \mathcal{O}(U/2 - W_{\text{UHB}}/2). \quad (5.41)$$

The energy W_{UHB} denotes the bandwidth of the so-called upper Hubbard band (UHB) which is formed since the extra electron is mobile: After having introduced a doubly occupied site, this defect can propagate through the lattice.

Extracting in turn an electron from the system, one requires the energy (remember that we are working with the particle-hole symmetric model (5.12))

$$\mu_{\text{LHB}}^- := E_0(L) - E_0(L-1) = \mathcal{O}(-U/2 + W_{\text{LHB}}/2), \quad (5.42)$$

where W_{LHB} denotes the bandwidth of the band, formed by the mobile hole. We will call this band the lower Hubbard band (LHB). What has been said in Sect. 5.3.2 about the energy spectrum of the atomic limit, also applies for the lower and upper Hubbard bands. They do not represent allowed single-particle states as in the case of band theory. This band structure is occupation-number dependent because the upper band can only be present if the lower band is filled. Additionally, we note that on a lattice with L sites, there are $2L$ states in a single-particle band but the lower Hubbard band can only hold L electrons: Having more than L electrons, there must be at least one doubly occupied site.

We will therefore find an energy gap $\Delta_C(U)$ for single-particle charge excitations which is given by

$$\Delta_C(U) := \mu_{\text{UHB}}^+ - \mu_{\text{LHB}}^- = \mathcal{O}(U - (W_{\text{UHB}} + W_{\text{LHB}})/2) > 0. \quad (5.43)$$

When we increase t further, e.g. by applying pressure to increase the overlap of the orbitals at neighboring lattice sites, we increase the tendency of the electrons to de-localize. The bandwidths of the UHB and LHB should increase and their separation should shrink. There should therefore be a critical value $(W/U)_{\text{cr}}$, where both bands touch and the gap Δ_C vanishes. This indicates an insulator-to-metal transition. According to figure 5.4b the upper and lower Hubbard bands for $U \gg W$ are just shifted versions of the density of states $\rho_\infty(\omega)$ of the non-interacting case which indicates that the motion of the hole or the double occupancy in loops is free in the limit $U \rightarrow \infty$. This is special for Bethe lattices. Due to the tree structure of the lattice, every path contributing to the local, single-particle Green function is background-restoring because there is only one path between two (different) lattice sites. Thus, the loop motion for an additional particle or hole is free.

Part II.
Methods

Being asked to calculate the stability of a table, a theoretical physicist quickly produces the result for tables with one leg and with infinitely many legs. He spends the rest of his life in futile attempts to generalize the results for tables with arbitrary many legs.

A popular wisdom



Dynamical Mean-Field Theory

Theoretical investigations of many-body systems are very difficult. This holds true for classical as well as for quantum-mechanical models. While trying to solve these models, one faces profound technical difficulties, especially for dimensions $d = 2$ and $d = 3$ which are of fundamental importance for applications. These difficulties consist mainly of the complicated and involved particle dynamics and additionally of the complicated fermionic or spin algebra in the quantum-mechanical case. Most of the interesting theoretical models are unsolved up to today, i.e., we do not know whether they are exactly solvable or how such a solution might look like. Therefore, we have to resort to reliable and controllable *approximations*. In classical physics, one often uses the concept of so-called ‘mean-field theories’. These approximation schemes are usually constructed in spirit of the Weiss molecular field theory for the Ising model which is the prototypical example of a mean-field theory [103]. For the description of quantum-mechanical systems, there also exist so-called mean-field theories as Hartree-Fock (see Sect. 2.2.2), random-phase approximation (RPA) [12], operator decoupling schemes [86], or evaluations of path integrals with the method of steepest decent (saddle-point approximation) [11]. Such mean-field theories will not be covered in this thesis, as they are not mean-field theories in the spirit of statistical mechanics, which should give a reliable and global description of the model under consideration [100]. In this chapter we will have a look at the solution of the one-dimensional Ising model and compare this with the solution of the corresponding mean-field theory. For the construction of this mean-field theory we follow the method of Weiss and Bragg-Williams as described for example in [104]. This will serve as a descriptive example for the construction of such a theory. Next, we will introduce the limit of high spatial dimensions, $d \rightarrow \infty$, for quantum-mechanical models of itinerant electrons, following the pioneering work of [105]. This leads to fundamental simplifications in the theoretical description of such models with local interactions. We will summarize a particular colorful interpretation of these results, the so-called ‘local impurity self-consistent approximation’ of [106] which allows to describe the original lattice model in terms of a quantum-impurity model.

6.1. Ising Model

6.1.1. Free Energy in One Dimension

The Ising model is one of the best known models in statistical mechanics. From 1969 to 2002 about 12000 articles have been published on it or referring to it [104]. It has been originally introduced by Wilhelm Lenz and has been treated in a short paper by Ernst Ising in 1925 [107] who was a PhD student of Lenz at that time. For a short treatise of the model and the life of Ising see [104]. In one spatial dimension the model is described by the Hamiltonian

$$H = -J \sum_{i=1}^{N-1} \sigma_i \sigma_{i+1} - h \sum_{i=1}^N \sigma_i. \quad (6.1)$$

Here σ_i denotes an Ising spin, i.e., a classical, commutative variable which might take on two values, for example $+1$ and -1 , h denotes an external magnetic field and J is the coupling strength of the Ising

6. Dynamical Mean-Field Theory

spins. Assuming periodic boundary conditions, $\sigma_i = \sigma_{N+i}$, the model can be solved by the transfer matrix method, which is based on the observation [104, 108] that the canonical partition function of the Ising model,

$$Z_N = \sum_{\{\sigma\}} e^{-\beta H}, \quad (6.2)$$

might as well be represented as a matrix product of 2×2 matrices,

$$Z_N = \sum_{\{\sigma\}} T(\sigma_1, \sigma_2) T(\sigma_2, \sigma_3) \dots T(\sigma_N, \sigma_1). \quad (6.3)$$

The matrix elements $T(\sigma, \sigma')$ are defined by

$$T(\sigma, \sigma') = e^{\mathcal{J}\sigma\sigma' + \frac{1}{2}\mathcal{H}(\sigma+\sigma')} \quad (6.4)$$

which can be written in the local basis $\{|\sigma = +1\rangle, |\sigma = -1\rangle\}$ as

$$\mathfrak{T} = \begin{pmatrix} e^{\mathcal{J}+\mathcal{H}} & e^{-\mathcal{J}} \\ e^{-\mathcal{J}} & e^{\mathcal{J}-\mathcal{H}} \end{pmatrix}. \quad (6.5)$$

We have used $\mathcal{J} := \beta J$ and $\mathcal{H} := \beta h$ as abbreviations. The partition function is therefore given as the trace

$$Z_N = \text{Tr } \mathfrak{T}^N. \quad (6.6)$$

The two eigenvalues of this symmetric matrix are given by [104]

$$\lambda_{\pm} = e^{\mathcal{J}} \cosh(\mathcal{H}) \pm \sqrt{e^{2\mathcal{J}} \cosh^2(\mathcal{H}) - 2 \sinh(2\mathcal{J})}. \quad (6.7)$$

The free energy density f ,

$$f(\beta, h) = -\frac{1}{\beta N} \ln Z_N = -\frac{1}{\beta} \left(\ln \lambda_+ + \frac{1}{N} \ln \left[1 + \left(\frac{\lambda_-}{\lambda_+} \right)^N \right] \right), \quad (6.8)$$

reads in the thermodynamic limit, $N \rightarrow \infty$,

$$f(\beta, h) = -\frac{1}{\beta} \ln \left[e^{\mathcal{J}} \cosh(\mathcal{H}) + \sqrt{e^{2\mathcal{J}} \cosh^2(\mathcal{H}) - 2 \sinh(2\mathcal{J})} \right]. \quad (6.9)$$

Taking the negative derivative with respect to the external field h , the mean magnetization density m becomes

$$m = \langle \sigma \rangle = \frac{e^{\mathcal{J}} \sinh(\mathcal{H})}{\sqrt{e^{2\mathcal{J}} \cosh^2(\mathcal{H}) - 2 \sinh(2\mathcal{J})}}. \quad (6.10)$$

The magnetization density m is plotted against the external field h at various temperatures T in figure 6.1. For all finite temperatures, the magnetization is an analytic function of the external field and always vanishes at zero h . This means that the system does not possess a phase transition at any finite temperature. This result of the one-dimensional Ising model is quite generic for models in one spatial dimension with short-range interactions. In particular, quantum-mechanical systems are special in one spatial dimension because quasi-particle excitations as in Landau's Fermi-Liquid theory are not possible [109]. The one-dimensional Hubbard model is a particular important example because it does not show a phase transition at all finite values of U [93]. This should be kept in mind when discussing the results of the limit $d \rightarrow \infty$.

In the zero-temperature limit, $T \rightarrow 0$, the magnetization develops a discontinuity,

$$m = \begin{cases} 1 & \text{if } h > 0, \\ 0 & \text{if } h = 0, \\ -1 & \text{if } h < 0. \end{cases} \quad (6.11)$$

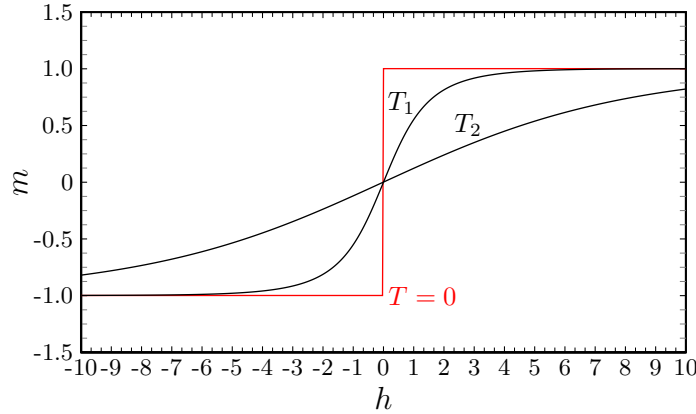


Figure 6.1.: The magnetization density (6.10) of the one-dimensional Ising model for various temperatures $T_1 < T_2$.

6.1.2. Mean-Field Theory of the Ising Model

The exact solution of the one-dimensional Ising model presented in the last section is one of the few examples for exact computations of interacting many-body problems. Especially in higher dimensions, such as $d = 2$ and $d = 3$, only very few models are solved exactly today. A particular important example is the two-dimensional Ising model without external magnetic field which has been solved for the first time by Lars Onsager [110]. The calculations in his work show that, in contrast to the one-dimensional case, the two-dimensional model forms a formidable mathematical problem. Therefore, for $d \geq 3$ dimensions, we have to rely on approximation methods. One such approximation scheme, already known before the solution of the one-dimensional Ising model, is the Weiss molecular field theory [103]. In the Ising model every spin interacts with an external magnetic field as well as with the (instantaneous) field of its neighboring spins. This latter field is a dynamical quantity which changes with every fluctuation of the spin configuration. The mean-field approximation now consists of replacing this instantaneous field by its thermal average. This replacement essentially introduces an interaction among *all* spins in the system. The resulting Hamiltonian therefore becomes exact in the (not so interesting) limit of an interaction with an infinite range and in the limit of infinite spatial dimension $d \rightarrow \infty$ [111, 112].

We consider the Ising Hamiltonian on a d -dimensional lattice with N spins,

$$H = -\frac{J}{2} \sum_{\langle i,j \rangle} \sigma_i \sigma_j - h \sum_i \sigma_i, \quad (6.12)$$

where the first sum extends over all nearest-neighbor pairs. The magnetization density m is again defined by

$$m = \frac{1}{N} \left\langle \sum_{i=1}^N \sigma_i \right\rangle, \quad (6.13)$$

where we assumed translational invariance. The product $\sigma_i \sigma_j$ can be written as

$$\sigma_i \sigma_j = (\sigma_i - m + m)(\sigma_j - m + m) \quad (6.14a)$$

$$= m^2 + m(\sigma_i - m) + m(\sigma_j - m) + (\sigma_i - m)(\sigma_j - m). \quad (6.14b)$$

The mean field approximation consist of neglecting the last term of (6.14b), also printed in red: All correlated fluctuations of spins at sites with index i and j are completely neglected.

Applying the mean-field decoupling (6.14b) to the Ising Hamiltonian we obtain

$$H \approx -\frac{J}{2} \sum_{\langle i,j \rangle} (-m^2 + m(\sigma_i + \sigma_j)) - h \sum_i \sigma_i. \quad (6.15)$$

6. Dynamical Mean-Field Theory

If we assume that the lattice has a coordination number Z , we may define

$$H^{\text{MF}} := \frac{1}{2}NJZm^2 - (JZm + h) \sum_i \sigma_i. \quad (6.16)$$

The mean field Hamiltonian H^{MF} describes a system of non-interacting spins σ_i in an external field $(JZm + h)$, the first part of which describes the mean field of all neighboring spins.

Though the Hamiltonian (6.16) describes a single-particle problem, we have to remember that the magnetization density m is a quantity to be determined from the equilibrium state of the system. We therefore need a *self-consistency* equation to fix the value of m . Since all spins are decoupled in H^{MF} , the calculation of the partition function is easy for a translational invariant system,

$$Z_N^{\text{MF}} = \sum_{\{\sigma\}} e^{-\beta H^{\text{MF}}} \quad (6.17a)$$

$$= e^{-\frac{1}{2}JNZm^2} \left(\sum_{\sigma=\pm} e^{(\beta JZm + \beta h)\sigma} \right)^N \quad (6.17b)$$

$$= e^{-\frac{1}{2}JNZm^2} (2 \cosh(\beta JZm + \beta h))^N. \quad (6.17c)$$

The free energy density f is therefore given by

$$f^{\text{MF}}(\beta, h) = -\frac{1}{\beta N} \ln Z_N^{\text{MF}} = \frac{1}{2}JZm^2 - \frac{1}{\beta} \ln (2 \cosh(\beta JZm + \beta h)). \quad (6.18)$$

The magnetization density can be obtained by taking the negative derivative of the free energy density with the external field and becomes

$$m = \tanh(\beta JZm + \beta h). \quad (6.19)$$

Equation (6.19) is the desired self-consistency condition for this mean-field theory. The equation can be solved numerically or graphically. To see whether there is spontaneous magnetization, i.e. $m \neq 0$ for $h \rightarrow 0$, we have plotted in figure 6.2 the straight line m and $\tanh(\beta JZm)$ for various temperatures. The value of JZ is finite.

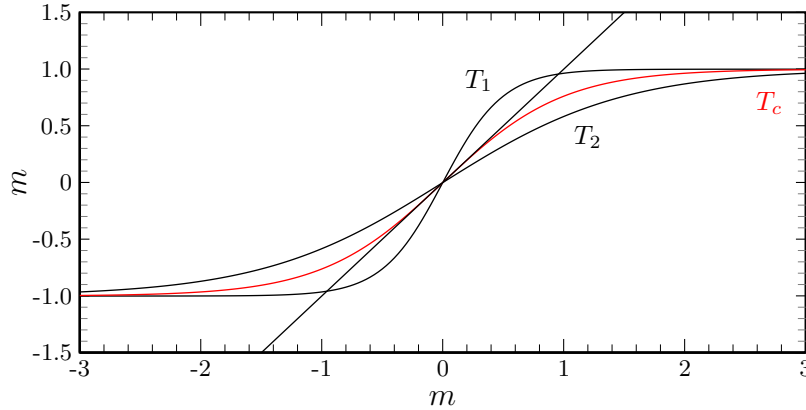


Figure 6.2.: The magnetization density $\tanh(\beta JZm)$ for various temperatures $T_1 < T_c < T_2$.

The value $m = 0$ is always a solution. But contrary to the result in one dimension, we find two solutions m^* and $-m^*$ provided the derivative of $\tanh(\beta JZm)$ at the origin is larger than unity. This analysis shows that the mean-field approximation predicts a phase transition from a disordered to an ordered phase at the critical temperature

$$T_c = JZ. \quad (6.20)$$

6.1.3. Limits of High Dimensions and Large Coordination Number

As we have pointed out in the beginning of Sect. 6.1.2, the mean-field approximation becomes exact in the limit of infinite spatial dimensions or, equivalently, in the limit where the coordination number Z diverges. Equation (6.20) shows that in the limit $Z \rightarrow \infty$ the critical temperature diverges. This is a consequence of the infinite number of mutually interacting nearest-neighbor spins in this limit. To get rid of this undesirable feature and to obtain meaningful results, we have to rescale the coupling J as

$$J \rightarrow \frac{\tilde{J}}{Z}, \quad \tilde{J} = \text{const.} \quad (6.21)$$

We note that this scaling is typical for localized spin models with isotropic coupling such that the spatial average over all couplings is finite. This holds true for classical as well as quantum-mechanical models [2, 41].

When one considers any regular lattice, one finds one important classification key, the *coordination number* Z , i.e., the number of nearest neighbors of every lattice site. On the other hand, one is accustomed to the somewhat abstract number of dimensions d which stems from the embedding of the lattice into the euclidean space (\mathbb{R}^d, \cdot) . Baxter [46] proposed a possibility to join the two terms: Consider a regular lattice and let $m_1 := Z$ denote the number of nearest neighbors per site, m_2 the number of next-nearest neighbor and so on. Then,

$$c_n := 1 + \sum_{i=1}^n m_i \quad (6.22)$$

is the number of sites within a topological distance $d = n$, see definition (3.3.6). In the case of the hypercubic lattices in d -dimensional euclidean space he shows further [46] that

$$\lim_{n \rightarrow \infty} \frac{\ln c_n}{\ln n} = d, \quad (6.23)$$

and claims that the relation is also valid for all regular two- and three-dimensional (Bravais) lattices. Applied to the Bethe lattice with Z nearest neighbors per site one finds, see (3.48),

$$\lim_{n \rightarrow \infty} \frac{\ln c_n}{\ln n} = \lim_{n \rightarrow \infty} \frac{\ln \frac{Z-2+Z[(Z-1)^n-1]}{(Z-2)}}{\ln n} = \begin{cases} 1 & \text{for } Z = 2, \\ \infty & \text{for } Z \geq 3. \end{cases} \quad (6.24)$$

Thus, the special case $Z = 2$ behaves again as expected but all Bethe lattices with $Z \geq 3$ have dimensionality $d = \infty$. This behavior shows again that the Bethe lattice is not comparable to Bravais lattices. It also indicates that the abstract quantity d as defined in (6.23) is not very helpful for classifying Bethe lattices.

When we look at Bravais lattices in three dimensions, $d = 3$, we find that a simple cubic lattice has $Z = 6$, a body-centered cubic lattice has $Z = 8$, and a face-centered cubic lattice even has $Z = 12$. Therefore, we may say that the dimensionality of a lattice can be directly described by the number Z of nearest neighbors of its sites [41]. Since a number of nearest neighbors of the order $\mathcal{O}(10)$ is already quite large, it seems to be a natural approach to start investigating the problem defined on such a lattice in the limit $Z \rightarrow \infty$ which we will call henceforth the limit of infinite dimensions. Later one may wish to use the small ratio $1/Z$ as an expansion parameter to calculate corrections for the problem (approximately) solved in $Z \rightarrow \infty$.

As we will only deal with hypercubic lattices where $Z = 2d$ and Bethe lattices which are classified according to Z , we will use the notions infinite dimensions d and infinite coordination number Z interchangeably in this thesis.

6.2. Limit of Infinite Dimensions for Itinerant Electron Systems

As we have seen in Sect. 6.1, the mathematical treatment of a classical system of interacting spins becomes simple in the limit of infinite dimensions while the physics it describes remains sensible. It therefore seems natural to ask whether a similar treatment of a quantum-mechanical model of interacting and itinerant electrons is possible and leads to non-trivial insights. As in models of itinerant electrons, the lattice structure plays an important role for such quantities as the density of states, we expect the influence of the lattice on the physics to remain in the limit $d \rightarrow \infty$. We therefore discuss the case of hypercubic and Bethe lattices separately.

6.2.1. Hypercubic Lattices

The dispersion relation of the tight-binding model on hypercubic lattices in d dimensions, (3.33), is given by

$$\epsilon(\mathbf{k}) = -2t \sum_{i=1}^d \cos(k_i), \quad \text{with } -\pi < k_i \leq \pi \text{ for all } i, \quad (6.25)$$

which shows that the band edges in every dimension are lying at $\pm 2td$. In other words, the kinetic energy would diverge in the limit $d \rightarrow \infty$. As the local Hubbard interaction is independent of dimension, the Hubbard model would be reduced to a trivial tight-binding model. To obtain non-trivial physics one has to scale the hopping amplitude t properly. Choosing the seemingly obvious scaling $t \rightarrow \tilde{t}/d$, does not lead to a sensible result as we will show below. The proper scaling

$$t \rightarrow \frac{\tilde{t}}{\sqrt{2d}} \quad (6.26)$$

has been obtained for the first time by Zaitsev and Dushenat in [113]. More systematic investigations of the scaling and its consequences started with the work of Metzner and Vollhardt in [105]. The following summary follows the derivation given in [42].

The density of states

$$\rho_{d\sigma}(\omega) = \frac{1}{L} \sum_{\mathbf{k}} \delta(\omega - \epsilon(\mathbf{k})) \quad (6.27)$$

can be written by expressing the delta distribution by its Fourier transform

$$\rho_{d\sigma}(\omega) = \frac{1}{2\pi} \prod_{i=1}^d \int_{-\pi}^{\pi} \frac{dk_i}{2\pi} \int_{-\infty}^{\infty} dx e^{ix(\omega - \epsilon(\mathbf{k}))} \quad (6.28a)$$

$$= \frac{1}{2\pi} \int_{-\infty}^{\infty} dx e^{i\omega x} (J_0(2xt))^d, \quad (6.28b)$$

with the zero-order Bessel function [37]

$$J_0(x) = \frac{1}{2\pi} \int_{-\pi}^{\pi} e^{ix \cos(k)} dk. \quad (6.29)$$

Note that the additivity of the kinetic energy is vital for the factorization. For $d \gg 1$, the main contribution to the integral comes from the first maximum of the Bessel function at the origin. Expanding the Bessel function according to $J_0(x) = 1 - x^2/4 + x^4/64 + \mathcal{O}(x^5)$ leads to

$$\rho_{d\sigma}(\omega) = \frac{1}{2\pi} \int_{-\infty}^{\infty} dx e^{i\omega x} \left(1 - (xt)^2 + \frac{(xt)^4}{4} + \mathcal{O}(x^5)\right)^d \quad (6.30a)$$

$$= \frac{1}{2\pi} \int_{-\infty}^{\infty} dx e^{i\omega x} e^{-\frac{(xt)^2}{2} - \frac{(xt)^4}{16d} + \mathcal{O}(x^5, d^{-2})} \quad (6.30b)$$

$$= \frac{1}{\sqrt{2\pi t^2}} e^{-\frac{\omega^2}{2t^2} - \frac{1}{16d} \left(\frac{\omega^4}{t^4} - \frac{6\omega^2}{t^2} + 3\right) + \mathcal{O}(d^{-2})}. \quad (6.30c)$$

6.2. Limit of Infinite Dimensions for Itinerant Electron Systems

Note that the scaling (6.26) is necessary because, otherwise, the density of states would either vanish exponentially (for $t \rightarrow \tilde{t}/Z$) or simply diverge. In the limit of infinite dimensions with the scaling (6.26) we obtain the density of states

$$\rho_{\infty\sigma}(\omega) = \frac{1}{\sqrt{2\pi\tilde{t}^2}} e^{-\frac{\omega^2}{2\tilde{t}^2}}, \quad (6.31)$$

which is Gaussian. Note that the smoothness of the density of states comes from the total neglect of the van-Hove singularities which result from the other maxima of J_0 and which give corrections of $\mathcal{O}(e^{-d})$ [42]. In figure 6.3 we show a comparison of the density of states for various d and the result (6.31).

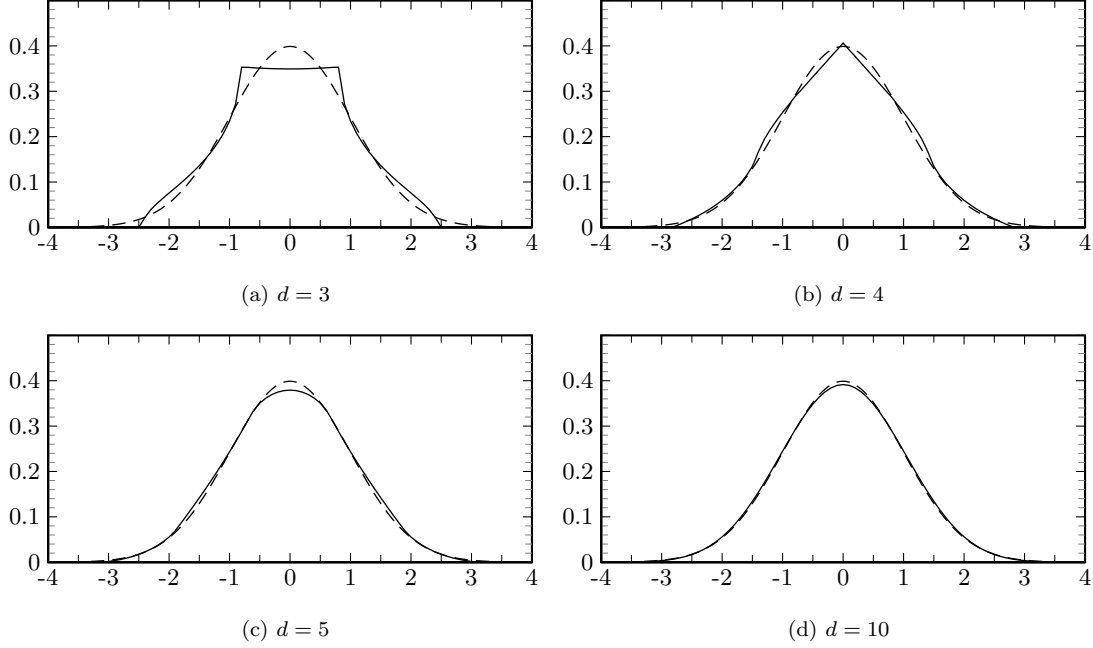


Figure 6.3.: The density of states $\rho_d(\omega)$, (3.42), has been scaled according to (6.26). The energy ω is measured in units of \tilde{t} . The dashed line represents the result (6.31) for $d \rightarrow \infty$.

One can see that the infinite- d result is approached rather quickly. Even the three-dimensional case deviates from (6.31) on average by only 10% [42]. The energy variable ω in (6.31) is unbounded due to special \mathbf{k} -values whose kinetic energy diverges $\propto \sqrt{d}$. One may define a bandwidth W through the second moment of the density [2],

$$W^2 = 16 \int \omega^2 \rho_{\infty\sigma}(\omega) d\omega. \quad (6.32)$$

To avoid problems with the exponential tails in the density of states, one wishes to perform calculations with a density of states with bounded support. One such possibility is the density of states on a Bethe lattice with an infinite number of nearest neighbors.

6.2.2. Bethe Lattices

As detailed in section 3.3.2, the local Green function $G_{\text{local},Z}(z)$, (3.61), on a Bethe lattice with Z nearest neighbors reads

$$G_{\text{local},Z}(z) = \frac{2(Z-1)}{(Z-2)z + Z\sqrt{z^2 - 4(Z-1)t^2}}, \quad (6.33)$$

6. Dynamical Mean-Field Theory

and leads to the density of states, (3.63),

$$\rho_Z(\omega) = \frac{Z\sqrt{4(Z-1)t^2 - \omega^2}}{2\pi(Z^2t^2 - \omega^2)}\Theta(4(Z-1)t^2 - \omega^2). \quad (6.34)$$

We use the scaling (6.26) and note that for hypercubic lattices in d dimensions the quantity $2d$ gives the number of nearest neighbors Z , so that we obtain

$$G_\infty(z) := \lim_{Z \rightarrow \infty} G_{\text{local},Z}(z) = \frac{2}{z + \sqrt{z^2 - 4\tilde{t}^2}} = \frac{1}{2\tilde{t}^2}(z - \sqrt{z^2 - 4\tilde{t}^2}) \quad (6.35)$$

and

$$\rho_\infty(\omega) := \lim_{Z \rightarrow \infty} \rho_Z(\omega) = \frac{1}{2\pi\tilde{t}^2}\sqrt{4\tilde{t}^2 - \omega^2}\Theta(4\tilde{t}^2 - \omega^2). \quad (6.36)$$

Note that (6.36) does as well follow from (A.35), if we insert (6.35). We express it in units of the bandwidth $W = 4\tilde{t}$ as

$$\rho_\infty(\omega) = \frac{4}{\pi W}\sqrt{1 - \left(\frac{2\omega}{W}\right)^2}\Theta(W^2/4 - \omega^2). \quad (6.37)$$

This density of states has compact support and a semi-elliptic shape. At its band-edges, the density of states (6.37) displays a typical three-dimensional behavior and is therefore a common model for such systems [32]. Note that Hubbard used the density of states (6.37) in his ‘Hubbard III’ approximation [85] which is why it is also called ‘Hubbard semi-ellipse’. We will use (6.37) as our density of band-states in this thesis.

6.2.3. Simplifications

We summarize some of the consequences of the scaling (6.26) and the limit of infinite dimensions which are important for this work.

The most important consequence of the scaling (6.26) is the spatial dependence of the single-particle Green function of the non-interacting model, which behaves as [2]

$$G_{ij}^{(0)} \xrightarrow{d \rightarrow \infty} \mathcal{O}(d^{-d(i,j)/2}). \quad (6.38)$$

Note, however, this does not imply that the particles are localized in the limit $d \rightarrow \infty$ as can be seen from a diagrammatic expansion. Here, one has to sum over all inner vertices of the self-energy which compensates partly for the decay of the non-interacting Green function [2]. As a result, the proper self-energy becomes local with corrections in $1/d$,

$$\Sigma_\sigma(\mathbf{R}, \mathbf{R}'; \omega) = \Sigma_\sigma(\mathbf{R}, \mathbf{R}; \omega)\delta_{\mathbf{R}, \mathbf{R}'} + \mathcal{O}(\sqrt{1/d}) \text{ as } d \rightarrow \infty. \quad (6.39)$$

This does unfortunately not imply that all vertices in the self-energy coincide: A complicated many-body problem still remains.

However, all vertices in the *skeleton* expansion of the self-energy are indeed identical, a property which is otherwise found in problems where the interaction is limited to one site such as in the Single Impurity Anderson Model (SIAM), see chapter 4. More precisely, we may state that the skeleton expansion of the infinite dimensional Hubbard model and that of the SIAM are identical [2].

The Fourier transform of the self-energy of the infinite-dimensional Hubbard model becomes independent of momentum,

$$\lim_{d \rightarrow \infty} \Sigma^*(\mathbf{k}, \omega) = \Sigma_\sigma^*(\omega). \quad (6.40)$$

One interesting consequence of the momentum independence of the self-energy is that, additionally to Luttinger’s theorem [114] which states that the volume within the Fermi surface is unaffected by the interaction, the shape of the Fermi surface is not altered by the interaction in the infinite-dimensional Hubbard model [96]. Note, however, that the whole concept of a $d - 1$ dimensional Fermi surface becomes questionable in $d \rightarrow \infty$ dimensions.

6.2.4. Remarks on the Correct Scaling

As we have pointed out, the scaling $t \rightarrow \tilde{t}/\sqrt{Z}$ is the only possibility for obtaining a Hubbard-type model with an infinite number of nearest neighbors such that there is a non-trivial competition between the kinetic and interaction part of the Hamiltonian [105]. Interactions beyond the on-site contribution such as the nearest-neighbor interaction

$$H_{\text{NN}} = \sum_{\langle i,j \rangle} V_{\sigma\sigma'} n_{i\sigma} n_{j\sigma'}, \quad (6.41)$$

have to be scaled according to the classical ‘spin-scaling’ $V \mapsto \tilde{V}/Z$. This implies [2, 41] that all terms in a diagrammatic perturbation theory except for the Hartree-terms vanish in infinite dimensions. One can therefore say that the Hubbard interaction is unique, as it is the only interaction in fermionic lattice models which shows correlation effects in the limit of infinite dimensions [42].

Another interesting remark is, that the scaling $t \mapsto \tilde{t}/\sqrt{Z}$ can also be inferred from the classical scaling $J \mapsto \tilde{J}/Z$ of spin models such as the Heisenberg model, since the Hubbard model maps to the Heisenberg model at half band-filling and $U \rightarrow \infty$ with coupling constant $J \propto t^2$, see (5.40). Though this is not a rigorous proof, it shows the consistency of the approaches. It should also be noted that the scaling $t \mapsto \tilde{t}/\sqrt{Z}$ can (a posteriori) be deduced from the bandwidth of the tight-binding model on the Bethe lattice (3.65) which was not possible for the hypercubic lattice.

6.3. Self-Consistency Equations of the Dynamical Mean-Field Theory

As has been discussed in Sect. 6.2.3, the proper self-energy of the Hubbard model in infinite dimensions is diagonal in position space. In this respect it corresponds to an impurity model, where the interaction between the electrons is limited to a single site. The idea for proceeding is therefore to construct an *effective* quantum impurity model which describes the same physics as the infinite-dimensional Hubbard model. This idea is visualized in figure 6.4.

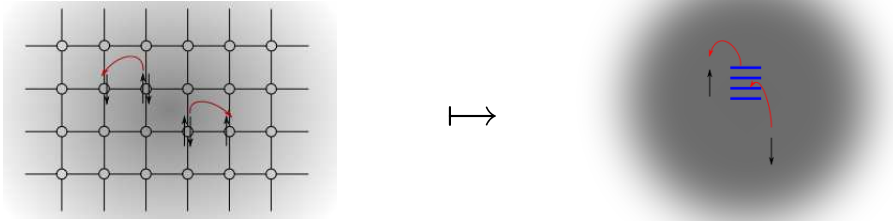


Figure 6.4.: Mapping of the lattice model with on-site interactions to an effective quantum impurity model.

This approach underlies the so-called Dynamical Mean-Field Theory (DMFT) [106, 115–118]. It is a mean-field theory in the sense of the Weiss molecular field theory [41] in which the static Weiss molecular field ($JZm + h$) is replaced by a local, frequency dependent, i.e., dynamic Green function of non-interacting electrons of an electron-bath. There are a lot of possibilities to derive and formulate the self-consistency equations of DMFT: In [117, 118] a derivation with the help of generating functionals analogously to the coherent potential approximation is presented (see also [41]); a perturbative derivation starting from the non-interacting Fermi gas is given in [119, 120]; the review [106] shows a derivation using an effective action in analogy to the ‘cavity’ method in classical statistical mechanics.

6. Dynamical Mean-Field Theory

The formulation in which the single-site problem is formulated as an effective SIAM is a notably colorful representation. In figure 6.4 we have drawn the impurity with a few levels. Such an impurity model is required if the lattice model is a multi-orbital Hubbard model. In this thesis we exclusively work with the one-orbital Hubbard model and therefore consider the one-orbital SIAM only.

6.3.1. Self-Consistency in the Paramagnetic Case

In the following, we limit ourselves to the paramagnetic case as it is the only case to be considered in this thesis. We will therefore drop spin indices wherever possible.

Let us assume that we know the interacting Green function $G_{\text{SIAM}}(\omega)$ of the SIAM (4.6) for a given (arbitrary) hybridization function (4.19). In a diagrammatic expansion in the interaction U of this Green function we find the same diagrams as for the local Green function G_{Hubbard} in the case of the infinite-dimensional Hubbard model. Therefore, our first self-consistency equation is

$$G_{\text{SIAM}}(\omega) = G_{\text{Hubbard}}(\omega). \quad (6.42a)$$

Since the skeleton diagrams of the local self-energy are identical for both models and (6.42a) is assumed to hold, we also have to demand that

$$\Sigma_{\text{SIAM}}^*(\omega) = \Sigma_{\text{Hubbard}}^*(\omega) \quad (6.42b)$$

which therefore serves as the second part of the self-consistency.

Equations (6.42a) and (6.42b) are the self-consistency equations which have to be fulfilled for the mapping of the infinite-dimensional Hubbard model onto the effective SIAM to work. The usual self-consistency cycle as for example described in [2, 106] and which is used in numerical studies will not be necessary for this thesis, so we do not go into further detail. Since we will work on a Bethe lattice with infinite connectivity, the self-consistency equation can be simplified considerably. We discuss it next.

6.3.2. Self-Consistency on the Infinitely Connected Bethe Lattice

The local Green function of the Hubbard model as the momentum average of the \mathbf{k} -resolved Green function, see (A.28) of appendix A, can be written as the following transform of the non-interacting density of states $\rho(\omega)$,

$$G_{\text{Hubbard}}(\omega) = \int_{-\infty}^{\infty} d\omega' \frac{\rho(\omega')}{\omega - \omega' - \Sigma^*(\omega)}. \quad (6.43)$$

The density of states of the non-interacting system is the only reference to the actual lattice structure. Note that due to the momentum independence of the self-energy, the interacting Green function can be expressed through the non-interacting one by

$$G_{\text{Hubbard}}(\omega) = G_{\text{Hubbard}}^{(0)}(\omega - \Sigma^*(\omega)). \quad (6.44)$$

For the Bethe lattice with $Z \rightarrow \infty$ we work with the density of states given in (6.37). The integral (6.43) can then be solved analytically, as we show in Sect. A.4 of appendix A, to give

$$G_{\text{Hubbard}}^{(0)}(z) = \frac{1}{2\tilde{t}^2} (z - \sqrt{z^2 - 4\tilde{t}^2}), \quad z \in \mathbb{C} \quad (6.45)$$

which is of course the non-interacting Green function of the tight-binding model on the infinitely connected Bethe lattice, (6.35). Substituting z in (6.45) by $s := \omega - \Sigma^*(\omega)$ and keeping in mind (6.44), we can solve (6.45) for s to obtain

$$s = \tilde{t}^2 G_{\text{Hubbard}}^{(0)}(s) + 1/G_{\text{Hubbard}}^{(0)}(s) \quad (6.46)$$

which means that

$$\Sigma_{\text{Hubbard}}^*(\omega) = \omega - \tilde{t}^2 G_{\text{Hubbard}}(\omega) - 1/G_{\text{Hubbard}}(\omega). \quad (6.47)$$

With the Green function of the SIAM (4.28) we can therefore write

$$G_{\text{Hubbard}}(\omega) = G_{\text{SIAM}}(\omega) = (\omega - \Delta(\omega) - \Sigma_{\text{SIAM}}^*(\omega))^{-1} \quad (6.48a)$$

$$= (\omega - \Delta(\omega) - \Sigma_{\text{Hubbard}}^*(\omega))^{-1}. \quad (6.48b)$$

The first equality stems from (6.42a) whereas the third equality is a consequence of (6.42b). Inserting (6.47) into (6.48b), we finally obtain the self-consistency condition on an infinitely connected Bethe lattice which reads

$$\tilde{t}^2 G_{\sigma}(\omega) = \Delta(\omega). \quad (6.49)$$

In this last equation we have included the spin index explicitly. The Green function $G_{\sigma}(\omega)$ is either the Green function of the SIAM or of the Hubbard model as they have to be identical according to (6.42a). Though the equations look rather innocent, they pose a formidable problem: In order to achieve self-consistency, one has to solve the SIAM with an arbitrary hybridization function. Thus far no such solution has been obtained. Only for a very limited number of special hybridization functions, an exact solution of the SIAM is known by means of the Bethe ansatz [80]. Since an exact solution is not available one has to proceed by means of perturbation theory or numerically. In this thesis we propose a perturbative way to solve the self-consistency equations in the limit of strong coupling.

6.4. Summary

The Weiss molecular field theory is a common approximation in classical statistical mechanics. It describes interacting spins, using a single-particle approach, the parameters of which have to be found via a self-consistency condition. Dynamical-Mean Field Theory (DMFT) uses and expands the concepts of the Weiss mean-field theory, so that they can be applied to quantum-mechanical problems of itinerant, locally interacting electrons.

As the Weiss theory becomes exact in the limit of infinite spatial dimensions, DMFT allows us to exactly formulate the infinite-dimensional Hubbard model, which is defined on a *lattice* with an infinite coordination number, in terms of a quantum impurity model. In this work we choose the Single Impurity Anderson model (SIAM). The impurity model, though still a complicated many-particle problem, is considerably easier to tackle: All temporal correlations of the lattice model are preserved but all spatial fluctuations are absent.

Unfortunately, it does not suffice to find a solution of the impurity model for special values of its parameters, but we need to solve it for arbitrary parameters. In order for the SIAM to describe the same physics as the infinite-dimensional, lattice Hubbard model, the variables of the SIAM have to be fixed self-consistently. On the Bethe lattice with infinite connectivity this is done by means of the self-consistency equation

$$\tilde{t}^2 G_{\sigma}(\omega) = \Delta(\omega). \quad (6.50)$$

In the thirties, under the demoralizing influence of quantum-theoretic perturbation theory, the mathematics required of a theoretical physicist was reduced to a rudimentary knowledge of the Latin and Greek alphabets.

Res Jost

7

Kato Perturbation Theory

In this chapter we give a summary of the foundations of the perturbation theory we will use in this work. The method has been formulated by Kato [121]. Contrary to the well known Rayleigh-Schrödinger perturbation theory, Kato's method is based on projections onto subspaces of the Hilbert space under consideration. This proves to be a major advantage in the case of degenerate spectra.

In the subsequent sections we follow [122]. A readable introduction into the method can also be found in [81]. The reader who does not wish to follow the derivation in detail can forward to Sect. 7.5 on page 71 in which we summarize the results.

7.1. Basic Definitions

Resolvent

Definition 7.1.1. Let H denote a Hamiltonian operator with spectrum $\sigma(H)$ and let $z \in \mathbb{C} \setminus \sigma(H)$. The quantity

$$R(z) := (z - H)^{-1} \equiv \frac{1}{z - H} \quad (7.1)$$

will be called the resolvent (operator) of H .

In this thesis we will assume the spectrum of H to be purely discrete, as is the case for finite lattices. Since H is a self-adjoint operator, its eigenvalues lie on the real axis. Let $E_i, i \in \mathbb{N}$ denote the eigenvalues of H and let $P_i, i \in \mathbb{N}$ denote the projection operators onto the corresponding eigenspaces,

$$HP_i = E_i P_i. \quad (7.2)$$

Another consequence of the self-adjointness of the Hamiltonian is the orthogonality condition

$$P_i P_j = P_i \delta_{ij}, \quad i, j \in \mathbb{N}, \quad (7.3)$$

where δ_{ij} denotes the Kronecker delta. Since we assume the spectrum of H to be purely discrete, we find the following decomposition of unity (closure relation),

$$\mathbb{1} = \sum_{i \in \mathbb{N}} P_i. \quad (7.4)$$

It follows that

$$R(z)P_i = P_i(z - E_i)^{-1} \equiv \frac{P_i}{z - E_i}, \quad i \in \mathbb{N}, \quad (7.5)$$

and we may write

$$R(z) = R(z)\mathbb{1} = R(z) \sum_{i \in \mathbb{N}} P_i = \sum_{i \in \mathbb{N}} \frac{P_i}{z - E_i}. \quad (7.6)$$

From this equation we may deduce the following lemma.

7. Kato Perturbation Theory

Lemma 7.1.1. *Every discrete eigenvalue of H is a simple pole of $R(z)$ (and vice versa) and the residue at each pole is the projection operator onto the corresponding eigenspace,*

$$R(z) = \sum_{i \in \mathbb{N}} \frac{P_i}{z - E_i}, \quad (7.7a)$$

$$P_i = \operatorname{Res}_{z \rightarrow E_i} R(z), \quad i \in \mathbb{N}. \quad (7.7b)$$

Resolvent and Projection Operators

Definition 7.1.2. Let γ_i denote that closed path in the complex z -plane which encloses the pole at $z = E_i$ but no other singularity of $R(z)$.

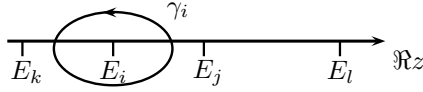


Figure 7.1.: Path γ_i of definition 7.1.2.

From this definition it immediately follows that the projection operator P_i can be written as a contour integral along the path γ_i ,

$$P_i = \frac{1}{2\pi i} \oint_{\gamma_i} R(z) dz. \quad (7.8)$$

Since the projectors are mutually orthogonal every $\sum_{i \in M} P_i$, $M \subset \mathbb{N}$ will be a projection operator.

General Projection Properties

Definition 7.1.3. Let γ denote a closed path in the complex z -plane which does not cross any singularity of H . Then, we define the projection operator

$$P_\gamma := \frac{1}{2\pi i} \oint_{\gamma} R(z) dz \quad (7.9)$$

which projects onto the direct sum of the eigenspaces corresponding to those eigenvalues of H lying within the area enclosed by γ .

Due to

$$(z - H)R(z) = R(z)(z - H) = \mathbb{1} \quad (7.10)$$

we obtain

$$HP_\gamma = \frac{1}{2\pi i} \oint_{\gamma} HR(z) dz \quad (7.11a)$$

$$= \frac{1}{2\pi i} \oint_{\gamma} (H - z + z)R(z) dz \quad (7.11b)$$

$$= -\frac{1}{2\pi i} \oint_{\gamma} \mathbb{1} dz + \frac{1}{2\pi i} \oint_{\gamma} zR(z) dz. \quad (7.11c)$$

Since this result is of profound importance for our further calculations we summarize it in the following

Lemma 7.1.2. *The action of the Hamiltonian H onto the direct sum of vector spaces represented by the projector P_γ is given by*

$$HP_\gamma = \frac{1}{2\pi i} \oint_{\gamma} zR(z) dz. \quad (7.12)$$

7.2. Perturbational Setup

Perturbation Operator and Coupling Constant

Suppose the eigenvalue problem corresponding to the operator H_0 is solved and suppose further that H_0 is slightly perturbed, i.e., we consider the operator

$$H = H_0 + \lambda V, \quad (7.13)$$

where λ is a formal parameter to keep track of the various orders of perturbation theory and V is some known operator.

Definition 7.2.1. The operator V in (7.13) is called the perturbation and λ the coupling constant.

Let us again assume that the spectrum of H_0 is purely discrete, and let us denote the eigenvalues of H_0 by $E_i^{(0)}$,

$$H_0 P_i^{(0)} = E_i^{(0)} P_i^{(0)}, \quad i \in \mathbb{N}. \quad (7.14)$$

The projection operators onto the corresponding eigenspaces will be denoted by $P_i^{(0)}$ and fulfill, due to self-adjointness, the relation

$$P_i^{(0)} P_j^{(0)} = P_i^{(0)} \delta_{ij}, \quad i \in \mathbb{N}. \quad (7.15)$$

The resolvent operator of H_0 will be denoted by

$$R_0(z) := (z - H_0)^{-1} \equiv \frac{1}{z - H_0}. \quad (7.16)$$

Performing the same steps as discussed in Sect. 7.1 for a general H , we find

$$R_0(z) = \sum_{i \in \mathbb{N}} \frac{P_i^{(0)}}{z - E_i^{(0)}}, \quad (7.17a)$$

$$P_i^{(0)} = \operatorname{Res}_{z \rightarrow E_i^{(0)}} R_0(z), \quad i \in \mathbb{N} \quad (7.17b)$$

and

$$H_0 P_\gamma^{(0)} = \frac{1}{2\pi i} \oint_\gamma z R_0(z) dz. \quad (7.17c)$$

Expansion of the Resolvent

For arbitrary operators A and B , for which the following algebraic operations are defined, we may write

$$(A - B)^{-1} = A^{-1} A (A - B)^{-1} \quad (7.18a)$$

$$= A^{-1} (A - B + B) (A - B)^{-1} \quad (7.18b)$$

$$= A^{-1} + A^{-1} B (A - B)^{-1}. \quad (7.18c)$$

Thus, we may formulate the

Lemma 7.2.1. *Operator Identity*

$$(A - B)^{-1} = A^{-1} + A^{-1} B (A - B)^{-1}. \quad (7.19)$$

Applying this lemma to the full resolvent operator of H , where we set $A = z - H_0$ and $B = \lambda V$, we obtain

7. Kato Perturbation Theory

Definition 7.2.2. The following ‘integral’ equation applies to the perturbation expansion of the projection operator P onto some eigenspace of the Hamiltonian and the quantity HP ,

$$R(z) = R_0(z) + R_0(z)\lambda VR(z). \quad (7.20)$$

It admits a (formal) solution by iteration,

$$R(z) = \sum_{n=0}^{\infty} \lambda^n R_0(z)(VR_0(z))^n. \quad (7.21)$$

7.3. Eigenvalues and Eigenspaces

Definition 7.3.1. Let $\mathcal{E}_i^{(0)}$ denote the eigenspace of H_0 corresponding to the eigenvalue $E_i^{(0)}$, $i \in \mathbb{N}$. Let $\mathcal{E}_a(i)$ and $E_a(i)$, $a \in S \subset \mathbb{N}$ denote all those eigenspaces and corresponding eigenenergies of H that tend to $\mathcal{E}_i^{(0)}$ and $E_i^{(0)}$ as $\lambda \rightarrow 0$.

Let γ_i^* denote a closed path in the complex z -plane which encloses the eigenvalue $E_i^{(0)}$ of H_0 and all the eigenvalues $E_a(i)$, $a \in S$. The area enclosed by γ_i^* must not contain any other eigenvalues of H_0 or H .

The existence of this path for a particular eigenvalue $E_i^{(0)}$ of H_0 is a necessary assumption for the applicability of the perturbation theory. Consider two distinct eigenvalues $E_a^{(0)}$ and $E_b^{(0)}$ of H_0 and let

$$\{E_1(k), \dots, E_{n_k}(k)\}, \quad k = a \vee k = b \quad (7.22)$$

denote those eigenvalues of H evolving for $\lambda \rightarrow 0$ to $E_k^{(0)}$, $k = a$ and $k = b$, respectively.

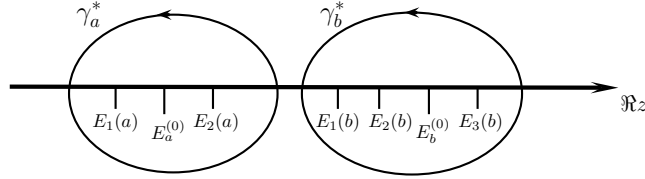


Figure 7.2.: Normal energy-level structure without level-crossing.

In the present thesis we will always assume the situation depicted in figure 7.2: For ‘small enough’ λ the various eigenenergies of H are well separated.

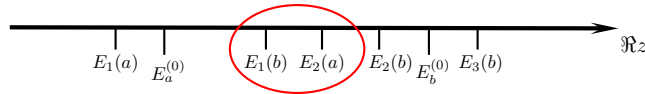


Figure 7.3.: Level-crossing at the energies $E_1(b)$ and $E_2(a)$.

Figure 7.3 shows a situation where two eigenstates of the a and b group have crossed (level-crossing). In such a case no path γ^* as described in definition (7.3.1) can exist.

If $a \neq b$ exist such that $E_a(i) \neq E_b(i)$ it follows that the degeneracy of $E_i^{(0)}$ is lifted and we have splitting of eigenvalues as λ is increased from zero. The projection operator

$$P_i(\lambda) = \frac{1}{2\pi i} \oint_{\gamma_i^*} R(z) dz \quad (7.23)$$

projects in such a situation onto the direct sum of the eigenspaces $\mathcal{E}_a(i)$ and $\mathcal{E}_b(i)$,

$$P_i(\lambda) : \mathcal{H} \rightarrow \bigoplus_a \mathcal{E}_a(i). \quad (7.24)$$

Lemma 7.3.1. *If the projection operator P_i was a projector onto one particular eigenspace of H corresponding to the energy $E_i(\lambda)$ (evolving continuously from its undisturbed value $E_i^{(0)}$) there must be no splitting of eigenvalues as λ increases from zero.*

As long as the perturbation series in λ for $P_i(\lambda)$ converges, the following lemma [122] holds.

Lemma 7.3.2. *Let $P(\lambda)$ be a projection depending continuously on a parameter λ varying in a (connected) region of real or complex numbers. The ranges of $P(\lambda)$ for different λ are isomorphic to one another. In particular, the dimension of the range of $P(\lambda)$ is constant.*

This implies especially that, for small enough λ such that we have convergence, the unperturbed eigenspace $\mathcal{E}_i^{(0)}$ and the subspace $\mathcal{E}_i = \bigoplus_{a=1}^m \mathcal{E}_a(i)$ are isomorphic, which we summarize in form of

Lemma 7.3.3. *The projection operators $P_i^{(0)}$ and $P_i(\lambda)$ map the Hilbert space \mathcal{H} onto the eigenspaces $\mathcal{E}_i^{(0)}$ and \mathcal{E}_i*

$$P_i^{(0)} : \mathcal{H} \rightarrow \mathcal{E}_i^{(0)}, \quad (7.25)$$

$$P_i : \mathcal{H} \rightarrow \mathcal{E}_i. \quad (7.26)$$

Let $r(P_i)$ denote the convergence radius of $P_i(\lambda)$ and let $U_r(P_i)$ be its region of convergence. For $\lambda \in U_r(P_i)$ we have

$$\mathcal{E}_i^{(0)} \simeq \mathcal{E}_i \quad (7.27)$$

which implies that P_i induces an isomorphism of vector spaces,

$$P_i|_{\mathcal{E}_i^{(0)}} : \mathcal{E}_i^{(0)} \rightarrow \mathcal{E}_i. \quad (7.28)$$

7.4. Perturbative Expansions

7.4.1. Projection Operator

To obtain the perturbative expansion of $P_i(\lambda)$ in powers of the coupling λ , we insert the iterative solution (7.21) for $R(z)$ into the defining equation of P_i and interchange integration and summation. This leads to

$$P_i = P_i^{(0)} + \sum_{n=1}^{\infty} \lambda^n A^{(n)}, \quad (7.29)$$

$$A^{(n)} := \frac{1}{2\pi i} \oint_{\gamma_i^*} R_0(z) (V R_0(z))^n dz. \quad (7.29a)$$

Due to the restrictions on the path γ_i^* , the function

$$F_n(\gamma_i^*, z) := R_0(z) (V R_0(z))^n \Big|_{\gamma_i^*} \quad (7.30)$$

is analytic within that part of the complex plane enclosed by γ_i^* except for a single pole of order $n+1$. It immediately follows that

$$A^{(n)} = \operatorname{Res}_{z \rightarrow E_i^{(0)}} F_n(\gamma_i^*, z). \quad (7.31)$$

7.4.2. Calculation of the Residue for the Projector

To calculate the residue $A^{(n)}$ explicitly, we expand $R_0(z)$ into a Laurent series about its pole $E_i^{(0)}$. Since in the part of the complex plane enclosed by γ_i^* , $R_0(z)$ has a single pole of order unity and no other singularity, we may write according to complex analysis [123]

$$R_0(z) = \sum_{n=-1}^{\infty} c_n (z - E_i^{(0)})^n, \quad (7.32)$$

where the coefficients in the above Laurent series are given by

$$c_n = \frac{1}{2\pi i} \oint_{\gamma_i^*} \frac{R_0(z)}{(z - E_i^{(0)})^{n+1}} dz \quad (7.33a)$$

$$= \sum_{a=0}^{\infty} P_a^{(0)} \frac{1}{2\pi i} \oint_{\gamma_i^*} \frac{dz}{(z - E_i^{(0)})^{n+1} (z - E_a^{(0)})}. \quad (7.33b)$$

Since

$$\oint_{\gamma_i^*} \frac{1}{(z - E_i^{(0)})^n} dz = \begin{cases} 2\pi i & \text{for } n = 1, \\ 0 & \text{for } n > 1, \end{cases} \quad (7.34)$$

we find $c_{-1} = P_i^{(0)}$ and for $n > -1$ that

$$c_n = \sum_{a \neq i}^{\infty} P_a^{(0)} \frac{1}{2\pi i} \oint_{\gamma_i^*} \frac{dz}{(z - E_i^{(0)})^{n+1} (z - E_a^{(0)})} \quad (7.35a)$$

$$= \sum_{a \neq i}^{\infty} P_a^{(0)} \operatorname{Res}_{z \rightarrow E_i^{(0)}} \frac{1}{(z - E_i^{(0)})^{n+1} (z - E_a^{(0)})} \quad (7.35b)$$

$$= \sum_{a \neq i}^{\infty} P_a^{(0)} \frac{1}{n!} \frac{d^n}{dz^n} \left[(z - E_i^{(0)})^{n+1} \frac{1}{(z - E_i^{(0)})^{n+1} (z - E_a^{(0)})} \right] \Big|_{z=E_i^{(0)}}. \quad (7.35c)$$

We use

$$\frac{d^{(n)}}{dz^{(n)}} (z - E)^{-1} = n! (-1)^n (z - E)^{-n-1} \quad (7.36)$$

to obtain

$$c_n = \begin{cases} P_i^{(0)} & \text{for } n = -1, \\ (-1)^n \sum_{a \neq i}^{\infty} \frac{P_a^{(0)}}{(E_i^{(0)} - E_a^{(0)})^{n+1}} & \text{for } n \geq 0. \end{cases} \quad (7.37)$$

After a shift of the index n in equation (7.32) and the insertion of (7.37) we obtain

Lemma 7.4.1. *The Laurent expansion of $R_0(z)$ about its pole at $z = E_i^{(0)}$ reads*

$$R_0(z) = \frac{P_i^{(0)}}{z - E_i^{(0)}} + \sum_{n=1}^{\infty} (-1)^{n-1} (z - E_i^{(0)})^{n-1} \sum_{a \neq i}^{\infty} \frac{P_a^{(0)}}{(E_i^{(0)} - E_a^{(0)})^n}. \quad (7.38)$$

Following the notation of Kato [121], we define

$$\tilde{S}^0 := -P_i^{(0)}, \quad (7.39a)$$

$$(E_i^{(0)} - H) \tilde{S} := 1 - P_i^{(0)}, \quad (7.39b)$$

so that we may write

$$R_0(z) = \sum_{n=0}^{\infty} (-1)^{n-1} (z - E_i^{(0)})^{n-1} \tilde{S}^n. \quad (7.40)$$

It remains to calculate $A^{(n)}$. We insert (7.40) into the expression for $F_n(\gamma_i^*, z)$, (7.30), and obtain the Laurent expansion

$$F_n(\gamma_i^*, z) = R_0(z)(VR_0(z))^n \quad (7.41)$$

$$= \sum_{k_1=0}^{\infty} \dots \sum_{k_{n+1}=0}^{\infty} (-1)^{k_1+\dots+k_{n+1}-n-1} (z - E_i^{(0)})^{k_1+\dots+k_{n+1}-n-1} \tilde{S}^{k_1} V \tilde{S}^{k_2} \dots V \tilde{S}^{k_{n+1}}. \quad (7.42)$$

Since $A^{(n)}$ is the residue of $F_n(\gamma_i^*, z)$, i.e. the coefficient of $(z - E_i^{(0)})^{-1}$ in a Laurent expansion of F_n , we can read off $A^{(n)}$ as

$$A^{(n)} = - \sum_{\substack{k_1, \dots, k_{n+1}=0 \\ k_1+\dots+k_{n+1}=n}}^n \tilde{S}^{k_1} V \tilde{S}^{k_2} \dots V \tilde{S}^{k_{n+1}} \quad (7.43a)$$

$$=: - \sum_{(n)} \tilde{S}^{k_1} V \tilde{S}^{k_2} \dots V \tilde{S}^{k_{n+1}}. \quad (7.43b)$$

The last line defines a convenient abbreviation for the sum in (7.43a).

7.4.3. Hamiltonian

We start with the expression (7.12),

$$HP_{\gamma_i^*} = \frac{1}{2\pi i} \oint_{\gamma_i^*} zR(z)dz. \quad (7.44)$$

From the derivation in Sect. 7.1 it is evident that

$$H_0P_{\gamma_i^*}^{(0)} = \frac{1}{2\pi i} \oint_{\gamma_i^*} zR_0(z)dz \quad (7.45)$$

and that

$$H_0P_{\gamma_i^*}^{(0)} = E_i^{(0)}P_{\gamma_i^*}^{(0)}. \quad (7.46)$$

$P_{\gamma_i^*}^{(0)}$ is of course nothing else but $P_i^{(0)}$. From the derivation of $P_i(\lambda)$ in Sect. 7.1 we know that

$$HP_i = \frac{1}{2\pi i} \oint_{\gamma_i^*} zR(z)dz \quad (7.47)$$

and, see (7.21),

$$R(z) = \sum_{n=0}^{\infty} R_0(z)(\lambda VR_0(z))^n. \quad (7.48)$$

We insert the last two equations into one another and interchange summation and integration to obtain

$$HP_i = H_0P_i^{(0)} + \sum_{n=1}^{\infty} \lambda^n \tilde{B}^{(n)}, \quad (7.49)$$

$$\tilde{B}^{(n)} := \frac{1}{2\pi i} \oint_{\gamma_i^*} zR_0(z)(VR_0(z))^n dz.$$

7.4.4. Calculation of the Residue for the Hamiltonian

The defining formula (7.49) can be simplified along the lines shown for $A^{(n)}$ in Sect. 7.4.2,

$$\tilde{B}^{(n)} = \frac{1}{2\pi i} \oint_{\gamma_i^*} z R_0(z) (V R_0(z))^n dz \quad (7.50a)$$

$$= \frac{1}{2\pi i} \oint_{\gamma_i^*} (z - E_i^{(0)} + E_i^{(0)}) R_0(z) (V R_0(z))^n dz \quad (7.50b)$$

$$= \frac{1}{2\pi i} \oint_{\gamma_i^*} (z - E_i^{(0)}) R_0(z) (V R_0(z))^n dz + E_i^{(0)} A^{(n)}. \quad (7.50c)$$

We may therefore write

$$\tilde{B}^{(n)} = B^{(n)} + E_i^{(0)} A^{(n)}, \quad (7.51)$$

where

$$B^{(n)} := \frac{1}{2\pi i} \oint_{\gamma_i^*} (z - E_i^{(0)}) R_0(z) (V R_0(z))^n dz \quad (7.52)$$

is the residue of $(z - E_i^{(0)}) F_n(\gamma_i^*, z)$ at $z = E_i^{(0)}$. The expansion of $F_n(\gamma_i^*, z)$ is already known from (7.42) and the expansion of $B^{(n)}$ can be read off to give

$$B^{(n)} = - \sum_{\substack{k_1, \dots, k_{n+1}=0 \\ k_1 + \dots + k_{n+1} = n-1}}^{n-1} \tilde{S}^{k_1} V \tilde{S}^{k_2} \dots V \tilde{S}^{k_{n+1}} \quad (7.53a)$$

$$=: - \sum_{(n-1)} \tilde{S}^{k_1} V \tilde{S}^{k_2} \dots V \tilde{S}^{k_{n+1}}. \quad (7.53b)$$

In the last line we introduced an abbreviation of the sum in (7.53a).

With (7.29),

$$P_i - P_i^{(0)} = \sum_{n=1}^{\infty} \lambda^n A^{(n)}, \quad (7.54)$$

we can write

$$H P_i = H_0 P_i^{(0)} + \sum_{n=1}^{\infty} \lambda^n \tilde{B}^{(n)} \quad (7.55a)$$

$$= E_i^{(0)} P_i^{(0)} + E_i^{(0)} \sum_{n=1}^{\infty} \lambda^n A^{(n)} + \sum_{n=1}^{\infty} \lambda^n B^{(n)} \quad (7.55b)$$

$$= E_i^{(0)} P_i^{(0)} + E_i^{(0)} (P_i - P_i^{(0)}) + \sum_{n=1}^{\infty} \lambda^n B^{(n)}, \quad (7.55c)$$

so that we end up with

$$(H - E_i^{(0)}) P_i = \sum_{n=1}^{\infty} \lambda^n B^{(n)}, \quad (7.56)$$

$$B^{(n)} := - \sum_{(n-1)} \tilde{S}^{k_1} V \tilde{S}^{k_2} \dots V \tilde{S}^{k_{n+1}}.$$

7.5. Summary

In this chapter we have introduced a perturbational technique developed by Kato [121]. It is a perturbation expansion of projection operators onto eigenspaces of the Hamiltonian

$$H = H_0 + \lambda V, \quad (7.57)$$

where V is the perturbation and λ a dimensionless coupling constant. The projection operator $P_i(\lambda)$ onto the direct sum

$$\mathcal{E}_i = \bigoplus_{a \in S} \mathcal{E}_a(i) \quad (7.58)$$

of those eigenspaces $\mathcal{E}_a(i)$, $a \in S \subset \mathbb{N}$ of the full H which tend to $\mathcal{E}_i^{(0)}$ for $\lambda \rightarrow 0$, is given as a contour integral

$$P_i(\lambda) = \frac{1}{2\pi i} \oint_{\gamma_i^*} R(z) dz \quad (7.59)$$

along a closed path γ_i^* defined in Sect. 7.3.1. $R(z)$ denotes the resolvent operator of the Hamiltonian. We have shown that the integral can be performed to yield an explicit expansion of $P_i(\lambda)$ which reads

$$\begin{aligned} P_i(\lambda) &= P_i^{(0)} + \sum_{n=1}^{\infty} \lambda^n A^{(n)}, \\ A^{(n)} &:= - \sum_{(n)} \tilde{S}^{k_1} V \tilde{S}^{k_2} \dots V \tilde{S}^{k_{n+1}}. \end{aligned} \quad (7.60)$$

The action of the Hamiltonian in the space defined by $P_i(\lambda)$ is given by a similar contour integral,

$$HP_i = \frac{1}{2\pi i} \oint_{\gamma_i^*} z R(z) dz, \quad (7.61)$$

which we have calculated explicitly,

$$\begin{aligned} (H - E_i^{(0)})P_i(\lambda) &= \sum_{n=1}^{\infty} \lambda^n B^{(n)}, \\ B^{(n)} &:= \sum_{(n-1)} \tilde{S}^{k_1} V \tilde{S}^{k_2} \dots V \tilde{S}^{k_{n+1}}. \end{aligned} \quad (7.62)$$

Following [121] we have introduced the notations

$$\begin{aligned} \tilde{S}^0 &= -P_i^{(0)}, \\ (E_i^{(0)} - H_0)\tilde{S} &= 1 - P_i^{(0)}, \end{aligned} \quad (7.63)$$

and the abbreviation

$$\sum_{(l)} f(k_1, \dots, k_m) = \sum_{\substack{k_1, \dots, k_m=0 \\ k_1 + \dots + k_m = l}}^l f(k_1, \dots, k_m). \quad (7.64)$$

*There is only one object on earth that frightens me:
a physicist working on a new trick.*

Nero Wolfe in **A Family Affair** by Rex Stout

8

Kato-Takahashi Formalism

Takahashi was the first to apply the general perturbation theory of Kato, developed in the last section, to the half-filled Hubbard model at zero temperature [124]. It is a systematic expansion in $1/U$. Takahashi used it to calculate the ground-state energy and various static correlation functions for the Hubbard model in low spatial dimensions. We will use the method in this thesis to calculate the (dynamic) one-particle Green function in the limit of high dimensions. We will introduce the technique in the first section of this chapter and give explicit formulae for the Hubbard model in the second section.

8.1. Fundamental Quantities

We know from chapter 7 that for sufficiently small λ the projection $P_i(\lambda)$,

$$P_i(\lambda) : \mathcal{H} \rightarrow \mathcal{E}_i = \bigoplus_a \mathcal{E}_a(i), \quad (8.1)$$

induces an isomorphism of vector spaces,

$$P_i(\lambda)|_{\mathcal{E}_i^{(0)}} : \mathcal{E}_i^{(0)} \rightarrow \mathcal{E}_i. \quad (8.2)$$

Instead of diagonalizing H in the full Hilbert space \mathcal{H} , we can examine its various eigenspaces separately. Under the assumption of the validity of the perturbation theory, the isomorphism (8.2) grants the description of the unknown spaces \mathcal{E}_i by the known eigenspaces $\mathcal{E}_i^{(0)}$ of H_0 .

It is a minor drawback that the projection $P_i(\lambda)$ does not preserve the norms of vectors. In the case of a finite-dimensional vector space this does not pose a big problem. Since $P_i(\lambda)|_{\mathcal{E}_i^{(0)}}$ as a Hermitian, invertible mapping is positive definite (as is true for its inverse), the square root of the operator $P_i(\lambda)|_{\mathcal{E}_i^{(0)}}$ exists and is unique [125]. We will assume that this remains true even in the thermodynamic limit, where linear algebra has to be substituted by (linear) functional analysis.

In order to work with norm-conserving operators, Takahashi introduced the following isometry $\Gamma_i(\lambda)$,

$$\Gamma_i(\lambda) := P_i(\lambda)|_{\mathcal{E}_i^{(0)}} \left(P_i(\lambda)|_{\mathcal{E}_i^{(0)}} \right)^{-\frac{1}{2}}. \quad (8.3)$$

In order to make the expansion in powers of the perturbation V more transparent we will write

$$\Gamma_i(\lambda) = P_i(\lambda) P_i^{(0)} \left(P_i^{(0)} P_i(\lambda) P_i^{(0)} \right)^{-\frac{1}{2}} \quad (8.4)$$

with $P_i^{(0)}$ denoting the projection

$$P_i^{(0)} : \mathcal{H} \rightarrow \mathcal{E}_i^{(0)} \quad (8.5)$$

onto the corresponding eigenspace of H_0 . It is implicitly understood that $\Gamma_i(\lambda)$ only acts on states belonging to $\mathcal{E}_i^{(0)}$. Note that this is a vital assumption because the projector is most certainly not

8. Kato-Takahashi Formalism

invertible on the full Hilbert space \mathcal{H} . The inverse square root will be considered to be given by its formal series expansion

$$\left(P_i(\lambda)\right)^{-\frac{1}{2}} \equiv \left(1 - [1 - P_i(\lambda)]\right)^{-\frac{1}{2}} = \sum_{n=0}^{\infty} \frac{(2n-1)!!}{(2n)!!} [1 - P_i(\lambda)]^n \quad (8.6)$$

which leads to

$$P_i^{(0)} \left(P_i^{(0)} P_i P_i^{(0)}\right)^{-\frac{1}{2}} = \sum_{n=0}^{\infty} \frac{(2n-1)!!}{(2n)!!} \left[P_i^{(0)} (P_i^{(0)} - P_i) P_i^{(0)}\right]^n. \quad (8.7)$$

We will abbreviate $P_i(\lambda)$ by P_i with similar abbreviations for the other mappings. When applying the mappings to many-particle quantum physics, we should also notify the number of particles as $P_i(N, \lambda) \equiv P_i(N)$.

In the following lemma we summarize some properties of Takahashi's mapping $\Gamma_i(\lambda)$.

Lemma 8.1.1. *Properties of Γ_i*

$$(i) \quad \Gamma_i^\dagger = \left(P_i^{(0)} P_i P_i^{(0)}\right)^{-\frac{1}{2}} P_i^{(0)} P_i \quad (8.8)$$

$$(ii) \quad \Gamma_i^2 = \Gamma_i \left(P_i^{(0)} P_i P_i^{(0)}\right)^{\frac{1}{2}} = P_i P_i^{(0)} \quad (8.9)$$

$$(iii) \quad \Gamma_i^\dagger \Gamma_i = P_i^{(0)} \quad (8.10)$$

$$(iv) \quad \Gamma_i \Gamma_i^\dagger = P_i \quad (8.11)$$

Proof.

(i) obvious

$$\begin{aligned} (ii) \quad \Gamma_i^2 &= P_i P_i^{(0)} \left(P_i^{(0)} P_i P_i^{(0)}\right)^{-\frac{1}{2}} P_i P_i^{(0)} \left(P_i^{(0)} P_i P_i^{(0)}\right)^{-\frac{1}{2}} \\ &= P_i P_i^{(0)} \left(P_i^{(0)} P_i P_i^{(0)}\right)^{-\frac{1}{2}} P_i^{(0)} P_i P_i^{(0)} \left(P_i^{(0)} P_i P_i^{(0)}\right)^{-\frac{1}{2}} \\ &= P_i P_i^{(0)} = \Gamma_i \left(P_i^{(0)} P_i P_i^{(0)}\right)^{\frac{1}{2}} \end{aligned}$$

$$\begin{aligned} (iii) \quad \Gamma_i^\dagger \Gamma_i &= \left(P_i^{(0)} P_i P_i^{(0)}\right)^{-\frac{1}{2}} P_i^{(0)} P_i P_i^{(0)} \left(P_i^{(0)} P_i P_i^{(0)}\right)^{-\frac{1}{2}} \\ &= id_{\mathcal{E}_i^{(0)}} = P_i^{(0)} \end{aligned}$$

$$\begin{aligned} (iv) \quad \Gamma_i \Gamma_i^\dagger &= P_i P_i^{(0)} \left(P_i^{(0)} P_i P_i^{(0)}\right)^{-1} P_i^{(0)} P_i \\ &\stackrel{*}{=} P_i P_i^{(0)} \left(P_i^{(0)} P_i P_i^{(0)}\right)^{-1} P_i^{(0)} P_i P_i^{(0)} \\ &= P_i P_i^{(0)} \stackrel{*}{=} P_i = id_{\mathcal{E}_i} \end{aligned}$$

Note that the inverse is only defined for $P_i : \mathcal{E}_i^{(0)} \rightarrow \mathcal{E}_i$ in which case the equality marked with * is valid.

□

In the finite-dimensional case we may identify \mathcal{E}_i and $\mathcal{E}_i^{(0)}$ which renders Γ_i unitary.

8.2. Leading-Order Terms

8.2.1. Takahashi's Operator

In this section we will show by example of the leading-order contributions how to obtain the expression of $\Gamma_i(\lambda)$. For a complete derivation we refer the reader to appendix C, where he can also find a complete summary of the resulting expansion.

From Kato perturbation theory we know that, see (7.60),

$$\begin{aligned} P_i &= P_i^{(0)} + \sum_{n=1}^{\infty} \lambda^n A^{(n)}, \\ A^{(n)} &= - \sum_{(n)} \tilde{S}^{k_1} V \tilde{S}^{k_2} \dots V \tilde{S}^{k_{n+1}}. \end{aligned} \quad (8.12)$$

In all subsequent expressions involving P_i it will always appear in combination with $P_i^{(0)}$ in the form $P_i P_i^{(0)}$. It follows that $\tilde{S}^{k_{n+1}}$ in the expansion of $A^{(n)}$ must always be set to $P_i^{(0)}$ which implies $k_{n+1} = 0$,

$$P_i P_i^{(0)} = P_i^{(0)} + \sum_{n=1}^{\infty} \lambda^n \tilde{A}^{(n)} \quad (8.13)$$

with the definition

$$\tilde{A}^{(n)} := A^{(n)} P_i^{(0)}. \quad (8.14)$$

Up to (and including) the first order in λ we thus have

$$P_i P_i^{(0)} = P_i^{(0)} + \lambda \tilde{S} V P_i^{(0)}. \quad (8.15)$$

We introduce

$$P_i^{(0)} P_i P_i^{(0)} = P_i^{(0)} + \sum_{n=1}^{\infty} \lambda^n \bar{A}^{(n)} \quad (8.16)$$

with the definition

$$\bar{A}^{(n)} := P_i^{(0)} \tilde{A} \equiv P_i^{(0)} A^{(n)} P_i^{(0)} \quad (8.17)$$

and find to first order that $\bar{A}^{(1)}$ vanishes. This means that

$$P_i^{(0)} - P_i^{(0)} P_i P_i^{(0)} = \mathcal{O}(\lambda^2). \quad (8.18)$$

It follows that

$$P_i^{(0)} (P_i^{(0)} P_i P_i^{(0)})^{-\frac{1}{2}} = P_i^{(0)} + \mathcal{O}(\lambda^2). \quad (8.19)$$

Using the defining equation (8.4) and the preceding results, we find

$$\Gamma_i = \left\{ P_i^{(0)} + \sum_{n=1}^{\infty} \lambda^n \tilde{A}^{(n)} \right\} \times \left\{ P_i^{(0)} + \mathcal{O}(\lambda^2) \right\} \quad (8.20a)$$

$$= P_i^{(0)} + \lambda \{ \tilde{A}^{(1)} \} + \mathcal{O}(\lambda^2), \quad (8.20b)$$

which can be rewritten as

$$\boxed{\Gamma_i(\lambda) = P_i^{(0)} + \lambda \tilde{S} V P_i^{(0)} + \mathcal{O}(\lambda^2)}. \quad (8.21)$$

8.2.2. Transformed Energy Operator

As we will explain in detail in Sect. 9.3.3, we need the expansion of the transformed energy operator

$$\Gamma_i^\dagger(\lambda, N)(H - E_i^{(0)}(N))\Gamma_i(\lambda, N) = \sum_{n=1}^{\infty} \lambda^n \tilde{R}_i^{(n)}(N) \quad (8.22)$$

to calculate the Green function. In (8.22) we have made the dependence of the operators on the total number of particles, N , explicit.

In chapter 7 we showed that, see (7.62),

$$(H - E_i^{(0)})P_i P_i^{(0)} = \sum_{n=1}^{\infty} \lambda^n \tilde{B}^{(n)} \quad (8.23)$$

where

$$\tilde{B}^{(n)} := - \sum_{(n-1)} \tilde{S}^{k_1} V \tilde{S}^{k_2} V \dots \tilde{S}^{k_n} V P_i^{(0)}. \quad (8.23a)$$

To first and second order we simply find $\tilde{B}^{(1)} = P_i^{(0)} V P_i^{(0)}$ and $\tilde{B}^{(2)} = \tilde{S} V P_i^{(0)} V P_i^{(0)} + P_i^{(0)} V \tilde{S} V P_i^{(0)}$. With the definition (8.4) and our finding

$$P_i^{(0)} (P_i^{(0)} P_i P_i^{(0)})^{-\frac{1}{2}} = P_i^{(0)} + \mathcal{O}(\lambda^2),$$

we define

$$(H - E_i^{(0)})\Gamma_i = \sum_{n=1}^2 \lambda^n C^{(n)} + \mathcal{O}(\lambda^3), \quad (8.24)$$

where $C^{(1)} := \tilde{B}^{(1)}$ and $C^{(2)} := \tilde{B}^{(2)}$. With the definition of Γ_i ,

$$\Gamma_i = \sum_{n=0}^{\infty} \lambda^n \tilde{\Gamma}_i^{(n)},$$

we obtain

$$\begin{aligned} \Gamma_i^\dagger (H - E_i^{(0)}) \Gamma_i &= \sum_{m=0}^1 \sum_{n=1}^2 \lambda^{m+n} \tilde{\Gamma}_i^{\dagger(m)} C^{(n)} + \mathcal{O}(\lambda^3) \\ &= \sum_{n=1}^2 \lambda^n \tilde{R}_i^{(n)} + \mathcal{O}(\lambda^3) \end{aligned} \quad (8.25)$$

and thus, to first and second order, $\tilde{R}_i^{(1)} = P_i^{(0)} V P_i^{(0)}$ and $\tilde{R}_i^{(2)} = P_i^{(0)} V \tilde{S} V P_i^{(0)}$. In summary we have to first and second order in λ

$$\boxed{\Gamma_i^\dagger (H - E_i^{(0)}) \Gamma_i = \lambda P_i^{(0)} V P_i^{(0)} + \lambda^2 P_i^{(0)} V \tilde{S} V P_i^{(0)} + \mathcal{O}(\lambda^3)}. \quad (8.26)$$

We present the explicit formulae and their derivation up to fifth order in appendix C.

Part III.

Calculations and Results

*The person who says it cannot be done
should not interrupt the person doing it.*

Chinese Saying

9

Theoretical Setup

In this chapter we explain how we utilize the methods described in the last chapters to calculate the Green function for the Hubbard model. First, we introduce the quantity of interest, namely the local, single-particle Green function of the Hubbard model. Second, we discuss the mapping of the Hubbard model onto the Single Impurity Anderson Model (SIAM), introduce the local impurity Green function of the SIAM, and discuss the mappings of the SIAM onto chain geometries, especially onto the two-chain geometry. Third, we explain our usage of the Kato-Takahashi perturbation theory on the SIAM in two-chain geometry, discuss the starting Hamiltonian of the perturbation theory, and analyze the perturbation. Finally, we show how we implement the self-consistency condition of the Dynamical Mean-Field Theory (DMFT) in matrix form for a multichain setup of the SIAM.

9.1. Hubbard Lattice Model

In this thesis we calculate the single-particle density of states for charge-carrying excitations of the Mott-Hubbard insulator, see Sect. 5.4, on a Bethe lattice with infinite coordination $Z \rightarrow \infty$. The Hubbard model we are working with is the particle-hole symmetric version (5.12),

$$H_{\text{Hubbard}} = -\frac{t}{\sqrt{Z}} \sum_{\langle i,j \rangle} (c_{i\sigma}^\dagger c_{j\sigma} + c_{j\sigma}^\dagger c_{i\sigma}) + U \sum_i (n_{i\uparrow} - 1/2)(n_{i\downarrow} - 1/2). \quad (9.1)$$

We use the electron transfer amplitude t as our unit of energy, thus $t \equiv 1$.

The charge gap can be read off the density of states which is given, see (A.35) of appendix A, in terms of the local, single-particle Green function, defined on the lattice as

$$iG_{\text{local}}(t) = \frac{1}{L} \sum_{i,\sigma} \langle T_s c_{i\sigma}(t) c_{i\sigma}^\dagger(0) \rangle, \quad (9.2)$$

where L denotes the number of lattice points. The brackets denote an average which we define now.

Average We start with the real-time Green function at finite, inverse temperature β ,

$$i\mathcal{G}(t) = \frac{1}{L} \sum_{i,\sigma} \frac{\text{Tr} e^{-\beta H_{\text{Hubbard}}} T_s c_{i\sigma}(t) c_{i\sigma}^\dagger}{\mathcal{Z}}, \quad (9.3)$$

with Tr denoting a trace over a complete set of N -particle states. \mathcal{Z} denotes the partition function. Only the ground states of H_{Hubbard} will contribute in the limit of zero temperature and \mathcal{Z} will simply be equal to their number. At half band-filling, $N = L$, the insulating, paramagnetic phase of the Hubbard model has the finite ground-state entropy density $s = \ln(2)$ in the thermodynamic limit [2]. Thus, the ground state is 2^L -fold degenerate and the average in (9.2) reads

$$iG_{\text{local}}(t) = \frac{1}{L} \sum_{i,\sigma} \frac{\text{tr} T_s c_{i\sigma}(t) c_{i\sigma}^\dagger}{2^L}, \quad (9.4)$$

where the trace tr is taken over the 2^L ground states.

9. Theoretical Setup

Hubbard Bands We take the Fourier transformation of (9.2) and, according to (A.30) of appendix A, obtain

$$G_{\text{local}}(\omega) = \frac{1}{L} \sum_{i,\sigma} \lim_{\eta \searrow 0} \left(\langle c_{i\sigma}(\omega - (H_{\text{Hubbard}} - E_0(L)) + i\eta)^{-1} c_{i\sigma}^\dagger \rangle + \langle c_{i\sigma}^\dagger(\omega + (H_{\text{Hubbard}} - E_0(L)) - i\eta)^{-1} c_{i\sigma} \rangle \right), \quad (9.5)$$

where $E_0(L)$ is the ground-state energy of the half-filled Hubbard model.

We know that, within the insulating phase, there is a gap in the density of states $D(\omega)$. Therefore, it is possible to separate the contributions of $G_{\text{local}}(\omega)$ to the lower (LHB) and upper (UHB) Hubbard bands. For the particle-hole symmetric model we denote the negative frequency part of the density of states with LHB, whereas the positive frequency part forms the UHB. In figure 9.1 we give a sketch of the situation in the Mott-Hubbard insulator. Note that there may be several sub-bands centered at the excitation energies of the atomic limit Hamiltonian (5.32) within the LHB and UHB. Then, the LHB denotes the union of the various sub-bands at negative frequencies. An analog statement holds for the UHB.

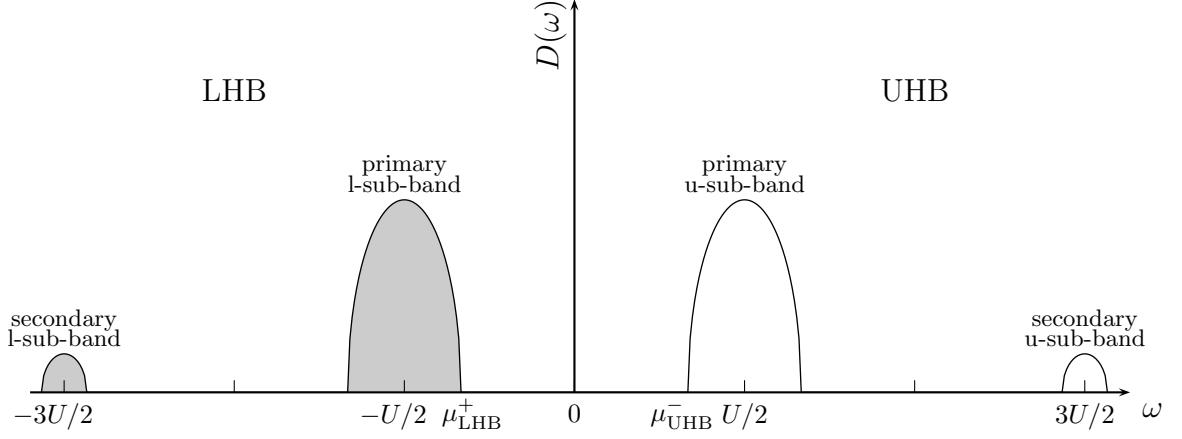


Figure 9.1.: Sketch of the density of states of the Mott-Hubbard insulator at strong coupling.

The poles of the expression in the first parenthesis in (9.5) lie at positive frequencies, whereas they are located at negative frequencies in the second term. Thus, for the insulator it is permissible to write

$$G_{\text{LHB}}(\omega) := \frac{1}{L} \sum_{i,\sigma} \lim_{\eta \searrow 0} \langle c_{i\sigma}^\dagger(\omega + (H_{\text{Hubbard}} - E_0(L)) - i\eta)^{-1} c_{i\sigma} \rangle, \quad (9.6)$$

$$G_{\text{UHB}}(\omega) := \frac{1}{L} \sum_{i,\sigma} \lim_{\eta \searrow 0} \langle c_{i\sigma}(\omega - (H_{\text{Hubbard}} - E_0(L)) + i\eta)^{-1} c_{i\sigma}^\dagger \rangle, \quad (9.7)$$

such that the Green function (9.5) is the sum

$$G_{\text{local}}(\omega) = G_{\text{LHB}}(\omega) + G_{\text{UHB}}(\omega). \quad (9.8)$$

Exploiting Particle-Hole Symmetry As we have explained in detail in Sect. 5.2.2, the Hubbard model (9.1) on the bipartite Bethe lattice is invariant under the particle-hole transformation \mathcal{T}_3 . We apply

this transformation to the Green function of the lower Hubbard band and get

$$G_{\text{LHB}}(\omega) = \frac{1}{L} \sum_{i,\sigma} \lim_{\eta \searrow 0} \langle c_{i\sigma}^\dagger (\omega + (H_{\text{Hubbard}} - E_0(L)) - i\eta)^{-1} c_{i\sigma} \rangle \quad (9.9a)$$

$$= \frac{1}{L} \sum_{i,\sigma} \lim_{\eta \searrow 0} \langle \mathcal{T}_3^\dagger c_{i\sigma}^\dagger \mathcal{T}_3 \mathcal{T}_3^\dagger (\omega + (H_{\text{Hubbard}} - E_0(L)) - i\eta)^{-1} \mathcal{T}_3 \mathcal{T}_3^\dagger c_{i\sigma} \mathcal{T}_3 \rangle \quad (9.9b)$$

$$= \frac{1}{L} \sum_{i,\sigma} \lim_{\eta \searrow 0} \langle c_{i\sigma}^\dagger (\mathcal{T}_3^\dagger (\omega + (H_{\text{Hubbard}} - E_0(L)) - i\eta) \mathcal{T}_3)^{-1} c_{i\sigma} \rangle \quad (9.9c)$$

$$= \frac{1}{L} \sum_{i,\sigma} \lim_{\eta \searrow 0} \langle c_{i\sigma} (\omega + (H_{\text{Hubbard}} - E_0(L)) - i\eta)^{-1} c_{i\sigma}^\dagger \rangle \quad (9.9d)$$

$$= -G_{\text{UHB}}(-\omega). \quad (9.9e)$$

Using equations (A.32) and (A.35) of appendix A, we can calculate the density of states as

$$D(\omega) = \frac{1}{\pi} \{ \Theta(-\omega) - \Theta(\omega) \} \Im G_{\text{local}}(\omega) \quad (9.10a)$$

$$= D_{\text{LHB}}(\omega) + D_{\text{UHB}}(\omega), \quad (9.10b)$$

where the density of the lower/upper Hubbard band is given by

$$D_{\text{UHB}}^{\text{LHB}}(\omega) = \pm \frac{1}{\pi} \Im G_{\text{UHB}}^{\text{LHB}}(\omega). \quad (9.11)$$

Due to (9.9e) the density of the UHB can be obtained via $D_{\text{UHB}}(\omega) = D_{\text{LHB}}(-\omega)$. This shows that it is sufficient to calculate $G_{\text{LHB}}(\omega)$.

Charge Gap $\Delta_{\text{C}}(U)$ At half band-filling, where the number of electrons N equals the number of sites L in the lattice, the LHB is filled which we have symbolized in figure 9.1 by the gray shading. To insert an additional electron into the system one must invest the energy, see Sect. 5.4,

$$\mu_{\text{UHB}}^- = E_0(L+1) - E_0(L) = \mathcal{O}(U/2 - W/2), \quad (9.12)$$

whereas the removal of an electron from the half-filled system requires the energy

$$\mu_{\text{LHB}}^+ = E_0(L) - E_0(L-1) = \mathcal{O}(-U/2 + W/2). \quad (9.13)$$

The gap for charge excitations therefore results in

$$\Delta_{\text{C}}(U) = \mu_{\text{UHB}}^- - \mu_{\text{LHB}}^+ = 2|\mu_{\text{LHB}}^+| = \mathcal{O}(U - W) > 0, \quad (9.14)$$

where we used the particle-hole symmetry in the second step.

9.2. Mapping onto the Impurity Problem

As described in detail in chapter 6, instead of approaching the lattice problem directly, we use the Dynamical Mean-Field Theory (DMFT) to map the Hubbard model (9.1) onto the symmetric Single Impurity Anderson Model (SIAM)

$$H_{\text{SIAM}} = \sum_{\mathbf{k},\sigma} \varepsilon_{\mathbf{k}} n_{\mathbf{k}\sigma} + \sum_{\mathbf{k},\sigma} V_{\mathbf{k}} (c_{\mathbf{k}\sigma}^\dagger d_\sigma + d_\sigma^\dagger c_{\mathbf{k}\sigma}) + U(n_{d\uparrow} - 1/2)(n_{d\downarrow} - 1/2). \quad (9.15)$$

9. Theoretical Setup

9.2.1. Local Impurity Green Function

The local, impurity Green function reads

$$G_{\text{local}}^{\text{SIAM}}(\omega) = \sum_{\sigma} \lim_{\eta \searrow 0} \left(\langle d_{\sigma}(\omega - (H_{\text{SIAM}} - \tilde{E}_0(L)) + i\eta)^{-1} d_{\sigma}^{\dagger} \rangle + \langle d_{\sigma}^{\dagger}(\omega + (H_{\text{SIAM}} - \tilde{E}_0(L)) - i\eta)^{-1} d_{\sigma} \rangle \right), \quad (9.16)$$

where $\tilde{E}_0(L)$ denotes the ground-state energy of the SIAM at half filling. In the insulating state at half band-filling, the ground state has total spin $|S_{\text{total}}^z| = 1/2$ and, as a consequence, is two-fold degenerate. The average in (9.15) is then given by

$$\langle \dots \rangle = \frac{\text{tr} \dots}{2}, \quad (9.17)$$

where the trace tr is taken over the two ground states $|\Psi_{\uparrow}\rangle$ and $|\Psi_{\downarrow}\rangle$ with total spin $S_{\text{total}}^z = 1/2$ and $S_{\text{total}}^z = -1/2$, respectively.

Spin-Rotational Invariance As in the case of the Hubbard model, the SIAM is invariant under rotations in spin space. We introduce the unitary operator J_S via

$$\begin{aligned} J_S c_{m\sigma}^{(\dagger)} J_S^{\dagger} &= c_{m-\sigma}^{(\dagger)}, \\ J_S d_{\sigma}^{(\dagger)} J_S^{\dagger} &= d_{-\sigma}^{(\dagger)}. \end{aligned} \quad (9.18)$$

Given that the Hamiltonian (9.15) transforms according to

$$J_S H_{\text{SIAM}} J_S^{\dagger} = H_{\text{SIAM}}, \quad (9.19)$$

we find the following symmetry of the Green function,

$$G_{\text{local},\sigma}^{\text{SIAM}}(\omega < 0) = \lim_{\eta \searrow 0} \langle J_S^{\dagger} J_S d_{\sigma}^{\dagger} J_S^{\dagger} J_S (\omega + (H_{\text{SIAM}} - \tilde{E}_0(L)) - i\eta)^{-1} J_S^{\dagger} J_S d_{\sigma} J_S^{\dagger} J_S \rangle \quad (9.20)$$

$$= \lim_{\eta \searrow 0} \langle d_{-\sigma}^{\dagger} (J_S [\omega + (H_{\text{SIAM}} - \tilde{E}_0(L)) - i\eta] J_S^{\dagger})^{-1} d_{-\sigma} \rangle \quad (9.21)$$

$$= G_{\text{local},-\sigma}^{\text{SIAM}}(\omega < 0). \quad (9.22)$$

It therefore suffices to calculate the Green function of one spin species. Then, we have

$$G_{\text{local}}^{\text{SIAM}}(\omega) = \sum_{\sigma} G_{\text{local},\sigma}^{\text{SIAM}}(\omega) = 2G_{\text{local},\sigma}^{\text{SIAM}}(\omega). \quad (9.23)$$

In particular, the z -component of the total spin is preserved, and we may calculate the Green function (9.16) as the expectation value in the state

$$|\Psi\rangle := \frac{1}{\sqrt{2}}(|\Psi_{\uparrow}\rangle + |\Psi_{\downarrow}\rangle), \quad (9.24)$$

because the cross terms $\langle \Psi_{\sigma} | R | \Psi_{-\sigma} \rangle$ do not contribute. Here, R denotes the resolvent operator in (9.16). The factor of $1/\sqrt{2}$ is included for normalization. The parameters $V_{\mathbf{k}}$ and $\varepsilon_{\mathbf{k}}$ of the SIAM have to be self-consistently fixed, such that the SIAM describes the same physics as the Hubbard model on the infinitely connected Bethe lattice. According to (6.49), self-consistency is achieved, if, for $t = 1$, $G_{\text{local},\sigma}^{\text{SIAM}}(\omega) = \Delta(\omega)$ with the hybridization function (4.19). Due to the symmetries (9.9e) and (9.22) we can restrict ourselves in the following to the Green function

$$G_{\text{SIAM}}(\omega < 0) = \langle \Psi | d_{\uparrow}^{\dagger} (\omega + H_{\text{SIAM}} - \tilde{E}_0(L) - i\eta)^{-1} d_{\uparrow} | \Psi \rangle. \quad (9.25)$$

9.2.2. Chain Geometry of the SIAM

The SIAM (9.15) describes the coupling of an impurity with a (continuous) band or ‘bath’ of single-particle states. The first step towards a solution consists of discretizing the model.

SIAM in Star Geometry The particular discretization scheme is not important for this thesis. For details, the reader may consult [126]. In principle, energy intervals of the band are presented by individual levels ξ_m . The hybridization between these levels and the impurity level is discretized accordingly. The result, as depicted in 9.2a, reads

$$H_{\text{SIAM}} = \sum_{m,\sigma} \xi_m a_{m\sigma}^\dagger a_{m\sigma} + \sum_{m,\sigma} V_m (a_{m\sigma}^\dagger d_\sigma + d_\sigma^\dagger a_{m\sigma}) + U(n_{d\uparrow} - 1/2)(n_{d\downarrow} - 1/2). \quad (9.26)$$

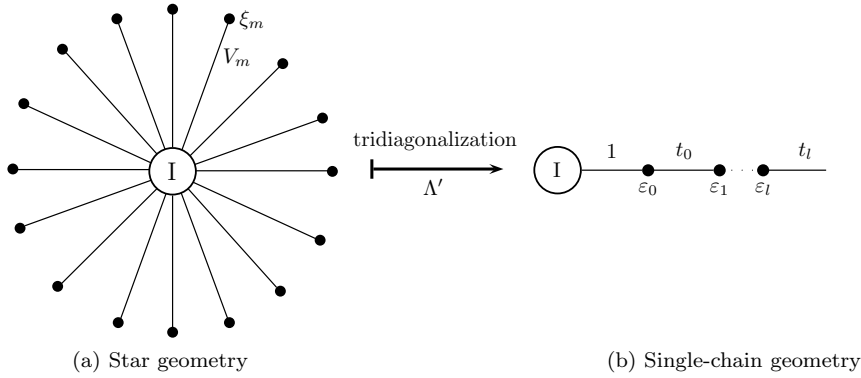


Figure 9.2.: Mapping of the discretized SIAM in star geometry to a semi-infinite chain.

Mapping of the SIAM onto a Single Chain Every method for solving the SIAM at zero temperature begins with mapping the discretized model (9.26) to a semi-infinite, one-dimensional chain [126]. By defining

$$\gamma_{0\sigma}^{(\dagger)} := \sum_{m=0}^{\infty} V_m a_{m\sigma}^{(\dagger)}, \quad (9.27)$$

we may write the hybridization part of (9.26) as

$$H_{\text{hyb}} = \sum_{\sigma} (d_{\sigma}^\dagger \gamma_{0\sigma} + \gamma_{0\sigma}^\dagger d_{\sigma}), \quad (9.28)$$

which describes the coupling of the impurity to the first site of the chain. Since the states, described by $\gamma_{0\sigma}$ and $\gamma_{0\sigma}^\dagger$, are not orthogonal to the band states described by $a_{m\sigma}$ and $a_{m\sigma}^\dagger$, one needs to find an orthogonalization transformation Λ' , as detailed in [126]. The result, as sketched in 9.2b, reads

$$\Lambda'^{\dagger} H_{\text{SIAM}} \Lambda' = \sum_{\sigma} \sum_{l=0}^{\infty} \{ \varepsilon_l \gamma_{l\sigma}^\dagger \gamma_{l\sigma} + t_l (\gamma_{l\sigma}^\dagger \gamma_{l+1\sigma} + \text{h.c.}) \} + H_{\text{hyb}} + U(n_{d\uparrow} - 1/2)(n_{d\downarrow} - 1/2). \quad (9.29)$$

The price we have to pay for the simplified geometry is the site-dependence of the electron transfer amplitudes t_l and of the on-site energies ε_l . The parameters t_l and ε_l of the one-dimensional chain are connected to the original parameters V_m and ξ_m by means of the transformation Λ' . Since we will not need the details of the mapping, we do not quote them here. The interested reader may find them in Ref. [126].

9. Theoretical Setup

Two-chain Geometry When we look at figure 9.1, we see that the lower and upper Hubbard bands are separated by an energy of the order $U - W$ and we realize that this decoupling of energy scales is lost after the mapping of the SIAM onto a single chain. It therefore seems desirable to introduce two discretized electron-baths which have to leading-order perturbation theory their centers of gravity located at $U/2$ and $-U/2$, respectively. This is sketched in figure 9.3a. Consequently, we map each group of discretized bath states to a single-chain separately, as has been proposed in [127]. These two chains are coupled via the impurity site, as can be seen in figure 9.3. The lower chain represents the LHB and analogously the upper chain the UHB. We call the transformation which achieves this Λ . The detailed form of the mapping Λ is not important for our calculations. In principle, it consists of two separate mappings of the electron baths onto single chains. The impurity connects these two chains. The transformed Hamiltonian reads

$$H_S := \Lambda H_{\text{SIAM}} \Lambda = H_0 + V, \quad (9.30)$$

$$H_0 := -\frac{U}{2} \sum_{l=0}^{\infty} (\alpha_{l\sigma}^\dagger \alpha_{l\sigma} - \beta_{l\sigma}^\dagger \beta_{l\sigma}) + U(n_{d\uparrow} - 1/2)(n_{d\downarrow} - 1/2), \quad (9.30a)$$

$$V := \sum_{l=-1}^{\infty} t_l \{ (\alpha_{l\sigma}^\dagger \alpha_{l+1\sigma} + \beta_{l\sigma}^\dagger \beta_{l+1\sigma}) + \text{h.c.} \} + \sum_{l=0}^{\infty} (\varepsilon_l + U/2) (\alpha_{l\sigma}^\dagger \alpha_{l\sigma} - \beta_{l\sigma}^\dagger \beta_{l\sigma}), \quad (9.30b)$$

with the abbreviations $t_{-1} := 1/\sqrt{2}$ and $\alpha_{-1\sigma}^{(\dagger)} = \beta_{-1\sigma}^{(\dagger)} := d_{\sigma}^{(\dagger)}$. The α -operators describe electrons in the lower chain and the β -operators those in the upper chain. Having in mind our later application of perturbation theory, we already separated the Hamiltonian into the starting Hamiltonian H_0 , (9.30a), and the perturbation V , (9.30b). Due to particle-hole symmetry, the electron transfer amplitudes in the lower and upper chain are equal, $t_l^- = t_l^+$, and the on-site energies in the lower chain are the negative of those in the upper chain, $\varepsilon_l^- = -\varepsilon_l^+$.

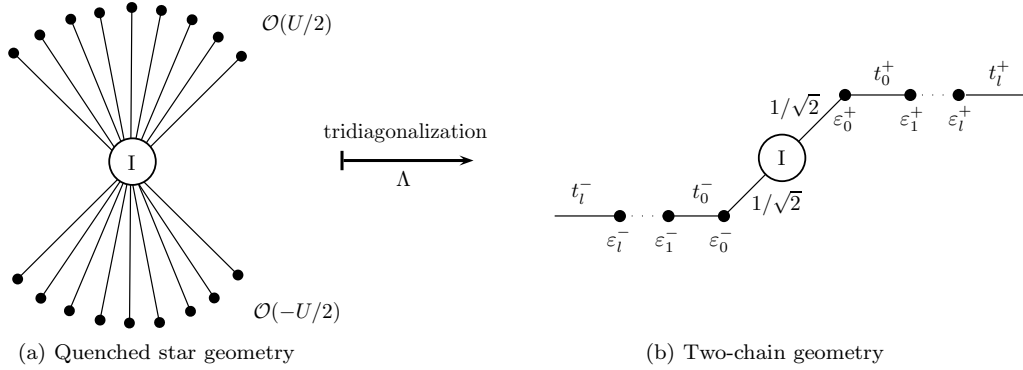


Figure 9.3.: Mapping of the discretized SIAM onto two semi-infinite chains, coupled via the impurity. The states which have in leading-order perturbation theory the energy $\mathcal{O}(U/2)$, are mapped onto the upper chain and analogously for the other group of states.

9.3. Application of Kato-Takahashi Perturbation Theory

In this section we present details on the application of Kato-Takahashi perturbation theory, as described in chapters 7 and 8, to calculate the Green function of the SIAM (9.25). For this purpose we split the SIAM Hamiltonian into two parts, the starting Hamiltonian H_0 and the perturbation V .

9.3.1. Starting Hamiltonian H_0

The starting Hamiltonian H_0 is the expression (9.30a) in two-chain geometry,

$$H_0 = -\frac{U}{2} \sum_{\substack{l=0 \\ \sigma}}^{\infty} (\alpha_{l\sigma}^\dagger \alpha_{l\sigma} - \beta_{l\sigma}^\dagger \beta_{l\sigma}) + U(n_{d\uparrow} - 1/2)(n_{d\downarrow} - 1/2). \quad (9.31)$$

Ground States at Half Band-Filling At half band-filling, H_0 has a two-fold degenerate ground state. We denote two linear independent ground-state vectors by

$$|\phi_\uparrow\rangle := \dots \alpha_{2\uparrow}^\dagger \alpha_{2\downarrow}^\dagger \alpha_{1\uparrow}^\dagger \alpha_{1\downarrow}^\dagger \alpha_{0\uparrow}^\dagger \alpha_{0\downarrow}^\dagger d_\uparrow^\dagger |\text{vac}\rangle \equiv |\dots \uparrow\downarrow \uparrow\downarrow \uparrow\downarrow \uparrow\downarrow \dots\rangle, \quad (9.32)$$

$$|\phi_\downarrow\rangle := \dots \alpha_{2\uparrow}^\dagger \alpha_{2\downarrow}^\dagger \alpha_{1\uparrow}^\dagger \alpha_{1\downarrow}^\dagger \alpha_{0\uparrow}^\dagger \alpha_{0\downarrow}^\dagger d_\downarrow^\dagger |\text{vac}\rangle \equiv |\dots \uparrow\downarrow \uparrow\downarrow \uparrow\downarrow \downarrow\uparrow \dots\rangle. \quad (9.33)$$

Note that the overall phase of the states is fixed: An electron on a particular site with spin up is placed to the left of an electron with spin down.

The ground-state energy at half filling is given by

$$\tilde{E}_0^{(0)}(L) = -(L-1)\frac{U}{2} - \frac{U}{4}. \quad (9.34)$$

Excited States at Half Band-Filling Starting with the two ground-state vectors (9.32) and (9.33), we can reach all excited states by applying one or a combination of the following processes successively, provided they are physically allowed:

- (a) Remove an α -electron and add an electron to an already singly occupied impurity site. The energy change ΔE of this process is

$$\Delta E = \frac{U}{4} - \left(-\frac{U}{4} - \frac{U}{2}\right) = U. \quad (9.35)$$

- (b) Remove an electron from a singly occupied impurity and add a β -electron:

$$\Delta E = \frac{U}{2} + \frac{U}{4} - \left(-\frac{U}{4}\right) = U. \quad (9.36)$$

- (c) Exchange an α - by a β -electron:

$$\Delta E = \frac{U}{2} - \left(-\frac{U}{2}\right) = U. \quad (9.37)$$

Note that due to particle-hole symmetry the process of removing an electron from a doubly occupied impurity site and adding a β -electron does not alter the energy.

With $P_j^{(0)}(L) : \mathcal{H} \rightarrow \mathcal{E}_i^{(0)}(L)$ denoting the projector onto the subspace of energy $\tilde{E}_j^{(0)}(L) = \tilde{E}_0^{(0)}(L) + jU$ we may write

$$H_0 = \tilde{E}_0^{(0)}(L) + U \sum_{j=1}^{\infty} j P_j^{(0)}(L), \quad (9.38)$$

which shows that the spectrum of H_0 at half filling is a ladder, starting at $\tilde{E}_0^{(0)}(L)$ with equidistant energy separations of magnitude U between adjacent levels.

9. Theoretical Setup

Spectrum of H_0 with One Particle less than Half Filling The $2L + 1$ ground-state vectors with $L - 1$ electrons and $S_{\text{total}}^z = 0$ are given by

$$|\phi_{-1}\rangle := \frac{1}{\sqrt{2}} |\dots \uparrow \uparrow \uparrow - \dots \rangle, \quad (9.39)$$

and, for $n \geq 0$,

$$|\phi_{nu}\rangle := \frac{1}{\sqrt{2}} |\dots \underbrace{\uparrow \uparrow \uparrow}_{\text{index } n} \dots \underbrace{\uparrow \uparrow \downarrow}_{\text{index } 0} - \dots \rangle, \quad (9.40)$$

$$|\phi_{nd}\rangle := \frac{1}{\sqrt{2}} |\dots \underbrace{\uparrow \downarrow \uparrow}_{\text{index } n} \dots \underbrace{\uparrow \uparrow \uparrow}_{\text{index } 0} - \dots \rangle. \quad (9.41)$$

The states with $S_{\text{total}}^z = -1$ which we will need, are denoted by

$$|\chi_n\rangle := \frac{1}{\sqrt{2}} |\dots \underbrace{\uparrow \downarrow \uparrow}_{\text{index } n} \dots \underbrace{\uparrow \uparrow \downarrow}_{\text{index } 0} - \dots \rangle \text{ with } n \geq 0. \quad (9.42)$$

Note that we include the square-root factor for convenience. The ground-state energy is given by $\tilde{E}_0^{(0)}(L - 1) = -(L - 1)U/2 + U/4$ and, with $P_j^{(0)}(L - 1)$ denoting the projector onto the subspace $\mathcal{E}_j^{(0)}(L - 1)$ of energy $\tilde{E}_j^{(0)}(L - 1) = \tilde{E}_0^{(0)}(L - 1) + jU$, we may write

$$H_0 = \tilde{E}_0^{(0)}(L - 1) + U \sum_{j=1}^{\infty} j P_j^{(0)}(L - 1), \quad (9.43)$$

which shows that the spectrum of H_0 at $N = L - 1$ is a ladder, too. It is shifted by $U/2$ to higher energies as compared to the case of half filling.

9.3.2. Perturbation V

As the perturbation V we take the part (9.30b) of the SIAM in two-chain geometry. We split it into the three distinct parts

$$V = V_0 + V_1 + V_2, \quad (9.44)$$

we discuss separately in the following.

Perturbation Part V_0 The part

$$V_0 = \frac{1}{\sqrt{2}} \sum_{\sigma} \{ (d_{\sigma}^{\dagger} \alpha_{0\sigma} + d_{\sigma}^{\dagger} \beta_{0\sigma}) + \text{h.c.} \} \quad (9.45)$$

describes the coupling of the impurity site to the two chains and is independent of the Hubbard interaction.

Perturbation Part V_1 This part describes the transfer of the electrons along the two chains,

$$V_1 = \sum_{\substack{l=0 \\ \sigma}}^{\infty} t_l \{ (\alpha_{l\sigma}^{\dagger} \alpha_{l+1\sigma} + \beta_{l\sigma}^{\dagger} \beta_{l+1\sigma}) + \text{h.c.} \}. \quad (9.46)$$

9.3. Application of Kato-Takahashi Perturbation Theory

V_1 does not connect the impurity site to the chains. Since the site-dependent hopping amplitudes have to be calculated self-consistently, they are functions of the interaction strength U . We assume the series expansion

$$t_l = \sum_{n=0}^{\infty} t_l^{(n)} \left(\frac{1}{U} \right)^n, \quad l \in \mathbb{N} \quad (9.47)$$

to be valid. This means that V_1 is dependent of U by itself, which we acknowledge by writing

$$V_1 = \sum_{n=0}^{\infty} V_1^{(n)} \left(\frac{1}{U} \right)^n \quad \text{with } V_1^{(n)} := \sum_{l,\sigma} t_l^{(n)} \{(\alpha_{l\sigma}^\dagger \alpha_{l+1\sigma} + \beta_{l\sigma}^\dagger \beta_{l+1\sigma}) + \text{h.c.}\}. \quad (9.48)$$

Perturbation Part V_2 Contrary to the other two parts, V_2 does not describe the motion of the electrons but accounts for the site-dependent energies ε_n as

$$V_2 = \sum_{l=0}^{\infty} \sum_{\sigma} \varepsilon_l (\alpha_{l\sigma}^\dagger \alpha_{l\sigma} - \beta_{l\sigma}^\dagger \beta_{l\sigma}). \quad (9.49)$$

For the same reason as in the case of the t_l , the parameters ε_l depend on U and we assume the validity of the series expansion

$$\varepsilon_l = \sum_{n=0}^{\infty} \varepsilon_l^{(n)} \left(\frac{1}{U} \right)^n, \quad l \in \mathbb{N}. \quad (9.50)$$

We therefore write

$$V_2 = \sum_{n=0}^{\infty} V_2^{(n)} \left(\frac{1}{U} \right)^n \quad \text{with } V_2^{(n)} := \sum_{l,\sigma} \varepsilon_l^{(n)} \{(\alpha_{l\sigma}^\dagger \alpha_{l\sigma} - \beta_{l\sigma}^\dagger \beta_{l\sigma}) + \text{h.c.}\}. \quad (9.51)$$

Note that it is vital to include the U -dependence of V_1 and V_2 . In a systematic expansion in $1/U$ the terms of $\mathcal{O}(U^{-n})$ contain corrections from all lower $\mathcal{O}(U^{-l})$ -terms containing $V_{1,2}^{n-l}$.

9.3.3. Systematic Expansion of the Green Function

According to chapter 8, there is an isometry $\Gamma_i(N)$ from the N -particle eigenspace $\mathcal{E}_i^{(0)}(N)$ of H_0 to the corresponding eigenspace $\mathcal{E}_i(N)$ of H_S ,

$$\Gamma_i(N) : \mathcal{E}_i^{(0)}(N) \rightarrow \mathcal{E}_i(N), \quad (9.52)$$

given in terms of Kato's projection operators by

$$\Gamma_i(N) = P_i P_i^{(0)} (P_i^{(0)} P_i P_i^{(0)})^{-\frac{1}{2}}. \quad (9.53)$$

$\Gamma_i(N)$ is unitary provided we may identify the isomorphic subspaces $\mathcal{E}_i^{(0)}(N)$ and $\mathcal{E}_i(N)$.

With these definitions we can write

$$|\Psi_\sigma\rangle = \Gamma_0(L) |\Phi_\sigma\rangle, \quad (9.54)$$

where $|\Phi_\sigma\rangle \in \mathcal{E}_0^{(0)}(L)$ and $|\Psi_\sigma\rangle \in \mathcal{E}_0(L)$. We introduce

$$|\Phi\rangle := \frac{1}{\sqrt{2}} (|\phi_\uparrow\rangle + |\phi_\downarrow\rangle) \quad (9.55)$$

to write (9.25) as

$$G_{\text{SIAM}}(\omega < 0) = \langle \Phi | \Gamma_0^\dagger(L) d_\uparrow^\dagger (\omega + H_S - \tilde{E}_0(L) - i\eta)^{-1} d_\uparrow \Gamma_0(L) | \Phi \rangle \quad (9.56)$$

which is an exact expression. The average can now be taken in the known ground states of H_0 . However, (9.56) is of little use because H_S is not yet projected onto the eigenspaces of H_0 . For lighter notation, we sometimes use the form $\Gamma_{0,L}$ instead of $\Gamma_0(L)$ and analogously for the other projectors.

9. Theoretical Setup

Separating the Contributions of the Sub-Bands We understand that the density of states of the Mott-Hubbard insulator at $W \ll U < \infty$ has the structure depicted in figure 9.1. There is the primary lower Hubbard sub-band, centered at $-U/2$, and there can be higher order sub-bands, centered at $-U/2 - nU$, $n \in \mathbb{N}$. We assume that

- (a) all these bands do not overlap,
- (b) are well separated in energy and, additionally, that
- (c) the degeneracies of the eigenspaces $\mathcal{E}_i^{(0)}$ are not lifted to all orders in perturbation theory, as is the case for the ground state [67].

With these assumptions the operators $P_{i,L-1}$ project onto those states, forming the i th lower sub-band. Since these projectors form a complete set,

$$\sum_i P_{i,L-1} = \mathbb{1}, \quad (9.57)$$

we may write the Green function (9.56) as

$$G_{\text{SIAM}}(\omega < 0) = \langle \Phi | \Gamma_{0,L}^\dagger d_\uparrow^\dagger (\omega + H_S - \tilde{E}_0(L) - i\eta)^{-1} d_\uparrow \Gamma_{0,L} | \Phi \rangle \quad (9.58a)$$

$$= \sum_{i,j} \langle \Phi | \Gamma_{0,L}^\dagger d_\uparrow^\dagger P_{i,L-1} (\omega + H_S - \tilde{E}_0(L) - i\eta)^{-1} P_{j,L-1} d_\uparrow \Gamma_{0,L} | \Phi \rangle \quad (9.58b)$$

$$\stackrel{(b)}{=} \sum_i \langle \Phi | \Gamma_{0,L}^\dagger d_\uparrow^\dagger P_{i,L-1} (\omega + H_S - \tilde{E}_0(L) - i\eta)^{-1} P_{i,L-1} d_\uparrow \Gamma_{0,L} | \Phi \rangle \quad (9.58c)$$

$$\stackrel{(8.11)}{=} \sum_i \langle \Phi | \Gamma_{0,L}^\dagger d_\uparrow^\dagger \Gamma_{i,L-1} \Gamma_{i,L-1}^\dagger (\omega + H_S - \tilde{E}_0(L) - i\eta)^{-1} \Gamma_{i,L-1} \Gamma_{i,L-1}^\dagger d_\uparrow \Gamma_{0,L} | \Phi \rangle \quad (9.58d)$$

$$\stackrel{(8.10)}{=} \sum_i \langle \Phi | \tilde{d}_{i\uparrow}^\dagger (\omega P_{i,L-1}^{(0)} + \tilde{h}_i - \tilde{E}_0(L) P_{i,L-1}^{(0)} - i\eta)^{-1} \tilde{d}_{i\uparrow} | \Phi \rangle, \quad (9.58e)$$

with the reduced operators

$$\tilde{d}_{i\sigma} := \Gamma_{i,L-1}^\dagger d_\sigma \Gamma_{0,L}, \quad (9.59a)$$

$$\tilde{d}_{i\sigma}^\dagger := (\tilde{d}_{i\sigma})^\dagger,$$

$$\tilde{h}_i := \Gamma_{i,L-1}^\dagger H_S \Gamma_{i,L-1}. \quad (9.59b)$$

For the primary Hubbard sub-band, we will drop the index $i = 0$ whenever possible.

Reduced Energy Operator As we explained in the last paragraph, we have to work with the reduced or ‘transformed energy operator’ in the resolvent of (9.58e),

$$\tilde{h}_i - \tilde{E}_0(L) P_{i,L-1}^{(0)} := \Gamma_{i,L-1}^\dagger H_S \Gamma_{i,L-1} - \tilde{E}_0(L) P_{i,L-1}^{(0)}. \quad (9.60)$$

The expansion of the related expression (C.73) reads

$$\Gamma_{i,N}^\dagger (H_S - \tilde{E}_i^{(0)}(N)) \Gamma_{i,N} = \sum_{n=1}^{\infty} \lambda^n \tilde{R}_{i,N}^{(n)}. \quad (9.61)$$

Taking the ground-state average at $N = L$, we can immediately derive the expansion of the ground-state energy of the SIAM at half filling,

$$\tilde{E}_0(L) = \tilde{E}_0^{(0)}(L) + \sum_{n=1}^{\infty} \lambda^n \tilde{E}_0^{[n]}(L), \quad (9.62)$$

9.4. Matrix Representation via the Lanczos Iteration

with

$$\tilde{E}_0^{[n]}(L) := \langle \phi_\uparrow | \tilde{R}_{0,L}^{(n)} | \phi_\uparrow \rangle \quad (9.63)$$

as the n th-order correction of the ground-state energy.

At $N = L - 1$ (9.61) becomes

$$\tilde{h}_i = \tilde{E}_i^{(0)}(L-1)P_{i,L-1}^{(0)} + \sum_{n=1}^{\infty} \lambda^n \tilde{R}_{i,L-1}^{(n)}, \quad (9.64)$$

which we insert together with the expansion of the ground-state energy (9.62) into (9.60), to obtain

$$\tilde{h}_i - \tilde{E}_0(L)P_{i,L-1}^{(0)} = (\tilde{E}_i^{(0)}(L-1) - \tilde{E}_0^{(0)}(L))P_{i,L-1}^{(0)} + \sum_{n=1}^{\infty} \lambda^n (\tilde{R}_{i,L-1}^{(n)} - \tilde{E}_0^{[n]}(L)P_{i,L-1}^{(0)}). \quad (9.65)$$

As explained in Sect. 9.3.1, $\tilde{E}_i^{(0)}(L-1) - \tilde{E}_0^{(0)}(L) = U/2 + iU$, thus

$$\tilde{h}_i - \tilde{E}_0(L)P_{i,L-1}^{(0)} = (U/2 + iU)P_{i,L-1}^{(0)} + \sum_{n=1}^{\infty} \lambda^n (\tilde{R}_{i,L-1}^{(n)} - \tilde{E}_0^{[n]}(L)P_{i,L-1}^{(0)}). \quad (9.66)$$

We introduce the abbreviation

$$\mathcal{L}_i := \tilde{h}_i - (\tilde{E}_0(L) + U/2 + iU)P_{i,L-1}^{(0)} = \sum_{n=1}^{\infty} \lambda^n \mathcal{L}_i^{(n)}, \quad (9.67)$$

where $\mathcal{L}_i^{(n)}$ can be read off (9.66) as

$$\mathcal{L}_i^{(n)} = \tilde{R}_{i,L-1}^{(n)} - \tilde{E}_0^{[n]}(L)P_{i,L-1}^{(0)}. \quad (9.68)$$

Then, we can express the local Green function (9.58e) in the form

$$G_{\text{SIAM}}(\omega < 0) = \lim_{\eta \searrow 0} \sum_i \langle \Phi | \tilde{d}_{i\uparrow}^\dagger ((\omega + U/2 + iU)P_{i,L-1}^{(0)} + \mathcal{L}_i - i\eta)^{-1} \tilde{d}_{i\uparrow} | \Phi \rangle. \quad (9.69)$$

9.4. Matrix Representation via the Lanczos Iteration

As we explain in Sect. 9.4.3, it is advantageous to represent the Green function (9.69) and the hybridization function (4.19) as suitable matrices. From a mathematical point of view, we employ a method originally invented by Lanczos [128] which transforms a symmetric matrix into a tridiagonal form. From a physical point of view these tridiagonal matrices can be interpreted as describing tight-binding Hamiltonians on infinite or semi-infinite chains. Especially Haydock and coworkers extended and applied Lanczos' method to map various models, in particular disordered systems and problems on surfaces, to tight-binding models in order to calculate the local electronic structure [129, 130].

Lanczos Iteration With the starting vector $|0\rangle$ and the Hermitian operator O , we use the following form of the Lanczos iteration:

$$|1\rangle = -O|0\rangle + a_0|0\rangle, \quad (9.70a)$$

$$|n+1\rangle = -O|n\rangle + a_n|n\rangle + b_{n-1}|n-1\rangle, \quad n \geq 1, \quad (9.70b)$$

where

$$a_n := \frac{\langle n|O|n\rangle}{\langle n|n\rangle}, \quad n \geq 0, \quad (9.70c)$$

$$b_{n-1} := \frac{\langle n-1|O|n\rangle}{\langle n-1|n-1\rangle} \equiv -\frac{\langle n|n\rangle}{\langle n-1|n-1\rangle}, \quad n \geq 1. \quad (9.70d)$$

9. Theoretical Setup

The matrix representation \mathfrak{D} of O within the Lanczos basis $\{|n\rangle\}$ is tridiagonal, symmetric, and we have

$$\mathfrak{D}_{nn} = \frac{\langle n|O|n\rangle}{\langle n|n\rangle} = a_n, \quad (9.71)$$

$$\mathfrak{D}_{n-1n} = \frac{\langle n-1|O|n\rangle}{\| |n-1\rangle \| \| |n\rangle \|} = -\sqrt{-b_n}. \quad (9.72)$$

We reserve fracture letters for the matrix representations of the corresponding operators in their Lanczos basis. Note that the parameters b_n can only be defined up to an arbitrary phase, which is a sign factor in the real case. Thus, the matrix \mathfrak{D}' , where we changed the sign of an arbitrary off-diagonal element and of its symmetric counterpart, still represents the same operator O ,

9.4.1. Hybridization Function

According to (D.4) of appendix D, we can write the hybridization function for negative frequencies as

$$\Delta(\omega < 0) = \lim_{\eta \searrow 0} \sum_{m,i} \frac{V_{m,i}^{-2}}{(\omega + U/2 + iU) - \bar{\xi}_{m,i}^- - i\eta} = \sum_i \Delta_i(\omega < 0), \quad (9.73)$$

where $\Delta_i(\omega)$ denotes the contribution of the i th sub-band. We cast each $\Delta_i(\omega)$ into matrix form by applying the Lanczos iteration with the starting vector

$$|0\rangle_i := \frac{1}{\sqrt{g_i}} \sum_{\xi_{m,i}^-} V_{m,i} c_{m\sigma}^\dagger |\text{vac}\rangle, \quad (9.74)$$

where the factor $1/\sqrt{g_i}$ comes from the normalization. With the Hamiltonian

$$H_{\Delta,i} = \sum_{m,\sigma} \bar{\xi}_{m,i}^- c_{m\sigma}^\dagger c_{m\sigma} \quad (9.75)$$

we may write

$$\Delta_i(\omega < 0) = \lim_{\eta \searrow 0} {}_i\langle 0 | ((\omega + U/2 + iU) - H_{\Delta,i} - i\eta)^{-1} | 0 \rangle_i \quad (9.76a)$$

$$\equiv \lim_{\eta \searrow 0} \left(((\omega + U/2 + iU)\mathbb{1} - \mathfrak{h}_{\Delta,i} - i\eta)^{-1} \right)_{00}. \quad (9.76b)$$

This form can be verified by noting that $H_{\Delta,i}^n |0\rangle = 1/\sqrt{g_i} \sum_{m,\sigma} V_{m,i} \bar{\xi}_{m,i}^{-n} c_{m\sigma}^\dagger |\text{vac}\rangle$.

According to (D.13) of appendix D, the starting vector $|0\rangle_i$ is identical to the first site, ${}^{(i)}\alpha_{0\sigma}^\dagger |\text{vac}\rangle$, of the i th lower chain in the multichain geometry. Thus, the Hamiltonian $H_{\Delta,i}$ can also be written as

$$H_{\Delta,i} := \sum_{\substack{l=0 \\ \sigma}}^{\infty} \left\{ {}^{(i)}t_l ({}^{(i)}\alpha_{l\sigma}^\dagger {}^{(i)}\alpha_{l+1\sigma} + \text{h.c.}) + {}^{(i)}\varepsilon_l ({}^{(i)}\alpha_{l\sigma}^\dagger {}^{(i)}\alpha_{l\sigma}) \right\}. \quad (9.77)$$

Then, the matrix $\mathfrak{h}_{\Delta,i}$ representing $H_{\Delta,i}$ in the Lanczos basis reads

$$\mathfrak{h}_{\Delta,i} = \begin{pmatrix} {}^{(i)}\varepsilon_0 & {}^{(i)}t_0 & & & \\ {}^{(i)}t_0 & {}^{(i)}\varepsilon_1 & {}^{(i)}t_1 & & \\ & {}^{(i)}t_1 & {}^{(i)}\varepsilon_2 & {}^{(i)}t_2 & \\ & & \ddots & \ddots & \ddots \end{pmatrix}, \quad (9.78)$$

where the entries not shown are zero.

9.4.2. Green Function

For the Green function

$$G_{\text{SIAM}}(\omega < 0) = \lim_{\eta \searrow 0} \sum_i \langle \Phi | \tilde{d}_{i\uparrow}^\dagger \left((\omega + U/2 + iU) P_{i,L-1}^{(0)} + \mathcal{L}_i - i\eta \right)^{-1} \tilde{d}_{i\uparrow} | \Phi \rangle, \quad (9.79)$$

we use $|\Psi_0\rangle = \tilde{d}_{i\uparrow} | \Phi \rangle$, (9.55), as the starting vector and \mathcal{L}_i , (9.67), as the operator O in the Lanczos iteration. In this way we obtain the matrix representation

$$G_{\text{SIAM}}(\omega < 0) = \lim_{\eta \searrow 0} \sum_i \left(\left((\omega + U/2 + iU) \mathbf{1} + \mathfrak{L}_i - i\eta \right)^{-1} \right)_{00}, \quad (9.80)$$

where the structure of \mathfrak{L}_i is identical for all i and is given by

$$\mathfrak{L}_i = \begin{pmatrix} e_0^{(i)} & \tau_0^{(i)} & & & & & \\ \tau_0^{(i)} & e_1^{(i)} & \tau_1^{(i)} & & & & \\ & \tau_1^{(i)} & e_2^{(i)} & \tau_2^{(i)} & & & \\ & & & \ddots & \ddots & \ddots & \\ & & & & & & \ddots \end{pmatrix}, \quad (9.81)$$

with parameters $e_n^{(i)}$, given by (9.71), and $\tau_n^{(i)}$, given by (9.72).

9.4.3. Self-Consistency Equation

For $t \equiv 1$ as our unit of energy, the self-consistency equation (6.49) reads

$$\lim_{\eta \searrow 0} \sum_i \left(\left((\omega + U/2 + iU) \mathbf{1} - \mathfrak{h}_{\Delta,i} - i\eta \right)^{-1} \right)_{00} = \lim_{\eta \searrow 0} \sum_i \left(\left((\omega + U/2 + iU) \mathbf{1} + \mathfrak{L}_i - i\eta \right)^{-1} \right)_{00}. \quad (9.82)$$

The two-chain setup is not sufficient to analyze the primary Hubbard sub-band and the higher-order sub-bands. One would run into the same problems which convinced us to use the two-chain geometry instead of the conventional single-chain setup, because we assumed that in the insulator the higher-order sub-bands are well separated in energy. As we discuss in more detail in appendix D, we should utilize a setup of the SIAM with $2n$ chains to analyze the primary LHB and $n - 1$ higher-order sub-bands. In this work we are mainly interested in the primary LHB which, as we show in Sect. D.2 of appendix D, is the only lower band with non-vanishing spectral weight up to $\mathcal{O}(1/U^4)$. Up to this order, we may therefore write

$$\lim_{\eta \searrow 0} \left(\left((\omega + U/2) \mathbf{1} - \mathfrak{h}_{\Delta} - i\eta \right)^{-1} \right)_{00} = \lim_{\eta \searrow 0} \left(\left((\omega + U/2) \mathbf{1} + \mathfrak{L} - i\eta \right)^{-1} \right)_{00} + \mathcal{O}\left(\frac{1}{U^4}\right), \quad \omega < 0, \quad (9.83)$$

where we have dropped the subscript $i = 0$. Reckoning (9.83), we realize that

$$\mathfrak{h}_{\Delta} = -\mathfrak{L} \quad (9.84)$$

is at least a sufficient condition to ensure the self-consistency.

Let us abbreviate $\omega + U/2 - i\eta \equiv a$ and let us consider the left-hand side of (9.83). According to Cramers rule [125], the 00-element, $\Delta(\omega < 0)$, of the inverse matrix can be calculated by means of

$$\Delta(\omega < 0) = \frac{\det_1(a\mathbf{1} - \mathfrak{h}_{\Delta})}{\det(a\mathbf{1} - \mathfrak{h}_{\Delta})}. \quad (9.85)$$

Here and in all subsequent formulae of this chapter, the limit $\lim_{\eta \searrow 0}$ is to be understood implicitly. The symbol $\det_n(\mathbf{m})$ denotes the determinant of the matrix \mathbf{m} , where the first n columns and rows have been deleted. Expanding the determinant $\det(a\mathbf{1} - \mathfrak{h}_{\Delta})$ according to its first column, we obtain

$$\det(a\mathbf{1} - \mathfrak{h}_{\Delta}) = (a - \varepsilon_0) \det_1(a\mathbf{1} - \mathfrak{h}_{\Delta}) - t_0^2 \det_2(a\mathbf{1} - \mathfrak{h}_{\Delta}), \quad (9.86)$$

9. Theoretical Setup

which leads with (9.85) to

$$\Delta(\omega < 0) = \frac{1}{(a - \varepsilon_0) - t_0^2 \frac{\det_2(a\mathbb{1} - \mathfrak{h}_\Delta)}{\det_1(a\mathbb{1} - \mathfrak{h}_\Delta)}}. \quad (9.87)$$

Generalizing by induction, we obtain the continued fraction

$$\Delta(\omega < 0) = \frac{1}{(\omega + U/2 - i\eta - \varepsilon_0) - \frac{t_0^2}{(\omega + U/2 - i\eta - \varepsilon_1) - \frac{t_1^2}{(\omega + U/2 - i\eta - \varepsilon_2) + \dots}}}. \quad (9.88)$$

Expanding the right-hand side of (9.83) in the same way,

$$G_{\text{SIAM}}(\omega < 0) = \frac{1}{(\omega + U/2 - i\eta + e_0) - \frac{\tau_0^2}{(\omega + U/2 - i\eta + e_1) - \frac{\tau_1^2}{(\omega + U/2 - i\eta + e_2) + \dots}}}, \quad (9.89)$$

we see that we obtain equality between these two continued fractions for all $\omega < 0$, and therefore self-consistency, only if for all $n \in \mathbb{N}$

$$\varepsilon_n = -e_n \quad (9.90a)$$

and

$$|t_n| = |\tau_n| \quad (9.90b)$$

holds. We already remarked that the off-diagonal Lanczos parameters are only defined up to a sign factor and, consequently, we find that (9.84) is a necessary condition for self-consistency, too.

Consequently, our self-consistency condition up to fourth order in $1/U$ reads

$$\begin{pmatrix} \varepsilon_0 & t_0 & & & \\ t_0 & \varepsilon_1 & t_1 & & \\ & t_1 & \varepsilon_2 & t_2 & \\ & & \ddots & \ddots & \ddots \end{pmatrix} = - \begin{pmatrix} e_0 & \tau_0 & & & \\ \tau_0 & e_1 & \tau_1 & & \\ & \tau_1 & e_2 & \tau_2 & \\ & & \ddots & \ddots & \ddots \end{pmatrix}. \quad (9.91)$$

Note that this is a vast simplification because, due to the matrix structure, we only have to equate numbers and not functions. Since all our calculations are implicitly done in the thermodynamic limit, there are countably infinite many parameters to fix. Due to locality of the Hubbard interaction, as we prove by induction in appendix E up to third order in $1/U$, there is an index l_n in n th order perturbation theory, such that the Lanczos parameters τ_m and e_m become constant for $m > l_n$.

*Achtung! Jetzt gibt es nur zwei Möglichkeiten:
Entweder es funktioniert oder es funktioniert nicht.*

Lukas in **Jim Knopf und Lukas, der Lokomotivführer** by Michael Ende

10

Results

In this chapter we finally present our results. We start by giving the solution to the DMFT self-consistency equation, (9.91), up to and including third order in $1/U$. We show explicitly how to obtain the self-consistent parameters ε_l and t_l of the effective SIAM in two-chain geometry, (9.30), to lowest order in $1/U$. We defer the detailed calculations for higher orders, being highly technical and rather tedious, to appendix E. Here, we restrict ourselves to some remarks on the higher-order calculations, but we do not go into detail.

Having obtained the parameters, the remaining single-particle scattering problem is defined on a one-dimensional, semi-infinite chain. We obtain the Green function of the problem which, due to the self-consistency, is identical with the Hubbard Green function. First, we solve the scattering problem by expanding its Green function systematically in $1/U$. However, since the scattering problem involves an *attractive* potential, we have to include the resonance contribution, a non-perturbative effect which is always present in such a situation. Therefore, we also provide the exact solution of the scattering problem. After having obtained the Green function, we derive the formulae for the single-particle gap Δ_C and the density of states. Then, we compare our results for the single-particle gap and the density of states with the DDMRG data of Ref. [131]. We finish the chapter with a comparison of our Green function with numerical data obtained via a Quantum Monte Carlo (QMC) analysis [132].

We perform all calculations with the unit of energy given in terms of the electron transfer amplitude t , see (9.1), which implies that we set $t \equiv 1$. As a consequence, the bare bandwidth reads $W = 4$.

10.1. Solution of the Self-Consistency Equation

10.1.1. Calculations to Leading Order

Transformed Ground-State Vector

We recall that $|\phi_\uparrow\rangle$ and $|\phi_\downarrow\rangle$ denote the ground states of the SIAM in two-chain geometry at $U = 0$, (9.30a). They are given by

$$|\phi_\uparrow\rangle = |\dots \uparrow \uparrow \uparrow \uparrow \uparrow \dots\rangle, \quad (10.1)$$

$$|\phi_\downarrow\rangle = |\dots \downarrow \downarrow \downarrow \downarrow \downarrow \dots\rangle. \quad (10.2)$$

We use Takahashi's operator $\Gamma(L) \equiv \Gamma_L$, (C.72) of appendix C, to relate the ground state $|\Psi_\sigma\rangle$ of the interacting SIAM H_S , see (9.30), with the non-interacting ground state $|\phi_\sigma\rangle$ of H_0 and define

$$|\Psi_\sigma\rangle = \Gamma_L |\phi_\sigma\rangle = \sum_{n=0}^{\infty} \left(\frac{1}{U}\right)^n |\Psi_\sigma^{(n)}\rangle. \quad (10.3)$$

10. Results

Here $|\Psi_\sigma^{(n)}\rangle := \Gamma_L^{(n)} |\phi_\sigma\rangle$, where $\Gamma_L^{(n)}$ can be found in Sect. C.3.2 of appendix C. With the simplifications of Sect. C.3.1 at half filling, we find to leading order in $1/U$ that $\Gamma_L = P + \mathcal{O}(1/U)$. This implies that the exact ground state reads

$$|\Psi_\sigma\rangle = |\phi_\sigma\rangle + \mathcal{O}(1/U). \quad (10.4)$$

Calculation of $|\bar{\Psi}_\sigma\rangle$

Defining the state

$$|\bar{\Psi}_\sigma\rangle := d_\uparrow |\Psi_\sigma\rangle = \sum_{n=0}^{\infty} \left(\frac{1}{U}\right)^n |\bar{\Psi}_\sigma^{(n)}\rangle, \quad (10.5)$$

we obtain

$$|\bar{\Psi}_\uparrow^{(0)}\rangle = d_\uparrow |\phi_\uparrow\rangle = |\dots \uparrow \uparrow \uparrow \dots\rangle = \sqrt{2} |\phi_{-1}\rangle, \quad (10.6)$$

$$|\bar{\Psi}_\downarrow^{(0)}\rangle = d_\uparrow |\phi_\downarrow\rangle = 0. \quad (10.7)$$

Starting Vector for the Lanczos Iteration

The starting vector $|\Psi_0\rangle$ for the Lanczos tridiagonalization is given by

$$|\Psi_0\rangle = \Gamma_{L-1}^\dagger d_\uparrow \Gamma_L |\Phi\rangle, \quad (10.8)$$

where $|\Phi\rangle = 1/\sqrt{2}(|\phi_\uparrow\rangle + |\phi_\downarrow\rangle)$. With (C.72) of appendix C we find to leading order that the projector $\Gamma_{L-1} = P + \mathcal{O}(1/U)$. Together with equations (10.6) and (10.7) we may write the starting vector as

$$|\Psi_0\rangle = |\phi_{-1}\rangle + \mathcal{O}(1/U). \quad (10.9)$$

Leading-Order Correction of the Ground-State Energy

The expansion of the ground-state energy $\tilde{E}_0(L)$ is given in (9.62). With the notation of Sect. C.3, the leading-order correction at half filling is given by

$$\tilde{E}_0^{[0]}(L) = \langle \phi_\uparrow | R_L^{(0)} | \phi_\uparrow \rangle. \quad (10.10)$$

Note that this correction is not the ground-state energy of H_0 which we denote by $\tilde{E}_0^{(0)}$. It is rather a consequence of the expansion (9.50), as detailed in Sect. 9.3, and we show in this chapter that for our model there is no correction to leading order in $1/U$. Looking at (C.73) we see that at arbitrary filling, $R^{(0)}$ is given by

$$R^{(0)} = P(V_0 + V_1^{(0)} + V_2^{(0)})P, \quad (10.11)$$

which can be simplified at half band-filling to read, see (C.78),

$$R_L^{(0)} = \xi^{(0)} P, \quad (10.12)$$

where $\xi^{(0)} := 2 \sum_{l \in \text{chain}}^{\text{lower}} \varepsilon_l^{(0)}$. Here $\varepsilon_l^{(0)}$ denotes the leading-order coefficient in $1/U$ of the on-site energy ε_l , see (9.50). Since the state $|\phi_\uparrow\rangle$ is normalized, we finally obtain

$$\tilde{E}_0^{[0]} = \xi^{(0)}. \quad (10.13)$$

Operator for the Lanczos Procedure

As we showed in chapter 9 for the calculation of the matrix representation of the Green function, the operator

$$\mathcal{L} = \sum_{n=0}^{\infty} \left(\frac{1}{U}\right)^n \mathcal{L}^{(n)} \quad (10.14)$$

with $\mathcal{L}^{(n)} = R_{L-1}^{(n)} - \tilde{E}_0^{[n]}P$ has to be tridiagonalized. Using equation (10.13) and equation (C.73) of appendix C, we find to leading order in $1/U$ that

$$\mathcal{L}^{(0)} = R_{L-1}^{(0)} - \tilde{E}_0^{[0]}(L)P \quad (10.15a)$$

$$= P(V_0 + V_1^{(0)} + V_2^{(0)})P - \xi^{(0)}P \quad (10.15b)$$

and, thus,

$$\mathcal{L}^{(0)} = P\bar{V}_0P + P(V_2^{(0)} - \xi^{(0)})P, \quad \bar{V}_0 := V_0 + V_1^{(0)}. \quad (10.16)$$

Lanczos Iteration to Leading Order

In order to obtain the parameters ε_l and t_l to leading order, we have to use the self-consistency equation (9.91). This necessitates to calculate the Lanczos basis $\{|\Psi_n\rangle\}$ of the operator \mathcal{L} , as described in detail in Sect. 9.4. To perform the Lanczos iteration, we need to calculate the effect of \mathcal{L} on the states which will appear during this iteration. To keep the notation as simple as possible, we have introduced in Sect. E.1 of appendix E some abbreviations for frequently appearing states. Here, we show by means of a few examples, how to work with the operators of the perturbation theory at hand. In appendix E we present the calculations up to third order in $1/U$ in detail.

Application of $\mathcal{L}^{(0)}$ As a first example consider the application of $P(V_0 + V_1^{(0)})P$ to $|\phi_{-1}\rangle$ which is one of the ground states of H_0 at $N = L - 1$. The first step is the application of P , which projects onto the ground states of H_0 at $N = L - 1$,

$$P(V_0 + V_1^{(0)})P|\phi_{-1}\rangle = P(V_0 + V_1^{(0)})P\frac{1}{\sqrt{2}}|\dots\uparrow\uparrow\uparrow\uparrow\text{---}\rangle \quad (10.17a)$$

$$= P(V_0 + V_1^{(0)})\frac{1}{\sqrt{2}}|\dots\uparrow\uparrow\uparrow\uparrow\text{---}\rangle. \quad (10.17b)$$

With V_1 given by (9.48), we realize that without a hole in the lower chain, there can be no contribution from V_1 . V_0 , (9.45), represents the coupling part of the Hamiltonian H_S , joining the impurity site and the chains. In the state $|\phi_{-1}\rangle$ either the electron with spin down or with spin up can jump from the first site of the lower chain to the impurity site. Due to the fermionic algebra, we need to include a minus sign when the electron with spin up jumps because it has to change places with the down-spin electron first. We therefore obtain the state

$$P(V_0 + V_1^{(0)})P|\phi_{-1}\rangle = P\frac{1}{2}\{|\dots\uparrow\uparrow\uparrow\downarrow\text{---}\rangle - |\dots\uparrow\uparrow\downarrow\uparrow\text{---}\rangle\}. \quad (10.17c)$$

10. Results

Note that we have described the process rather figuratively. With V_0 and $|\phi_{-1}\rangle$ given in second-quantized form, e.g. (9.32), we can derive the same results purely algebraically, only relying on the fundamental fermionic anti-commutation relations. At last, P checks whether the state belongs to the ground state of H_0 which is the case for both states here,

$$P(V_0 + V_1^{(0)})P|\phi_{-1}\rangle = \frac{1}{2} \{ |\dots \uparrow\uparrow \uparrow\uparrow \uparrow \downarrow \text{---} \rangle - |\dots \uparrow\uparrow \uparrow\uparrow \downarrow \uparrow \text{---} \rangle \} \quad (10.17d)$$

$$= |\gamma_0\rangle. \quad (10.17e)$$

The application of $V_2^{(0)}$ is even easier because it is diagonal in the states we are working with and which are all eigenstates of the local number operators. According to (9.51), V_2 provides a factor of $\varepsilon_l / -\varepsilon_l$ for every electron on site l in the lower/upper chain,

$$PV_2^{(0)}P|\phi_{-1}\rangle = PV_2^{(0)}P \frac{1}{\sqrt{2}} |\dots \uparrow\uparrow \uparrow\uparrow \uparrow \text{---} \rangle \quad (10.18a)$$

$$= 2 \sum_{\substack{l \in \text{lower} \\ \text{chain}}} \varepsilon_l^{(0)} |\phi_{-1}\rangle \quad (10.18b)$$

$$= \xi^{(0)} |\phi_{-1}\rangle. \quad (10.18c)$$

In order to exemplify the action of the operator $PV_1^{(0)}P$, we apply it to the state $|\phi_{0u}\rangle$,

$$PV_1^{(0)}P|\phi_{0u}\rangle = PV_1^{(0)}P \frac{1}{\sqrt{2}} |\dots \uparrow\uparrow \uparrow\uparrow \uparrow \downarrow \text{---} \rangle \quad (10.19a)$$

$$= PV_1^{(0)} \frac{1}{\sqrt{2}} |\dots \uparrow\uparrow \uparrow\uparrow \uparrow \downarrow \text{---} \rangle. \quad (10.19b)$$

As there is no electron in the upper chain, the β -part of V_1 does not contribute. However, due to the hole at the first site in the lower chain, we get a contribution from the α -part. Since V_1 , as defined in (9.48), moves particles, we can describe the process as follows. The electron with spin down on the second site and, thus, index $l = 1$ can jump with hopping amplitude $t_0^{(0)}$ to the first site with index $l = 0$. Here, we have to interchange it with the up-spin electron due to our phase convention, see the discussion below (9.33), which produces a minus sign. The process continues for a spin-down electron from the third site which can jump to the second site and so on. Here, we are making use of the fact that all our calculations are implicitly understood to be carried out in the thermodynamic limit, such that there are no boundary contributions coming from the left site of the lower chain. Because V_1 does not couple the chain with the impurity, no hole motion to the right is possible in this case, and we obtain in the end

$$PV_1^{(0)}P|\phi_{0u}\rangle = -t_0^{(0)} \frac{1}{\sqrt{2}} |\dots \uparrow\uparrow \uparrow\uparrow \downarrow \text{---} \rangle \quad (10.19c)$$

$$= -t_0^{(0)} |\phi_{1u}\rangle. \quad (10.19d)$$

10.1. Solution of the Self-Consistency Equation

Contrary to the case of $|\phi_{0u}\rangle$, in the states $|\phi_{nu}\rangle$ with $n \geq 1$ we can shift the hole to the right as well,

$$PV_1^{(0)}P|\phi_{nu}\rangle = PV_1^{(0)}P\frac{1}{\sqrt{2}}|\dots\uparrow\uparrow\uparrow\uparrow\dots\uparrow\uparrow\downarrow\dots\rangle \quad (10.20a)$$

$$= P\frac{1}{\sqrt{2}}\{-t_n^{(0)}|\dots\uparrow\uparrow\uparrow\dots\uparrow\uparrow\downarrow\dots\rangle \quad (10.20b)$$

$$-t_{n-1}^{(0)}|\dots\uparrow\uparrow\uparrow\dots\uparrow\uparrow\downarrow\dots\rangle\}$$

$$= -t_n^{(0)}|\phi_{n+1u}\rangle - t_{n-1}^{(0)}|\phi_{n-1u}\rangle. \quad (10.20c)$$

Obviously, it is the presence of the impurity site which prohibits hole motion further to the right. As we show by example below, the operators which constitute \mathcal{L} act locally in a certain sense: If the hole in the lower chain has been shifted a certain distance from the impurity, the action of \mathcal{L} becomes stationary, i.e., identical for all states having the hole located further to the left.

As these examples demonstrate, it is straightforward to calculate the effect of $\mathcal{L}^{(0)}$ on the various states. The calculations can be found in Sect. E.5 of appendix E. Here, we only summarize the results.

Summary The action of $\mathcal{L}^{(0)}$ can be summarized as follows:

$$\mathcal{L}^{(0)}|\phi_{-1}\rangle = |\gamma_0\rangle, \quad (10.21a)$$

$$\mathcal{L}^{(0)}|\gamma_n\rangle = \begin{cases} |\phi_{-1}\rangle - \varepsilon_0^{(0)}|\gamma_0\rangle + t_0^{(0)}|\gamma_1\rangle & n = 0, \\ t_{n-1}^{(0)}|\gamma_{n-1}\rangle - \varepsilon_n^{(0)}|\gamma_n\rangle + t_n^{(0)}|\gamma_{n+1}\rangle & n \geq 1, \end{cases} \quad (10.21b)$$

$$\mathcal{L}^{(0)}|m_{nu}\rangle = \begin{cases} \frac{1}{2}|\phi_{-1}\rangle - \varepsilon_0^{(0)}|m_{0u}\rangle + t_0^{(0)}|m_{1u}\rangle & n = 0, \\ t_{n-1}^{(0)}|m_{n-1u}\rangle - \varepsilon_n^{(0)}|m_{nu}\rangle + t_n^{(0)}|m_{n+1u}\rangle & n \geq 1, \end{cases} \quad (10.21c)$$

$$\mathcal{L}^{(0)}|m_{nd}\rangle = \begin{cases} -\frac{1}{2}|\phi_{-1}\rangle - \varepsilon_0^{(0)}|m_{0d}\rangle + t_0^{(0)}|m_{1d}\rangle & n = 0, \\ t_{n-1}^{(0)}|m_{n-1d}\rangle - \varepsilon_n^{(0)}|m_{nd}\rangle + t_n^{(0)}|m_{n+1d}\rangle & n \geq 1. \end{cases} \quad (10.21d)$$

Note that the effect of $\mathcal{L}^{(0)}$ on all states with index $n \geq 1$ is identical. This is a consequence of the locality of the operator and remains true to all orders in perturbation theory. Only the value of the index n at which this happens increases with increasing order.

With the starting vector $|\Psi_0\rangle$ to leading order, (10.9), and the knowledge of the action of $\mathcal{L}^{(0)}$ we can perform the Lanczos iteration. Here, we explain how to perform the procedure on the basis of the first two iterations only. The complete iterations, including the proof by induction, can be found in Sect. E.6.1 of appendix E.

First Iteration

In the first iteration we determine the state

$$|\Psi_1\rangle := -\mathcal{L}|\Psi_0\rangle + e_0|\Psi_0\rangle \quad (10.22)$$

to leading order. First, we calculate

$$|\tilde{\Psi}_1^{(0)}\rangle := -\mathcal{L}^{(0)}|\Psi_0^{(0)}\rangle = -\mathcal{L}^{(0)}|\phi_{-1}\rangle \stackrel{(10.21a)}{=} -|\gamma_0\rangle, \quad (10.23)$$

which we summarize as

$$|\tilde{\Psi}_1\rangle = -|\gamma_0\rangle + \mathcal{O}(1/U). \quad (10.24)$$

10. Results

Next, we need to calculate

$$e_0 = \frac{\langle \Psi_0 | \mathcal{L} | \Psi_0 \rangle}{\langle \Psi_0 | \Psi_0 \rangle} = -2 \langle \Psi_0 | \tilde{\Psi}_1 \rangle + \mathcal{O}(1/U) = 2 \langle \phi_{-1} | \gamma_0 \rangle + \mathcal{O}(1/U) = 0 \quad (10.25)$$

and therefore

$$e_0 = \mathcal{O}(1/U) \stackrel{(9.91)}{\Rightarrow} \varepsilon_0^{(0)} = 0. \quad (10.26)$$

In the last step we made use of the self-consistency condition (9.91). As one can see, we perform the Lanczos iteration and, at the same time, use the self-consistency equation. This is a consequence of the matrix form of the self-consistency equation because matrices are identical if all their entries are. This property is of vital importance because we need the correct value of $\varepsilon_0^{(0)}$ in the next iteration. With (10.22) the first Lanczos vector reads

$$|\Psi_1\rangle = -|\gamma_0\rangle + \mathcal{O}(1/U). \quad (10.27)$$

It remains to calculate the hopping parameter

$$\tau_0 = \frac{\langle \Psi_0 | \mathcal{L} | \Psi_1 \rangle}{\langle \Psi_0 | \Psi_0 \rangle} = -2 \langle \tilde{\Psi}_1 | \Psi_1 \rangle + \mathcal{O}(1/U) = -2 \langle \gamma_0 | \gamma_0 \rangle + \mathcal{O}(1/U) = -1 + \mathcal{O}(1/U), \quad (10.28)$$

which results in

$$\tau_0 = -1 + \mathcal{O}(1/U) \stackrel{(9.91)}{\Rightarrow} t_0^{(0)} = 1. \quad (10.29)$$

Second Iteration

With the results of the last iteration we can calculate the second Lanczos state,

$$|\Psi_2\rangle := -\mathcal{L}|\Psi_1\rangle + e_1|\Psi_1\rangle + \tau_0|\Psi_0\rangle. \quad (10.30)$$

Since

$$|\tilde{\Psi}_2^{(0)}\rangle := -\mathcal{L}^{(0)}|\Psi_1^{(0)}\rangle = \mathcal{L}^{(0)}|\gamma_0\rangle \stackrel{(10.21b)}{=} |\phi_{-1}\rangle - \varepsilon_0^{(0)}|\gamma_0\rangle + t_0^{(0)}|\gamma_1\rangle, \quad (10.31)$$

we realize that we need the values of $\varepsilon_0^{(0)}$ and $t_0^{(0)}$ from the last iteration. With (10.26) and (10.29) we can write

$$|\tilde{\Psi}_2\rangle = |\phi_{-1}\rangle + |\gamma_1\rangle + \mathcal{O}(1/U). \quad (10.32)$$

Next, the parameter e_1 can be obtained via

$$e_1 = \frac{\langle \Psi_1 | \mathcal{L} | \Psi_1 \rangle}{\langle \Psi_1 | \Psi_1 \rangle} = -2 \langle \Psi_1 | \tilde{\Psi}_2 \rangle + \mathcal{O}(1/U) = 2 \langle \gamma_0 | (|\phi_{-1}\rangle + |\gamma_1\rangle) \rangle + \mathcal{O}(1/U) = 0, \quad (10.33)$$

and, thus,

$$e_1 = \mathcal{O}(1/U) \stackrel{(9.91)}{\Rightarrow} \varepsilon_1^{(0)} = 0. \quad (10.34)$$

This implies for the second Lanczos vector that

$$|\Psi_2^{(0)}\rangle = |\tilde{\Psi}_2^{(0)}\rangle + e_1^{(0)}|\Psi_1^{(0)}\rangle + \tau_0^{(0)}|\Psi_0^{(0)}\rangle = |\phi_{-1}\rangle + |\gamma_1\rangle - |\phi_{-1}\rangle \quad (10.35)$$

which therefore becomes

$$|\Psi_2\rangle = |\gamma_1\rangle + \mathcal{O}(1/U). \quad (10.36)$$

The hopping parameter

$$\tau_1 = \frac{\langle \Psi_1 | \mathcal{L} | \Psi_2 \rangle}{\langle \Psi_1 | \Psi_1 \rangle} = -2 \langle \tilde{\Psi}_2 | \Psi_2 \rangle + \mathcal{O}(1/U) = -1 + \mathcal{O}(1/U) \quad (10.37)$$

reads

$$\tau_1 = -1 + \mathcal{O}(1/U) \stackrel{(9.91)}{\Rightarrow} t_1^{(0)} = 1. \quad (10.38)$$

The remaining calculations, being straightforward, can be found in Sect. E.6.1 of appendix E and shall not be repeated here. The only (slight) complication is the inductive proof of the n th iteration.

Summary of the Results to Leading Order in $1/U$

To leading order, the matrix \mathfrak{h}_Δ , (9.78), is given by

$$\mathfrak{h}_\Delta = \begin{pmatrix} 0 & 1 & & & \\ 1 & 0 & 1 & & \\ & 1 & 0 & 1 & \\ & & \ddots & \ddots & \ddots \end{pmatrix} + \mathcal{O}\left(\frac{1}{U}\right), \quad (10.39)$$

which we recognize as the matrix representation of the simple tight-binding Hamiltonian

$$H_{\text{TB}'} = \sum_{l=0}^{\infty} (\alpha_l^\dagger \alpha_{l+1} + \alpha_{l+1}^\dagger \alpha_l) \quad (10.40)$$

with constant electron transfer amplitudes $t_l = 1$ and vanishing on-site energies $\varepsilon_l = 0$. It therefore does not surprise us that to leading order in $1/U$ the Green function and, thus, the density of states are identical with (shifted versions of) the free quantities. We prove this claim in Sect. 10.3.

10.1.2. Remarks on the Higher-Order Calculations

As we have already noted, we are not going into detail of the higher-order calculations here. However, as we mentioned in the last section, the action of the operator $\mathcal{L}^{(n)}$ becomes stationary: When the hole in the lower chain is moved sufficiently far from the impurity, say to site with index l_n , $\mathcal{L}^{(n)}$ acts on all states which have the hole at position $l \geq l_n$ as if there was no impurity site. From the calculations presented in Sect. C.3.2 of appendix C we see that $\mathcal{L}^{(n)}$ is build up of fundamental parts, namely

$$h_0 := P\bar{V}_0P, \quad (10.41a)$$

$$h_1 := PV_0SV_0P, \quad (10.41b)$$

$$h_2 := PV_0S\bar{V}_0SV_0P, \quad (10.41c)$$

$$h_3 := PV_0S\bar{V}_0S\bar{V}_0SV_0P. \quad (10.41d)$$

For completeness we include the expressions of $\mathcal{L}^{(n)}$ up to third order, see E.5.4 of appendix E,

$$\mathcal{L}^{(0)} = h_0 + PV_1^{(0)}P, \quad (10.42)$$

$$\mathcal{L}^{(1)} = -h_1 + P + PV_1^{(1)}P + P(V_2^{(1)} - \xi^{(1)})P, \quad (10.43)$$

$$\mathcal{L}^{(2)} = h_2 - \frac{1}{2}\{h_1h_0 + h_0h_1\} + PV_1^{(2)}P + P(V_2^{(2)} - \xi^{(2)})P, \quad (10.44)$$

$$\mathcal{L}^{(3)} = -h_3 - \frac{1}{2}\{h_2h_0 + h_0h_2\} - \frac{1}{2}\{h_1h_0^2 + h_0^2h_1\} + \frac{3}{2}P + PV_1^{(3)}P + P(V_2^{(3)} - \xi^{(3)})P. \quad (10.45)$$

They can be derived analogously to the lowest- and first-order expressions, as shown in appendix E. Note that (10.42) already includes the result $V_2^{(0)} \equiv 0$, derived in the last section and appendix E. From the defining equations of h_n and $\mathcal{L}^{(n)}$ we see that $\mathcal{L}^{(n)}$ contains parts which admit at most $n+1$ electron transfers. Thus, it is obvious that, whenever the hole in the lower chain is located at sites with index $l \geq n$ (remember that the first site has index zero), the impurity cannot be reached. The only exception to this rule is $\mathcal{L}^{(0)}$, where $l_0 = n+1 = 1$.

Examples

For a better understanding of the explanations above, we consider some examples here.

10. Results

$\mathcal{L}^{(1)}$

Consider the application of $-h_1$ to $|\phi_{0u}\rangle$,

$$-PV_0SV_0P|\phi_{0u}\rangle = -PV_0SV_0P\frac{1}{\sqrt{2}}|\dots\uparrow\uparrow\uparrow\downarrow\dots\rangle, \quad (10.46a)$$

where after the application of V_0 , the operator S checks whether the state is an excited one,

$$-PV_0SV_0P|\phi_{0u}\rangle = -PV_0\frac{1}{2}\{|\dots\uparrow\uparrow\uparrow\downarrow\dots\rangle + |\dots\uparrow\uparrow\downarrow\dots\rangle\}. \quad (10.46b)$$

Now V_0 has to be applied in order to return to a ground state,

$$-PV_0SV_0P|\phi_{0u}\rangle = -\frac{1}{2\sqrt{2}}\{2|\dots\uparrow\uparrow\uparrow\downarrow\dots\rangle - |\dots\uparrow\uparrow\downarrow\uparrow\dots\rangle\} \quad (10.46c)$$

$$= -|\phi_{0u}\rangle + \frac{1}{2}|\phi_{0d}\rangle. \quad (10.46d)$$

Note that, due the presence of the impurity, a spin-flip process has occurred. The effect of the other parts of $\mathcal{L}^{(1)}$ is given by

$$P|\phi_{0u}\rangle = |\phi_{0u}\rangle, \quad (10.46e)$$

$$PV_1^{(1)}P|\phi_{0u}\rangle = -t_0^{(1)}|\phi_{1u}\rangle, \quad (10.46f)$$

where, due to the presence of the impurity, there is no motion to the right and

$$P(V_2^{(1)} - \xi^{(1)})P|\phi_{0u}\rangle = -\varepsilon_0^{(1)}|\phi_{0u}\rangle, \quad (10.46g)$$

so that the effect of $\mathcal{L}^{(1)}$ on $|\phi_{0u}\rangle$ reads

$$\mathcal{L}^{(1)}|\phi_{0u}\rangle = -\varepsilon_0^{(1)}|\phi_{0u}\rangle - t_0^{(1)}|\phi_{1u}\rangle + \frac{1}{2}|\phi_{0d}\rangle. \quad (10.47)$$

Next, consider its effect on $|\phi_{nu}\rangle$, $n \geq 1$, where the hole is at least at the second site,

$$-PV_0SV_0P|\phi_{nu}\rangle = -PV_0SV_0P\frac{1}{\sqrt{2}}|\dots\uparrow\uparrow\uparrow\dots\uparrow\uparrow\downarrow\dots\rangle \quad (10.48a)$$

$$= -PV_0\frac{1}{2}\{|\dots\uparrow\uparrow\uparrow\dots\uparrow\uparrow\downarrow\dots\rangle - |\dots\uparrow\uparrow\uparrow\dots\uparrow\downarrow\uparrow\dots\rangle\}. \quad (10.48b)$$

10.1. Solution of the Self-Consistency Equation

In all intermediate states the first site in the lower chain is always at least singly occupied. Thus, no spin-flip processes can occur and we finally find

$$-PV_0SV_0P|\phi_{nu}\rangle = -|\phi_{nu}\rangle. \quad (10.48c)$$

Concerning the other parts of $\mathcal{L}^{(1)}$, we can state that only the effect of V_1 deviates from the last case,

$$P|\phi_{nu}\rangle = |\phi_{nu}\rangle, \quad (10.48d)$$

$$PV_1^{(1)}P|\phi_{nu}\rangle = -t_{n-1}^{(1)}|\phi_{n-1u}\rangle - t_n^{(1)}|\phi_{n+1u}\rangle, \quad (10.48e)$$

$$P(V_2^{(1)} - \xi^{(1)})P|\phi_{nu}\rangle = -\varepsilon_n^{(1)}|\phi_{nu}\rangle, \quad (10.48f)$$

and we finally obtain

$$\mathcal{L}^{(1)}|\phi_{nu}\rangle = -t_{n-1}^{(1)}|\phi_{n-1u}\rangle - \varepsilon_n^{(1)}|\phi_{nu}\rangle - t_n^{(1)}|\phi_{n+1u}\rangle, \quad n \geq 1. \quad (10.49)$$

$\mathcal{L}^{(2)}$

As a second example we consider the application of $\mathcal{L}^{(2)}$ to the states $|\phi_{nu}\rangle$. Since the effects of h_0 and h_1 are already known, we only show the behavior of h_2 .

$|\phi_{0u}\rangle$

$$h_2|\phi_{0u}\rangle = PV_0S\bar{V}_0SV_0P|\phi_{0u}\rangle \quad (10.50a)$$

$$= \frac{1}{2}PV_0S\bar{V}_0\left\{|\dots \uparrow \uparrow \uparrow - \downarrow - \dots\rangle + |\dots \uparrow \uparrow - \uparrow - \dots\rangle\right\} \quad (10.50b)$$

$$= \frac{1}{2}PV_0\left\{-|\dots \uparrow \uparrow \uparrow - \downarrow - \dots\rangle + |\dots \uparrow \uparrow \downarrow \uparrow - \dots\rangle\right. \quad (10.50c)$$

$$\left. - |\dots \uparrow \downarrow \uparrow \uparrow - \dots\rangle + \text{terms not contributing (t.n.c.)}\right\}$$

$$= -\frac{1}{2}|\phi_{1u}\rangle - \frac{1}{2}|\phi_{1u}\rangle + \frac{1}{2}|\phi_{1d}\rangle = -|\phi_{1u}\rangle + \frac{1}{2}|\phi_{1d}\rangle \quad (10.50d)$$

With t.n.c. we abbreviate all those terms which cannot relax to a ground state by means of one-electron transfer.

$|\phi_{1u}\rangle$

$$h_2|\phi_{1u}\rangle = PV_0S\bar{V}_0SV_0P|\phi_{1u}\rangle \quad (10.51a)$$

$$= \frac{1}{2}PV_0S\bar{V}_0\left\{|\dots \uparrow \uparrow \uparrow - \downarrow - \dots\rangle - |\dots \uparrow \uparrow \downarrow \uparrow - \dots\rangle\right\} \quad (10.51b)$$

10. Results

$$= \frac{1}{2}PV_0 \left\{ - \left| \dots \uparrow \uparrow \uparrow \uparrow - \downarrow - \dots \right\rangle - \left| \dots \uparrow \uparrow \uparrow \uparrow - \downarrow - \dots \right\rangle \right. \quad (10.51c)$$

$$\left. + \left| \dots \uparrow \uparrow \downarrow \uparrow - \dots \right\rangle - \left| \dots \uparrow \uparrow - \uparrow - \dots \right\rangle + \text{t.n.c.} \right\}$$

$$= \frac{1}{2} \{ -|\phi_{2u}\rangle - |\phi_{0u}\rangle - |\phi_{2u}\rangle - |\phi_{0u}\rangle + |\phi_{0d}\rangle \} = -|\phi_{0u}\rangle - |\phi_{2u}\rangle + \frac{1}{2}|\phi_{0d}\rangle. \quad (10.51d)$$

For $n \geq 2$ there is no possibility for a spin-flip process and also the effect of the other operators is not influenced by the presence of the impurity.

We can therefore summarize

$$\mathcal{L}^{(2)}|\phi_{0u}\rangle = -\frac{3}{4\sqrt{2}}|\phi_{-1}\rangle - \varepsilon_0^{(2)}|\phi_{0u}\rangle - t_0^{(2)}|\phi_{1u}\rangle + \frac{1}{4}|\phi_{1d}\rangle, \quad (10.52)$$

$$\mathcal{L}^{(2)}|\phi_{1u}\rangle = -t_0^{(2)}|\phi_{0u}\rangle - \varepsilon_1^{(2)}|\phi_{1u}\rangle - t_1^{(2)}|\phi_{2u}\rangle + \frac{1}{4}|\phi_{0d}\rangle, \quad (10.53)$$

$$\mathcal{L}^{(2)}|\phi_{nu}\rangle = -t_{n-1}^{(2)}|\phi_{n-1u}\rangle - \varepsilon_n^{(2)}|\phi_{nu}\rangle - t_n^{(2)}|\phi_{n+1u}\rangle, \quad n \geq 2. \quad (10.54)$$

We have indicated all terms in red which stem from the presence of the impurity. These are especially due to the spin-flip processes, stemming from h_n but also due to the impossibility of shifting the hole from site with index $l = 0$ to the impurity with V_1 . Note that for $n \geq 2$, $\mathcal{L}^{(1)}$ and $\mathcal{L}^{(2)}$ both act like the same hopping operator (with different parameters).

The stationarity of $\mathcal{L}^{(n)}$ implies that the Lanczos parameters $e_l^{(n)}$ and $\tau_l^{(n)}$ and therefore the parameters $\varepsilon_l^{(n)}$ and $t_l^{(n)}$ of the effective SIAM become stationary. This is also proven up to third order in $1/U$ in appendix E.

10.1.3. Results up to Third Order

According to our calculations in Sect. E.6.1 to E.6.4 of appendix E, the on-site energies ε_l of the effective SIAM are given up to third order in $1/U$ by

$$\varepsilon_0 = \frac{14}{8U^3} + \mathcal{O}\left(\frac{1}{U^5}\right), \quad (10.55a)$$

$$\varepsilon_1 = \frac{1}{2U} + \frac{31}{8U^3} + \mathcal{O}\left(\frac{1}{U^5}\right), \quad (10.55b)$$

$$\varepsilon_l = \frac{1}{2U} + \frac{35}{8U^3} + \mathcal{O}\left(\frac{1}{U^5}\right) =: \bar{\varepsilon} \quad \forall l \geq 2, \quad (10.55c)$$

while the hopping amplitudes t_l read

$$t_0 = 1 + \frac{1}{8U^2} + \mathcal{O}\left(\frac{1}{U^4}\right), \quad (10.56a)$$

$$t_l = 1 + \frac{3}{8U^2} + \mathcal{O}\left(\frac{1}{U^4}\right) =: \bar{t} \quad \forall l \geq 1. \quad (10.56b)$$

Note that for all sites with index $l \geq 2$ the on-site energies are constant, $\varepsilon_{l \geq 2} = \bar{\varepsilon}$, and that for all sites with index $l \geq 1$ so are the electron transfer amplitudes, $t_{l \geq 1} = \bar{t}$. Additionally, we like to draw attention to the fact that the expansion (9.50) of the on-site energies contains odd powers of $1/U$ only. The corresponding expansion (9.47) of the electron transfer amplitudes on the other hand contains only even powers.

10.2. Impurity Scattering Model

With the results given in the last section, the matrix \mathfrak{h}_Δ reads

$$\mathfrak{h}_\Delta = \begin{pmatrix} \bar{\varepsilon} & \bar{t} & & & \\ \bar{t} & \bar{\varepsilon} & \bar{t} & & \\ & \bar{t} & \bar{\varepsilon} & \bar{t} & \\ & & & \ddots & \ddots & \ddots \end{pmatrix} + \begin{pmatrix} \varepsilon_0 - \bar{\varepsilon} & t_0 - \bar{t} & & & \\ t_0 - \bar{t} & \varepsilon_1 - \bar{\varepsilon} & 0 & & \\ & 0 & 0 & 0 & \\ & & & \ddots & \ddots & \ddots \end{pmatrix} =: \bar{\mathfrak{h}}_\Delta + \mathfrak{V}^*. \quad (10.57)$$

Here, we have introduced the matrix $\bar{\mathfrak{h}}_\Delta$ which is the representation of the tight-binding Hamiltonian

$$\bar{H}_{\text{TB}} := \sum_{\substack{n=0 \\ \sigma}}^{\infty} \{ \bar{t} (\alpha_{n\sigma}^\dagger \alpha_{n+1\sigma} + \text{h.c.}) + \bar{\varepsilon} \alpha_{n\sigma}^\dagger \alpha_{n\sigma} \} \quad (10.58)$$

in the states $|l\rangle = \alpha_{l\sigma}^\dagger |\text{vac}\rangle$, as discussed in Sect. 9.4.1. In the basis $\{|l\rangle\}$, the matrix \mathfrak{V}^* represents the one-particle potential

$$V^* := \sum_{\substack{n=0 \\ \sigma}}^1 \{ \varepsilon_n^* \alpha_{n\sigma}^\dagger \alpha_{n\sigma} + \delta_{n,0} t_n^* (\alpha_{n\sigma}^\dagger \alpha_{n+1\sigma} + \text{h.c.}) \} \quad (10.59)$$

with the abbreviations

$$\varepsilon_0^* := \varepsilon_0 - \bar{\varepsilon} = -\frac{1}{2U} - \frac{21}{8U^3} + \mathcal{O}\left(\frac{1}{U^5}\right), \quad (10.59a)$$

$$\varepsilon_1^* := \varepsilon_1 - \bar{\varepsilon} = -\frac{1}{2U^3} + \mathcal{O}\left(\frac{1}{U^5}\right), \quad (10.59b)$$

$$t_0^* := t_0 - \bar{t} = -\frac{1}{4U^2} + \mathcal{O}\left(\frac{1}{U^4}\right). \quad (10.59c)$$

Thus, \mathfrak{h}_Δ defines a single-particle problem with Hamiltonian

$$H_{\text{Scatter}} = \bar{H}_{\text{TB}} + V^* \quad (10.60)$$

on a semi-infinite chain. The perturbing potential V^* can be thought of as arising by substituting the first two orbitals in the lower chain for new ones with different energies and a new electron transfer amplitude between them. As the new orbitals have lower on-site energies, the potential is attractive. See figure 10.1 for a visualization. Thus, there is a scattering resonance within the band and perhaps a bound state outside of it. Note that we are working with a semi-infinite chain, we assume to extend to infinity to the left. This means that the wave functions of the electrons need to be identically zero to the right of the first site. This corresponds exactly to the case of s-wave scattering in three dimensions: Here, only the radial part matters which is also defined on the semi-infinite interval $[0, \infty[$. We know that in such a situation, there will only be a bound state if the potential is strong enough [81].

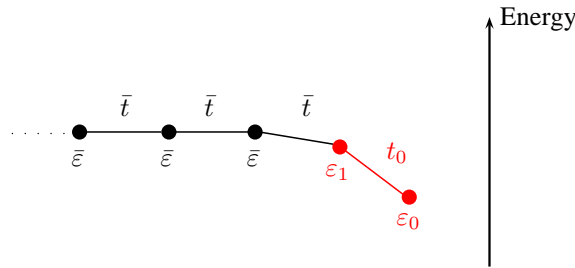


Figure 10.1.: Impurity scattering model to third order in $1/U$.

10.3. Green Function

As detailed in Sect. 9.2.1 the Green function of the primary lower Hubbard band is given in terms of the scattering model as

$$G_{\text{LHB},\sigma}(\omega) = \Delta(\omega) \stackrel{(9.76b)}{=} \lim_{\eta \searrow 0} \left(((\omega + U/2)\mathbb{1} - \mathfrak{h}_\Delta - i\eta)^{-1} \right)_{00} \quad (10.61)$$

$$\stackrel{(9.76a)}{=} \lim_{\eta \searrow 0} \langle 0 | ((\omega + U/2) - H_{\text{Scatter}} - i\eta)^{-1} | 0 \rangle.$$

As we discuss in Sect. F.3 of appendix F, we can write the last equation as

$$G_{\text{LHB},\sigma}(\omega) = \lim_{\eta \searrow 0} \langle 0 | (\tilde{\omega} - \bar{t}K - V^* - i\eta)^{-1} | 0 \rangle, \quad (10.62)$$

with the definitions

$$K := \sum_{\substack{n=0 \\ \sigma}}^{\infty} (\alpha_{n\sigma}^\dagger \alpha_{n+1\sigma} + \alpha_{n+1\sigma}^\dagger \alpha_{n\sigma}), \quad (10.62a)$$

$$V^* := \sum_{\substack{n=0 \\ \sigma}}^1 \{ \varepsilon_n^* \alpha_{n\sigma}^\dagger \alpha_{n\sigma} + \delta_{n,0} t_n^* (\alpha_{n\sigma}^\dagger \alpha_{n+1\sigma} + \text{h.c.}) \}, \quad (10.62b)$$

$$\tilde{\omega} := \omega + U/2 - \bar{\varepsilon}. \quad (10.62c)$$

Due to the simplicity of the scattering model (10.60), we can calculate its Green function (10.62) by perturbation theory as well as exactly. We have to keep in mind that the scattering model does only describe the physics of the infinite-dimensional Hubbard model up to third order in $1/U$. Thus, it may not seem appropriate to discuss the exact Green function of the scattering model but only its perturbative expansion up to third order. We remark on two issues.

- (a) A simple Taylor-expansion of (10.62), where we expand the energy denominator systematically in $1/U$, is out of the question. It would lead to a Taylor series of the Green function, every term of which would be a Green function of the atomic-limit Hamiltonian H_0 of the form

$$G(\omega) = \frac{1}{\omega - H_0}. \quad (10.63)$$

This implies that the information of the spectrum of H_{Hubbard} would be lost. What we actually need is a finite-order expansion of the self-energy, see Sect. A.3.1 of appendix A and [12]. Thus, when we expand (10.62), we have to make sure that we do not expand $\tilde{\omega}$.

- (b) Every expansion of the Green function (10.62) will not cover the resonance contribution due to the scattering potential, because this is a non-perturbative effect. Even if the scattering model does describe the physics of Hubbard model only down to some critical value of the on-site interaction U , the resonance will be part of that physics.

To cope with these two points we proceed as follows. In Sect. 10.3.1 we expand the Green function (10.62) in terms of the functions

$$\Delta_{lm}^{(0)}(\omega) := \lim_{\eta \rightarrow 0} \langle l | (\tilde{\omega} - \bar{t}K - i\eta)^{-1} | m \rangle \quad (10.64)$$

and obtain what we call ‘band-part contribution’ to the Green function. In Sect. 10.3.2 we use the expansion of the scattering potential V^* and solve the resulting equations for the Green function in each order exactly. We call this result the ‘full Green function’.

10.3.1. Band-Part Contribution

In the following subsection we expand the Green function (10.62) with the help of lemma (7.2.1),

$$(A - B)^{-1} = A^{-1} + A^{-1}B(A - B)^{-1}, \quad (10.65)$$

perturbatively by setting $A \equiv (\tilde{\omega} - \bar{t}K - i\eta)$, where the limit $\lim_{\eta \searrow 0}$ is to be understood implicitly, and $B \equiv V^*$. This leads to

$$\begin{aligned} G_{\text{LHB},\sigma}^{(n)}(\omega) &= \sum_{p=0}^n \langle 0 | (\tilde{\omega} - \bar{t}K)^{-1} (V^* (\tilde{\omega} - \bar{t}K)^{-1})^p | 0 \rangle \\ &= \sum_{p=0}^n \sum_l \Delta_{0l}^{(0)}(\omega) \langle l | (V^* (\tilde{\omega} - \bar{t}K)^{-1})^p | 0 \rangle. \end{aligned} \quad (10.66)$$

The Green functions

$$\Delta_{lm}^{(0)}(\omega) := \lim_{\eta \searrow 0} \langle l | (\tilde{\omega} - \bar{t}K - i\eta)^{-1} | m \rangle \quad (10.67)$$

and their powers have been calculated in Sect. F.3 of appendix F. We expand the perturbation V^* accordingly to obtain a systematic expansion in $1/U$. The potential V^* admits, according to (10.59a)-(10.59c), the expansion

$$V^* = V_1^* + V_2^* + V_3^* \quad (10.68)$$

with the abbreviations

$$V_1^* := -\frac{1}{2U} |0\rangle\langle 0|, \quad (10.68a)$$

$$V_2^* := -\frac{1}{4U^2} (|1\rangle\langle 0| + |0\rangle\langle 1|), \quad (10.68b)$$

$$V_3^* := -\frac{21}{8U^3} |0\rangle\langle 0| - \frac{1}{2U^3} |1\rangle\langle 1|. \quad (10.68c)$$

We will expand only the ‘shape corrections’, i.e., the contributions stemming from the numerator in (10.66).

Leading Order To leading order in $1/U$ the expansion (10.66) results in $G_{\text{LHB},\sigma}^{(0)}(\omega) = \Delta_{00}^{(0)}(\omega)$. With (F.69) of appendix F the Green function is given by

$$\bar{t}G_{\text{LHB},\sigma}^{(0)}(\omega) = \Theta(x^2 - 1) \{x - \text{sgn}(x)\sqrt{x^2 - 1}\} + \Theta(1 - x^2) \{x + i\sqrt{1 - x^2}\} \quad (10.69)$$

with

$$2\bar{t}x = \omega + \frac{U}{2} + \mathcal{O}\left(\frac{1}{U}\right) \quad \text{and} \quad \bar{t} = 1 + \mathcal{O}\left(\frac{1}{U^2}\right). \quad (10.69a)$$

Recall that the bare electron transfer amplitude t , as defined in (9.1), is our unit of energy, $t \equiv 1$. Therefore (10.69) can be cast into the form

$$G_{\text{LHB},\sigma}^{(0)}(\omega) = \lim_{\eta \searrow 0} \frac{1}{2} \left\{ \left(\omega + \frac{U}{2} + i\eta \right) - \sqrt{\left(\omega + \frac{U}{2} + i\eta \right)^2 - 4} \right\}, \quad (10.70)$$

which we recognize as the Green function $G_\infty(\omega + U/2 + i\eta)$, (6.35), of the non-interacting tight-binding model on the infinitely connected Bethe lattice, shifted by $U/2$ to lower energies. For completeness we provide a plot of the real and the imaginary part of the Green function (10.69) in figure 10.2.

This confirms our earlier claim that in the limit $U \rightarrow \infty$ the loop motion of a hole resembles that of a free particle on this lattice. Due to particle-hole symmetry, an analog statement holds for the motion of a double occupancy, i.e., for the Green function of the upper Hubbard band $G_{\text{UHB},\sigma}^{(0)}(\omega)$.

10. Results

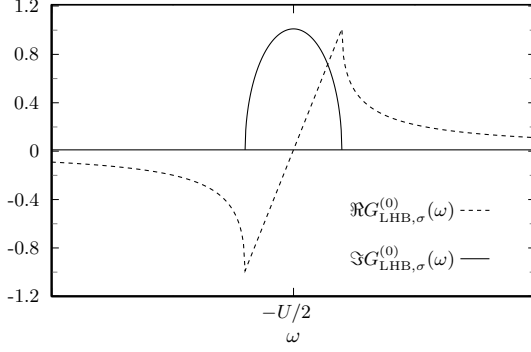


Figure 10.2: Real and imaginary part of the Green function of the lower Hubbard band in the limit $U \rightarrow \infty$.

First Order First, we expand according to (10.66) and find

$$G_{\text{LHB},\sigma}^{(1)}(\omega) = \sum_{p=0}^1 \sum_l \Delta_{0l}^{(0)}(\omega) \langle l | (V_1^* (\tilde{\omega} - \bar{t}K)^{-1})^p | 0 \rangle \quad (10.71a)$$

$$= \Delta_{00}^{(0)}(\omega) + \sum_{l,m} \Delta_{0l}^{(0)}(\omega) V_{1,lm}^* \Delta_{m0}^{(0)}(\omega) \quad (10.71b)$$

which, due to (10.68a), simplifies and becomes

$$\bar{t}G_{\text{LHB},\sigma}^{(1)}(\omega) = \bar{t}\Delta_{00}^{(0)}(\omega) - \frac{1}{2U\bar{t}} (\bar{t}\Delta_{00}^{(0)}(\omega))^2. \quad (10.72)$$

Second, with (F.70) of appendix F we finally arrive at

$$\bar{t}G_{\text{LHB},\sigma}^{(1)}(\omega) = \sum_{n=0}^1 \lambda_n^{(1)} (\tilde{g}_n(x) + g_n(x)), \quad (10.73)$$

where we have defined

$$\begin{aligned} \tilde{g}_n(x) &:= \Theta(x^2 - 1) (T_{n+1}(x) - \tilde{w}_2(x) U_n(x)), \\ g_n(x) &:= \Theta(1 - x^2) (T_{n+1}(x) + i w_2(x) U_n(x)), \end{aligned} \quad (10.73a)$$

with the Chebyshev polynomials of the first kind, $T_l(x)$, and of the second kind, $U_l(x)$, as covered in appendix F. Note that we use the following definition of the step function,

$$\Theta(x) := \begin{cases} 0 & x < 0, \\ 1/2 & x = 0, \\ 1 & \text{otherwise.} \end{cases} \quad (10.73b)$$

The function $w_2(x) = \sqrt{1 - x^2}$ is the weight function of the $U_l(x)$ and $\tilde{w}_2(x)$ is the related function $\tilde{w}_2(x) = \sqrt{x^2 - 1}$. We note in passing that the functions $\tilde{g}_n(x)$ are real for all $x \in \mathbb{R}$.

Up to first order in $1/U$, the parameters \bar{t} and x read

$$2\bar{t}x := \omega + \frac{U}{2} - \frac{1}{2U} + \mathcal{O}\left(\frac{1}{U^2}\right) \quad \text{and} \quad \bar{t} = 1 + \mathcal{O}\left(\frac{1}{U^2}\right). \quad (10.73c)$$

Thus, to first order in $1/U$ the expansion coefficients $\lambda_n^{(1)}$ are given by

$$\begin{aligned} \lambda_0^{(1)} &= 1 + \mathcal{O}\left(\frac{1}{U^2}\right), \\ \lambda_1^{(1)} &= -\frac{1}{2U\bar{t}} + \mathcal{O}\left(\frac{1}{U^2}\right) = -\frac{1}{2U} + \mathcal{O}\left(\frac{1}{U^2}\right). \end{aligned} \quad (10.73d)$$

In figure 10.3 we have plotted (10.73) together with a comparison with the lowest-order result (10.69).

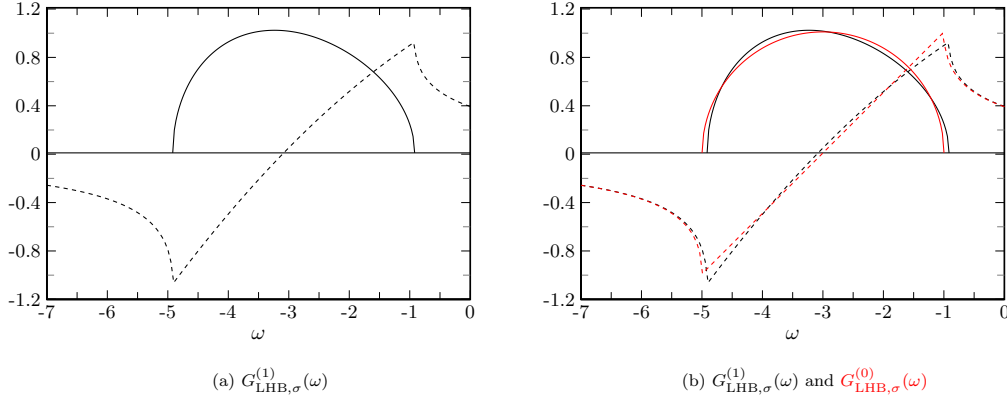


Figure 10.3.: Band-part contribution to first order, $G_{\text{LHB},\sigma}^{(1)}(\omega)$, for $U = 6$. For comparison we include in 10.3b the result to leading order.

Second Order According to (10.66) we get

$$G_{\text{LHB},\sigma}^{(2)}(\omega) = \sum_{p=0}^2 \sum_l \Delta_{0l}^{(0)}(\omega) \langle l | ((V_1^* + V_2^*)(\tilde{\omega} - \bar{t}K)^{-1})^p | 0 \rangle \quad (10.74a)$$

$$= \Delta_{00}^{(0)}(\omega) - \frac{1}{2U} (\Delta_{00}^{(0)}(\omega))^2 + \sum_{l,m} \Delta_{0l}^{(0)}(\omega) V_{2,lm}^* \Delta_{m0}^{(0)}(\omega) \quad (10.74b)$$

$$+ \sum_{k,l,m,n} \Delta_{0k}^{(0)}(\omega) V_{1,kl}^* \Delta_{lm}^{(0)}(\omega) V_{1,mn}^* \Delta_{n0}^{(0)}(\omega)$$

$$\stackrel{(10.68a)}{=} \stackrel{(10.68b)}{=} \Delta_{00}^{(0)}(\omega) - \frac{1}{2U} (\Delta_{00}^{(0)}(\omega))^2 - \frac{1}{4U^2} \{ 2\Delta_{00}^{(0)}(\omega)\Delta_{10}^{(0)}(\omega) - (\Delta_{00}^{(0)}(\omega))^3 \}. \quad (10.74c)$$

Note that because K is Hermitian, we find $\Delta_{lm}^{(0)}(\omega) = \Delta_{ml}^{(0)}(\omega)$. All terms in (10.74c) can be found in Sect. F.3.2 of appendix F. Thus, we finally obtain

$$\bar{t}G_{\text{LHB},\sigma}^{(2)}(\omega) = \sum_{n=0}^2 \lambda_n^{(2)} (\tilde{g}(x)_n + g_n(x)), \quad (10.75)$$

where the functions $\tilde{g}_n(x)$ and $g_n(x)$ are defined in (10.73a). To second order the parameters \bar{t} and x are given by

$$2\bar{t}x := \omega + \frac{U}{2} - \frac{1}{2U} + \mathcal{O}\left(\frac{1}{U^3}\right) \quad \text{and} \quad \bar{t} = 1 + \frac{3}{8U^2} + \mathcal{O}\left(\frac{1}{U^4}\right), \quad (10.75a)$$

which implies that the expansion coefficients $\lambda_n^{(2)}$ to second order in $1/U$ read

$$\lambda_0^{(2)} = 1 + \mathcal{O}\left(\frac{1}{U^3}\right),$$

$$\lambda_1^{(2)} = -\frac{1}{2U\bar{t}} + \mathcal{O}\left(\frac{1}{U^3}\right) = -\frac{1}{2U} + \mathcal{O}\left(\frac{1}{U^3}\right), \quad (10.75b)$$

$$\lambda_2^{(2)} = -\frac{1}{4U^2\bar{t}^2}(2\bar{t} - 1) + \mathcal{O}\left(\frac{1}{U^3}\right) = -\frac{1}{4U^2} + \mathcal{O}\left(\frac{1}{U^3}\right).$$

In figure 10.4 we show the second-order band-part contribution $G_{\text{LHB},\sigma}^{(2)}(\omega)$ and a comparison with the first-order result for $U = 5.5$. Note the small difference between these two functions despite the rather small value of the on-site interaction U .

10. Results

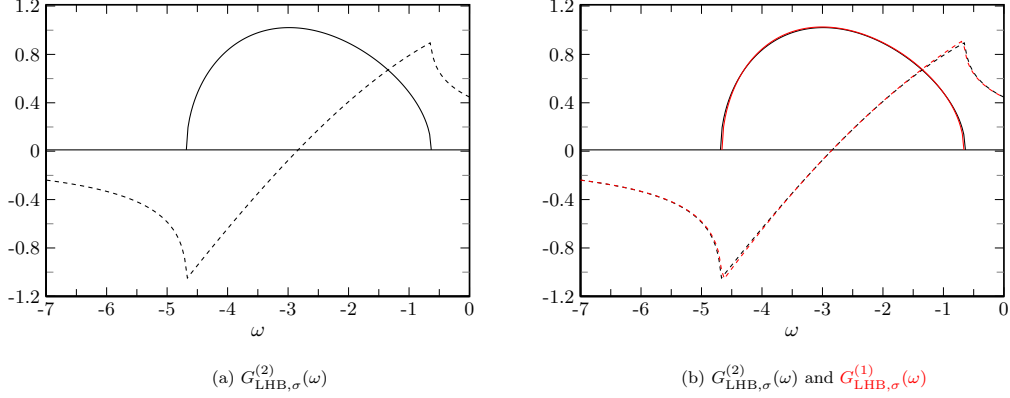


Figure 10.4.: This figure shows the band-part contribution to second order, $G_{\text{LHB},\sigma}^{(2)}(\omega)$, for $U = 5.5$. For comparison we include in 10.4b the result to first order.

Our result for the Green function to second order, $G_{\text{LHB},\sigma}^{(2)}(\omega)$, agrees with the result of Gebhard, Kalinowski et al. [67] who obtained the Green function by means of a different analytical approach.

Third Order To third order in $1/U$ we finally obtain with the help of (10.66)

$$G_{\text{LHB},\sigma}^{(3)}(\omega) = \sum_{p=0}^3 \sum_l \Delta_{0l}^{(0)}(\omega) \langle l | ((V_1^* + V_2^* + V_3^*)(\tilde{\omega} - \bar{t}K)^{-1})^p | 0 \rangle \quad (10.76a)$$

$$\begin{aligned} &= \Delta_{00}^{(0)}(\omega) - \frac{1}{2U} (\Delta_{00}^{(0)}(\omega))^2 - \frac{1}{4U^2} \left\{ 2\Delta_{00}^{(0)}(\omega)\Delta_{10}^{(0)}(\omega) - (\Delta_{00}^{(0)}(\omega))^3 \right\} \\ &\quad + \sum_{k,l} \Delta_{0k}^{(0)}(\omega) V_{3,kl}^* \Delta_{l0}^{(0)}(\omega) \\ &\quad + \sum_{k,\dots,n} \left\{ \Delta_{0k}^{(0)}(\omega) V_{1,kl}^* \Delta_{lm}^{(0)}(\omega) V_{2,mn}^* \Delta_{n0}^{(0)}(\omega) + \Delta_{0k}^{(0)}(\omega) V_{2,kl}^* \Delta_{lm}^{(0)}(\omega) V_{1,mn}^* \Delta_{n0}^{(0)}(\omega) \right\} \end{aligned} \quad (10.76b)$$

$$\begin{aligned} &\quad + \sum_{k,\dots,p} \Delta_{0k}^{(0)}(\omega) V_{1,kl}^* \Delta_{lm}^{(0)}(\omega) V_{1,mn}^* \Delta_{no}^{(0)}(\omega) V_{1,op}^* \Delta_{p0}^{(0)}(\omega) \\ &= \Delta_{00}^{(0)}(\omega) - \frac{1}{2U} (\Delta_{00}^{(0)}(\omega))^2 - \frac{1}{4U^2} \left\{ 2\Delta_{00}^{(0)}(\omega)\Delta_{10}^{(0)}(\omega) - (\Delta_{00}^{(0)}(\omega))^3 \right\} \\ &\quad + \frac{1}{8U^3} \left\{ -21(\Delta_{00}^{(0)}(\omega))^2 - 4(\Delta_{10}^{(0)}(\omega))^2 + 4(\Delta_{00}^{(0)}(\omega))^2 \Delta_{10}^{(0)}(\omega) - (\Delta_{00}^{(0)}(\omega))^4 \right\}. \end{aligned} \quad (10.76c)$$

The last equality follows from the definition of the V_n^* , (10.68a), (10.68b) and (10.68c). We have calculated the powers of the Green functions appearing in (10.76c) in Sect. F.3.2 of appendix F. With the defining equation (10.73a) of the $\tilde{g}_n(x)$ and $g_n(x)$ we can cast (10.76c) into the form

$$\bar{t}G_{\text{LHB},\sigma}^{(3)}(\omega) = \sum_{n=0}^3 \lambda_n^{(3)}(\tilde{g}_n(x) + g_n(x)). \quad (10.77)$$

The parameters x and \bar{t} are given by

$$\begin{aligned} 2\bar{t}x &= \omega + \frac{U}{2} - \frac{1}{2U} - \frac{35}{8U^3} + \mathcal{O}\left(\frac{1}{U^5}\right), \\ \bar{t} &= 1 + \frac{3}{8U^2} + \mathcal{O}\left(\frac{1}{U^4}\right), \end{aligned} \quad (10.77a)$$

and the expansion coefficients $\lambda_n^{(3)}$ to third order read

$$\begin{aligned}
\lambda_0^{(3)} &= 1 + \mathcal{O}\left(\frac{1}{U^4}\right), \\
\lambda_1^{(3)} &= -\frac{1}{2U\bar{t}} - \frac{21}{8U^3\bar{t}} + \mathcal{O}\left(\frac{1}{U^4}\right) = -\frac{1}{2U} - \frac{39}{16U^3} + \mathcal{O}\left(\frac{1}{U^4}\right), \\
\lambda_2^{(3)} &= -\frac{1}{4U^2\bar{t}^2}(2\bar{t} - 1) + \mathcal{O}\left(\frac{1}{U^4}\right) = -\frac{1}{4U^2} + \mathcal{O}\left(\frac{1}{U^4}\right), \\
\lambda_3^{(3)} &= \frac{1}{8U^3\bar{t}^3}(-4\bar{t}^2 + 4\bar{t} - 1) + \mathcal{O}\left(\frac{1}{U^4}\right) = -\frac{1}{8U^3} + \mathcal{O}\left(\frac{1}{U^4}\right).
\end{aligned} \tag{10.77b}$$

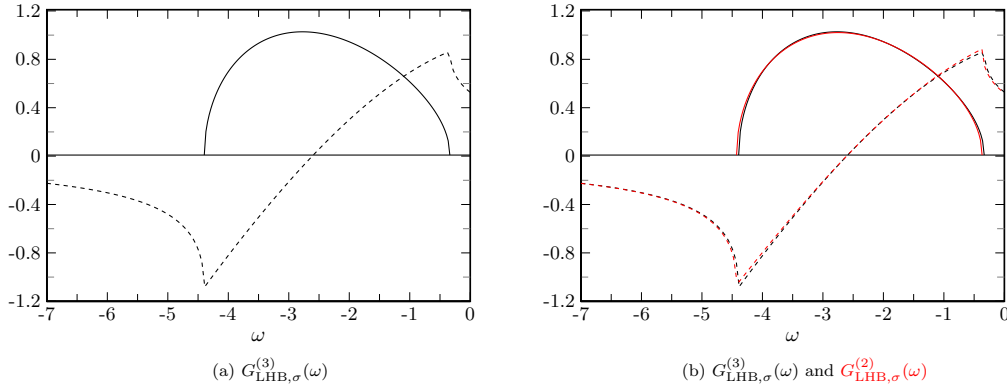


Figure 10.5.: Band-part contribution to third order for $U = 5$. For comparison we include in 10.5b the result to second order.

We depicted the function (10.77) together with a comparison of the second-order result, (10.75), in figure 10.5. Our result for the Green function to third order exceeds the calculations of [67]. This is the first time that an analytical expression for the Green function of the Mott-Hubbard insulator up to third order in strong-coupling has been obtained.

10.3.2. Full Green Function

In this section we use lemma (7.2.1) again. This time, however, we do not seek an iterative solution but solve the emerging equations exactly. Therefore, we write

$$G_{ij}^{[n]}(\omega) = \Delta_{ij}^{(0)}(\omega) + \sum_{l,m} \Delta_{il}^{(0)}(\omega) V_{lm}^* G_{mj}^{[n]}(\omega). \tag{10.78}$$

The superscript $[n]$ signals that we use V^* up to n th order in $1/U$. The Green function of the lower Hubbard band is then given by

$$G_{\text{LHB},\sigma}^{[n]}(\omega) \equiv G_{00}^{[n]}(\omega). \tag{10.79}$$

Solution to Leading Order Since the lowest-order result, (10.69) and (10.70), is also the solution of (10.78) to lowest order, i.e., for $V^* = 0$, we can state that

$$G_{\text{LHB},\sigma}^{[0]}(\omega) \equiv G_{\text{LHB},\sigma}^{(0)}(\omega). \tag{10.80}$$

We proceed with the higher-order solutions.

10. Results

Solution to First Order With (10.66) and V^* to first order, (10.68a), we obtain

$$G_{\text{LHB},\sigma}^{[1]}(\omega) \equiv G_{00}^{[1]}(\omega) = \Delta_{00}^{(0)}(\omega) + \sum_{k,l} \Delta_{0k}^{(0)}(\omega) V_{1,kl} G_{k0}^{[1]}(\omega) \quad (10.81a)$$

$$= \Delta_{00}^{(0)}(\omega) - \frac{1}{2U} \Delta_{00}^{(0)}(\omega) G_{00}^{[1]}(\omega). \quad (10.81b)$$

This equation has the solution

$$G_{\text{LHB},\sigma}^{[1]}(\omega) = \frac{\Delta_{00}^{(0)}(\omega)}{1 + \frac{1}{2U} \Delta_{00}^{(0)}(\omega)}. \quad (10.82)$$

Solution to Second Order With V^* to second order, we obtain from (10.78) the system of coupled equations

$$G_{00}^{[2]}(\omega) = \Delta_{00}^{(0)}(\omega) + (\varepsilon_0^* \Delta_{00}^{(0)}(\omega) + t_0^* \Delta_{10}^{(0)}(\omega)) G_{00}^{[2]}(\omega) + t_0^* \Delta_{00}^{(0)} G_{10}^{[2]}(\omega), \quad (10.83a)$$

$$G_{10}^{[2]}(\omega) = \Delta_{10}^{(0)}(\omega) + (\varepsilon_0^* \Delta_{10}^{(0)}(\omega) + t_0^* \Delta_{11}^{(0)}(\omega)) G_{00}^{[2]}(\omega) + t_0^* \Delta_{10}^{(0)} G_{10}^{[2]}(\omega). \quad (10.83b)$$

The parameters ε_0^* and t_0^* are defined in (10.59a) and (10.59c) and read up to second order in $1/U$

$$\varepsilon_0^* = -\frac{1}{2U} + \mathcal{O}\left(\frac{1}{U^3}\right), \quad (10.84)$$

$$t_0^* = -\frac{1}{4U^2} + \mathcal{O}\left(\frac{1}{U^3}\right). \quad (10.85)$$

From (10.83b) we obtain $G_{10}^{[2]}(\omega)$ in terms of $G_{00}^{[2]}(\omega)$,

$$G_{10}^{[2]}(\omega) = \frac{\Delta_{10}^{(0)}(\omega) + (\varepsilon_0^* \Delta_{10}^{(0)}(\omega) + t_0^* \Delta_{11}^{(0)}(\omega)) G_{00}^{[2]}(\omega)}{1 - t_0^* \Delta_{10}^{(0)}(\omega)}. \quad (10.86)$$

Next, we insert (10.86) into (10.83a) and after some simple algebraic manipulations we get

$$G_{\text{LHB},\sigma}^{[2]}(\omega) = \Delta_{00}^{(0)}(\omega) \frac{1}{1 - 2t_0^* \Delta_{10}^{(0)}(\omega) - \varepsilon_0^* \Delta_{00}^{(0)}(\omega) + (t_0^*)^2 \{(\Delta_{10}^{(0)}(\omega))^2 - \Delta_{11}^{(0)}(\omega) \Delta_{00}^{(0)}(\omega)\}}. \quad (10.87)$$

With the help of (F.62a) of appendix F and (10.73a) we can express $\Delta_{11}^{(0)}(\omega)$ in form of

$$\bar{t} \Delta_{11}^{(0)}(\omega) = \bar{g}_0(x) + \bar{g}_2(x) + g_0(x) + g_2(x) \equiv \bar{t} \Delta_{00}^{(0)}(\omega) + (\bar{t} \Delta_{00}^{(0)}(\omega))^3 \quad (10.88)$$

which, according to Sect. F.3.2 of appendix F, implies that

$$\bar{t} \Delta_{00}^{(0)}(\omega) \bar{t} \Delta_{11}^{(0)}(\omega) = (\bar{t} \Delta_{00}^{(0)}(\omega))^2 + (\bar{t} \Delta_{00}^{(0)}(\omega))^4 \equiv \bar{t} \Delta_{10}^{(0)}(\omega) + (\bar{t} \Delta_{10}^{(0)}(\omega))^2. \quad (10.89)$$

Thus,

$$\bar{t} \Delta_{00}^{(0)}(\omega) \bar{t} \Delta_{11}^{(0)}(\omega) - (\bar{t} \Delta_{10}^{(0)}(\omega))^2 = \bar{t} \Delta_{10}^{(0)}(\omega) \equiv (\bar{t} \Delta_{00}^{(0)}(\omega))^2, \quad (10.90)$$

and we can cast the second-order solution (10.87) into the form

$$G_{\text{LHB},\sigma}^{[2]}(\omega) = \Delta_{00}^{(0)}(\omega) \frac{1}{1 - \varepsilon_0^* \Delta_{00}^{(0)}(\omega) - t_0^* (t_0^* + 2\bar{t}) (\Delta_{00}^{(0)}(\omega))^2}. \quad (10.91)$$

Solution to Third Order V^* is given to third order by (10.68c). We obtain from (10.78) the system of coupled equations

$$G_{00}^{[3]}(\omega) = \Delta_{00}^{(0)}(\omega) + \{\varepsilon_0^* \Delta_{00}^{(0)}(\omega) + t_0^* \Delta_{10}^{(0)}(\omega)\} G_{00}^{[3]}(\omega) + \{\varepsilon_1^* \Delta_{10}^{(0)}(\omega) + t_0^* \Delta_{00}^{(0)}(\omega)\} G_{10}^{[3]}(\omega), \quad (10.92a)$$

$$G_{10}^{[3]}(\omega) = \Delta_{10}^{(0)}(\omega) + \{\varepsilon_0^* \Delta_{10}^{(0)}(\omega) + t_0^* \Delta_{11}^{(0)}(\omega)\} G_{00}^{[3]}(\omega) + \{\varepsilon_1^* \Delta_{11}^{(0)}(\omega) + t_0^* \Delta_{10}^{(0)}(\omega)\} G_{10}^{[3]}(\omega), \quad (10.92b)$$

where the parameters ε_0^* , ε_1^* and t_0^* are defined in (10.59a), (10.59b) and (10.59c), respectively. The solution for $G_{00}^{[3]}(\omega) \equiv G_{\text{LHB},\sigma}^{[3]}(\omega)$ reads

$$G_{\text{LHB},\sigma}^{[3]}(\omega) = \frac{\Delta_{00}^{(0)}(\omega) - \varepsilon_1^* \{\Delta_{00}^{(0)}(\omega) \Delta_{11}^{(0)}(\omega) - (\Delta_{10}^{(0)}(\omega))^2\}}{1 - \varepsilon_0^* \Delta_{00}^{(0)}(\omega) - 2t_0^* \Delta_{10}^{(0)}(\omega) - \varepsilon_1^* \Delta_{11}^{(0)}(\omega) + (\varepsilon_0^* \varepsilon_1^* - (t_0^*)^2) \{\Delta_{00}^{(0)}(\omega) \Delta_{11}^{(0)}(\omega) - (\Delta_{10}^{(0)}(\omega))^2\}}. \quad (10.93)$$

With the simplifications (10.88) and (10.90) we can finally state that

$$G_{\text{LHB},\sigma}^{[3]}(\omega) = \frac{\Delta_{00}^{(0)}(\omega) - \varepsilon_1^* (\Delta_{00}^{(0)}(\omega))^2}{1 - (\varepsilon_0^* + \varepsilon_1^*) \Delta_{00}^{(0)}(\omega) + (\varepsilon_0^* \varepsilon_1^* - 2t_0^* \bar{t} - (t_0^*)^2) (\Delta_{00}^{(0)}(\omega))^2 - \varepsilon_1^* \bar{t}^2 (\Delta_{00}^{(0)}(\omega))^3}. \quad (10.94)$$

Note that we can obtain the lower-order solutions from (10.94) by simply inserting the values of the parameters ε^* and t^* as appropriate for the desired order. This may serve as a convenient check.

10.3.3. Summary

Up to third order in $1/U$ the Green function of the lower Hubbard band on the Bethe lattice with infinite connectivity is given in terms of the scattering model (10.60) and reads

$$G_{\text{LHB},\sigma}(\omega) = \lim_{\eta \searrow 0} \langle 0 | (\omega + U/2 - \bar{\varepsilon} - \bar{t}K - V^* - i\eta)^{-1} | 0 \rangle. \quad (10.95)$$

The operator K denotes the simple tight-binding Hamiltonian (10.62a), and the scattering potential V^* reads

$$V^* := \varepsilon_0^* |0\rangle \langle 0| + \varepsilon_1 |1\rangle \langle 1| + t_0^* (|0\rangle \langle 1| + |1\rangle \langle 0|). \quad (10.96)$$

Its parameters are functions of $1/U$ and are given by

$$\varepsilon_0^* = -\frac{1}{2U} - \frac{21}{8U^3} + \mathcal{O}\left(\frac{1}{U^5}\right), \quad (10.97)$$

$$\varepsilon_1^* = -\frac{1}{2U^3} + \mathcal{O}\left(\frac{1}{U^5}\right), \quad (10.98)$$

$$t_0^* = -\frac{1}{4U^2} + \mathcal{O}\left(\frac{1}{U^4}\right). \quad (10.99)$$

Up to third order in $1/U$ the parameters \bar{t} and $\bar{\varepsilon}$ read

$$\bar{t} = 1 + \frac{3}{8U^2} + \mathcal{O}\left(\frac{1}{U^4}\right), \quad (10.100)$$

$$\bar{\varepsilon} = \frac{1}{2U} + \frac{35}{8U^3} + \mathcal{O}\left(\frac{1}{U^4}\right). \quad (10.101)$$

Band-Part Contribution

Expanding the Green function (10.95) by iteration of lemma 7.2.1 we obtain the functions $G_{\text{LHB},\sigma}^{(n)}(\omega)$, we call ‘band-part contributions’ of order n to the Green function. Up to third order in $1/U$ we found that

$$\bar{t} G_{\text{LHB},\sigma}^{(3)}(\omega) = \sum_{n=0}^3 \lambda_n^{(3)} (\tilde{g}_n(x) + g_n(x)), \quad (10.102)$$

10. Results

where the parameter x is defined by

$$2\bar{t}x := \omega + \frac{U}{2} - \frac{1}{2U} - \frac{35}{8U^3} + \mathcal{O}\left(\frac{1}{U^5}\right). \quad (10.103)$$

The functions $\tilde{g}_n(x)$ and $g_n(x)$ are given in terms of Chebyshev polynomials, see appendix F for details, and read

$$\tilde{g}_n(x) := \Theta(x^2 - 1)(T_{n+1}(x) - \tilde{w}_2(x)U_n(x)), \quad (10.104)$$

$$g_n(x) := \Theta(1 - x^2)(T_{n+1}(x) + iw_2(x)U_n(x)). \quad (10.105)$$

Here, we use the following variant of the unit step function $\Theta(x)$,

$$\Theta(x) = \begin{cases} 0 & x < 0, \\ 1/2 & x = 0, \\ 1 & \text{otherwise.} \end{cases} \quad (10.106)$$

The expansion coefficients $\lambda_n^{(3)}$ to third order read

$$\lambda_0^{(3)} = 1 + \mathcal{O}\left(\frac{1}{U^4}\right), \quad (10.107)$$

$$\lambda_1^{(3)} = -\frac{1}{2U} - \frac{39}{16U^3} + \mathcal{O}\left(\frac{1}{U^4}\right), \quad (10.108)$$

$$\lambda_2^{(3)} = -\frac{1}{4U^2} + \mathcal{O}\left(\frac{1}{U^4}\right), \quad (10.109)$$

$$\lambda_3^{(3)} = -\frac{1}{8U^3} + \mathcal{O}\left(\frac{1}{U^4}\right). \quad (10.110)$$

Full Green Function

Expanding the scattering potential (10.96) in $1/U$ and solving in each order for $G_{\text{LHB},\sigma}(\omega)$ exactly, we obtain the functions $G_{\text{LHB},\sigma}^{[n]}$, we call ‘full Green functions’ of order n . Additionally to the information encoded in the band-part contributions $G_{\text{LHB},\sigma}^{(n)}$, the full Green functions contain the information about the scattering resonance. Up to third order in $1/U$ we find

$$G_{\text{LHB},\sigma}^{[3]}(\omega) = \frac{\Delta_{00}^{(0)}(\omega) - \varepsilon_1^*(\Delta_{00}^{(0)}(\omega))^2}{1 - (\varepsilon_0^* + \varepsilon_1^*)\Delta_{00}^{(0)}(\omega) + (\varepsilon_0^*\varepsilon_1^* - 2t_0^*\bar{t} - (t_0^*)^2)(\Delta_{00}^{(0)}(\omega))^2 - \varepsilon_1^*\bar{t}^2(\Delta_{00}^{(0)}(\omega))^3}. \quad (10.111)$$

The Green function $\Delta_{00}^{(0)}(\omega)$ and its powers are expressible in terms of Chebyshev polynomials as detailed in appendix F. They read

$$(\bar{t}\Delta_{00}^{(0)}(\omega))^p = \tilde{g}_{p-1}(x) + g_{p-1}(x), \quad (10.112)$$

with x given in (10.103) and \tilde{g} and g summarized in (10.104) and (10.105), respectively.

10.4. Single-Particle Gap

As the finite potential V^* cannot change the energy of the standing waves of \bar{H}_{TB} , it does not alter the support of the imaginary part of the Green function

$$\Delta_{00}^{(0)}(\omega) = \langle 0 | (\tilde{\omega}^- - \bar{t}K)^{-1} | 0 \rangle. \quad (10.113)$$

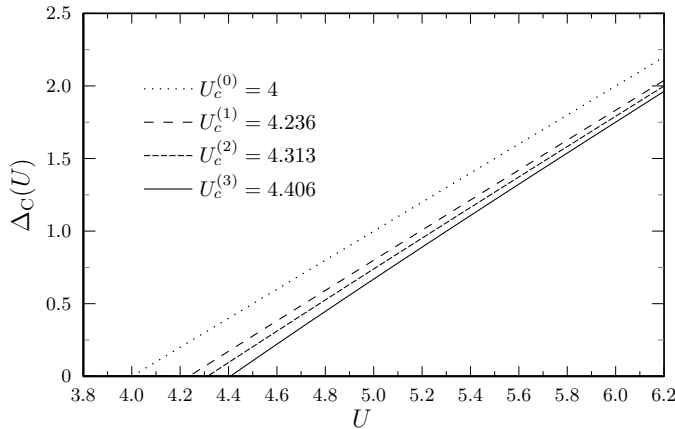


Figure 10.6: The single-particle gap for charge excitations $\Delta_C(U)$. Each line corresponds to a particular order in $1/U$ as shown in the figure.

Thus, it follows that the single-particle gap $\Delta_C(U)$ as a function of the interaction U is given by the simple expression

$$\Delta_C(U) = 2 \left| -\frac{U}{2} + \bar{\varepsilon} + 2\bar{t} \right| = U - 4 - \frac{1}{U} - \frac{3}{2U^2} - \frac{35}{4U^3} + \mathcal{O}\left(\frac{1}{U^4}\right). \quad (10.114)$$

In figure 10.6 we plotted $\Delta_C(U)$, (10.114), for each order in $1/U$ separately.

First, we note that with decreasing interaction U , the magnitude of the single-particle gap shrinks for every order of perturbation theory. This behavior was to be expected as we already discussed in Sect. 5.4. Furthermore, we can state that on the Bethe lattice with an infinite number of nearest neighbors the closure of the gap is a consequence of

- (a) the increase of the bandwidth $W = 4\bar{t}$, see (10.100), and
- (b) a shift of the center of gravity of the band described by (10.101).

Let U_c denote the critical value of the on-site interaction U , where the single-particle gap closes, i.e., $\Delta_C(U_c) = 0$. Up to third order in $1/U$ we find

$$U_c^{(0)} = 4, \quad (10.115)$$

$$U_c^{(1)} = 4.236 [5.90\%], \quad (10.116)$$

$$U_c^{(2)} = 4.313 [1.82\%], \quad (10.117)$$

$$U_c^{(3)} = 4.406 [2.16\%]. \quad (10.118)$$

The numbers in the square brackets give the percentage change to the result from the previous order. We like to remark that our results up to *second* order agree with data obtained via a different perturbative treatment of the Mott-Hubbard insulator [67]. Unfortunately, the method used in [67] is rather unsystematic and could not be extended to third order in $1/U$. The authors of [67] *conjectured* a very fast decay in the percentage change and, thus, estimated a value of $U_c^{(3)} \approx 4.357$. Our result shows that at least the percentage change of the third-order contribution is still of the same magnitude as the previous one.

Let us finally note that the $1/U$ expansion provides an excellent estimate of the support of the density of states of the Mott-Hubbard insulator. This makes it highly valuable for comparisons with numerical methods. All of those deal necessarily with finite systems and, as a consequence, can only obtain the support of the density of states and therefore the single-particle gap by means of more or less well defined extrapolations. Comparing the numerical data with our analytical results provides a reliable test of the accuracy of the numerical methods. We will return to this subject in Sect. 10.6.

10.5. Density of States

The density of states of the lower Hubbard band is given by (9.11) and reads

$$D_{\text{LHB},\sigma}(\omega) = \frac{1}{\pi} \Im G_{\text{LHB},\sigma}(\omega). \quad (10.119)$$

According to Sect. 10.3 we have for each order n in $1/U$ two Green functions: the band-part contribution $G_{\text{LHB},\sigma}^{(n)}(\omega)$ and the full Green function $G_{\text{LHB},\sigma}^{[n]}(\omega)$. Thus, we obtain two density of states: the band-part contribution

$$D_{\text{LHB},\sigma}^{(n)}(\omega) = \frac{1}{\pi} \Im G_{\text{LHB},\sigma}^{(n)}(\omega) \quad (10.120)$$

and the full density of states

$$D_{\text{LHB},\sigma}^{[n]}(\omega) = \frac{1}{\pi} \Im G_{\text{LHB},\sigma}^{[n]}(\omega). \quad (10.121)$$

We discuss the full density of state in the following subsection. We postpone the discussion of the band-part contribution to Sect. 10.5.2.

10.5.1. Full Density of States

According to (10.111), the full Green function up to third order in $1/U$ reads

$$G_{\text{LHB},\sigma}^{[3]}(\omega) = \frac{\Delta_{00}^{(0)}(\omega) - \varepsilon_1^* (\Delta_{00}^{(0)}(\omega))^2}{1 - (\varepsilon_0^* + \varepsilon_1^*) \Delta_{00}^{(0)}(\omega) + (\varepsilon_0^* \varepsilon_1^* - 2t_0^* \bar{t} - (t_0^*)^2) (\Delta_{00}^{(0)}(\omega))^2 - \varepsilon_1^* \bar{t}^2 (\Delta_{00}^{(0)}(\omega))^3}. \quad (10.122)$$

By inserting the parameters ε^* and t^* valid for the order of interest, we can obtain the full density of states to that order. In figure 10.7 we show the evolution of the density of states as the on-site interaction U decreases. We have plotted the first-order result in black, the second-order result in blue and the third-order Green function in red.

First, we like to note that the change in the shape of the density of states in the various orders for constant U is small. The change in the support is clearly visible. With decreasing U the center of gravity of the band is shifted to lower values of $|\omega|$, as we already discussed in Sect. 10.4.

Second, the elliptic shape of the lowest-order solution, see 10.2, is deformed. With decreasing U we recognize a redshift in the spectral weight. This has a very simple explanation in terms of the scattering model. Let us discuss it by means of the first-order result.

The Green function to first order reads

$$G_{\text{LHB},\sigma}^{[1]}(\omega) = \frac{\Delta_{00}^{(0)}(\omega)}{1 - \varepsilon_0^* \Delta_{00}^{(0)}(\omega)}, \quad (10.123)$$

and the density of states is therefore given by

$$D_{\text{LHB},\sigma}^{[1]}(\omega) = \frac{D_{\text{LHB},\sigma}^{(0)}(\omega)}{|1 - \varepsilon_0^* \Delta_{00}^{(0)}(\omega)|^2}. \quad (10.124)$$

A pole in the Green function signals the occurrence of a discrete eigenvalue of the underlying Hamiltonian which is here the scattering Hamiltonian (10.60) to first order. A pole can only occur for vanishing imaginary part, thus, outside the band. Inspection of figures 10.2 and 10.3 assures us that the real part of $\Delta_{00}^{(0)}(\omega)$ is minimal at the lower band edge $\mu \equiv \mu_{\text{LHB}}^-$. A pole and thus a bound state will therefore only occur for values of $U < U_b$. The critical interaction U_b is defined by

$$\Delta_{00}^{(0)}(\mu, U_b) = \frac{1}{\varepsilon_0^*(U_b)}. \quad (10.125)$$

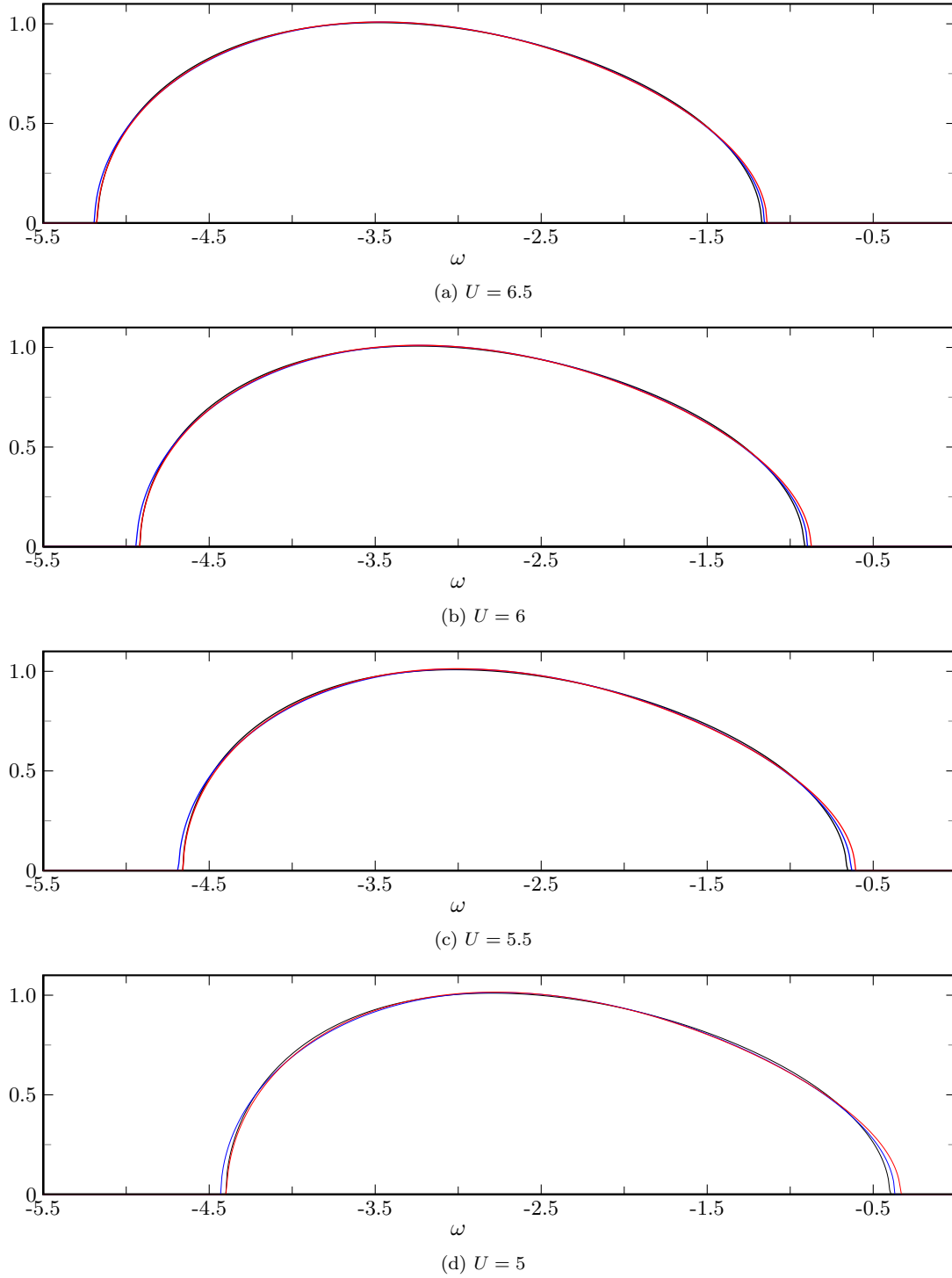


Figure 10.7.: Dependence of the full density of states of the lower Hubbard band, $D_{\text{LHB},\sigma}^{[n]}(\omega)$, on the on-site interaction U . We have plotted $\pi D_{\text{LHB},\sigma}^{[n]}(\omega)$. We depicted the first-order result with a black line, used a blue line for $n = 2$ and a red one for $n = 3$. The value of the interaction U used to generate the graphs is given below each figure.

10. Results

At the critical U_b the bound state will first appear at the lower band edge and by decreasing U it will be pushed towards lower frequencies. Because the sum rule

$$\int_{-\infty}^0 D_{\text{LHB},\sigma}(\omega) d\omega = 1 \quad (10.126)$$

holds, spectral weight leaves the band together with the bound state.

For larger values of U , there is no solution of (10.125) and therefore no bound state. However, upon approaching U_b from above, the shape of the density of states is modified. Spectral weight is transferred to lower frequencies to prepare for the formation of the bound state at the lower band edge at $U = U_b$. For a detailed discussion we refer the reader to the book by Economou [32], who discusses the formation of bound states and scattering resonances for a simple model-scattering problem in great detail.

Upon inspection of figure 10.7 we can state that up to third order, there is no bound state in the Hubbard model for $U > U_c$.

10.5.2. Resonance Contribution

As resonance contribution of order n in $1/U$ we denote the difference

$$D_{\text{res},\sigma}^{[n]}(\omega) := D_{\text{LHB},\sigma}^{[n]}(\omega) - D_{\text{LHB},\sigma}^{(n)}(\omega), \quad (10.127)$$

as it gives the strength of the resonance which emerges due to the attractive potential V^* .

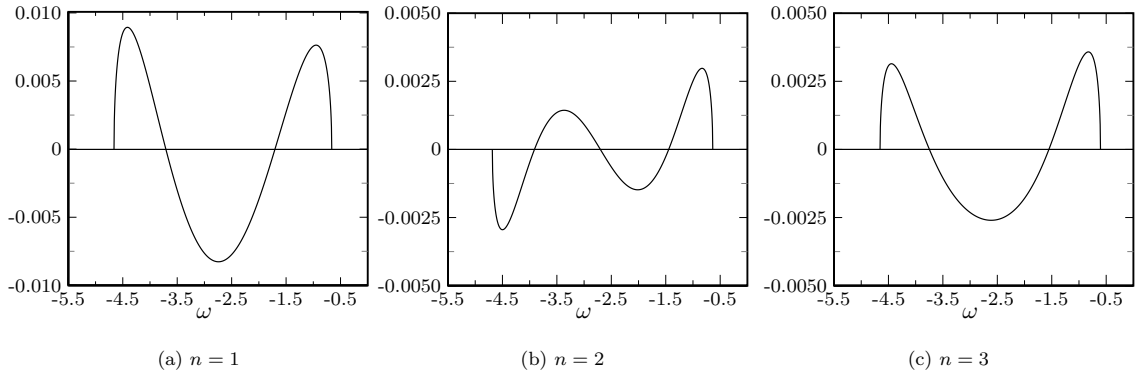


Figure 10.8.: The figure shows the resonance contribution to the density of states of the lower Hubbard band, $D_{\text{res},\sigma}^{[n]}(\omega)$, for values of n of the order in perturbation theory as shown in the figure. For the on-site interaction U we used $U = 5.5$.

In figure 10.8 we show the resonance contribution to first, second and third order for $U = 5.5$. Note that the first-order and third-order result show the same shape. The second-order contribution differs noticeably. The reason is simple. In first and third order the diagonal part of V^* changes. In second order we get an off-diagonal perturbation, see (10.68b). Note that the resonance contributions are at most of the order of $1/U^3$ which was to be expected because the attractive potential as well as the off-diagonal perturbation V_2^* are very small for values of the interaction down to $U = 5$.

10.6. Comparisons

In the following we compare our analytical results with data from numerical methods. In Sect. 10.6.1 and 10.6.2 we compare the single-particle gap $\Delta_C(U)$ and the density of states with DDMRG data from

Nishimoto et al. [131]. In Sect. 10.6.3 we calculate an approximation of the Matsubara Green function for small but finite (inverse) temperature β and compare with recent QMC results of Blümer [132]. In all cases we find excellent agreement with our results down to values of $U \approx 5$.

10.6.1. Charge Gap

Figure 10.9 shows again a plot of the single-particle charge gap $\Delta_C(U)$, (10.114). This time, we have additionally included the data obtained by Nishimoto et al. in [131].

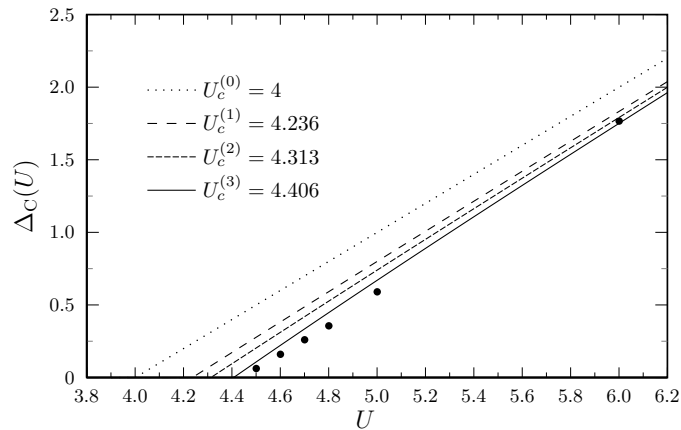


Figure 10.9.: Single-particle gap for charge excitations $\Delta_C(U)$. Each line corresponds to a particular order in $1/U$ as shown in the figure. The black dots represent DDMRG data of [131].

The authors of [131] also employed the DMFT to map the Hubbard lattice model onto the SIAM but then used the Dynamical Density Matrix Renormalization Group (DDMRG) [133] as an ‘impurity solver’. They performed their calculations on a finite chain with 65 sites and gave an estimation of the critical value of the interaction U which reads $U_c^{\text{DDMRG}} = 4.45$, in excellent agreement with our third-order result. Note that their values for the charge gap are always a bit larger than our third-order result except for the point at $U = 6$. We can certainly not expect to find perfect agreement. In particular, it is difficult and ambiguous to extract the support of the density of states from the finite-system numerical data. All Dirac-distributions are approximated by Lorentz functions, leading to a broadening of the support of the density of states which depends on system size. One therefore has to extrapolate to an infinite system. Though our analytical results are not exact, they do not suffer from these kind of problems and, especially, provide unique estimates of the support of the density of states for the infinite system. Thus, they provide a convenient means to test the validity of the numerical extrapolation schemes.

10.6.2. Density of States

In this subsection we compare our full density of states $D_{\text{LHB},\sigma}^{[n]}(\omega)$ with the DDMRG data [131]. We start with a fairly large value of the interaction U , namely $U = 6$. In figures 10.10a, 10.10b and 10.10c we show a comparison of our results to first, second and third order with the DDMRG data. Whereas the first-order result deviates considerably, the second-order and, in particular, the third-order density of states agree very well with the DDMRG data.

In figures 10.10d, 10.10e and 10.10f we compare our full Green function to first, second and third order, respectively, with DDMRG data for $U = 5$. As was to be expected, the density of states to first order deviates considerably from the DDMRG result. This clearly indicates that the our first-order result is not valid at such small values of U . Though the shape of the second-order density of states resembles the shape of the DDMRG result quite well, its support deviates considerably at frequencies near $\omega \approx 0.6$.

10. Results

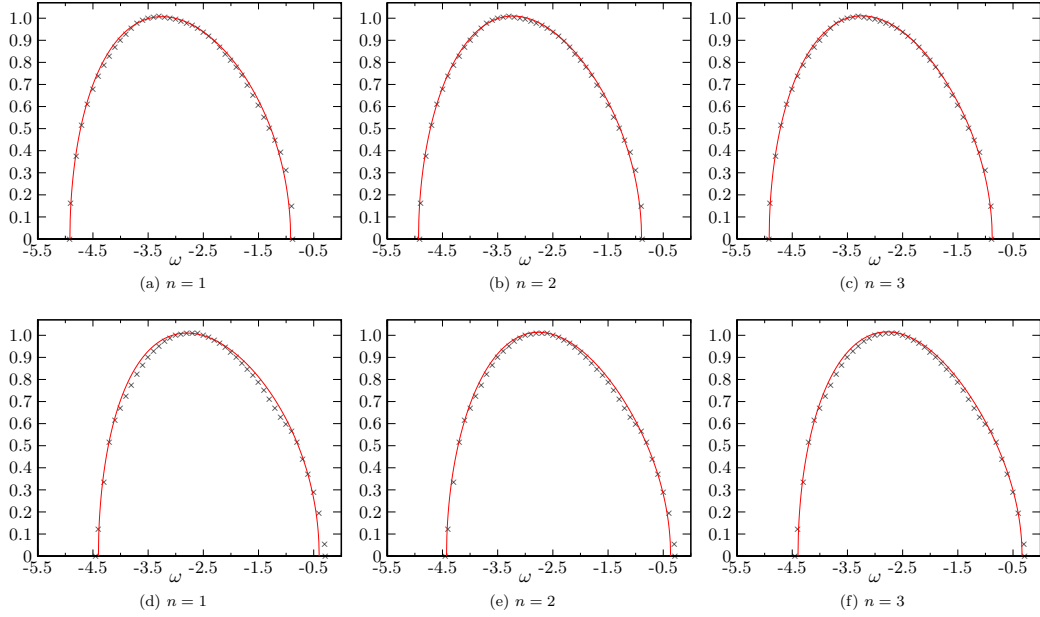


Figure 10.10.: The figures show a comparison of the density of states of the lower Hubbard band, $\pi D_{\text{LHB},\sigma}^{[n]}(\omega)$, and the DDMRG data [131]. Our analytical results are plotted in red while we used black crosses for the DDMRG data. The values of n of the order in perturbation theory are given below each figure. In the first row the interaction is $U = 6$, and in the second row it is $U = 5$.

The agreement of our third-order expression with the DDMRG data is much better. Our result gives slightly larger spectral weight at frequencies around $\omega \approx -3.5$ and $\omega \approx -1.2$. Otherwise both data sets are nearly congruent.

A glance at figure 10.11 reminds us that our density of states $D_{\text{LHB},\sigma}^{[n]}(\omega)$ is a perturbative result after all. The DDMRG data for $U = 4.8$ shows a clear peak in the spectral weight around $\omega \approx -0.5$. This behavior could already been anticipated in the case of $U = 5$. Our density of states does not show this feature. Even for much smaller values of U there is no sign of this peak in our results. We conjecture that it describes a non-perturbative effect. Note, however, that the support of our density of states and that of the DDMRG result still agree very well.

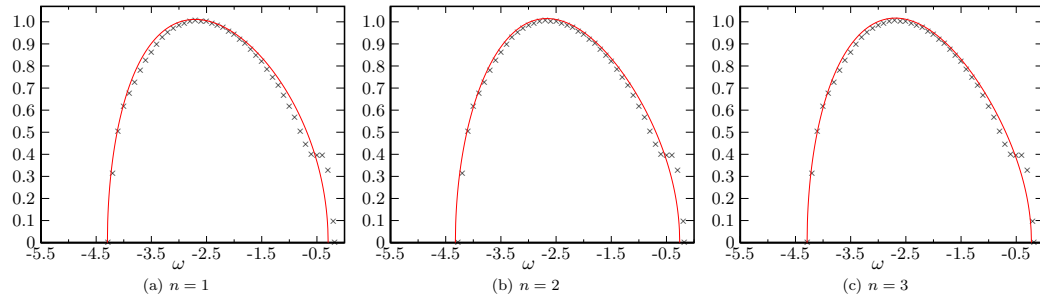


Figure 10.11.: The red line represents the density of states of the lower Hubbard band, $\pi D_{\text{LHB},\sigma}^{[n]}(\omega)$, for values of n as shown in the figure. The black crosses represent DDMRG data of [131]. The data are shown for $U = 4.8$.

10.6.3. Matsubara Green Function

In the following subsection we compare our result with data from recent Quantum Monte Carlo (QMC) studies of Blümer [132]. QMC calculations are done at non-zero temperatures and lead naturally to Matsubara Green functions [134]

$$\mathcal{G}_\sigma(\tau) = -\frac{1}{L} \sum_i \text{Tr} e^{\beta(\Omega-H)} \mathcal{T}_\tau c_{i\sigma}(\tau) c_{i\sigma}^\dagger, \quad (10.128)$$

where β is the inverse temperature, Ω the grand-canonical potential and \mathcal{T}_τ orders the operators in imaginary time. The operators are given in imaginary-time Heisenberg representation

$$c_a^{(\dagger)}(\tau) := e^{\tau H} c_a^{(\dagger)} e^{-\tau H}. \quad (10.129)$$

For general complex τ the creator $c_a^\dagger(\tau)$ is not the adjoint of $c_a(\tau)$. For convergence we need $-\beta \leq \tau \leq \beta$. Note that we only introduce a few concepts here as we do not wish to develop the methods of quantum field theory at finite temperature. For a detailed account of the Green function's technique at finite temperature we refer the reader to the relevant books of many-particle theory, e.g. [4, 12, 28].

The algorithm used in most implementations of QMC for solving quantum impurity problems is the so-called Hirsch-Fye Impurity Algorithm [135, 136]. Its computational effort scales with the third power of the inverse temperature β [135]. Thus, it is numerically expensive to obtain results for very low temperatures, $\beta \rightarrow \infty$. A second problem with the QMC data involves the analytic properties of the Matsubara functions. For a comparison with experiment, e.g. for linear response theory, we need retarded Green functions. For example, according to (A.35) of appendix A, we need the retarded single-particle Green function to obtain the density of states. There exists a very simple connection between the Matsubara functions and the corresponding retarded ones. Let $\mathcal{G}(i\omega)$ denote the Fourier transform of the Matsubara function (10.128). Provided $\mathcal{G}(i\omega)$ is written as a rational function which is analytic in the complex upper half-plane [28], we can obtain the retarded Green function $G_{\text{ret}}(\omega)$ by means of the analytical continuation [4, 12, 28]

$$G_{\text{ret}}(\omega) = \lim_{\eta \searrow 0} \mathcal{G}(i\omega \rightarrow \omega + i\eta). \quad (10.130)$$

Though (10.130) is easy to deal with if $\mathcal{G}(i\omega)$ is given in the form of an analytic function, the situation is much more involved if we know $\mathcal{G}(i\omega)$ only for a finite set of points in the complex plane as is the case in QMC calculations. No unique way exists to perform the analytic continuation (10.130).

For all these reasons we need a controllable and reliable method to compare the QMC data for $\mathcal{G}(\tau)$ (no numerical analytic continuation) at finite inverse temperature. According to [28] we can calculate the Matsubara Green function by means of the following formula,

$$\mathcal{G}(\tau) = -\frac{1}{\pi} \int_{-\infty}^{\infty} \Im G_{\text{ret}}(x, \beta) \frac{e^{-x\tau}}{e^{\beta x} + 1} dx, \quad (10.131)$$

where τ is restricted to the interval $\tau \in [0, \beta]$. Note that the retarded Green function in (10.131) is the *temperature-dependent* function (10.130). We approximate (10.131) by using our third-order result of the *zero-temperature* full Green function, (10.111). In this way we obtain

$$\mathcal{G}(\tau) \approx -\frac{1}{2} \int_{-\infty}^{\infty} (D_{\text{LHB},\sigma}^{[3]}(x) + D_{\text{LHB},\sigma}^{[3]}(-x)) \frac{e^{-x\tau}}{e^{\beta x} + 1} dx, \quad (10.132)$$

where the factor 1/2 has been included for comparison with the data from [132]. Note that this is not such a drastic approximation as it might appear at first glance. Remember that our result for the density of states is valid for the Mott-Hubbard insulator which shows a gap in its spectrum of single-particle excitations. The charge gap $\Delta_C(U)$ is of the order U , see Sect. 10.4. This implies that for $U \gg W$ the excited states of the Mott-Hubbard insulator are exponentially suppressed according to the Boltzmann

10. Results

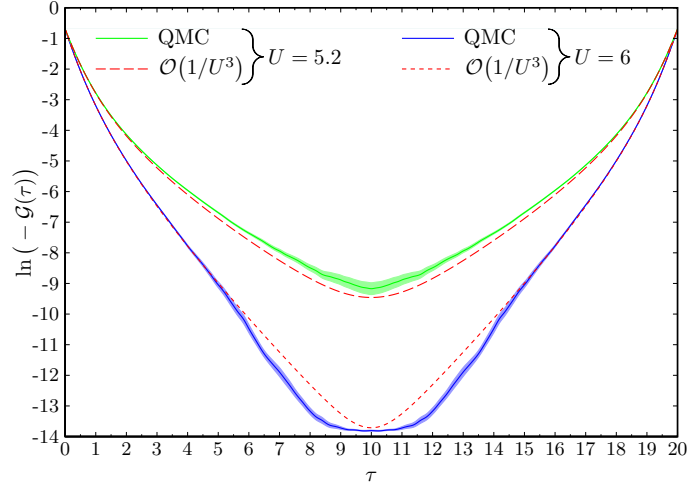


Figure 10.12.: Comparison of the logarithm of our Matsubara Green function (10.128) with the QMC data [132] at $U = 5.2$ and $U = 6$, respectively. The value of the inverse temperature is $\beta = 20$, i.e., $T = 0.05$. The charge gap to third order is $\Delta_C(U = 6) \approx 1.75$ and $\Delta_C(U = 5.2) \approx 0.89$, respectively. Note that the lighter color gives an indication of the error of the QMC calculations.

factor $\exp(-\beta\Delta_C)$. Thus, for temperatures $T \ll \Delta_C(U)$ the excited states of our model should only lead to exponentially small corrections to (10.131).

In figure 10.12 we show a comparison of the logarithm of our Matsubara Green function (10.128) and the QMC data [132]. The inverse temperature in both plots is $\beta = 20$. We see that down to values of $U = 5.2$ we have excellent agreement of both methods; note the logarithmic scale of the ordinate. The flattening of the numerical curve at values of $\ln(-\mathcal{G}) < -13$ is due to a cutoff in the QMC code [132].

In figure 10.13 we depict the difference between the QMC-Matsubara function and our result. The blue curve shows the data for $U = 6$ while the result for $U = 5.2$ is plotted in green. The value of the inverse temperature is $\beta = 20$. Note that the scale of the ordinate is enlarged by a factor of thousand. The fact that the difference at small τ for $U = 5.2$ is larger than for $U = 6$ indicates that the deviation at small τ is due to the higher-order contributions in perturbation theory. Nevertheless, for $U = 6$ as well as for $U = 5.2$ the difference is always smaller than $1/U^3$.

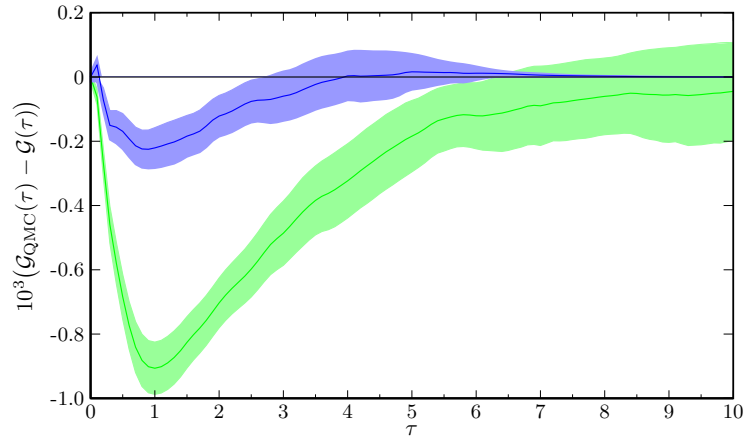


Figure 10.13.: Deviation of our third-order result from QMC data for $U = 6$ (blue) and $U = 5.2$ (green). The value of the inverse temperature is $\beta = 20$.

So eine Arbeit wird eigentlich nie fertig, man muß sie für fertig erklären, wenn man nach Zeit und Umständen das möglichste getan hat.

Italienische Reise by Johann Wolfgang von Goethe

11

Conclusions

In this chapter we summarize our results and give a short outlook of what remains to be done.

11.1. Achievements

In this thesis we provided a new method to obtain the local Green function of the Hubbard model on the Bethe lattice with infinite connectivity in analytic form.

We started with the Dynamical Mean-Field Theory (DMFT) to map the lattice Hubbard model onto an effective Single Impurity Anderson Model (SIAM), the parameters of which we had to fix by means of the DMFT self-consistency equations. For the SIAM we used a setup with two electron baths which are well separated in energy and mapped each bath onto a separate chain. Both such bands are coupled via the impurity site. Next, we invoked the Kato-Takahashi perturbation theory to calculate the local impurity Green function of the SIAM. By means of the Lanczos algorithm we were able to cast the self-consistency equation of the DMFT into a matrix form. This was mainly possible due to the two-chain geometry of the SIAM and the particle-hole symmetry of the Hubbard model under investigation. Because matrices are identical if all their entries are, we achieved a major simplification: We only needed to equate two countable set of numbers. Thus, we were able to use mathematical induction to prove the values of these numbers which we derived from low orders. With the solution of the DMFT equation up to third order in $1/U$ we obtained the parameters of the effective SIAM. Next, we were able to interpret the hybridization function of the SIAM as the local Green function of the first site of a single-particle scattering problem on a semi-infinite chain. We solved this problem and calculated its Green function. Because, due to the DMFT self-consistency, the hybridization function of the SIAM equals the local Green function of the Hubbard model, we obtained the desired analytical result we were aiming at. We like to highlight that this work provides the first analytical solution to the DMFT self-consistency equation for the insulating state, certainly a remarkable result on its own.

With the knowledge of the local Green function we calculated the local density of states of the Mott-Hubbard insulator which is the imaginary part of the Green function. From the density of states we were able to draw conclusions about the magnitude of the single-particle gap for charge-carrying excitations as a function of the ‘Hubbard’-interaction U . We gave an estimate of the critical value for the insulator-to-metal transition.

Finally, we compared our analytical results with two independent numerical methods, namely the Dynamical Density Matrix Renormalization Group (DDMRG) method and the Quantum Monte Carlo (QMC) method. We found excellent agreement between the DDMRG data and our results down to interaction strengths of $U \approx 5$, where $W = 4$ is the bare bandwidth. For the comparison with the QMC results, we approximately calculated the local Matsubara Green function at finite temperature from our zero-temperature local density of states. This was possible due to the substantial single-particle charge gap in the insulator. For values of $U \approx 5$ we found excellent agreement for inverse temperatures $\beta = 20$. As QMC calculations are numerically expensive for small temperatures [135], our result provides a convenient and reliable benchmark test.

11.2. Outlook

In the following section we give a short outlook on future developments concerning our method.

1. First and foremost, the fourth-order calculations seem to be feasible. They would not only provide a quantitative improvement of the results. To fourth order we could prove our assertion about the higher-order sub-bands which, to our understanding, should appear with center of gravity at the excitation energies of the atomic-limit Hamiltonian. According to our results so far, we expect the secondary lower (and upper) Hubbard sub-band to have spectral weight proportional to $1/U^4$. The calculations to fourth order should reveal it. We like to note that we started a first attempt to perform the calculations but, most certainly due to a mistake in the calculations, this did not lead to a solution. We like to stress that the effort we have to invest for the fourth-order calculations corresponds to the combined efforts of the first four orders taken together.
2. If the fourth-order calculation was successful and confirmed our assertion, an implementation of our method as a symbolic computer algorithm would be a possibility to obtain results up to an even higher order in $1/U$. Note, however, that the number of terms in the expansion for the operators increases exponentially with the order in perturbation theory. Even if one takes all simplifications into account, one could only hope for a solution up to approximately the tenth order. At any rate, this is a rather ambitious goal.
3. A third possible extension would be the extension to a Hubbard model with two orbitals per site. The main difficulty will be the additional degeneracy which makes it unclear if the perturbation theory can still be applied.
4. In the SIAM there is always spectral weight at $\omega = 0$ in the metallic phase which vanishes in all numerical DMFT calculations upon entering the insulating phase. In order to study a metallic solution of the DMFT equations, we must include a third electron bath in the effective SIAM and test whether a self-consistent solution for the insulator exists with weight at zero frequency. This would imply that in infinite dimensions there is no insulator except for $U \rightarrow \infty$. Though we do not believe this to happen, a negative result would prove that the DMFT does not constrict the parameter space for the insulator.

Appendices

A

Use of Green Functions

A.1. Classical Green Functions

We assume the reader to be familiar with the theory of Green functions in classical physics such as classical electrodynamics. To recapitulate the ideas of the method we consider Poisson's equation [137]

$$\Delta\Phi(\mathbf{r}) = -4\pi\rho(\mathbf{r}), \quad (\text{A.1})$$

which is a linear partial differential equation. $\rho(\mathbf{r})$ denotes the known charge distribution. To solve (A.1) one first tries to find a solution to the equation

$$\Delta G(\mathbf{r}) = \delta(\mathbf{r}), \quad (\text{A.2})$$

where $G(\mathbf{r})$ is subject to the same boundary conditions as $\Phi(\mathbf{r})$ and $\delta(\mathbf{r})$ denotes the Dirac delta distribution. For simplicity let us assume that $\Phi(|\mathbf{r}| \rightarrow \infty) = 0$. Equation (A.2) defines the Green function for the Laplace operator. By transforming (A.2) to reciprocal space we obtain

$$-k^2\tilde{G}(k) = 1 \quad (\text{A.3})$$

and thus

$$G(\mathbf{r}) = \int \frac{d^3r}{(2\pi)^3} e^{i\mathbf{k}\mathbf{r}} \tilde{G}(\mathbf{k}) = -\frac{1}{4\pi|\mathbf{r}|}. \quad (\text{A.4})$$

Having found the Green function of the problem, we obtain its solution via

$$\Phi(\mathbf{r}) = -4\pi \int d^3r' G(\mathbf{r} - \mathbf{r}') \rho(\mathbf{r}') = \int d^3r' \frac{\rho(\mathbf{r}')}{|\mathbf{r} - \mathbf{r}'|}. \quad (\text{A.5})$$

With the knowledge of the Green function of the Laplace operator one can easily solve inhomogeneous equations such as (A.1).

A.2. Green Functions in Single-Particle Quantum Mechanics

Consider the one-particle Schrödinger equation

$$(i\partial_t - H(\mathbf{r}))\Psi(\mathbf{r}, t) = 0. \quad (\text{A.6})$$

The corresponding Green function $G(\mathbf{r}, \mathbf{r}'; t, t')$ is the solution of

$$(i\partial_t - H(\mathbf{r}))G(\mathbf{r}, \mathbf{r}'; t, t') = \delta(\mathbf{r} - \mathbf{r}')\delta(t - t'), \quad (\text{A.7})$$

subject to the same boundary conditions as $\Psi(\mathbf{r}, t)$. Assuming a closed system, which implies time-translational invariance, $t - t' = \tau$, we may introduce the Fourier transform formally by

$$G(\mathbf{r}, \mathbf{r}'; \tau) = \frac{1}{2\pi} \int_{-\infty}^{\infty} d\omega e^{-i\omega\tau} G(\mathbf{r}, \mathbf{r}'; \omega). \quad (\text{A.8})$$

A. Use of Green Functions

Note that we have, as is common practice in physics, used the same symbol for the Green function and its transform. Transforming (A.7) to the frequency domain leads to

$$(\omega - H(\mathbf{r}))G(\mathbf{r}, \mathbf{r}'; \omega) = \delta(\mathbf{r} - \mathbf{r}'). \quad (\text{A.9})$$

In physics the operator H is local

$$\langle \mathbf{r} | H | \mathbf{r}' \rangle = H(\mathbf{r})\delta(\mathbf{r} - \mathbf{r}'), \quad (\text{A.10})$$

self-adjoint with a purely real spectrum $\sigma(H)$, and possesses an orthonormal and complete set of eigenfunctions

$$H(\mathbf{r})\Phi_n(\mathbf{r}) = E_n\Phi_n(\mathbf{r}). \quad (\text{A.11})$$

Introducing the resolvent operator

$$R(z) = (z - H)^{-1}, \quad (\text{A.12})$$

defined for all $z \in \mathbb{C} \setminus \sigma(H)$, we can write the Green function as the matrix

$$G(\mathbf{r}, \mathbf{r}'; z) = \langle \mathbf{r} | R(z) | \mathbf{r}' \rangle. \quad (\text{A.13})$$

Note in particular that the resolvent is the quantity of interest and can be studied in any single-particle basis

$$G(\alpha, \beta; z) = \langle \alpha | R(z) | \beta \rangle \equiv \langle \text{vac} | c_\alpha R(z) c_\beta^\dagger | \text{vac} \rangle. \quad (\text{A.14})$$

Using the completeness of the eigenstates $\Phi_n(\mathbf{r}) = \langle \mathbf{r} | \Phi_n \rangle$, we obtain the Lehmann representation of the resolvent [12, 138]

$$R(z) = \sum_n \frac{|\Phi_n\rangle\langle\Phi_n|}{z - E_n}. \quad (\text{A.15})$$

Since the eigenvalues E_n are real, the Green function is a meromorphic function with simple poles at the points E_n of the real axis. In principle, the spectrum of H might contain a continuum of eigenenergies. This continuous part produces branch cuts and natural boundaries in $G(\mathbf{r}, \mathbf{r}'; z)$ on the real axis [32]. Since in this thesis no such problems arise, we do not go into further details of this issue.

Due to the singularities of the Green function on the real axis, the integral (A.8) is not well defined and one has to use a limiting procedure to unambiguously define $G(\mathbf{r}, \mathbf{r}'; \tau)$ [32]. We start by writing

$$G_C(\mathbf{r}, \mathbf{r}'; \tau) = \lim_{C \rightarrow \mathbb{R}} \int_C \frac{dz}{2\pi} G(\mathbf{r}, \mathbf{r}'; z) e^{-iz\tau}. \quad (\text{A.16})$$

Depending on how the contour C approaches the real axis \mathbb{R} one obtains different Green functions. Of particular importance in physics are the *retarded* and *advanced* functions, which can be obtained by choosing the path C to lie infinitesimal above or below the real axis:

$$G_{\text{adv}}(\mathbf{r}, \mathbf{r}'; \tau) = \lim_{\eta \searrow 0} \int_{-\infty}^{\infty} \frac{d\omega}{2\pi} \sum_n \frac{e^{-i(\omega \pm i\eta)\tau}}{\omega - E_n \pm i\eta} \Phi_n(\mathbf{r}) \Phi_n^*(\mathbf{r}') \quad (\text{A.17a})$$

$$= \mp i \sum_n \Phi_n(\mathbf{r}) \Phi_n^*(\mathbf{r}') e^{-iE_n\tau} \lim_{\eta \searrow 0} (\mp) \int_{-\infty}^{\infty} \frac{d\omega}{2\pi i} \frac{e^{-i(\omega - E_n \pm i\eta)\tau}}{\omega - E_n \pm i\eta} \quad (\text{A.17b})$$

$$= \mp i \sum_n \Phi_n(\mathbf{r}) \Phi_n^*(\mathbf{r}') e^{-iE_n\tau} \Theta(\pm\tau) \quad (\text{A.17c})$$

$$= \mp i \Theta(\pm\tau) \langle \mathbf{r} | e^{-iH\tau} | \mathbf{r}' \rangle. \quad (\text{A.17d})$$

Note that $e^{-iH\tau}$ is the time evolution operator. This property explains why the Green function is also called ‘propagator’.

The retarded Green function can thus be obtained by making the substitution $z \mapsto \omega + i\eta$ in (A.14). Applying the Dirac identity

$$\lim_{\eta \searrow 0} \frac{1}{\omega \pm i\eta} = \mathcal{P} \frac{1}{\omega} \mp i\pi\delta(\omega) \text{ for } \omega \in \mathbb{R}, \quad (\text{A.18})$$

where we denote the principal value by \mathcal{P} , gives

$$-\frac{1}{\pi}\Im R(\omega + i\eta) = \sum_n |\Phi_n\rangle\delta(\omega - E_n)\langle\Phi_n| = \delta(\omega - H). \quad (\text{A.19})$$

Taking the trace eventually results in

$$N(\omega) := -\frac{1}{\pi}\Im \text{Tr} R(\omega + i\eta) = \sum_n \delta(\omega - E_n). \quad (\text{A.20})$$

$N(\omega)d\omega$ gives the number of states in the energy interval $[\omega, \omega + d\omega]$ and $N(\omega)$ is called the total ‘density of states’. In problems defined on lattices one often likes to know the density of states per unit volume at a particular lattice site. This information can be obtained by taking matrix elements of (A.15) with the position eigenstates $|\mathbf{r}\rangle$ and substituting as above. One obtains in this way

$$\rho(\mathbf{r}, \omega) = -\frac{1}{\pi}\Im G(\mathbf{r}, \mathbf{r}; \omega) = \sum_n \delta(\omega - E_n)\Phi_n(\mathbf{r})\Phi_n^*(\mathbf{r}), \quad (\text{A.21})$$

the density of states per unit volume at position \mathbf{r} . Note that if H is a lattice Hamiltonian, diagonalizable by Bloch states, equation (A.21) simplifies to

$$\rho_\sigma(\omega) = \frac{1}{L} \sum_{\mathbf{k}} \delta(\omega - \epsilon(\mathbf{k})). \quad (\text{A.22})$$

In the last formula we have explicitly included the spin variable, which so far has been suppressed.

A.3. Green Functions in Many-Body Problems

We present some material in this section which is of importance for this work. We follow [11, 12], where the material is presented in great detail. In the following we focus on electrons defined on a lattice with vertices denoted by integer numbers like i, j . In this section we set the chemical potential μ to zero. At zero temperature the causal, single-particle Green function is defined by

$$G_{\sigma\sigma'}(i, j; t) = -i\langle T_s c_{i\sigma}(t) c_{j\sigma'}^\dagger(0) \rangle, \quad (\text{A.23})$$

where the operators are given in the Heisenberg picture and we have assumed a closed system such that only time differences matter. The expectation value is to be taken in the N -particle ground state

$$\langle \dots \rangle = \frac{\langle \Psi_0 | \dots | \Psi_0 \rangle}{\langle \Psi_0 | \Psi_0 \rangle}. \quad (\text{A.24})$$

The symbol T_s denotes the time-ordering operator which includes a sign change,

$$T_s c(t) d(t') = \begin{cases} c(t) d(t') & \text{for } t > t', \\ -d(t') c(t) & \text{for } t' > t. \end{cases} \quad (\text{A.25})$$

For a translational invariant system we may profit from Fourier transformation

$$G_{\sigma\sigma'}(\mathbf{k}, \omega) = \frac{1}{L} \sum_{\mathbf{k}} \int dt e^{-i(\mathbf{k}\cdot(\mathbf{R}_i - \mathbf{R}_j) - \omega t)} G_{\sigma\sigma'}(i, j; t). \quad (\text{A.26})$$

Of particular importance in this work is the local Green function $G_{\text{local},\sigma}(t)$ which, using the identity

$$\frac{1}{L} \sum_{\mathbf{k}} e^{i\mathbf{k}\cdot(\mathbf{R}_i - \mathbf{R}_j)} = \delta_{\mathbf{R}_i, \mathbf{R}_j}, \quad (\text{A.27})$$

A. Use of Green Functions

can be obtained from the \mathbf{k} -resolved function as

$$G_{\text{local},\sigma}(t) := G_{\sigma\sigma}(i, i; t) = \frac{1}{L} \sum_{\mathbf{k}} G_{\sigma\sigma}(\mathbf{k}, t). \quad (\text{A.28})$$

The time-frequency Fourier transformation of the local function can be written as

$$iG_{\text{local},\sigma}(\omega) = \int_{-\infty}^{\infty} dt e^{i\omega t} \langle T_s c_{i\sigma}(t) c_{i\sigma}^\dagger(0) \rangle \quad (\text{A.29a})$$

$$= \int_{-\infty}^{\infty} dt e^{i\omega t} \{ \Theta(t) \langle c_{i\sigma}(t) c_{i\sigma}^\dagger(0) \rangle - \Theta(-t) \langle c_{i\sigma}^\dagger(0) c_{i\sigma}(t) \rangle \} \quad (\text{A.29b})$$

$$= \int_0^{\infty} dt \langle c_{i\sigma} e^{i(\omega+E_0-H)t} c_{i\sigma}^\dagger \rangle - \int_{-\infty}^0 dt \langle c_{i\sigma}^\dagger e^{i(\omega-E_0+H)t} c_{i\sigma} \rangle \quad (\text{A.29c})$$

and thus

$$G_{\text{local},\sigma}(\omega) = \lim_{\eta \searrow 0} \left\{ \langle c_{i\sigma} \frac{1}{\omega - (H - E_0(N)) + i\eta} c_{i\sigma}^\dagger \rangle + \langle c_{i\sigma}^\dagger \frac{1}{\omega + (H - E_0(N)) - i\eta} c_{i\sigma} \rangle \right\}. \quad (\text{A.30})$$

$E_0(N)$ denotes the energy of the N -particle ground state $|\Psi_0\rangle$.

Contrary to the retarded or advanced functions, this Green function is neither analytic in the lower nor in the upper half-plane of \mathbb{C} . Note that (A.30) has the same structure as (A.14) except that we now need both operator orderings and the expectation value is taken in the interacting ground state instead of the vacuum.

The retarded and advanced functions can be introduced according to

$$G_{\text{local},\sigma}^{\text{adv}}(t) = \pm \Theta(\pm t) \langle \{ c_{i\sigma}(t), c_{i\sigma}^\dagger(0) \} \rangle, \quad (\text{A.31})$$

and therefore have Fourier transforms

$$G_{\text{local},\sigma}^{\text{adv}}(\omega) = \lim_{\eta \searrow 0} \left\{ \langle c_{i\sigma} \frac{1}{\omega - (H - E_0(N)) \pm i\eta} c_{i\sigma}^\dagger \rangle + \langle c_{i\sigma}^\dagger \frac{1}{\omega + (H - E_0(N)) \pm i\eta} c_{i\sigma} \rangle \right\}, \quad (\text{A.32})$$

with the usual analytic behavior. In particular we find

$$G_{\text{local},\sigma}^{\text{ret}}(\omega) = G_{\text{local},\sigma}(\omega) \quad \text{for } \omega > 0, \quad (\text{A.33})$$

$$G_{\text{local},\sigma}^{\text{adv}}(\omega) = G_{\text{local},\sigma}(\omega) \quad \text{for } \omega < 0, \quad (\text{A.34})$$

so that it is sufficient to calculate the causal function. In complete analogy to the case of one-particle quantum mechanics one introduces the density of states $D_\sigma(\omega)$ as the imaginary part of the retarded or advanced, local Green function

$$D_\sigma(\omega) = -\frac{1}{\pi} \Im G_{\text{local},\sigma}^{\text{ret}}(\omega) = \frac{1}{\pi} \Im G_{\text{local},\sigma}^{\text{adv}}(\omega). \quad (\text{A.35})$$

To distinguish this density of allowed one-particle excitations of the many-body problem from the density of one-particle levels in the single-particle problem, we will use the symbol $D(\omega)$ instead of $\rho(\omega)$.

Since

$$\int_{-\infty}^{\infty} D_\sigma(\omega) d\omega = \int_{-\infty}^{\infty} d\omega \{ \langle c_{i\sigma} \delta(\omega + E_0 - H) c_{i\sigma}^\dagger \rangle + \langle c_{i\sigma}^\dagger \delta(\omega - E_0 + H) c_{i\sigma} \rangle \} = \langle \{ c_{i\sigma}^\dagger, c_{i\sigma} \} \rangle, \quad (\text{A.36})$$

where $\{a, b\}$ denotes the anti-commutator, the density of states fulfills the important sum rule

$$\int_{-\infty}^{\infty} D_\sigma(\omega) d\omega = 1. \quad (\text{A.37})$$

A.3.1. Self-Energy

The causal Green function of a non-interacting Fermi gas is given by [12]

$$G_{\sigma\sigma'}^{(0)}(\mathbf{k}, \omega) = \delta_{\sigma,\sigma'} \lim_{\eta \searrow 0} \left\{ \frac{\Theta(|\mathbf{k}| - k_F)}{\omega - \epsilon(\mathbf{k}) + i\eta} + \frac{\Theta(k_F - |\mathbf{k}|)}{\omega - \epsilon(\mathbf{k}) - i\eta} \right\}. \quad (\text{A.38})$$

According to Dyson's equation

$$G_{\sigma\sigma'}(\mathbf{k}, \omega) = G_{\sigma\sigma'}^{(0)}(\mathbf{k}, \omega) + \sum_{\sigma'', \sigma'''} G_{\sigma\sigma''}^{(0)}(\mathbf{k}, \omega) \Sigma_{\sigma''\sigma'''}^*(\mathbf{k}, \omega) G_{\sigma'''\sigma'}(\mathbf{k}, \omega) \quad (\text{A.39})$$

the Green function of an interacting problem, which is diagonal in the spin variables, can be written as

$$G_{\sigma}(\mathbf{k}, \omega) = \frac{1}{\omega - \epsilon(\mathbf{k}) - \Sigma_{\sigma}^*(\mathbf{k}, \omega)}. \quad (\text{A.40})$$

Equation (A.40) shows the meaning of the proper, i.e. one-particle irreducible, self-energy $\Sigma_{\sigma}^*(\mathbf{k}, \omega)$. It is a complex function, which includes all the effects of the interaction. The local Green function of the interacting system is therefore given by

$$G_{\text{local},\sigma}(\omega) = \frac{1}{L} \sum_{\mathbf{k}} \frac{1}{\omega - \epsilon(\mathbf{k}) - \Sigma_{\sigma}^*(\mathbf{k}, \omega)}, \quad (\text{A.41})$$

which can be written with the density of one-particle band states $\rho_{\sigma}(\omega)$ as the integral

$$G_{\text{local},\sigma}(\omega) = \int_{-\infty}^{\infty} \frac{\rho_{\sigma}(\omega')}{\omega - \omega' - \Sigma_{\sigma}^*(\omega', \omega)}, \quad (\text{A.42})$$

provided the dependence on momentum of the self-energy is solely given through the dispersion,

$$\Sigma_{\sigma}^*(\mathbf{k}, \omega) = \Sigma_{\sigma}^*(\epsilon(\mathbf{k}), \omega). \quad (\text{A.43})$$

Note that the momentum-dependence of the self-energy complicates the expression considerably. A common approximation is therefore to neglect this dependence [41]. In chapter 6 we show that this approximation becomes exact for Hubbard models in infinite dimensions.

A.3.2. Summary of Diagrammatic Notions

In chapter 6 we will need a few concepts from diagrammatic perturbation theory for the self-energy. Expanding the self-energy up to second order in the interaction strength leads to the diagrams given in figures A.1 and A.2.

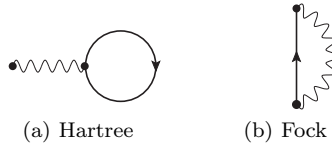


Figure A.1.: Diagrams contributing to $\Sigma_{\sigma}^*(\mathbf{k}, \omega)$ to first order in the interaction.

If only these two diagrams are retained in the proper self-energy, one recovers the Hartree-Fock theory of chapter 2 under the assumption that the Green functions are calculated from the Hartree-Fock Hamiltonian.

The diagrams to second order are shown in figure A.2.

A. Use of Green Functions

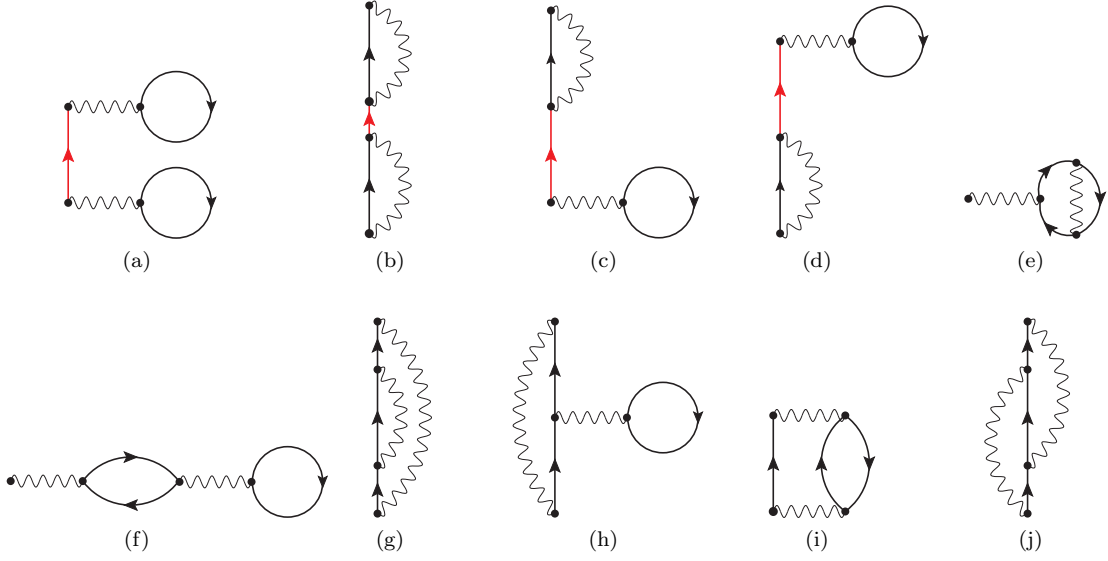


Figure A.2.: Diagrams contributing to $\Sigma_\sigma(\mathbf{k}, \omega)$ in second order perturbation theory.

As one can see, diagrams A.2a to A.2d are one-particle reducible as they separate into two first-order diagrams upon cutting the single-particle lines printed in red. Thus, in second order, only diagrams A.2e to A.2j contribute to the proper self-energy. Note that this reordering of the perturbation series as described by Dyson's equation is of great help since it reduces the number of diagrams one has to calculate.

Another concept of great value for the understanding of chapter 6 is the so-called *skeleton* expansion of the self-energy. Without going into detail, we give a hint of this reordering scheme.

As we can see from figure A.3, diagrams A.2f and A.2e are the leading-order terms in an expansion of diagram A.1a in which one has substituted the bare Green function $G^{(0)}$ with the full interacting Green function, printed as a double line in figure A.3. Figuratively speaking, one takes the 'skeleton' A.1a and adds the 'flesh', namely the full Green function. As a consequence, one calls A.1a a skeleton diagram.

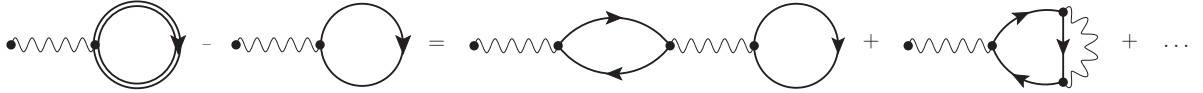


Figure A.3.: Some diagrams contributing to $\Sigma_\sigma^*(\mathbf{k}, \omega)$ and how they can be reordered.

Thus one obtains the skeleton expansion of the proper-self energy if one removes order by order all diagrams containing self-energy insertions, which already exist (without these insertions of course) in lower orders.

We like to draw the readers attention to the beautiful book of Mattuck [139], where he, among other things, can find a very readable and amusing introduction into these concepts.

A.4. Local Green Function of the Infinitely Connected Bethe Lattice

In this section we give the explicit calculation of the non-interacting, local Green function of the Hubbard model on the Bethe lattice with $Z \rightarrow \infty$, starting from the integral expression (6.43).

A.4. Local Green Function of the Infinitely Connected Bethe Lattice

The non-interacting density of states of the tight-binding model on the Bethe lattice with $Z \rightarrow \infty$, (6.36), reads

$$\rho_\infty(\omega) = \frac{1}{2\pi\tilde{t}^2} \sqrt{4\tilde{t}^2 - \omega^2} \Theta(4\tilde{t}^2 - \omega^2). \quad (\text{A.44})$$

We have to insert this expression into (6.43) with $\Sigma^*(\omega) = 0$. We obtain

$$G_{\text{Hubbard}}^{(0)}(z) = \int_{-\infty}^{\infty} \frac{\rho_\infty(\omega')}{z - \omega'} d\omega' \quad (\text{A.45a})$$

$$= \frac{2}{\pi} \int_{-1}^1 \frac{\sqrt{1-u^2}}{z - 2\tilde{t}u} du \quad (\text{A.45b})$$

$$= \frac{2}{\pi} \int_0^\pi \frac{\sin^2(x)}{z - 2\tilde{t}\cos(x)} dx. \quad (\text{A.45c})$$

The last integral, (A.45c), can be found as equation (3.644), no. 4 of [140]. The result thus reads

$$G_{\text{Hubbard}}^{(0)}(z) = \frac{1}{2\tilde{t}^2} (z - \sqrt{z^2 - 4\tilde{t}^2}). \quad (\text{A.46})$$

B

Applications of Symmetries of the Hubbard Model

In this appendix we discuss some important consequences of the various symmetries of the Hubbard Hamiltonian as described in Sect. 5.2.

B.1. Irrelevance of the Sign of the Electron Transfer Amplitude

Let us consider the Hubbard Hamiltonian (5.12) on a bipartite lattice. The transformation \mathcal{T}_2 , (5.25), leads to

$$\mathcal{T}_2^\dagger H(t) \mathcal{T}_2 = \sum_{\substack{l,m \\ \sigma}} (-1)^{l+m} t(l-m) c_{l\sigma}^\dagger c_{m\sigma} + U \sum_i (n_{i\uparrow} - 1/2)(n_{i\downarrow} - 1/2) \quad (\text{B.1a})$$

$$= - \sum_{\substack{l,m \\ \sigma}} t(l-m) c_{l\sigma}^\dagger c_{m\sigma} + U \sum_i (n_{i\uparrow} - 1/2)(n_{i\downarrow} - 1/2) \quad (\text{B.1b})$$

$$= H(-t). \quad (\text{B.1c})$$

As a consequence, the free energy is given by

$$F(t) = \frac{\text{Tr} H(t) e^{-\beta(H(t) - \mu N)}}{\text{Tr} e^{-\beta(H(t) - \mu N)}} \quad (\text{B.2a})$$

$$= \frac{\text{Tr} \mathcal{T}_2^\dagger H(t) \mathcal{T}_2 \mathcal{T}_2^\dagger e^{-\beta(H(t) - \mu N)} \mathcal{T}_2}{\text{Tr} \mathcal{T}_2^\dagger e^{-\beta(H(t) - \mu N)} \mathcal{T}_2} \quad (\text{B.2b})$$

$$= \frac{\text{Tr} \mathcal{T}_2^\dagger H(t) \mathcal{T}_2 e^{-\beta \mathcal{T}_2^\dagger (H(t) - \mu N) \mathcal{T}_2}}{\text{Tr} e^{-\beta \mathcal{T}_2^\dagger (H(t) - \mu N) \mathcal{T}_2}} \quad (\text{B.2c})$$

$$= \frac{\text{Tr} H(-t) e^{-\beta(H(-t) - \mu N)}}{\text{Tr} e^{-\beta(H(-t) - \mu N)}} \quad (\text{B.2d})$$

$$= F(-t), \quad (\text{B.2e})$$

which shows that the spectrum and the thermodynamic quantities of $H(t)$ and $H(-t)$ coincide.

B.2. Chemical Potential at Half Band-Filling

All models in this section are defined on a bipartite lattice. The band is half filled for all temperatures for a fixed chemical potential μ . In order to prove this statement we start with the application of the transformation $\mathcal{T}_{3,\sigma}$ introduced in Sect. 5.2.2.

The kinetic energy is invariant under the $\mathcal{T}_{3,\sigma}$ transformations, as shown in Sect. 5.2.2. The local number operators $n_{l\sigma}$ transform according to

$$\mathcal{T}_{3\sigma}^\dagger n_{l\sigma} \mathcal{T}_{3\sigma} = 1 - n_{l\sigma}, \quad (\text{B.3})$$

B. Applications of Symmetries of the Hubbard Model

which leads to the following transformations of the total number operator and the interaction:

$$\mathcal{T}_{3\sigma}^\dagger N_\sigma \mathcal{T}_{3\sigma} = L - N_\sigma, \quad (\text{B.4})$$

$$\mathcal{T}_{3\sigma}^\dagger N \mathcal{T}_{3\sigma} = \begin{cases} L + 2S^z & \text{for } \sigma = \downarrow, \\ L - 2S^z & \text{for } \sigma = \uparrow, \end{cases} \quad (\text{B.5})$$

$$\mathcal{T}_{3\sigma}^\dagger 2S^z \mathcal{T}_{3\sigma} = \begin{cases} N - L & \text{for } \sigma = \downarrow, \\ L - N & \text{for } \sigma = \uparrow, \end{cases} \quad (\text{B.6})$$

$$\mathcal{T}_3^\dagger N \mathcal{T}_3 = 2L - N, \quad (\text{B.7})$$

$$\mathcal{T}_{3\sigma'}^\dagger \frac{1}{2} \sum_{l,\sigma} n_{l\sigma} n_{l,-\sigma} \mathcal{T}_{3\sigma'} = -D + N_{-\sigma'}, \quad (\text{B.8})$$

$$\mathcal{T}_3^\dagger D \mathcal{T}_3 = D + (L - N). \quad (\text{B.9})$$

The modified Hubbard interaction (5.12) on the other hand just changes its sign, see (5.30a). For Hubbard's original model, (5.10), one finds

$$\langle N \rangle_H(\mu, T) = \frac{1}{\beta} \frac{\partial}{\partial \mu} \ln \text{Tr} \left[e^{-\beta(H - \mu N)} \right] \quad (\text{B.10a})$$

$$= \frac{1}{\beta} \frac{\partial}{\partial \mu} \ln \text{Tr} \left[\mathcal{T}_3^\dagger e^{-\beta(H - \mu N)} \mathcal{T}_3 \right] \quad (\text{B.10b})$$

$$= \frac{1}{\beta} \frac{\partial}{\partial \mu} \ln \text{Tr} \left[e^{-\beta \mathcal{T}_3^\dagger (H - \mu N) \mathcal{T}_3} \right] \quad (\text{B.10c})$$

$$= \frac{1}{\beta} \frac{\partial}{\partial \mu} \ln \text{Tr} \left[e^{-\beta(H + U(L - N) - \mu(2L - N))} \right] \quad (\text{B.10d})$$

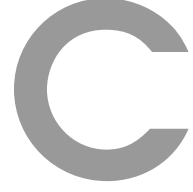
$$= 2L + \frac{1}{\beta} \frac{\partial}{\partial \mu} \ln \text{Tr} \left[e^{-\beta(H - (U - \mu)N)} \right] \quad (\text{B.10e})$$

$$= 2L - \langle N \rangle_H(U - \mu, T). \quad (\text{B.10f})$$

This shows that for the original Hubbard model (5.10) the choice of $\mu = U/2$ for the chemical potential ensures a half-filled band, i.e. $\langle N \rangle_H = L$, for all temperatures. For the modified Hubbard model H_{Hubbard} on the other hand, an analogous calculation leads to the result

$$\langle N \rangle_{H_{\text{Hubbard}}}(\mu, T) = 2L - \langle N \rangle_{H_{\text{Hubbard}}}(-\mu, T), \quad (\text{B.11})$$

which in turn proves, making the choice of $\mu = 0$ for the chemical potential ensures a half-filled band, $\langle N \rangle_{H_{\text{Hubbard}}} = L$, for all temperatures.



Calculation of the Mappings in the Kato-Takahashi Formalism

In this appendix we calculate explicit expressions for Takahashi's operator Γ_i and the 'transformed energy operator' $\Gamma_i^\dagger(H - E_i^{(0)})\Gamma_i$, defined in chapter 8. We begin with deriving the formulae for the expansion in the general coupling constant λ , see (7.13). Then, we apply the expansion in λ to the Single Impurity Anderson Model (SIAM) in two-chain geometry, (9.30). We will see that the expansion in $1/U$ differs from the expansion in the general coupling λ . This is a consequence of the implicit $1/U$ dependence of the perturbation V in the case of the SIAM.

C.1. Expansion of Takahashi's operator

In this section we derive the expression up to fourth order in the coupling λ , (7.13), for Takahashi's operator (8.4),

$$\Gamma_i(\lambda, N) = \sum_{n=0}^{\infty} \lambda^n \tilde{\Gamma}_i^{(n)}(N), \quad (\text{C.1})$$

as introduced in chapter 8. We suppress the dependence on the total number of particles from now on.

C.1.1. Calculations

Explicit Expansion of $P_i(\lambda)P_i^{(0)}(\lambda)$

As shown in chapter 7, we know that

$$P_i = P_i^{(0)} + \sum_{n=1}^{\infty} \lambda^n A^{(n)}, \quad (\text{C.2a})$$

$$A^{(n)} = - \sum_{(n)} \tilde{S}^{k_1} V \tilde{S}^{k_2} \dots V \tilde{S}^{k_{n+1}}. \quad (\text{C.2b})$$

Here, we have used the abbreviations (7.64)

$$\sum_{(n)} F(k_1, \dots, k_m) = \sum_{\substack{k_1, \dots, k_m=0 \\ k_1 + \dots + k_m = n}}^n F(k_1, \dots, k_m) \quad (\text{C.3})$$

and (7.63)

$$\tilde{S}^0 = -P_i^{(0)} \quad \wedge \quad (E_i^{(0)} - H_0)\tilde{S} = \mathbb{1} - P_i^{(0)}. \quad (\text{C.4})$$

C. Calculation of the Mappings in the Kato-Takahashi Formalism

In all subsequent expressions involving P_i it will always appear in combination with $P_i^{(0)}$ in the form $P_i P_i^{(0)}$. It follows that $\tilde{S}^{k_{n+1}}$ in the expansion of $A^{(n)}$ must always be set to $P_i^{(0)}$ which implies $k_{n-1} = 0$,

$$P_i P_i^{(0)} = P_i^{(0)} + \sum_{n=1}^{\infty} \lambda^n \tilde{A}^{(n)}, \text{ where } \tilde{A}^{(n)} := A^{(n)} P_i^{(0)}. \quad (\text{C.5})$$

In order to save space we will simply write

$$A^{(n)} = - \sum_{(n)} k_1 k_2 \dots k_{n+1}, \quad (\text{C.6})$$

i.e., we will only write down the exponents of \tilde{S} . Since $\tilde{S}^0 = -P_i^{(0)}$ we must include a minus sign for every '0'.

First Order

$$\begin{aligned} \tilde{A}^{(1)} &= - \sum_{(1)} k_1 k_2 \cdot 0 = \sum_{(1)} k_1 0 \\ &\boxed{\tilde{A}^{(1)} = 10} \end{aligned} \quad (\text{C.7})$$

Second Order

$$\begin{aligned} \tilde{A}^{(2)} &= - \sum_{(2)} k_1 k_2 k_3 \cdot 0 = \sum_{(2)} k_1 k_2 0 \\ &\boxed{\tilde{A}^{(2)} = -200 - 020 + 110} \end{aligned} \quad (\text{C.8})$$

Third Order

$$\begin{aligned} \tilde{A}^{(3)} &= - \sum_{(3)} k_1 k_2 k_3 k_4 \cdot 0 = \sum_{(3)} k_1 k_2 k_3 0 \\ &\boxed{\tilde{A}^{(3)} = 3000 + 0300 + 0030 - 2100 - 2010 \\ &\quad - 1200 - 0210 - 1020 - 0120 + 1110} \end{aligned} \quad (\text{C.9})$$

Fourth Order

$$\begin{aligned} \tilde{A}^{(4)} &= - \sum_{(4)} k_1 k_2 k_3 k_4 k_5 \cdot 0 = \sum_{(4)} k_1 k_2 k_3 k_4 0 \\ &\boxed{\begin{aligned} \tilde{A}^{(4)} &= - 40000 - 04000 - 00400 - 00040 + 31000 + 30100 + 30010 \\ &\quad + 13000 + 03100 + 03010 + 10300 + 01300 + 00310 + 10030 \\ &\quad + 01030 + 00130 + 22000 + 20200 + 20020 + 02200 + 02020 \\ &\quad + 00220 - 21100 - 21010 - 20110 - 12100 - 12010 - 02110 \\ &\quad - 11200 - 10210 - 01210 - 11020 - 10120 - 01120 + 11110 \end{aligned}} \end{aligned} \quad (\text{C.10})$$

Expansion of $P_i^{(0)}(\lambda)P_i(\lambda)P_i^{(0)}(\lambda)$

We define

$$P_i^{(0)} P_i P_i^{(0)} = P_i^{(0)} + \sum_{n=1}^{\infty} \lambda^n \bar{A}^{(n)}, \text{ where } \bar{A}^{(n)} := P_i^{(0)} \tilde{A} \equiv P_i^{(0)} A^{(n)} P_i^{(0)} \quad (\text{C.11})$$

and find,

First Order

$$\boxed{\bar{A}^{(1)} \text{ vanishes,}} \quad (\text{C.12})$$

Second Order

$$\boxed{\bar{A}^{(2)} = -020,} \quad (\text{C.13})$$

Third Order

$$\boxed{\bar{A}^{(3)} = 0300 + 0030 - 0210 - 0120,} \quad (\text{C.14})$$

Fourth Order

$$\boxed{\begin{aligned} \bar{A}^{(4)} = & -04000 - 00400 - 00040 + 03100 + 03010 \\ & + 01300 + 00310 + 01030 + 00130 + 02200 \\ & + 02020 + 00220 - 02110 - 01210 - 01120. \end{aligned}} \quad (\text{C.15})$$

Expansion of $(P_i^{(0)}(\lambda)P_i(\lambda)P_i^{(0)}(\lambda))^{-\frac{1}{2}}$

With

$$P_i^{(0)} - P_i^{(0)}P_iP_i^{(0)} = -\sum_{n=2}^{\infty} \lambda^n \bar{A}^{(n)}, \quad (\text{C.16})$$

it readily follows that

$$P_i^{(0)}(P_i^{(0)}P_iP_i^{(0)})^{-\frac{1}{2}} = P_i^{(0)} + \sum_{m=1}^{\infty} (-1)^m \frac{(2m-1)!!}{(2m)!!} \prod_{i=1}^m \left\{ \sum_{l_i=2}^{\infty} \lambda^{l_i} \bar{A}^{(l_i)} \right\}. \quad (\text{C.17})$$

Thus, up to fourth order in λ , we have

$$P_i^{(0)}(P_i^{(0)}P_iP_i^{(0)})^{-\frac{1}{2}} = P_i^{(0)} + \lambda^2 \left\{ -\frac{1}{2} \bar{A}^{(2)} \right\} + \lambda^3 \left\{ -\frac{1}{2} \bar{A}^{(3)} \right\} + \lambda^4 \left\{ \frac{3}{8} (\bar{A}^{(2)})^2 - \frac{1}{2} \bar{A}^{(4)} \right\}. \quad (\text{C.18})$$

Explicit Expansion of $\Gamma_i(\lambda)$

Using the defining equation (8.4),

$$\Gamma_i = P_i P_i^{(0)} \left(P_i^{(0)} P_i P_i^{(0)} \right)^{-\frac{1}{2}}, \quad (\text{C.19})$$

and the results of the preceding subsections, we find

$$\begin{aligned} \Gamma_i &= \left\{ P_i^{(0)} + \sum_{n=1}^{\infty} \lambda^n \bar{A}^{(n)} \right\} \times \left\{ P_i^{(0)} + \lambda^2 \left\{ -\frac{1}{2} \bar{A}^{(2)} \right\} + \lambda^3 \left\{ -\frac{1}{2} \bar{A}^{(3)} \right\} \right. \\ &\quad \left. + \lambda^4 \left\{ \frac{3}{8} (\bar{A}^{(2)})^2 - \frac{1}{2} \bar{A}^{(4)} \right\} + \mathcal{O}(\lambda^5) \right\} \\ &= P_i^{(0)} + \lambda \{ \bar{A}^{(1)} \} + \lambda^2 \{ \bar{A}^{(2)} - 1/2 \bar{A}^{(2)} \} + \lambda^3 \{ \bar{A}^{(3)} - 1/2 \bar{A}^{(1)} \bar{A}^{(2)} - 1/2 \bar{A}^{(3)} \} \\ &\quad + \lambda^4 \{ \bar{A}^{(4)} - 1/2 \bar{A}^{(2)} \bar{A}^{(2)} - 1/2 \bar{A}^{(1)} \bar{A}^{(3)} + 3/8 (\bar{A}^{(2)})^2 - 1/2 \bar{A}^{(4)} \} + \mathcal{O}(\lambda^5). \end{aligned} \quad (\text{C.20})$$

With the definition

$$\Gamma_i = \sum_{n=0}^{\infty} \lambda^n \tilde{\Gamma}_i^{(n)}, \quad (\text{C.21})$$

C. Calculation of the Mappings in the Kato-Takahashi Formalism

where

$$\tilde{\Gamma}_i^{(0)} := P_i^{(0)}, \quad (\text{C.22a})$$

$$\tilde{\Gamma}_i^{(1)} := \tilde{A}^{(1)}, \quad (\text{C.22b})$$

$$\tilde{\Gamma}_i^{(2)} := \tilde{A}^{(2)} - 1/2\bar{A}^{(2)}, \quad (\text{C.22c})$$

$$\tilde{\Gamma}_i^{(3)} := \tilde{A}^{(3)} - 1/2\tilde{A}^{(1)}\bar{A}^{(2)} - 1/2\bar{A}^{(3)}, \quad (\text{C.22d})$$

$$\tilde{\Gamma}_i^{(4)} := \tilde{A}^{(4)} - 1/2\tilde{A}^{(2)}\bar{A}^{(2)} - 1/2\tilde{A}^{(1)}\bar{A}^{(3)} + 3/8(\bar{A}^{(2)})^2 - 1/2\bar{A}^{(4)}, \quad (\text{C.22e})$$

we obtain,

Leading Order

$$\boxed{\tilde{\Gamma}_i^{(0)} = P_i^{(0)},} \quad (\text{C.23})$$

First Order

$$\boxed{\tilde{\Gamma}_i^{(1)} = 10,} \quad (\text{C.24})$$

Second Order

$$\boxed{\tilde{\Gamma}_i^{(2)} = -200 - \frac{1}{2}020 + 110,} \quad (\text{C.25})$$

Third Order

$$-\frac{1}{2}\tilde{A}^{(1)}\bar{A}^2 = -\frac{1}{2}(10)(-020) = \frac{1}{2}1020,$$

$$\boxed{\begin{aligned} \tilde{\Gamma}_i^{(3)} &= 3000 + \frac{1}{2}0300 + \frac{1}{2}0030 - 2100 - 2010 \\ &\quad - 1200 - \frac{1}{2}0210 - \frac{1}{2}1020 - \frac{1}{2}0120 + 1110, \end{aligned}} \quad (\text{C.26})$$

Fourth Order

$$\begin{aligned} -\frac{1}{2}\tilde{A}^{(2)}\bar{A}^{(2)} &= -\frac{1}{2}(-200 - 020 + 110)(-020) \\ &= -\frac{1}{2}20020 - \frac{1}{2}02020 + \frac{1}{2}11020, \\ -\frac{1}{2}\tilde{A}^{(1)}\bar{A}^{(3)} &= -\frac{1}{2}10300 - \frac{1}{2}10030 + \frac{1}{2}10210 + \frac{1}{2}10120, \\ \frac{3}{8}(\bar{A}^{(2)})^2 &= \frac{3}{8}02020, \end{aligned}$$

$$\boxed{\begin{aligned} \tilde{\Gamma}_i^{(4)} &= -40000 - \frac{1}{2}04000 - \frac{1}{2}00400 - \frac{1}{2}00040 + 31000 + 30100 \\ &\quad + 30010 + 13000 + \frac{1}{2}03100 + \frac{1}{2}03010 + \frac{1}{2}10300 + \frac{1}{2}01300 \\ &\quad + \frac{1}{2}00310 + \frac{1}{2}10030 + \frac{1}{2}01030 + \frac{1}{2}00130 + 22000 + 20200 \\ &\quad + \frac{1}{2}20020 + \frac{1}{2}02200 + \frac{3}{8}02020 + \frac{1}{2}00220 - 21100 - 21010 \\ &\quad - 20110 - 12100 - 12010 - \frac{1}{2}02110 - 11200 - \frac{1}{2}10210 \\ &\quad - \frac{1}{2}01210 - \frac{1}{2}11020 - \frac{1}{2}10120 - \frac{1}{2}01120 + 11110. \end{aligned}} \quad (\text{C.27})$$

C.1.2. Summary

The expansion of Takahashi's operator

$$\Gamma_i = \sum_{n=0}^{\infty} \lambda^n \tilde{\Gamma}_i^{(n)} \quad (\text{C.28})$$

reads up to fourth order in the coupling λ ,

$$\tilde{\Gamma}_i^{(0)} := P_i^{(0)}, \quad (\text{C.29a})$$

$$\tilde{\Gamma}_i^{(1)} := \tilde{S} V P_i^{(0)}, \quad (\text{C.29b})$$

$$\tilde{\Gamma}_i^{(2)} := -\tilde{S}^2 V P_i^{(0)} V P_i^{(0)} - \frac{1}{2} P_i^{(0)} V \tilde{S}^2 V P_i^{(0)} + \tilde{S} V \tilde{S} V P_i^{(0)}, \quad (\text{C.29c})$$

$$\begin{aligned} \tilde{\Gamma}_i^{(3)} := & \tilde{S}^3 V P_i^{(0)} V P_i^{(0)} V P_i^{(0)} + \frac{1}{2} P_i^{(0)} V \tilde{S}^3 V P_i^{(0)} V P_i^{(0)} + \frac{1}{2} P_i^{(0)} V P_i^{(0)} V \tilde{S}^3 V P_i^{(0)} \\ & - \tilde{S}^2 V \tilde{S} V P_i^{(0)} V P_i^{(0)} - \tilde{S}^2 V P_i^{(0)} V \tilde{S} V P_i^{(0)} - \tilde{S} V \tilde{S}^2 V P_i^{(0)} V P_i^{(0)} - \frac{1}{2} P_i^{(0)} V \tilde{S}^2 V \tilde{S} V P_i^{(0)} \\ & - \frac{1}{2} \tilde{S} V P_i^{(0)} V \tilde{S}^2 V P_i^{(0)} - \frac{1}{2} P_i^{(0)} V \tilde{S} V \tilde{S}^2 V P_i^{(0)} + \tilde{S} V \tilde{S} V \tilde{S} V P_i^{(0)}, \end{aligned} \quad (\text{C.29d})$$

$$\begin{aligned} \tilde{\Gamma}_i^{(4)} := & -\tilde{S}^4 V P_i^{(0)} V P_i^{(0)} V P_i^{(0)} V P_i^{(0)} - \frac{1}{2} P_i^{(0)} V \tilde{S}^4 V P_i^{(0)} V P_i^{(0)} V P_i^{(0)} - \frac{1}{2} P_i^{(0)} V P_i^{(0)} V \tilde{S}^4 V P_i^{(0)} V P_i^{(0)} \\ & - \frac{1}{2} P_i^{(0)} V P_i^{(0)} V P_i^{(0)} V \tilde{S}^4 V P_i^{(0)} + \tilde{S}^3 V \tilde{S} V P_i^{(0)} V P_i^{(0)} V P_i^{(0)} + \tilde{S}^3 V P_i^{(0)} V \tilde{S} V P_i^{(0)} V P_i^{(0)} \\ & + \tilde{S}^3 V P_i^{(0)} V P_i^{(0)} V \tilde{S} V P_i^{(0)} + \tilde{S} V \tilde{S}^3 V P_i^{(0)} V P_i^{(0)} V P_i^{(0)} + \frac{1}{2} P_i^{(0)} V \tilde{S}^3 V \tilde{S} V P_i^{(0)} V P_i^{(0)} \\ & + \frac{1}{2} P_i^{(0)} V \tilde{S}^3 V P_i^{(0)} V \tilde{S} V P_i^{(0)} + \frac{1}{2} \tilde{S} V P_i^{(0)} V \tilde{S}^3 V P_i^{(0)} V P_i^{(0)} + \frac{1}{2} P_i^{(0)} V \tilde{S} V \tilde{S}^3 V P_i^{(0)} V P_i^{(0)} \\ & + \frac{1}{2} P_i^{(0)} V P_i^{(0)} V \tilde{S}^3 V \tilde{S} V P_i^{(0)} + \frac{1}{2} \tilde{S} V P_i^{(0)} V P_i^{(0)} V \tilde{S}^3 V P_i^{(0)} + \frac{1}{2} P_i^{(0)} V \tilde{S} V P_i^{(0)} V \tilde{S}^3 V P_i^{(0)} \\ & + \frac{1}{2} P_i^{(0)} V P_i^{(0)} V \tilde{S} V \tilde{S}^3 V P_i^{(0)} + \tilde{S}^2 V \tilde{S}^2 V P_i^{(0)} V P_i^{(0)} V P_i^{(0)} + \tilde{S}^2 V P_i^{(0)} V \tilde{S}^2 V P_i^{(0)} V P_i^{(0)} \\ & + \frac{1}{2} \tilde{S}^2 V P_i^{(0)} V P_i^{(0)} V \tilde{S}^2 V P_i^{(0)} + \frac{1}{2} P_i^{(0)} V \tilde{S}^2 V \tilde{S}^2 V P_i^{(0)} V P_i^{(0)} + \frac{3}{8} P_i^{(0)} V \tilde{S}^2 V P_i^{(0)} V \tilde{S}^2 V P_i^{(0)} \\ & + \frac{1}{2} P_i^{(0)} V P_i^{(0)} V \tilde{S}^2 V \tilde{S}^2 V P_i^{(0)} - \tilde{S}^2 V \tilde{S} V \tilde{S} V P_i^{(0)} V P_i^{(0)} - \tilde{S}^2 V \tilde{S} V P_i^{(0)} V \tilde{S} V P_i^{(0)} \\ & - \tilde{S}^2 V P_i^{(0)} V \tilde{S} V \tilde{S} V P_i^{(0)} - \tilde{S} V \tilde{S}^2 V \tilde{S} V P_i^{(0)} V P_i^{(0)} - \tilde{S} V \tilde{S}^2 V P_i^{(0)} V \tilde{S} V P_i^{(0)} \\ & - \frac{1}{2} P_i^{(0)} V \tilde{S}^2 V \tilde{S} V \tilde{S} V P_i^{(0)} - \tilde{S} V \tilde{S} V \tilde{S}^2 V P_i^{(0)} V P_i^{(0)} - \frac{1}{2} \tilde{S} V P_i^{(0)} V \tilde{S}^2 V \tilde{S} V P_i^{(0)} \\ & - \frac{1}{2} P_i^{(0)} V \tilde{S} V \tilde{S}^2 V \tilde{S} V P_i^{(0)} - \frac{1}{2} \tilde{S} V \tilde{S} V P_i^{(0)} V \tilde{S}^2 V P_i^{(0)} - \frac{1}{2} \tilde{S} V P_i^{(0)} V \tilde{S} V \tilde{S}^2 V P_i^{(0)} \\ & - \frac{1}{2} P_i^{(0)} V \tilde{S} V \tilde{S} V \tilde{S}^2 V P_i^{(0)} + \tilde{S} V \tilde{S} V \tilde{S} V \tilde{S} V P_i^{(0)}. \end{aligned} \quad (\text{C.29e})$$

C.2. Expansion of the Transformed Energy Operator

In this section we derive the formulae for the reduced energy operator (8.22),

$$\Gamma_i^\dagger(\lambda, N)(H - E_i^{(0)}(N))\Gamma_i(\lambda, N) =: \sum_{n=1}^{\infty} \lambda^n \tilde{R}_i^{(n)}(N), \quad (\text{C.30})$$

as introduced in chapter 8. Note that we will usually suppress the dependence on the total number N of particles.

C.2.1. Calculations

Expansion of $(H - E_i^{(0)})P_i(\lambda)P_i^{(0)}(\lambda)$

Kato perturbation theory tells us that

$$(H - E_i^{(0)})P_i P_i^{(0)} = \sum_{n=1}^{\infty} \lambda^n \tilde{B}^{(n)}, \quad (\text{C.31})$$

where

$$\tilde{B}^{(n)} := - \sum_{(n-1)} \tilde{S}^{k_1} V \tilde{S}^{k_2} V \dots \tilde{S}^{k_n} V P_i^{(0)}. \quad (\text{C.31a})$$

Writing down only the exponents, we arrive at:

First Order

$$\tilde{B}^{(1)} = - \sum_{(0)} k_1 0,$$

$$\boxed{\tilde{B}^{(1)} = 00}, \quad (\text{C.32})$$

Second Order

$$\tilde{B}^{(2)} = - \sum_{(1)} k_1 k_2 0,$$

$$\boxed{\tilde{B}^{(2)} = 100 + 010}, \quad (\text{C.33})$$

Third Order

$$\tilde{B}^{(3)} = - \sum_{(2)} k_1 k_2 k_3 0,$$

$$\boxed{\tilde{B}^{(3)} = -2000 - 0200 - 0020 + 1100 + 1010 + 0110}, \quad (\text{C.34})$$

Fourth Order

$$\tilde{B}^{(4)} = - \sum_{(3)} k_1 k_2 k_3 k_4 0,$$

$$\boxed{\begin{aligned} \tilde{B}^{(4)} = & 30000 + 03000 + 00300 + 00030 - 21000 - 20100 - 20010 \\ & - 12000 - 02100 - 02010 - 10200 - 01200 - 00210 - 10020 \\ & - 01020 - 00120 + 11100 + 11010 + 10110 + 01110. \end{aligned}} \quad (\text{C.35})$$

Fifth Order

$$\tilde{B}^{(5)} = - \sum_{(4)} k_1 k_2 k_3 k_4 k_5 0,$$

$\begin{aligned} \tilde{B}^{(5)} = & -400000 - 040000 - 004000 - 000400 - 000040 + 310000 \\ & + 301000 + 300100 + 300010 + 130000 + 031000 + 030100 \\ & + 030010 + 103000 + 013000 + 003100 + 003010 + 100300 \\ & + 010300 + 001300 + 000310 + 100030 + 010030 + 001030 \\ & + 000130 + 220000 + 202000 + 200200 + 200020 + 022000 \\ & + 020200 + 020020 + 002200 + 002020 + 000220 - 211000 \\ & - 210100 - 210010 - 201100 - 201010 - 200110 - 121000 \\ & - 120100 - 120010 - 021100 - 021010 - 020110 - 112000 \\ & - 102100 - 102010 - 012100 - 012010 - 002110 - 110200 \\ & - 101200 - 100210 - 011200 - 010210 - 001210 - 110020 \\ & - 101020 - 100120 - 011020 - 010120 - 001120 + 111100 \\ & + 111010 + 110110 + 101110 + 011110. \end{aligned}$	(C.36)
--	--------

Expansion of $(H - E_i^{(0)})\Gamma_i(\lambda)$

Recalling that

$$\begin{aligned} P_i^{(0)}(P_i^{(0)}P_iP_i^{(0)})^{-\frac{1}{2}} = & P_i^{(0)} + \lambda^2 \left\{ -\frac{1}{2}\bar{A}^{(2)} \right\} + \lambda^3 \left\{ -\frac{1}{2}\bar{A}^{(3)} \right\} \\ & + \lambda^4 \left\{ \frac{3}{8}(\bar{A}^{(2)})^2 - \frac{1}{2}\bar{A}^{(4)} \right\} + \mathcal{O}(\lambda^5), \end{aligned} \quad (C.37)$$

we define

$$(H - E_i^{(0)})\Gamma_i = \sum_{n=1}^5 \lambda^n C^{(n)} + \mathcal{O}(\lambda^6), \quad (C.38)$$

where

$$C^{(1)} := \tilde{B}^{(1)}, \quad (C.39a)$$

$$C^{(2)} := \tilde{B}^{(2)}, \quad (C.39b)$$

$$C^{(3)} := \tilde{B}^{(3)} - \frac{1}{2}\tilde{B}^{(1)}\bar{A}^{(2)}, \quad (C.39c)$$

$$C^{(4)} := \tilde{B}^{(4)} - \frac{1}{2}\tilde{B}^{(2)}\bar{A}^{(2)} - \frac{1}{2}\tilde{B}^{(1)}\bar{A}^{(3)}, \quad (C.39d)$$

$$C^{(5)} := \tilde{B}^{(5)} - \frac{1}{2}\tilde{B}^{(3)}\bar{A}^{(2)} - \frac{1}{2}\tilde{B}^{(2)}\bar{A}^{(3)} + \tilde{B}^{(1)} \left\{ \frac{3}{8}(\bar{A}^{(2)})^2 - \frac{1}{2}\bar{A}^{(4)} \right\}. \quad (C.39e)$$

This results in

First Order

$$\boxed{C^{(1)} = 00}, \quad (C.40)$$

Second Order

$$\boxed{C^{(2)} = 100 + 010}, \quad (C.41)$$

C. Calculation of the Mappings in the Kato-Takahashi Formalism

Third Order

$$-\frac{1}{2}\tilde{B}^{(1)}\bar{A}^{(2)} = \frac{1}{2}0020,$$

$$C^{(3)} = -2000 - 0200 - \frac{1}{2}0020 + 1100 + 1010 + 0110,$$

(C.42)

Fourth Order

$$-\frac{1}{2}\tilde{B}^{(2)}\bar{A}^{(2)} = \frac{1}{2}10020 + \frac{1}{2}01020,$$

$$-\frac{1}{2}\tilde{B}^{(1)}\bar{A}^{(3)} = -\frac{1}{2}00300 - \frac{1}{2}00030 + \frac{1}{2}00210 + \frac{1}{2}00120,$$

$$C^{(4)} = 30000 + 0300 + \frac{1}{2}00300 + \frac{1}{2}00030 - 21000 - 20100 - 20010 \\ -12000 - 02100 - 020100 - 10200 - 01200 - \frac{1}{2}00210 - \frac{1}{2}10020 \\ - \frac{1}{2}01020 - \frac{1}{2}00120 + 11100 + 11010 + 10110 + 01110,$$

(C.43)

Fifth Order

$$-\frac{1}{2}\tilde{B}^{(3)}\bar{A}^{(2)} = -\frac{1}{2}200020 - \frac{1}{2}020020 - \frac{1}{2}002020 + \frac{1}{2}110020 \\ + \frac{1}{2}101020 + \frac{1}{2}011020,$$

$$-\frac{1}{2}\tilde{B}^{(2)}\bar{A}^{(3)} = -\frac{1}{2}100300 - \frac{1}{2}100030 + \frac{1}{2}100210 + \frac{1}{2}100120 \\ - \frac{1}{2}010300 - \frac{1}{2}010030 + \frac{1}{2}010210 + \frac{1}{2}010120,$$

$$-\frac{3}{8}\tilde{B}^{(1)}(\bar{A}^{(2)})^2 = \frac{3}{8}002020,$$

$$-\frac{1}{2}\tilde{B}^{(1)}\bar{A}^{(4)} = \frac{1}{2}004000 + \frac{1}{2}000400 + \frac{1}{2}000040 - \frac{1}{2}003100 \\ - \frac{1}{2}003010 - \frac{1}{2}001300 - \frac{1}{2}000310 - \frac{1}{2}001030 \\ - \frac{1}{2}000130 - \frac{1}{2}002200 - \frac{1}{2}002020 - \frac{1}{2}000220 \\ + \frac{1}{2}002110 + \frac{1}{2}001210 + \frac{1}{2}001120,$$

$$\sum \text{above terms} = \frac{1}{2}00400 + \frac{1}{2}000400 + \frac{1}{2}000040 - \frac{1}{2}003100 \\ - \frac{1}{2}003010 - \frac{1}{2}100300 - \frac{1}{2}010300 - \frac{1}{2}001300 \\ - \frac{1}{2}000310 - \frac{1}{2}100030 - \frac{1}{2}010030 - \frac{1}{2}001030 \\ - \frac{1}{2}000130 - \frac{1}{2}200020 - \frac{1}{2}020020 - \frac{1}{2}002200 \\ - \frac{5}{8}002020 - \frac{1}{2}000220 + \frac{1}{2}002110 + \frac{1}{2}100210$$

C.2. Expansion of the Transformed Energy Operator

$$\begin{aligned}
& + \frac{1}{2}010210 + \frac{1}{2}001210 + \frac{1}{2}110020 + \frac{1}{2}101020 \\
& + \frac{1}{2}100120 + \frac{1}{2}011020 + \frac{1}{2}010120 + \frac{1}{2}001120,
\end{aligned}$$

$$\begin{aligned}
C^{(5)} = & -400000 - 040000 - \frac{1}{2}004000 - \frac{1}{2}000400 - \frac{1}{2}000040 \\
& + 310000 + 301000 + 300100 + 300010 + 130000 \\
& + 031000 + 030100 + 030010 + 103000 + 013000 \\
& + \frac{1}{2}003100 + \frac{1}{2}003010 + \frac{1}{2}100300 + \frac{1}{2}010300 + \frac{1}{2}001300 \\
& + \frac{1}{2}000310 + \frac{1}{2}100030 + \frac{1}{2}010030 + \frac{1}{2}001030 + \frac{1}{2}000130 \\
& + 220000 + 202000 + 200200 + \frac{1}{2}200020 + 022000 \\
& + 020200 + \frac{1}{2}020020 + \frac{1}{2}002200 + \frac{3}{8}002020 + \frac{1}{2}000220 \\
& - 211000 - 210100 - 210010 - 201100 - 201010 \\
& - 200110 - 121000 - 120100 - 120010 - 021100 \\
& - 021010 - 020110 - 112000 - 102100 - 102010 \\
& - 012100 - 012010 - \frac{1}{2}002110 - 110200 - 101200 \\
& - \frac{1}{2}100210 - 011200 - \frac{1}{2}010210 - \frac{1}{2}001210 - \frac{1}{2}110020 \\
& - \frac{1}{2}101020 - \frac{1}{2}100120 - \frac{1}{2}011020 - \frac{1}{2}010120 - \frac{1}{2}001120 \\
& + 111100 + 111010 + 110110 + 101110 + 011110.
\end{aligned} \tag{C.44}$$

Explicit Expansion of $\Gamma_i^\dagger(\lambda)(H - E_i^{(0)})\Gamma_i(\lambda)$

With (C.21) we can formulate

$$\begin{aligned}
\Gamma_i^\dagger(H - E_i^{(0)})\Gamma_i &= \sum_{m=0}^4 \sum_{n=1}^5 \lambda^{m+n} \tilde{\Gamma}_i^{\dagger(m)} C^{(n)} + \mathcal{O}(\lambda^6) \\
&= \sum_{n=1}^5 \lambda^n \tilde{R}_i^{(n)} + \mathcal{O}(\lambda^6),
\end{aligned} \tag{C.45}$$

where

$$\tilde{R}_i^{(1)} = \tilde{\Gamma}_i^{\dagger(1)} C^{(1)}, \tag{C.46a}$$

$$\tilde{R}_i^{(2)} = \tilde{\Gamma}_i^{\dagger(0)} C^{(2)} + \tilde{\Gamma}_i^{\dagger(1)} C^{(1)}, \tag{C.46b}$$

$$\tilde{R}_i^{(3)} = \tilde{\Gamma}_i^{\dagger(0)} C^{(3)} + \tilde{\Gamma}_i^{\dagger(1)} C^{(2)} + \tilde{\Gamma}_i^{\dagger(2)} C^{(1)}, \tag{C.46c}$$

$$\tilde{R}_i^{(4)} = \tilde{\Gamma}_i^{\dagger(0)} C^{(4)} + \tilde{\Gamma}_i^{\dagger(1)} C^{(3)} + \tilde{\Gamma}_i^{\dagger(2)} C^{(2)} + \tilde{\Gamma}_i^{\dagger(3)} C^{(1)}, \tag{C.46d}$$

$$\tilde{R}_i^{(5)} = \tilde{\Gamma}_i^{\dagger(0)} C^{(5)} + \tilde{\Gamma}_i^{\dagger(1)} C^{(4)} + \tilde{\Gamma}_i^{\dagger(2)} C^{(3)} + \tilde{\Gamma}_i^{\dagger(3)} C^{(2)} + \tilde{\Gamma}_i^{\dagger(4)} C^{(1)}. \tag{C.46e}$$

First Order

$$\begin{aligned}
\tilde{R}_i^{(1)} &= \tilde{\Gamma}_i^{\dagger(1)} C^{(1)} \\
\boxed{\tilde{R}_i^{(1)} = 00} &
\end{aligned} \tag{C.47}$$

C. Calculation of the Mappings in the Kato-Takahashi Formalism

Second Order

$$\tilde{R}_i^{(2)} = \tilde{\Gamma}_i^{\dagger(0)} C^{(2)} + \tilde{\Gamma}_i^{\dagger(1)} C^{(1)} = 0C^{(2)} + 01(00)$$

$$\boxed{\tilde{R}_i^{(2)} = 010}$$

(C.48)

Third Order

$$\begin{aligned} \tilde{R}_i^{(3)} &= \tilde{\Gamma}_i^{\dagger(0)} C^{(3)} + \tilde{\Gamma}_i^{\dagger(1)} C^{(2)} + \tilde{\Gamma}_i^{\dagger(2)} C^{(1)} = 0C^{(3)} + 01(100) - \frac{1}{2}020(00) \\ &= 0C^{(3)} + 0200 - \frac{1}{2}0200 = 0C^{(3)} + \frac{1}{2}0200 \end{aligned}$$

$$\boxed{\tilde{R}_i^{(3)} = -\frac{1}{2}0200 - \frac{1}{2}0020 + 0110}$$

(C.49)

Fourth Order

$$\begin{aligned} \tilde{R}_i^{(4)} &= \tilde{\Gamma}_i^{\dagger(0)} C^{(4)} + \tilde{\Gamma}_i^{\dagger(1)} C^{(3)} + \tilde{\Gamma}_i^{\dagger(2)} C^{(2)} + \tilde{\Gamma}_i^{\dagger(3)} C^{(1)} \\ &= 0C^{(4)} + 01(-2000 + 1100 + 1010) + (-002 + 011)(100) - \frac{1}{2}020(010) \\ &\quad + \frac{1}{2}00300 + \frac{1}{2}03000 - \frac{1}{2}01200 - \frac{1}{2}02100 \\ &= 0C^{(4)} - 03000 + 02100 + 02010 - 00300 + 01200 - \frac{1}{2}02010 \\ &\quad + \frac{1}{2}00300 + \frac{1}{2}03000 - \frac{1}{2}01200 - \frac{1}{2}02100 \\ &= 0C^{(4)} - \frac{1}{2}03000 - \frac{1}{2}00300 + \frac{1}{2}02100 + \frac{1}{2}02010 + \frac{1}{2}01200 \end{aligned}$$

$$\boxed{\begin{aligned} \tilde{R}_i^{(4)} &= \frac{1}{2}03000 + \frac{1}{2}00030 - \frac{1}{2}02100 - \frac{1}{2}02010 - \frac{1}{2}01200 - \frac{1}{2}00210 \\ &\quad - \frac{1}{2}01020 - \frac{1}{2}00120 + 01110 \end{aligned}}$$

(C.50)

Fifth Order

$$\tilde{R}_i^{(5)} = \tilde{\Gamma}_i^{\dagger(0)} C^{(5)} + \tilde{\Gamma}_i^{\dagger(1)} C^{(4)} + \tilde{\Gamma}_i^{\dagger(2)} C^{(3)} + \tilde{\Gamma}_i^{\dagger(3)} C^{(2)} + \tilde{\Gamma}_i^{\dagger(4)} C^{(1)}$$

$$\begin{aligned} \tilde{\Gamma}_i^{\dagger(1)} C^{(4)} &= 040000 - 031000 - 030100 - 030010 - 022000 - 020200 \\ &\quad - \frac{1}{2}020020 + 021100 + 021010 + 020110 \end{aligned}$$

$$\begin{aligned} \tilde{\Gamma}_i^{\dagger(2)} C^{(3)} &= 004000 - 003100 - 003010 + \frac{1}{2}020200 + \frac{1}{4}020020 \\ &\quad - \frac{1}{2}020110 - 013000 + 012100 + 012010 \end{aligned}$$

$$\begin{aligned} \tilde{\Gamma}_i^{\dagger(3)} C^{(2)} &= 000400 - 001300 - 010300 - 002200 - \frac{1}{2}020200 + 011200 \\ &\quad + \frac{1}{2}003010 + \frac{1}{2}030010 - \frac{1}{2}012010 - \frac{1}{2}021010 \end{aligned}$$

$$\begin{aligned} \tilde{\Gamma}_i^{\dagger(4)} C^{(1)} &= -\frac{1}{2}000400 - \frac{1}{2}004000 - \frac{1}{2}040000 + \frac{1}{2}001300 + \frac{1}{2}010300 \\ &\quad + \frac{1}{2}003100 + \frac{1}{2}013000 + \frac{1}{2}030100 + \frac{1}{2}031000 + \frac{1}{2}002200 \end{aligned}$$

C.2. Expansion of the Transformed Energy Operator

$$\begin{aligned}
& + \frac{3}{8}020200 + \frac{1}{2}022000 - \frac{1}{2}011200 - \frac{1}{2}012100 - \frac{1}{2}021100 \\
\sum_{m=1}^4 \tilde{\Gamma}_i^{(m)} C^{(5-m)} = & \frac{1}{2}040000 + \frac{1}{2}004000 + \frac{1}{2}000400 - \frac{1}{2}031000 - \frac{1}{2}030100 \\
& - \frac{1}{2}030010 - \frac{1}{2}013000 - \frac{1}{2}003100 - \frac{1}{2}003010 - \frac{1}{2}010300 \\
& - \frac{1}{2}001300 - \frac{1}{2}022000 - \frac{5}{8}020200 - \frac{1}{4}020020 - \frac{1}{2}002200 \\
& + \frac{1}{2}021100 + \frac{1}{2}021010 + \frac{1}{2}020110 + \frac{1}{2}012100 + \frac{1}{2}012010 \\
& + \frac{1}{2}011200
\end{aligned}$$

$ \begin{aligned} \tilde{R}_i^{(5)} = & -\frac{1}{2}040000 - \frac{1}{2}000040 + \frac{1}{2}031000 + \frac{1}{2}030100 + \frac{1}{2}030010 \\ & + \frac{1}{2}013000 + \frac{1}{2}000310 + \frac{1}{2}010030 + \frac{1}{2}001030 + \frac{1}{2}000130 \\ & + \frac{1}{2}022000 + \frac{3}{8}020200 + \frac{1}{4}020020 + \frac{3}{8}002020 + \frac{1}{2}000220 \\ & - \frac{1}{2}021100 - \frac{1}{2}021010 - \frac{1}{2}020110 - \frac{1}{2}012100 - \frac{1}{2}012010 \\ & - \frac{1}{2}002110 - \frac{1}{2}011200 - \frac{1}{2}010210 - \frac{1}{2}001210 - \frac{1}{2}011020 \\ & - \frac{1}{2}010120 - \frac{1}{2}001120 + 011110 \end{aligned} $
--

(C.51)

C.2.2. Summary

The expansion of the transformed energy operator (C.45),

$$\Gamma_i^\dagger (H - E_i^{(0)}) \Gamma_i = \sum_{n=1}^{\infty} \lambda^n \tilde{R}_i^{(n)}, \quad (\text{C.52})$$

reads up to fifth order in the coupling λ ,

$$\tilde{R}_i^{(1)} := P_i^{(0)} V P_i^{(0)} \quad (\text{C.53a})$$

$$\tilde{R}_i^{(2)} := P_i^{(0)} V \tilde{S} V P_i^{(0)} \quad (\text{C.53b})$$

$$\tilde{R}_i^{(3)} := P_i^{(0)} V \tilde{S} V \tilde{S} V P_i^{(0)} + \frac{1}{2} \left\{ -P_i^{(0)} V \tilde{S}^2 V P_i^{(0)} V P_i^{(0)} - P_i^{(0)} V P_i^{(0)} V \tilde{S}^2 V P_i^{(0)} \right\} \quad (\text{C.53c})$$

$$\begin{aligned} \tilde{R}_i^{(4)} := & P_i^{(0)} V \tilde{S} V \tilde{S} V \tilde{S} V P_i^{(0)} + \frac{1}{2} \left\{ P_i^{(0)} V \tilde{S}^3 V P_i^{(0)} V P_i^{(0)} V P_i^{(0)} \right. \\ & + P_i^{(0)} V P_i^{(0)} V P_i^{(0)} V \tilde{S}^3 V P_i^{(0)} - P_i^{(0)} V \tilde{S}^2 V \tilde{S} V P_i^{(0)} V P_i^{(0)} \\ & - P_i^{(0)} V \tilde{S}^2 V P_i^{(0)} V \tilde{S} V P_i^{(0)} - P_i^{(0)} V \tilde{S} V \tilde{S}^2 V P_i^{(0)} V P_i^{(0)} \\ & - P_i^{(0)} V P_i^{(0)} V \tilde{S}^2 V \tilde{S} V P_i^{(0)} - P_i^{(0)} V \tilde{S} V P_i^{(0)} V \tilde{S}^2 V P_i^{(0)} \\ & \left. - P_i^{(0)} V P_i^{(0)} V \tilde{S} V \tilde{S}^2 V P_i^{(0)} \right\} \end{aligned} \quad (\text{C.53d})$$

$$\begin{aligned} \tilde{R}_i^{(5)} := & P_i^{(0)} V \tilde{S} V \tilde{S} V \tilde{S} V \tilde{S} V P_i^{(0)} + \frac{1}{2} \left\{ -P_i^{(0)} V \tilde{S}^4 V P_i^{(0)} V P_i^{(0)} V P_i^{(0)} V P_i^{(0)} \right. \\ & - P_i^{(0)} V P_i^{(0)} V P_i^{(0)} V P_i^{(0)} V \tilde{S}^4 V P_i^{(0)} + P_i^{(0)} V \tilde{S}^3 V \tilde{S} V P_i^{(0)} V P_i^{(0)} V P_i^{(0)} \\ & + P_i^{(0)} V \tilde{S}^3 V P_i^{(0)} V \tilde{S} V P_i^{(0)} V P_i^{(0)} + P_i^{(0)} V \tilde{S}^3 V P_i^{(0)} V P_i^{(0)} V \tilde{S} V P_i^{(0)} \\ & + P_i^{(0)} V \tilde{S} V \tilde{S}^3 V P_i^{(0)} V P_i^{(0)} V P_i^{(0)} + P_i^{(0)} V P_i^{(0)} V P_i^{(0)} V \tilde{S}^3 V \tilde{S} V P_i^{(0)} \\ & + P_i^{(0)} V \tilde{S} V P_i^{(0)} V P_i^{(0)} V \tilde{S}^3 V P_i^{(0)} + P_i^{(0)} V P_i^{(0)} V \tilde{S} V P_i^{(0)} V \tilde{S}^3 V P_i^{(0)} \\ & + P_i^{(0)} V P_i^{(0)} V P_i^{(0)} V \tilde{S} V \tilde{S}^3 V P_i^{(0)} + P_i^{(0)} V \tilde{S}^2 V \tilde{S}^2 V P_i^{(0)} V P_i^{(0)} V P_i^{(0)} \\ & + \frac{3}{4} P_i^{(0)} V \tilde{S}^2 V P_i^{(0)} V \tilde{S}^2 V P_i^{(0)} V P_i^{(0)} + \frac{1}{2} P_i^{(0)} V \tilde{S}^2 V P_i^{(0)} V P_i^{(0)} V \tilde{S}^2 V P_i^{(0)} \\ & + \frac{3}{4} P_i^{(0)} V P_i^{(0)} V \tilde{S}^2 V P_i^{(0)} V \tilde{S}^2 V P_i^{(0)} + P_i^{(0)} V P_i^{(0)} V P_i^{(0)} V \tilde{S}^2 V \tilde{S}^2 V P_i^{(0)} \\ & - P_i^{(0)} V \tilde{S}^2 V \tilde{S} V \tilde{S} V P_i^{(0)} V P_i^{(0)} - P_i^{(0)} V \tilde{S}^2 V \tilde{S} V P_i^{(0)} V \tilde{S} V P_i^{(0)} \\ & - P_i^{(0)} V \tilde{S}^2 V P_i^{(0)} V \tilde{S} V \tilde{S} V P_i^{(0)} - P_i^{(0)} V \tilde{S} V \tilde{S}^2 V \tilde{S} V P_i^{(0)} V P_i^{(0)} \\ & - P_i^{(0)} V \tilde{S} V \tilde{S}^2 V P_i^{(0)} V \tilde{S} V P_i^{(0)} - P_i^{(0)} V P_i^{(0)} V \tilde{S}^2 V \tilde{S} V \tilde{S} V P_i^{(0)} \\ & - P_i^{(0)} V \tilde{S} V \tilde{S} V \tilde{S}^2 V P_i^{(0)} V P_i^{(0)} - P_i^{(0)} V \tilde{S} V P_i^{(0)} V \tilde{S}^2 V \tilde{S} V P_i^{(0)} \\ & - P_i^{(0)} V P_i^{(0)} V \tilde{S} V \tilde{S}^2 V \tilde{S} V P_i^{(0)} - P_i^{(0)} V \tilde{S} V \tilde{S} V P_i^{(0)} V \tilde{S}^2 V P_i^{(0)} \\ & \left. - P_i^{(0)} V \tilde{S} V P_i^{(0)} V \tilde{S} V \tilde{S}^2 V P_i^{(0)} - P_i^{(0)} V P_i^{(0)} V \tilde{S} V \tilde{S} V \tilde{S}^2 V P_i^{(0)} \right\} \end{aligned} \quad (\text{C.53e})$$

C.3. Implementation of the SIAM

In this section we present the expansions of Takahashi's operator Γ_i , (C.28), and of the reduced energy operator $\Gamma_i^\dagger(H_S - \tilde{E}_i^{(0)})\Gamma_i$, (C.52), in $1/U$ for the Single Impurity Anderson Model (SIAM) in two-chain geometry, (9.30), as described in chapter 9. Due to the U -dependence of the on-site energies ε_l , (9.50), and of the electron transfer amplitudes t_l , (9.47), of the SIAM, the expansion in $1/U$ differs somewhat from the expansion in the general coupling constant λ as presented in the last sections.

Simplifying the Notation In order to get more transparent expressions, we introduce the following new conventions:

- (a) For calculations involving only the primary lower Hubbard band, we work with $P_0^{(0)}$ exclusively, which we denote by

$$P := P_0^{(0)}. \quad (\text{C.54})$$

- (b) Using (a), we write the operator \tilde{S} , (7.63), as

$$\tilde{S}^0 = -P \text{ and } (\tilde{E}_0^{(0)} - H_0)\tilde{S} = 1 - P. \quad (\text{C.55})$$

With the spectrum of H_0 at half-filling, (9.38), and at $N = L - 1$, (9.43), we can write

$$\tilde{S}^k = \sum_{j=1}^{\infty} \frac{P_j}{(E_0^{(0)} - E_j^{(0)})^k} = (-1)^k \frac{1}{U^k} \sum_{j=1}^{\infty} \frac{P_j}{j^k}, \quad k > 0. \quad (\text{C.56})$$

Thus, we introduce a new operator S , defined by

$$S^0 := -P \quad \text{and} \quad S^k := \sum_{j=1}^{\infty} \frac{P_j}{j^k}. \quad (\text{C.57})$$

C.3.1. Simplifications in Two-Chain Geometry

Here, we summarize some remarkable simplifications in two-chain geometry which reduce the computational effort.

- (1) Hopping to or from the impurity site always involves a factor of $1/\sqrt{2}$.
- (2) The part V_2 of the perturbation, (9.51), is diagonal within the eigenstates of the local number operators. In particular, this implies that V_2 cannot alter such a state and, as a consequence, we are able to state that

$$\dots S^k V_2 P \dots = \dots P V_2 S^k \dots = 0, \quad k > 0, \quad (\text{C.58a})$$

$$\dots S^k V_2 S^m \dots = \dots S^{k+m} V_2 \dots = \dots V_2 S^{k+m} \dots, \quad k, m > 0. \quad (\text{C.58b})$$

- (3) Since the part V_1 , (9.48), does *not* couple the impurity site to any of the two chains and because the energy of the eigenstates of H_0 does not depend on the location of electrons in the lower or upper chain, V_1 cannot connect different subspaces of H_0 . Thus, we note that

$$\dots S^k V_1 P \dots = \dots P V_1 S^k \dots = 0, \quad k > 0, \quad (\text{C.59a})$$

$$\dots S^k V_1 S^m \dots = \dots V_1 S^{k+m} \dots = \dots S^{k+m} V_1, \quad k, m > 0. \quad (\text{C.59b})$$

This claim would be violated if for any l , see (9.50),

$$\varepsilon_l = \varepsilon_l^{(0)} + \frac{1}{U} \varepsilon_l^{(1)} + \dots,$$

$\varepsilon_l^{(0)} \neq 0$ would be a finite correction. In chapter 10 and appendix E we show that $\varepsilon_l^{(0)} = 0$ for all sites l .

C. Calculation of the Mappings in the Kato-Takahashi Formalism

- (4) If we start with a ground state at arbitrary filling and apply V_0 , we can reach at most a first excited state which implies that

$$\dots S^k V_0 P \dots = \dots S V_0 P \dots, \quad k > 0. \quad (\text{C.60})$$

- (5) Consider the following sequences of hopping processes where we start in a ground state at arbitrary filling:

$$|\dots \star \uparrow\uparrow \uparrow \text{---}\dots\rangle \xrightarrow{\Delta E=U} |\dots \star \uparrow \uparrow\uparrow \text{---}\dots\rangle \xrightarrow{\Delta E=0} |\dots \star \uparrow \uparrow \downarrow \text{---}\dots\rangle, \quad (\text{C.61a})$$

$$|\dots \star \downarrow \uparrow \text{---}\dots\rangle \xrightarrow{\Delta E=U} |\dots \star \text{---} \uparrow\uparrow \text{---}\dots\rangle \xrightarrow{\Delta E=0} |\dots \star \text{---} \uparrow \downarrow \text{---}\dots\rangle, \quad (\text{C.61b})$$

$$|\dots \star \uparrow\uparrow \uparrow \text{---}\dots\rangle \xrightarrow{\Delta E=U} |\dots \star \uparrow\uparrow \text{---} \uparrow \text{---}\dots\rangle \xrightarrow{\Delta E=0} |\dots \star \uparrow \downarrow \uparrow \text{---}\dots\rangle, \quad (\text{C.61c})$$

$$|\dots \star \downarrow \uparrow \text{---}\dots\rangle \xrightarrow{\Delta E=U} |\dots \star \downarrow \text{---} \uparrow \text{---}\dots\rangle \xrightarrow{\Delta E=0} |\dots \star \text{---} \downarrow \uparrow \text{---}\dots\rangle. \quad (\text{C.61d})$$

In all the processes shown, the last step is no excitation. This is another consequence of the particle-hole symmetry of the model. Because every excitation from a ground state has to involve the impurity site in one of the shown processes (or one with flipped spins), it follows that

$$\dots S^k \bar{V}_0 S^m V_0 P \dots = \dots S \bar{V}_0 S V_0 P \dots, \quad k, m > 0, \quad (\text{C.62})$$

where $\bar{V}_0 := V_0 + V_1^{(0)} + V_2^{(0)}$.

- (6) Additionally, we state without its simple but tedious proof that

$$\dots [S V_0 P, V_2^{(n)}] \dots = \varepsilon_0^{(n)} \dots S V_0 P \dots \quad (\text{C.63})$$

Here, $[\cdot, \cdot]$ denotes the commutator.

Half-Filling At half band-filling, there are only the two ground states (9.32) and (9.33). Thus, we readily find the following simplifications (l.c. \equiv lower chain),

$$\dots P V_0 P \dots = 0, \quad (\text{C.64a})$$

$$\dots P V_1 P \dots = 0, \quad (\text{C.64b})$$

$$\dots P V_2^{(n)} P \dots = 2 \sum_{l \in \text{l.c.}} \varepsilon_l^{(n)} \dots P \dots =: \xi^{(n)} \dots P \dots, \quad (\text{C.64c})$$

$$\dots P V_0 S V_0 P \dots = \dots P \dots, \quad (\text{C.64d})$$

$$\dots S V_2^{(n)} S V_0 P \dots = (\xi^{(n)} - \varepsilon_0^{(n)}) \dots S V_0 P \dots, \quad n \geq 0. \quad (\text{C.64e})$$

Using the simplifications (1) to (6) and using the expansions of V_1 , (9.48), and V_2 , (9.51), we can derive the explicit expansions of $\Gamma_0 \equiv \Gamma$ and $\Gamma^\dagger (H_S - \tilde{E}_0^{(0)}) \Gamma$. We state the results on the following pages.

C.3.2. Operators at Arbitrary Filling

First, let us introduce

$$\bar{V}_0 := V_0 + V_1^{(0)} + V_2^{(0)}. \quad (\text{C.65})$$

We show in chapter 10 that the leading-order result leads to $\varepsilon_l^{(0)} = 0$ for all sites l and, thus, $V_2^{(0)} \equiv 0$. For all $n \geq 1$ we make use of this fact and, as a consequence, we write

$$\bar{V}_0 = V_0 + V_1^{(0)}, \quad n \geq 1. \quad (\text{C.66})$$

Second, we define the operators

$$\Upsilon_1 := SV_0P, \quad (\text{C.67a})$$

$$\Upsilon_2 := S\bar{V}_0SV_0P, \quad (\text{C.67b})$$

$$\Upsilon_3 := S\bar{V}_0S\bar{V}_0SV_0P, \quad (\text{C.67c})$$

$$\Upsilon_4 := S\bar{V}_0S\bar{V}_0S\bar{V}_0SV_0P, \quad (\text{C.67d})$$

together with

$$h_0 := P\bar{V}_0P, \quad (\text{C.68a})$$

$$h_1 := PV_0SV_0P, \quad (\text{C.68b})$$

$$h_2 := PV_0S\bar{V}_0SV_0P, \quad (\text{C.68c})$$

$$h_3 := PV_0S\bar{V}_0S\bar{V}_0SV_0P, \quad (\text{C.68d})$$

$$h_4 := PV_0S\bar{V}_0S\bar{V}_0S\bar{V}_0SV_0P. \quad (\text{C.68e})$$

Finally, we introduce

$$v^{(n)} := P(V_1^{(n)} + V_2^{(n)})P. \quad (\text{C.69})$$

For later computations we note that for $n \geq 1$ we have

$$\Upsilon_n = S\bar{V}_0\Upsilon_{n-1}, \quad (\text{C.70})$$

$$h_n = PV_0\Upsilon_n. \quad (\text{C.71})$$

Takahashi's Operator Γ

The expansion of Takahashi's operator

$$\Gamma = \sum_{n=0}^{\infty} \left(\frac{1}{U}\right)^n \Gamma^{(n)} \quad (\text{C.72})$$

for the primary Hubbard band at arbitrary filling is given up to fourth order in $1/U$ by

$$\Gamma^{(0)} := P, \quad (\text{C.72a})$$

$$\Gamma^{(1)} := -\Upsilon_1, \quad (\text{C.72b})$$

$$\Gamma^{(2)} := \Upsilon_2 - \Upsilon_1 h_0 - \frac{1}{2} h_1, \quad (\text{C.72c})$$

$$\Gamma^{(3)} := -\Upsilon_3 + 2\Upsilon_2 h_0 + \Upsilon_1 \left(\frac{3}{2} h_1 - h_0^2 - \varepsilon_0^{(1)} P\right) + h_2 - \frac{1}{2} (h_1 h_0 + h_0 h_1) + [V_1^{(1)}, \Upsilon_1], \quad (\text{C.72d})$$

$$\begin{aligned} \Gamma^{(4)} := & \Upsilon_4 - S\Upsilon_3 h_0 - 2\Upsilon_2 h_0 + \Upsilon_2 \left(-\frac{5}{2} h_1 + 3h_0^2\right) + \Upsilon_1 \left(-2h_2 + \frac{5}{2} h_1 h_0 + 2h_0 h_1 - h_0^3 - \varepsilon_0^{(2)} P\right) \\ & + \varepsilon_0^{(1)} \Gamma^{(2)} - \frac{3}{2} h_3 + \frac{3}{2} (h_2 h_0 + h_0 h_2) + \frac{11}{8} h_1^2 - \frac{1}{2} (h_1 h_0^2 + h_0 h_1 h_0 + h_0^2 h_1) - \frac{1}{2} \varepsilon_0^{(1)} h_1 \\ & + [V_1^{(1)}, \Upsilon_1] h_0 + S\bar{V}_0 S [\Upsilon_1, V_1^{(1)}] - \frac{1}{2} \{ \Upsilon_1^\dagger [\Upsilon_1, V_1^{(1)}] + [V_1^{(1)}, \Upsilon_1^\dagger] \Upsilon_1 \} \\ & + [(\Upsilon_2 - \Upsilon_1 h_0), (V_1^{(1)} + V_2^{(1)})] + [V_1^{(2)}, \Upsilon_1]. \end{aligned} \quad (\text{C.72e})$$

C. Calculation of the Mappings in the Kato-Takahashi Formalism

Transformed Energy Operator

The expansion of the transformed energy operator, (C.45),

$$\Gamma^\dagger(H_S - \tilde{E}_0^{(0)})\Gamma = \sum_{n=1}^{\infty} \left(\frac{1}{U}\right)^n R^{(n)} \quad (\text{C.73})$$

for the primary Hubbard band, reads up to fourth order in $1/U$,

$$R^{(0)} := h_0, \quad (\text{C.73a})$$

$$R^{(1)} := -h_1 + v^{(1)}, \quad (\text{C.73b})$$

$$R^{(2)} := h_2 - \frac{1}{2}(h_1 h_0 + h_0 h_1) + v^{(2)}, \quad (\text{C.73c})$$

$$R^{(3)} := -h_3 + (h_2 h_0 + h_0 h_2) - \frac{1}{2}(h_1 h_0^2 + h_0^2 h_1) + h_1^2 - \varepsilon_0^{(1)} h_1 + v^{(3)} \\ - \frac{1}{2}\{\Upsilon_1^\dagger[\Upsilon_1, V_1^{(1)}] + [V_1^{(1)}, \Upsilon_1^\dagger]\Upsilon_1\}, \quad (\text{C.73d})$$

$$R^{(4)} := h_4 - \frac{3}{2}(h_3 h_0 + h_0 h_3) - \frac{3}{2}(h_2 h_1 + h_1 h_2) + \frac{3}{2}(h_2 h_0^2 + h_0^2 h_2) + \frac{7}{8}(h_1^2 h_0 + h_0 h_1^2) \\ + \frac{5}{4}h_1 h_0 h_1 - \frac{1}{2}(h_1 h_0^3 + h_0^3 h_1) - \frac{1}{2}\varepsilon_0^{(1)}(h_1 h_0 + h_0 h_1) + 2\varepsilon_0^{(1)}h_2 - \varepsilon_0^{(2)}h_1 + v^{(4)} \\ + \Upsilon_2^\dagger[\Upsilon_1, V_1^{(1)}]P + P[V_1^{(1)}, \Upsilon_1^\dagger]\Upsilon_2 - \frac{1}{2}\{\Upsilon_1^\dagger[\Upsilon_1, V_1^{(2)}] + [V_1^{(2)}, \Upsilon_1^\dagger]\Upsilon_1\} \\ + \frac{1}{2}\{\Upsilon_1^\dagger[(V_1^{(1)} + V_2^{(1)}), \Upsilon_1 h_0]P - P[(V_1^{(1)} + V_2^{(1)}), h_0 \Upsilon_1^\dagger]\Upsilon_1\} \\ - \frac{1}{2}\{h_0[V_1^{(1)}, \Upsilon_1^\dagger]\Upsilon_1 - \Upsilon_1^\dagger[V_1^{(1)}, \Upsilon_1]h_0\}. \quad (\text{C.73e})$$

C.3.3. Operators at Half Band-Filling

At half band-filling the ground state of H_0 , (9.30a), is only two-fold degenerate. Therefore, according to (C.64a) to (C.64e), we can simplify drastically to obtain

$$h_0 = \begin{cases} \xi^{(0)}P & \text{for calculations to lowest order,} \\ 0 & \text{otherwise,} \end{cases} \quad (\text{C.74})$$

$$h_1 = P, \quad (\text{C.75})$$

$$v^{(n)} = \xi^{(n)}P. \quad (\text{C.76})$$

Here, we again made use of the result to lowest order: In the expressions of $\mathcal{O}(n)$ with $n \geq 1$ we use that all on-site energies $\varepsilon_l^{(0)}$ vanish.

Takahashi's Operator Γ_L

The expansion of Takahashi's operator

$$\Gamma_L = \sum_{n=0}^{\infty} \left(\frac{1}{U}\right)^n \Gamma_L^{(n)} \quad (\text{C.77})$$

for the primary Hubbard band at half band-filling reads up to fourth order in $1/U$,

$$\Gamma_L^{(0)} := P, \quad (\text{C.77a})$$

$$\Gamma_L^{(1)} := -\Upsilon_1, \quad (\text{C.77b})$$

$$\Gamma_L^{(2)} := \Upsilon_2 - \frac{1}{2}P, \quad (\text{C.77c})$$

$$\Gamma_L^{(3)} := -\Upsilon_3 + \Upsilon_1 \left(\frac{3}{2} - \varepsilon_0^{(1)} \right) P + h_2 + V_1^{(1)} \Upsilon_1, \quad (\text{C.77d})$$

$$\begin{aligned} \Gamma_L^{(4)} := & \Upsilon_4 - \frac{5}{2} \Upsilon_2 + \Upsilon_1 (-2h_2 - \varepsilon_0^{(2)} P) + \varepsilon_0^{(1)} \Gamma^{(2)} - \frac{3}{2} h_3 + \left(\frac{11}{8} - \frac{1}{2} \varepsilon_0^{(1)} \right) P \\ & - S \bar{V}_0 S V_1^{(1)} \Upsilon_1 + \Upsilon_1^\dagger V_1^{(1)} \Upsilon_1 + [\Upsilon_2, (V_1^{(1)} + V_2^{(1)})] + [V_1^{(2)}, \Upsilon_1]. \end{aligned} \quad (\text{C.77e})$$

Transformed Energy Operator

At half band-filling, the expansion of the transformed energy operator, (C.45),

$$\Gamma_L^\dagger (H_S - \tilde{E}_0^{(0)}(L)) \Gamma_L = \sum_{n=1}^{\infty} \left(\frac{1}{U} \right)^n R_L^{(n)} \quad (\text{C.78})$$

for the primary Hubbard band up to fourth order in $1/U$ is given by

$$R_L^{(0)} := \xi^{(0)} P, \quad (\text{C.78a})$$

$$R_L^{(1)} := (\xi^{(1)} - 1) P, \quad (\text{C.78b})$$

$$R_L^{(2)} := h_2 + \xi^{(2)} P, \quad (\text{C.78c})$$

$$R_L^{(3)} := -h_3 + (1 - \varepsilon_0^{(1)} + \xi^{(3)}) P + \Upsilon_1^\dagger V_1^{(1)} \Upsilon_1, \quad (\text{C.78d})$$

$$R_L^{(4)} := h_4 + h_2 (-3 + 2\varepsilon_0^{(1)}) + (\xi^{(4)} - \varepsilon_0^{(2)}) P - \Upsilon_2^\dagger V_1^{(1)} \Upsilon_1 - \Upsilon_1^\dagger V_1^{(1)} \Upsilon_2 + \Upsilon_1^\dagger V_1^{(2)} \Upsilon_1. \quad (\text{C.78e})$$

D

Multichain Approach to the SIAM

The hybridization function of the discretized Single Impurity Anderson Model (SIAM) reads

$$\Delta(\omega) = \lim_{\eta \searrow 0} \sum_m \frac{V_m^2}{\omega - \xi_m + i \operatorname{sgn}(\omega)\eta} \quad (\text{D.1})$$

We introduce n electron baths located at the energies $\pm nU \pm U/2$ with parameters V_m^\pm and ξ_m^\pm of the SIAM such that

$$\xi_{m,n}^- =: -U/2 - nU + \bar{\xi}_{m,n}^-, \quad (\text{D.2})$$

$$\xi_{m,n}^+ =: +U/2 + nU + \bar{\xi}_{m,n}^+. \quad (\text{D.3})$$

This scheme will be of importance for the SIAM in the insulating state, where we assume that the various bands introduced above are well separated with non-overlapping supports. In this case, we may immediately write

$$\Delta(\omega) = \lim_{\eta \searrow 0} \sum_n \sum_m \left\{ \frac{V_{m,n}^{-2}}{(\omega + U/2 + nU) - \bar{\xi}_{m,n}^- + i \operatorname{sgn}(\omega)\eta} + \frac{V_{m,n}^{+2}}{(\omega - U/2 - nU) - \bar{\xi}_{m,n}^+ + i \operatorname{sgn}(\omega)\eta} \right\}. \quad (\text{D.4})$$

The density of states looks therefore like the one we depicted in figure 9.1 on page 80. The first term in parenthesis in (D.4) describes the n th lower sub-band, whereas the second term denotes the n th upper sub-band. For $t \equiv 1$ as our unit of energy, the self-consistency equation on the Bethe lattice is given by

$$\Delta(\omega) = G_\sigma(\omega), \quad (\text{D.5})$$

where $G_\sigma(\omega)$ denotes the one-particle, local impurity Green function for spin σ . For the paramagnetic insulator we have

$$G_\sigma(\omega) = \frac{1}{2}G(\omega), \quad (\text{D.6})$$

with $G(\omega)$ being the spin-summed Green function. This means that the sum rule, see (A.37),

$$1 = -\frac{1}{\pi} \int_{-\infty}^{\infty} \Im \Delta^{\text{ret}}(\omega) d\omega = \sum_n \left\{ \sum_m V_{m,n}^{-2} + \sum_m V_{m,n}^{+2} \right\} \stackrel{\text{p.h.}}{=} 2 \sum_n \left\{ \sum_m V_{m,n}^{-2} \right\}$$

holds and, thus,

$$\frac{1}{2} = \sum_n \left\{ \sum_m V_{m,n}^{-2} \right\}. \quad (\text{D.7})$$

As long as we are in the insulating phase with no overlap between the different sub-bands we can identify

$$\sum_m V_{m,n}^{-2} = g_n^-, \quad (\text{D.8})$$

where g_n^- denotes the weight per spin of the negative frequency part of sub-band n . Due to particle-hole symmetry we find $g_n^+ = g_n^- \equiv g_n$.

D.1. Multichain Setup of the SIAM Hamiltonian

The discretized Hamiltonian of the SIAM (9.26) reads

$$H_{\text{SIAM}} = H_{\text{imp}} + \sum_{m,\sigma} \xi_m a_{m\sigma}^\dagger a_{m\sigma} + \sum_{\sigma} \left\{ d_{\sigma}^\dagger \sum_m V_m a_{m\sigma} + \sum_m V_m a_{m\sigma}^\dagger \right\}. \quad (\text{D.9})$$

In the multichain setup we introduce the operators ${}^{(n)}\alpha_{j\sigma}^\dagger$ and ${}^{(n)}\beta_{j\sigma}^\dagger$ such that

- (i) the new set of operators is orthogonal,
- (ii) obey a fermionic algebra,
- (iii) the operators for the first site in the corresponding chains are given by (as can in fact be read off the SIAM Hamiltonian)

$${}^{(n)}\alpha_{0\sigma}^\dagger = N_n^- \sum_m V_{m,n}^- a_{m\sigma}^\dagger, \quad (\text{D.10})$$

$${}^{(n)}\beta_{0\sigma}^\dagger = N_n^+ \sum_m V_{m,n}^+ a_{m\sigma}^\dagger. \quad (\text{D.11})$$

Due to particle-hole symmetry the normalization constants N_n^+ and N_n^- are identical and can be fixed as follows. In order for the new operators to represent fermions, they must obey the canonical anti-commutation relations. Invoking these, we find

$$1 = \{ {}^{(n)}\alpha_{0\sigma}, {}^{(n)}\alpha_{0\sigma}^\dagger \} = N_n^{-2} \sum_m V_{m,n}^{-2} \quad (\text{D.12a})$$

$$= N_n^{-2} g_n. \quad (\text{D.12b})$$

In the first step we have used that the operators are fermions. The normalization constants are therefore given by the square root of the weights of the corresponding sub-bands. Thus, the operators read

$${}^{(n)}\alpha_{0\sigma}^\dagger = \frac{1}{\sqrt{g_n}} \sum_m V_{m,n}^- a_{m\sigma}^\dagger, \quad (\text{D.13})$$

$${}^{(n)}\beta_{0\sigma}^\dagger = \frac{1}{\sqrt{g_n}} \sum_m V_{m,n}^+ a_{m\sigma}^\dagger. \quad (\text{D.14})$$

The hybridization part of the Hamiltonian becomes

$$\sum_n \sqrt{g_n} \left\{ \sum_{\sigma} (d_{\sigma}^\dagger {}^{(n)}\alpha_{0\sigma} + \text{h.c.}) + \sum_{\sigma} (d_{\sigma}^\dagger {}^{(n)}\beta_{0\sigma} + \text{h.c.}) \right\}. \quad (\text{D.15})$$

The remaining operators are obtained by means of an orthogonalization procedure. The resulting SIAM Hamiltonian in multichain geometry reads

$$\begin{aligned} H_{\text{SIAM}} = & H_{\text{imp}} + \sum_{n,\sigma} \sqrt{g_n} \left\{ (d_{\sigma}^\dagger {}^{(n)}\alpha_{0\sigma} + \text{h.c.}) + (d_{\sigma}^\dagger {}^{(n)}\beta_{0\sigma} + \text{h.c.}) \right\} \\ & + \sum_{n,j,\sigma} {}^{(n)}t_j \left\{ {}^{(n)}\alpha_{j\sigma}^\dagger {}^{(n)}\alpha_{j+1\sigma} + {}^{(n)}\beta_{j\sigma}^\dagger {}^{(n)}\beta_{j+1\sigma} + \text{h.c.} \right\} \\ & + \sum_{n,j,\sigma} {}^{(n)}\varepsilon_j \left\{ {}^{(n)}\alpha_{j\sigma}^\dagger {}^{(n)}\alpha_{j\sigma} - {}^{(n)}\beta_{j\sigma}^\dagger {}^{(n)}\beta_{j\sigma} \right\}. \end{aligned} \quad (\text{D.16})$$

D.2. Calculation of the Weights g_n by Perturbation Theory

The local impurity Green function for a single spin is defined by

$$G_{\text{SIAM}}(\omega < 0) = \langle \Psi | d_{\uparrow}^{\dagger} (\omega + (H_S - \tilde{E}_0(L)) - i\eta)^{-1} d_{\uparrow} | \Psi \rangle. \quad (\text{D.17})$$

By means of Kato-Takahashi perturbation theory we find

$$G_{\text{SIAM}}(\omega) = \langle \Phi | \Gamma_L^{\dagger} d_{\uparrow}^{\dagger} (\omega + (H_S - \tilde{E}_0(L)) - i\eta)^{-1} d_{\uparrow} \Gamma_L | \Phi \rangle, \quad (\text{D.18})$$

with $|\Phi\rangle = 1/\sqrt{2}(|\phi_{\uparrow}\rangle + |\phi_{\downarrow}\rangle)$. Thus, due to (D.7) and particle-hole symmetry, we have

$$\frac{1}{2} = \frac{1}{\pi} \int_{-\infty}^0 \Im G_{\text{SIAM}}(\omega) d\omega = \|d_{\uparrow} \Gamma_L \Phi\|^2. \quad (\text{D.19})$$

We will denote the vector $d_{\uparrow} \Gamma_L |\Phi\rangle$ by $|\bar{\Psi}\rangle$. It admits the expansion

$$|\bar{\Psi}\rangle = \sum_{n=0}^{\infty} \left(\frac{1}{U}\right)^n |\bar{\Psi}^{(n)}\rangle, \quad (\text{D.20})$$

where $|\bar{\Psi}^{(n)}\rangle := d_{\uparrow} \Gamma_L^{(n)} |\Phi\rangle$, see (E.21) of appendix E but note that the state $|\bar{\Psi}\rangle$ in appendix E has to be multiplied by $1/\sqrt{2}$ to correspond to our present definition. The states $|\bar{\Psi}^{(n)}\rangle$ might be expanded into the contributions from $P_i^{(0)} \mathcal{H}$ according to

$$|\bar{\Psi}^{(n)}\rangle = \sum_i |\bar{\Psi}_i^{(n)}\rangle, \quad (\text{D.21})$$

where the state $|\bar{\Psi}_i^{(n)}\rangle$ is part of the i th excited eigenspace of H_0 ,

$$|\bar{\Psi}_i^{(n)}\rangle \in P_i^{(0)} \mathcal{H}. \quad (\text{D.22})$$

With the expansions (D.20) and (D.22) we find

$$\frac{1}{2} = \langle \bar{\Psi} | \bar{\Psi} \rangle = \sum_{n=0}^{\infty} \sum_{m=0}^{\infty} \left(\frac{1}{U}\right)^{n+m} \langle \bar{\Psi}^{(n)} | \bar{\Psi}^{(m)} \rangle \quad (\text{D.23a})$$

$$= \sum_{n=0}^{\infty} \sum_{m=0}^{\infty} \left(\frac{1}{U}\right)^{n+m} \sum_{i,j} \langle \bar{\Psi}_i^{(n)} | \bar{\Psi}_j^{(m)} \rangle \quad (\text{D.23b})$$

$$= \sum_{n=0}^{\infty} \sum_{m=0}^{\infty} \left(\frac{1}{U}\right)^{n+m} \sum_j \langle \bar{\Psi}_j^{(n)} | \bar{\Psi}_j^{(m)} \rangle \quad (\text{D.23c})$$

$$= \sum_n g_n. \quad (\text{D.23d})$$

To obtain the third equality we used the fact that the different sub-bands do not overlap. The weights of the various sub-bands therefore satisfy the sum rule

$$\sum_n g_n = \frac{1}{2} \quad (\text{D.24})$$

and, according to (D.23c), can be expanded in powers of $1/U$ as follows,

$$g_n = \sum_{l=0}^{\infty} \left(\frac{1}{U}\right)^n g_{n,l}, \quad (\text{D.25})$$

where

$$g_{n,l} := \sum_{m=0}^l \langle \bar{\Psi}_n^{(m)} | \bar{\Psi}_n^{(l-m)} \rangle. \quad (\text{D.25a})$$

D. Multichain Approach to the SIAM

Results for g_n up to Fourth Order in $1/U$

For the state $|\bar{\Psi}\rangle$ we found up to third order in $1/U$, see Sect. E.2.2,

$$|\bar{\Psi}^{(0)}\rangle = |\bar{\Psi}_0^{(0)}\rangle, \quad (\text{D.26})$$

$$|\bar{\Psi}^{(1)}\rangle = |\bar{\Psi}_0^{(1)}\rangle, \quad (\text{D.27})$$

$$|\bar{\Psi}^{(2)}\rangle = |\bar{\Psi}_0^{(2)}\rangle + |\bar{\Psi}_1^{(2)}\rangle, \quad (\text{D.28})$$

$$|\bar{\Psi}^{(3)}\rangle = |\bar{\Psi}_0^{(3)}\rangle + |\bar{\Psi}_1^{(3)}\rangle. \quad (\text{D.29})$$

With the definitions (E.22a) to (E.22c) and (E.23a) to (E.23c) the various states in (D.26) to (D.29) read, see Sect. E.1 as well as (E.64a), (E.64d) and (E.64e) for details on the notation,

$$|\bar{\Psi}_0^{(0)}\rangle = |\phi_{-1}\rangle, \quad (\text{D.30})$$

$$|\bar{\Psi}_0^{(1)}\rangle = -|m_{0u}\rangle, \quad (\text{D.31})$$

$$|\bar{\Psi}_0^{(2)}\rangle = -\frac{1}{2}|\phi_{-1}\rangle + |m_{1u}\rangle, \quad (\text{D.32})$$

$$|\bar{\Psi}_1^{(2)}\rangle = \frac{1}{2}|\phi_{0u}^*\rangle + \frac{1}{2}|\phi_{0d}^*\rangle + |\chi_0^*\rangle, \quad (\text{D.33})$$

$$|\bar{\Psi}_0^{(3)}\rangle = -|m_{2u}\rangle - |m_{0u}\rangle. \quad (\text{D.34})$$

With the scalar products given in table E.1 and the sum rule (D.24) we finally obtain for the weights up to fourth order in $1/U$,

$$g_0(U) = \frac{1}{2} - \frac{3}{4U^4} + \mathcal{O}\left(\frac{1}{U^5}\right), \quad (\text{D.35})$$

$$g_1(U) = \frac{3}{4U^4} + \mathcal{O}\left(\frac{1}{U^5}\right), \quad (\text{D.36})$$

$$g_i(U) = \mathcal{O}\left(\frac{1}{U^5}\right) \text{ for } i \geq 2. \quad (\text{D.37})$$

To calculate $g_0(U)$ up to fourth order we used the sum rule (D.24). In order to show the consistency of (D.35) to fourth order in $1/U$ we need to calculate $|\bar{\Psi}_0^{(4)}\rangle$. As a consequence, we need a four-chain setup starting from fourth order in the $1/U$ -expansion.

E

Explicit Calculations

In this appendix we present the calculations up to and including third order in $1/U$ explicitly. After introducing some abbreviations we calculate the starting vector for the Lanczos iteration of the operator \mathcal{L} , introduced in Sect. 9.3.3. Then, we perturbatively determine the ground-state energy $\tilde{E}_0(L)$ of the SIAM, (9.30), to derive in the next step the explicit form of the ‘Green function’-operator \mathcal{L} . To facilitate the Lanczos iterations, we calculate the effects of some commonly appearing operators. Finally, we calculate the complete Lanczos basis of the operator \mathcal{L} . To leading order in $1/U$ we determine the Lanczos basis of $\mathcal{L}^{(0)}$ and, at the same time, fix the on-site energies $\varepsilon_i^{(0)}$ and the electron transfer amplitudes $t_i^{(0)}$ by means of the DMFT self-consistency equation (9.91). Then, we proceed with the first-order calculations, where we obtain the Lanczos basis of $\mathcal{L}^{(1)}$ and fix the parameters $\varepsilon_i^{(1)}$ and $t_i^{(1)}$. We continue in this way up to third order in $1/U$.

This appendix is highly technical and has been included for completeness and documentary purposes.

E.1. Definitions

In order to be able to state the various formulae in concise form, we introduce the states

$$|\phi_{-1}\rangle := \frac{1}{\sqrt{2}} |\dots \uparrow \uparrow \uparrow \text{---} \dots \rangle, \quad (\text{E.1a})$$

and, for $n \geq 0$,

$$|\phi_{nu}\rangle := \frac{1}{\sqrt{2}} |\dots \underbrace{\uparrow \uparrow \uparrow}_{\text{index } n} \dots \underbrace{\uparrow \uparrow \downarrow}_{\text{index } 0} \text{---} \dots \rangle, \quad (\text{E.1b})$$

$$|\phi_{nd}\rangle := \frac{1}{\sqrt{2}} |\dots \underbrace{\uparrow \downarrow \uparrow}_{\text{index } n} \dots \underbrace{\uparrow \uparrow \uparrow}_{\text{index } 0} \text{---} \dots \rangle, \quad (\text{E.1c})$$

$$|\chi_n\rangle := \frac{1}{\sqrt{2}} |\dots \underbrace{\uparrow \downarrow \uparrow}_{\text{index } n} \dots \underbrace{\uparrow \uparrow \downarrow}_{\text{index } 0} \text{---} \dots \rangle. \quad (\text{E.1d})$$

Additionally, we define the vectors

$$|\gamma_n\rangle := (-1)^n \frac{1}{\sqrt{2}} (|\phi_{nu}\rangle - |\phi_{nd}\rangle) \quad \text{for } n \geq 0, \quad (\text{E.2a})$$

$$|m_{nx}\rangle := (-1)^n \frac{1}{\sqrt{2}} (|\phi_{nx}\rangle + |\chi_n\rangle) \quad \text{for } n \geq 0 \text{ and } x \in \{u, d\}. \quad (\text{E.2b})$$

The scalar products of the vectors introduced above are given in table E.1.

E. Explicit Calculations

States	$ \phi_{-1}\rangle$	$ \phi_{nu}\rangle$	$ \phi_{nd}\rangle$	$ \chi_n\rangle$	$ \gamma_n\rangle$	$ m_{nu}\rangle$	$ m_{nd}\rangle$
$\langle\phi_{-1} $	$\frac{1}{2}$	0	0	0	0	0	0
$\langle\phi_{lu} $		$\frac{\delta_{l,n}}{2}$	0	0	$\frac{(-1)^n \delta_{l,n}}{2\sqrt{2}}$	$\frac{(-1)^n \delta_{l,n}}{2\sqrt{2}}$	0
$\langle\phi_{ld} $			$\frac{\delta_{l,n}}{2}$	0	$\frac{(-1)^{n+1} \delta_{l,n}}{2\sqrt{2}}$	0	$\frac{(-1)^n \delta_{l,n}}{2\sqrt{2}}$
$\langle\chi_l $				$\frac{\delta_{l,n}}{2}$	0	$\frac{(-1)^n \delta_{l,n}}{2\sqrt{2}}$	$\frac{(-1)^n \delta_{l,n}}{2\sqrt{2}}$
$\langle\gamma_l $					$\frac{\delta_{l,n}}{2}$	$\frac{\delta_{l,n}}{4}$	$\frac{-\delta_{l,n}}{4}$
$\langle m_{lu} $						$\frac{\delta_{l,n}}{2}$	$\frac{\delta_{l,n}}{4}$
$\langle m_{ld} $							$\frac{\delta_{l,n}}{2}$

Table E.1.: Scalar products of the states introduced in Sect. E.1. Since the scalar product is symmetric, the table is symmetric with respect to a reflection at its main diagonal. Thus, we only show its upper half.

E.2. Starting Vector for the Lanczos Iteration

As we showed in Sect. 9.4, we have to perform the Lanczos iteration, (9.70a) to (9.70d), with

$$|\Psi_0\rangle := \Gamma_{L-1}^\dagger d_\uparrow \Gamma_L |\Phi\rangle \quad (\text{E.3})$$

as the starting vector. Here, $|\Phi\rangle$ denotes the linear combination

$$|\Phi\rangle = \frac{1}{\sqrt{2}}(|\phi_\uparrow\rangle + |\phi_\downarrow\rangle) \quad (\text{E.4})$$

of the two degenerate ground states, (9.32) and (9.33), of H_0 . We calculated the operator Γ for the (SIAM) in Sect. C.3.

E.2.1. Ground-State Vectors at Half Filling

As a first step, we apply Γ_L , given in (C.77), to the states $|\phi_\uparrow\rangle$ and $|\phi_\downarrow\rangle$. For convenience, we introduce the notation

$$|\Psi_\sigma\rangle := \Gamma_L |\phi_\sigma\rangle = \sum_{n=0}^{\infty} \left(\frac{1}{U}\right)^n |\Psi_\sigma^{(n)}\rangle \quad (\text{E.5})$$

with $|\Psi_\sigma^{(n)}\rangle := \Gamma_L^{(n)} |\phi_\sigma\rangle$, see (C.77).

Consequences of Spin-Rotational Invariance

With the help of the spin-flip operator J_S , (9.18), we need to carry out the calculations for the spin-up sector only. Since the Hamiltonian H_S , (9.30), commutes with J_S , so does Γ . Thus, we obtain

$$|\Psi_\sigma\rangle = \Gamma_L J_S |\phi_{-\sigma}\rangle = J_S \Gamma_L |\phi_{-\sigma}\rangle = J_S |\Psi_{-\sigma}\rangle. \quad (\text{E.6})$$

The application of J_S to the states defined in Sect. E.1 is straightforward. However, we have to remember our phase convention: We always put electrons with spin up on a site before those with spin down. Let us consider an example.

For definiteness, we assume, without loss of generality, that the number of sites in the lower chain as well as in the upper chain is even. Then, we find that

$$J_S |\phi_\uparrow\rangle = J_S \dots \alpha_{1\uparrow}^\dagger \alpha_{1\downarrow}^\dagger \alpha_{0\uparrow}^\dagger \alpha_{0\downarrow}^\dagger d_\uparrow^\dagger |\text{vac}\rangle \quad (\text{E.7a})$$

$$= J_S \dots J_S^\dagger J_S \alpha_{0\uparrow}^\dagger J_S^\dagger J_S \alpha_{0\downarrow}^\dagger J_S^\dagger J_S d_\uparrow^\dagger J_S^\dagger J_S |\text{vac}\rangle \quad (\text{E.7b})$$

E.2. Starting Vector for the Lanczos Iteration

$$= \dots \alpha_{1\downarrow}^\dagger \alpha_{1\uparrow}^\dagger \alpha_{0\downarrow}^\dagger \alpha_{0\uparrow}^\dagger d_{\downarrow}^\dagger |\text{vac}\rangle \quad (\text{E.7c})$$

$$= \dots (-\alpha_{1\uparrow}^\dagger \alpha_{1\downarrow}^\dagger) (-\alpha_{0\uparrow}^\dagger \alpha_{0\downarrow}^\dagger) d_{\downarrow}^\dagger |\text{vac}\rangle \quad (\text{E.7d})$$

$$= |\phi_{\downarrow}\rangle. \quad (\text{E.7e})$$

In the second equality we made use of the unitarity of J_S , in the third we used its defining properties (9.18), and in the final step we used our assumption that the number of sites in the lower chain is even. When we perform the above steps with a state $|\phi_{nu}\rangle$, we obtain

$$J_S |\phi_{nu}\rangle = -|\phi_{nd}\rangle, \quad (\text{E.8})$$

where the minus comes from the odd number of $\alpha_{l\uparrow}^\dagger \leftrightarrow \alpha_{l\downarrow}^\dagger$ interchanges.

Calculation of $|\Psi_{\uparrow}\rangle$

With Γ_L given by (C.77) we can perform the calculations. We discuss each order in $1/U$ separately.

Leading Order To leading order we found $\Gamma_L^{(0)}$ to be identical to the ground-state projector P , see (C.77a). Thus, we may state that

$$\boxed{|\Psi_{\uparrow}^{(0)}\rangle = |\phi_{\uparrow}\rangle.} \quad (\text{E.9})$$

First Order To first order in $1/U$ Takahashi's operator is given by (C.77b), $\Gamma_L^{(1)} = -\Upsilon_1$, and we need to calculate

$$-\Upsilon_1 |\phi_{\uparrow}\rangle = -S V_0 P |\dots \uparrow \uparrow \uparrow \uparrow \uparrow \dots\rangle. \quad (\text{E.10})$$

Thus, we get

$$\boxed{|\Psi_{\uparrow}^{(1)}\rangle = \frac{1}{\sqrt{2}} \left(|\dots \uparrow \uparrow \uparrow \uparrow \uparrow \dots\rangle - |\dots \uparrow \uparrow \uparrow \uparrow \downarrow \dots\rangle \right).} \quad (\text{E.11})$$

Second Order The self-consistent calculation to lowest order, as we show in Sect. E.6.1, leads to

$$\varepsilon_l^{(0)} = 0 \quad \text{and} \quad t_l^{(0)} = 1 \quad (\text{E.12})$$

for all sites l . As the higher-order calculations can only be done after the lowest-order calculations have been performed, we can use (E.12) for all $n \geq 1$. This does not affect the lowest-order results at all.

The operator $\Gamma_L^{(2)}$ is given by (C.77c) of appendix C and reads

$$\Gamma_L^{(2)} = \Upsilon_2 - \frac{1}{2}P. \quad (\text{E.13})$$

We start with the calculation of the state $\Upsilon_2 |\phi_{\uparrow}\rangle$, see (C.67b), and obtain

$$\begin{aligned} \Upsilon_2 |\phi_{\uparrow}\rangle &= S \bar{V}_0 \Upsilon_1 |\phi_{\uparrow}\rangle = \frac{1}{\sqrt{2}} S \bar{V}_0 \left(|\dots \uparrow \uparrow \uparrow \uparrow \downarrow \dots\rangle - |\dots \uparrow \uparrow \uparrow \uparrow \uparrow \dots\rangle \right) \\ &= \frac{1}{\sqrt{2}} |\dots \uparrow \uparrow \uparrow \uparrow \uparrow \dots\rangle + |\dots \uparrow \uparrow \uparrow \uparrow \downarrow \dots\rangle \\ &\quad - \frac{1}{2} |\dots \uparrow \uparrow \uparrow \uparrow \uparrow \downarrow \dots\rangle - \frac{1}{2} |\dots \uparrow \uparrow \uparrow \uparrow \downarrow \uparrow \dots\rangle \\ &\quad + \frac{1}{\sqrt{2}} |\dots \uparrow \uparrow \uparrow \uparrow \dots\rangle. \end{aligned} \quad (\text{E.14})$$

E. Explicit Calculations

Since the action of P on $|\phi_\uparrow\rangle$ is trivial, we finally arrive at

$$\begin{aligned}
 |\Psi_\uparrow^{(2)}\rangle = & -\frac{1}{2}|\phi_\uparrow\rangle + \frac{1}{\sqrt{2}}|\dots\uparrow\uparrow\uparrow\uparrow\downarrow\downarrow\downarrow\downarrow\dots\rangle + |\dots\uparrow\uparrow\uparrow\uparrow\downarrow\uparrow\downarrow\dots\rangle \\
 & -\frac{1}{2}|\dots\uparrow\uparrow\uparrow\uparrow\downarrow\downarrow\dots\rangle - \frac{1}{2}|\dots\uparrow\uparrow\downarrow\uparrow\uparrow\downarrow\dots\rangle \\
 & + \frac{1}{\sqrt{2}}|\dots\uparrow\uparrow\uparrow\downarrow\uparrow\dots\rangle.
 \end{aligned} \tag{E.15}$$

Third Order According to (C.77d) of appendix C, $\Gamma_L^{(3)}$ reads

$$\Gamma_L^{(3)} = -\Upsilon_3 + \frac{3}{2}\Upsilon_1 + h_2, \tag{E.16}$$

where we have used of the result to first order, see Sect. E.6.2, especially that $V_1^{(1)} \equiv 0$ and $\varepsilon_0^{(1)} = 0$. Since the operator Υ_3 is identical to $S\bar{V}_0\Upsilon_2$, see Sect. C.3.2, and since we already calculated the effect of Υ_2 on the ground state $|\phi_\uparrow\rangle$ in (E.14), we can easily derive the effect of Υ_3 on the state $|\phi_\uparrow\rangle$. The result reads

$$\begin{aligned}
 -\Upsilon_3|\phi_\uparrow\rangle = & -S\bar{V}_0\Upsilon_2|\phi_\uparrow\rangle \\
 = & \frac{1}{\sqrt{2}}|\dots\uparrow\uparrow\uparrow\uparrow\downarrow\downarrow\downarrow\downarrow\dots\rangle + \frac{5}{2\sqrt{2}}|\dots\uparrow\uparrow\uparrow\uparrow\downarrow\downarrow\dots\rangle \\
 & - |\dots\uparrow\uparrow\uparrow\uparrow\downarrow\uparrow\downarrow\dots\rangle + \frac{3}{2}|\dots\uparrow\uparrow\uparrow\uparrow\downarrow\uparrow\uparrow\downarrow\dots\rangle \\
 & - \frac{3}{2}|\dots\uparrow\uparrow\uparrow\uparrow\downarrow\downarrow\uparrow\dots\rangle - \frac{5}{2\sqrt{2}}|\dots\uparrow\uparrow\uparrow\uparrow\downarrow\uparrow\dots\rangle \\
 & - \frac{3}{4\sqrt{2}}|\dots\uparrow\uparrow\uparrow\uparrow\downarrow\uparrow\uparrow\downarrow\dots\rangle + \frac{3}{4\sqrt{2}}|\dots\uparrow\uparrow\uparrow\uparrow\downarrow\uparrow\downarrow\dots\rangle \\
 & + \frac{1}{2}|\dots\uparrow\uparrow\uparrow\uparrow\downarrow\uparrow\downarrow\dots\rangle - \frac{1}{2}|\dots\uparrow\uparrow\downarrow\uparrow\uparrow\uparrow\downarrow\dots\rangle \\
 & + |\dots\uparrow\uparrow\uparrow\uparrow\downarrow\uparrow\uparrow\uparrow\downarrow\dots\rangle - \frac{1}{\sqrt{2}}|\dots\uparrow\uparrow\uparrow\uparrow\downarrow\uparrow\dots\rangle.
 \end{aligned} \tag{E.17}$$

It remains to calculate $h_2|\phi_\uparrow\rangle$. The operator h_2 , as defined in (C.68c), is identical to $PV_0\Upsilon_2$. The action of Υ_2 on the ground state $|\phi_\uparrow\rangle$ is given by (E.14). Applying PV_0 to (E.14), we obtain

$$h_2|\phi_\uparrow\rangle = 0. \tag{E.18}$$

With the known state $\Upsilon_1|\phi_\uparrow\rangle$, (E.10), we therefore conclude that

$$\begin{aligned}
 |\Psi_\uparrow^{(3)}\rangle = & \frac{1}{\sqrt{2}}|\dots\uparrow\uparrow\uparrow\uparrow\text{---}\rangle + \frac{1}{\sqrt{2}}|\dots\uparrow\uparrow\uparrow\uparrow\text{---}\rangle \\
 & - |\dots\uparrow\uparrow\uparrow\downarrow\text{---}\rangle + \frac{3}{2}|\dots\uparrow\uparrow\uparrow\downarrow\uparrow\text{---}\rangle \\
 & - \frac{3}{2}|\dots\uparrow\uparrow\uparrow\downarrow\text{---}\rangle - \frac{1}{\sqrt{2}}|\dots\uparrow\uparrow\uparrow\text{---}\rangle \\
 & - \frac{3}{4\sqrt{2}}|\dots\uparrow\uparrow\text{---}\rangle + \frac{3}{4\sqrt{2}}|\dots\uparrow\uparrow\uparrow\text{---}\rangle \\
 & + \frac{1}{2}|\dots\uparrow\uparrow\uparrow\downarrow\text{---}\rangle - \frac{1}{2}|\dots\uparrow\downarrow\uparrow\uparrow\text{---}\rangle \\
 & + |\dots\uparrow\uparrow\downarrow\uparrow\text{---}\rangle - \frac{1}{\sqrt{2}}|\dots\uparrow\uparrow\uparrow\text{---}\rangle.
 \end{aligned} \tag{E.19}$$

Calculation of $|\Psi_\downarrow\rangle$

With the help of the spin-flip operator J_S , see (E.6), we can immediately state the expressions for $|\Psi_\downarrow^{(n)}\rangle$. They read

$$|\Psi_\downarrow^{(0)}\rangle = |\phi_\downarrow\rangle, \tag{E.20a}$$

$$|\Psi_\downarrow^{(1)}\rangle = \frac{1}{\sqrt{2}}\left(|\dots\uparrow\uparrow\downarrow\uparrow\text{---}\rangle - |\dots\uparrow\uparrow\uparrow\text{---}\rangle\right), \tag{E.20b}$$

$$\begin{aligned}
 |\Psi_\downarrow^{(2)}\rangle = & -\frac{1}{2}|\phi_\downarrow\rangle + \frac{1}{\sqrt{2}}|\dots\uparrow\downarrow\uparrow\uparrow\text{---}\rangle - |\dots\uparrow\uparrow\downarrow\uparrow\text{---}\rangle \\
 & + \frac{1}{2}|\dots\uparrow\uparrow\downarrow\uparrow\text{---}\rangle + \frac{1}{2}|\dots\uparrow\uparrow\uparrow\downarrow\text{---}\rangle \\
 & + \frac{1}{\sqrt{2}}|\dots\uparrow\uparrow\uparrow\text{---}\rangle,
 \end{aligned} \tag{E.20c}$$

$$\begin{aligned}
 |\Psi_\downarrow^{(3)}\rangle = & \frac{1}{\sqrt{2}}|\dots\downarrow\uparrow\uparrow\uparrow\text{---}\rangle + \frac{1}{\sqrt{2}}|\dots\uparrow\uparrow\downarrow\uparrow\text{---}\rangle \\
 & + |\dots\uparrow\downarrow\uparrow\uparrow\text{---}\rangle - \frac{3}{2}|\dots\uparrow\downarrow\uparrow\uparrow\text{---}\rangle \\
 & + \frac{3}{2}|\dots\uparrow\uparrow\downarrow\uparrow\text{---}\rangle - \frac{1}{\sqrt{2}}|\dots\uparrow\uparrow\uparrow\text{---}\rangle \\
 & - \frac{3}{4\sqrt{2}}|\dots\uparrow\uparrow\text{---}\rangle + \frac{3}{4\sqrt{2}}|\dots\uparrow\uparrow\downarrow\text{---}\rangle \\
 & - \frac{1}{2}|\dots\uparrow\uparrow\downarrow\uparrow\text{---}\rangle + \frac{1}{2}|\dots\uparrow\uparrow\uparrow\downarrow\text{---}\rangle \\
 & - |\dots\uparrow\uparrow\uparrow\downarrow\text{---}\rangle - \frac{1}{\sqrt{2}}|\dots\uparrow\uparrow\uparrow\text{---}\rangle.
 \end{aligned} \tag{E.20d}$$

E.2.2. Transformed Hole States

Next, we calculate the transformed hole-state vectors

$$|\bar{\Psi}_\sigma\rangle := d_\uparrow|\Psi_\sigma\rangle = \sum_{n=0}^{\infty} \left(\frac{1}{U}\right)^n |\bar{\Psi}_\sigma^{(n)}\rangle \quad (\text{E.21})$$

with $|\bar{\Psi}_\sigma^{(n)}\rangle := d_\uparrow|\Psi_\sigma^{(n)}\rangle$. It is trivial to apply the operator d_\uparrow to the states $|\Psi_\sigma\rangle$ because these are given in terms of eigenstates of the local number operators. But we have to remember that we work with fermions and, as a consequence, must include a minus sign for every interchange of d_\uparrow with an operator $\alpha_{l\sigma}^\dagger$ of the chain. Therefore, we obtain

$$|\bar{\Psi}_\uparrow^{(0)}\rangle = |\dots \uparrow \uparrow \uparrow - \dots\rangle, \quad (\text{E.22a})$$

$$|\bar{\Psi}_\uparrow^{(1)}\rangle = -\frac{1}{\sqrt{2}}|\dots \uparrow \uparrow \uparrow \downarrow - \dots\rangle, \quad (\text{E.22b})$$

$$\begin{aligned} |\bar{\Psi}_\uparrow^{(2)}\rangle &= -\frac{1}{2}|\dots \uparrow \uparrow \uparrow - \dots\rangle - \frac{1}{\sqrt{2}}|\dots \uparrow \uparrow \uparrow \downarrow - \dots\rangle \\ &+ \frac{1}{2}|\dots \uparrow \uparrow \uparrow \downarrow - \dots\rangle + \frac{1}{2}|\dots \uparrow \uparrow \downarrow - \dots\rangle, \end{aligned} \quad (\text{E.22c})$$

$$\begin{aligned} |\bar{\Psi}_\uparrow^{(3)}\rangle &= -\frac{1}{\sqrt{2}}|\dots \uparrow \uparrow \uparrow \downarrow - \dots\rangle - \frac{1}{\sqrt{2}}|\dots \uparrow \uparrow \uparrow \downarrow - \dots\rangle \\ &+ |\dots \uparrow \uparrow \uparrow \downarrow - \dots\rangle - \frac{3}{4\sqrt{2}}|\dots \uparrow \uparrow \downarrow - \dots\rangle \\ &- \frac{1}{2}|\dots \uparrow \uparrow \uparrow \downarrow - \dots\rangle + \frac{1}{2}|\dots \uparrow \uparrow \downarrow - \dots\rangle \\ &- |\dots \uparrow \uparrow \downarrow - \dots\rangle. \end{aligned} \quad (\text{E.22d})$$

The corresponding expressions for spin down read

$$|\bar{\Psi}_\downarrow^{(0)}\rangle = 0, \quad (\text{E.23a})$$

$$|\bar{\Psi}_\downarrow^{(1)}\rangle = -\frac{1}{\sqrt{2}}|\dots \uparrow \uparrow \downarrow \downarrow - \dots\rangle, \quad (\text{E.23b})$$

$$|\bar{\Psi}_\downarrow^{(2)}\rangle = -\frac{1}{\sqrt{2}}|\dots \uparrow \downarrow \uparrow \downarrow - \dots\rangle + |\dots \uparrow \uparrow \downarrow - \dots\rangle \quad (\text{E.23c})$$

$$\begin{aligned} |\bar{\Psi}_\downarrow^{(3)}\rangle &= -\frac{1}{\sqrt{2}}|\dots \downarrow \uparrow \uparrow \downarrow - \dots\rangle - \frac{1}{\sqrt{2}}|\dots \uparrow \uparrow \downarrow \downarrow - \dots\rangle \\ &+ \frac{3}{2}|\dots \uparrow \downarrow \uparrow - \dots\rangle - \frac{3}{2}|\dots \uparrow \uparrow \downarrow - \dots\rangle \\ &- \frac{3}{4\sqrt{2}}|\dots \uparrow \uparrow - \dots\rangle. \end{aligned} \quad (\text{E.23d})$$

E.2.3. Starting Vector

Finally, to obtain the starting vector $|\Psi_0\rangle$ for the Lanczos iteration, (E.3), we need to calculate

$$|\tilde{\Psi}_\sigma\rangle := \Gamma_{L-1}^\dagger |\bar{\Psi}_\sigma\rangle = \sum_{n=0}^{\infty} \left(\frac{1}{U}\right)^n |\tilde{\Psi}_\sigma^{(n)}\rangle. \quad (\text{E.24})$$

To obtain the state $|\tilde{\Psi}_\sigma^{(n)}\rangle$ we have to expand $|\bar{\Psi}_\sigma\rangle$ as well as the operator Γ_{L-1}^\dagger . With the expansion of the state $|\bar{\Psi}_\sigma\rangle$, (E.21), and the expansion of Γ_{L-1} , (C.72), we may conclude that

$$|\tilde{\Psi}_\sigma^{(n)}\rangle = \sum_{l=0}^n \left(\Gamma_{L-1}^{(n-l)}\right)^\dagger |\bar{\Psi}_\sigma^{(l)}\rangle. \quad (\text{E.25})$$

Leading Order To leading order we find

$$|\tilde{\Psi}_\sigma^{(0)}\rangle = \left(\Gamma_{L-1}^{(0)}\right)^\dagger |\bar{\Psi}_\sigma^{(0)}\rangle = P|\bar{\Psi}_\sigma^{(0)}\rangle, \quad (\text{E.26})$$

and therefore, with (E.22a) and (E.23a),

$$|\tilde{\Psi}_\uparrow^{(0)}\rangle = |\dots \uparrow \uparrow \uparrow \uparrow \dots\rangle = \sqrt{2}|\phi_{-1}\rangle, \quad (\text{E.27a})$$

$$|\tilde{\Psi}_\downarrow^{(0)}\rangle = 0. \quad (\text{E.27b})$$

First Order Only $\left(\Gamma_{L-1}^{(0)}\right)^\dagger |\bar{\Psi}_\sigma\rangle = P|\bar{\Psi}_\sigma\rangle$ contributes to the sum (E.25) in first order. We obtain

$$|\tilde{\Psi}_\uparrow^{(1)}\rangle = -\frac{1}{\sqrt{2}}|\dots \uparrow \uparrow \uparrow \downarrow \dots\rangle = -|\phi_{0u}\rangle, \quad (\text{E.28a})$$

$$|\tilde{\Psi}_\downarrow^{(1)}\rangle = -\frac{1}{\sqrt{2}}|\dots \uparrow \uparrow \downarrow \downarrow \dots\rangle = -|\chi_0\rangle. \quad (\text{E.28b})$$

Second Order According to (E.25), we have to calculate

$$|\tilde{\Psi}_\sigma^{(1)}\rangle = \left(\Gamma_{L-1}^{(2)}\right)^\dagger |\bar{\Psi}_\sigma^{(0)}\rangle + \left(\Gamma_{L-1}^{(1)}\right)^\dagger |\bar{\Psi}_\sigma^{(1)}\rangle + \left(\Gamma_{L-1}^{(0)}\right)^\dagger |\bar{\Psi}_\sigma^{(2)}\rangle. \quad (\text{E.29})$$

The only non-vanishing contribution stems from $P|\bar{\Psi}_\sigma^{(2)}\rangle$ and we get, see (E.22c) and (E.23c),

$$|\tilde{\Psi}_\uparrow^{(2)}\rangle = -\frac{\sqrt{2}}{2}|\phi_{-1}\rangle - |\phi_{1u}\rangle, \quad (\text{E.30a})$$

$$|\tilde{\Psi}_\downarrow^{(2)}\rangle = -|\chi_1\rangle. \quad (\text{E.30b})$$

Third Order With Γ_{L-1} , (C.72), and the sum (E.25) we obtain without difficulty

$$|\tilde{\Psi}_\uparrow^{(3)}\rangle = -\frac{1}{\sqrt{2}}|\dots \uparrow \uparrow \uparrow \downarrow \dots\rangle - \frac{7}{4\sqrt{2}}|\dots \uparrow \uparrow \uparrow \downarrow \dots\rangle = -|\phi_{2u}\rangle - \frac{7}{4}|\phi_{0u}\rangle, \quad (\text{E.31a})$$

$$|\tilde{\Psi}_\downarrow^{(3)}\rangle = -\frac{1}{\sqrt{2}}|\dots \downarrow \uparrow \uparrow \downarrow \dots\rangle - \frac{7}{4\sqrt{2}}|\dots \uparrow \uparrow \downarrow \downarrow \dots\rangle = -|\chi_2\rangle - \frac{7}{4}|\chi_0\rangle. \quad (\text{E.31b})$$

E. Explicit Calculations

Summary for the Starting Vector

The starting vector for the Lanczos iteration,

$$|\Psi_0\rangle = \Gamma_{L-1}^\dagger d_\uparrow \Gamma_L |\Phi\rangle, \quad (\text{E.32})$$

admits the expansion

$$|\Psi_0\rangle = \sum_{n=0}^{\infty} \left(\frac{1}{U}\right)^n |\Psi_0^{(n)}\rangle, \quad (\text{E.33})$$

where, according to (E.24), the states $|\Psi_0^{(n)}\rangle$ read

$$|\Psi_0^{(n)}\rangle = \frac{1}{\sqrt{2}} (|\tilde{\Psi}_\uparrow^{(n)}\rangle + |\tilde{\Psi}_\downarrow^{(n)}\rangle). \quad (\text{E.34})$$

With the states $|\tilde{\Psi}_\sigma^{(n)}\rangle$ given by (E.27a) to (E.31b), we can state the starting vector $|\Psi_0\rangle$ up to third order in $1/U$ as

$$\boxed{|\Psi_0\rangle = |\phi_{-1}\rangle - \frac{1}{U} |m_{0u}\rangle + \frac{1}{U^2} \left(-\frac{1}{2} |\phi_{-1}\rangle + |m_{1u}\rangle\right) - \frac{1}{U^3} \left(\frac{7}{4} |m_{0u}\rangle + |m_{2u}\rangle\right) + \mathcal{O}\left(\frac{1}{U^4}\right)}. \quad (\text{E.35})$$

E.3. Ground-State Energy of the SIAM at Half Filling

In the following section we calculate the ground-state energy, $\tilde{E}_0(L)$, of the half-filled Single Impurity Anderson Model (SIAM) by means of Kato-Takahashi perturbation theory. With this perturbation theory, as described in chapter 8, we can transform the time-independent, ground-state Schrödinger equation

$$H_S |\Psi\rangle = \tilde{E}_0(L) |\Psi\rangle \quad (\text{E.36})$$

for the SIAM Hamiltonian, (9.30), at half band-filling into the equivalent eigenvalue problem

$$\Gamma_L^\dagger H_S \Gamma_L |\Phi\rangle = \tilde{E}_0(L) |\Phi\rangle, \quad (\text{E.37})$$

defined in the ground-state eigenspace of H_0 , (9.30a). The state $|\Phi\rangle$ can be any ground-state vector of H_0 , for example $|\phi_\uparrow\rangle$, see (9.32). In chapter 8 we introduced the reduced energy operator (8.22). For the SIAM at half band-filling it admits the expansion (C.78),

$$\Gamma_L^\dagger (H_S - \tilde{E}_0^{(0)}(L)) \Gamma_L = \sum_{n=0}^{\infty} \left(\frac{1}{U}\right)^n R_L^{(n)}, \quad (\text{E.38})$$

with $\tilde{E}_0^{(0)}(L)$ denoting the ground-state energy of H_0 at half filling, see (9.34). We take the expectation value of (E.38) in the normalized ground state $|\phi_\uparrow\rangle$ and obtain the expansion

$$\tilde{E}_0(L) = \tilde{E}_0^{(0)}(L) + \sum_{n=0}^{\infty} \left(\frac{1}{U}\right)^n \tilde{E}_0^{[n]}(L) \quad (\text{E.39})$$

for the ground-state energy $\tilde{E}_0(L)$. We defined the n th order corrections $\tilde{E}_0^{[n]}(L)$ by

$$\tilde{E}_0^{[n]}(L) = \langle \phi_\uparrow | R_L^{(n)} | \phi_\uparrow \rangle. \quad (\text{E.40})$$

Thus, with the $R_L^{(n)}$ given by (C.78), we can immediately calculate the expressions $\tilde{E}_0^{[n]}(L)$.

Leading Order To lowest order in $1/U$ we find with $R_L^{(0)} = \xi^{(0)}P$, see (C.78), that

$$\boxed{\tilde{E}_0^{[0]}(L) = \xi^{(0)}} \quad (\text{E.41})$$

The $\xi^{(n)}$ were introduced in Sect. C.3.1 and read

$$\xi^{(n)} = 2 \sum_{l \in \text{lower chain}} \varepsilon_l^{(n)}. \quad (\text{E.42})$$

First Order With $R_L^{(1)} = (\xi^{(1)} - 1)P$ we obtain the correction to first order which reads

$$\boxed{\tilde{E}_0^{[1]}(L) = \xi^{(1)} - 1}. \quad (\text{E.43})$$

Second Order According to (C.78), we have to evaluate

$$\tilde{E}_0^{[2]}(L) = \langle \phi_\uparrow | R_L^{(2)}(L) | \phi_\uparrow \rangle = \langle \phi_\uparrow | \Upsilon_1^\dagger \bar{V}_0 \Upsilon_1 | \phi_\uparrow \rangle + \xi^{(2)} = \xi^{(2)} \quad (\text{E.44})$$

in second order which we can summarize as

$$\boxed{\tilde{E}_0^{[2]}(L) = \xi^{(2)}}. \quad (\text{E.45})$$

Third Order To third order, $R_L^{(3)}$ is given by

$$R_L^{(3)} = -h_3 + (1 + \xi^{(3)})P, \quad (\text{E.46})$$

where we already used the results of the lower orders.

Only the expectation value of $h_3 = PV_0 \Upsilon_3$ is non-trivial. We already calculated the action of Υ_3 on the ground state at half filling. Applying PV_0 to (E.17) results in

$$-PV_0 \Upsilon_3 | \phi_\uparrow \rangle = -\frac{5}{2} | \dots \uparrow \uparrow \uparrow \uparrow \uparrow \dots \rangle = -\frac{5}{2} | \phi_\uparrow \rangle. \quad (\text{E.47})$$

Thus, we can finally state that

$$\boxed{\tilde{E}_0^{[3]}(L) = \xi^{(3)} - \frac{3}{2}}. \quad (\text{E.48})$$

E.4. Operator for the Lanczos Procedure

In Sect. 9.3.3 and 9.4.2 we showed that we need to submit the operator (9.67),

$$\mathcal{L} = \sum_{n=0}^{\infty} \left(\frac{1}{U} \right)^n \mathcal{L}^{(n)}, \quad (\text{E.49})$$

to the Lanczos iteration (9.70a) to (9.70d) in order to obtain the matrix representation (9.80) of the Green function. The $\mathcal{L}^{(n)}$ are defined by (9.68) and read

$$\mathcal{L}^{(n)} = R_{L-1}^{(n)} - \tilde{E}_0^{[n]}(L)P. \quad (\text{E.50})$$

We derived the expressions for the energy corrections $\tilde{E}_0^{[n]}(L)$ in Sect. E.3. The formulae for $R_{L-1}^{(n)}$ are given by (C.73). Thus, we can calculate the $\mathcal{L}^{(n)}$.

E. Explicit Calculations

Leading Order With $R_{L-1}^{(0)} = h_0$, see (C.73) and (C.68a), and with $\tilde{E}_0^{[0]}(L) = \xi^{(0)}$, (E.41), we obtain

$$\mathcal{L}^{(0)} = P\bar{V}_0P + P(V_2^{(0)} - \xi^{(0)})P, \quad \bar{V}_0 := V_0 + V_1^{(0)}. \quad (\text{E.51})$$

Note that we changed the definition of \bar{V}_0 . In the remainder of this appendix we use this new definition.

First Order To first order we find with (E.43) and (C.73) that

$$\mathcal{L}^{(1)} = -h_1 + P + PV_1^{(1)}P + P(V_2^{(1)} - \xi^{(1)})P. \quad (\text{E.52})$$

Second Order According to (E.45) and (C.73), $\mathcal{L}^{(2)}$ can be cast into the form

$$\mathcal{L}^{(2)} = h_2 - \frac{1}{2}(h_1h_0 + h_0h_1) + PV_1^{(2)}P + P(V_2^{(2)} - \xi^{(2)})P. \quad (\text{E.53})$$

Third Order Finally, to obtain the expression to third order, we make use of $R_{L-1}^{(3)}$, given in (C.73), and $\tilde{E}_0^{[3]}(L)$, (E.48). Thus, $\mathcal{L}^{(3)}$ reads

$$\mathcal{L}^{(3)} = -h_3 + (h_2h_0 + h_0h_2) - \frac{1}{2}(h_1h_0^2 + h_0^2h_1) + h_1^2 + \frac{3}{2}P + PV_1^{(3)}P + P(V_2^{(3)} - \xi^{(3)})P. \quad (\text{E.54})$$

We used the first-order result, see Sect. E.6.2, that $V_1^{(1)} \equiv 0$ and $\varepsilon_0^{(1)} = 0$.

E.5. Action of Operators

In this section we analyze the effect of the various operators which constitute \mathcal{L} on the states defined in Sect. E.1. We discuss separately the action of the ‘restricted on-site energy operator’ $P(V_2^{(l)} - \xi^{(l)})P$, the ‘restricted intra-chain hopping’ $PV_1^{(l)}P$, and of the ‘restricted Hamiltonians’ h_0 , h_1 , h_2 and h_3 , as introduced in (C.68a) to (C.68d) of appendix C. We call them restricted because they act within the ground-state eigenspace of H_0 and only allow for virtual excitations, if any.

E.5.1. On-site Energy Operator

The effect of $P(V_2^{(l)} - \xi^{(l)})P$, $l \in \mathbb{N}$ on eigenstates of the local number operators is trivial because $V_2^{(l)}$ is given in terms of these operators, see (9.51). Since the numbers $\xi^{(l)}$ are simply equal to the sum of all on-site energies $\varepsilon_n^{(l)}$ of the lower chain, see (E.42), we can immediately state the action of the l th-order energy operator as

$$P(V_2^{(l)} - \xi^{(l)})P|\phi_{-1}\rangle = 0, \quad (\text{E.55a})$$

$$P(V_2^{(l)} - \xi^{(l)})P|\omega_n\rangle = -\varepsilon_n^{(l)}|\omega_n\rangle. \quad (\text{E.55b})$$

Here, $|\omega_n\rangle$ is a wild-card for the states (E.1b) to (E.2b) with site index n .

E.5.2. Intra-Chain Hopping

Hopping within the lower chain is described by the restricted hopping Hamiltonians $PV_1^{(l)}P$, $l \in \mathbb{N}$. They move a hole in the lower chain. Thus, a state without a hole in the lower chain is annihilated by them. The only difficulty in deriving their action are the site-dependent electron transfer amplitudes

$t_n^{(l)}$. Since the $V_1^{(l)}$ do not couple the impurity to the chain, we expect different behavior for states with small and large site indices n , respectively. Since the calculations are trivial after all, let us summarize:

$$PV_1^{(l)}P|\phi_{-1}\rangle = 0, \quad (\text{E.56a})$$

$$PV_1^{(l)}P|\omega_n\rangle = \begin{cases} -t_0^{(l)}|\omega_1\rangle & n = 0, \\ -t_{n-1}^{(l)}|\omega_{n-1}\rangle - t_n^{(l)}|\omega_{n+1}\rangle & n \geq 1, \end{cases} \quad (\text{E.56b})$$

$$PV_1^{(l)}P|\tilde{\omega}_n\rangle = \begin{cases} t_0^{(l)}|\tilde{\omega}_1\rangle & n = 0, \\ t_{n-1}^{(l)}|\tilde{\omega}_{n-1}\rangle + t_n^{(l)}|\tilde{\omega}_{n+1}\rangle & n \geq 1, \end{cases} \quad (\text{E.56c})$$

where we have made use of the wild card $|\omega_n\rangle$ for the states (E.1b) to (E.1d) with site index n and the wild card $|\tilde{\omega}_n\rangle$ for the states (E.2a) and (E.2b) with site index n .

E.5.3. Restricted Hamiltonians

The restricted Hamiltonians are defined by (C.68a) to (C.68d) of appendix C. We analyze them separately.

Restricted Hamiltonian h_0

The restricted Hamiltonian h_0 is, according to (C.68a), given by

$$h_0 = P\bar{V}_0P \quad (\text{E.57})$$

with

$$\bar{V}_0 = V_0 + V_1^{(0)} + V_2^{(0)}. \quad (\text{E.57a})$$

According to (E.51), we separated the contribution to $\mathcal{L}^{(0)}$ which is due to $V_2^{(0)}$ and which we have already discussed in Sect. E.5.1. Therefore, we can use the definition of \bar{V}_0 given in (E.51). Since we discussed the effect of the $V_1^{(0)}$ -part in Sect. E.5.2 as well, we can limit ourselves to the discussion of PV_0P .

The operator V_0 couples the first site in the lower chain, the impurity and the first site in the upper chain, see (9.45). Thus, it follows that

$$PV_0P|\phi_{-1}\rangle = \frac{1}{\sqrt{2}}|\gamma_0\rangle, \quad (\text{E.58a})$$

$$PV_0P|\phi_{0u}\rangle = \frac{1}{\sqrt{2}}|\phi_{-1}\rangle, \quad (\text{E.58b})$$

$$PV_0P|\phi_{0d}\rangle = -\frac{1}{\sqrt{2}}|\phi_{-1}\rangle, \quad (\text{E.58c})$$

$$PV_0P|\gamma_0\rangle = |\phi_{-1}\rangle, \quad (\text{E.58d})$$

$$PV_0P|m_{0u}\rangle = \frac{1}{2}|\phi_{-1}\rangle, \quad (\text{E.58e})$$

$$PV_0P|m_{0d}\rangle = -\frac{1}{2}|\phi_{-1}\rangle, \quad (\text{E.58f})$$

with all other states from Sect. E.1 being annihilated by PV_0P . With the result of Sect. E.5.2 for $n = 0$ we can therefore summarize the action of h_0 .

E. Explicit Calculations

Summary for $h_0 = P\bar{V}_0P$ with $\bar{V}_0 = V_0 + V_1^{(0)}$

$$h_0|\phi_{-1}\rangle = |\gamma_0\rangle, \quad (\text{E.59a})$$

$$h_0|\phi_{nu}\rangle = \begin{cases} \frac{1}{\sqrt{2}}|\phi_{-1}\rangle - t_0^{(0)}|\phi_{1u}\rangle & n = 0, \\ -t_{n-1}^{(0)}|\phi_{n-1u}\rangle - t_n^{(0)}|\phi_{n+1u}\rangle & n \geq 1, \end{cases} \quad (\text{E.59b})$$

$$h_0|\phi_{nd}\rangle = \begin{cases} -\frac{1}{\sqrt{2}}|\phi_{-1}\rangle - t_0^{(0)}|\phi_{1d}\rangle & n = 0, \\ -t_{n-1}^{(0)}|\phi_{n-1d}\rangle - t_n^{(0)}|\phi_{n+1d}\rangle & n \geq 1, \end{cases} \quad (\text{E.59c})$$

$$h_0|\chi_n\rangle = \begin{cases} -t_0^{(0)}|\chi_1\rangle & n = 0, \\ -t_{n-1}^{(0)}|\chi_{n-1}\rangle - t_n^{(0)}|\chi_{n+1}\rangle & n \geq 1, \end{cases} \quad (\text{E.59d})$$

$$h_0|\gamma_n\rangle = \begin{cases} |\phi_{-1}\rangle + t_0^{(0)}|\gamma_1\rangle & n = 0, \\ t_{n-1}^{(0)}|\gamma_{n-1}\rangle + t_n^{(0)}|\gamma_{n+1}\rangle & n \geq 1, \end{cases} \quad (\text{E.59e})$$

$$h_0|m_{nu}\rangle = \begin{cases} \frac{1}{2}|\phi_{-1}\rangle + t_0^{(0)}|m_{1u}\rangle & n = 0, \\ t_{n-1}^{(0)}|m_{n-1u}\rangle + t_n^{(0)}|m_{n+1u}\rangle & n \geq 1, \end{cases} \quad (\text{E.59f})$$

$$h_0|m_{nd}\rangle = \begin{cases} -\frac{1}{2}|\phi_{-1}\rangle + t_0^{(0)}|m_{1d}\rangle & n = 0, \\ t_{n-1}^{(0)}|m_{n-1d}\rangle + t_n^{(0)}|m_{n+1d}\rangle & n \geq 1. \end{cases} \quad (\text{E.59g})$$

Restricted Hamiltonian h_1

According to (C.68b), the restricted Hamiltonian h_1 reads

$$h_1 = PV_0SV_0P. \quad (\text{E.60})$$

We calculate its effect on the states of Sect. E.1 and summarize it in the end.

$|\phi_{-1}\rangle$

$$h_1|\phi_{-1}\rangle = PV_0SV_0P|\phi_{-1}\rangle = 0$$

$|\phi_{0u}\rangle$

$$\begin{aligned} h_1|\phi_{0u}\rangle &= PV_0SV_0P \frac{1}{\sqrt{2}} |\dots \uparrow \uparrow \uparrow \downarrow \dots \rangle \\ &= PV_0 \frac{1}{2} (|\dots \uparrow \uparrow \uparrow \downarrow \dots \rangle + |\dots \uparrow \uparrow \downarrow \uparrow \dots \rangle) \\ &= |\phi_{0u}\rangle - \frac{1}{2} |\phi_{0d}\rangle \end{aligned}$$

$|\phi_{nu}\rangle, n \geq 1$

$$\begin{aligned} h_1|\phi_{nu}\rangle &= PV_0SV_0P \frac{1}{\sqrt{2}} |\dots \uparrow \uparrow \dots \uparrow \uparrow \downarrow \dots \rangle \\ &= PV_0 \frac{1}{2} (|\dots \uparrow \uparrow \dots \uparrow \uparrow \downarrow \dots \rangle - |\dots \uparrow \uparrow \dots \uparrow \downarrow \uparrow \dots \rangle) \\ &= |\phi_{nu}\rangle \end{aligned}$$

Instead of calculating $h_1|\phi_{nd}\rangle$ in the same tedious way, we use the fact that the Hamiltonian H_S and, thus, h_n commute with the spin-flip operator J_S , see (9.18) and our discussion in Sect. E.2.1. Additionally, we use that $J_S|\phi_{nu}\rangle = -|\phi_{nd}\rangle$ and can proceed as follows,

$$h_3|\phi_{nd}\rangle = -h_3J_S|\phi_{nu}\rangle = -J_S h_3|\phi_{nu}\rangle. \quad (\text{E.61})$$

We state the results in the summary below.

$|\chi_0\rangle$

$$\begin{aligned} h_1|\chi_0\rangle &= PV_0SV_0P\frac{1}{\sqrt{2}}|\dots\uparrow\uparrow\downarrow\downarrow\dots\rangle \\ &= PV_0\frac{1}{2}|\dots\uparrow\uparrow\downarrow-\downarrow\dots\rangle \\ &= \frac{1}{2}|\chi_0\rangle \end{aligned}$$

$|\chi_n\rangle, n \geq 1$

$$\begin{aligned} h_1|\chi_n\rangle &= PV_0SV_0P\frac{1}{\sqrt{2}}|\dots\uparrow\downarrow\uparrow\dots\uparrow\uparrow\downarrow\dots\rangle \\ &= PV_0\frac{1}{2}\left(|\dots\uparrow\downarrow\uparrow\dots\uparrow\uparrow-\downarrow\dots\rangle - |\dots\uparrow\downarrow\uparrow\dots\uparrow\downarrow\uparrow\dots\rangle\right) \\ &= |\chi_n\rangle \end{aligned}$$

With the effect of h_1 on the states (E.1b) to (E.1d) and with the definitions of the composite states (E.2a) and (E.2b) we can calculate $|\gamma_n\rangle$ and $|m_{nx}\rangle$ with ease. We state the result in the following summary.

Summary for h_1

$$h_1|\phi_{-1}\rangle = 0, \quad (\text{E.62a})$$

$$h_1|\phi_{nu}\rangle = \begin{cases} |\phi_{0u}\rangle - \frac{1}{2}|\phi_{0d}\rangle & n = 0, \\ |\phi_{nu}\rangle & n \geq 1, \end{cases} \quad (\text{E.62b})$$

$$h_1|\phi_{nd}\rangle = \begin{cases} |\phi_{0d}\rangle - \frac{1}{2}|\phi_{0u}\rangle & n = 0, \\ |\phi_{nd}\rangle & n \geq 1, \end{cases} \quad (\text{E.62c})$$

$$h_1|\chi_n\rangle = \begin{cases} \frac{1}{2}|\chi_0\rangle & n = 0, \\ |\chi_n\rangle & n \geq 1, \end{cases} \quad (\text{E.62d})$$

$$h_1|\gamma_n\rangle = \begin{cases} \frac{3}{2}|\gamma_0\rangle & n = 0, \\ |\gamma_n\rangle & n \geq 1, \end{cases} \quad (\text{E.62e})$$

$$h_1|m_{nu}\rangle = \begin{cases} \frac{1}{2}(|\gamma_0\rangle + |m_{0u}\rangle) & n = 0, \\ |m_{nu}\rangle & n \geq 1, \end{cases} \quad (\text{E.62f})$$

$$h_1|m_{nd}\rangle = \begin{cases} \frac{1}{2}(-|\gamma_0\rangle + |m_{0d}\rangle) & n = 0, \\ |m_{nd}\rangle & n \geq 1. \end{cases} \quad (\text{E.62g})$$

E. Explicit Calculations

Restricted Hamiltonian h_2

In second order in $1/U$ we have to deal with

$$h_2 = PV_0S\bar{V}_0SV_0P. \quad (\text{E.63})$$

For the calculations involving h_2 and h_3 we introduce some additional abbreviations for frequently appearing excited states. First, we define for $n \geq 0$

$$|\phi_{nu}^*\rangle := \frac{1}{\sqrt{2}} \left| \dots \underbrace{\uparrow \uparrow \uparrow}_{\text{index } n} \dots \underbrace{\uparrow \uparrow}_{\text{index } 0} - \downarrow - \dots \right\rangle, \quad (\text{E.64a})$$

$$|\bar{\phi}_{nu}\rangle := \frac{1}{\sqrt{2}} \left| \dots \underbrace{\uparrow \uparrow \uparrow}_{\text{index } n} \dots \underbrace{\uparrow \downarrow \uparrow}_{\text{index } 0} - \dots \right\rangle, \quad (\text{E.64b})$$

$$|\phi_{nd}^*\rangle := \frac{1}{\sqrt{2}} \left| \dots \underbrace{\uparrow \downarrow \uparrow}_{\text{index } n} \dots \underbrace{\uparrow \uparrow}_{\text{index } 0} - \uparrow - \dots \right\rangle, \quad (\text{E.64c})$$

$$|\bar{\phi}_{nd}\rangle := \frac{1}{\sqrt{2}} \left| \dots \underbrace{\uparrow \downarrow \uparrow}_{\text{index } n} \dots \underbrace{\uparrow \uparrow \uparrow}_{\text{index } 0} - \dots \right\rangle, \quad (\text{E.64d})$$

$$|\chi_n^*\rangle := \frac{1}{\sqrt{2}} \left| \dots \underbrace{\uparrow \downarrow \uparrow}_{\text{index } n} \dots \underbrace{\uparrow \uparrow}_{\text{index } 0} - \downarrow - \dots \right\rangle. \quad (\text{E.64e})$$

Second, we introduce for $n \geq 1$

$$|\bar{\chi}_n\rangle := \frac{1}{\sqrt{2}} \left| \dots \underbrace{\uparrow \downarrow \uparrow}_{\text{index } n} \dots \underbrace{\uparrow \downarrow \uparrow}_{\text{index } 0} - \dots \right\rangle. \quad (\text{E.64f})$$

We proceed as in the case of h_1 : We start with the calculations of the effect of h_2 on the states (E.1b) to (E.1d). Then, we are able to derive, according to the definitions (E.2a) and (E.2b), the composite states. Finally, we summarize.

$|\phi_{-1}\rangle$

$$h_2|\phi_{-1}\rangle = PV_0S\bar{V}_0SV_0P|\phi_{-1}\rangle = 0$$

$|\phi_{0u}\rangle$

$$\begin{aligned} h_2|\phi_{0u}\rangle &= \frac{1}{\sqrt{2}} PV_0S\bar{V}_0SV_0P \left| \dots \uparrow \uparrow \uparrow \uparrow \downarrow - \dots \right\rangle \\ &= \frac{1}{2} PV_0S\bar{V}_0 \left(\left| \dots \uparrow \uparrow \uparrow \uparrow - \downarrow - \dots \right\rangle + \left| \dots \uparrow \uparrow - \uparrow - \dots \right\rangle \right) \\ &= \frac{1}{2} PV_0 \left(- \left| \dots \uparrow \uparrow \uparrow \uparrow - \downarrow - \dots \right\rangle + \left| \dots \uparrow \uparrow \downarrow \uparrow - \dots \right\rangle \right. \\ &\quad \left. - \left| \dots \uparrow \downarrow \uparrow \uparrow - \dots \right\rangle + \text{terms not contributing (t.n.c.)} \right) \\ &= -|\phi_{1u}\rangle + \frac{1}{2}|\phi_{1d}\rangle \end{aligned}$$

With t.n.c. we abbreviate all those states which cannot relax to a ground state by application of a single V_0 .

$|\phi_{1u}\rangle$

$$\begin{aligned}
 h_2|\phi_{1u}\rangle &= \frac{1}{\sqrt{2}}PV_0S\bar{V}_0SV_0P|\dots\uparrow\uparrow\uparrow\downarrow\text{---}\rangle \\
 &= \frac{1}{2}PV_0S\bar{V}_0(|\dots\uparrow\uparrow\uparrow\downarrow\text{---}\rangle - |\dots\uparrow\uparrow\downarrow\uparrow\text{---}\rangle) \\
 &= \frac{1}{2}PV_0(-|\dots\uparrow\uparrow\uparrow\downarrow\text{---}\rangle - |\dots\uparrow\uparrow\uparrow\downarrow\text{---}\rangle \\
 &\quad + |\dots\uparrow\uparrow\downarrow\uparrow\text{---}\rangle - |\dots\uparrow\uparrow\downarrow\uparrow\text{---}\rangle + \text{t.n.c.}) \\
 &= \frac{1}{2}(-|\phi_{2u}\rangle - |\phi_{0u}\rangle - |\phi_{2u}\rangle - |\phi_{0u}\rangle + |\phi_{0d}\rangle) \\
 &= -|\phi_{0u}\rangle - |\phi_{2u}\rangle + \frac{1}{2}|\phi_{0d}\rangle
 \end{aligned}$$

$|\phi_{nu}\rangle, n \geq 2$

$$\begin{aligned}
 h_2|\phi_{nu}\rangle &= \frac{1}{\sqrt{2}}PV_0S\bar{V}_0SV_0P|\dots\uparrow\uparrow\uparrow\dots\uparrow\uparrow\downarrow\text{---}\rangle \\
 &= \frac{1}{\sqrt{2}}PV_0S\bar{V}_0(|\phi_{nu}^*\rangle - |\bar{\phi}_{nu}\rangle) \\
 &= \frac{1}{\sqrt{2}}PV_0(-|\phi_{n+1u}^*\rangle - |\phi_{n-1u}^*\rangle - [|\bar{\phi}_{n+1u}\rangle - |\bar{\phi}_{n-1u}\rangle] + \text{t.n.c.}) \\
 &= \frac{1}{2}(-|\phi_{n+1u}\rangle - |\phi_{n-1u}\rangle - |\phi_{n+1u}\rangle - |\phi_{n-1u}\rangle) \\
 &= -|\phi_{n-1u}\rangle - |\phi_{n+1u}\rangle
 \end{aligned}$$

Note again that we obtain the effect of h_2 on the states $|\phi_{nd}\rangle$ with the help of (E.61) and give the result in the summary.

$|\chi_0\rangle$

$$\begin{aligned}
 h_2|\chi_0\rangle &= PV_0S\bar{V}_0SV_0P|\chi_0\rangle \\
 &= \frac{1}{\sqrt{2}}PV_0S\bar{V}_0|\chi_0^*\rangle = \frac{1}{\sqrt{2}}PV_0(-|\chi_1^*\rangle + \text{t.n.c.}) \\
 &= -\frac{1}{2}|\chi_1\rangle
 \end{aligned}$$

E. Explicit Calculations

$|\chi_1\rangle$

$$\begin{aligned}
h_2|\chi_1\rangle &= PV_0S\bar{V}_0SV_0P|\chi_1\rangle \\
&= \frac{1}{\sqrt{2}}PV_0S\bar{V}_0(|\chi_1^*\rangle - |\bar{\chi}_1\rangle) = \frac{1}{\sqrt{2}}PV_0(-|\chi_2^*\rangle - |\chi_0^*\rangle + |\bar{\chi}_2\rangle + \text{t.n.c.}) \\
&= -\frac{1}{2}|\chi_0\rangle - |\chi_2\rangle
\end{aligned}$$

$|\chi_n\rangle, n \geq 2$

$$\begin{aligned}
h_2|\chi_n\rangle &= PV_0S\bar{V}_0SV_0P|\chi_n\rangle \\
&= \frac{1}{\sqrt{2}}PV_0S\bar{V}_0(|\chi_n^*\rangle - |\bar{\chi}_n\rangle) \\
&= \frac{1}{\sqrt{2}}PV_0(-|\chi_{n+1}^*\rangle - |\chi_{n-1}^*\rangle - \{ -|\bar{\chi}_{n+1}\rangle - |\bar{\chi}_{n-1}\rangle \} + \text{t.n.c.}) \\
&= \frac{1}{2}(-|\chi_{n+1}\rangle - |\chi_{n-1}\rangle - |\chi_{n+1}\rangle - |\chi_{n-1}\rangle) = -|\chi_{n-1}\rangle - |\chi_{n+1}\rangle
\end{aligned}$$

With the defining equations (E.2a) and (E.2b) and the known effect of the operator on the states $|\phi_{nu}\rangle$, $|\phi_{nd}\rangle$ and $|\chi_n\rangle$, we can calculate the effect of h_2 on the states $|\gamma_n\rangle$ and $|m_{nx}\rangle$. Since the calculations are simple, we state the results in the following summary.

Summary for h_2

$h_2 \phi_{-1}\rangle = 0,$	(E.65a)
$h_2 \phi_{nu}\rangle = \begin{cases} - \phi_{1u}\rangle + \frac{1}{2} \phi_{1d}\rangle & n = 0, \\ - \phi_{0u}\rangle - \phi_{2u}\rangle + \frac{1}{2} \phi_{0d}\rangle & n = 1, \\ - \phi_{n-1u}\rangle - \phi_{n+1u}\rangle & n \geq 2, \end{cases}$	(E.65b)
$h_2 \phi_{nd}\rangle = \begin{cases} - \phi_{1d}\rangle + \frac{1}{2} \phi_{1u}\rangle & n = 0, \\ - \phi_{0d}\rangle - \phi_{2d}\rangle + \frac{1}{2} \phi_{0u}\rangle & n = 1, \\ - \phi_{n-1d}\rangle - \phi_{n+1d}\rangle & n \geq 2, \end{cases}$	(E.65c)
$h_2 \chi_n\rangle = \begin{cases} -\frac{1}{2} \chi_1\rangle & n = 0, \\ -\frac{1}{2} \chi_0\rangle - \chi_2\rangle & n = 1, \\ - \chi_{n-1}\rangle - \chi_{n+1}\rangle & n \geq 2, \end{cases}$	(E.65d)
$h_2 \gamma_n\rangle = \begin{cases} \frac{3}{2} \gamma_1\rangle & n = 0, \\ \frac{3}{2} \gamma_0\rangle + \gamma_2\rangle & n = 1, \\ \gamma_{n-1}\rangle + \gamma_{n+1}\rangle & n \geq 2, \end{cases}$	(E.65e)
$h_2 m_{nu}\rangle = \begin{cases} \frac{1}{2} m_{1u}\rangle + \frac{1}{2} \gamma_1\rangle & n = 0, \\ \frac{1}{2} m_{0u}\rangle + m_{2u}\rangle + \frac{1}{2} \gamma_0\rangle & n = 1, \\ m_{n-1u}\rangle + m_{n+1u}\rangle & n \geq 2, \end{cases}$	(E.65f)
$h_2 m_{nd}\rangle = \begin{cases} \frac{1}{2} m_{1d}\rangle - \frac{1}{2} \gamma_1\rangle & n = 0, \\ \frac{1}{2} m_{0d}\rangle + m_{2d}\rangle - \frac{1}{2} \gamma_0\rangle & n = 1, \\ m_{n-1d}\rangle + m_{n+1d}\rangle & n \geq 2. \end{cases}$	(E.65g)

Restricted Hamiltonian h_3

In third order we need to consider the restricted Hamiltonian (C.68d),

$$h_3 = PV_0S\bar{V}_0S\bar{V}_0SV_0P. \quad (\text{E.66})$$

In the following, we apply h_3 to the states $|\phi_{-1}\rangle$, (E.1a), $|\phi_{nu}\rangle$, (E.1b), and $|\chi_n\rangle$, (E.1d). We do not calculate the effect of h_3 on the states $|\phi_{nd}\rangle$ explicitly because we can use (E.61) to obtain it. Then, the composite states, (E.2a) and (E.2b), can be obtained. In the end we summarize the results.

$|\phi_{-1}\rangle$

$$h_3|\phi_{-1}\rangle = PV_0S\bar{V}_0S\bar{V}_0SV_0P|\phi_{-1}\rangle = 0$$

$|\phi_{0u}\rangle$

$$\begin{aligned} h_3|\phi_{0u}\rangle &= \frac{1}{\sqrt{2}}PV_0S\bar{V}_0S\bar{V}_0SV_0P|\dots\uparrow\uparrow\uparrow\downarrow\text{---}\rangle \\ &= \frac{1}{2}PV_0S\bar{V}_0S\bar{V}_0\left\{|\dots\uparrow\uparrow\uparrow\downarrow\text{---}\rangle + |\dots\uparrow\uparrow\downarrow\uparrow\text{---}\rangle\right\} \\ &= \frac{1}{2}PV_0S\bar{V}_0\left\{-|\dots\uparrow\uparrow\uparrow\downarrow\text{---}\rangle + \frac{1}{\sqrt{2}}|\dots\uparrow\uparrow\downarrow\uparrow\text{---}\rangle\right. \\ &\quad + |\dots\uparrow\uparrow\uparrow\text{---}\downarrow\text{---}\rangle + |\dots\uparrow\uparrow\downarrow\uparrow\text{---}\rangle - |\dots\uparrow\downarrow\uparrow\uparrow\text{---}\rangle \\ &\quad \left. + \frac{1}{\sqrt{2}}|\dots\uparrow\uparrow\downarrow\uparrow\text{---}\rangle - \frac{1}{\sqrt{2}}|\dots\uparrow\uparrow\downarrow\uparrow\text{---}\rangle\right\} \\ &= \frac{1}{\sqrt{2}}PV_0\left\{|\phi_{2u}^*\rangle + |\phi_{0u}^*\rangle + \frac{1}{2}|\phi_{0u}^*\rangle + \frac{1}{2}|\bar{\phi}_{0u}\rangle + |\phi_{0u}^*\rangle - |\bar{\phi}_{2u}\rangle + |\bar{\phi}_{0u}\rangle + |\bar{\phi}_{2d}\rangle + |\bar{\phi}_{0u}\rangle\right. \\ &\quad \left. + \frac{1}{2}|\phi_{0u}^*\rangle + \frac{1}{2}|\bar{\phi}_{0u}\rangle - \frac{1}{2}|\phi_{0d}^*\rangle + \frac{1}{2}|\bar{\phi}_{0u}\rangle + \text{t.n.c.}\right\} \\ &= \frac{13}{4}|\phi_{0u}\rangle + |\phi_{2u}\rangle - 2|\phi_{0d}\rangle - \frac{1}{2}|\phi_{2d}\rangle \end{aligned}$$

In the last step we used $V_0|\bar{\phi}_{0u}\rangle = 1/\sqrt{2}(|\phi_{1u}\rangle - |\phi_{1d}\rangle)$.

$|\phi_{1u}\rangle$

$$\begin{aligned} h_3|\phi_{1u}\rangle &= \frac{1}{\sqrt{2}}PV_0S\bar{V}_0S\bar{V}_0SV_0P|\dots\uparrow\uparrow\uparrow\downarrow\text{---}\rangle \\ &= \frac{1}{2}PV_0S\bar{V}_0S\bar{V}_0\left\{|\dots\uparrow\uparrow\uparrow\downarrow\text{---}\rangle - |\dots\uparrow\uparrow\downarrow\uparrow\text{---}\rangle\right\} \\ &= \frac{1}{2}PV_0S\bar{V}_0\left\{-|\dots\uparrow\uparrow\uparrow\downarrow\text{---}\rangle - |\dots\uparrow\uparrow\uparrow\text{---}\downarrow\text{---}\rangle\right. \\ &\quad \left. + \frac{1}{\sqrt{2}}|\dots\uparrow\uparrow\uparrow\downarrow\text{---}\rangle - \frac{1}{\sqrt{2}}|\dots\uparrow\uparrow\downarrow\uparrow\text{---}\rangle + |\dots\uparrow\uparrow\uparrow\text{---}\downarrow\text{---}\rangle\right\} \end{aligned}$$

E. Explicit Calculations

$$\begin{aligned}
& + |\dots \uparrow \uparrow \downarrow \uparrow \uparrow \dots \rangle - |\dots \uparrow \uparrow \uparrow \uparrow \dots \rangle - |\dots \uparrow \uparrow \uparrow \uparrow \dots \rangle \\
& - \frac{1}{\sqrt{2}} |\dots \uparrow \uparrow \downarrow \uparrow \downarrow \dots \rangle + \frac{1}{\sqrt{2}} |\dots \uparrow \uparrow \downarrow \downarrow \uparrow \dots \rangle \} \\
= & \frac{1}{\sqrt{2}} PV_0 \{ |\phi_{3u}^* \rangle + |\phi_{1u}^* \rangle + |\phi_{1u}^* \rangle + \frac{1}{2} |\phi_{1u}^* \rangle + \frac{1}{2} |\phi_{1u}^* \rangle - \frac{1}{2} |\bar{\phi}_{1u} \rangle + |\phi_{1u}^* \rangle - |\bar{\phi}_{3u} \rangle - |\bar{\phi}_{1u} \rangle \\
& - |\bar{\phi}_{1u} \rangle + |\bar{\phi}_{1d} \rangle - |\bar{\phi}_{1u} \rangle + |\bar{\phi}_{1d} \rangle + \frac{1}{2} |\phi_{1u}^* \rangle - \frac{1}{2} |\bar{\phi}_{1u} \rangle - \frac{1}{2} |\bar{\phi}_{1u} \rangle + \text{t.n.c.} \} \\
= & \frac{9}{2} |\phi_{1u} \rangle + |\phi_{3u} \rangle - |\phi_{1d} \rangle
\end{aligned}$$

$|\phi_{2u} \rangle$

$$\begin{aligned}
h_3 |\phi_{2u} \rangle & = \frac{1}{\sqrt{2}} PV_0 S \bar{V}_0 S \bar{V}_0 S V_0 P |\dots \uparrow \uparrow \uparrow \downarrow \dots \rangle \\
& = \frac{1}{2} PV_0 S \bar{V}_0 S \bar{V}_0 \{ |\dots \uparrow \uparrow \uparrow \downarrow \dots \rangle - |\dots \uparrow \uparrow \downarrow \uparrow \dots \rangle \} \\
& = \frac{1}{2} PV_0 S \bar{V}_0 \{ -|\phi_{3u}^* \rangle - |\dots \uparrow \uparrow \uparrow \downarrow \dots \rangle + \frac{1}{\sqrt{2}} |\dots \uparrow \uparrow \uparrow \downarrow \downarrow \dots \rangle \\
& \quad - \frac{1}{\sqrt{2}} |\dots \uparrow \uparrow \downarrow \uparrow \downarrow \dots \rangle + |\dots \uparrow \uparrow \uparrow \uparrow \dots \rangle + |\bar{\phi}_{3u} \rangle \\
& \quad + |\dots \uparrow \uparrow \downarrow \uparrow \dots \rangle + |\dots \uparrow \downarrow \uparrow \uparrow \dots \rangle - \frac{1}{\sqrt{2}} |\dots \uparrow \uparrow \downarrow \uparrow \downarrow \dots \rangle \\
& \quad + \frac{1}{\sqrt{2}} |\dots \uparrow \uparrow \downarrow \downarrow \uparrow \dots \rangle \} \\
& = \frac{1}{\sqrt{2}} PV_0 \{ |\phi_{4u}^* \rangle + |\phi_{2u}^* \rangle + |\phi_{2u}^* \rangle + |\phi_{0u}^* \rangle + \frac{1}{2} |\phi_{2u}^* \rangle + \frac{1}{2} |\phi_{2u}^* \rangle - \frac{1}{2} |\bar{\phi}_{2u} \rangle + |\phi_{2u}^* \rangle - |\bar{\phi}_{4u} \rangle \\
& \quad - |\bar{\phi}_{2u} \rangle - |\bar{\phi}_{2u} \rangle + |\bar{\phi}_{0u} \rangle - |\bar{\phi}_{2u} \rangle + \frac{1}{2} |\phi_{2u}^* \rangle - \frac{1}{2} |\bar{\phi}_{2u} \rangle - \frac{1}{2} |\bar{\phi}_{2u} \rangle + \text{t.n.c.} \} \\
& = |\phi_{0u} \rangle + \frac{9}{2} |\phi_{2u} \rangle + |\phi_{4u} \rangle - \frac{1}{2} |\phi_{0d} \rangle
\end{aligned}$$

$|\phi_{nu} \rangle, n \geq 3$

$$\begin{aligned}
h_3 |\phi_{nu} \rangle & = \frac{1}{\sqrt{2}} PV_0 S \bar{V}_0 S \bar{V}_0 S V_0 P |\dots \uparrow \uparrow \uparrow \dots \uparrow \uparrow \downarrow \dots \rangle \\
& = \frac{1}{2} PV_0 S \bar{V}_0 S \bar{V}_0 \{ |\dots \uparrow \uparrow \uparrow \dots \uparrow \uparrow \downarrow \dots \rangle - |\dots \uparrow \uparrow \uparrow \dots \uparrow \downarrow \uparrow \dots \rangle \} \\
& = \frac{1}{2} PV_0 S \bar{V}_0 \{ -|\phi_{n+1u}^* \rangle - |\phi_{n-1u}^* \rangle + \frac{1}{\sqrt{2}} |\dots \uparrow \uparrow \uparrow \dots \uparrow \uparrow \downarrow \downarrow \dots \rangle \\
& \quad - \frac{1}{\sqrt{2}} |\dots \uparrow \uparrow \uparrow \dots \uparrow \downarrow \uparrow \downarrow \dots \rangle + |\dots \uparrow \uparrow \uparrow \dots \uparrow \uparrow \uparrow \dots \rangle + |\bar{\phi}_{n+1u} \rangle
\end{aligned}$$

$$\begin{aligned}
 & + |\bar{\phi}_{n-1u}\rangle - \frac{1}{\sqrt{2}} |\dots \uparrow \uparrow \uparrow \dots \uparrow \downarrow \uparrow \downarrow \dots \rangle + \frac{1}{\sqrt{2}} |\dots \uparrow \uparrow \uparrow \dots \uparrow \downarrow \downarrow \uparrow \dots \rangle \\
 & + |\dots \uparrow \uparrow \uparrow \dots \uparrow \uparrow \uparrow \dots \rangle \} \\
 & = \frac{1}{\sqrt{2}} PV_0 \{ |\phi_{n+2u}^*\rangle + |\phi_{nu}^*\rangle + |\phi_{nu}^*\rangle + |\phi_{n-2u}^*\rangle + \frac{1}{2} |\phi_{nu}^*\rangle + \frac{1}{2} |\phi_{nu}^*\rangle - \frac{1}{2} |\bar{\phi}_{nu}\rangle + |\phi_{nu}^*\rangle \\
 & \quad - |\bar{\phi}_{n+2u}\rangle - |\bar{\phi}_{nu}\rangle - |\bar{\phi}_{nu}\rangle - |\bar{\phi}_{n-2u}\rangle + \frac{1}{2} |\phi_{nu}^*\rangle - \frac{1}{2} |\bar{\phi}_{nu}\rangle - \frac{1}{2} |\bar{\phi}_{nu}\rangle - |\bar{\phi}_{nu}\rangle + \text{t.n.c.} \} \\
 & = |\phi_{n-2u}\rangle + \frac{9}{2} |\phi_{nu}\rangle + |\phi_{n+2u}\rangle
 \end{aligned}$$

As we have already stated, we obtain the effect of h_3 on the states $|\phi_{nd}\rangle$ with the help of (E.61). We give the results in the summary.

$|\chi_0\rangle$

$$\begin{aligned}
 h_3|\chi_0\rangle & = \frac{1}{\sqrt{2}} PV_0 S \bar{V}_0 S \bar{V}_0 S V_0 P |\dots \uparrow \uparrow \downarrow \downarrow \dots \rangle \\
 & = \frac{1}{2} PV_0 S \bar{V}_0 S \bar{V}_0 |\dots \uparrow \uparrow \downarrow \downarrow \dots \rangle \\
 & = \frac{1}{2} PV_0 S \bar{V}_0 \{ - |\dots \uparrow \downarrow \uparrow \downarrow \dots \rangle + \frac{1}{\sqrt{2}} |\dots \uparrow \uparrow \downarrow \downarrow \dots \rangle \\
 & \quad + |\dots \uparrow \uparrow \downarrow \dots \downarrow \dots \rangle \} = \frac{1}{\sqrt{2}} PV_0 \{ |\chi_2^*\rangle + |\chi_0^*\rangle + \frac{1}{2} |\chi_0^*\rangle + |\chi_0^*\rangle + \text{t.n.c.} \} \\
 & = \frac{5}{4} |\chi_0\rangle + \frac{1}{2} |\chi_2\rangle
 \end{aligned}$$

$|\chi_1\rangle$

$$\begin{aligned}
 h_3|\chi_1\rangle & = \frac{1}{\sqrt{2}} PV_0 S \bar{V}_0 S \bar{V}_0 S V_0 P |\dots \uparrow \downarrow \uparrow \downarrow \dots \rangle \\
 & = \frac{1}{2} PV_0 S \bar{V}_0 S \bar{V}_0 \{ |\dots \uparrow \downarrow \uparrow \downarrow \dots \rangle - |\dots \uparrow \downarrow \downarrow \uparrow \dots \rangle \} \\
 & = \frac{1}{2} PV_0 S \bar{V}_0 \{ - |\dots \downarrow \uparrow \uparrow \downarrow \dots \rangle - |\dots \uparrow \uparrow \downarrow \downarrow \dots \rangle \\
 & \quad + \frac{1}{\sqrt{2}} |\dots \uparrow \downarrow \uparrow \downarrow \downarrow \dots \rangle - \frac{1}{\sqrt{2}} |\dots \uparrow \downarrow \downarrow \uparrow \downarrow \dots \rangle + |\dots \uparrow \downarrow \uparrow \dots \downarrow \dots \rangle \\
 & \quad + |\dots \downarrow \uparrow \uparrow \uparrow \dots \rangle - \frac{1}{\sqrt{2}} |\dots \uparrow \downarrow \downarrow \uparrow \downarrow \dots \rangle + \frac{1}{\sqrt{2}} |\dots \uparrow \downarrow \downarrow \downarrow \uparrow \dots \rangle \} \\
 & = \frac{1}{\sqrt{2}} PV_0 \{ |\chi_3^*\rangle + |\chi_1^*\rangle + |\chi_1^*\rangle + \frac{1}{2} |\chi_1^*\rangle + \frac{1}{2} |\chi_1^*\rangle - \frac{1}{2} |\bar{\chi}_1\rangle \}
 \end{aligned}$$

E. Explicit Calculations

$$\begin{aligned}
& + |\bar{\chi}_1\rangle - |\bar{\chi}_3\rangle - |\bar{\chi}_1\rangle + \frac{1}{2}|\chi_1^*\rangle - \frac{1}{2}|\bar{\chi}_1\rangle - \frac{1}{2}|\bar{\chi}_1\rangle + \text{t.n.c.}\} \\
& = \frac{7}{2}|\chi_1\rangle + |\chi_3\rangle
\end{aligned}$$

$|\chi_2\rangle$

$$\begin{aligned}
h_3|\chi_2\rangle &= \frac{1}{\sqrt{2}}PV_0S\bar{V}_0S\bar{V}_0SV_0P|\dots\downarrow\uparrow\uparrow\uparrow\downarrow\text{---}\rangle \\
&= \frac{1}{2}PV_0S\bar{V}_0S\bar{V}_0\{|\dots\downarrow\uparrow\uparrow\uparrow\text{---}\rangle - |\dots\downarrow\uparrow\uparrow\downarrow\text{---}\rangle\} \\
&= \frac{1}{2}PV_0S\bar{V}_0\left\{-|\chi_3^*\rangle - |\chi_1^*\rangle + \frac{1}{\sqrt{2}}|\dots\downarrow\uparrow\uparrow\downarrow\text{---}\rangle\right. \\
&\quad - \frac{1}{\sqrt{2}}|\dots\downarrow\uparrow\uparrow\downarrow\uparrow\text{---}\rangle + |\dots\uparrow\uparrow\uparrow\text{---}\downarrow\text{---}\rangle + |\bar{\chi}_3\rangle + |\bar{\chi}_1\rangle \\
&\quad + |\dots\downarrow\downarrow\uparrow\uparrow\text{---}\rangle - \frac{1}{\sqrt{2}}|\dots\downarrow\uparrow\uparrow\downarrow\uparrow\text{---}\rangle \\
&\quad \left. + \frac{1}{\sqrt{2}}|\dots\downarrow\uparrow\uparrow\downarrow\uparrow\text{---}\rangle\right\} \\
&= \frac{1}{\sqrt{2}}PV_0\{|\chi_4^*\rangle + |\chi_2^*\rangle + |\chi_2^*\rangle + |\chi_0^*\rangle + \frac{1}{2}|\chi_2^*\rangle + \frac{1}{2}|\chi_2^*\rangle - \frac{1}{2}|\bar{\chi}_2\rangle \\
&\quad + |\chi_2^*\rangle - |\bar{\chi}_4\rangle - |\bar{\chi}_2\rangle - |\bar{\chi}_2\rangle - |\bar{\chi}_2\rangle + \frac{1}{2}|\chi_2^*\rangle - \frac{1}{2}|\bar{\chi}_2\rangle - \frac{1}{2}|\bar{\chi}_2\rangle + \text{t.n.c.}\} \\
&= \frac{1}{2}|\chi_0\rangle + \frac{9}{2}|\chi_2\rangle + |\chi_4\rangle
\end{aligned}$$

$|\chi_n\rangle, n \geq 3$

$$\begin{aligned}
h_3|\chi_n\rangle &= \frac{1}{\sqrt{2}}PV_0S\bar{V}_0S\bar{V}_0SV_0P|\dots\uparrow\downarrow\uparrow\text{---}\uparrow\uparrow\downarrow\text{---}\rangle \\
&= \frac{1}{2}PV_0S\bar{V}_0S\bar{V}_0\{|\dots\uparrow\downarrow\uparrow\text{---}\uparrow\uparrow\text{---}\rangle - |\dots\uparrow\downarrow\uparrow\text{---}\uparrow\downarrow\text{---}\rangle\} \\
&= \frac{1}{2}PV_0S\bar{V}_0\left\{-|\chi_{n+1}^*\rangle - |\chi_{n-1}^*\rangle + \frac{1}{\sqrt{2}}|\dots\uparrow\downarrow\uparrow\text{---}\uparrow\downarrow\text{---}\rangle\right. \\
&\quad - \frac{1}{\sqrt{2}}|\dots\uparrow\downarrow\uparrow\text{---}\uparrow\downarrow\uparrow\text{---}\rangle + |\dots\uparrow\downarrow\uparrow\text{---}\uparrow\uparrow\text{---}\downarrow\text{---}\rangle + |\bar{\chi}_{n+1}\rangle \\
&\quad + |\bar{\chi}_{n-1}\rangle + |\dots\uparrow\downarrow\uparrow\text{---}\downarrow\uparrow\uparrow\text{---}\rangle - \frac{1}{\sqrt{2}}|\dots\uparrow\downarrow\uparrow\text{---}\uparrow\downarrow\uparrow\text{---}\rangle \\
&\quad \left. + \frac{1}{\sqrt{2}}|\dots\uparrow\downarrow\uparrow\text{---}\uparrow\downarrow\uparrow\text{---}\rangle\right\}
\end{aligned}$$

$$\begin{aligned}
 &= \frac{1}{\sqrt{2}} PV_0 \{ |\chi_{n+2}^* \rangle + |\chi_n^* \rangle + |\chi_n^* \rangle + |\chi_{n-2}^* \rangle + \frac{1}{2} |\chi_n^* \rangle + \frac{1}{2} |\chi_n^* \rangle - \frac{1}{2} |\bar{\chi}_n \rangle \\
 &\quad + |\chi_n^* \rangle - |\bar{\chi}_{n+2} \rangle - |\bar{\chi}_n \rangle - |\bar{\chi}_n \rangle - |\bar{\chi}_{n-2} \rangle - |\bar{\chi}_n \rangle + \frac{1}{2} |\chi_n^* \rangle - \frac{1}{2} |\bar{\chi}_n \rangle - \frac{1}{2} |\bar{\chi}_n \rangle + \text{t.n.c.} \} \\
 &= |\chi_{n-2} \rangle + \frac{9}{2} |\chi_n \rangle + |\chi_{n+2} \rangle
 \end{aligned}$$

Summary for h_3

$$h_3 |\phi_{-1} \rangle = 0, \quad (\text{E.67a})$$

$$h_3 |\phi_{nu} \rangle = \begin{cases} \frac{13}{4} |\phi_{0u} \rangle + |\phi_{2u} \rangle - 2 |\phi_{0d} \rangle - \frac{1}{2} |\phi_{2d} \rangle & n = 0, \\ \frac{9}{2} |\phi_{1u} \rangle + |\phi_{3u} \rangle - |\phi_{1d} \rangle & n = 1, \\ |\phi_{0u} \rangle + \frac{9}{2} |\phi_{2u} \rangle + |\phi_{4u} \rangle - \frac{1}{2} |\phi_{0d} \rangle & n = 2, \\ |\phi_{n-2u} \rangle + \frac{9}{2} |\phi_{nu} \rangle + |\phi_{n+2u} \rangle & n \geq 3, \end{cases} \quad (\text{E.67b})$$

$$h_3 |\phi_{nd} \rangle = \begin{cases} \frac{13}{4} |\phi_{0d} \rangle + |\phi_{2d} \rangle - 2 |\phi_{0u} \rangle - \frac{1}{2} |\phi_{2u} \rangle & n = 0, \\ \frac{9}{2} |\phi_{1d} \rangle + |\phi_{3d} \rangle - |\phi_{1u} \rangle & n = 1, \\ |\phi_{0d} \rangle + \frac{9}{2} |\phi_{2d} \rangle + |\phi_{4d} \rangle - \frac{1}{2} |\phi_{0u} \rangle & n = 2, \\ |\phi_{n-2d} \rangle + \frac{9}{2} |\phi_{nd} \rangle + |\phi_{n+2d} \rangle & n \geq 3, \end{cases} \quad (\text{E.67c})$$

$$h_3 |\chi_n \rangle = \begin{cases} \frac{5}{4} |\chi_0 \rangle + \frac{1}{2} |\chi_2 \rangle & n = 0, \\ \frac{7}{2} |\chi_1 \rangle + |\chi_3 \rangle & n = 1, \\ \frac{1}{2} |\chi_0 \rangle + \frac{9}{2} |\chi_2 \rangle + |\chi_4 \rangle & n = 2, \\ |\chi_{n-2} \rangle + \frac{9}{2} |\chi_n \rangle + |\chi_{n+2} \rangle & n \geq 3, \end{cases} \quad (\text{E.67d})$$

$$h_3 |\gamma_n \rangle = \begin{cases} \frac{21}{4} |\gamma_0 \rangle + \frac{3}{2} |\gamma_2 \rangle & n = 0, \\ \frac{11}{2} |\gamma_1 \rangle + |\gamma_3 \rangle & n = 1, \\ \frac{3}{2} |\gamma_0 \rangle + \frac{9}{2} |\gamma_2 \rangle + |\gamma_4 \rangle & n = 2, \\ |\gamma_{n-2} \rangle + \frac{9}{2} |\gamma_n \rangle + |\gamma_{n+2} \rangle & n \geq 3, \end{cases} \quad (\text{E.67e})$$

$$h_3 |m_{nu} \rangle = \begin{cases} \frac{5}{4} |m_{0u} \rangle + \frac{1}{2} |m_{2u} \rangle + 2 |\gamma_0 \rangle + \frac{1}{2} |\gamma_2 \rangle & n = 0, \\ \frac{7}{2} |m_{1u} \rangle + |m_{3u} \rangle + |\gamma_1 \rangle & n = 1, \\ \frac{1}{2} |m_{0u} \rangle + \frac{9}{2} |m_{2u} \rangle + |m_{4u} \rangle + \frac{1}{2} |\gamma_0 \rangle & n = 2, \\ |m_{n-2u} \rangle + \frac{9}{2} |m_{nu} \rangle + |m_{n+2u} \rangle & n \geq 3, \end{cases} \quad (\text{E.67f})$$

$$h_3 |m_{nd} \rangle = \begin{cases} \frac{5}{4} |m_{0d} \rangle + \frac{1}{2} |m_{2d} \rangle - 2 |\gamma_0 \rangle - \frac{1}{2} |\gamma_2 \rangle & n = 0, \\ \frac{7}{2} |m_{1d} \rangle + |m_{3d} \rangle - |\gamma_1 \rangle & n = 1, \\ \frac{1}{2} |m_{0d} \rangle + \frac{9}{2} |m_{2d} \rangle + |m_{4d} \rangle - \frac{1}{2} |\gamma_0 \rangle & n = 2, \\ |m_{n-2d} \rangle + \frac{9}{2} |m_{nd} \rangle + |m_{n+2d} \rangle & n \geq 3. \end{cases} \quad (\text{E.67g})$$

E.5.4. Operator for the Lanczos Procedure

With the action of the restricted Hamiltonians h_0 , h_1 , h_2 and h_3 and the expressions for the operators $\mathcal{L}^{(n)}$ given in Sect. E.4, we can derive the effect of $\mathcal{L}^{(n)}$ on the composite states (E.2a) and (E.2b). Since the calculations only involve the application of h_n and basic arithmetics, we just present the results.

E. Explicit Calculations

Action of $\mathcal{L}^{(0)}$

The action of the operator $\mathcal{L}^{(0)}$,

$$\mathcal{L}^{(0)} = P\bar{V}_0P + P(V_2^{(0)} - \xi^{(0)})P \text{ with } \bar{V}_0 = V_0 + V_1^{(0)}, \quad (\text{E.68})$$

can be summarized as follows:

$$\mathcal{L}^{(0)}|\phi_{-1}\rangle = |\gamma_0\rangle, \quad (\text{E.69a})$$

$$\mathcal{L}^{(0)}|\gamma_n\rangle = \begin{cases} |\phi_{-1}\rangle - \varepsilon_0^{(0)}|\gamma_0\rangle + t_0^{(0)}|\gamma_1\rangle & n = 0, \\ t_{n-1}^{(0)}|\gamma_{n-1}\rangle - \varepsilon_n^{(0)}|\gamma_n\rangle + t_n^{(0)}|\gamma_{n+1}\rangle & n \geq 1, \end{cases} \quad (\text{E.69b})$$

$$\mathcal{L}^{(0)}|m_{nu}\rangle = \begin{cases} \frac{1}{2}|\phi_{-1}\rangle - \varepsilon_0^{(0)}|m_{0u}\rangle + t_0^{(0)}|m_{1u}\rangle & n = 0, \\ t_{n-1}^{(0)}|m_{n-1u}\rangle - \varepsilon_n^{(0)}|m_{nu}\rangle + t_n^{(0)}|m_{n+1u}\rangle & n \geq 1, \end{cases} \quad (\text{E.69c})$$

$$\mathcal{L}^{(0)}|m_{nd}\rangle = \begin{cases} -\frac{1}{2}|\phi_{-1}\rangle - \varepsilon_0^{(0)}|m_{0d}\rangle + t_0^{(0)}|m_{1d}\rangle & n = 0, \\ t_{n-1}^{(0)}|m_{n-1d}\rangle - \varepsilon_n^{(0)}|m_{nd}\rangle + t_n^{(0)}|m_{n+1d}\rangle & n \geq 1. \end{cases} \quad (\text{E.69d})$$

Action of $\mathcal{L}^{(1)}$

We give a summary of the effect of the operator

$$\mathcal{L}^{(1)} = -h_1 + P + PV_1^{(1)}P + P(V_2^{(1)} - \xi^{(1)})P, \quad (\text{E.70})$$

on the states of Sect. E.1:

$$\mathcal{L}^{(1)}|\phi_{-1}\rangle = |\phi_{-1}\rangle, \quad (\text{E.71a})$$

$$\mathcal{L}^{(1)}|\gamma_n\rangle = \begin{cases} -(\frac{1}{2} + \varepsilon_0^{(1)})|\gamma_0\rangle + t_0^{(1)}|\gamma_1\rangle & n = 0, \\ t_{n-1}^{(1)}|\gamma_{n-1}\rangle - \varepsilon_n^{(1)}|\gamma_n\rangle + t_n^{(1)}|\gamma_{n+1}\rangle & n \geq 1, \end{cases} \quad (\text{E.71b})$$

$$\mathcal{L}^{(1)}|m_{nu}\rangle = \begin{cases} -\varepsilon_0^{(1)}|m_{0u}\rangle + t_0^{(1)}|m_{1u}\rangle + \frac{1}{2}|m_{0d}\rangle & n = 0, \\ t_{n-1}^{(1)}|m_{n-1u}\rangle - \varepsilon_n^{(1)}|m_{nu}\rangle + t_n^{(1)}|m_{n+1u}\rangle & n \geq 1, \end{cases} \quad (\text{E.71c})$$

$$\mathcal{L}^{(1)}|m_{nd}\rangle = \begin{cases} -\varepsilon_0^{(1)}|m_{0d}\rangle + t_0^{(1)}|m_{1d}\rangle + \frac{1}{2}|m_{0u}\rangle & n = 0, \\ t_{n-1}^{(1)}|m_{n-1d}\rangle - \varepsilon_n^{(1)}|m_{nd}\rangle + t_n^{(1)}|m_{n+1d}\rangle & n \geq 1. \end{cases} \quad (\text{E.71d})$$

Action of $\mathcal{L}^{(2)}$

According to (E.53), the operator $\mathcal{L}^{(2)}$ is given by

$$\mathcal{L}^{(2)} = h_2 - \frac{1}{2}(h_1h_0 + h_0h_1) + PV_1^{(2)}P + P(V_2^{(2)} - \xi^{(2)})P, \quad (\text{E.72})$$

and acts on the states $|\phi_{-1}\rangle$, $|\gamma_n\rangle$ and $|m_{nx}\rangle$ as follows:

$$L^{(2)}|\phi_{-1}\rangle = -\frac{3}{4}|\gamma_0\rangle, \quad (\text{E.73a})$$

$$L^{(2)}|\gamma_n\rangle = \begin{cases} -\frac{3}{4}|\phi_{-1}\rangle - \varepsilon_0^{(2)}|\gamma_0\rangle + (\frac{1}{4} + t_0^{(2)})|\gamma_1\rangle & n = 0, \\ (t_0^{(2)} + \frac{1}{4})|\gamma_0\rangle - \varepsilon_1^{(2)}|\gamma_1\rangle + t_1^{(2)}|\gamma_2\rangle & n = 1, \\ t_{n-1}^{(2)}|\gamma_{n-1}\rangle - \varepsilon_n^{(2)}|\gamma_n\rangle + t_n^{(2)}|\gamma_{n+1}\rangle & n \geq 2, \end{cases} \quad (\text{E.73b})$$

$$L^{(2)}|m_{nu}\rangle = \begin{cases} -\frac{3}{8}|\phi_{-1}\rangle - \varepsilon_0^{(2)}|m_{0u}\rangle + t_0^{(2)}|m_{1u}\rangle - \frac{1}{4}|m_{1d}\rangle & n = 0, \\ t_0^{(2)}|m_{0u}\rangle - \varepsilon_1^{(2)}|m_{1u}\rangle + t_1^{(2)}|m_{2u}\rangle - \frac{1}{4}|m_{0d}\rangle & n = 1, \\ t_{n-1}^{(2)}|m_{n-1u}\rangle - \varepsilon_n^{(2)}|m_{nu}\rangle + t_n^{(2)}|m_{n+1u}\rangle & n \geq 2, \end{cases} \quad (\text{E.73c})$$

$$L^{(2)}|m_{nd}\rangle = \begin{cases} \frac{3}{8}|\phi_{-1}\rangle - \varepsilon_0^{(2)}|m_{0d}\rangle + t_0^{(2)}|m_{1d}\rangle - \frac{1}{4}|m_{1u}\rangle & n = 0, \\ t_0^{(2)}|m_{0d}\rangle - \varepsilon_1^{(2)}|m_{1d}\rangle + t_1^{(2)}|m_{2d}\rangle - \frac{1}{4}|m_{0u}\rangle & n = 1, \\ t_{n-1}^{(2)}|m_{n-1d}\rangle - \varepsilon_n^{(2)}|m_{nd}\rangle + t_n^{(2)}|m_{n+1d}\rangle & n \geq 2. \end{cases} \quad (\text{E.73d})$$

Action of $\mathcal{L}^{(3)}$

Finally, we state the effect of $\mathcal{L}^{(3)}$,

$$\mathcal{L}^{(3)} = -h_3 + (h_2h_0 + h_0h_2) - \frac{1}{2}(h_1h_0^2 + h_0^2h_1) + h_1^2 + \frac{3}{2}P + PV_1^{(3)}P + P(V_2^{(3)} - \xi^{(3)})P, \quad (\text{E.74})$$

on the states $|\phi_{-1}\rangle$ and $|\gamma_n\rangle$. For calculations up to and including the third order in $1/U$, we do not need $\mathcal{L}^{(3)}|m_{nx}\rangle$ and, thus, we do not include the formulae in this summary.

$$L^{(3)}|\phi_{-1}\rangle = \frac{3}{2}|\phi_{-1}\rangle + |\gamma_1\rangle, \quad (\text{E.75a})$$

$$L^{(3)}|\gamma_n\rangle = \begin{cases} -(\varepsilon_0^{(3)} + \frac{3}{2})|\gamma_0\rangle + t_0^{(3)}|\gamma_1\rangle - \frac{1}{4}|\gamma_2\rangle & n = 0, \\ |\phi_{-1}\rangle + t_0^{(3)}|\gamma_0\rangle - \varepsilon_1^{(3)}|\gamma_1\rangle + t_1^{(3)}|\gamma_2\rangle & n = 1, \\ -\frac{1}{4}|\gamma_0\rangle + t_1^{(3)}|\gamma_1\rangle - \varepsilon_2^{(3)}|\gamma_2\rangle + t_2^{(3)}|\gamma_3\rangle & n = 2, \\ t_{n-1}^{(3)}|\gamma_{n-1}\rangle - \varepsilon_n^{(3)}|\gamma_n\rangle + t_n^{(3)}|\gamma_{n+1}\rangle & n \geq 3, \end{cases} \quad (\text{E.75b})$$

$$(\text{E.75c})$$

E.6. Lanczos Iteration

Here, we calculate the Lanczos basis, (9.70a) and (9.70b), for the operator \mathcal{L} ,

$$|\Psi_1\rangle = -\mathcal{L}|\Psi_0\rangle + \tilde{e}_0|\Psi_0\rangle, \quad (\text{E.76a})$$

$$|\Psi_n\rangle = -\mathcal{L}|\Psi_n\rangle + \tilde{e}_n|\Psi_n\rangle + \tilde{\tau}_{n-1}|\Psi_{n-1}\rangle \quad n \in \mathbb{N} \setminus \{0\}, \quad (\text{E.76b})$$

with the parameters given, see (9.70c) and (9.70d), by

$$\tilde{e}_n = \frac{\langle \Psi_n | \mathcal{L} | \Psi_n \rangle}{\langle \Psi_n | \Psi_n \rangle} \quad \text{for } n \geq 0, \quad (\text{E.77a})$$

$$\tilde{\tau}_{n-1} = -\frac{\langle \Psi_n | \Psi_n \rangle}{\langle \Psi_{n-1} | \Psi_{n-1} \rangle} \quad \text{for } n \geq 1. \quad (\text{E.77b})$$

According to the self-consistency condition (9.91),

$$\begin{pmatrix} \varepsilon_0 & t_0 & & & \\ t_0 & \varepsilon_1 & t_1 & & \\ & t_1 & \varepsilon_2 & t_2 & \\ & & & \ddots & \ddots & \ddots \end{pmatrix} = - \begin{pmatrix} e_0 & \tau_0 & & & \\ \tau_0 & e_1 & \tau_1 & & \\ & \tau_1 & e_2 & \tau_2 & \\ & & & \ddots & \ddots & \ddots \end{pmatrix}, \quad (\text{E.78})$$

we fix the parameters t_l and ε_l of the SIAM up to third order in $1/U$. The parameters e_l and τ_l are the matrix elements of \mathcal{L} in its Lanczos basis and, according to (9.71) and (9.72), are given by

$$e_n = \tilde{e}_n, \quad (\text{E.79})$$

$$\tau_n = -\sqrt{-\tilde{\tau}_n}. \quad (\text{E.80})$$

\mathcal{L} admits the expansion

$$\mathcal{L} = \sum_{n=0}^{\infty} \left(\frac{1}{U}\right)^n \mathcal{L}^{(n)}. \quad (\text{E.81})$$

E. Explicit Calculations

We derived the formulae for each $\mathcal{L}^{(n)}$ in Sect. E.4. According to (9.47) and (9.50), we assume that the electron transfer amplitudes and on-site energies of the SIAM in two-chain geometry, (9.30), admit the series expansions

$$t_l = \sum_{n=0}^{\infty} \left(\frac{1}{U}\right)^n t_l^{(n)}, \quad (\text{E.82})$$

$$\varepsilon_l = \sum_{n=0}^{\infty} \left(\frac{1}{U}\right)^n \varepsilon_l^{(n)}. \quad (\text{E.83})$$

Therefore, we proceed as follows. To obtain the electron transfer amplitudes $t_l^{(n)}$ and on-site energies $\varepsilon_l^{(n)}$ we calculate the complete Lanczos basis of \mathcal{L} up to n th order in $1/U$. For convenience we introduce for $l \geq 1$

$$|\tilde{\Psi}_l\rangle := -\mathcal{L}|\Psi_{l-1}\rangle = \sum_{n=0}^{\infty} \left(\frac{1}{U}\right)^n |\tilde{\Psi}_l^{(n)}\rangle. \quad (\text{E.84})$$

To calculate $|\tilde{\Psi}_l^{(n)}\rangle$ we need to expand \mathcal{L} as well as the state $|\Psi_{l-1}\rangle$,

$$|\tilde{\Psi}_l^{(n)}\rangle = -\sum_{j=0}^n \mathcal{L}^{(j)} |\Psi_{l-1}^{(n-j)}\rangle. \quad (\text{E.85})$$

With (E.84) we calculate the diagonal Lanczos parameters e_l as

$$e_{l-1} = -\frac{\langle\Psi_{l-1}|\tilde{\Psi}_l\rangle}{\langle\Psi_{l-1}|\Psi_{l-1}\rangle} =: \sum_{n=0}^{\infty} \left(\frac{1}{U}\right)^n e_{l-1}^{(n)}, \quad (\text{E.86})$$

which we have to expand systematically in $1/U$ to obtain the coefficients $e_{l-1}^{(n)}$ to n th order in $1/U$. Note that in the l th iteration, we already know all states $|\Psi_{m<l}\rangle$, in particular their norm. With e_{l-1} and the already known τ_{l-2} we can calculate the l th Lanczos vector $|\Psi_l\rangle$ according to (E.76b). Finally, with $|\Psi_l\rangle$ and (E.77b) we can calculate $\tilde{\tau}_{l-1}$. To obtain the matrix element τ_{l-1} , we use (E.80), where we expand the square root in its Taylor series about zero,

$$\sqrt{1+x} = \sum_{n=0}^{\infty} \frac{(-1)^n (2n)!}{(1-2n)(n!)^2 (4^n)} x^n = 1 + \frac{1}{2}x - \frac{1}{8}x^2 \dots, \quad (\text{E.87})$$

to get the expansion

$$\tau_n = \sum_{n=0}^{\infty} \left(\frac{1}{U}\right)^n \tau_l^{(n)}. \quad (\text{E.88})$$

Finally, we use the self-consistency equation (E.78) to fix the parameters $\varepsilon_l^{(n)}$ and $t_l^{(n)}$ of the SIAM as

$$t_l^{(n)} \equiv -\tau_l^{(n)}, \quad (\text{E.89a})$$

$$\varepsilon_l^{(n)} \equiv -e_l^{(n)}. \quad (\text{E.89b})$$

We use these parameters to obtain the Lanczos basis to first order and, thus, fix the parameters $t_l^{(1)}$ and $\varepsilon_l^{(1)}$ we need in second order. We continue in this way up to third order in $1/U$.

E.6.1. Leading Order

As we showed in Sect. E.4, we have to tridiagonalize the operator (E.51),

$$\mathcal{L}^{(0)} = P\bar{V}_0P + P(V_2^{(0)} - \xi^{(0)})P \text{ with } \bar{V}_0 = V_0 + V_1^{(0)}, \quad (\text{E.90})$$

with the starting vector (E.35),

$$|\Psi_0\rangle = |\phi_{-1}\rangle + \mathcal{O}\left(\frac{1}{U}\right). \quad (\text{E.91})$$

With the action of $\mathcal{L}^{(0)}$, given by (E.69a) to (E.69d), we can begin with the first iteration.

First Iteration: $|\Psi_1\rangle := -\mathcal{L}|\Psi_0\rangle + e_0|\Psi_0\rangle$

$$\begin{aligned} |\tilde{\Psi}_1^{(0)}\rangle &:= -\mathcal{L}^{(0)}|\Psi_0^{(0)}\rangle = -\mathcal{L}^{(0)}|\phi_{-1}\rangle \\ &= -|\gamma_0\rangle \end{aligned}$$

$$\boxed{|\tilde{\Psi}_1\rangle = -|\gamma_0\rangle + \mathcal{O}(1/U)} \quad (\text{E.92})$$

$$e_0 = \frac{\langle\Psi_0|\mathcal{L}|\Psi_0\rangle}{\langle\Psi_0|\Psi_0\rangle} = -2\langle\Psi_0|\tilde{\Psi}_1\rangle + \mathcal{O}(1/U) = 2\langle\phi_{-1}|\gamma_0\rangle + \mathcal{O}(1/U) = 0$$

Note that $\tilde{e}_n = e_n$ and, for this reason, we do not need to discriminate between them.

$$\boxed{e_0 = \mathcal{O}(1/U) \stackrel{(E.78)}{\Rightarrow} \varepsilon_0^{(0)} = 0} \quad (\text{E.93})$$

$$\boxed{|\Psi_1\rangle = -|\gamma_0\rangle + \mathcal{O}(1/U)} \quad (\text{E.94})$$

$$\begin{aligned} \tilde{\tau}_0 &= \frac{\langle\Psi_0|\mathcal{L}|\Psi_1\rangle}{\langle\Psi_0|\Psi_0\rangle} = -2\langle\tilde{\Psi}_1|\Psi_1\rangle + \mathcal{O}(1/U) = -2\langle\gamma_0|\gamma_0\rangle + \mathcal{O}(1/U) \\ &= -1 + \mathcal{O}(1/U) \end{aligned}$$

$$\boxed{\tau_0 = -1 + \mathcal{O}(1/U) \stackrel{(E.78)}{\Rightarrow} t_0^{(0)} = 1} \quad (\text{E.95})$$

Second Iteration: $|\Psi_2\rangle := -\mathcal{L}|\Psi_1\rangle + e_1|\Psi_1\rangle + \tau_0|\Psi_0\rangle$

$$\begin{aligned} |\tilde{\Psi}_2^{(0)}\rangle &:= -\mathcal{L}^{(0)}|\Psi_1^{(0)}\rangle \quad (\text{use } \varepsilon_0^{(0)} = 0 \text{ and } t_0^{(0)} = 1) \\ &= \mathcal{L}^{(0)}|\gamma_0\rangle \\ &= |\phi_{-1}\rangle + |\gamma_1\rangle \end{aligned}$$

$$\boxed{|\tilde{\Psi}_2\rangle = |\phi_{-1}\rangle + |\gamma_1\rangle + \mathcal{O}(1/U)} \quad (\text{E.96})$$

$$\begin{aligned} e_1 &= \frac{\langle\Psi_1|\mathcal{L}|\Psi_1\rangle}{\langle\Psi_1|\Psi_1\rangle} = -2\langle\Psi_1|\tilde{\Psi}_2\rangle + \mathcal{O}(1/U) \\ &= 2\langle\gamma_0|(|\phi_{-1}\rangle + |\gamma_1\rangle) + \mathcal{O}(1/U) = 0 \end{aligned}$$

$$\boxed{e_1 = \mathcal{O}(1/U) \stackrel{(E.78)}{\Rightarrow} \varepsilon_1^{(0)} = 0} \quad (\text{E.97})$$

$$\begin{aligned} |\Psi_2^{(0)}\rangle &= |\tilde{\Psi}_2^{(0)}\rangle + e_1^{(0)}|\Psi_1^{(0)}\rangle + \tau_0^{(0)}|\Psi_0^{(0)}\rangle \\ &= |\phi_{-1}\rangle + |\gamma_1\rangle - |\phi_{-1}\rangle \end{aligned}$$

$$\boxed{|\Psi_2\rangle = |\gamma_1\rangle + \mathcal{O}(1/U)} \quad (\text{E.98})$$

$$\tilde{\tau}_1 = \frac{\langle\Psi_1|\mathcal{L}|\Psi_2\rangle}{\langle\Psi_1|\Psi_1\rangle} = -2\langle\tilde{\Psi}_2|\Psi_2\rangle + \mathcal{O}(1/U) = -1 + \mathcal{O}(1/U)$$

$$\boxed{\tau_1 = -1 + \mathcal{O}(1/U) \stackrel{(E.78)}{\Rightarrow} t_1^{(0)} = 1} \quad (\text{E.99})$$

Now go on by induction.

E. Explicit Calculations

Induction Hypothesis to Leading Order

Let $N \geq 3$, then we find for all $1 \leq n < N$

$$|\Psi_n\rangle = (-1)^n |\gamma_{n-1}\rangle + \mathcal{O}(1/U), \quad (\text{E.100})$$

$$e_{n-1} = \mathcal{O}(1/U), \quad (\text{E.101})$$

$$\tau_{n-1} = -1 + \mathcal{O}(1/U), \quad (\text{E.102})$$

which implies

$$\varepsilon_{n-1} = \mathcal{O}(1/U), \quad (\text{E.103})$$

$$t_{n-1} = 1 + \mathcal{O}(1/U). \quad (\text{E.104})$$

Induction Step Since the induction hypothesis (i.h.) has been proven for $n = 1$ and $n = 2$, we may go on with the induction step.

$$\begin{aligned} |\tilde{\Psi}_N^{(0)}\rangle &= -\mathcal{L}^{(0)}|\Psi_{N-1}^{(0)}\rangle \stackrel{\text{i.h.}}{=} (-1)^N \mathcal{L}^{(0)}|\gamma_{N-2}\rangle \\ &= (-1)^N \left\{ \tau_{N-3}^{(0)}|\gamma_{N-3}\rangle - e_{N-2}^{(0)}|\gamma_{N-2}\rangle + \tau_{N-2}^{(0)}|\gamma_{N-1}\rangle \right\} \\ &\stackrel{\text{i.h.}}{=} (-1)^N \{ |\gamma_{N-3}\rangle + |\gamma_{N-1}\rangle \} \end{aligned}$$

$$\boxed{|\tilde{\Psi}_N\rangle = |\gamma_{N-3}\rangle + |\gamma_{N-1}\rangle + \mathcal{O}(1/U)} \quad (\text{E.105})$$

$$e_{N-1} = \frac{\langle \Psi_{N-1} | \mathcal{L} | \Psi_{N-1} \rangle}{\langle \Psi_{N-1} | \Psi_{N-1} \rangle} = -2\langle \Psi_{N-1} | \tilde{\Psi}_N \rangle + \mathcal{O}(1/U) \stackrel{\text{i.h.}}{=} 0 + \mathcal{O}(1/U)$$

$$\boxed{e_{N-1} = \mathcal{O}(1/U) \stackrel{(E.78)}{\Rightarrow} \varepsilon_{N-1}^{(0)} = 0} \quad (\text{E.106})$$

$$\begin{aligned} |\Psi_N^{(0)}\rangle &= |\tilde{\Psi}_N^{(0)}\rangle + e_{N-1}^{(0)}|\Psi_{N-1}^{(0)}\rangle + \tau_{N-2}^{(0)}|\Psi_{N-2}^{(0)}\rangle \\ &\stackrel{\text{i.h.}}{=} |\tilde{\Psi}_N^{(0)}\rangle - |\Psi_{N-2}^{(0)}\rangle \\ &\stackrel{\text{i.h.}}{=} (-1)^N \{ |\gamma_{N-3}\rangle + |\gamma_{N-1}\rangle \} - (-1)^{N-2} |\gamma_{N-3}\rangle \end{aligned}$$

$$\boxed{|\Psi_N\rangle = (-1)^N |\gamma_{N-1}\rangle + \mathcal{O}(1/U)} \quad (\text{E.107})$$

$$\tilde{\tau}_{N-1} = \frac{\langle \Psi_{N-1} | \mathcal{L} | \Psi_N \rangle}{\langle \Psi_{N-1} | \Psi_{N-1} \rangle} \stackrel{\text{i.h.}}{=} -(-1)^{N-1} \frac{\langle \tilde{\Psi}_N | \Psi_N \rangle}{\langle \gamma_{N-2} | \gamma_{N-2} \rangle} = -1 + \mathcal{O}(1/U)$$

$$\boxed{\tau_{N-1} = -1 + \mathcal{O}(1/U) \stackrel{(E.78)}{\Rightarrow} t_{N-1}^{(0)} = 1} \quad (\text{E.108})$$

□

Summary of the Results to Leading Order

Let us summarize the Lanczos vectors in leading-order perturbation theory:

$$|\Psi_0^{(0)}\rangle = |\phi_{-1}\rangle, \quad (\text{E.109a})$$

$$|\tilde{\Psi}_1^{(0)}\rangle = -|\gamma_0\rangle, \quad (\text{E.109b})$$

$$|\Psi_1^{(0)}\rangle = -|\gamma_0\rangle, \quad (\text{E.109c})$$

$$|\tilde{\Psi}_2^{(0)}\rangle = |\phi_{-1}\rangle + |\gamma_1\rangle, \quad (\text{E.109d})$$

$$|\Psi_2^{(0)}\rangle = |\gamma_1\rangle, \quad (\text{E.109e})$$

$$|\tilde{\Psi}_n^{(0)}\rangle = (-1)^n \{|\gamma_{n-3}\rangle + |\gamma_{n-1}\rangle\}, \quad (\text{E.109f})$$

$$|\Psi_n^{(0)}\rangle = (-1)^n |\gamma_{n-1}\rangle. \quad (\text{E.109g})$$

Thus, we have for all $n \in \mathbb{N}$

$$e_n^{(0)} = 0 \wedge \tau_n^{(0)} = -1, \quad (\text{E.110})$$

which results for all $n \in \mathbb{N}$ in

$$\varepsilon_n^{(0)} = 0 \wedge t_n^{(0)} = 1. \quad (\text{E.111})$$

We note in particular that the result implies that $V_2^{(0)} \equiv 0$.

E.6.2. First Order

Here, we perform the Lanczos iteration to first order. The starting vector is given by (E.35),

$$|\Psi_0\rangle = |\phi_{-1}\rangle - \frac{1}{U}|m_{0u}\rangle + \mathcal{O}\left(\frac{1}{U^2}\right). \quad (\text{E.112})$$

With the action of $\mathcal{L}^{(1)}$ given by (E.71a) to (E.71d) we can perform the tridiagonalization easily.

First Iteration: $|\Psi_1\rangle := -\mathcal{L}|\Psi_0\rangle + e_0|\Psi_0\rangle$

$$\begin{aligned} |\tilde{\Psi}_1\rangle &:= |\tilde{\Psi}_1^{(0)}\rangle + 1/U\{-\mathcal{L}^{(0)}|\Psi_0^{(1)}\rangle - \mathcal{L}^{(1)}|\Psi_0^{(0)}\rangle\} + \mathcal{O}(1/U^2) \\ &= |\tilde{\Psi}_1^{(0)}\rangle + 1/U\{\mathcal{L}^{(0)}|m_{0u}\rangle - \mathcal{L}^{(1)}|\phi_{-1}\rangle\} + \mathcal{O}(1/U^2) \\ &= |\tilde{\Psi}_1^{(0)}\rangle + 1/U\{1/2|\phi_{-1}\rangle + |m_{1u}\rangle - |\phi_{-1}\rangle\} + \mathcal{O}(1/U^2) \\ &= |\tilde{\Psi}_1^{(0)}\rangle + 1/U\{-1/2|\phi_{-1}\rangle + |m_{1u}\rangle\} + \mathcal{O}(1/U^2) \end{aligned}$$

$$\boxed{|\tilde{\Psi}_1\rangle = -|\gamma_0\rangle + \frac{1}{U}\left\{-\frac{1}{2}|\phi_{-1}\rangle + |m_{1u}\rangle\right\} + \mathcal{O}\left(\frac{1}{U^2}\right)} \quad (\text{E.113})$$

$$\begin{aligned} e_0 &= \frac{\langle\Psi_0|\mathcal{L}|\Psi_0\rangle}{\langle\Psi_0|\Psi_0\rangle} = -\frac{\langle\Psi_0|\tilde{\Psi}_1\rangle}{1/2 + \mathcal{O}(1/U^2)} \\ &= e_0^{(0)} + 1/U^2\left\{-\langle\Psi_0^{(0)}|\tilde{\Psi}_1^{(1)}\rangle - \langle\Psi_0^{(1)}|\tilde{\Psi}_1^{(0)}\rangle\right\} + \mathcal{O}(1/U^2) \\ &= 1/U^2\left\{\langle\phi_{-1}|(1/2|\phi_{-1}\rangle - |m_{1u}\rangle) - \langle m_{0u}|\gamma_0\rangle + \mathcal{O}(1/U^2)\right\} \\ &= 1/U\{1/2 - 1/2\} + \mathcal{O}(1/U^2) \end{aligned}$$

$$\boxed{e_0 = \mathcal{O}(1/U^2) \stackrel{(E.78)}{\Rightarrow} \varepsilon_0^{(0)} = 0 \wedge \varepsilon_0^{(1)} = 0} \quad (\text{E.114})$$

$$\boxed{|\Psi_1\rangle = -|\gamma_0\rangle + \frac{1}{U}\left\{-\frac{1}{2}|\phi_{-1}\rangle + |m_{1u}\rangle\right\} + \mathcal{O}\left(\frac{1}{U^2}\right)} \quad (\text{E.115})$$

E. Explicit Calculations

Norm of $|\Psi_1\rangle$

$$\boxed{\|\Psi_1\|^2 = \langle\Psi_1|\Psi_1\rangle = 1/2 + \mathcal{O}(1/U^2)} \quad (\text{E.116})$$

$$\tilde{\tau}_0 = -\frac{\langle\Psi_1|\Psi_1\rangle}{\langle\Psi_0|\Psi_0\rangle} = -2\langle\Psi_1|\Psi_1\rangle + \mathcal{O}(1/U^2) = -1 + \mathcal{O}(1/U^2)$$

$$\boxed{\tau_0 = -1 + \mathcal{O}(1/U^2) \stackrel{(E.78)}{\Rightarrow} t_0^{(0)} = 1 \wedge t_0^{(1)} = 0} \quad (\text{E.117})$$

Second Iteration: $|\Psi_2\rangle := -\mathcal{L}|\Psi_1\rangle + e_1|\Psi_1\rangle + \tau_0|\Psi_0\rangle$

$$\begin{aligned} |\tilde{\Psi}_2\rangle &:= |\tilde{\Psi}_2^{(0)}\rangle + 1/U\{-\mathcal{L}^{(0)}|\Psi_1^{(1)}\rangle - \mathcal{L}^{(1)}|\Psi_1^{(0)}\rangle\} + \mathcal{O}(1/U^2) \\ &= |\tilde{\Psi}_2^{(0)}\rangle + 1/U\{\mathcal{L}^{(0)}(1/2|\phi_{-1}\rangle - |m_{1u}\rangle) + \mathcal{L}^{(1)}|\gamma_0\rangle\} + \mathcal{O}(1/U^2) \\ &= |\tilde{\Psi}_2^{(0)}\rangle + 1/U\{1/2|\gamma_0\rangle - |m_{0u}\rangle - |m_{2u}\rangle - 1/2|\gamma_0\rangle - \varepsilon_0^{(1)}|\gamma_0\rangle + t_0^{(1)}|\gamma_1\rangle\} + \mathcal{O}(1/U^2) \end{aligned}$$

We use $\varepsilon_0^{(1)} = 0$ and $t_0^{(1)} = 0$ to obtain

$$\boxed{|\tilde{\Psi}_2\rangle = |\phi_{-1}\rangle + |\gamma_1\rangle + \frac{1}{U}\{-|m_{0u}\rangle - |m_{2u}\rangle\} + \mathcal{O}(1/U^2)}. \quad (\text{E.118})$$

$$\begin{aligned} e_1 &= \frac{\langle\Psi_1|\mathcal{L}|\Psi_1\rangle}{\langle\Psi_1|\Psi_1\rangle} = -\frac{\langle\Psi_1|\tilde{\Psi}_2\rangle}{1/2 + \mathcal{O}(1/U^2)} \\ &= e_1^{(0)} + 1/U2\{-\langle\Psi_1^{(0)}|\tilde{\Psi}_2^{(1)}\rangle - \langle\Psi_1^{(1)}|\tilde{\Psi}_2^{(0)}\rangle\} + \mathcal{O}(1/U^2) \\ &= 1/U2\{-\langle\gamma_0|(|m_{0u}\rangle + |m_{2u}\rangle) + (1/2\langle\phi_{-1}| - \langle m_{1u}|)(|\phi_{-1}\rangle + |\gamma_1\rangle)\} + \mathcal{O}(1/U^2) \\ &= 1/U\{-2\langle\gamma_0|m_{0u}\rangle + 1/2 - 2\langle m_{1u}|\gamma_1\rangle\} + \mathcal{O}(1/U^2) \\ &= 1/U\{-1/2 + 1/2 - 1/2\} + \mathcal{O}(1/U^2) = -1/2U + \mathcal{O}(1/U^2) \end{aligned}$$

$$\boxed{e_1 = -\frac{1}{2U} + \mathcal{O}(1/U^2) \stackrel{(E.78)}{\Rightarrow} \varepsilon_1^{(0)} = 0 \wedge \varepsilon_1^{(1)} = \frac{1}{2}} \quad (\text{E.119})$$

$$\begin{aligned} |\Psi_2\rangle &= |\gamma_1\rangle + 1/U\{|\tilde{\Psi}_2^{(1)}\rangle + e_1^{(1)}|\Psi_1^{(0)}\rangle + \tau_0^{(0)}|\Psi_0^{(1)}\rangle\} + \mathcal{O}(1/U^2) \\ &= |\gamma_1\rangle + 1/U\{-|m_{0u}\rangle - |m_{2u}\rangle + 1/2|\gamma_0\rangle + |m_{0u}\rangle\} \end{aligned}$$

$$\boxed{|\Psi_2\rangle = |\gamma_1\rangle + \frac{1}{U}\{1/2|\gamma_0\rangle - |m_{2u}\rangle\} + \mathcal{O}(1/U^2)} \quad (\text{E.120})$$

Norm of $|\Psi_2\rangle$

$$\boxed{\|\Psi_2\|^2 = \langle\Psi_2|\Psi_2\rangle = 1/2 + \mathcal{O}(1/U^2)} \quad (\text{E.121})$$

$$\tilde{\tau}_1 = -\frac{\langle\Psi_2|\Psi_2\rangle}{\langle\Psi_1|\Psi_1\rangle} = -2\langle\Psi_2|\Psi_2\rangle + \mathcal{O}(1/U^2) = -1 + \mathcal{O}(1/U^2)$$

$$\boxed{\tau_1 = -1 + \mathcal{O}(1/U^2) \stackrel{(E.78)}{\Rightarrow} t_1^{(0)} = 1 \wedge t_1^{(1)} = 0} \quad (\text{E.122})$$

Third Iteration: $|\Psi_3\rangle := -\mathcal{L}|\Psi_2\rangle + e_2|\Psi_2\rangle + \tau_1|\Psi_1\rangle$

$$\begin{aligned} |\tilde{\Psi}_3\rangle &:= |\tilde{\Psi}_3^{(0)}\rangle + 1/U\{-\mathcal{L}^{(0)}|\Psi_2^{(1)}\rangle - \mathcal{L}^{(1)}|\Psi_2^{(0)}\rangle\} + \mathcal{O}(1/U^2) \\ &= |\tilde{\Psi}_3^{(0)}\rangle + 1/U\{\mathcal{L}^{(0)}(-1/2|\gamma_0\rangle + |m_{2u}\rangle) - \mathcal{L}^{(1)}|\gamma_1\rangle\} + \mathcal{O}(1/U^2) \\ &= |\tilde{\Psi}_3^{(0)}\rangle + 1/U\{-1/2|\phi_{-1}\rangle - 1/2|\gamma_1\rangle + |m_{1u}\rangle + |m_{3u}\rangle - t_0^{(1)}|\gamma_0\rangle + \varepsilon_1^{(1)}|\gamma_1\rangle - t_1^{(1)}|\gamma_2\rangle\} + \mathcal{O}(1/U^2) \end{aligned}$$

With $\varepsilon_1^{(1)} = 1/2$ and $t_0^{(1)} = t_1^{(1)} = 0$ we obtain

$$\boxed{|\tilde{\Psi}_3\rangle = -|\gamma_0\rangle - |\gamma_2\rangle + \frac{1}{U}\{-\frac{1}{2}|\phi_{-1}\rangle + |m_{1u}\rangle + |m_{3u}\rangle\} + \mathcal{O}(1/U^2)}. \quad (\text{E.123})$$

$$\begin{aligned} e_2 &= \frac{\langle\Psi_2|\mathcal{L}|\Psi_2\rangle}{\langle\Psi_2|\Psi_2\rangle} = -\frac{\langle\Psi_2|\tilde{\Psi}_3\rangle}{1/2 + \mathcal{O}(1/U^2)} \\ &= e_2^{(0)} + 1/U^2\{-\langle\Psi_2^{(0)}|\tilde{\Psi}_3^{(1)}\rangle - \langle\Psi_2^{(1)}|\tilde{\Psi}_3^{(0)}\rangle\} + \mathcal{O}(1/U^2) \\ &= 1/U^2\{-\langle\gamma_1|(-1/2|\phi_{-1}\rangle + |m_{1u}\rangle + |m_{3u}\rangle) - (1/2\langle\gamma_0| - \langle m_{2u}|)(-|\gamma_0\rangle - |\gamma_2\rangle)\} + \mathcal{O}(1/U^2) \\ &= 1/U^2\{-\langle\gamma_1|m_{1u}\rangle + 1/2\langle\gamma_0|\gamma_0\rangle - \langle m_{2u}|\gamma_2\rangle\} + \mathcal{O}(1/U^2) \\ &= 1/U\{-1/2 + 1/2 - 1/2\} + \mathcal{O}(1/U^2) = -1/2U + \mathcal{O}(1/U^2) \end{aligned}$$

$$\boxed{e_2 = -\frac{1}{2U} + \mathcal{O}(1/U) \stackrel{(E.78)}{\Rightarrow} \varepsilon_2^{(0)} = 0 \wedge \varepsilon_2^{(1)} = \frac{1}{2}} \quad (\text{E.124})$$

$$\begin{aligned} |\Psi_3\rangle &= -|\gamma_2\rangle + 1/U\{|\tilde{\Psi}_3^{(1)}\rangle + e_2^{(1)}|\Psi_2^{(0)}\rangle + \tau_1^{(0)}|\Psi_1^{(1)}\rangle\} + \mathcal{O}(1/U^2) \\ &= -|\gamma_2\rangle + 1/U\{-1/2|\phi_{-1}\rangle + |m_{1u}\rangle + |m_{3u}\rangle - 1/2|\gamma_1\rangle - (-1/2|\phi_{-1}\rangle + |m_{1u}\rangle)\} + \mathcal{O}(1/U^2) \end{aligned}$$

$$\boxed{|\Psi_3\rangle = -|\gamma_2\rangle + \frac{1}{U}\{-\frac{1}{2}|\gamma_1\rangle + |m_{3u}\rangle\} + \mathcal{O}(1/U^2)} \quad (\text{E.125})$$

Norm of $|\Psi_3\rangle$

$$\boxed{\|\Psi_3\|^2 = \langle\Psi_3|\Psi_3\rangle = 1/2 + \mathcal{O}(1/U^2)} \quad (\text{E.126})$$

$$\tilde{\tau}_2 = -\frac{\langle\Psi_3|\Psi_3\rangle}{\langle\Psi_2|\Psi_2\rangle} = -2\langle\Psi_3|\Psi_3\rangle + \mathcal{O}(1/U^2) = -1 + \mathcal{O}(1/U^2)$$

$$\boxed{\tau_2 = -1 + \mathcal{O}(1/U^2) \stackrel{(E.78)}{\Rightarrow} t_2^{(0)} = 1 \wedge t_2^{(1)} = 0} \quad (\text{E.127})$$

Fourth Iteration: $|\Psi_4\rangle := -\mathcal{L}|\Psi_3\rangle + e_3|\Psi_3\rangle + \tau_2|\Psi_2\rangle$

$$\begin{aligned} |\tilde{\Psi}_4\rangle &:= |\tilde{\Psi}_4^{(0)}\rangle + 1/U\{-\mathcal{L}^{(0)}|\Psi_3^{(1)}\rangle - \mathcal{L}^{(1)}|\Psi_3^{(0)}\rangle\} + \mathcal{O}(1/U^2) \\ &= |\tilde{\Psi}_4^{(0)}\rangle + 1/U\{\mathcal{L}^{(0)}(1/2|\gamma_1\rangle - |m_{3u}\rangle) + \mathcal{L}^{(1)}|\gamma_2\rangle\} + \mathcal{O}(1/U^2) \\ &= |\tilde{\Psi}_4^{(0)}\rangle + 1/U\{1/2|\gamma_0\rangle + 1/2|\gamma_2\rangle - |m_{2u}\rangle - |m_{4u}\rangle + t_1^{(1)}|\gamma_1\rangle - \varepsilon_2^{(1)}|\gamma_2\rangle + t_2^{(1)}|\gamma_3\rangle\} + \mathcal{O}(1/U^2) \end{aligned}$$

With the help of $\varepsilon_2^{(1)} = 1/2$, $t_0^{(1)} = t_1^{(1)} = 0$ we obtain

$$\boxed{|\tilde{\Psi}_4\rangle = |\gamma_1\rangle + |\gamma_3\rangle + \frac{1}{U}\{\frac{1}{2}|\gamma_0\rangle - |m_{2u}\rangle - |m_{4u}\rangle\} + \mathcal{O}(1/U^2)}. \quad (\text{E.128})$$

E. Explicit Calculations

$$\begin{aligned}
e_3 &= \frac{\langle \Psi_3 | \mathcal{L} | \Psi_3 \rangle}{\langle \Psi_3 | \Psi_3 \rangle} = -\frac{\langle \Psi_3 | \tilde{\Psi}_4 \rangle}{1/2 + \mathcal{O}(1/U^2)} \\
&= e_3^{(0)} + 1/U \{ -\langle \Psi_3^{(0)} | \tilde{\Psi}_4^{(1)} \rangle - \langle \Psi_3^{(1)} | \tilde{\Psi}_4^{(0)} \rangle \} + \mathcal{O}(1/U^2) \\
&= 1/U \{ \langle \gamma_2 | (1/2) \gamma_0 \rangle - |m_{2u}\rangle - |m_{4u}\rangle \} - (-1/2 \langle \gamma_1 | + \langle m_{3u} |) (|\gamma_1\rangle + |\gamma_3\rangle) \} + \mathcal{O}(1/U^2) \\
&= 1/U \{ -\langle \gamma_2 | m_{2u} \rangle + 1/2 \langle \gamma_1 | \gamma_1 \rangle - \langle m_{3u} | \gamma_3 \rangle \} + \mathcal{O}(1/U^2) \\
&= 1/U \{ -1/2 + 1/2 - 1/2 \} + \mathcal{O}(1/U^2) = -1/2U + \mathcal{O}(1/U^2)
\end{aligned}$$

$$\boxed{e_3 = -\frac{1}{2U} + \mathcal{O}(1/U) \stackrel{(E.78)}{\Rightarrow} \varepsilon_3^{(0)} = 0 \wedge \varepsilon_3^{(1)} = \frac{1}{2}} \quad (E.129)$$

$$\begin{aligned}
|\Psi_4\rangle &= |\gamma_3\rangle + 1/U \{ |\tilde{\Psi}_4^{(1)}\rangle + e_3^{(1)} |\Psi_3^{(0)}\rangle + \tau_2^{(0)} |\Psi_2^{(1)}\rangle \} + \mathcal{O}(1/U^2) \\
&= |\gamma_3\rangle + 1/U \{ 1/2 |\gamma_0\rangle - |m_{2u}\rangle - |m_{4u}\rangle + 1/2 |\gamma_2\rangle - 1/2 |\gamma_0\rangle + |m_{2u}\rangle \} + \mathcal{O}(1/U^2)
\end{aligned}$$

$$\boxed{|\Psi_4\rangle = |\gamma_3\rangle + \frac{1}{U} \{ \frac{1}{2} |\gamma_2\rangle - |m_{4u}\rangle \} + \mathcal{O}(1/U^2)} \quad (E.130)$$

Norm of $|\Psi_4\rangle$

$$\boxed{\| |\Psi_4\rangle \|^2 = \langle \Psi_4 | \Psi_4 \rangle = 1/2 + \mathcal{O}(1/U^2)} \quad (E.131)$$

$$\tilde{\tau}_3 = -\frac{\langle \Psi_4 | \Psi_4 \rangle}{\langle \Psi_3 | \Psi_3 \rangle} = -2 \langle \Psi_4 | \Psi_4 \rangle + \mathcal{O}(1/U^2) = -1 + \mathcal{O}(1/U^2)$$

$$\boxed{\tau_3 = -1 + \mathcal{O}(1/U^2) \stackrel{(E.78)}{\Rightarrow} t_3^{(0)} = 1 \wedge t_3^{(1)} = 0} \quad (E.132)$$

Now go on by induction.

Induction Hypothesis to First Order

Let $N \geq 4$, then we have for all $2 \leq n < N$

$$|\Psi_n\rangle = (-1)^n \left(|\gamma_{n-1}\rangle + \frac{1}{U} \left\{ \frac{1}{2} |\gamma_{n-2}\rangle - |m_{nu}\rangle \right\} \right) + \mathcal{O}(1/U^2), \quad (E.133)$$

$$e_{n-1} = -\frac{1}{2U} + \mathcal{O}(1/U^2), \quad (E.134)$$

$$\tau_{n-1} = -1 + \mathcal{O}(1/U^2), \quad (E.135)$$

which implies

$$\varepsilon_{n-1} = \frac{1}{2U} + \mathcal{O}(1/U^2), \quad (E.136)$$

$$t_{n-1} = 1 + \mathcal{O}(1/U^2). \quad (E.137)$$

Induction Step Since the induction hypothesis (i.h.) has been proven for $n = 2, 3, 4$, we proceed with the induction step.

$$\begin{aligned}
|\tilde{\Psi}_N\rangle &:= -\mathcal{L} |\Psi_{N-1}\rangle = |\tilde{\Psi}_N^{(0)}\rangle + 1/U \{ -\mathcal{L}^{(0)} |\Psi_{N-1}^{(1)}\rangle - \mathcal{L}^{(1)} |\Psi_{N-1}^{(0)}\rangle \} + \mathcal{O}(1/U^2) \\
&\stackrel{\text{i.h.}}{=} |\tilde{\Psi}_N^{(0)}\rangle + 1/U (-1)^{N-1} \{ -\mathcal{L}^{(0)} (1/2 |\gamma_{N-3}\rangle - |m_{N-1u}\rangle) - \mathcal{L}^{(1)} |\gamma_{N-2}\rangle \} + \mathcal{O}(1/U^2)
\end{aligned}$$

$$\begin{aligned}
&= |\tilde{\Psi}_N^{(0)}\rangle + 1/U(-1)^{N-1}\{-1/2|\gamma_{N-4}\rangle - 1/2|\gamma_{N-2}\rangle + |m_{N-2u}\rangle + |m_{Nu}\rangle \\
&\quad - (t_{N-3}^{(1)}|\gamma_{N-3}\rangle - \varepsilon_{N-2}^{(1)}|\gamma_{N-2}\rangle + t_{N-2}^{(1)}|\gamma_{N-1}\rangle)\} + \mathcal{O}(1/U^2) \\
&\stackrel{\text{i.h.}}{=} |\tilde{\Psi}_N^{(0)}\rangle + 1/U(-1)^N\{1/2|\gamma_{N-4}\rangle - |m_{N-2u}\rangle - |m_{Nu}\rangle\} + \mathcal{O}(1/U^2)
\end{aligned}$$

$$\boxed{|\tilde{\Psi}_N\rangle = (-1)^N\left(\{|\gamma_{N-3}\rangle + |\gamma_{N-1}\rangle\} + \frac{1}{U}\left\{\frac{1}{2}|\gamma_{N-4}\rangle - |m_{N-2u}\rangle - |m_{Nu}\rangle\right\}\right) + \mathcal{O}(1/U^2)} \quad (\text{E.138})$$

$$\begin{aligned}
e_{N-1} &= \frac{\langle\Psi_{N-1}|\mathcal{L}|\Psi_{N-1}\rangle}{\langle\Psi_{N-1}|\Psi_{N-1}\rangle} = -\frac{\langle\Psi_{N-1}|\tilde{\Psi}_N\rangle}{1/2 + \mathcal{O}(1/U^2)} \\
&= e_{N-1}^{(0)} + 1/U^2\left\{-\langle\Psi_{N-1}^{(0)}|\tilde{\Psi}_N^{(1)}\rangle - \langle\Psi_{N-1}^{(1)}|\tilde{\Psi}_N^{(0)}\rangle\right\} + \mathcal{O}(1/U^2) \\
&= 1/U^2\left\{\langle\gamma_{N-2}|(1/2|\gamma_{N-4}\rangle - |m_{N-2u}\rangle - |m_{Nu}\rangle)\right. \\
&\quad \left.- \left[-(1/2\langle\gamma_{N-3}| - \langle m_{N-1u}|)(|\gamma_{N-3}\rangle + |\gamma_{N-1}\rangle)\right]\right\} + \mathcal{O}(1/U^2) \\
&= 1/U^2\{-\langle\gamma_{N-2}|m_{N-2u}\rangle + 1/2\langle\gamma_{N-3}|\gamma_{N-3}\rangle - \langle m_{N-1u}|\gamma_{N-1}\rangle\} + \mathcal{O}(1/U^2) \\
&= 1/U\{-1/2 + 1/2 - 1/2\} + \mathcal{O}(1/U^2) = -1/2U + \mathcal{O}(1/U^2)
\end{aligned}$$

$$\boxed{e_{N-1} = -\frac{1}{2U} + \mathcal{O}(1/U^2) \stackrel{(E.78)}{\Rightarrow} \varepsilon_{N-1}^{(0)} = 0 \wedge \varepsilon_{N-1}^{(1)} = \frac{1}{2}} \quad (\text{E.139})$$

$$\begin{aligned}
|\Psi_N\rangle &= |\tilde{\Psi}_N^{(0)}\rangle + 1/U\{|\tilde{\Psi}_N^{(1)}\rangle + e_{N-1}^{(1)}|\Psi_{N-1}^{(0)}\rangle + \tau_{N-2}^{(0)}|\Psi_{N-2}^{(1)}\rangle\} + \mathcal{O}(1/U^2) \\
&= |\tilde{\Psi}_N^{(0)}\rangle + 1/U\{(-1)^N(1/2|\gamma_{N-4}\rangle - |m_{N-2u}\rangle - |m_{Nu}\rangle) \\
&\quad - 1/2(-1)^{N-1}|\gamma_{N-2}\rangle - (-1)^{N-2}(1/2|\gamma_{N-4}\rangle - |m_{N-2u}\rangle)\} + \mathcal{O}(1/U^2)
\end{aligned}$$

$$\boxed{|\Psi_N\rangle = (-1)^N\left(|\gamma_{N-1}\rangle + \frac{1}{U}\left\{\frac{1}{2}|\gamma_{N-2}\rangle - |m_{Nu}\rangle\right\}\right) + \mathcal{O}(1/U^2)} \quad (\text{E.140})$$

Norm of $|\Psi_N\rangle$

$$\boxed{\|\Psi_N\|^2 = \langle\Psi_N|\Psi_N\rangle = 1/2 + \mathcal{O}(1/U^2)} \quad (\text{E.141})$$

$$\tilde{\tau}_{N-1} = -\frac{\langle\Psi_N|\Psi_N\rangle}{\langle\Psi_{N-1}|\Psi_{N-1}\rangle} = -2\langle\Psi_N|\Psi_N\rangle + \mathcal{O}(1/U^2) = -1 + \mathcal{O}(1/U^2)$$

$$\boxed{\tau_{N-1} = -1 + \mathcal{O}(1/U^2) \stackrel{(E.78)}{\Rightarrow} t_{N-1}^{(0)} = 1 \wedge t_{N-1}^{(1)} = 0} \quad (\text{E.142})$$

□

Summary of the Results to First Order

To first order, the Lanczos Iteration may be summarized as follows:

$$|\Psi_0\rangle = |\phi_{-1}\rangle + \frac{1}{U}\{-|m_{0u}\rangle\} + \mathcal{O}(1/U^2), \quad (\text{E.143a})$$

$$|\tilde{\Psi}_1\rangle = -|\gamma_0\rangle + \frac{1}{U}\left\{-\frac{1}{2}|\phi_{-1}\rangle + |m_{1u}\rangle\right\} + \mathcal{O}(1/U^2), \quad (\text{E.143b})$$

$$|\Psi_1\rangle = -|\gamma_0\rangle + \frac{1}{U}\left\{-\frac{1}{2}|\phi_{-1}\rangle + |m_{1u}\rangle\right\} + \mathcal{O}(1/U^2), \quad (\text{E.143c})$$

E. Explicit Calculations

$$|\tilde{\Psi}_2\rangle = |\phi_{-1}\rangle + |\gamma_1\rangle + \frac{1}{U}\{-|m_{0u}\rangle - |m_{2u}\rangle\} + \mathcal{O}(1/U^2), \quad (\text{E.143d})$$

$$|\Psi_2\rangle = |\gamma_1\rangle + \frac{1}{U}\left\{\frac{1}{2}|\gamma_0\rangle - |m_{2u}\rangle\right\} + \mathcal{O}(1/U^2), \quad (\text{E.143e})$$

$$|\tilde{\Psi}_3\rangle = -|\gamma_0\rangle - |\gamma_2\rangle + \frac{1}{U}\left\{-\frac{1}{2}|\phi_{-1}\rangle + |m_{1u}\rangle + |m_{3u}\rangle\right\} + \mathcal{O}(1/U^2), \quad (\text{E.143f})$$

$$|\Psi_3\rangle = -|\gamma_2\rangle + \frac{1}{U}\left\{-\frac{1}{2}|\gamma_1\rangle + |m_{3u}\rangle\right\} + \mathcal{O}(1/U^2), \quad (\text{E.143g})$$

and for $n \geq 4$

$$|\tilde{\Psi}_n\rangle = (-1)^n \left(\{|\gamma_{n-3}\rangle + |\gamma_{n-1}\rangle\} + \frac{1}{U} \left\{ \frac{1}{2}|\gamma_{n-4}\rangle - |m_{n-2u}\rangle - |m_{nu}\rangle \right\} \right) + \mathcal{O}(1/U^2), \quad (\text{E.143h})$$

$$|\tilde{\Psi}_n\rangle = (-1)^n \left(|\gamma_{n-1}\rangle + \frac{1}{U} \left\{ \frac{1}{2}|\gamma_{n-2}\rangle - |m_{nu}\rangle \right\} \right) + \mathcal{O}(1/U^2). \quad (\text{E.143i})$$

Thus, we have

$$e_0 = \mathcal{O}(1/U^2) \quad \wedge \quad e_n = -\frac{1}{2U} + \mathcal{O}(1/U^2), \quad (\text{E.144a})$$

$$\tau_0 = -1 + \mathcal{O}(1/U^2) \quad \wedge \quad \tau_n = -1 + \mathcal{O}(1/U^2) \quad n \geq 1, \quad (\text{E.144b})$$

and

$$\varepsilon_0 = \mathcal{O}(1/U^2) \quad \wedge \quad \varepsilon_n = \frac{1}{2U} + \mathcal{O}(1/U^2), \quad (\text{E.145a})$$

$$t_0 = 1 + \mathcal{O}(1/U^2) \quad \wedge \quad t_n = 1 + \mathcal{O}(1/U^2) \quad n \geq 1. \quad (\text{E.145b})$$

This shows especially that $V_1^{(1)} \equiv 0$.

E.6.3. Second Order

Up to second order the starting vector is given by, see (E.35),

$$|\Psi_0\rangle = |\phi_{-1}\rangle - \frac{1}{U}|m_{0u}\rangle + \frac{1}{U^2}\left\{-\frac{1}{2}|\phi_{-1}\rangle + |m_{1u}\rangle\right\} + \mathcal{O}(1/U^3) \quad (\text{E.146})$$

and has the norm

$$\|\Psi_0\|^2 = \langle\Psi_0|\Psi_0\rangle = \frac{1}{2} + \frac{1}{U^2}\left\{\langle m_{1u}|m_{1u}\rangle + 2\left(-\frac{1}{2}\langle\phi_{-1}|\phi_{-1}\rangle\right)\right\} + \mathcal{O}(1/U^3),$$

and therefore

$$\boxed{\|\Psi_0\|^2 = \frac{1}{2} + \mathcal{O}(1/U^3)}. \quad (\text{E.147})$$

First Iteration: $|\Psi_1\rangle := -\mathcal{L}|\Psi_0\rangle + e_0|\Psi_0\rangle$

$$\begin{aligned} |\tilde{\Psi}_1^{(2)}\rangle &:= -\mathcal{L}^{(0)}|\Psi_0^{(2)}\rangle - \mathcal{L}^{(1)}|\Psi_0^{(1)}\rangle - \mathcal{L}^{(2)}|\Psi_0^{(0)}\rangle \\ &= \mathcal{L}^{(0)}\left\{\frac{1}{2}|\phi_{-1}\rangle - |m_{1u}\rangle\right\} + \mathcal{L}^{(1)}|m_{0u}\rangle - \mathcal{L}^{(2)}|\phi_{-1}\rangle \\ &= \frac{1}{2}|\gamma_0\rangle - |m_{0u}\rangle - |m_{2u}\rangle + \frac{1}{2}|m_{0d}\rangle + \frac{3}{4}|\gamma_0\rangle \\ &= \frac{5}{4}|\gamma_0\rangle - \frac{1}{2}|m_{0u}\rangle - |m_{2u}\rangle - \frac{1}{2}\underbrace{\{|m_{0u}\rangle - |m_{0d}\rangle\}}_{|\gamma_0\rangle} \end{aligned}$$

$$\boxed{|\tilde{\Psi}_1\rangle = -|\gamma_0\rangle + \frac{1}{U}\{-\frac{1}{2}|\phi_{-1}\rangle + |m_{1u}\rangle\} + \frac{1}{U^2}\{\frac{3}{4}|\gamma_0\rangle - \frac{1}{2}|m_{0u}\rangle - |m_{2u}\rangle\} + \mathcal{O}(1/U^3)} \quad (\text{E.148})$$

$$\begin{aligned} e_0 &= \frac{\langle\Psi_0|\mathcal{L}|\Psi_0\rangle}{\langle\Psi_0|\Psi_0\rangle} = -\frac{\langle\Psi_0|\tilde{\Psi}_1\rangle}{1/2 + \mathcal{O}(1/U^3)} \\ &= 1/U^2\{ -\langle\Psi_0^{(0)}|\tilde{\Psi}_1^{(2)}\rangle - \langle\Psi_0^{(1)}|\tilde{\Psi}_1^{(1)}\rangle - \langle\Psi_0^{(2)}|\tilde{\Psi}_1^{(0)}\rangle\} + \mathcal{O}(1/U^3) \\ &= 1/U^2\{ -\langle\phi_{-1}|(3/4|\gamma_0\rangle - 1/2|m_{0u}\rangle - |m_{2u}\rangle) + \langle m_{0u}|(-1/2|\phi_{-1}\rangle + |m_{1u}\rangle) \\ &\quad - (-1/2\langle\phi_{-1}| + \langle m_{1u}|)(-|\gamma_0\rangle)\} + \mathcal{O}(1/U^3) = \mathcal{O}(1/U^3) \end{aligned}$$

$$\boxed{e_0 = \mathcal{O}(1/U^3) \stackrel{(E.78)}{\Rightarrow} \varepsilon_0^{(0)} = \varepsilon_0^{(1)} = \varepsilon_0^{(2)} = 0} \quad (\text{E.149})$$

$$\boxed{|\Psi_1\rangle = -|\gamma_0\rangle + \frac{1}{U}\{-\frac{1}{2}|\phi_{-1}\rangle + |m_{1u}\rangle\} + \frac{1}{U^2}\{\frac{3}{4}|\gamma_0\rangle - \frac{1}{2}|m_{0u}\rangle - |m_{2u}\rangle\} + \mathcal{O}(1/U^3)} \quad (\text{E.150})$$

Norm of $|\Psi_1\rangle$

$$\begin{aligned} 2\langle\Psi_1|\Psi_1\rangle &= 1 + 1/U^2\{(-1/2\langle\phi_{-1}| + \langle m_{1u}|)(-1/2|\phi_{-1}\rangle + |m_{1u}\rangle) + 2(-3/4\langle\gamma_0|\gamma_0\rangle + 1/2\langle\gamma_0|m_{0u}\rangle)\} \\ &\quad + \mathcal{O}(1/U^3) \\ &= 1 + 1/U^2\{1/4 + 1 - 3/2 + 1/2\} + \mathcal{O}(1/U^3) \end{aligned}$$

$$\boxed{\|\Psi_1\|^2 = \langle\Psi_1|\Psi_1\rangle = \frac{1}{2} + \frac{1}{8U^2} + \mathcal{O}(1/U^3)} \quad (\text{E.151})$$

$$\tilde{\tau}_0 = -\frac{\langle\Psi_1|\Psi_1\rangle}{\langle\Psi_0|\Psi_0\rangle} = -2\langle\Psi_1|\Psi_1\rangle + \mathcal{O}(1/U^3) = -1 - \frac{1}{4U^2} + \mathcal{O}(1/U^3)$$

$$\boxed{\tilde{\tau}_0 = -1 - \frac{1}{4U^2} + \mathcal{O}(1/U^3)} \quad (\text{E.152})$$

Off-Diagonal Element τ_0

$$\tau_0 := -\sqrt{-\tilde{\tau}_0} = -\sqrt{1 + \frac{1}{4U^2} + \mathcal{O}(1/U^3)} = -(1 + \frac{1}{8U^2} + \mathcal{O}(1/U^3))$$

$$\boxed{\tau_0 = -1 - \frac{1}{8U^2} + \mathcal{O}(1/U^3) \stackrel{(E.78)}{\Rightarrow} t_0^{(0)} = 1 \wedge t_0^{(1)} = 0 \wedge t_0^{(2)} = \frac{1}{8}} \quad (\text{E.153})$$

Second Iteration: $|\Psi_2\rangle := -\mathcal{L}|\Psi_1\rangle + e_1|\Psi_1\rangle + \tau_0|\Psi_0\rangle$

$$\begin{aligned} |\tilde{\Psi}_2^{(2)}\rangle &:= -\mathcal{L}^{(0)}|\Psi_1^{(2)}\rangle - \mathcal{L}^{(1)}|\Psi_1^{(1)}\rangle - \mathcal{L}^{(2)}|\Psi_1^{(0)}\rangle \\ &= \mathcal{L}^{(0)}\{-3/4|\gamma_0\rangle + 1/2|m_{0u}\rangle + |m_{2u}\rangle\} + \mathcal{L}^{(1)}\{1/2|\phi_{-1}\rangle - |m_{1u}\rangle\} + \mathcal{L}^{(2)}|\gamma_0\rangle \\ &= -3/4|\phi_{-1}\rangle - 3/4|\gamma_1\rangle + 1/4|\phi_{-1}\rangle + 1/2|m_{1u}\rangle + |m_{1u}\rangle + |m_{3u}\rangle + 1/2|\phi_{-1}\rangle + 1/2|m_{1u}\rangle - 3/4|\phi_{-1}\rangle \\ &\quad - \varepsilon_0^{(2)}|\gamma_0\rangle + 1/4|\gamma_1\rangle + t_0^{(2)}|\gamma_1\rangle \end{aligned}$$

use $\varepsilon_0^{(2)} = 0$ and $t_0^{(2)} = 1/8$

$$= -3/4|\phi_{-1}\rangle - 3/8|\gamma_1\rangle + 2|m_{1u}\rangle + |m_{3u}\rangle$$

E. Explicit Calculations

$$\begin{aligned} |\tilde{\Psi}_2\rangle &= |\phi_{-1}\rangle + |\gamma_1\rangle + \frac{1}{U}\{-|m_{0u}\rangle - |m_{2u}\rangle\} \\ &\quad + \frac{1}{U^2}\{-\frac{3}{4}|\phi_{-1}\rangle - \frac{3}{8}|\gamma_1\rangle + 2|m_{1u}\rangle + |m_{3u}\rangle\} + \mathcal{O}(1/U^3) \end{aligned} \quad (\text{E.154})$$

$$\begin{aligned} e_1 &= \frac{\langle \Psi_1 | \mathcal{L} | \Psi_1 \rangle}{\langle \Psi_1 | \Psi_1 \rangle} = -\frac{\langle \Psi_1 | \tilde{\Psi}_2 \rangle}{\frac{1}{2} + \frac{1}{8U^2} + \mathcal{O}(1/U^3)} = -2\langle \Psi_1 | \tilde{\Psi}_2 \rangle (1 - 1/4U^2) + \mathcal{O}(1/U^3) \\ &= -\frac{1}{2U} + \frac{1}{U^2} 2(-\langle \Psi_1^{(0)} | \tilde{\Psi}_2^{(2)} \rangle - \langle \Psi_1^{(1)} | \tilde{\Psi}_2^{(1)} \rangle - \langle \Psi_1^{(2)} | \tilde{\Psi}_2^{(0)} \rangle) (1 - \frac{1}{4U^2}) + \mathcal{O}(1/U^3) \\ &= -1/2U + \mathcal{O}(1/U^3) \end{aligned}$$

$$e_1 = -\frac{1}{2U} + \mathcal{O}(1/U^3) \stackrel{(E.78)}{\Rightarrow} \varepsilon_1^{(0)} = 0 \wedge \varepsilon_1^{(1)} = \frac{1}{2} \wedge \varepsilon_1^{(2)} = 0 \quad (\text{E.155})$$

$$\begin{aligned} |\Psi_2^{(2)}\rangle &= |\tilde{\Psi}_2^{(2)}\rangle + e_1^{(1)}|\Psi_1^{(1)}\rangle + \tau_0^{(0)}|\Psi_0^{(2)}\rangle + \tau_0^{(2)}|\Psi_0^{(0)}\rangle \\ &= |\tilde{\Psi}_2^{(2)}\rangle - 1/2\{-1/2|\phi_{-1}\rangle + |m_{1u}\rangle\} - \{-1/2|\phi_{-1}\rangle + |m_{1u}\rangle\} - \frac{1}{4}|\phi_{-1}\rangle \\ &= |\tilde{\Psi}_2^{(2)}\rangle + 1/2|\phi_{-1}\rangle - 3/2|m_{1u}\rangle \end{aligned}$$

$$|\Psi_2\rangle = |\gamma_1\rangle + \frac{1}{U}\{\frac{1}{2}|\gamma_0\rangle - |m_{2u}\rangle\} + \frac{1}{U^2}\{-\frac{1}{4}|\phi_{-1}\rangle - \frac{3}{8}|\gamma_1\rangle + \frac{1}{2}|m_{1u}\rangle + |m_{3u}\rangle\} + \mathcal{O}(1/U^3) \quad (\text{E.156})$$

Norm of $|\Psi_2\rangle$

$$2\langle \Psi_2 | \Psi_2 \rangle = 1 + 1/U^2\{2(-3/8 + 1/4) + 1/4 + 1\} + \mathcal{O}(1/U^3) = 1 + 1/U^2 + \mathcal{O}(1/U^3)$$

$$\|\Psi_2\|^2 = \langle \Psi_2 | \Psi_2 \rangle = \frac{1}{2} + \frac{1}{2U^2} + \mathcal{O}(1/U^3) \quad (\text{E.157})$$

$$\begin{aligned} \tilde{\tau}_1 &= -\frac{\langle \Psi_2 | \Psi_2 \rangle}{\langle \Psi_1 | \Psi_1 \rangle} = -\left(\frac{1}{2} + 1/2U^2\right) 2(1 + 1/4U^2)^{-1} + \mathcal{O}(1/U^3) \\ &= -(1 + 1/U^2)(1 - 1/4U^2) + \mathcal{O}(1/U^3) \\ &= -1 - (1/U^2 - 1/4U^2) + \mathcal{O}(1/U^3) \\ &= -1 - 3/4U^2 + \mathcal{O}(1/U^3) \end{aligned}$$

$$\tilde{\tau}_1 = -1 - \frac{3}{4U^2} + \mathcal{O}(1/U^3) \quad (\text{E.158})$$

Off-Diagonal Element τ_1

$$\tau_1 := -\sqrt{-\tilde{\tau}_1} = -\sqrt{1 + \frac{3}{4U^2} + \mathcal{O}(1/U^3)} = -(1 + \frac{3}{8U^2} + \mathcal{O}(1/U^3))$$

$$\tau_1 = -1 - \frac{3}{8U^2} + \mathcal{O}(1/U^3) \stackrel{(E.78)}{\Rightarrow} t_1^{(0)} = 1 \wedge t_1^{(1)} = 0 \wedge t_1^{(2)} = \frac{3}{8} \quad (\text{E.159})$$

Third Iteration: $|\Psi_3\rangle := -\mathcal{L}|\Psi_2\rangle + e_2|\Psi_2\rangle + \tau_1|\Psi_1\rangle$

$$\begin{aligned}
|\tilde{\Psi}_3^{(2)}\rangle &:= -\mathcal{L}^{(0)}|\Psi_2^{(2)}\rangle - \mathcal{L}^{(1)}|\Psi_2^{(1)}\rangle - \mathcal{L}^{(2)}|\Psi_2^{(0)}\rangle \\
&= \mathcal{L}^{(0)}\{1/4|\phi_{-1}\rangle + 3/8|\gamma_1\rangle - 1/2|m_{1u}\rangle - |m_{3u}\rangle\} + \mathcal{L}^{(1)}\{-1/2|\gamma_0\rangle + |m_{2u}\rangle\} - \mathcal{L}^{(2)}|\gamma_1\rangle \\
&= 1/4|\gamma_0\rangle + 3/8|\gamma_0\rangle + 3/8|\gamma_2\rangle - 1/2|m_{0u}\rangle - 1/2|m_{2u}\rangle - |m_{2u}\rangle - |m_{4u}\rangle + 1/4|\gamma_0\rangle - 1/2|m_{2u}\rangle \\
&\quad - (t_0^{(2)} + 1/4)|\gamma_0\rangle + \varepsilon_1^{(2)}|\gamma_1\rangle - t_1^{(2)}|\gamma_2\rangle \\
&= (5/8 - t_0^{(2)})|\gamma_0\rangle + \varepsilon_1^{(2)}|\gamma_1\rangle - (t_1^{(2)} - 3/8)|\gamma_2\rangle - 1/2|m_{0u}\rangle - 2|m_{2u}\rangle - |m_{4u}\rangle
\end{aligned}$$

We use $\varepsilon_1^{(2)} = 0$, $t_0^{(2)} = 1/8$ and $t_1^{(2)} = 3/8$ to obtain

$$\begin{aligned}
|\tilde{\Psi}_3\rangle &= -|\gamma_0\rangle - |\gamma_2\rangle + \frac{1}{U}\{-\frac{1}{2}|\phi_{-1}\rangle + |m_{1u}\rangle + |m_{3u}\rangle\} \\
&\quad + \frac{1}{U^2}\{\frac{1}{2}|\gamma_0\rangle - \frac{1}{2}|m_{0u}\rangle - 2|m_{2u}\rangle - |m_{4u}\rangle\} + \mathcal{O}(1/U^3).
\end{aligned} \tag{E.160}$$

$$\begin{aligned}
e_2 &= \frac{\langle\Psi_2|\mathcal{L}|\Psi_2\rangle}{\langle\Psi_2|\Psi_2\rangle} = -\frac{\langle\Psi_2|\tilde{\Psi}_3\rangle}{\frac{1}{2} + \frac{1}{2U^2} + \mathcal{O}(1/U^3)} = -2\langle\Psi_2|\tilde{\Psi}_3\rangle(1 - 1/U^2) + \mathcal{O}(1/U^3) \\
&= -\frac{1}{2U} + \frac{1}{U^2}2(-\langle\Psi_2^{(0)}|\tilde{\Psi}_3^{(2)}\rangle - \langle\Psi_2^{(1)}|\tilde{\Psi}_3^{(1)}\rangle - \langle\Psi_2^{(2)}|\tilde{\Psi}_3^{(0)}\rangle)(1 - \frac{1}{U^2}) + \mathcal{O}(1/U^3) \\
&= -1/2U + \mathcal{O}(1/U^3)
\end{aligned}$$

$$e_2 = -\frac{1}{2U} + \mathcal{O}(1/U^3) \stackrel{(E.78)}{\Rightarrow} \varepsilon_2^{(0)} = 0 \wedge \varepsilon_2^{(1)} = \frac{1}{2} \wedge \varepsilon_2^{(2)} = 0 \tag{E.161}$$

$$\begin{aligned}
|\Psi_3^{(2)}\rangle &= |\tilde{\Psi}_3^{(2)}\rangle + e_2^{(1)}|\Psi_2^{(1)}\rangle + \tau_1^{(0)}|\Psi_1^{(2)}\rangle + \tau_1^{(2)}|\Psi_1^{(0)}\rangle \\
&= |\tilde{\Psi}_3^{(2)}\rangle - 1/4|\gamma_0\rangle + 1/2|m_{2u}\rangle - 3/4|\gamma_0\rangle + 1/2|m_{0u}\rangle + |m_{2u}\rangle + 3/4|\gamma_0\rangle \\
&= |\tilde{\Psi}_3^{(2)}\rangle - 1/4|\gamma_0\rangle + 1/2|m_{0u}\rangle + 3/2|m_{2u}\rangle
\end{aligned}$$

$$|\Psi_3\rangle = -|\gamma_2\rangle + \frac{1}{U}\{-\frac{1}{2}|\gamma_1\rangle + |m_{3u}\rangle\} + \frac{1}{U^2}\{\frac{1}{4}|\gamma_0\rangle - \frac{1}{2}|m_{2u}\rangle - |m_{4u}\rangle\} + \mathcal{O}(1/U^3) \tag{E.162}$$

Norm of $|\Psi_3\rangle$

$$2\langle\Psi_3|\Psi_3\rangle = 1 + 1/U^2\{2(1/4) + 1/4 + 1\} + \mathcal{O}(1/U^3) = 1 + 1/U^2\{7/4\} + \mathcal{O}(1/U^3)$$

$$\|\Psi_3\|^2 = \langle\Psi_3|\Psi_3\rangle = \frac{1}{2} + \frac{7}{8U^2} + \mathcal{O}(1/U^3) \tag{E.163}$$

$$\begin{aligned}
\tilde{\tau}_2 &= -\frac{\langle\Psi_3|\Psi_3\rangle}{\langle\Psi_2|\Psi_2\rangle} = -\left(\frac{1}{2} + 7/8U^2\right)2(1 + 1/U^2)^{-1} + \mathcal{O}(1/U^3) = -(1 + 7/4U^2)(1 - 1/U^2) + \mathcal{O}(1/U^3) \\
&= -1 - (-1/U^2 + 7/4U^2) + \mathcal{O}(1/U^3) = -1 - 3/4U^2 + \mathcal{O}(1/U^3)
\end{aligned}$$

$$\tilde{\tau}_2 = -1 - \frac{3}{4U^2} + \mathcal{O}(1/U^3) \tag{E.164}$$

E. Explicit Calculations

Off-Diagonal Element τ_2

$$\tau_2 := -\sqrt{-\tilde{\tau}_2} = -\sqrt{1 + \frac{3}{4U^2} + \mathcal{O}(1/U^3)} = -(1 + \frac{3}{8U^2} + \mathcal{O}(1/U^3))$$

$$\boxed{\tau_2 = -1 - \frac{3}{8U^2} + \mathcal{O}(1/U^3) \stackrel{(E.78)}{\Rightarrow} t_2^{(0)} = 1 \wedge t_2^{(1)} = 0 \wedge t_2^{(2)} = \frac{3}{8}}$$
 (E.165)

Fourth Iteration: $|\Psi_4\rangle := -\mathcal{L}|\Psi_3\rangle + e_3|\Psi_3\rangle + \tau_2|\Psi_2\rangle$

$$\begin{aligned} |\tilde{\Psi}_4^{(2)}\rangle &:= -\mathcal{L}^{(0)}|\Psi_3^{(2)}\rangle - \mathcal{L}^{(1)}|\Psi_3^{(1)}\rangle - \mathcal{L}^{(2)}|\Psi_3^{(0)}\rangle \\ &= \mathcal{L}^{(0)}\{-1/4|\gamma_0\rangle + 1/2|m_{2u}\rangle + |m_{4u}\rangle\} + \mathcal{L}^{(1)}\{1/2|\gamma_1\rangle - |m_{3u}\rangle\} + \mathcal{L}^{(2)}|\gamma_2\rangle \\ &= -1/4|\phi_{-1}\rangle - 1/4|\gamma_1\rangle + 1/2|m_{1u}\rangle + 1/2|m_{3u}\rangle + |m_{3u}\rangle \\ &\quad + |m_{5u}\rangle - 1/4|\gamma_1\rangle + 1/2|m_{3u}\rangle + t_1^{(2)}|\gamma_1\rangle - \varepsilon_2^{(2)}|\gamma_2\rangle + t_2^{(2)}|\gamma_3\rangle \\ &= -1/4|\phi_{-1}\rangle - (1/2 - t_1^{(2)})|\gamma_1\rangle - \varepsilon_2^{(2)}|\gamma_2\rangle + t_2^{(2)}|\gamma_3\rangle + 1/2|m_{1u}\rangle + 2|m_{3u}\rangle + |m_{5u}\rangle \end{aligned}$$

With $\varepsilon_2^{(2)} = 0$, $t_1^{(2)} = t_2^{(2)} = 3/8$ we obtain

$$\boxed{|\tilde{\Psi}_4\rangle = |\gamma_1\rangle + |\gamma_3\rangle + \frac{1}{U}\left\{\frac{1}{2}|\gamma_0\rangle - |m_{2u}\rangle - |m_{4u}\rangle\right\} + \frac{1}{U^2}\left\{-\frac{1}{4}|\phi_{-1}\rangle - \frac{1}{8}|\gamma_1\rangle + \frac{3}{8}|\gamma_3\rangle + \frac{1}{2}|m_{1u}\rangle + 2|m_{3u}\rangle + |m_{5u}\rangle\right\} + \mathcal{O}(1/U^3).}$$
 (E.166)

$$\begin{aligned} e_3 &= \frac{\langle\Psi_3|\mathcal{L}|\Psi_3\rangle}{\langle\Psi_3|\Psi_3\rangle} = -\frac{\langle\Psi_3|\tilde{\Psi}_4\rangle}{\frac{1}{2} + \frac{7}{8U^2} + \mathcal{O}(1/U^3)} = -2\langle\Psi_3|\tilde{\Psi}_4\rangle(1 - 7/4U^2) + \mathcal{O}(1/U^3) \\ &= -\frac{1}{2U} + \frac{1}{U^2}2(-\langle\Psi_3^{(0)}|\tilde{\Psi}_4^{(2)}\rangle - \langle\Psi_3^{(1)}|\tilde{\Psi}_4^{(1)}\rangle - \langle\Psi_3^{(2)}|\tilde{\Psi}_4^{(0)}\rangle)(1 - \frac{7}{4U^2}) + \mathcal{O}(1/U^3) \\ &= -1/2U + \mathcal{O}(1/U^3) \end{aligned}$$

$$\boxed{e_3 = -\frac{1}{2U} + \mathcal{O}(1/U^3) \stackrel{(E.78)}{\Rightarrow} \varepsilon_3^{(0)} = 0 \wedge \varepsilon_3^{(1)} = \frac{1}{2} \wedge \varepsilon_3^{(2)} = 0}$$
 (E.167)

$$\begin{aligned} |\Psi_4^{(2)}\rangle &= |\tilde{\Psi}_4^{(2)}\rangle + e_3^{(1)}|\Psi_3^{(1)}\rangle + \tau_2^{(0)}|\Psi_2^{(2)}\rangle + \tau_2^{(2)}|\Psi_2^{(0)}\rangle \\ &= |\tilde{\Psi}_4^{(2)}\rangle + 1/4|\gamma_1\rangle - 1/2|m_{3u}\rangle + 1/4|\phi_{-1}\rangle + 3/8|\gamma_1\rangle - 1/2|m_{1u}\rangle - |m_{3u}\rangle - 3/4|\gamma_1\rangle \\ &= |\tilde{\Psi}_4^{(2)}\rangle + 1/4|\phi_{-1}\rangle - 1/8|\gamma_1\rangle - 1/2|m_{1u}\rangle - 3/2|m_{3u}\rangle \end{aligned}$$

$$\boxed{|\Psi_4\rangle = |\gamma_3\rangle + \frac{1}{U}\left\{\frac{1}{2}|\gamma_2\rangle - |m_{4u}\rangle\right\} + \frac{1}{U^2}\left\{-\frac{1}{4}|\gamma_1\rangle + \frac{3}{8}|\gamma_3\rangle + \frac{1}{2}|m_{3u}\rangle + |m_{5u}\rangle\right\} + \mathcal{O}(1/U^3)}$$
 (E.168)

Norm of $|\Psi_4\rangle$

$$2\langle\Psi_4|\Psi_4\rangle = 1 + 1/U^2\{2(3/8 + 1/4) + 1/4 + 1\} + \mathcal{O}(1/U^3) = 1 + 1/U^2\{10/4\} + \mathcal{O}(1/U^3)$$

$$\boxed{\|\Psi_4\|^2 = \langle\Psi_4|\Psi_4\rangle = \frac{1}{2} + \frac{5}{4U^2} + \mathcal{O}(1/U^3)}$$
 (E.169)

$$\begin{aligned}
\tilde{\tau}_3 &= -\frac{\langle \Psi_4 | \Psi_4 \rangle}{\langle \Psi_3 | \Psi_3 \rangle} = -(1/2 + 5/4U^2)2(1 + 7/4U^2)^{-1} + \mathcal{O}(1/U^3) = -(1 + 10/4U^2)(1 - 7/4U^2) + \mathcal{O}(1/U^3) \\
&= -1 - [-7/4U^2 + 10/4U^2] + \mathcal{O}(1/U^3) = -1 - 3/4U^2 + \mathcal{O}(1/U^3)
\end{aligned}$$

$$\tilde{\tau}_3 = -1 - \frac{3}{4U^2} + \mathcal{O}(1/U^3)$$

(E.170)

Off-Diagonal Element τ_3

$$\tau_3 := -\sqrt{-\tilde{\tau}_3} = -\sqrt{1 + \frac{3}{4U^2} + \mathcal{O}(1/U^3)} = -(1 + \frac{3}{8U^2} + \mathcal{O}(1/U^3))$$

$$\tau_3 = -1 - \frac{3}{8U^2} + \mathcal{O}(1/U^3) \stackrel{(E.78)}{\Rightarrow} t_3^{(0)} = 1 \wedge t_3^{(1)} = 0 \wedge t_3^{(2)} = \frac{3}{8}$$

(E.171)

Fifth Iteration: $|\Psi_5\rangle := -\mathcal{L}|\Psi_4\rangle + e_4|\Psi_4\rangle + \tau_3|\Psi_3\rangle$

$$\begin{aligned}
|\tilde{\Psi}_5^{(2)}\rangle &:= -\mathcal{L}^{(0)}|\Psi_4^{(2)}\rangle - \mathcal{L}^{(1)}|\Psi_4^{(1)}\rangle - \mathcal{L}^{(2)}|\Psi_4^{(0)}\rangle \\
&= \mathcal{L}^{(0)}\{1/4|\gamma_1\rangle - 3/8|\gamma_3\rangle - 1/2|m_{3u}\rangle - |m_{5u}\rangle\} + \mathcal{L}^{(1)}\{-1/2|\gamma_2\rangle + |m_{4u}\rangle\} - \mathcal{L}^{(2)}|\gamma_3\rangle \\
&= 1/4|\gamma_0\rangle + 1/4|\gamma_2\rangle - 3/8|\gamma_2\rangle - 3/8|\gamma_4\rangle - 1/2|m_{2u}\rangle - 1/2|m_{4u}\rangle - |m_{4u}\rangle - |m_{6u}\rangle \\
&\quad + 1/4|\gamma_2\rangle - 1/2|m_{4u}\rangle - t_2^{(2)}|\gamma_2\rangle + \varepsilon_3^{(2)}|\gamma_3\rangle - t_3^{(2)}|\gamma_4\rangle \\
&= 1/4|\gamma_0\rangle + (1/8 - t_2^{(2)})|\gamma_2\rangle + \varepsilon_3^{(2)}|\gamma_3\rangle - (3/8 + t_3^{(2)})|\gamma_4\rangle - 1/2|m_{2u}\rangle - 2|m_{4u}\rangle - |m_{6u}\rangle
\end{aligned}$$

We use $\varepsilon_3^{(2)} = 0$, $t_2^{(2)} = t_3^{(2)} = 3/8$ and obtain

$$\begin{aligned}
|\tilde{\Psi}_5\rangle &= -|\gamma_2\rangle - |\gamma_4\rangle + \frac{1}{U}\{-\frac{1}{2}|\gamma_1\rangle + |m_{3u}\rangle + |m_{5u}\rangle\} \\
&\quad + \frac{1}{U^2}\{\frac{1}{4}|\gamma_0\rangle - \frac{1}{4}|\gamma_2\rangle - \frac{3}{4}|\gamma_4\rangle - \frac{1}{2}|m_{2u}\rangle - 2|m_{4u}\rangle - |m_{6u}\rangle\} + \mathcal{O}(1/U^3).
\end{aligned}$$

(E.172)

$$\begin{aligned}
e_4 &= \frac{\langle \Psi_4 | \mathcal{L} | \Psi_4 \rangle}{\langle \Psi_4 | \Psi_4 \rangle} = -\frac{\langle \Psi_4 | \tilde{\Psi}_5 \rangle}{\frac{1}{2} + \frac{5}{4U^2} + \mathcal{O}(1/U^3)} = -\langle \Psi_4 | \tilde{\Psi}_5 \rangle 2(1 - 10/4U^2) + \mathcal{O}(1/U^3) \\
&= -\frac{1}{2U} + \frac{1}{U^2}2(-\langle \Psi_4^{(0)} | \tilde{\Psi}_5^{(2)} \rangle - \langle \Psi_4^{(1)} | \tilde{\Psi}_5^{(1)} \rangle - \langle \Psi_4^{(2)} | \tilde{\Psi}_5^{(0)} \rangle)(1 - \frac{10}{4U^2}) + \mathcal{O}(1/U^3) \\
&= -1/2U + \mathcal{O}(1/U^3)
\end{aligned}$$

$$e_4 = -\frac{1}{2U} + \mathcal{O}(1/U^3) \stackrel{(E.78)}{\Rightarrow} \varepsilon_4^{(0)} = 0 \wedge \varepsilon_4^{(1)} = \frac{1}{2} \wedge \varepsilon_4^{(2)} = 0$$

(E.173)

$$\begin{aligned}
|\Psi_5^{(2)}\rangle &= |\tilde{\Psi}_5^{(2)}\rangle + e_4^{(1)}|\Psi_4^{(1)}\rangle + \tau_3^{(0)}|\Psi_3^{(2)}\rangle + \tau_3^{(2)}|\Psi_3^{(0)}\rangle \\
&= |\tilde{\Psi}_5^{(2)}\rangle - 1/4|\gamma_2\rangle + 1/2|m_{4u}\rangle - 1/4|\gamma_0\rangle + 1/2|m_{2u}\rangle + |m_{4u}\rangle + 3/4|\gamma_2\rangle \\
&= |\tilde{\Psi}_5^{(2)}\rangle - 1/4|\gamma_0\rangle + 1/4|\gamma_2\rangle + 1/2|m_{2u}\rangle + 3/2|m_{4u}\rangle
\end{aligned}$$

$$|\Psi_5\rangle = -|\gamma_4\rangle + \frac{1}{U}\{-\frac{1}{2}|\gamma_3\rangle + |m_{5u}\rangle\} + \frac{1}{U^2}\{\frac{1}{4}|\gamma_2\rangle - \frac{3}{4}|\gamma_4\rangle - \frac{1}{2}|m_{4u}\rangle - |m_{6u}\rangle\} + \mathcal{O}(1/U^3)$$

(E.174)

E. Explicit Calculations

Norm of $|\Psi_5\rangle$

$$2\langle\Psi_5|\Psi_5\rangle = 1 + 1/U^2\{2[3/4 + 1/4] + 1/4 + 1\} + \mathcal{O}(1/U^3) = 1 + 1/U^2\{13/4\} + \mathcal{O}(1/U^3)$$

$$\boxed{\|\Psi_5\|^2 = \langle\Psi_5|\Psi_5\rangle = \frac{1}{2} + \frac{13}{8U^2} + \mathcal{O}(1/U^3)} \quad (\text{E.175})$$

$$\begin{aligned} \tilde{\tau}_4 &= -\frac{\langle\Psi_5|\Psi_5\rangle}{\langle\Psi_4|\Psi_4\rangle} = -(1/2 + 13/8U^2)2(1 + 10/4U^2)^{-1} + \mathcal{O}(1/U^3) = -(1 + 13/4U^2)(1 - 10/4U^2) + \mathcal{O}(1/U^3) \\ &= -1 - [-10/4U^2 + 13/4U^2] + \mathcal{O}(1/U^3) = -1 - 3/4U^2 + \mathcal{O}(1/U^3) \end{aligned}$$

$$\boxed{\tilde{\tau}_4 = -1 - \frac{3}{4U^2} + \mathcal{O}(1/U^3)} \quad (\text{E.176})$$

Off-Diagonal Element τ_4

$$\tau_4 := -\sqrt{-\tilde{\tau}_4} = -\sqrt{1 + \frac{3}{4U^2} + \mathcal{O}(1/U^3)} = -(1 + \frac{3}{8U^2} + \mathcal{O}(1/U^3))$$

$$\boxed{\tau_4 = -1 - \frac{3}{8U^2} + \mathcal{O}(1/U^3) \stackrel{(E.78)}{\Rightarrow} t_4^{(0)} = 1 \wedge t_4^{(1)} = 0 \wedge t_4^{(2)} = \frac{3}{8}} \quad (\text{E.177})$$

No go on by induction.

Induction Hypothesis to Second Order

Let $N \geq 6$, then we find for all $3 \leq n < N$

$$\begin{aligned} |\Psi_n\rangle &= (-1)^n \left(|\gamma_{n-1}\rangle + \frac{1}{U} \left\{ \frac{1}{2} |\gamma_{n-2}\rangle - |m_{nu}\rangle \right\} \right. \\ &\quad \left. + \frac{1}{U^2} \left\{ -\frac{1}{4} |\gamma_{n-3}\rangle + a_n |\gamma_{n-1}\rangle + \frac{1}{2} |m_{n-1u}\rangle + |m_{n+1u}\rangle \right\} \right) + \mathcal{O}(1/U^3), \end{aligned} \quad (\text{E.178})$$

$$a_n := (n-3)\frac{3}{8} \quad (\text{E.179})$$

$$e_{n-1} = -\frac{1}{2U} + \mathcal{O}(1/U^3), \quad (\text{E.180})$$

$$\tau_{n-1} = -1 - \frac{3}{4U^2} + \mathcal{O}(1/U^3), \quad (\text{E.181})$$

which implies

$$\varepsilon_{n-1} = \frac{1}{2U} + \mathcal{O}(1/U^3), \quad (\text{E.182})$$

$$t_{n-1} = 1 + \frac{3}{8U^2} + \mathcal{O}(1/U^3). \quad (\text{E.183})$$

We further have

$$\langle\Psi_n|\Psi_n\rangle = \frac{1}{2} + \frac{1}{U^2} \left\{ a_n + \frac{7}{8} \right\} + \mathcal{O}(1/U^3). \quad (\text{E.184})$$

We note in passing that a_n linearly increases with order n .

Induction Step The induction hypothesis (i.h.) has been proven for $n = 3, 4, 5$ and, thus, we may proceed with the induction step. Since we already proved that $|\Psi_N^{(0)}\rangle$ and $|\Psi_N^{(1)}\rangle$ obey the formula, we go on with the proof for $|\Psi_N^{(2)}\rangle$.

$$\begin{aligned}
 |\tilde{\Psi}_N^{(2)}\rangle &:= -\mathcal{L}^{(0)}|\Psi_{N-1}^{(2)}\rangle - \mathcal{L}^{(1)}|\Psi_{N-1}^{(1)}\rangle - \mathcal{L}^{(2)}|\Psi_{N-1}^{(0)}\rangle \\
 &\stackrel{\text{i.h.}}{=} (-1)^N \left(\mathcal{L}^{(0)} \{ -1/4|\gamma_{N-4}\rangle + (N-4)^{3/8}|\gamma_{N-2}\rangle + 1/2|m_{N-2u}\rangle + |m_{Nu}\rangle \} \right. \\
 &\quad \left. + \mathcal{L}^{(1)} \{ 1/2|\gamma_{N-3}\rangle - |m_{N-1u}\rangle \} + \mathcal{L}^{(2)}|\gamma_{N-2}\rangle \right) \\
 &= (-1)^N \left(-1/4|\gamma_{N-5}\rangle - 1/4|\gamma_{N-3}\rangle + (N-4)^{3/8}(|\gamma_{N-3}\rangle + |\gamma_{N-1}\rangle) \right. \\
 &\quad \left. + 1/2|m_{N-3u}\rangle + 1/2|m_{N-1u}\rangle + |m_{N-1u}\rangle + |m_{N+1u}\rangle - 1/4|\gamma_{N-3}\rangle \right. \\
 &\quad \left. + 1/2|m_{N-1u}\rangle + t_{N-3}^{(2)}|\gamma_{N-3}\rangle - \varepsilon_{N-2}^{(2)}|\gamma_{N-2}\rangle + t_{N-2}^{(2)}|\gamma_{N-1}\rangle \right) \\
 &= (-1)^N \left(-1/4|\gamma_{N-5}\rangle + ((N-4)^{3/8} - 1/2 + t_{N-3}^{(2)})|\gamma_{N-3}\rangle \right. \\
 &\quad \left. - \varepsilon_{N-2}^{(2)}|\gamma_{N-2}\rangle + ((N-4)^{3/8} + t_{N-2}^{(2)})|\gamma_{N-1}\rangle \right. \\
 &\quad \left. + 1/2|m_{N-3u}\rangle + 2|m_{N-1u}\rangle + |m_{N+1u}\rangle \right) \\
 &\stackrel{\text{i.h.}}{=} (-1)^N \left(-1/4|\gamma_{N-5}\rangle + ((N-3)^{3/8} - 4/8)|\gamma_{N-3}\rangle \right. \\
 &\quad \left. + (N-3)^{3/8}|\gamma_{N-1}\rangle + 1/2|m_{N-3u}\rangle + 2|m_{N-1u}\rangle + |m_{N+1u}\rangle \right)
 \end{aligned}$$

$$\boxed{|\tilde{\Psi}_N^{(2)}\rangle = (-1)^N \left\{ -\frac{1}{4}|\gamma_{N-5}\rangle + \left(a_n - \frac{4}{8}\right)|\gamma_{N-3}\rangle + a_N|\gamma_{N-1}\rangle + \frac{1}{2}|m_{N-3u}\rangle + 2|m_{N-1u}\rangle + |m_{N+1u}\rangle \right\}} \quad (\text{E.185})$$

$$\begin{aligned}
 e_{N-1} &= \frac{\langle \Psi_{N-1} | \mathcal{L} | \Psi_{N-1} \rangle}{\langle \Psi_{N-1} | \Psi_{N-1} \rangle} = -\frac{\langle \Psi_{N-1} | \tilde{\Psi}_N \rangle}{\frac{1}{2} + (N-4)\frac{3}{8U^2} + \frac{7}{8U^2} + \mathcal{O}(1/U^3)} \\
 &= -\langle \Psi_{N-1} | \tilde{\Psi}_N \rangle 2 \left(1 - (N-4)\frac{3}{4U^2} - \frac{7}{4U^2} \right) + \mathcal{O}(1/U^3) \\
 &= -\frac{1}{2U} + \frac{1}{U^2} 2 \left(-\langle \Psi_{N-1}^{(0)} | \tilde{\Psi}_N^{(2)} \rangle - \langle \Psi_{N-1}^{(1)} | \tilde{\Psi}_N^{(1)} \rangle - \langle \Psi_{N-1}^{(2)} | \tilde{\Psi}_N^{(0)} \rangle \right) \\
 &\quad \times \left(1 - (N-4)\frac{3}{4U^2} - \frac{7}{4U^2} \right) + \mathcal{O}(1/U^3) \\
 &= -1/2U + \mathcal{O}(1/U^3)
 \end{aligned}$$

$$\boxed{e_{N-1} = -\frac{1}{2U} + \mathcal{O}(1/U^3) \stackrel{(\text{E.78})}{\Rightarrow} \varepsilon_{N-1}^{(0)} = 0 \wedge \varepsilon_{N-1}^{(1)} = \frac{1}{2} \wedge \varepsilon_{N-1}^{(2)} = 0} \quad (\text{E.186})$$

$$\begin{aligned}
 |\Psi_N^{(2)}\rangle &= |\tilde{\Psi}_N^{(2)}\rangle + e_{N-1}^{(1)}|\Psi_{N-1}^{(1)}\rangle + \tau_{N-2}^{(0)}|\Psi_{N-2}^{(2)}\rangle + \tau_{N-2}^{(2)}|\Psi_{N-2}^{(0)}\rangle \\
 &= |\tilde{\Psi}_N^{(2)}\rangle + (-1)^N \{ 1/4|\gamma_{N-3}\rangle - 1/2|m_{N-1u}\rangle \} + (-1)^{N-1} \{ -1/4|\gamma_{N-5}\rangle + a_{N-2}|\gamma_{N-3}\rangle \\
 &\quad + 1/2|m_{N-3u}\rangle + |m_{N-1u}\rangle \} + (-1)^{N-1} 3/4|\gamma_{N-3}\rangle \\
 &= |\tilde{\Psi}_N^{(2)}\rangle + (-1)^N \{ 1/4|\gamma_{N-5}\rangle - (a_{N-2} + 1/2)|\gamma_{N-3}\rangle - 1/2|m_{N-3u}\rangle - 3/2|m_{N-1u}\rangle \}
 \end{aligned}$$

E. Explicit Calculations

Norm of $|\Psi_N\rangle$ Together with $|\Psi_N^{(0)}\rangle$ and $|\Psi_N^{(1)}\rangle$ it follows that the norm of $|\Psi_N\rangle$ is given by

$$2\langle\Psi_N|\Psi_N\rangle = 1 + \frac{1}{U^2}\left\{2\left[(N-3)\frac{3}{8} + \frac{1}{4}\right] + \frac{5}{4}\right\} + \mathcal{O}(1/U^3)$$

$$\boxed{\langle\Psi_N|\Psi_N\rangle = \frac{1}{2} + \frac{1}{U^2}\left\{a_N + \frac{7}{8}\right\} + \mathcal{O}(1/U^3)} \quad (\text{E.187})$$

and, thus,

$$\tilde{\tau}_{N-1} = -\frac{\langle\Psi_N|\Psi_N\rangle}{\langle\Psi_{N-1}|\Psi_{N-1}\rangle} = -(1 + \frac{1}{U^2}\left\{(N-3)\frac{3}{8} + \frac{7}{8}\right\})2\left(1 - \frac{1}{U^2}\left\{(N-4)\frac{3}{4} + \frac{7}{4}\right\}\right) + \mathcal{O}(1/U^3),$$

$$\boxed{\tilde{\tau}_{N-1} = -1 - \frac{3}{4U^2} + \mathcal{O}(1/U^3)}. \quad (\text{E.188})$$

Off-Diagonal Element τ_{N-1}

$$\tau_{N-1} := -\sqrt{-\tilde{\tau}_{N-1}} = -\sqrt{1 + \frac{3}{4U^2} + \mathcal{O}(1/U^3)} = -(1 + \frac{3}{8U^2} + \mathcal{O}(1/U^3))$$

$$\boxed{\tau_{N-1} = -1 - \frac{3}{8U^2} + \mathcal{O}(1/U^3) \stackrel{(\text{E.78})}{\Rightarrow} t_{N-1}^{(0)} = 1 \wedge t_{N-1}^{(1)} = 0 \wedge t_{N-1}^{(2)} = \frac{3}{8}} \quad (\text{E.189})$$

□

Summary of the Results to Second Order

To second order we may summarize the Lanczos iteration in the following form:

$$|\Psi_0\rangle = |\phi_{-1}\rangle - \frac{1}{U}|m_{0u}\rangle + \frac{1}{U^2}\left\{-\frac{1}{2}|\phi_{-1}\rangle + |m_{1u}\rangle\right\} + \mathcal{O}(1/U^3), \quad (\text{E.190a})$$

$$|\tilde{\Psi}_1\rangle = -|\gamma_0\rangle + \frac{1}{U}\left\{-\frac{1}{2}|\phi_{-1}\rangle + |m_{1u}\rangle\right\} + \frac{1}{U^2}\left\{\frac{3}{4}|\gamma_0\rangle - \frac{1}{2}|m_{0u}\rangle - |m_{2u}\rangle\right\} + \mathcal{O}(1/U^3), \quad (\text{E.190b})$$

$$|\Psi_1\rangle = -|\gamma_0\rangle + \frac{1}{U}\left\{-\frac{1}{2}|\phi_{-1}\rangle + |m_{1u}\rangle\right\} + \frac{1}{U^2}\left\{\frac{3}{4}|\gamma_0\rangle - \frac{1}{2}|m_{0u}\rangle - |m_{2u}\rangle\right\} + \mathcal{O}(1/U^3), \quad (\text{E.190c})$$

$$\begin{aligned} |\tilde{\Psi}_2\rangle &= |\phi_{-1}\rangle + |\gamma_1\rangle + \frac{1}{U}\left\{-|m_{0u}\rangle - |m_{2u}\rangle\right\} \\ &+ \frac{1}{U^2}\left\{-\frac{3}{4}|\phi_{-1}\rangle - \frac{3}{8}|\gamma_1\rangle + 2|m_{1u}\rangle + |m_{3u}\rangle\right\} + \mathcal{O}(1/U^3), \end{aligned} \quad (\text{E.190d})$$

$$|\Psi_2\rangle = |\gamma_1\rangle + \frac{1}{U}\left\{\frac{1}{2}|\gamma_0\rangle - |m_{2u}\rangle\right\} + \frac{1}{U^2}\left\{-\frac{1}{4}|\phi_{-1}\rangle - \frac{3}{8}|\gamma_1\rangle + \frac{1}{2}|m_{1u}\rangle + |m_{3u}\rangle\right\} + \mathcal{O}(1/U^3), \quad (\text{E.190e})$$

$$\begin{aligned} |\tilde{\Psi}_3\rangle &= -|\gamma_0\rangle - |\gamma_2\rangle + \frac{1}{U}\left\{-\frac{1}{2}|\phi_{-1}\rangle + |m_{1u}\rangle + |m_{3u}\rangle\right\} \\ &+ \frac{1}{U^2}\left\{\frac{1}{2}|\gamma_0\rangle - \frac{1}{2}|m_{0u}\rangle - 2|m_{2u}\rangle - |m_{4u}\rangle\right\} + \mathcal{O}(1/U^3), \end{aligned} \quad (\text{E.190f})$$

$$|\Psi_3\rangle = -|\gamma_2\rangle + \frac{1}{U}\left\{-\frac{1}{2}|\gamma_1\rangle + |m_{3u}\rangle\right\} + \frac{1}{U^2}\left\{\frac{1}{4}|\gamma_0\rangle - \frac{1}{2}|m_{2u}\rangle - |m_{4u}\rangle\right\} + \mathcal{O}(1/U^3), \quad (\text{E.190g})$$

$$\begin{aligned} |\tilde{\Psi}_4\rangle &= |\gamma_1\rangle + |\gamma_3\rangle + \frac{1}{U}\left\{\frac{1}{2}|\gamma_0\rangle - |m_{2u}\rangle - |m_{4u}\rangle\right\} \\ &+ \frac{1}{U^2}\left\{-\frac{1}{4}|\phi_{-1}\rangle - \frac{1}{8}|\gamma_1\rangle + \frac{3}{8}|\gamma_3\rangle + \frac{1}{2}|m_{1u}\rangle + 2|m_{3u}\rangle + |m_{5u}\rangle\right\} + \mathcal{O}(1/U^3), \end{aligned} \quad (\text{E.190i})$$

$$|\Psi_4\rangle = |\gamma_3\rangle + \frac{1}{U}\left\{\frac{1}{2}|\gamma_2\rangle - |m_{4u}\rangle\right\} + \frac{1}{U^2}\left\{-\frac{1}{4}|\gamma_1\rangle + \frac{3}{8}|\gamma_3\rangle + \frac{1}{2}|m_{3u}\rangle + |m_{5u}\rangle\right\} + \mathcal{O}(1/U^3), \quad (\text{E.190j})$$

and for $n \geq 5$

$$\begin{aligned} |\tilde{\Psi}_n\rangle &= (-1)^n \left(\{|\gamma_{n-3}\rangle + |\gamma_{n-1}\rangle\} + \frac{1}{U} \left\{ \frac{1}{2}|\gamma_{n-4}\rangle - |m_{n-2u}\rangle - |m_{nu}\rangle \right\} \right. \\ &\quad + \frac{1}{U^2} \left\{ -\frac{1}{4}|\gamma_{n-5}\rangle + \left(a_n - \frac{4}{8}\right)|\gamma_{n-3}\rangle \right. \\ &\quad \left. \left. + a_n|\gamma_{n-1}\rangle + \frac{1}{2}|m_{n-3u}\rangle + 2|m_{n-1u}\rangle + |m_{n+1u}\rangle \right\} \right), \end{aligned} \quad (\text{E.190k})$$

$$\begin{aligned} |\Psi_n\rangle &= (-1)^n \left(|\gamma_{n-1}\rangle + \frac{1}{U} \left\{ \frac{1}{2}|\gamma_{n-2}\rangle - |m_{nu}\rangle \right\} \right. \\ &\quad \left. + \frac{1}{U^2} \left\{ -\frac{1}{4}|\gamma_{n-3}\rangle + a_n|\gamma_{n-1}\rangle + \frac{1}{2}|m_{n-1u}\rangle + |m_{n+1u}\rangle \right\} \right). \end{aligned} \quad (\text{E.190l})$$

Thus, we have

$$e_0 = \mathcal{O}(1/U^3) \quad \wedge \quad e_n = -\frac{1}{2U} + \mathcal{O}(1/U^3), \quad (\text{E.191a})$$

$$\tau_0 = -1 - \frac{1}{4U^2} + \mathcal{O}(1/U^3) \quad \wedge \quad \tau_n = -1 - \frac{3}{4U^2} + \mathcal{O}(1/U^3) \quad n \geq 1, \quad (\text{E.191b})$$

and for the parameters of the SIAM

$$\varepsilon_0 = \mathcal{O}(1/U^3) \quad \wedge \quad \varepsilon_n = \frac{1}{2U} + \mathcal{O}(1/U^3), \quad (\text{E.192a})$$

$$t_0 = 1 + \frac{1}{4U^2} + \mathcal{O}(1/U^3) \quad \wedge \quad t_n = 1 + \frac{3}{4U^2} + \mathcal{O}(1/U^3) \quad n \geq 1. \quad (\text{E.192b})$$

E.6.4. Third Order

The starting vector to third order reads, according to (E.35),

$$|\Psi_0\rangle = |\phi_{-1}\rangle - \frac{1}{U}|m_{0u}\rangle + \frac{1}{U^2} \left\{ -\frac{1}{2}|\phi_{-1}\rangle + |m_{1u}\rangle \right\} - \frac{1}{U^3} \left\{ \frac{7}{4}|m_{0u}\rangle + |m_{2u}\rangle \right\} + \mathcal{O}\left(\frac{1}{U^4}\right) \quad (\text{E.193})$$

and has the norm

$$\|\Psi_0\|^2 = \frac{1}{2} + \mathcal{O}\left(\frac{1}{U^4}\right). \quad (\text{E.194})$$

With $\mathcal{L}^{(3)}$ given by (E.54) and its action, see (E.75a) and (E.75b), we can do the Lanczos iteration to third order.

First Iteration: $|\Psi_1\rangle := -\mathcal{L}|\Psi_0\rangle + e_0|\Psi_0\rangle$

$$\begin{aligned} |\tilde{\Psi}_1^{(3)}\rangle &:= -\mathcal{L}^{(0)}|\Psi_0^{(3)}\rangle - \mathcal{L}^{(1)}|\Psi_0^{(2)}\rangle - \mathcal{L}^{(2)}|\Psi_0^{(1)}\rangle - \mathcal{L}^{(3)}|\Psi_0^{(0)}\rangle \\ &= 7/4\mathcal{L}^{(0)}|m_{0u}\rangle + \mathcal{L}^{(0)}|m_{2u}\rangle + 1/2\mathcal{L}^{(1)}|\phi_{-1}\rangle - \mathcal{L}^{(1)}|m_{1u}\rangle + \mathcal{L}^{(2)}|m_{0u}\rangle - \mathcal{L}^{(3)}|\phi_{-1}\rangle \\ &= -1/2|\phi_{-1}\rangle - |\gamma_1\rangle + \frac{1}{4} \underbrace{\{|m_{1u}\rangle - |m_{1d}\rangle\}}_{|\gamma_1\rangle} + 25/8|m_{1u}\rangle + |m_{3u}\rangle \\ &= -1/2|\phi_{-1}\rangle - 3/4|\gamma_1\rangle + 25/8|m_{1u}\rangle + |m_{3u}\rangle \end{aligned}$$

$$\boxed{|\tilde{\Psi}_1\rangle = -|\gamma_0\rangle + \frac{1}{U} \left\{ -\frac{1}{2}|\phi_{-1}\rangle + |m_{1u}\rangle \right\} + \frac{1}{U^2} \left\{ \frac{3}{4}|\gamma_0\rangle - \frac{1}{2}|m_{0u}\rangle - |m_{2u}\rangle \right\} + \frac{1}{U^3} \left\{ -\frac{1}{2}|\phi_{-1}\rangle - \frac{3}{4}|\gamma_1\rangle + \frac{25}{8}|m_{1u}\rangle + |m_{3u}\rangle \right\} + \mathcal{O}(1/U^4)} \quad (\text{E.195})$$

E. Explicit Calculations

$$e_0 = \frac{\langle \Psi_0 | \mathcal{L} | \Psi_0 \rangle}{\langle \Psi_0 | \Psi_0 \rangle} = -\frac{\langle \Psi_0 | \tilde{\Psi}_1 \rangle}{1/2 + \mathcal{O}(1/U^4)}$$

$$= \frac{1}{U^3} \{ -(-1/2) - (-3/8 + 1/2) - (1/4 + 1) - 7/8 \} + \mathcal{O}(1/U^4) = -14/8U^3 + \mathcal{O}(1/U^4)$$

$$\boxed{e_0 = -\frac{7}{4U^3} + \mathcal{O}(1/U^4) \stackrel{(E.78)}{\Rightarrow} \varepsilon_0^{(0)} = \varepsilon_0^{(1)} = \varepsilon_0^{(2)} = 0 \wedge \varepsilon_0^{(3)} = \frac{7}{4}} \quad (\text{E.196})$$

$$\boxed{|\Psi_1\rangle = -|\gamma_0\rangle + \frac{1}{U} \left\{ -\frac{1}{2}|\phi_{-1}\rangle + |m_{1u}\rangle \right\} + \frac{1}{U^2} \left\{ \frac{3}{4}|\gamma_0\rangle - \frac{1}{2}|m_{0u}\rangle - |m_{2u}\rangle \right\}$$

$$+ \frac{1}{U^3} \left\{ -\frac{9}{4}|\phi_{-1}\rangle - \frac{3}{4}|\gamma_1\rangle + \frac{25}{8}|m_{1u}\rangle + |m_{3u}\rangle \right\} + \mathcal{O}(1/U^4)} \quad (\text{E.197})$$

Norm of $|\Psi_1\rangle$

$$\boxed{\|\Psi_1\|^2 = \langle \Psi_1 | \Psi_1 \rangle = \frac{1}{2} + \frac{1}{8U^2} + \mathcal{O}(1/U^4)} \quad (\text{E.198})$$

$$\tilde{\tau}_0 = -\frac{\langle \Psi_1 | \Psi_1 \rangle}{\langle \Psi_0 | \Psi_0 \rangle} = -2\langle \Psi_1 | \Psi_1 \rangle + \mathcal{O}(1/U^4) = -1 - \frac{1}{4U^2} + \mathcal{O}(1/U^4)$$

$$\boxed{\tilde{\tau}_0 = -1 - \frac{1}{4U^2} + \mathcal{O}(1/U^4)} \quad (\text{E.199})$$

Off-Diagonal Element τ_0

$$\tau_0 := -\sqrt{-\tilde{\tau}_0} = -\sqrt{1 + \frac{1}{4U^2} + \mathcal{O}(1/U^4)} = -(1 + \frac{1}{8U^2} + \mathcal{O}(1/U^4))$$

$$\boxed{\tau_0 = -1 - \frac{1}{8U^2} + \mathcal{O}(1/U^4) \stackrel{(E.78)}{\Rightarrow} t_0^{(0)} = 1 \wedge t_0^{(1)} = 0 \wedge t_0^{(2)} = \frac{1}{8} \wedge t_0^{(3)} = 0} \quad (\text{E.200})$$

Second Iteration: $|\Psi_2\rangle := -\mathcal{L}|\Psi_1\rangle + e_1|\Psi_1\rangle + \tau_0|\Psi_0\rangle$

$$|\tilde{\Psi}_2^{(3)}\rangle := -\mathcal{L}^{(0)}|\Psi_1^{(3)}\rangle - \mathcal{L}^{(1)}|\Psi_1^{(2)}\rangle - \mathcal{L}^{(2)}|\Psi_1^{(1)}\rangle - \mathcal{L}^{(3)}|\Psi_1^{(0)}\rangle$$

$$= 9/4\mathcal{L}^{(0)}|\phi_{-1}\rangle + 3/4\mathcal{L}^{(0)}|\gamma_1\rangle - 25/8\mathcal{L}^{(0)}|m_{1u}\rangle - \mathcal{L}^{(0)}|m_{3u}\rangle - 3/4\mathcal{L}^{(1)}|\gamma_0\rangle + 1/2\mathcal{L}^{(1)}|m_{0u}\rangle + \mathcal{L}^{(1)}|m_{2u}\rangle$$

$$+ 1/2\mathcal{L}^{(2)}|\phi_{-1}\rangle - \mathcal{L}^{(2)}|m_{1u}\rangle + \mathcal{L}^{(3)}|\gamma_0\rangle$$

$$= -1/4|\gamma_0\rangle + 1/2|\gamma_2\rangle - 1/2 \underbrace{\{|m_{0u}\rangle - |m_{0d}\rangle\}}_{|\gamma_0\rangle} - 11/4|m_{0u}\rangle - 5|m_{2u}\rangle - |m_{4u}\rangle$$

$$\boxed{|\tilde{\Psi}_2\rangle = |\phi_{-1}\rangle + |\gamma_1\rangle + \frac{1}{U} \{-|m_{0u}\rangle - |m_{2u}\rangle\} + \frac{1}{U^2} \{-\frac{3}{4}|\phi_{-1}\rangle - \frac{3}{8}|\gamma_1\rangle + 2|m_{1u}\rangle + |m_{3u}\rangle\}$$

$$+ \frac{1}{U^3} \{-\frac{3}{4}|\gamma_0\rangle + \frac{1}{2}|\gamma_2\rangle - \frac{11}{4}|m_{0u}\rangle - 5|m_{2u}\rangle - |m_{4u}\rangle\} + \mathcal{O}(1/U^4)} \quad (\text{E.201})$$

$$e_1 = \frac{\langle \Psi_1 | \mathcal{L} | \Psi_1 \rangle}{\langle \Psi_1 | \Psi_1 \rangle} = -\frac{\langle \Psi_1 | \tilde{\Psi}_2 \rangle}{\frac{1}{2} + \frac{1}{8U^2} + \mathcal{O}(1/U^4)} = -2\langle \Psi_1 | \tilde{\Psi}_2 \rangle (1 - 1/4U^2) + \mathcal{O}(1/U^4)$$

$$= \left\{ -\frac{1}{2U} + \frac{2}{U^3} (-\langle \Psi_1^{(0)} | \tilde{\Psi}_2^{(3)} \rangle - \langle \Psi_1^{(1)} | \tilde{\Psi}_2^{(2)} \rangle - \langle \Psi_1^{(2)} | \tilde{\Psi}_2^{(1)} \rangle - \langle \Psi_1^{(3)} | \tilde{\Psi}_2^{(0)} \rangle) \right\} (1 - \frac{1}{4U^2}) + \mathcal{O}(1/U^4)$$

$$= \left(-\frac{1}{2U} - \frac{32}{8U^3}\right)\left(1 - \frac{1}{4U^2}\right) + \mathcal{O}(1/U^4) = -\frac{1}{2U} - \frac{31}{8U^3} + \mathcal{O}(1/U^4)$$

$$\boxed{e_1 = -\frac{1}{2U} - \frac{31}{8U^3} + \mathcal{O}(1/U^4) \stackrel{(E.78)}{\Rightarrow} \varepsilon_1^{(0)} = 0 \wedge \varepsilon_1^{(1)} = \frac{1}{2} \wedge \varepsilon_1^{(2)} = 0 \wedge \varepsilon_1^{(3)} = \frac{31}{8}} \quad (E.202)$$

$$\begin{aligned} |\Psi_2^{(3)}\rangle &= |\tilde{\Psi}_2^{(3)}\rangle + e_1^{(1)}|\Psi_2^{(2)}\rangle + e_1^{(3)}|\Psi_1^{(0)}\rangle + \tau_0^{(0)}|\Psi_0^{(3)}\rangle + \tau_0^{(2)}|\Psi_0^{(1)}\rangle \\ &= \frac{11}{4}|\gamma_0\rangle + \frac{1}{2}|\gamma_2\rangle - \frac{1}{2}|m_{0u}\rangle - \frac{7}{2}|m_{2u}\rangle - |m_{4u}\rangle \end{aligned}$$

$$\boxed{|\Psi_2\rangle = |\gamma_1\rangle + \frac{1}{U}\left\{\frac{1}{2}|\gamma_0\rangle - |m_{2u}\rangle\right\} + \frac{1}{U^2}\left\{-\frac{1}{4}|\phi_{-1}\rangle - \frac{3}{8}|\gamma_1\rangle + \frac{1}{2}|m_{1u}\rangle + |m_{3u}\rangle\right\} + \frac{1}{U^3}\left\{\frac{11}{4}|\gamma_0\rangle + \frac{1}{2}|\gamma_2\rangle - \frac{1}{2}|m_{0u}\rangle - \frac{7}{2}|m_{2u}\rangle - |m_{4u}\rangle\right\} + \mathcal{O}(1/U^4)} \quad (E.203)$$

Norm of $|\Psi_2\rangle$

$$\boxed{\|\Psi_2\|^2 = \langle\Psi_2|\Psi_2\rangle = \frac{1}{2} + \frac{1}{2U^2} + \mathcal{O}(1/U^4)} \quad (E.204)$$

$$\begin{aligned} \tilde{\tau}_1 &= -\frac{\langle\Psi_2|\Psi_2\rangle}{\langle\Psi_1|\Psi_1\rangle} = -(1/2 + 1/2U^2)2(1 + 1/4U^2)^{-1} + \mathcal{O}(1/U^4) \\ &= -(1 + 1/U^2)(1 - 1/4U^2) + \mathcal{O}(1/U^4) \\ &= -1 - 3/4U^2 + \mathcal{O}(1/U^4) \end{aligned}$$

$$\boxed{\tilde{\tau}_1 = -1 - \frac{3}{4U^2} + \mathcal{O}(1/U^4)} \quad (E.205)$$

Off-Diagonal Element τ_1

$$\tau_1 := -\sqrt{-\tilde{\tau}_1} = -\sqrt{1 + \frac{3}{4U^2} + \mathcal{O}(1/U^4)} = -(1 + \frac{3}{8U^2} + \mathcal{O}(1/U^4))$$

$$\boxed{\tau_1 = -1 - \frac{3}{8U^2} + \mathcal{O}(1/U^4) \stackrel{(E.78)}{\Rightarrow} t_1^{(0)} = 1 \wedge t_1^{(1)} = 0 \wedge t_1^{(2)} = \frac{3}{8} \wedge t_1^{(3)} = 0} \quad (E.206)$$

Third Iteration: $|\Psi_3\rangle := -\mathcal{L}|\Psi_2\rangle + e_2|\Psi_2\rangle + \tau_1|\Psi_1\rangle$

$$\begin{aligned} |\tilde{\Psi}_3^{(3)}\rangle &:= -\mathcal{L}^{(0)}|\Psi_2^{(3)}\rangle - \mathcal{L}^{(1)}|\Psi_2^{(2)}\rangle - \mathcal{L}^{(2)}|\Psi_2^{(1)}\rangle - \mathcal{L}^{(3)}|\Psi_2^{(0)}\rangle \\ &= -11/4\mathcal{L}^{(0)}|\gamma_0\rangle - 1/2\mathcal{L}^{(0)}|\gamma_2\rangle + 1/2\mathcal{L}^{(0)}|m_{0u}\rangle + 7/2\mathcal{L}^{(0)}|m_{2u}\rangle + \mathcal{L}^{(0)}|m_{4u}\rangle + 1/4\mathcal{L}^{(1)}|\phi_{-1}\rangle \\ &\quad + 3/8\mathcal{L}^{(1)}|\gamma_1\rangle - 1/2\mathcal{L}^{(1)}|m_{1u}\rangle - \mathcal{L}^{(1)}|m_{3u}\rangle - 1/2\mathcal{L}^{(2)}|\gamma_0\rangle + \mathcal{L}^{(2)}|m_{2u}\rangle - \mathcal{L}^{(3)}|\gamma_1\rangle \\ &= -23/8|\phi_{-1}\rangle + 1/4|\gamma_1\rangle - 1/2|\gamma_3\rangle + 37/8|m_{1u}\rangle + 43/8|m_{3u}\rangle + |m_{5u}\rangle \end{aligned}$$

$$\boxed{|\tilde{\Psi}_3\rangle = -|\gamma_0\rangle - |\gamma_2\rangle + \frac{1}{U}\left\{-\frac{1}{2}|\phi_{-1}\rangle + |m_{1u}\rangle + |m_{3u}\rangle\right\} + \frac{1}{U^2}\left\{\frac{1}{2}|\gamma_0\rangle - \frac{1}{2}|m_{0u}\rangle - 2|m_{2u}\rangle - |m_{4u}\rangle\right\} + \frac{1}{U^3}\left\{-\frac{23}{8}|\phi_{-1}\rangle + \frac{1}{4}|\gamma_1\rangle - \frac{1}{2}|\gamma_3\rangle + \frac{37}{8}|m_{1u}\rangle + \frac{43}{8}|m_{3u}\rangle + |m_{5u}\rangle\right\} + \mathcal{O}(1/U^4)} \quad (E.207)$$

$$e_2 = \frac{\langle\Psi_2|\mathcal{L}|\Psi_2\rangle}{\langle\Psi_2|\Psi_2\rangle} = -\frac{\langle\Psi_2|\tilde{\Psi}_3\rangle}{\frac{1}{2} + \frac{1}{2U^2} + \mathcal{O}(1/U^4)} = -2\langle\Psi_2|\tilde{\Psi}_3\rangle(1 - 1/U^2) + \mathcal{O}(1/U^4)$$

E. Explicit Calculations

$$\begin{aligned}
&= \left\{ -\frac{1}{2U} + \frac{2}{U^3} \left(-\langle \Psi_2^{(0)} | \tilde{\Psi}_3^{(3)} \rangle - \langle \Psi_2^{(1)} | \tilde{\Psi}_3^{(2)} \rangle - \langle \Psi_2^{(2)} | \tilde{\Psi}_3^{(1)} \rangle - \langle \Psi_2^{(3)} | \tilde{\Psi}_3^{(0)} \rangle \right) \right\} \left(1 - \frac{1}{U^2} \right) + \mathcal{O}(1/U^4) \\
&= \left(-\frac{1}{2U} - \frac{39}{8U^3} \right) \left(1 - \frac{1}{U^2} \right) + \mathcal{O}(1/U^4) = -\frac{1}{2U} - \frac{35}{8U^3} + \mathcal{O}(1/U^4)
\end{aligned}$$

$$\boxed{e_2 = -\frac{1}{2U} - \frac{35}{8U^3} + \mathcal{O}(1/U^4) \stackrel{(E.78)}{\Rightarrow} \varepsilon_2^{(0)} = 0 \wedge \varepsilon_2^{(1)} = \frac{1}{2} \wedge \varepsilon_2^{(2)} = 0 \wedge \varepsilon_2^{(3)} = \frac{35}{8}} \quad (E.208)$$

$$\begin{aligned}
|\Psi_3^{(3)}\rangle &= |\tilde{\Psi}_3^{(3)}\rangle + e_2^{(1)} |\Psi_3^{(2)}\rangle + e_2^{(3)} |\Psi_2^{(0)}\rangle + \tau_1^{(0)} |\Psi_1^{(3)}\rangle + \tau_1^{(2)} |\Psi_1^{(1)}\rangle \\
&= -1/8 |\phi_{-1}\rangle - 51/16 |\gamma_1\rangle - 1/2 |\gamma_3\rangle + 1/2 |m_{1u}\rangle + 31/8 |m_{3u}\rangle + |m_{5u}\rangle
\end{aligned}$$

$$\boxed{|\Psi_3\rangle = -|\gamma_2\rangle + \frac{1}{U} \left\{ -\frac{1}{2} |\gamma_1\rangle + |m_{3u}\rangle \right\} + \frac{1}{U^2} \left\{ \frac{1}{4} |\gamma_0\rangle - \frac{1}{2} |m_{2u}\rangle - |m_{4u}\rangle \right\} + \frac{1}{U^3} \left\{ -\frac{1}{8} |\phi_{-1}\rangle - \frac{51}{16} |\gamma_1\rangle - \frac{1}{2} |\gamma_3\rangle + \frac{1}{2} |m_{1u}\rangle + \frac{31}{8} |m_{3u}\rangle + |m_{5u}\rangle \right\} + \mathcal{O}(1/U^4)} \quad (E.209)$$

Norm of $|\Psi_3\rangle$

$$\boxed{\|\Psi_3\|^2 = \langle \Psi_3 | \Psi_3 \rangle = \frac{1}{2} + \frac{7}{8U^2} + \mathcal{O}(1/U^4)} \quad (E.210)$$

$$\begin{aligned}
\tilde{\tau}_2 &= -\frac{\langle \Psi_3 | \Psi_3 \rangle}{\langle \Psi_2 | \Psi_2 \rangle} = -(1/2 + 7/8U^2) 2(1 + 1/U^2)^{-1} + \mathcal{O}(1/U^4) = -(1 + 7/4U^2)(1 - 1/U^2) + \mathcal{O}(1/U^4) \\
&= -1 - (-1/U^2 + 7/4U^2) + \mathcal{O}(1/U^4) = -1 - 3/4U^2 + \mathcal{O}(1/U^4)
\end{aligned}$$

$$\boxed{\tilde{\tau}_2 = -1 - \frac{3}{4U^2} + \mathcal{O}(1/U^4)} \quad (E.211)$$

Off-Diagonal Element τ_2

$$\tau_2 := -\sqrt{-\tilde{\tau}_2} = -\sqrt{1 + \frac{3}{4U^2} + \mathcal{O}(1/U^4)} = -(1 + \frac{3}{8U^2} + \mathcal{O}(1/U^4))$$

$$\boxed{\tau_2 = -1 - \frac{3}{8U^2} + \mathcal{O}(1/U^4) \stackrel{(E.78)}{\Rightarrow} t_2^{(0)} = 1 \wedge t_2^{(1)} = 0 \wedge t_2^{(2)} = \frac{3}{8} \wedge t_2^{(3)} = 0} \quad (E.212)$$

Fourth Iteration: $|\Psi_4\rangle := -\mathcal{L}|\Psi_3\rangle + e_3|\Psi_3\rangle + \tau_2|\Psi_2\rangle$

$$\begin{aligned}
|\tilde{\Psi}_4^{(3)}\rangle &:= -\mathcal{L}^{(0)}|\Psi_3^{(3)}\rangle - \mathcal{L}^{(1)}|\Psi_3^{(2)}\rangle - \mathcal{L}^{(2)}|\Psi_3^{(1)}\rangle - \mathcal{L}^{(3)}|\Psi_3^{(0)}\rangle \\
&= 1/8\mathcal{L}^{(0)}|\phi_{-1}\rangle + 51/16\mathcal{L}^{(0)}|\gamma_1\rangle + 1/2\mathcal{L}^{(0)}|\gamma_3\rangle - 1/2\mathcal{L}^{(0)}|m_{1u}\rangle - 31/8\mathcal{L}^{(0)}|m_{3u}\rangle - \mathcal{L}^{(0)}|m_{5u}\rangle \\
&\quad - 1/4\mathcal{L}^{(1)}|\gamma_0\rangle + 1/2\mathcal{L}^{(1)}|m_{2u}\rangle + \mathcal{L}^{(1)}|m_{4u}\rangle + 1/2\mathcal{L}^{(2)}|\gamma_1\rangle - \mathcal{L}^{(2)}|m_{3u}\rangle + \mathcal{L}^{(3)}|\gamma_2\rangle \\
&= 27/8|\gamma_0\rangle - 1/2|\gamma_2\rangle + 1/2|\gamma_4\rangle - 1/2|m_{0u}\rangle - 5|m_{2u}\rangle - 23/4|m_{4u}\rangle - |m_{6u}\rangle
\end{aligned}$$

$$\boxed{|\tilde{\Psi}_4\rangle = |\gamma_1\rangle + |\gamma_3\rangle + \frac{1}{U} \left\{ \frac{1}{2} |\gamma_0\rangle - |m_{2u}\rangle - |m_{4u}\rangle \right\} + \frac{1}{U^2} \left\{ -\frac{1}{4} |\phi_{-1}\rangle - \frac{1}{8} |\gamma_1\rangle + \frac{3}{8} |\gamma_3\rangle + \frac{1}{2} |m_{1u}\rangle + 2|m_{3u}\rangle + |m_{5u}\rangle \right\} + \frac{1}{U^3} \left\{ \frac{27}{8} |\gamma_0\rangle - \frac{1}{2} |\gamma_2\rangle + \frac{1}{2} |\gamma_4\rangle - \frac{1}{2} |m_{0u}\rangle - 5|m_{2u}\rangle - \frac{23}{4} |m_{4u}\rangle - |m_{6u}\rangle \right\} + \mathcal{O}(1/U^4)} \quad (E.213)$$

$$\begin{aligned}
e_3 &= \frac{\langle \Psi_3 | \mathcal{L} | \Psi_3 \rangle}{\langle \Psi_3 | \Psi_3 \rangle} = -\frac{\langle \Psi_3 | \tilde{\Psi}_4 \rangle}{\frac{1}{2} + \frac{7}{8U^2} + \mathcal{O}(1/U^4)} = -2\langle \Psi_3 | \tilde{\Psi}_4 \rangle (1 - 7/4U^2) + \mathcal{O}(1/U^4) \\
&= \left\{ -\frac{1}{2U} + \frac{2}{U^3} \left(-\langle \Psi_3^{(0)} | \tilde{\Psi}_4^{(3)} \rangle - \langle \Psi_3^{(1)} | \tilde{\Psi}_4^{(2)} \rangle - \langle \Psi_3^{(2)} | \tilde{\Psi}_4^{(1)} \rangle - \langle \Psi_3^{(3)} | \tilde{\Psi}_4^{(0)} \rangle \right) \right\} \left(1 - \frac{7}{4U^2} \right) + \mathcal{O}(1/U^4) \\
&= \left(-\frac{1}{2U} - \frac{42}{8U^3} \right) \left(1 - \frac{7}{4U^2} \right) + \mathcal{O}(1/U^4) = -\frac{1}{2U} - \frac{35}{8U^3} + \mathcal{O}(1/U^4)
\end{aligned}$$

$$e_3 = -\frac{1}{2U} - \frac{35}{8U^3} + \mathcal{O}(1/U^4) \stackrel{(E.78)}{\Rightarrow} \varepsilon_3^{(0)} = 0 \wedge \varepsilon_3^{(1)} = \frac{1}{2} \wedge \varepsilon_3^{(2)} = 0 \wedge \varepsilon_3^{(3)} = \frac{35}{8} \quad (E.214)$$

$$\begin{aligned}
|\Psi_4^{(3)}\rangle &= |\tilde{\Psi}_4^{(3)}\rangle + e_3^{(1)}|\Psi_3^{(2)}\rangle + e_3^{(3)}|\Psi_3^{(0)}\rangle + \tau_2^{(0)}|\Psi_2^{(3)}\rangle + \tau_2^{(2)}|\Psi_2^{(1)}\rangle \\
&= 1/8|\gamma_0\rangle + 27/8|\gamma_2\rangle + 1/2|\gamma_4\rangle - 1/2|m_{2u}\rangle - 17/4|m_{4u}\rangle - |m_{6u}\rangle
\end{aligned}$$

$$\begin{aligned}
|\Psi_4\rangle &= |\gamma_3\rangle + \frac{1}{U} \left\{ \frac{1}{2}|\gamma_2\rangle - |m_{4u}\rangle \right\} + \frac{1}{U^2} \left\{ -\frac{1}{4}|\gamma_1\rangle + \frac{3}{8}|\gamma_3\rangle + \frac{1}{2}|m_{3u}\rangle + |m_{5u}\rangle \right\} \\
&\quad + \frac{1}{U^3} \left\{ \frac{1}{8}|\gamma_0\rangle + \frac{27}{8}|\gamma_2\rangle + \frac{1}{2}|\gamma_4\rangle - \frac{1}{2}|m_{2u}\rangle - \frac{17}{4}|m_{4u}\rangle - |m_{6u}\rangle \right\} + \mathcal{O}(1/U^4)
\end{aligned}$$

(E.215)

Norm of $|\Psi_4\rangle$

$$\|\Psi_4\|^2 = \langle \Psi_4 | \Psi_4 \rangle = \frac{1}{2} + \frac{5}{4U^2} + \mathcal{O}(1/U^4) \quad (E.216)$$

$$\begin{aligned}
\tilde{\tau}_3 &= -\frac{\langle \Psi_4 | \Psi_4 \rangle}{\langle \Psi_3 | \Psi_3 \rangle} = -(1/2 + 5/4U^2)2(1 + 7/4U^2)^{-1} + \mathcal{O}(1/U^4) = -(1 + 10/4U^2)(1 - 7/4U^2) + \mathcal{O}(1/U^4) \\
&= -1 - [-7/4U^2 + 10/4U^2] + \mathcal{O}(1/U^4) = -1 - 3/4U^2 + \mathcal{O}(1/U^4)
\end{aligned}$$

$$\tilde{\tau}_3 = -1 - \frac{3}{4U^2} + \mathcal{O}(1/U^4) \quad (E.217)$$

Off-Diagonal Element τ_3

$$\tau_3 := -\sqrt{-\tilde{\tau}_3} = -\sqrt{1 + \frac{3}{4U^2} + \mathcal{O}(1/U^4)} = -\left(1 + \frac{3}{8U^2} + \mathcal{O}(1/U^4) \right)$$

$$\tau_3 = -1 - \frac{3}{8U^2} + \mathcal{O}(1/U^4) \stackrel{(E.78)}{\Rightarrow} t_3^{(0)} = 1 \wedge t_3^{(1)} = 0 \wedge t_3^{(2)} = \frac{3}{8} \wedge t_3^{(3)} = 0 \quad (E.218)$$

Fifth Iteration: $|\Psi_5\rangle := -\mathcal{L}|\Psi_4\rangle + e_4|\Psi_4\rangle + \tau_3|\Psi_3\rangle$

$$\begin{aligned}
|\tilde{\Psi}_5^{(3)}\rangle &:= -\mathcal{L}^{(0)}|\Psi_4^{(3)}\rangle - \mathcal{L}^{(1)}|\Psi_4^{(2)}\rangle - \mathcal{L}^{(2)}|\Psi_4^{(1)}\rangle - \mathcal{L}^{(3)}|\Psi_4^{(0)}\rangle \\
&= -1/8\mathcal{L}^{(0)}|\gamma_0\rangle - 27/8\mathcal{L}^{(0)}|\gamma_2\rangle - 1/2\mathcal{L}^{(0)}|\gamma_4\rangle + 1/2\mathcal{L}^{(0)}|m_{2u}\rangle + 17/4\mathcal{L}^{(0)}|m_{4u}\rangle \\
&\quad + \mathcal{L}^{(0)}|m_{6u}\rangle + 1/4\mathcal{L}^{(1)}|\gamma_1\rangle - 3/8\mathcal{L}^{(1)}|\gamma_3\rangle - 1/2\mathcal{L}^{(1)}|m_{3u}\rangle - \mathcal{L}^{(1)}|m_{5u}\rangle - 1/2\mathcal{L}^{(2)}|\gamma_2\rangle \\
&\quad + \mathcal{L}^{(2)}|m_{4u}\rangle - \mathcal{L}^{(3)}|\gamma_3\rangle \\
&= -1/8|\phi_{-1}\rangle - 61/16|\gamma_1\rangle + 1/2|\gamma_3\rangle - 1/2|\gamma_5\rangle + 1/2|m_{1u}\rangle + 43/8|m_{3u}\rangle + 49/8|m_{5u}\rangle + |m_{7u}\rangle
\end{aligned}$$

E. Explicit Calculations

$$\begin{aligned}
|\tilde{\Psi}_5\rangle &= -|\gamma_2\rangle - |\gamma_4\rangle + \frac{1}{U}\{-\frac{1}{2}|\gamma_1\rangle + |m_{3u}\rangle + |m_{5u}\rangle\} \\
&+ \frac{1}{U^2}\{\frac{1}{4}|\gamma_0\rangle - \frac{1}{4}|\gamma_2\rangle - \frac{3}{4}|\gamma_4\rangle - \frac{1}{2}|m_{2u}\rangle - 2|m_{4u}\rangle - |m_{6u}\rangle\} \\
&+ \frac{1}{U^3}\{-\frac{1}{8}|\phi_{-1}\rangle - \frac{61}{16}|\gamma_1\rangle + \frac{1}{2}|\gamma_3\rangle - \frac{1}{2}|\gamma_5\rangle + \frac{1}{2}|m_{1u}\rangle + \frac{43}{8}|m_{3u}\rangle + \frac{49}{8}|m_{5u}\rangle + |m_{7u}\rangle\} \\
&+ \mathcal{O}(1/U^4)
\end{aligned} \tag{E.219}$$

$$\begin{aligned}
e_4 &= \frac{\langle\Psi_4|\mathcal{L}|\Psi_4\rangle}{\langle\Psi_4|\Psi_4\rangle} = -\frac{\langle\Psi_4|\tilde{\Psi}_5\rangle}{\frac{1}{2} + \frac{5}{4U^2} + \mathcal{O}(1/U^4)} = -2\langle\Psi_4|\tilde{\Psi}_5\rangle(1 - 10/4U^2) + \mathcal{O}(1/U^4) \\
&= \{-\frac{1}{2U} + \frac{2}{U^3}(-\langle\Psi_4^{(0)}|\tilde{\Psi}_5^{(3)}\rangle - \langle\Psi_4^{(1)}|\tilde{\Psi}_5^{(2)}\rangle - \langle\Psi_4^{(2)}|\tilde{\Psi}_5^{(1)}\rangle - \langle\Psi_4^{(3)}|\tilde{\Psi}_5^{(0)}\rangle)\}(1 - \frac{10}{4U^2}) + \mathcal{O}(1/U^4) \\
&= (-\frac{1}{2U} - \frac{45}{8U^3})(1 - \frac{10}{4U^2}) + \mathcal{O}(1/U^4) = -\frac{1}{2U} - \frac{35}{8U^3} + \mathcal{O}(1/U^4)
\end{aligned}$$

$$e_4 = -\frac{1}{2U} - \frac{35}{8U^3} + \mathcal{O}(1/U^4) \stackrel{(E.78)}{\Rightarrow} \varepsilon_4^{(0)} = 0 \wedge \varepsilon_4^{(1)} = \frac{1}{2} \wedge \varepsilon_4^{(2)} = 0 \wedge \varepsilon_4^{(3)} = \frac{35}{8} \tag{E.220}$$

$$\begin{aligned}
|\Psi_5^{(3)}\rangle &= |\tilde{\Psi}_5^{(3)}\rangle + e_4^{(1)}|\Psi_4^{(2)}\rangle + e_4^{(3)}|\Psi_4^{(0)}\rangle + \tau_3^{(0)}|\Psi_3^{(3)}\rangle + \tau_3^{(2)}|\Psi_3^{(1)}\rangle \\
&= -1/8|\gamma_1\rangle - 57/16|\gamma_3\rangle - 1/2|\gamma_5\rangle + 1/2|m_{3u}\rangle + 37/8|m_{5u}\rangle + |m_{7u}\rangle
\end{aligned}$$

$$\begin{aligned}
|\Psi_5\rangle &= -|\gamma_4\rangle + \frac{1}{U}\{-\frac{1}{2}|\gamma_3\rangle + |m_{5u}\rangle\} + \frac{1}{U^2}\{\frac{1}{4}|\gamma_2\rangle - \frac{3}{4}|\gamma_4\rangle - \frac{1}{2}|m_{4u}\rangle - |m_{6u}\rangle\} \\
&+ \frac{1}{U^3}\{-\frac{1}{8}|\gamma_1\rangle - \frac{57}{16}|\gamma_3\rangle - \frac{1}{2}|\gamma_5\rangle + \frac{1}{2}|m_{3u}\rangle + \frac{37}{8}|m_{5u}\rangle + |m_{7u}\rangle\} + \mathcal{O}(1/U^4)
\end{aligned} \tag{E.221}$$

Norm of $|\Psi_5\rangle$

$$\|\Psi_5\|^2 = \langle\Psi_5|\Psi_5\rangle = \frac{1}{2} + \frac{13}{8U^2} + \mathcal{O}(1/U^4) \tag{E.222}$$

$$\begin{aligned}
\tilde{\tau}_4 &= -\frac{\langle\Psi_5|\Psi_5\rangle}{\langle\Psi_4|\Psi_4\rangle} = -(1/2 + 13/8U^2)2(1 + 10/4U^2)^{-1} + \mathcal{O}(1/U^4) = -(1 + 13/4U^2)(1 - 10/4U^2) + \mathcal{O}(1/U^4) \\
&= -1 - [-10/4U^2 + 13/4U^2] + \mathcal{O}(1/U^4) = -1 - 3/4U^2 + \mathcal{O}(1/U^4)
\end{aligned}$$

$$\tilde{\tau}_4 = -1 - \frac{3}{4U^2} + \mathcal{O}(1/U^4) \tag{E.223}$$

Off-Diagonal Element τ_4

$$\tau_4 := -\sqrt{-\tilde{\tau}_4} = -\sqrt{1 + \frac{3}{4U^2} + \mathcal{O}(1/U^4)} = -(1 + \frac{3}{8U^2} + \mathcal{O}(1/U^4))$$

$$\tau_4 = -1 - \frac{3}{8U^2} + \mathcal{O}(1/U^4) \stackrel{(E.78)}{\Rightarrow} t_4^{(0)} = 1 \wedge t_4^{(1)} = 0 \wedge t_4^{(2)} = \frac{3}{8} \wedge t_4^{(3)} = 0 \tag{E.224}$$

Sixth Iteration: $|\Psi_6\rangle := -\mathcal{L}|\Psi_6\rangle + e_5|\Psi_5\rangle + \tau_4|\Psi_4\rangle$

$$\begin{aligned} |\tilde{\Psi}_6^{(3)}\rangle &:= -\mathcal{L}^{(0)}|\Psi_5^{(3)}\rangle - \mathcal{L}^{(1)}|\Psi_5^{(2)}\rangle - \mathcal{L}^{(2)}|\Psi_5^{(1)}\rangle - \mathcal{L}^{(3)}|\Psi_5^{(0)}\rangle \\ &= 1/8\mathcal{L}^{(0)}|\gamma_1\rangle + 57/16\mathcal{L}^{(0)}|\gamma_3\rangle + 1/2\mathcal{L}^{(0)}|\gamma_5\rangle - 1/2\mathcal{L}^{(0)}|m_{3u}\rangle - 37/8\mathcal{L}^{(0)}|m_{5u}\rangle \\ &\quad - \mathcal{L}^{(0)}|m_{7u}\rangle - 1/4\mathcal{L}^{(1)}|\gamma_2\rangle + 3/4\mathcal{L}^{(1)}|\gamma_4\rangle + 1/2\mathcal{L}^{(1)}|m_{4u}\rangle + \mathcal{L}^{(1)}|m_{6u}\rangle + 1/2\mathcal{L}^{(2)}|\gamma_3\rangle \\ &\quad - \mathcal{L}^{(2)}|m_{5u}\rangle + \mathcal{L}^{(3)}|\gamma_4\rangle \\ &= 1/8|\gamma_0\rangle + 4|\gamma_2\rangle - 1/2|\gamma_4\rangle + 1/2|\gamma_6\rangle - 1/2|m_{2u}\rangle - 23/4|m_{4u}\rangle - 13/2|m_{6u}\rangle - |m_{8u}\rangle \end{aligned}$$

$$\begin{aligned} |\tilde{\Psi}_6\rangle &= |\gamma_3\rangle + |\gamma_5\rangle + \frac{1}{U}\left\{\frac{1}{2}|\gamma_2\rangle - |m_{4u}\rangle - |m_{6u}\rangle\right\} \\ &\quad + \frac{1}{U^2}\left\{-\frac{1}{4}|\gamma_1\rangle + \frac{5}{8}|\gamma_3\rangle + \frac{9}{8}|\gamma_5\rangle + \frac{1}{2}|m_{3u}\rangle + 2|m_{5u}\rangle + |m_{7u}\rangle\right\} \\ &\quad + \frac{1}{U^3}\left\{\frac{1}{8}|\gamma_0\rangle + 4|\gamma_2\rangle - \frac{1}{2}|\gamma_4\rangle + \frac{1}{2}|\gamma_6\rangle - \frac{1}{2}|m_{2u}\rangle - \frac{23}{4}|m_{4u}\rangle - \frac{13}{2}|m_{6u}\rangle - |m_{8u}\rangle\right\} \\ &\quad + \mathcal{O}(1/U^4) \end{aligned} \tag{E.225}$$

$$\begin{aligned} e_5 &= \frac{\langle\Psi_5|\mathcal{L}|\Psi_5\rangle}{\langle\Psi_5|\Psi_5\rangle} = -\frac{\langle\Psi_5|\tilde{\Psi}_6\rangle}{\frac{1}{2} + \frac{13}{8U^2} + \mathcal{O}(1/U^4)} = -2\langle\Psi_5|\tilde{\Psi}_6\rangle(1 - 13/4U^2) + \mathcal{O}(1/U^4) \\ &= \left\{-\frac{1}{2U} + \frac{2}{U^3}\left(-\langle\Psi_5^{(0)}|\tilde{\Psi}_6^{(3)}\rangle - \langle\Psi_5^{(1)}|\tilde{\Psi}_6^{(2)}\rangle - \langle\Psi_5^{(2)}|\tilde{\Psi}_6^{(1)}\rangle - \langle\Psi_5^{(3)}|\tilde{\Psi}_6^{(0)}\rangle\right)\right\}(1 - \frac{13}{4U^2}) + \mathcal{O}(1/U^4) \\ &= \left(-\frac{1}{2U} - \frac{48}{8U^3}\right)(1 - \frac{13}{4U^2}) + \mathcal{O}(1/U^4) = -\frac{1}{2U} - \frac{35}{8U^3} + \mathcal{O}(1/U^4) \end{aligned}$$

$$e_5 = -\frac{1}{2U} - \frac{35}{8U^3} + \mathcal{O}(1/U^4) \stackrel{(E.78)}{\Rightarrow} \varepsilon_5^{(0)} = 0 \wedge \varepsilon_5^{(1)} = \frac{1}{2} \wedge \varepsilon_5^{(2)} = 0 \wedge \varepsilon_5^{(3)} = \frac{35}{8} \tag{E.226}$$

$$\begin{aligned} |\Psi_6^{(3)}\rangle &= |\tilde{\Psi}_6^{(3)}\rangle + e_5^{(1)}|\Psi_5^{(2)}\rangle + e_5^{(3)}|\Psi_5^{(0)}\rangle + \tau_4^{(0)}|\Psi_4^{(3)}\rangle + \tau_4^{(2)}|\Psi_4^{(1)}\rangle \\ &= 1/8|\gamma_2\rangle + 15/4|\gamma_4\rangle + 1/2|\gamma_6\rangle - 1/2|m_{4u}\rangle - 5|m_{6u}\rangle - |m_{8u}\rangle \end{aligned}$$

$$\begin{aligned} |\Psi_6\rangle &= |\gamma_5\rangle + \frac{1}{U}\left\{\frac{1}{2}|\gamma_4\rangle - |m_{6u}\rangle\right\} + \frac{1}{U^2}\left\{-\frac{1}{4}|\gamma_3\rangle + \frac{9}{8}|\gamma_5\rangle + \frac{1}{2}|m_{5u}\rangle + |m_{7u}\rangle\right\} \\ &\quad + \frac{1}{U^3}\left\{\frac{1}{8}|\gamma_2\rangle + \frac{15}{4}|\gamma_4\rangle + \frac{1}{2}|\gamma_6\rangle - \frac{1}{2}|m_{4u}\rangle - 5|m_{6u}\rangle - |m_{8u}\rangle\right\} + \mathcal{O}(1/U^4) \end{aligned} \tag{E.227}$$

Norm of $|\Psi_6\rangle$

$$\|\Psi_6\|^2 = \langle\Psi_6|\Psi_6\rangle = \frac{1}{2} + \frac{16}{8U^2} + \mathcal{O}(1/U^4) \tag{E.228}$$

$$\begin{aligned} \tilde{\tau}_5 &= -\frac{\langle\Psi_6|\Psi_6\rangle}{\langle\Psi_5|\Psi_5\rangle} = -(1/2 + 16/8U^2)2(1 + 13/4U^2)^{-1} + \mathcal{O}(1/U^4) = -(1 + 16/4U^2)(1 - 13/4U^2) + \mathcal{O}(1/U^4) \\ &= -1 - [16/4U^2 - 13/4U^2] + \mathcal{O}(1/U^4) = -1 - 3/4U^2 + \mathcal{O}(1/U^4) \end{aligned}$$

$$\tilde{\tau}_5 = -1 - \frac{3}{4U^2} + \mathcal{O}(1/U^4) \tag{E.229}$$

E. Explicit Calculations

Off-Diagonal Element τ_5

$$\tau_5 := -\sqrt{-\tilde{\tau}_5} = -\sqrt{1 + \frac{3}{4U^2} + \mathcal{O}(1/U^4)} = -(1 + \frac{3}{8U^2} + \mathcal{O}(1/U^4))$$

$$\tau_5 = -1 - \frac{3}{8U^2} + \mathcal{O}(1/U^4) \stackrel{(E.78)}{\Rightarrow} t_5^{(0)} = 1 \wedge t_5^{(1)} = 0 \wedge t_5^{(2)} = \frac{3}{8} \wedge t_5^{(3)} = 0 \quad (E.230)$$

Seventh Iteration: $|\Psi_7\rangle := -\mathcal{L}|\Psi_6\rangle + e_6|\Psi_6\rangle + \tau_5|\Psi_5\rangle$

$$\begin{aligned} |\tilde{\Psi}_7^{(3)}\rangle &:= -\mathcal{L}^{(0)}|\Psi_6^{(3)}\rangle - \mathcal{L}^{(1)}|\Psi_6^{(2)}\rangle - \mathcal{L}^{(2)}|\Psi_6^{(1)}\rangle - \mathcal{L}^{(3)}|\Psi_6^{(0)}\rangle \\ &= -1/8\mathcal{L}^{(0)}|\gamma_2\rangle - 15/4\mathcal{L}^{(0)}|\gamma_4\rangle - 1/2\mathcal{L}^{(0)}|\gamma_6\rangle + 1/2\mathcal{L}^{(0)}|m_{4u}\rangle + 5\mathcal{L}^{(0)}|m_{6u}\rangle \\ &\quad + \mathcal{L}^{(0)}|m_{8u}\rangle + 1/4\mathcal{L}^{(1)}|\gamma_3\rangle - 9/8\mathcal{L}^{(1)}|\gamma_5\rangle - 1/2\mathcal{L}^{(1)}|m_{5u}\rangle - \mathcal{L}^{(1)}|m_{7u}\rangle - 1/2\mathcal{L}^{(2)}|\gamma_4\rangle \\ &\quad + \mathcal{L}^{(2)}|m_{6u}\rangle - \mathcal{L}^{(3)}|\gamma_5\rangle \\ &= -1/8|\gamma_1\rangle - 67/16|\gamma_3\rangle + 1/2|\gamma_5\rangle - 1/2|\gamma_7\rangle + 1/2|m_{3u}\rangle + 49/8|m_{5u}\rangle + 55/8|m_{7u}\rangle + |m_{9u}\rangle \end{aligned}$$

$$\begin{aligned} |\tilde{\Psi}_7\rangle &= -|\gamma_4\rangle - |\gamma_6\rangle + \frac{1}{U}\{-\frac{1}{2}|\gamma_3\rangle + |m_{5u}\rangle + |m_{7u}\rangle\} \\ &\quad + \frac{1}{U^2}\{\frac{1}{4}|\gamma_2\rangle - |\gamma_4\rangle - \frac{3}{2}|\gamma_6\rangle - \frac{1}{2}|m_{4u}\rangle - 2|m_{6u}\rangle - |m_{8u}\rangle\} \\ &\quad + \frac{1}{U^3}\{-\frac{1}{8}|\gamma_1\rangle - \frac{67}{16}|\gamma_3\rangle + \frac{1}{2}|\gamma_5\rangle - \frac{1}{2}|\gamma_7\rangle + \frac{1}{2}|m_{3u}\rangle + \frac{49}{8}|m_{5u}\rangle + \frac{55}{8}|m_{7u}\rangle + |m_{9u}\rangle\} \\ &\quad + \mathcal{O}(1/U^4) \end{aligned} \quad (E.231)$$

$$\begin{aligned} e_6 &= \frac{\langle\Psi_6|\mathcal{L}|\Psi_6\rangle}{\langle\Psi_6|\Psi_6\rangle} = -\frac{\langle\Psi_6|\tilde{\Psi}_7\rangle}{\frac{1}{2} + \frac{16}{8U^2} + \mathcal{O}(1/U^4)} = -2\langle\Psi_6|\tilde{\Psi}_7\rangle(1 - 16/4U^2) + \mathcal{O}(1/U^4) \\ &= \{-\frac{1}{2U} + \frac{2}{U^3}(-\langle\Psi_6^{(0)}|\tilde{\Psi}_7^{(3)}\rangle - \langle\Psi_6^{(1)}|\tilde{\Psi}_7^{(2)}\rangle - \langle\Psi_6^{(2)}|\tilde{\Psi}_7^{(1)}\rangle - \langle\Psi_6^{(3)}|\tilde{\Psi}_7^{(0)}\rangle)\}(1 - \frac{16}{4U^2}) + \mathcal{O}(1/U^4) \\ &= (-\frac{1}{2U} - \frac{51}{8U^3})(1 - \frac{16}{8U^2}) + \mathcal{O}(1/U^4) = -\frac{1}{2U} - \frac{35}{8U^3} + \mathcal{O}(1/U^4) \end{aligned}$$

$$e_6 = -\frac{1}{2U} - \frac{35}{8U^3} + \mathcal{O}(1/U^4) \stackrel{(E.78)}{\Rightarrow} \varepsilon_6^{(0)} = 0 \wedge \varepsilon_6^{(1)} = \frac{1}{2} \wedge \varepsilon_6^{(2)} = 0 \wedge \varepsilon_6^{(3)} = \frac{35}{8} \quad (E.232)$$

$$\begin{aligned} |\Psi_7^{(3)}\rangle &= |\tilde{\Psi}_7^{(3)}\rangle + e_6^{(1)}|\Psi_6^{(2)}\rangle + e_6^{(3)}|\Psi_6^{(0)}\rangle + \tau_5^{(0)}|\Psi_5^{(3)}\rangle + \tau_5^{(2)}|\Psi_5^{(1)}\rangle \\ &= -1/8|\gamma_3\rangle - 63/16|\gamma_5\rangle - 1/2|\gamma_7\rangle + 1/2|m_{5u}\rangle + 43/8|m_{7u}\rangle + |m_{9u}\rangle \end{aligned}$$

$$\begin{aligned} |\Psi_7\rangle &= -|\gamma_6\rangle + \frac{1}{U}\{-\frac{1}{2}|\gamma_5\rangle + |m_{7u}\rangle\} + \frac{1}{U^2}\{\frac{1}{4}|\gamma_4\rangle - \frac{3}{2}|\gamma_6\rangle - \frac{1}{2}|m_{6u}\rangle - |m_{8u}\rangle\} \\ &\quad + \frac{1}{U^3}\{-\frac{1}{8}|\gamma_3\rangle - \frac{63}{16}|\gamma_5\rangle - \frac{1}{2}|\gamma_7\rangle + \frac{1}{2}|m_{5u}\rangle + \frac{43}{8}|m_{7u}\rangle + |m_{9u}\rangle\} + \mathcal{O}(1/U^4) \end{aligned} \quad (E.233)$$

Norm of $|\Psi_7\rangle$

$$\|\Psi_7\|^2 = \langle\Psi_7|\Psi_7\rangle = \frac{1}{2} + \frac{19}{8U^2} + \mathcal{O}(1/U^4) \quad (E.234)$$

$$\tilde{\tau}_6 = -\frac{\langle\Psi_7|\Psi_7\rangle}{\langle\Psi_6|\Psi_6\rangle} = -(1/2 + 19/8U^2)2(1 + 16/4U^2)^{-1} + \mathcal{O}(1/U^4) = -(1 + 19/4U^2)(1 - 16/4U^2) + \mathcal{O}(1/U^4)$$

$$= -1 - [19/4U^2 - 16/4U^2] + \mathcal{O}(1/U^4) = -1 - 3/4U^2 + \mathcal{O}(1/U^4)$$

$$\boxed{\tilde{\tau}_6 = -1 - \frac{3}{4U^2} + \mathcal{O}(1/U^4)} \quad (\text{E.235})$$

Off-Diagonal Element τ_6

$$\tau_6 := -\sqrt{-\tilde{\tau}_6} = -\sqrt{1 + \frac{3}{4U^2} + \mathcal{O}(1/U^4)} = -\left(1 + \frac{3}{8U^2} + \mathcal{O}(1/U^4)\right)$$

$$\boxed{\tau_6 = -1 - \frac{3}{8U^2} + \mathcal{O}(1/U^4) \stackrel{(\text{E.78})}{\Rightarrow} t_6^{(0)} = 1 \wedge t_6^{(1)} = 0 \wedge t_6^{(2)} = \frac{3}{8} \wedge t_6^{(3)} = 0} \quad (\text{E.236})$$

No go on by induction.

Induction Hypothesis to Third Order

Let $N \geq 8$, then we find for all $5 \leq n < N$

$$\begin{aligned} |\Psi_n\rangle &= (-1)^n \left(|\gamma_{n-1}\rangle + \frac{1}{U} \left\{ \frac{1}{2} |\gamma_{n-2}\rangle - |m_{nu}\rangle \right\} \right. \\ &\quad + \frac{1}{U^2} \left\{ -\frac{1}{4} |\gamma_{n-3}\rangle + a_n |\gamma_{n-1}\rangle + \frac{1}{2} |m_{n-1u}\rangle + |m_{n+1u}\rangle \right\} \\ &\quad \left. + \frac{1}{U^3} \left\{ \frac{1}{8} |\gamma_{n-4}\rangle + b_n |\gamma_{n-2}\rangle + \frac{1}{2} |\gamma_n\rangle - \frac{1}{2} |m_{n-2u}\rangle - c_n |m_{nu}\rangle - |m_{n+2u}\rangle \right\} \right) + \mathcal{O}(1/U^4), \end{aligned} \quad (\text{E.237})$$

with parameters

$$a_n := (n-3) \frac{3}{8}, \quad (\text{E.238})$$

$$b_n := (n-4) \frac{3}{16} + \frac{54}{16}, \quad (\text{E.239})$$

$$c_n := (n-4) \frac{3}{8} + \frac{34}{8}, \quad (\text{E.240})$$

$$e_{n-1} = -\frac{1}{2U} - \frac{35}{8U^3} + \mathcal{O}(1/U^4), \quad (\text{E.241})$$

$$\tau_{n-1} = -1 - \frac{3}{4U^2} + \mathcal{O}(1/U^4). \quad (\text{E.242})$$

Note the linear increase of the coefficients a_n , b_n and c_n with n . This implies

$$\varepsilon_{n-1} = \frac{1}{2U} + \frac{35}{8U^3} + \mathcal{O}(1/U^4), \quad (\text{E.243})$$

$$t_{n-1} = 1 + \frac{3}{8U^2} + \mathcal{O}(1/U^4). \quad (\text{E.244})$$

We further have

$$\langle \Psi_n | \Psi_n \rangle = \frac{1}{2} + \frac{1}{U^2} \left\{ a_n + \frac{7}{8} \right\} + \mathcal{O}(1/U^4). \quad (\text{E.245})$$

E. Explicit Calculations

Induction Step The induction hypothesis (i.h.) has been proven for $n = 5, 6, 7$. Thus, we proceed with the induction step. Since we already proved that $|\Psi_N^{(0)}\rangle$, $|\Psi_N^{(1)}\rangle$ and $|\Psi_N^{(2)}\rangle$ obey the formula, we go on with the proof for $|\Psi_N^{(3)}\rangle$.

$$\begin{aligned}
|\tilde{\Psi}_N^{(3)}\rangle &:= -\mathcal{L}^{(0)}|\Psi_{N-1}^{(3)}\rangle - \mathcal{L}^{(1)}|\Psi_{N-1}^{(2)}\rangle - \mathcal{L}^{(2)}|\Psi_{N-1}^{(1)}\rangle - \mathcal{L}^{(3)}|\Psi_{N-1}^{(0)}\rangle \\
&\stackrel{\text{i.h.}}{=} (-1)^N \left(\mathcal{L}^{(0)} \left\{ \frac{1}{8}|\gamma_{N-5}\rangle + b_{N-1}|\gamma_{N-3}\rangle + \frac{1}{2}|\gamma_{N-1}\rangle - \frac{1}{2}|m_{N-3u}\rangle - c_{N-1}|m_{N-1u}\rangle - |m_{N+1u}\rangle \right\} \right. \\
&\quad + \mathcal{L}^{(1)} \left\{ -\frac{1}{4}|\gamma_{N-4}\rangle + a_{N-1}|\gamma_{N-2}\rangle + \frac{1}{2}|m_{N-2u}\rangle + |m_{Nu}\rangle \right\} \\
&\quad + \mathcal{L}^{(2)} \left\{ \frac{1}{2}|\gamma_{N-3}\rangle - |m_{N-1u}\rangle \right\} \\
&\quad \left. + \mathcal{L}^{(3)}|\gamma_{N-2}\rangle \right) \\
&\stackrel{\text{i.h.}}{=} (-1)^N \left(\left\{ \frac{1}{8}|\gamma_{N-6}\rangle + (b_{N-1} + \frac{1}{8})|\gamma_{N-4}\rangle + (b_{N-1} + \frac{1}{2})|\gamma_{N-2}\rangle + \frac{1}{2}|\gamma_N\rangle \right. \right. \\
&\quad \left. \left. - \frac{1}{2}|m_{N-4u}\rangle - (c_{N-2} + \frac{1}{2})|m_{N-2u}\rangle - (c_{N-1} + 1)|m_{Nu}\rangle - |m_{N+2u}\rangle \right\} \right. \\
&\quad + \left\{ \frac{1}{8}|\gamma_{N-4}\rangle - \frac{1}{2}a_{N-1}|\gamma_{N-2}\rangle - \frac{1}{4}|m_{N-2u}\rangle + \frac{1}{2}|m_{Nu}\rangle \right\} \\
&\quad + \left\{ \frac{3}{16}|\gamma_{N-4}\rangle + \frac{3}{16}|\gamma_{N-2}\rangle + \frac{1}{4}|m_{N-2u}\rangle + \frac{1}{2}|m_{Nu}\rangle \right\} \\
&\quad \left. + \left\{ -\frac{35}{8}|\gamma_{N-2}\rangle \right\} \right)
\end{aligned}$$

$$\boxed{|\tilde{\Psi}_N^{(3)}\rangle = (-1)^N \left(\frac{1}{8}|\gamma_{N-6}\rangle + (b_N + \frac{1}{4})|\gamma_{N-4}\rangle - \frac{1}{2}|\gamma_{N-2}\rangle + \frac{1}{2}|\gamma_N\rangle - \frac{1}{2}|m_{N-4u}\rangle - (c_N + \frac{3}{4})|m_{N-2u}\rangle - (c_N + \frac{3}{2})|m_{Nu}\rangle - |m_{N+2u}\rangle \right)} \quad (\text{E.246})$$

$$\begin{aligned}
e_{N-1} &= \frac{\langle \Psi_{N-1} | L | \Psi_{N-1} \rangle}{\langle \Psi_{N-1} | \Psi_{N-1} \rangle} \stackrel{\text{i.h.}}{=} -\frac{\langle \Psi_{N-1} | \tilde{\Psi}_N \rangle}{\frac{1}{2} + (a_{N-1} + \frac{7}{8})/U^2 + \mathcal{O}(1/U^4)} \\
&= -2 \langle \Psi_{N-1} | \tilde{\Psi}_N \rangle \left(1 - \frac{1}{U^2} (N \frac{3}{4} - \frac{5}{4}) \right) + \mathcal{O}(1/U^4) \\
&= \left(-\frac{1}{2U} + \frac{2}{U^3} \left(-\langle \Psi_{N-1}^{(0)} | \tilde{\Psi}_N^{(3)} \rangle - \langle \Psi_{N-1}^{(1)} | \tilde{\Psi}_N^{(2)} \rangle - \langle \Psi_{N-1}^{(2)} | \tilde{\Psi}_N^{(1)} \rangle - \langle \Psi_{N-1}^{(3)} | \tilde{\Psi}_N^{(0)} \rangle \right) \right) \\
&\quad \times \left(1 - \frac{1}{U^2} (N \frac{3}{4} - \frac{5}{4}) \right) + \mathcal{O}(1/U^4) \\
&= \left(-\frac{1}{2U} + \frac{1}{U^3} \left(-\frac{60}{16} - N \frac{3}{8} \right) \right) \left(1 - \frac{1}{U^2} (N \frac{3}{4} - \frac{5}{4}) \right) + \mathcal{O}(1/U^4)
\end{aligned}$$

$$\boxed{e_{N-1} = -\frac{1}{2U} - \frac{35}{8U^3} + \mathcal{O}(1/U^4) \stackrel{(\text{E.78})}{\Rightarrow} \varepsilon_{N-1}^{(0)} = 0 \wedge \varepsilon_{N-1}^{(1)} = \frac{1}{2} \wedge \varepsilon_{N-1}^{(2)} = 0 \wedge \varepsilon_{N-1}^{(3)} = -\frac{35}{8}} \quad (\text{E.247})$$

$$\begin{aligned}
|\Psi_N^{(3)}\rangle &= |\tilde{\Psi}_N^{(3)}\rangle + e_{N-1}^{(1)}|\Psi_{N-1}^{(2)}\rangle + e_{N-1}^{(3)}|\Psi_{N-1}^{(0)}\rangle + \tau_{N-2}^{(0)}|\Psi_{N-2}^{(3)}\rangle + \tau_{N-2}^{(2)}|\Psi_{N-2}^{(1)}\rangle \\
&= |\tilde{\Psi}_N^{(3)}\rangle + (-1)^N \left\{ -\frac{1}{8}|\gamma_{N-6}\rangle + \left(-\frac{1}{2} - b_{N-2} \right) |\gamma_{N-4}\rangle + \left(\frac{31}{8} + \frac{a_{N-1}}{2} \right) |\gamma_{N-2}\rangle \right. \\
&\quad \left. + \frac{1}{2}|m_{N-4u}\rangle + (c_{N-2} + 1)|m_{N-2u}\rangle + \frac{3}{2}|m_{Nu}\rangle \right\} \\
&= (-1)^N \left(\frac{1}{8}|\gamma_{N-4}\rangle + b_n|\gamma_{N-2}\rangle + \frac{1}{2}|\gamma_N\rangle - \frac{1}{2}|m_{N-2u}\rangle - c_N|m_{Nu}\rangle - |m_{N+2u}\rangle \right)
\end{aligned}$$

Norm of $|\Psi_N\rangle$ Up to third order in $1/U$ the norm of $|\Psi_N\rangle$ is given by

$$\langle \Psi_N | \Psi_N \rangle = \frac{1}{2} + \frac{1}{U^2} \left\{ a_n + \frac{7}{8} \right\} + \frac{1}{U^3} \sum_{l=0}^3 \langle \Psi_N^{(l)} | \Psi_N^{(3-l)} \rangle.$$

We see that we do not get a contribution in third order and, thus,

$$\boxed{\langle \Psi_N | \Psi_N \rangle = \frac{1}{2} + \frac{1}{U^2} \left\{ a_N + \frac{7}{8} \right\} + \mathcal{O}(1/U^4)}. \quad (\text{E.248})$$

Therefore we have additionally

$$\boxed{\tilde{\tau}_{N-1} = -1 - \frac{3}{4U^2} + \mathcal{O}(1/U^4)}. \quad (\text{E.249})$$

Off-Diagonal Element τ_{N-1}

$$\tau_{N-1} := -\sqrt{-\tilde{\tau}_{N-1}} = -\sqrt{1 + \frac{3}{4U^2} + \mathcal{O}(1/U^4)} = -\left(1 + \frac{3}{8U^2} + \mathcal{O}(1/U^4)\right)$$

$$\boxed{\tau_{N-1} = -1 - \frac{3}{8U^2} + \mathcal{O}(1/U^4) \stackrel{(\text{E.78})}{\Rightarrow} t_{N-1}^{(0)} = 1 \wedge t_{N-1}^{(1)} = 0 \wedge t_{N-1}^{(2)} = \frac{3}{8} \wedge t_{N-1}^{(3)} = 0} \quad (\text{E.250})$$

□

Summary of the Results to Third Order

To third order we may summarize the Lanczos iteration in the following form:

$$\begin{aligned} |\tilde{\Psi}_1\rangle &= -|\gamma_0\rangle + \frac{1}{U} \left\{ -\frac{1}{2}|\phi_{-1}\rangle + |m_{1u}\rangle \right\} + \frac{1}{U^2} \left\{ \frac{3}{4}|\gamma_0\rangle - \frac{1}{2}|m_{0u}\rangle - |m_{2u}\rangle \right\} \\ &\quad + \frac{1}{U^3} \left\{ -\frac{1}{2}|\phi_{-1}\rangle - \frac{3}{4}|\gamma_1\rangle + \frac{25}{8}|m_{1u}\rangle + |m_{3u}\rangle \right\} + \mathcal{O}(1/U^4), \end{aligned} \quad (\text{E.251a})$$

$$\begin{aligned} |\Psi_1\rangle &= -|\gamma_0\rangle + \frac{1}{U} \left\{ -\frac{1}{2}|\phi_{-1}\rangle + |m_{1u}\rangle \right\} + \frac{1}{U^2} \left\{ \frac{3}{4}|\gamma_0\rangle - \frac{1}{2}|m_{0u}\rangle - |m_{2u}\rangle \right\} \\ &\quad + \frac{1}{U^3} \left\{ -\frac{9}{4}|\phi_{-1}\rangle - \frac{3}{4}|\gamma_1\rangle + \frac{25}{8}|m_{1u}\rangle + |m_{3u}\rangle \right\} + \mathcal{O}(1/U^4), \end{aligned} \quad (\text{E.251b})$$

$$\begin{aligned} |\tilde{\Psi}_2\rangle &= |\phi_{-1}\rangle + |\gamma_1\rangle + \frac{1}{U} \left\{ -|m_{0u}\rangle - |m_{2u}\rangle \right\} + \frac{1}{U^2} \left\{ -\frac{3}{4}|\phi_{-1}\rangle - \frac{3}{8}|\gamma_1\rangle + 2|m_{1u}\rangle + |m_{3u}\rangle \right\} \\ &\quad + \frac{1}{U^3} \left\{ -\frac{3}{4}|\gamma_0\rangle + \frac{1}{2}|\gamma_2\rangle - \frac{11}{4}|m_{0u}\rangle - 5|m_{2u}\rangle - |m_{4u}\rangle \right\} + \mathcal{O}(1/U^4), \end{aligned} \quad (\text{E.251c})$$

$$\begin{aligned} |\Psi_2\rangle &= |\gamma_1\rangle + \frac{1}{U} \left\{ \frac{1}{2}|\gamma_0\rangle - |m_{2u}\rangle \right\} + \frac{1}{U^2} \left\{ -\frac{1}{4}|\phi_{-1}\rangle - \frac{3}{8}|\gamma_1\rangle + \frac{1}{2}|m_{1u}\rangle + |m_{3u}\rangle \right\} \\ &\quad + \frac{1}{U^3} \left\{ \frac{11}{4}|\gamma_0\rangle + \frac{1}{2}|\gamma_2\rangle - \frac{1}{2}|m_{0u}\rangle - \frac{7}{2}|m_{2u}\rangle - |m_{4u}\rangle \right\} + \mathcal{O}(1/U^4), \end{aligned} \quad (\text{E.251d})$$

$$\begin{aligned} |\tilde{\Psi}_3\rangle &= -|\gamma_0\rangle - |\gamma_2\rangle + \frac{1}{U} \left\{ -\frac{1}{2}|\phi_{-1}\rangle + |m_{1u}\rangle + |m_{3u}\rangle \right\} + \frac{1}{U^2} \left\{ \frac{1}{2}|\gamma_0\rangle - \frac{1}{2}|m_{0u}\rangle - 2|m_{2u}\rangle - |m_{4u}\rangle \right\} \\ &\quad + \frac{1}{U^3} \left\{ -\frac{23}{8}|\phi_{-1}\rangle + \frac{1}{4}|\gamma_1\rangle - \frac{1}{2}|\gamma_3\rangle + \frac{37}{8}|m_{1u}\rangle + \frac{43}{8}|m_{3u}\rangle + |m_{5u}\rangle \right\} + \mathcal{O}(1/U^4), \end{aligned} \quad (\text{E.251e})$$

$$\begin{aligned} |\Psi_3\rangle &= -|\gamma_2\rangle + \frac{1}{U} \left\{ -\frac{1}{2}|\gamma_1\rangle + |m_{3u}\rangle \right\} + \frac{1}{U^2} \left\{ \frac{1}{4}|\gamma_0\rangle - \frac{1}{2}|m_{2u}\rangle - |m_{4u}\rangle \right\} \\ &\quad + \frac{1}{U^3} \left\{ -\frac{1}{8}|\phi_{-1}\rangle - \frac{51}{16}|\gamma_1\rangle - \frac{1}{2}|\gamma_3\rangle + \frac{1}{2}|m_{1u}\rangle + \frac{31}{8}|m_{3u}\rangle + |m_{5u}\rangle \right\} + \mathcal{O}(1/U^4), \end{aligned} \quad (\text{E.251f})$$

E. Explicit Calculations

$$\begin{aligned}
|\tilde{\Psi}_4\rangle &= |\gamma_1\rangle + |\gamma_3\rangle + \frac{1}{U} \left\{ \frac{1}{2} |\gamma_0\rangle - |m_{2u}\rangle - |m_{4u}\rangle \right\} \\
&+ \frac{1}{U^2} \left\{ -\frac{1}{4} |\phi_{-1}\rangle - \frac{1}{8} |\gamma_1\rangle + \frac{3}{8} |\gamma_3\rangle + \frac{1}{2} |m_{1u}\rangle + 2|m_{3u}\rangle + |m_{5u}\rangle \right\} \\
&+ \frac{1}{U^3} \left\{ \frac{27}{8} |\gamma_0\rangle - \frac{1}{2} |\gamma_2\rangle + \frac{1}{2} |\gamma_4\rangle - \frac{1}{2} |m_{0u}\rangle - 5|m_{2u}\rangle - \frac{23}{4} |m_{4u}\rangle - |m_{6u}\rangle \right\} + \mathcal{O}(1/U^4),
\end{aligned} \tag{E.251g}$$

$$\begin{aligned}
|\Psi_4\rangle &= |\gamma_3\rangle + \frac{1}{U} \left\{ \frac{1}{2} |\gamma_2\rangle - |m_{4u}\rangle \right\} + \frac{1}{U^2} \left\{ -\frac{1}{4} |\gamma_1\rangle + \frac{3}{8} |\gamma_3\rangle + \frac{1}{2} |m_{3u}\rangle + |m_{5u}\rangle \right\} \\
&+ \frac{1}{U^3} \left\{ \frac{1}{8} |\gamma_0\rangle + \frac{27}{8} |\gamma_2\rangle + \frac{1}{2} |\gamma_4\rangle - \frac{1}{2} |m_{2u}\rangle - \frac{17}{4} |m_{4u}\rangle - |m_{6u}\rangle \right\} + \mathcal{O}(1/U^4),
\end{aligned} \tag{E.251h}$$

$$\begin{aligned}
|\tilde{\Psi}_5\rangle &= -|\gamma_2\rangle - |\gamma_4\rangle + \frac{1}{U} \left\{ -\frac{1}{2} |\gamma_1\rangle + |m_{3u}\rangle + |m_{5u}\rangle \right\} \\
&+ \frac{1}{U^2} \left\{ \frac{1}{4} |\gamma_0\rangle - \frac{1}{4} |\gamma_2\rangle - \frac{3}{4} |\gamma_4\rangle - \frac{1}{2} |m_{2u}\rangle - 2|m_{4u}\rangle - |m_{6u}\rangle \right\} \\
&+ \frac{1}{U^3} \left\{ -\frac{1}{8} |\phi_{-1}\rangle - \frac{61}{16} |\gamma_1\rangle + \frac{1}{2} |\gamma_3\rangle - \frac{1}{2} |\gamma_5\rangle + \frac{1}{2} |m_{1u}\rangle + \frac{43}{8} |m_{3u}\rangle + \frac{49}{8} |m_{5u}\rangle + |m_{7u}\rangle \right\} \\
&+ \mathcal{O}(1/U^4),
\end{aligned} \tag{E.251i}$$

$$\begin{aligned}
|\Psi_5\rangle &= -|\gamma_4\rangle + \frac{1}{U} \left\{ -\frac{1}{2} |\gamma_3\rangle + |m_{5u}\rangle \right\} + \frac{1}{U^2} \left\{ \frac{1}{4} |\gamma_2\rangle - \frac{3}{4} |\gamma_4\rangle - \frac{1}{2} |m_{4u}\rangle - |m_{6u}\rangle \right\} \\
&+ \frac{1}{U^3} \left\{ -\frac{1}{8} |\gamma_1\rangle - \frac{57}{16} |\gamma_3\rangle - \frac{1}{2} |\gamma_5\rangle + \frac{1}{2} |m_{3u}\rangle + \frac{37}{8} |m_{5u}\rangle + |m_{7u}\rangle \right\} + \mathcal{O}(1/U^4),
\end{aligned} \tag{E.251j}$$

$$\begin{aligned}
|\tilde{\Psi}_6\rangle &= |\gamma_3\rangle + |\gamma_5\rangle + \frac{1}{U} \left\{ \frac{1}{2} |\gamma_2\rangle - |m_{4u}\rangle - |m_{6u}\rangle \right\} \\
&+ \frac{1}{U^2} \left\{ -\frac{1}{4} |\gamma_1\rangle + \frac{5}{8} |\gamma_3\rangle + \frac{9}{8} |\gamma_5\rangle + \frac{1}{2} |m_{3u}\rangle + 2|m_{5u}\rangle + |m_{7u}\rangle \right\} \\
&+ \frac{1}{U^3} \left\{ \frac{1}{8} |\gamma_0\rangle + 4|\gamma_2\rangle - \frac{1}{2} |\gamma_4\rangle + \frac{1}{2} |\gamma_6\rangle - \frac{1}{2} |m_{2u}\rangle - \frac{23}{4} |m_{4u}\rangle - \frac{13}{2} |m_{6u}\rangle - |m_{8u}\rangle \right\} \\
&+ \mathcal{O}(1/U^4),
\end{aligned} \tag{E.251k}$$

$$\begin{aligned}
|\Psi_6\rangle &= |\gamma_5\rangle + \frac{1}{U} \left\{ \frac{1}{2} |\gamma_4\rangle - |m_{6u}\rangle \right\} + \frac{1}{U^2} \left\{ -\frac{1}{4} |\gamma_3\rangle + \frac{9}{8} |\gamma_5\rangle + \frac{1}{2} |m_{5u}\rangle + |m_{7u}\rangle \right\} \\
&+ \frac{1}{U^3} \left\{ \frac{1}{8} |\gamma_2\rangle + \frac{15}{4} |\gamma_4\rangle + \frac{1}{2} |\gamma_6\rangle - \frac{1}{2} |m_{4u}\rangle - 5|m_{6u}\rangle - |m_{8u}\rangle \right\} + \mathcal{O}(1/U^4),
\end{aligned} \tag{E.251l}$$

and for $n \geq 7$

$$\begin{aligned}
|\tilde{\Psi}_n\rangle &= (-1)^n \left(\{ |\gamma_{n-3}\rangle + |\gamma_{n-1}\rangle \} + \frac{1}{U} \left\{ \frac{1}{2} |\gamma_{n-4}\rangle - |m_{n-2u}\rangle - |m_{nu}\rangle \right\} \right. \\
&+ \frac{1}{U^2} \left\{ -\frac{1}{4} |\gamma_{n-5}\rangle + (a_n - \frac{4}{8}) |\gamma_{n-3}\rangle + a_n |\gamma_{n-1}\rangle + \frac{1}{2} |m_{n-3u}\rangle + 2|m_{n-1u}\rangle + |m_{n+1u}\rangle \right\} \\
&\left. \frac{1}{U^3} \left\{ \frac{1}{8} |\gamma_{N-6}\rangle + (b_N + \frac{1}{4}) |\gamma_{N-4}\rangle - \frac{1}{2} |\gamma_{N-2}\rangle + \frac{1}{2} |\gamma_N\rangle \right. \right. \\
&\quad \left. \left. - \frac{1}{2} |m_{n-4u}\rangle - (c_n + \frac{3}{4}) |m_{n-2u}\rangle - (c_n + \frac{3}{2}) |m_{nu}\rangle - |m_{n+2u}\rangle \right\} \right) + \mathcal{O}(1/U^4),
\end{aligned} \tag{E.251m}$$

$$\begin{aligned}
|\Psi_n\rangle &= (-1)^n \left(|\gamma_{n-1}\rangle + \frac{1}{U} \left\{ \frac{1}{2} |\gamma_{n-2}\rangle - |m_{nu}\rangle \right\} \right. \\
&+ \frac{1}{U^2} \left\{ -\frac{1}{4} |\gamma_{n-3}\rangle + a_n |\gamma_{n-1}\rangle + \frac{1}{2} |m_{n-1u}\rangle + |m_{n+1u}\rangle \right\} \\
&\left. + \frac{1}{U^3} \left\{ \frac{1}{8} |\gamma_{n-4}\rangle + b_n |\gamma_{n-2}\rangle + \frac{1}{2} |\gamma_n\rangle - \frac{1}{2} |m_{n-2u}\rangle - c_n |m_{nu}\rangle - |m_{n+2u}\rangle \right\} \right) + \mathcal{O}(1/U^4).
\end{aligned} \tag{E.251n}$$

Up to third order in $1/U$, we have found for the matrix elements e_n of the operator \mathcal{L} in its Lanczos basis that

$$e_0 = -\frac{14}{8U^3} + \mathcal{O}(1/U^4), \quad (\text{E.252a})$$

$$e_1 = -\frac{1}{2U} - \frac{31}{8U^3} + \mathcal{O}(1/U^4), \quad (\text{E.252b})$$

$$e_n = -\frac{1}{2U} - \frac{35}{8U^3} + \mathcal{O}(1/U^4) \quad n \geq 2. \quad (\text{E.252c})$$

The off-diagonal elements τ_n read

$$\tau_0 = -1 - \frac{1}{8U^2} + \mathcal{O}(1/U^4), \quad (\text{E.253a})$$

$$\tau_n = -1 - \frac{3}{8U^2} + \mathcal{O}(1/U^4) \quad n \geq 1. \quad (\text{E.253b})$$

According to the self-consistency condition (E.78), the on-site energies ε_n of the SIAM therefore read

$$\varepsilon_0 = \frac{14}{8U^3} + \mathcal{O}(1/U^4), \quad (\text{E.254a})$$

$$\varepsilon_1 = \frac{1}{2U} + \frac{31}{8U^3} + \mathcal{O}(1/U^4), \quad (\text{E.254b})$$

$$\varepsilon_n = \frac{1}{2U} + \frac{35}{8U^3} + \mathcal{O}(1/U^4) \quad n \geq 2, \quad (\text{E.254c})$$

and the electron transfer amplitudes t_n are given up to third order by

$$t_0 = 1 + \frac{1}{8U^2} + \mathcal{O}(1/U^4), \quad (\text{E.255a})$$

$$t_n = 1 + \frac{3}{8U^2} + \mathcal{O}(1/U^4) \quad n \geq 1. \quad (\text{E.255b})$$

F

Chebyshev Polynomials

We begin this appendix with a short overview of the properties of the Chebyshev polynomials of the first and of the second kind. The information presented summarizes some of their features we need. All the formulae in the first two sections can be found in [37], if not otherwise stated. We conclude the appendix by deriving the Green functions and some of their products for tight-binding Hamiltonians on a one-dimensional, semi-infinite chain.

F.1. Chebyshev Polynomials of the First Kind

The orthogonal polynomials $T_n(x)$, $n \in \mathbb{N}$ with respect to the weight function $w_1(x) = 1/\sqrt{1-x^2}$, defined on the real interval $-1 \leq x \leq 1$, are called Chebyshev polynomials of the first kind. They obey the orthogonality condition

$$\int_{-1}^1 w_1(x) T_n(x) T_m(x) dx = \frac{\pi}{2} \delta_{n,m} (1 + \delta_{n,0}). \quad (\text{F.1})$$

They are standardized as $T_n(1) = 1$ which implies that

$$\forall n \quad |T_n(x)| \leq 1, \quad x \in [-1, 1]. \quad (\text{F.2})$$

In terms of trigonometric functions, the $T_n(x)$ may be expressed as

$$T_n(\cos(\vartheta)) = \cos(n\vartheta). \quad (\text{F.3})$$

They have alternating parity

$$T_n(-x) = (-1)^n T_n(x). \quad (\text{F.4})$$

The Chebyshev polynomials of the first kind satisfy the recurrence relation

$$T_{n+1}(x) = 2xT_n(x) - T_{n-1}(x) \quad (\text{F.5})$$

with the starting values

$$T_0(x) = 1, \quad (\text{F.5a})$$

$$T_1(x) = x. \quad (\text{F.5b})$$

The first few polynomials read

$$T_0(x) = 1, \quad (\text{F.6})$$

$$T_1(x) = x, \quad (\text{F.7})$$

$$T_2(x) = 2x^2 - 1, \quad (\text{F.8})$$

$$T_3(x) = 4x^3 - 3x, \quad (\text{F.9})$$

$$T_4(x) = 8x^4 - 8x^2 + 1. \quad (\text{F.10})$$

F.2. Chebyshev Polynomials of the Second Kind

The Chebyshev polynomials of the second kind, $U_n(x)$ with $n \in \mathbb{N}$, are a system of orthogonal polynomials on the real interval $[-1, 1]$ with respect to the weight function $w_2(x) = \sqrt{1-x^2}$. They obey the orthogonality relation

$$\int_{-1}^1 w_2(x) U_n(x) U_m(x) dx = \frac{\pi}{2} \delta_{n,m}. \quad (\text{F.11})$$

They are standardized such that $U_n(1) = n + 1$, from which it follows that

$$\forall n \in \mathbb{N} \quad |U_n(x)| \leq n + 1 \text{ for } x \in [-1, 1]. \quad (\text{F.12})$$

The Chebyshev polynomial $U_n(x)$ has degree n and alternating parity,

$$U_n(-x) = (-1)^n U_n(x). \quad (\text{F.13})$$

There exists an explicit representation of the Chebyshev polynomial $U_n(x)$ in terms of trigonometric functions which reads

$$U_n(\cos(\vartheta)) = \frac{\sin((n+1)\vartheta)}{\sin(\vartheta)}. \quad (\text{F.14})$$

The $U_n(x)$ satisfy the recurrence relation

$$U_{n+1}(x) = 2xU_n(x) - U_{n-1}(x) \quad (\text{F.15})$$

with the starting values

$$U_0(x) = 1, \quad (\text{F.15a})$$

$$U_1(x) = 2x. \quad (\text{F.15b})$$

The first few polynomials $U_n(x)$ are given by

$$U_0(x) = 1, \quad (\text{F.16})$$

$$U_1(x) = 2x, \quad (\text{F.17})$$

$$U_2(x) = 4x^2 - 1, \quad (\text{F.18})$$

$$U_3(x) = 8x^3 - 4x, \quad (\text{F.19})$$

$$U_4(x) = 16x^4 - 12x^2 + 1. \quad (\text{F.20})$$

The following relations between the $U_n(x)$ and $T_n(x)$ are useful and might be found as equation (7.344) in [140],

$$J_n(x) := \mathcal{P} \int_{-1}^1 \frac{T_n(y)}{\pi(y-x)\sqrt{1-y^2}} dy \stackrel{|x| \leq 1}{=} U_{n-1}(x), \quad (\text{F.21})$$

$$I_{n-1}(x) := \mathcal{P} \int_{-1}^1 \frac{U_{n-1}(y)\sqrt{1-y^2}}{\pi(x-y)} dy \stackrel{|x| \leq 1}{=} T_n(x), \quad (\text{F.22})$$

where $\mathcal{P} \int$ denotes the principal value. Both equations are valid for $n \in \mathbb{N} \setminus \{0\}$. Additionally, we will need the following recurrence relations,

$$2T_m(x)T_n(x) = T_{n+m}(x) + T_{n-m}(x) \quad \text{for } n \geq m, \quad (\text{F.23})$$

$$2T_n(x)U_{n-1}(x) = U_{2n-1}(x), \quad (\text{F.24})$$

$$2T_m(x)U_{n-1}(x) = U_{n+m-1}(x) + U_{n-m-1}(x) \quad \text{for } n > m, \quad (\text{F.25})$$

$$2T_n(x)U_{m-1}(x) = U_{n+m-1}(x) - U_{n-m-1}(x) \quad \text{for } n > m, \quad (\text{F.26})$$

$$2(x^2 - 1)U_{m-1}(x)U_{n-1}(x) = T_{n+m}(x) - T_{n-m}(x) \quad \text{for } n \geq m. \quad (\text{F.27})$$

Expansion in Terms of Chebyshev Polynomials The Chebyshev polynomials form a complete set on an appropriate vector space (Sobolev space) of functions $f : [-1, 1] \rightarrow \mathbb{R}$, so that any such function can be expanded in a Chebyshev series [141],

$$f(x) = \sum_{n=0}^{\infty} \lambda_n(f) U_n(x), \quad (\text{F.28a})$$

with coefficients, the so-called Chebyshev moments of the second kind, given by

$$\lambda_n(f) = \frac{2}{\pi} \int_{-1}^1 w_2(x) U_n(x) f(x) dx. \quad (\text{F.28b})$$

For the purpose of this thesis it is advantageous to define the Chebyshev moments of the second kind $\mu_n(f)$ of a function $f : [-1, 1] \rightarrow \mathbb{R}$ by

$$f(x) = \frac{2}{\pi} \sqrt{1-x^2} \sum_{n=0}^{\infty} \mu_n(f) U_n(x), \quad (\text{F.29a})$$

$$\mu_n(f) = \int_{-1}^1 U_n(x) f(x) dx. \quad (\text{F.29b})$$

F.3. Electron Transport Along a Semi-Infinite Chain

Let K denote the tight-binding Hamiltonian on a semi-infinite chain,

$$K = \sum_{l=0}^{\infty} (c_l^\dagger c_{l+1} + c_{l+1}^\dagger c_l), \quad (\text{F.30})$$

and let $|\phi_l\rangle$ denote the state with one electron at site with index l ,

$$|\phi_l\rangle := c_l^\dagger |\text{vac}\rangle. \quad (\text{F.31})$$

Let the index of the first site be zero. It follows that

$$\begin{aligned} K|\phi_0\rangle &= |\phi_1\rangle, \\ K|\phi_l\rangle &= |\phi_{l-1}\rangle + |\phi_{l+1}\rangle \text{ for } l \geq 1. \end{aligned} \quad (\text{F.32})$$

We need the following lemma.

Lemma F.3.1 (Movement on a Semi-Infinite Chain).

(i) For all $n \in \mathbb{N}$ we find

$$U_n(K/2)|\phi_0\rangle = |\phi_n\rangle. \quad (\text{F.33})$$

(ii) For all $n, l \in \mathbb{N} \setminus \{0\}$ we have

$$U_n(K/2)|\phi_l\rangle = \sum_{i=0}^n \Theta_{2(l-n)+2i} |\phi_{l-n+2i}\rangle. \quad (\text{F.34})$$

The $U_n(x)$ are the Chebyshev polynomials of the second kind and Θ_l denotes the discrete unit-step function $\Theta : \mathbb{Z} \rightarrow \{0, 1\}$,

$$\Theta_l := \begin{cases} 1 & \text{for } l \geq 0, \\ 0 & \text{otherwise.} \end{cases} \quad (\text{F.35})$$

F. Chebyshev Polynomials

Proof.

- (i) Since $U_0(x) = 1$ and $U_1(x) = 2x$, we can verify the lemma for $n = 0$ and $n = 1$ with the help of (F.32). Let it be true for all $0 \leq n < N$ with $N > 1$. Then, it follows that

$$U_N(K/2)|\phi_0\rangle \stackrel{(F.15)}{=} KU_{N-1}(K/2)|\phi_0\rangle - U_{N-2}(K/2)|\phi_0\rangle \quad (\text{F.36a})$$

$$\stackrel{\text{i.h.}}{=} K|\phi_{N-1}\rangle - |\phi_{N-2}\rangle \stackrel{(F.32)}{=} |\phi_N\rangle. \quad (\text{F.36b})$$

- (ii) First, we prove the assertion for $n = 1, 2$ and all $l \in \mathbb{N} \setminus \{0\}$. With (F.32) it immediately follows that

$$U_1(K/2)|\phi_l\rangle = K|\phi_l\rangle \stackrel{(F.32)}{=} \sum_{i=0}^1 \Theta_{2(l-1)+2i}|\phi_{l-1+2i}\rangle. \quad (\text{F.37})$$

For $n = 2$ we have

$$U_2(K/2)|\phi_1\rangle \stackrel{(F.15)}{=} (KU_1(K/2) - U_0(K/2))|\phi_1\rangle \stackrel{(F.32)}{=} K(|\phi_0\rangle + |\phi_2\rangle) - |\phi_1\rangle \quad (\text{F.38a})$$

$$\stackrel{(F.32)}{=} |\phi_1\rangle + |\phi_3\rangle = \sum_{i=0}^2 \Theta_{-2+2i}|\phi_{-1+2i}\rangle \quad (\text{F.38b})$$

and for $l \geq 2$

$$U_2(K/2)|\phi_l\rangle \stackrel{(F.15)}{=} (KU_1(K/2) - U_0(K/2))|\phi_l\rangle \stackrel{(F.32)}{=} K(|\phi_{l-1}\rangle + |\phi_{l+1}\rangle) - |\phi_l\rangle \quad (\text{F.38c})$$

$$\stackrel{(F.32)}{=} |\phi_{l-2}\rangle + |\phi_l\rangle + |\phi_{l+2}\rangle = \sum_{i=0}^2 \Theta_{2(l-2)+2i}|\phi_{l-2+2i}\rangle. \quad (\text{F.38d})$$

Second, let the assertion be true for all $l \in \mathbb{N} \setminus \{0\}$ and for all $1 \leq n < N$. Then, we find

$$U_N(K/2)|\phi_l\rangle \stackrel{(F.15)}{=} (KU_{N-1}(K/2) - U_{N-2}(K/2))|\phi_l\rangle \quad (\text{F.39a})$$

$$\stackrel{\text{i.h.}}{=} K \sum_{i=0}^{N-1} \Theta_{2(l-N+1)+2i}|\phi_{l-N+1+2i}\rangle - \sum_{i=0}^{N-2} \Theta_{2(l-N+2)+2i}|\phi_{l-N+2+2i}\rangle \quad (\text{F.39b})$$

$$= \sum_{i=0}^{N-1} \Theta_{2(l-N+1)+2i}(|\phi_{l-N+2+2i}\rangle + \Theta_{l-N+2i}|\phi_{l-N+2i}\rangle) \quad (\text{F.39c})$$

$$- \sum_{i=0}^{N-2} \Theta_{2(l-N+2)+2i}|\phi_{l-N+2+2i}\rangle; \quad (\text{F.39d})$$

now, we change the summation index in the first sum to $j = i + 1$ and separate the term with $i = 0$ from the second sum,

$$= \sum_{j=1}^N \Theta_{2(l-N)+2j}|\phi_{l-N+2j}\rangle + \Theta_{2(l-N+1)}\Theta_{l-N}|\phi_{l-N}\rangle \quad (\text{F.39e})$$

$$+ \sum_{i=1}^{N-1} \Theta_{2(l-N+1)+2i}\Theta_{l-N+2i}|\phi_{l-N+2i}\rangle \quad (\text{F.39f})$$

$$- \sum_{i=0}^{N-2} \Theta_{2(l-N+2)+2i}|\phi_{l-N+2+2i}\rangle; \quad (\text{F.39g})$$

next, we change the summation index in (F.39f) to $j = i - 1$,

$$= \sum_{j=1}^N \Theta_{2(l-N)+2j} |\phi_{l-N+2j}\rangle + \Theta_{2(l-N+1)} \Theta_{l-N} |\phi_{l-N}\rangle \quad (\text{F.39h})$$

$$+ \sum_{j=0}^{N-2} \Theta_{2(l-N+2)+2j} \Theta_{l-N+2+2j} |\phi_{l-N+2+2j}\rangle \quad (\text{F.39i})$$

$$- \sum_{i=0}^{N-2} \Theta_{2(l-N+2)+2i} |\phi_{l-N+2+2i}\rangle; \quad (\text{F.39j})$$

finally, we note that for $l \geq N$ as well as for $l < N$ we can set $\Theta_{2(l-N+1)} \Theta_{l-N} \equiv \Theta_{2(l-N)}$ in (F.39h) and $\Theta_{2(l-N+2)+2j} \Theta_{l-N+2+2j} \equiv \Theta_{2(l-N+2)+2i}$ in (F.39i), leading to

$$U_N(K/2) |\phi_l\rangle = \sum_{j=0}^N \Theta_{2(l-N)+2j} |\phi_{l-N+2j}\rangle. \quad (\text{F.39k})$$

□

F.3.1. Green Functions

The Green functions of the Hamiltonian $H' = \bar{t}K + \bar{\varepsilon}N$, with N denoting the total number operator, are the expectation values

$$G_{lm}(\omega) = \lim_{\eta \searrow 0} \langle \phi_l | (\omega - H' \pm i\eta)^{-1} | \phi_m \rangle \quad (\text{F.40})$$

taken in the states (F.31). Note that since $[K, N] = 0$ and $N|\phi_l\rangle = |\phi_l\rangle$ for any l , we can immediately write

$$G_{lm}(\omega) = \lim_{\eta \searrow 0} \langle \phi_l | (\omega - \bar{t}K - \bar{\varepsilon}N \pm i\eta)^{-1} | \phi_m \rangle = \lim_{\eta \searrow 0} \langle \phi_l | (\omega - \bar{t}K - \bar{\varepsilon} \pm i\eta)^{-1} | \phi_m \rangle, \quad (\text{F.41})$$

and we take care of $\bar{\varepsilon}$ by including it in ω . It therefore suffices to investigate on $H = \bar{t}K$.

Imaginary Part

Since the eigenvalues E_i of $\bar{t}K$ fulfill $|E_i| \leq 2\bar{t}$, see (3.33), it follows that the support of

$$\Im G_{lm}(\omega) = \mp \pi \langle \phi_l | \delta(\omega - \bar{t}K) | \phi_m \rangle \quad (\text{F.42})$$

is given by the interval $-2\bar{t} \leq \omega \leq 2\bar{t}$. We use the property of the Dirac distribution $\delta(ax) = 1/|a|\delta(x)$, see for example [81], to write for positive \bar{t}

$$\Im G_{lm}(\omega) = \mp \frac{\pi}{2\bar{t}} \langle \phi_l | \delta\left(\frac{\omega}{2\bar{t}} - \frac{K}{2}\right) | \phi_m \rangle. \quad (\text{F.43})$$

Now, we expand the ‘function’ $f(x) := \pi\delta(x - z)$ in a Chebyshev series according to (F.29a),

$$\mu_n(f) = \pi \int_{-1}^1 \delta(x - z) U_n(x) dx = \pi U_n(z) \quad (\text{F.44a})$$

which leads to

$$\pi\delta(x - z) = 2\sqrt{1 - x^2} \sum_{n=0}^{\infty} U_n(x) U_n(z). \quad (\text{F.44b})$$

F. Chebyshev Polynomials

The imaginary part of (F.40) is therefore given by

$$\Im G_{lm}(\omega) = \mp \Theta \left(1 - \left(\frac{\omega}{2t} \right)^2 \right) \frac{1}{t} \sqrt{1 - \left(\frac{\omega}{2t} \right)^2} \sum_{n=0}^{\infty} U_n \left(\frac{\omega}{2t} \right) \langle \phi_l | U_n(K/2) | \phi_m \rangle. \quad (\text{F.45})$$

Because H is Hermitian, it suffices to examine the case $l \geq m$. With the help of lemma F.3.1, we can simplify the above expression. The case $m = 0$ is trivial. For $m > 0$ let $l = m + h$ with $h \in \mathbb{N}$ and let $y \in \mathbb{N}$, then

$$\sum_{n=0}^{\infty} U_n(x) \langle \phi_{m+h} | U_n(K/2) | \phi_m \rangle = \sum_{n=0}^{\infty} U_n(x) \sum_{i=0}^n \Theta_{2(m-n)+2i} \delta_{m+h, m-n+2i} \quad (\text{F.46a})$$

$$= \sum_{k=0}^{\infty} \left\{ U_{2k}(x) \sum_{i=0}^{2k} \Theta_{2(m-2k)+2i} \delta_{2i, h+2k} \right. \quad (\text{F.46b})$$

$$\left. + U_{2k+1}(x) \sum_{i=0}^{2k+1} \Theta_{2(m-2k-1)+2i} \delta_{2i, h+2k+1} \right\}$$

$$= \sum_{k=0}^{\infty} \left\{ U_{2k}(x) \delta_{h, 2y} \sum_{i=0}^{2k} \Theta_{2(m-2k)+2i} \delta_{2i, 2y+2k} \right. \quad (\text{F.46c})$$

$$\left. + U_{2k+1}(x) \delta_{h, 2y+1} \sum_{i=0}^{2k+1} \Theta_{2(m-2k-1)+2i} \delta_{2i, 2y+2k+2} \right\}$$

$$= \sum_{k=0}^{\infty} \Theta_{m+y-k} \Theta_{k-y} \left\{ U_{2k}(x) \delta_{h, 2y} + U_{2k+1}(x) \delta_{h, 2y+1} \right\}. \quad (\text{F.46d})$$

Thus, we can write for $h, m \in \mathbb{N}$,

$$\begin{aligned} \bar{t} \Im G_{m+h, m}(\omega) &= \mp \Theta(1-x^2) w_2(x) \left\{ \delta_{m,0} U_h(x) \right. \\ &\quad \left. + (1 - \delta_{m,0}) \sum_{k=0}^{\infty} \Theta_{m+y-k} \Theta_{k-y} \left\{ U_{2k}(x) \delta_{h, 2y} + U_{2k+1}(x) \delta_{h, 2y+1} \right\} \right\} \end{aligned} \quad (\text{F.47})$$

with the abbreviation $x := \omega/(2\bar{t})$ and the discrete unit-step function Θ_l , see (F.35). The function $w_2(x)$ is defined in Sect. F.2 and denotes the weight function of the Chebyshev polynomials of the second kind, $w_2(x) = \sqrt{1-x^2}$.

Real Part

The real part of (F.40),

$$\Re G_{lm}(\omega) = \mathcal{P} \langle \phi_l | (\omega - \bar{t}K)^{-1} | \phi_m \rangle, \quad (\text{F.48})$$

can be obtained, see (F.42), by means of

$$\bar{t} \Re G_{lm}(\omega) = \mp \frac{1}{\pi} \mathcal{P} \int_{-\infty}^{\infty} \frac{\bar{t} \Im G_{lm}(\omega')}{\omega - \omega'} d\omega'. \quad (\text{F.49})$$

Due to

$$\frac{1}{\pi} \mathcal{P} \int_{-2\bar{t}}^{2\bar{t}} \frac{w_2 \left(\frac{\omega'}{2\bar{t}} \right) U_l \left(\frac{\omega'}{2\bar{t}} \right)}{\omega - \omega'} d\omega' = \frac{1}{\pi} \mathcal{P} \int_{-1}^1 \frac{w_2(y) U_l(y)}{\frac{\omega}{2\bar{t}} - y} dy \stackrel{(\text{F.22})}{=} \frac{1}{t} I_l \left(\frac{\omega}{2t} \right), \quad (\text{F.50})$$

we can evaluate the real part. We obtain

$$\bar{t} \Re G_{m+h, m}(x) \stackrel{(\text{F.22})}{=} \delta_{m,0} I_h(x) + (1 - \delta_{m,0}) \sum_{k=0}^{\infty} \Theta_{m+y-k} \Theta_{k-y} \left\{ I_{2k}(x) \delta_{h, 2y} + I_{2k+1}(x) \delta_{h, 2y+1} \right\} \quad (\text{F.51})$$

with the abbreviation $x := \omega/(2\bar{t})$.

Properties of the $I_n(x)$

For the calculation of the real part (F.51) of the Green function (F.40) we need explicit expressions for the functions $I_n(x)$, see (F.22), for $n \in \mathbb{N}$. Let us therefore summarize their properties in form of the following lemma.

Lemma F.3.2 (Properties of the $I_n(x)$).

The functions (F.22),

$$I_n : \mathbb{R} \rightarrow \mathbb{R},$$

$$I_n(x) = \mathcal{P} \int_{-1}^1 \frac{w_2(y)U_n(y)}{\pi(x-y)} dy, \quad (\text{F.52})$$

with index $n \in \mathbb{N}$ have the following properties:

(i) For $n \geq 1$ the $I_n(x)$ obey the recurrence relation

$$I_{n+1}(x) = 2xI_n(x) - I_{n-1}(x). \quad (\text{F.53})$$

(ii) For $|x| < 1$ they evaluate to

$$I_n(x) = T_{n+1}(x). \quad (\text{F.54})$$

(iii) For $|x| > 1$ the functions $I_n(x)$ are expressible in terms of Chebyshev polynomials and read

$$I_n(x) = T_{n+1}(x) - \tilde{w}_2(x)U_n(x) \quad (\text{F.55})$$

with the abbreviation

$$\tilde{w}_2(x) := \text{sgn}(x)\sqrt{x^2 - 1}. \quad (\text{F.55a})$$

(iv) The powers $I_n^p(x)$, $p \in \mathbb{N} \setminus \{0\}$, of the functions $I_n(x)$ are given by

$$I_n^p(x) = \Theta(x^2 - 1)\{T_{p(n+1)}(x) - \tilde{w}_2(x)U_{p(n+1)-1}(x)\} + \Theta(1 - x^2)T_{n+1}^p(x). \quad (\text{F.56})$$

Proof.

(i) For $n \in \mathbb{N}$ we find

$$I_{n+1}(x) = \mathcal{P} \int_{-1}^1 \frac{w_2(y)U_{n+1}(y)}{\pi(x-y)} dy \quad (\text{F.57a})$$

$$\stackrel{(\text{F.15})}{=} \mathcal{P} \int_{-1}^1 \frac{w_2(y)2yU_n(y)}{\pi(x-y)} dy - I_{n-1}(x) \quad (\text{F.57b})$$

$$\stackrel{(\text{F.15})}{=} 2\mathcal{P} \int_{-1}^1 \frac{w_2(y)U_n(y)(y-x+x)}{\pi(x-y)} dy - I_{n-1}(x) \quad (\text{F.57c})$$

$$\stackrel{(\text{F.15})}{=} -\frac{2}{\pi} \int_{-1}^1 w_2(y)U_n(y) dy + 2xI_n(x) - I_{n-1}(x) \quad (\text{F.57d})$$

$$\stackrel{(\text{F.15})}{=} -\delta_{n,0} + 2xI_n(x) - I_{n-1}(x) \quad (\text{F.57e})$$

(ii) See equation (7.344) in [140].

F. Chebyshev Polynomials

- (iii) First, we prove (F.55) for $n = 0$ and $n = 1$. Then, we generalize with the aid of (F.53) by means of induction over n . For $n = 0$ we find

$$I_0(x) = \frac{1}{\pi} \int_{-1}^1 \frac{\sqrt{1-y^2}}{(x-y)} dy \quad (\text{F.58a})$$

$$= \frac{1}{\pi} \int_0^\pi \frac{\sin^2(x)}{x - \cos(x)} dx \quad (\text{F.58b})$$

$$= x \left(1 - \sqrt{1 - \frac{1}{x^2}} \right) \quad (\text{F.58c})$$

$$\equiv T_1(x) - \tilde{w}_2(x)U_0(x), \quad (\text{F.58d})$$

where the third equality follows from equation (3.644), no. 4 of [140]. Then, the case of $n = 1$ follows immediately,

$$I_1(x) = \frac{2}{\pi} \int_{-1}^1 \frac{w_2(y)y}{x-y} dy \quad (\text{F.59a})$$

$$= \frac{2}{\pi} \int_{-1}^1 \frac{w_2(y)(y-x+x)}{x-y} dy \quad (\text{F.59b})$$

$$= -\frac{2}{\pi} \int_{-1}^1 w_2(y) dy + 2xI_0(x) \quad (\text{F.59c})$$

$$= -1 + 2xI_0(x) \quad (\text{F.59d})$$

$$= T_2(x) - \tilde{w}_2(x)U_1(x). \quad (\text{F.59e})$$

Now, let $N > 2$ and let (F.55) be true for all $1 \leq n < N$, then

$$I_N(x) \stackrel{(\text{F.53})}{=} 2xI_{N-1}(x) - I_{N-2}(x) \quad (\text{F.60a})$$

$$\stackrel{\text{i.h.}}{=} 2x(T_N(x) - \tilde{w}_2(x)U_{N-1}(x)) - (T_{N-1}(x) - \tilde{w}_2(x)U_{N-2}(x)) \quad (\text{F.60b})$$

$$= 2xT_N(x) - T_{N-1}(x) - \tilde{w}_2(x)(2xU_{N-1}(x) - U_{N-2}(x)) \quad (\text{F.60c})$$

$$\stackrel{(\text{F.53})}{=} T_{N+1}(x) - \tilde{w}_2(x)U_N(x). \quad (\text{F.60d})$$

- (iv) For $|x| < 1$ there is nothing to show. For $|x| > 1$ we prove (F.56) by induction over p . The formula is valid for $p = 1$. Let it be valid for $p \geq 1$, then, we find

$$I_n^{p+1}(|x| > 1) \stackrel{\text{i.h.}}{=} (T_{p(n+1)}(x) - \tilde{w}_2(x)U_{p(n+1)-1}(x))I_n(x) \quad (\text{F.61a})$$

$$= T_{p(n+1)}(x)T_{n+1}(x) + (x^2 - 1)U_{p(n+1)-1}(x)U_n(x) - \tilde{w}_2(x)\{T_{p(n+1)}(x)U_n(x) + U_{p(n+1)-1}(x)T_{n+1}(x)\} \quad (\text{F.61b})$$

$$= \frac{1}{2}\{T_{(p+1)(n+1)}(x) + T_{(p-1)(n+1)}(x) + T_{(p+1)(n+1)}(x) - T_{(p-1)(n+1)}(x)\} - \frac{1}{2}\tilde{w}_2(x)\{U_{(p+1)(n+1)-1}(x) - U_{(p-1)(n+1)-1}(x) + U_{(p+1)(n+1)-1}(x) + U_{(p-1)(n+1)-1}(x)\} \quad (\text{F.61c})$$

$$= T_{(p+1)(n+1)}(x) - \tilde{w}_2(x)U_{(p+1)(n+1)-1}(x), \quad (\text{F.61d})$$

where the first parenthesis in (F.61c) follows from (F.23) and (F.27). For $p = 1$, the second parenthesis in (F.61b) leads directly to (F.61d) with the help of (F.24). For $p > 1$, the second parenthesis in (F.61c) follows from (F.25) and (F.26).

□

Summary

The Green functions of the single-particle Hamiltonian $H' = \bar{t}K + \bar{\varepsilon}N$,

$$G_{lm}(\omega) = \lim_{\eta \searrow 0} \langle \phi_l | (\omega - \bar{t}K - \bar{\varepsilon}N \pm i\eta)^{-1} | \phi_m \rangle, \quad (\text{F.62})$$

where K is the simple tight-binding Hamiltonian on a semi-infinite chain, (F.30), N the operator for the total number of particles and where the states $|\phi_l\rangle$ are defined in (F.31), are given by

$$\begin{aligned} \bar{t}G_{m+h,m}(\omega) &= \delta_{m,0}I_h(x) + (1 - \delta_{m,0}) \sum_{k=0}^{\infty} \Theta_{m+y-k} \Theta_{k-y} \{ I_{2k}(x)\delta_{h,2y} + I_{2k+1}(x)\delta_{h,2y+1} \} \\ &\mp i\Theta(1-x^2)w_2(x) \left\{ \delta_{m,0}U_h(x) \right. \\ &\quad \left. + (1 - \delta_{m,0}) \sum_{k=0}^{\infty} \Theta_{m+y-k} \Theta_{k-y} \{ U_{2k}(x)\delta_{h,2y} + U_{2k+1}(x)\delta_{h,2y+1} \} \right\}, \end{aligned} \quad (\text{F.62a})$$

where $2\bar{t}x = \omega - \bar{\varepsilon}$ and $w_2(x) = \sqrt{1-x^2}$ is the weight function of the Chebyshev polynomials of the second kind, see Sect. F.2. The $T_l(x)$ and $U_l(x)$ are the Chebyshev polynomials of the first and second kind, respectively. The explicit expressions of the functions $I_l(x)$ in terms of Chebyshev polynomials can be found in lemma F.3.2 and read

$$I_n(x) = \Theta(x^2 - 1)(T_{n+1}(x) - \tilde{w}_2(x)U_n(x)) + \Theta(1-x^2)T_{n+1}(x). \quad (\text{F.63})$$

We have proven expression (F.62a) only for $l \geq m$. However, since H' is Hermitian, we find the symmetry $G_{lm}(\omega) = G_{ml}(\omega)$.

F.3.2. Products of Green Functions

In the last section we found that for $n \in \mathbb{N}$ the Green function (F.40),

$$G_{n0}(\omega) = \lim_{\eta \searrow 0} \langle \phi_n | (\omega - \bar{t}K - \bar{\varepsilon}N - i\eta)^{-1} | \phi_0 \rangle \quad (\text{F.64})$$

$$= \frac{1}{2\bar{t}} \lim_{\eta \searrow 0} \langle \phi_n | (x - K/2 - i\eta)^{-1} | \phi_0 \rangle, \quad (\text{F.64a})$$

where we abbreviated $2\bar{t}x := \omega - \bar{\varepsilon}$, is according to (F.62a) given by

$$\bar{t}G_{n0}(\omega) = \Theta(x^2 - 1)I_n(x) + \Theta(1-x^2)\{T_{n+1}(x) + iw_2(x)U_n(x)\}, \quad (\text{F.65})$$

where the functions $I_n(x)$ can be found in (F.55). In chapter 10 we need the the following lemma.

Lemma F.3.3 (Powers of Green Functions).

For $n \in \mathbb{N}$ and $p \in \mathbb{N} \setminus \{0\}$ we have

$$\bar{t}^p G_{n0}^p(\omega) = \Theta(x^2 - 1)I_n^p(x) + \Theta(1-x^2)\{T_{p(n+1)}(x) + iw_2(x)U_{p(n+1)-1}(x)\}. \quad (\text{F.66})$$

Proof.

We prove the assertion by induction over p . As the proof of the first term in (F.66) is trivial and since we already expressed the powers $I_n^p(x)$ in terms of Chebyshev polynomials, see lemma F.3.2, we concentrate on the part which is non-zero for $x^2 < 1$. The assertion is clearly true for $p = 1$, see (F.65), and for $p = 2$ we find

$$\Theta(1-x^2)\bar{t}^2 G_{n0}^2(\omega) = (T_{n+1}(x) + iw_2(x)U_n(x))^2 \quad (\text{F.67a})$$

F. Chebyshev Polynomials

$$= (T_{n+1}^2(x) - (1-x^2)U_n^2(x)) + iw_2(x)2U_n(x)T_{n+1}(x) \quad (\text{F.67b})$$

$$\stackrel{(\text{F.27})}{=} T_{2(n+1)}(x) + iw_2(x)2U_n(x)T_{n+1}(x) \quad (\text{F.67c})$$

$$\stackrel{(\text{F.24})}{=} T_{2(n+1)}(x) + iw_2(x)U_{2(n+1)-1} \quad (\text{F.67d})$$

which proves (F.66) for $p = 2$. Next, we can continue with the induction step. Let the assertion be true for $p \geq 2$, then

$$\Theta(1-x^2)\bar{t}^{p+1}G_{n_0}^{p+1}(\omega) = \Theta(1-x^2)\bar{t}^p G_{n_0}^p(\omega)\bar{t}G_{n_0}(\omega) \quad (\text{F.67e})$$

$$\stackrel{\text{i.h.}}{=} (T_{p(n+1)}(x) + iw_2(x)U_{p(n+1)-1}(x))\Theta(1-x^2)\bar{t}G_{n_0}(\omega) \quad (\text{F.67f})$$

$$= T_{p(n+1)}(x)T_{n+1}(x) - (1-x^2)U_{p(n+1)-1}(x)U_n(x) \quad (\text{F.67g})$$

$$+ iw_2(x)(U_{p(n+1)-1}(x)T_{n+1}(x) + T_{p(n+1)}U_n(x)) \quad (\text{F.67h})$$

$$= T_{(p+1)(n+1)}(x) + iw_2(x)U_{(p+1)(n+1)-1}(x),$$

where the last equality follows again from equations (F.23) to (F.26). \square

Summary

For $n \in \mathbb{N}$ and $p \in \mathbb{N} \setminus \{0\}$ we find for the powers $G_{n_0}^p(\omega)$ of the Green functions (F.64) that

$$\begin{aligned} \bar{t}^p G_{n_0}^p(\omega) &= \Theta(x^2 - 1)\{T_{p(n+1)}(x) - \tilde{w}_2(x)U_{p(n+1)-1}(x)\} \\ &\quad + \Theta(1-x^2)\{T_{p(n+1)}(x) + iw_2(x)U_{p(n+1)-1}(x)\}, \end{aligned} \quad (\text{F.68})$$

where we abbreviated $2\bar{t}x := \omega - \bar{\varepsilon}$. The function $w_2(x)$ denotes the weight function of the Chebyshev polynomials of the second kind, $w_2(x) = \sqrt{1-x^2}$, and $\tilde{w}_2(x) = \text{sgn}(x)\sqrt{x^2-1}$, see (F.55a).

For convenience, we state some of the functions for small n and p , we need in chapter 10 explicitly. We find for $n = 0$,

$$\bar{t}G_{00}(\omega) = \Theta(x^2 - 1)\{T_1(x) - \tilde{w}_2(x)U_0(x)\} + \Theta(1-x^2)\{T_1(x) + iw_2(x)U_0(x)\}, \quad (\text{F.69})$$

$$\bar{t}^2 G_{00}^2(\omega) = \Theta(x^2 - 1)\{T_2(x) - \tilde{w}_2(x)U_1(x)\} + \Theta(1-x^2)\{T_2(x) + iw_2(x)U_1(x)\}, \quad (\text{F.70})$$

$$\bar{t}^3 G_{00}^3(\omega) = \Theta(x^2 - 1)\{T_3(x) - \tilde{w}_2(x)U_2(x)\} + \Theta(1-x^2)\{T_3(x) + iw_2(x)U_2(x)\}, \quad (\text{F.71})$$

$$\bar{t}^4 G_{00}^4(\omega) = \Theta(x^2 - 1)\{T_4(x) - \tilde{w}_2(x)U_3(x)\} + \Theta(1-x^2)\{T_4(x) + iw_2(x)U_3(x)\}. \quad (\text{F.72})$$

For $n = 1$ we have

$$\bar{t}G_{10}(\omega) = \Theta(x^2 - 1)\{T_2(x) - \tilde{w}_2(x)U_1(x)\} + \Theta(1-x^2)\{T_2(x) + iw_2(x)U_1(x)\}, \quad (\text{F.73})$$

$$\bar{t}^2 G_{10}^2(\omega) = \Theta(x^2 - 1)\{T_4(x) - \tilde{w}_2(x)U_3(x)\} + \Theta(1-x^2)\{T_4(x) + iw_2(x)U_3(x)\}. \quad (\text{F.74})$$

Additionally, we state the formulae for two products which arise in chapter 10. First, we have

$$\bar{t}^2 G_{00}(\omega)G_{10}(\omega) = \Theta(x^2 - 1)\{T_3(x) - \tilde{w}_2(x)U_2(x)\} + \Theta(1-x^2)\{T_3(x) + iw_2(x)U_2(x)\}, \quad (\text{F.75})$$

and second, we find

$$\bar{t}^3 G_{00}^2(\omega)G_{10}(\omega) = \Theta(x^2 - 1)\{T_4(x) - \tilde{w}_2(x)U_3(x)\} + \Theta(1-x^2)\{T_4(x) + iw_2(x)U_3(x)\}. \quad (\text{F.76})$$

Bibliography

- [1] M. Imada, A. Fujimori, and Y. Tokura, “Metal-insulator transitions”, *Reviews of Modern Physics*, vol. 70, no. 4, pp. 1039–1263, 1998.
- [2] F. Gebhard, *The Mott Metal-Insulator Transition*, vol. 137 of *Springer Tracts in Modern Physics*. Springer, 1997.
- [3] N. W. Ashcroft and N. D. Mermin, *Solid State Physics*. Thomson Learning, 1975.
- [4] G. D. Mahan, *Many-Particle Physics*. Physics of Solids and Liquids, Plenum Press, second ed., 1990.
- [5] J. H. de Boer and E. J. W. Verwey, “Semi-conductors with partially and with completely filled 3d-lattice bands”, *Proceedings of the Physical Society*, vol. 49, no. 4S, p. 59, 1937.
- [6] N. F. Mott and R. Peierls, “Discussion of the paper by de Boer and Verwey”, *Proceedings of the Physical Society*, vol. 49, no. 4S, p. 72, 1937.
- [7] N. F. Mott, *Metal-Insulator Transitions*. Taylor & Franics Ltd, second ed., 1990.
- [8] N. F. Mott, “The basis of the electron theory of metals, with special reference to the transition metals”, *Proceedings of the Physical Society. Section A*, vol. 62, no. 7, pp. 416–422, 1949.
- [9] N. F. Mott, “On the transition to metallic conduction in semiconductors”, *Canadian Journal of Physics*, vol. 34, pp. 1356–1368, 1956.
- [10] N. F. Mott, “The transition to the metallic state”, *Philosophical Magazine*, vol. 6, pp. 287–309, 1961.
- [11] J. W. Negele and H. Orland, *Quantum Many-Particle Systems*. Advanced Book Classics, Westview Press, 1998.
- [12] A. L. Fetter and J. D. Walecka, *Quantum Theory of Many-Particle Systems*. Dover Publications Inc., 2003.
- [13] P. Drude, “Zur Elektronentheorie der Metalle”, *Annalen der Physik*, vol. 306, no. 3, pp. 566–613, 1900.
- [14] M. Born and R. Oppenheimer, “Zur Quantentheorie der Molekeln”, *Annalen der Physik*, vol. 389, no. 20, pp. 457–484, 1927.
- [15] D. R. Hartree, “The wave mechanics of an atom with a non-coulomb central field. Part I. Theory and methods”, *Mathematical Proceedings of the Cambridge Philosophical Society*, vol. 24, no. 01, pp. 89–110, 1928.
- [16] D. R. Hartree, “The wave mechanics of an atom with a non-coulomb central field. Part II. Some results and discussion”, *Mathematical Proceedings of the Cambridge Philosophical Society*, vol. 24, no. 01, pp. 111–132, 1928.
- [17] V. Fock, “Näherungsmethode zur Lösung des quantenmechanischen Mehrkörperproblems”, *Zeitschrift für Physik*, vol. 61, pp. 126–148, 1930.
- [18] O. Madelung, *Introduction to Solid-State Theory*. Springer Series in Solid-State Sciences, Springer, 1995.
- [19] P. L. Taylor and O. Heinonen, *A Quantum Approach to Condensed Matter Physics*. Cambridge University Press, 2002.

Bibliography

- [20] G. Czycholl, *Theoretische Festkörperphysik*. Springer, 2004.
- [21] J. M. Ziman, *Electrons and Phonons*. Oxford Classic Texts in the Physical Sciences, Oxford University Press, 2004.
- [22] L. N. Cooper, “Bound electron pairs in a degenerate Fermi gas”, *Physical Review*, vol. 104, pp. 1189–1190, 1956.
- [23] J. Bardeen, L. N. Cooper, and J. R. Schrieffer, “Microscopic theory of superconductivity”, *Physical Review*, vol. 106, pp. 162–164, 1957.
- [24] J. Bardeen, L. N. Cooper, and J. R. Schrieffer, “Theory of superconductivity”, *Physical Review*, vol. 108, pp. 1175–1204, 1957.
- [25] J. C. Slater, “Note on Hartree’s method”, *Physical Review*, vol. 35, pp. 210–211, 1930.
- [26] G. C. Wick, “The evaluation of the collision matrix”, *Physical Review*, vol. 80, pp. 268–272, 1950.
- [27] T. Koopmans, “Über die Zuordnung von Wellenfunktionen und Eigenwerten zu den einzelnen Elektronen eines Atoms”, *Physica*, vol. 1, no. 1-6, pp. 104–113, 1934.
- [28] H. Bruus and K. Flensberg, *Many-Body Quantum Theory in Condensed Matter Physics*. Oxford Graduate Texts, Oxford University Press, first ed., 2004.
- [29] P. Fazekas, *Lecture Notes on Electron Correlation and Magnetism*, vol. 5 of *Series in Modern Condensed Matter Physics*. World Scientific Publishing Co. Pte. Ltd, 1999.
- [30] E. Wigner and F. Seitz, “On the constitution of metallic sodium”, *Physical Review*, vol. 43, pp. 804–810, 1933.
- [31] E. Wigner and F. Seitz, “On the constitution of metallic sodium. II”, *Physical Review*, vol. 46, pp. 509–524, 1934.
- [32] E. N. Economou, *Green’s Functions in Quantum Physics*. Springer Series in Solid-State Sciences, Springer, third ed., 2006.
- [33] F. Bloch, “Über die Quantenmechanik der Elektronen in Kristallgittern”, *Zeitschrift für Physik*, vol. 52, pp. 555–600, 1929.
- [34] W. Kohn, “Analytic properties of Bloch waves and Wannier functions”, *Physical Review*, vol. 115, pp. 809–821, 1959.
- [35] J. D. Cloizeaux, “Energy bands and projection operators in a crystal: Analytic and asymptotic properties”, *Physical Review*, vol. 135, pp. A685–A697, 1964.
- [36] J. D. Cloizeaux, “Analytical properties of n -dimensional energy bands and Wannier functions”, *Physical Review*, vol. 135, pp. A698–A707, 1964.
- [37] M. Abramowitz and I. A. Stegun, eds., *Handbook of Mathematical Functions*. Dover Publications Inc., 1972.
- [38] T. Hanisch, B. Kleine, and E. Müller-Hartmann, “Ferromagnetism in the Hubbard model: instability of the Nagaoka state on the triangular, honeycomb and kagome lattices”, *Annalen der Physik*, vol. 507, no. 4, pp. 303–328, 1995.
- [39] T. Morita and T. Horiguchi, “Lattice Green’s functions for the cubic lattices in terms of the complete elliptic integral”, *Journal of Mathematical Physics*, vol. 12, no. 6, pp. 981–986, 1971.

- [40] G. S. Joyce, “Lattice Green function for the simple cubic lattice”, *Journal of Physics A: General Physics*, vol. 5, no. 8, pp. L65–L68, 1972.
- [41] D. Vollhardt, “Investigation of correlated electron systems using the limit of high dimensions”, in *Correlated Electron Systems: Jerusalem, Israel, 30 Dec 91-8 Jan 92 (Jerusalem Winter School for Theoretical Physics)* (V. J. Emery, ed.), p. 57, World Scientific Publishing Co. Pte. Ltd, 1993.
- [42] E. Müller-Hartmann, “Correlated fermions on a lattice in high dimensions”, *Zeitschrift für Physik B: Condensed Matter*, vol. 74, pp. 507–512, 1989.
- [43] L. Kantorovich, *Quantum Theory of the Solid State: An Introduction*, vol. 136 of *Fundamental Theories of Physics*. Kluwer Academic Publishers, 2004.
- [44] J. L. Gross and J. Yellen, *Graph Theory and its Applications*. Discrete Mathematics and its Applications, Chapman & Hall/CRC, second ed., 2006.
- [45] P. Tittmann, *Einführung in die Kombinatorik*. Spektrum-Hochschultaschenbuch, Spektrum Akademischer Verlag, 2007.
- [46] R. J. Baxter, *Exactly Solved Models in Statistical Mechanics*. Dover Publications, Inc., 2007.
- [47] T. P. Eggarter, “Cayley trees, the Ising problem, and the thermodynamic limit”, *Physical Review B*, vol. 9, pp. 2989–2992, 1974.
- [48] E. Müller-Hartmann and J. Zittartz, “New type of phase transition”, *Physical Review Letters*, vol. 33, pp. 893–897, 1974.
- [49] F. Yndurain, “Surface magnetic order in the Ising model: A Cayley tree approximation”, *Physics Letters A*, vol. 62, no. 2, pp. 93–94, 1977.
- [50] F. Yndurain, R. Barrio, R. J. Elliott, and M. F. Thorpe, “Long-range correlations in Bethe lattices”, *Physical Review B*, vol. 28, pp. 3576–3578, 1983.
- [51] C. Domb, “On the theory of cooperative phenomena in crystals”, *Advances in Physics*, vol. 9, pp. 149–244, 1960.
- [52] C. Domb, “On the theory of cooperative phenomena in crystals”, *Advances in Physics*, vol. 9, pp. 245–361, 1960.
- [53] H. A. Bethe, “Statistical theory of superlattices”, *Proceedings of the Royal Society of London. Series A - Mathematical and Physical Sciences*, vol. 150, no. 871, pp. 552–575, 1935.
- [54] C.-K. Hu and N. S. Izmailian, “Exact correlation functions of Bethe lattice spin models in external magnetic fields”, *Physical Review E*, vol. 58, pp. 1644–1653, 1998.
- [55] M. E. Fisher and J. W. Essam, “Some cluster size and percolation problems”, *Journal of Mathematical Physics*, vol. 2, no. 4, pp. 609–619, 1961.
- [56] J. Chalupa, P. L. Leath, and G. R. Reich, “Bootstrap percolation on a Bethe lattice”, *Journal of Physics C: Solid State Physics*, vol. 12, no. 1, pp. L31–L35, 1979.
- [57] Z. Q. Zhang, T. C. Li, and F. C. Pu, “Percolation on a Bethe lattice with multi-neighbour bonds—exact results”, *Journal of Physics A: Mathematical and General*, vol. 16, no. 10, pp. 2267–2280, 1983.
- [58] R. Abou-Chacra, D. J. Thouless, and P. W. Anderson, “A selfconsistent theory of localization”, *Journal of Physics C: Solid State Physics*, vol. 6, no. 10, pp. 1734–1752, 1973.

Bibliography

- [59] R. Abou-Chacra and D. J. Thouless, “Self-consistent theory of localization: II. Localization near the band edges”, *Journal of Physics C: Solid State Physics*, vol. 7, no. 1, pp. 65–75, 1974.
- [60] J. L. Beeby, “Localization on a Bethe lattice”, *Journal of Physics C: Solid State Physics*, vol. 6, no. 14, pp. L283–L287, 1973.
- [61] M. R. Zirnbauer, “Localization transition on the Bethe lattice”, *Physical Review B*, vol. 34, pp. 6394–6408, 1986.
- [62] G. D. Mahan, “Energy bands of the Bethe lattice”, *Physical Review B*, vol. 63, p. 155110, 2001.
- [63] M. Kollar, M. Eckstein, K. Byczuk, N. Blümer, P. van Dongen, M. R. de Cuba, W. Metzner, D. Tanasković, V. Dobrosavljević, G. Kotliar, and D. Vollhardt, “Green functions for nearest- and next-nearest-neighbor hopping on the Bethe lattice”, *Annalen der Physik*, vol. 14, no. 9-10, pp. 642–657, 2005.
- [64] M. Eckstein, M. Kollar, K. Byczuk, and D. Vollhardt, “Hopping on the Bethe lattice: Exact results for densities of states and Dynamical Mean-Field Theory”, *Physical Review B*, vol. 71, p. 235119, 2005.
- [65] M.-B. Lepetit, M. Cousy, and G. Pastor, “Density-matrix renormalization study of the Hubbard model on a Bethe lattice”, *European Physical Journal B*, vol. 13, no. 3, pp. 421–427, 2000.
- [66] E. Kalinowski and F. Gebhard, “Mott-Hubbard insulator in infinite dimensions”, *Journal of Low Temperature Physics*, vol. 126, pp. 979–1007, 2002.
- [67] M. P. Eastwood, F. Gebhard, E. Kalinowski, S. Nishimoto, and R. M. Noack, “Analytical and numerical treatment of the Mott-Hubbard insulator in infinite dimensions”, *The European Physical Journal B*, vol. 35, pp. 155–175, 2003.
- [68] F. Harary, *Graph theory and theoretical physics*. Academic Press, 1967.
- [69] W. F. Brinkman and T. M. Rice, “Single-particle excitations in magnetic insulators”, *Physical Review B*, vol. 2, pp. 1324–1338, 1970.
- [70] M.-S. Chen, L. Onsager, J. Bonner, and J. Nagle, “Hopping of ions in ice”, *The Journal of Chemical Physics*, vol. 60, no. 2, pp. 405–419, 1974.
- [71] B. T. Matthias, M. Peter, H. J. Williams, A. M. Clogston, E. Corenzwit, and R. C. Sherwood, “Magnetic moment of transition metal atoms in dilute solution and their effect on superconducting transition temperature”, *Physical Review Letters*, vol. 5, pp. 542–544, 1960.
- [72] A. M. Clogston, B. T. Matthias, M. Peter, H. J. Williams, E. Corenzwit, and R. C. Sherwood, “Local magnetic moment associated with an iron atom dissolved in various transition metal alloys”, *Physical Review*, vol. 125, pp. 541–552, 1962.
- [73] P. de Faget de Casteljau and J. Friedel, “Étude de la résistivité et du pouvoir thermoélectrique des impuretés dissoutes dans les métaux nobles”, *Journal de Physique et Le Radium*, vol. 17, no. 1, pp. 27–32, 1956.
- [74] J. Friedel, “Sur la structure électronique des métaux et alliages de transition et des métaux lourds”, *Journal de Physique et Le Radium*, vol. 19, no. 6, pp. 573–581, 1958.
- [75] J. Friedel, “Metallic alloys”, *Supplemento del Il Nuovo Cimento*, vol. 7, no. 0, pp. 287–311, 1958.
- [76] S. Doniach and E. H. Sondheimer, *Green’s Functions for Solid State Physicists*. Imperial College Press, Imperial College Press ed., 1998.

- [77] P. W. Anderson, “Localized magnetic states in metals”, *Physical Review*, vol. 124, pp. 41–53, 1961.
- [78] P. Phillips, *Advanced Solid State Physics*. Advanced Book Program, Westview Press, 2003.
- [79] U. Fano, “Effects of configuration interaction on intensities and phase shifts”, *Physical Review*, vol. 124, pp. 1866–1878, 1961.
- [80] A. C. Hewson, *The Kondo Problem to Heavy Fermions*. Cambridge Studies in Magnetism, Cambridge University Press, 1997.
- [81] A. Messiah, *Quantum Mechanics*. Dover Publications, Inc., 1999.
- [82] M. C. Gutzwiller, “Effect of correlation on the ferromagnetism of transition metals”, *Physical Review Letters*, vol. 10, pp. 159–162, 1963.
- [83] J. Kanamori, “Electron correlation and ferromagnetism of transition metals”, *Progress of Theoretical Physics*, vol. 30, pp. 275–289, 1963.
- [84] J. Hubbard, “Electron correlations in narrow energy bands.”, *Proceedings of the Royal Society*, vol. 276, pp. 238–257, 1963.
- [85] J. Hubbard, “Electron correlations in narrow energy bands. II. The degenerate band case”, *Proceedings of the Royal Society*, vol. 277, pp. 237–259, 1964.
- [86] J. Hubbard, “Electron correlations in narrow energy bands. III. An improved solution”, *Proceedings of the Royal Society*, vol. 281, pp. 401–419, 1964.
- [87] J. Hubbard, “Electron correlations in narrow energy bands. IV. The atomic representation”, *Proceedings of the Royal Society*, vol. 285, pp. 542–560, 1965.
- [88] J. Hubbard, “Electron correlations in narrow energy bands. V. A perturbation expansion about the atomic limit”, *Proceedings of the Royal Society*, vol. 296, pp. 82–99, 1967.
- [89] J. Hubbard, “Electron correlations in narrow energy bands. VI. The connexion with many-body perturbation theory”, *Proceedings of the Royal Society*, vol. 296, pp. 100–112, 1967.
- [90] E. H. Lieb and F. Y. Wu, “Absence of Mott transition in an exact solution of the short-range, one-band model in one dimension”, *Physical Review Letters*, vol. 20, pp. 1445–1448, 1968.
- [91] F. H. L. Essler, V. E. Korepin, and K. Schoutens, “Complete solution of the one-dimensional Hubbard model”, *Physical Review Letters*, vol. 67, pp. 3848–3851, 1991.
- [92] A. M. Zagoskin, *Quantum Theory of Many-Body Systems*. Graduate Texts in Contemporary Physics, Springer, 1998.
- [93] F. H. L. Essler, H. Frahm, F. Göhmann, A. Klümper, and V. E. Korepin, *The One-Dimensional Hubbard Model*. Cambridge University Press, 2005.
- [94] M. Takahashi, *Thermodynamics of One-Dimensional Solvable Models*. Cambridge University Press, 1999.
- [95] A. Bohm, *Quantum Mechanics—Foundations and Applications*. Texts and Monographs in Physics, Springer, third ed., 2001.
- [96] E. Müller-Hartmann, “The Hubbard model at high dimensions: some exact results and weak coupling theory”, *Zeitschrift für Physik B: Condensed Matter*, vol. 76, pp. 211–217, 1989.

Bibliography

- [97] W. Metzner, “Linked-cluster expansion around the atomic limit of the Hubbard model”, *Physical Review B*, vol. 43, pp. 8549–8563, 1991.
- [98] S. Pairault, D. Sénéchal, and A.-M. S. Tremblay, “Strong-coupling expansion for the Hubbard model”, *Physical Review Letters*, vol. 80, pp. 5389–5392, 1998.
- [99] S. Pairault, D. Sénéchal, and A.-M. S. Tremblay, “Strong-coupling perturbation theory of the Hubbard model”, *European Physical Journal B*, vol. 16, pp. 85–105, 2000.
- [100] D. Vollhardt, “Strong-coupling approaches to correlated fermions.”, in *Proceedings of the International School of Physics ‘Enrico Fermi’, Course CXXI: ‘Perspectives in many-particle physics’ (Varenna on Lake Como, Villa Monastero, 7-17 July 1992)* (R. A. Broglia, J. R. Schrieffer, and P. F. Bortignon, eds.), p. 31, North-Holland Publishing Co., 1994.
- [101] A. B. Harris and R. V. Lange, “Single-particle excitations in narrow energy bands”, *Physical Review*, vol. 157, pp. 295–314, 1967.
- [102] W. Heisenberg, “Mehrkörperproblem und Resonanz in der Quantenmechanik”, *Zeitschrift für Physik*, vol. 38, pp. 411–426, 1926.
- [103] P. Weiss, “L’hypothèse du champ moléculaire et la propriété ferromagnétique”, *Journal de Physique Théorique et Appliquée*, vol. 6, no. 1, pp. 661–690, 1907.
- [104] G. Mussardo, *Statistical Field Theory*. Oxford University Press, 2009.
- [105] W. Metzner and D. Vollhardt, “Correlated lattice fermions in $d = \infty$ dimensions”, *Physical Review Letters*, vol. 62, pp. 324–327, 1989.
- [106] A. Georges, G. Kotliar, W. Krauth, and M. J. Rozenberg, “Dynamical Mean-Field Theory of strongly correlated Fermion systems and the limit of infinite dimensions”, *Reviews of Modern Physics*, vol. 68, pp. 13–125, 1996.
- [107] E. Ising, “Beitrag zur Theorie des Ferromagnetismus”, *Zeitschrift für Physik*, vol. 31, pp. 253–258, 1925.
- [108] C. Itzykson and J.-M. Drouffe, *Statistical Field Theory, Volume 1: From Brownian Motion to Renormalization and Lattice Gauge Theory*. Cambridge University Press, 1991.
- [109] T. Giamarchi, *Quantum Physics in One Dimension*. The International Series of Monographs in Physics, Oxford University Press, 2004.
- [110] L. Onsager, “Crystal statistics. I. A two-dimensional model with an order-disorder transition”, *Physical Review*, vol. 65, pp. 117–149, 1944.
- [111] R. Brout, “Statistical mechanical theory of ferromagnetism. High density behavior”, *Physical Review*, vol. 118, pp. 1009–1019, 1960.
- [112] C. J. Thompson, “Ising model in the high density limit”, *Communications in Mathematical Physics*, vol. 36, pp. 255–262, 1974.
- [113] R. O. Zaitsev and M. I. Dushenat, “Magnetic and Mott transition in the Hubbard model”, *Soviet physics–Solid state*, vol. 25, no. 11, p. 1979, 1984.
- [114] J. M. Luttinger, “Fermi surface and some simple equilibrium properties of a system of interacting fermions”, *Physical Review*, vol. 119, pp. 1153–1163, 1960.
- [115] M. Jarrell, “Hubbard model in infinite dimensions: A quantum Monte Carlo study”, *Physical Review Letters*, vol. 69, pp. 168–171, 1992.

- [116] A. Georges and G. Kotliar, “Hubbard model in infinite dimensions”, *Physical Review B*, vol. 45, pp. 6479–6483, 1992.
- [117] V. Janiš and D. Vollhardt, “Construction of analytically tractable mean-field theories for quantum models: I. General formalism with application to the Hubbard model at strong coupling”, *Zeitschrift für Physik B: Condensed Matter*, vol. 91, pp. 317–323, 1993.
- [118] V. Janiš, J. Mašek, and D. Vollhardt, “Construction of analytically tractable mean-field theories for quantum models: II. Susceptibilities and energy bounds for the Hubbard model”, *Zeitschrift für Physik B: Condensed Matter*, vol. 91, pp. 325–336, 1993.
- [119] D. M. Edwards and L. A. Hertz, “The breakdown of Fermi liquid theory in the Hubbard model”, *Physica B: Condensed Matter*, vol. 163, no. 1-3, pp. 527–529, 1990.
- [120] D. M. Edwards, “The breakdown of Fermi liquid theory in the Hubbard model: II”, *Journal of Physics: Condensed Matter*, vol. 5, pp. 161–170, 1993.
- [121] T. Kato, “On the convergence of the perturbation method I”, *Progress of Theoretical Physics*, vol. 4, pp. 514–523, 1949.
- [122] T. Kato, *Perturbation theory for linear operators*, vol. 132 of *Die Grundlehren der mathematischen Wissenschaften in Einzeldarstellung mit besonderer Berücksichtigung der Anwendungsgebiete*. Springer, 1966.
- [123] S. Lang, ed., *Complex Analysis*, vol. 103 of *Graduate Texts in Mathematics*. Springer, fourth ed., 1999.
- [124] M. Takahashi, “Half-filled Hubbard model at low temperature”, *Journal of Physics C: Solid State Physics*, vol. 10, pp. 1289–1301, 1977.
- [125] M. Koecher, *Lineare Algebra und analytische Geometrie*. Springer, 1997.
- [126] R. Bulla, T. A. Costi, and T. Pruschke, “Numerical renormalization group method for quantum impurity systems”, *Reviews of Modern Physics*, vol. 80, pp. 395–450, 2008.
- [127] M. Nahrgang, “Multichain Approach to the Single-Impurity Anderson Model in the Dynamical Mean-Field Theory”, Diplomarbeit, Philipps-Universität Marburg, 2008.
- [128] C. Lanczos, “An iteration method for the solution of the eigenvalue problem of linear differential and integral operators”, *Journal of Research of the National Bureau of Standards*, vol. 45, pp. 255–282, 1950.
- [129] R. Haydock, V. Heine, and M. J. Kelly, “Electronic structure based on the local atomic environment for tight-binding bands”, *Journal of Physics C: Solid State Physics*, vol. 5, no. 20, p. 2845, 1972.
- [130] R. Haydock, V. Heine, and M. J. Kelly, “Electronic structure based on the local atomic environment for tight-binding bands. II”, *Journal of Physics C: Solid State Physics*, vol. 8, no. 16, p. 2591, 1975.
- [131] S. Nishimoto, F. Gebhard, and E. Jeckelmann, “Dynamical density-matrix renormalization group for the Mott-Hubbard insulator in high dimensions”, *Journal of Physics: Condensed Matter*, vol. 16, pp. 7063–7081, 2004.
- [132] N. Blümer, private communication, 2010.
- [133] E. Jeckelmann, “Dynamical density-matrix renormalization-group method”, *Physical Review B*, vol. 66, no. 4, p. 045114, 2002.

Bibliography

- [134] T. Matsubara, “A new approach to quantum-statistical mechanics”, *Progress of Theoretical Physics*, vol. 14, no. 4, pp. 351–378, 1955.
- [135] H. Fehske, R. Schneider, and A. Weiße, eds., *Computational Many-Particle Physics*, vol. 739 of *The Lecture Notes in Physics*. Springer, 2008.
- [136] J. E. Hirsch and R. M. Fye, “Monte Carlo method for magnetic impurities in metals”, *Physical Review Letters*, vol. 56, no. 23, pp. 2521–2524, 1986.
- [137] J. D. Jackson, *Classical Electrodynamics*. John Wiley & Sons Inc., second ed., 1975.
- [138] H. Lehmann, “Über Eigenschaften von Ausbreitungsfunktionen und Renormierungskonstanten quantisierter Felder”, *Il Nuovo Cimento*, vol. 11, no. 4, pp. 342–357, 1954.
- [139] R. D. Mattuck, *A Guide to Feynman Diagrams in the Many-Body Problem*. Dover Publications Inc., second ed., 1992.
- [140] I. S. Gradshteyn and I. M. Ryzhik, *Table of Integrals, Series, and Products*. Academic Press, sixth ed., 2000.
- [141] J. P. Boyd, *Chebyshev and Fourier Spectral Methods*. Dover Publications, second ed., 2001.

I can no other answer make, but, thanks, and thanks.

William Shakespeare

Acknowledgements

Zum Abschluss meiner Arbeit bleibt mir nur mehr die angenehme Aufgabe, mich bei allen Personen zu bedanken, die, sei es direkt oder indirekt, zum Gelingen dieser Arbeit beigetragen haben.

Großen Dank schulde ich meinem Doktorvater Florian Gebhard, ohne dessen freundliche Aufnahme in seine Arbeitsgruppe, zunächst als Diplomand und später als Doktorand, ich diese Arbeit niemals hätte durchführen können. Durch viele inspirierende Diskussionen über spannende Fragestellungen hat er mir viele Ideen nahegebracht, die sehr zu meinem Verständnis der Physik im allgemeinen und korrelierter Elektronensysteme im speziellen beigetragen haben. Florian Gebhard hatte stets ein offenes Ohr für alle meine Probleme und stand mir stets mit Rat und Tat zur Seite – Vielen lieben Dank!

Besonders bedanken möchte ich mich auch bei Jörg Bünemann, der für physikalischen Fragestellungen stets ein offenes Ohr hatte und mir wichtige Anstöße für meine Arbeit geliefert hat. Auch die gemeinsamen Übungsbetreuungen und die vielen Diskussionen über Physik fernab dieser Arbeit werden mir in angenehmer Erinnerung bleiben.

Herzlich danken möchte ich auch Peter Lenz für seine Bereitschaft, meine Arbeit zu begutachten.

Bei Fabian Essler bedanke ich mich für die Einladung an das Rudolf Peierls Centre for Theoretical Physics in Oxford, wo ich 2009 drei Monate verbringen durfte und so einiges lernen konnte.

Mein Dank geht auch an Satoshi Nishimoto, der mir freundlicherweise seine DDMRG-Daten zur Verfügung gestellt hat. Für die Bereitstellung seiner QMC-Rohdaten sowie einiger Gnuplot-Skripte für deren Auswertung danke ich Nils Bluemer ganz herzlich.

Ein spezieller Dank an dieser Stelle geht auch an meinen Freund Cornelius Mund, mit dem ich oft und gerne über Fragestellungen aus Physik und Mathematik diskutieren konnte. Auch seine immerwährende Bereitschaft, mir sein Wissen über Computer, insbesondere über Linux-Systemadministration, weiterzugeben, darf hier nicht unerwähnt bleiben.

Meinem Freund Thomas Peters danke ich für die gewissenhaft Durchsicht von Teilen des Manuskripts und seine vielen wertvollen Tipps. Natürlich verbleibt die Verantwortung für verbleibende Fehler bei mir.

Dankend erwähne ich auch das internationale Graduiertenkolleg *Electron-Electron Interactions in Solids* der DFG für die Bereitstellung meines Promotionsstipendiums. Darüberhinaus hatte ich durch die Seminare des Graduiertenkollegs in Deutschland und Ungarn Gelegenheit, in internationalem Rahmen Vorträge zu halten.

Ein ganz besonderes Dankeschön geht an meine Familie, ohne deren liebe und uneingeschränkte Unterstützung meine Studien mir niemals möglich gewesen wären.

Curriculum Vitae

Persönliches

Name Daniel Friedrich Ruhl
Geburtstag 18.10.1978
Geburtsort Kassel
Nationalität Deutsch

Wissenschaftlicher Werdegang

1985–1989 Grundschule, Heiligenbergschule, Felsberg-Gensungen
1989–1995 Gymnasialstufe, Gesamtschule Felsberg, Felsberg
1995–1998 Oberstufengymnasium, Geschwister-Scholl-Schule, Melsungen
06/1998 Abitur, Geschwister-Scholl-Schule, Melsungen
10/1999–10/2001 Studium der Chemie, Fachbereich Chemie der Philipps-Universität Marburg
10/2001 Vordiplom für Chemie (“sehr gut”)
10/2001–12/2006 Studium der Physik an der Philipps-Universität Marburg
04/2004 Vordiplom für Physik (“sehr gut”)
2006 Diplomarbeit mit dem Titel
*Ground-State Properties of Correlated Electron Systems
in the Limit of High Spatial Dimensions*
in der AG Vielteilchentheorie des Fachbereichs Physik der Philipps-Universität
Marburg unter der Betreuung von Prof. Dr. Florian Gebhard
12/2006 Diplom für Physik (“sehr gut – mit Auszeichnung”)
seit 01/2007 Doktorand in der AG Vielteilchentheorie des Fachbereichs Physik der
Philipps-Universität Marburg
01/2007–03/2010 Stipendiat des Europäischen Graduiertenkollegs *Electron-Electron Interactions in
Solids* der DFG
08/2009–10/2009 Forschungsaufenthalt mit Prof. Dr. Fabian Essler am *Rudolf Peierls Centre for Theo-
retical Physics* in Oxford, United Kingdom
seit 04/2010 Wissenschaftlicher Mitarbeiter in der Arbeitsgruppe Vielteilchentheorie am Fachbe-
reich Physik der Philipps-Universität Marburg

Marburg, den 19.04.2010